# Cycles de vie de deux crevettes hydrothermales de la dorsale médio-atlantique : Rimicaris exoculata et Rimicaris chacei

Pierre Methou

UNIVERSITE SCIENCES
BRETAGNE DE LA MER
LOIRE ET DU LITTORAL

# THESE DE DOCTORAT DE

L'UNIVERSITE
DE BRETAGNE OCCIDENTALE
COMUE UNIVERSITE BRETAGNE LOIRE

ECOLE DOCTORALE N° 598
*Sciences de la Mer et du littoral*
Spécialité : Biologie Marine

Par
**Pierre METHOU**

## Lifecycles of two hydrothermal vent shrimps from the Mid-Atlantic Ridge: *Rimicaris exoculata* and *Rimicaris chacei*

"Embryonic development, Larva dispersal, Recruitment, Reproduction & Symbioses Acquisition"

**Thèse présentée et soutenue à Brest, le 10 Décembre 2019**
**Unité de recherche : Unité Étude des Écosystèmes Profonds (EEP) aux laboratoires LMEE & LEP**

**Rapporteurs:**

DUPERRON Sébastien
Professeur, MNHN Paris

HILARIO Ana
Assistant Researcher, Universidade de Aveiro (UA)

**Composition du Jury :**

DUPERRON Sébastien (Président)
Professeur, MNHN Paris

HILARIO Ana (Rapporteur)
Assistant Researcher, Universidade de Aveiro (UA)

JOLLIVET Didier (Examinateur)
Directeur de Recherche CNRS

ZBINDEN Magali (Examinateur)
Maître de Conférence, Sorbonne Université (SU)

CAMBON-BONAVITA Marie-Anne (Directrice de thèse)
Cadre de Recherche, Ifremer Brest

PRADILLON Florence (Co-directrice de thèse)
Cadre de Recherche, Ifremer Brest

**Invité(s)**

SEGONZAC Michel
Chercheur Emérite, MNHN Paris

Ifremer LM2E UBO - CNRS - IFREMER
cnrs INEE iuem UBO université de bretagne occidentale Région BRETAGNE
ISblue The interdisciplinary graduate school for the blue planet

# Remerciements and Acknowledgments

Par où commencer... Tout d'abord, il est tard, très tard, comme on le suppose et comme cela se doit pour tous bons remerciements de fin de thèse après un si long parcours. Mes pensées se mélangent donc un peu et les différentes langues aussi. Je pense donc que chacun recevra sa part dans la langue qui lui sied le mieux, ou tout du moins une dans laquelle je puisse m'exprimer.

Je pense que les plus évidents vont bien sûr à Marie Anne et Florence, sans qui ce travail n'aurait jamais atteint le stade de l'imprimerie. Elles y ont passé beaucoup de temps, beaucoup d'énergie et je n'ose imaginer comment j'aurais fait sans elles. Peut-être aurais-je laissé tout tomber ? Merci du fond du cœur pour tout ce que vous avez pu m'apporter, de l'encadrement de rêve que vous m'avez donné, un parfait équilibre entre vous deux, vos deux personnalités, comme un Ying et son Yang. Ces trois années, bien qu'épuisantes, ont sûrement été parmi les plus belles de ma vie, m'entraînant du fond des océans jusqu'aux deux extrémités du monde, des Etats-Unis au Japon.

A propos des Etats-Unis, merci à tous ceux avec qui j'ai pu partager ce magnifique appartement près de l'aquarium de Monterrey : Fanny, Julien, Sven – I will come to you later ;-) – Arunima, Sam, Joan et d'une certaine façon Leila, pour qui ce fut de belles retrouvailles, après tout ce temps en master. C'était un congrès palpitant, qui aura d'ailleurs peut-être changé ma vie.

Joan, mon jumeau de thèse, j'ai ce soir une petite pensée pour toi, d'ici quelques jours tu rendras ton manuscrit. On aura commencé ensemble, et nous finirons en beauté le même jour, enfin je l'espère. J'ai passé avec toi, Fanny et Julien des moments incroyables et chaque visite dans votre bureau a toujours été une bouffée d'air réanimant une journée assommée par la rédaction. En un mois d'absence seulement, ces journées me manquent déjà beaucoup. J'aurai beaucoup appris de toi, Joan, et je pense que j'en suis devenu un meilleur scientifique grâce à cela.

A gigantic thanks to you Sven, as well. If Joan is my twin, you are definitely my big brother. I think that I found in you a vision of the kind of scientist I would like to become after this thesis, always passionate, never afraid of challenges and that is always willing to share and help anyone he could. I have learn so many things with you, I really miss our conversations, either scientific or personnal. I was so glad when I hear you were coming to my defense. Writing these lines, I realize that I would like to keep and maintain contact with you and your family; you are definitely on the ones that matter for me.

Lors de mon arrivée à l'Ifremer, il y a déjà trois ans de cela, deux autres personnes furent particulièrement importantes pour moi : Sébastien et Valérie. Seb, j'espère que tu te plais dans ce que tu fais aujourd'hui et je te souhaite beaucoup de bonheur pour la suite. J'attends avec impatience nos retrouvailles le 10 décembre. Valérie, tu es sans doute l'une des personnes les plus incroyables et les plus étonnantes que je connaisse, tu es une source d'inspiration chaque jour, tu me manqueras beaucoup quand je partirai, et sans trop m'avancer je crois que ce sera réciproque, enfin je l'espère. Bonne chance pour ta thèse, je suis persuadé que tu relèveras ce nouveau défi haut la main une fois de plus. Lucile, on n'a pas eu la chance de partager autant qu'avec les autres, tu es arrivée lorsque j'ai quitté le FISH et ses salles noires. Néanmoins, tu as toujours été là pour moi surtout sur la fin. Merci de m'avoir renseigné sur tout le fonctionnement infernal du système des qualifications, désolé je n'ai pas réussi à trouver le temps de m'y inscrire cette année mais ça n'est que partie remise.

## REMERCIEMENTS AND ACKNOWLEDGMENTS

Bien sûr je voudrais aussi adresser des remerciements tout particuliers aux membres de mon Jury de thèse, notamment à mes deux rapporteurs, Sébastien Duperron, Professeur au Muséum d'Histoire Naturelle de Paris et Ana Hilário, Chercheuse à l'Université d'Aveiro, pour le temps qu'ils auront consacré à la relecture de ce manuscrit, sûrement trop long en l'état. Je remercie aussi évidement le reste de mon jury, Gwenaëlle Le Blay, Professeur à l'Université de Bretagne Occidentale, Didier Jollivet, Directeur de Recherche CNRS à la station biologique et Michel Segonzac, Chercheur émérite au Muséum d'Histoire Naturelle de Paris, pour l'intérêt qu'ils ont porté à mon sujet de recherche. Enfin, plus que tous les autres, un grand merci à Magali Zbinden, Maître de conférences à l'Université Pierre et Marie Curie, qui en plus de faire partie de mon jury, a suivi mon travail du début jusqu'à la fin lors de mes comités mais aussi à bord du *Pourquoi Pas ?*. Merci pour tes conseils, j'espère que tu trouveras ce travail intéressant et que ton modèle de recherche sera bien mis à l'honneur tout au long de ces pages.

Quelques autres personnes méritent amplement leur nom en particulier ici : Johanne, Michel, Loïc et Lyndsay. Johanne si je peux me targuer d'avoir sorti mon premier papier, c'est bien grâce à toi. Peu de figures et peu d'analyses statistiques de ces bactéries auraient pu se faire sans ta précieuse aide. Michel, je ne sais pas si tu réalises tout à fait, mais lorsque j'ai commencé à m'intéresser aux environnements profonds, tu es rapidement devenu un de mes héros, de ceux qu'on regarde d'en bas et qui nous seront toujours inaccessibles. Et pourtant, je ne sais par quel miracle mais on a fini par se rencontrer et surtout travailler ensemble. Ce furent des moments particulièrement privilégiés bien que trop rares. Et à défaut de se voir régulièrement, je garde bien en mémoire tous nos débats et nos succulents échanges de mails, c'est toujours avec joie que je découvre un nouveau message de toi parmi la souvente banalité de ma boite mail. Je suis fier de t'avoir dans mon jury et je t'attends de pied ferme d'ici moins de deux mois. Autrement, Loïc, le deuxième article sortira bientôt et c'est clairement aussi grâce à toi s'il peut être dans cet état aujourd'hui. Toujours disponible pour une question, toujours clair et concis dans tes explications, tu t'es véritablement investi dans ma thèse et mon projet et ça a été un véritable bonheur de collaborer avec toi. Lyndsay, je ne sais vraiment pas comment je m'en serais sorti sans toi, le troisième chapitre de ce travail n'aurait clairement pas pu avoir la même saveur sans tes connaissances en modélisation. Ton amitié me reste chère malgré nos différends cinématographiques, je te souhaite beaucoup de chance pour la suite de ta thèse, qu'elle finisse sur cette lancée actuelle et non sur une fausse note comme c'était le cas tout au début. Merci à Cécile aussi pour tout son travail sur les données environnementales, qui ont grandement amélioré ce chapitre aussi.

Nonetheless, there is still, one very important person between all these collaborators, Chong. I cannot believed you trusted me enough with only five minutes of conversation to give me samples from your lab, but also to accept to welcome me at the Jamstec for a month. Hiromi, you are the best! I heard a lot of good about you by Florence and others before coming to Japan but I could not imagine how wonderful you were. A lot of other people at Jamstec were also really welcoming, in particular Hidetaka. It was an amazing experience to meet you all, and I really hope, the project we send to your institution, will cross the pitfalls and be accepted. The idea of spending three years there is an exciting thought.

## REMERCIEMENTS AND ACKNOWLEDGMENTS

Evidemment, cette thèse n'aurait pu se faire sans la précieuse aide administrative des différentes secrétaires qui ont su me récupérer de mes errances et incompréhensions face à tous ces dossiers auxquels j'ai eu affaire. Parmi les plus importants, Annaïg qui a su se battre avec l'administration lors des justifications de paiements de la mission BICOSE 2 qui ne faisaient pas l'affaire, ou encore Anne-Laure que j'ai peu rencontré mais qui s'est occupé – et s'occupe encore ardemment – de l'organisation des trajets pour que tous les membres du jury puissent assister à ma future soutenance. Cependant, je tiens à remercier tout particulièrement Christine et son sourire avec qui j'ai pu partager ma passion de Jack London.

Parmi ceux qui manquait encore, beaucoup de gens de la mission BICOSE 2, Laurent, Françoise, Erwan, Aurélie, Christian, Marc, Laure, Inma, Bruce, Louis, Ivan, Lowick et tant d'autres que j'ai sûrement oublié. Je vous ai rencontré ou j'ai appris à vous connaître sur ce bateau et ce fut de belles rencontres. Toute l'équipe du bateau comme l'équipe du Nautile étaient au top de A à Z, une super expédition loin d'être sans embuches mais tellement enrichissante. Un merci tout spécial à Julien et Guillaume avec lesquels je suis allé rencontrer mes crevettes tout au fond, c'était renversant, je n'oublierai jamais ce jour. Encore merci à toi, Marie-Anne, de m'avoir offert cette opportunité. Je crois que c'est à ce moment précis, sur le pont entre deux conteneurs, que j'ai compris que c'était vraiment cela que je voulais faire tout ma vie.

Je crois que c'est le moment maintenant de remercier tout le laboratoire, tous les oubliés que je n'ai pas cité mais qui sont dans mon cœur, aussi bien ceux du LMEE que ceux du LEP, je ne fais pas la différence, vous êtes pour moi tous aussi géniaux.

Merci aussi à mes deux stagiaires, Leela et Marion, j'espère avoir été à la hauteur de ma tâche. Leela tu as fait un travail de tri formidable, j'espère que tu as pu trouver ton intérêt dans ce stage et que j'ai réussi à te transmettre des choses, malgré la différence culturelle qui nous sépare. Marion, tu as été incroyable, une bombe de positivité, et toujours l'envie de savoir la suite, c'est un bon moteur, tu tiens le bon bout. Bonne chance pour ta thèse, les choses ne font que commencer. Je te charge d'une mission, celle de maintenir la cohésion entre les doctorants LEP et LMEE, organiser des sorties au bar ou d'autre choses ensemble, j'ai tenté d'assurer ce rôle plusieurs années avec moins de succès sur la fin à mesure que la thèse avançait mais je pense que ça reste quelque chose d'important. Melissa, Julien et Camille sont des personnes formidables et vous auriez tort de passer à côté.

Merci à tous les doctorants du LMEE pour ceux que je n'aurai pas cité, Elodie, Jordan, Maurane, Sarah, maxime, Marc, David, Jie, Melanie, Charlène, Yang, Simon, Florian et Vincent, une belle troupe qui malheureusement se rétrécit avec le temps mais qui je l'espère gardera sa force. Bonne chance à tous ceux qui s'approchent de la ligne d'arrivée, vous verrez c'est grisant.

Merci à tous mes amis de Brest, de Paris ou d'ailleurs, je ne peux pas tous vous citer mais si vous êtes en train de lire ces lignes c'est que vous m'êtes indéniablement très chers. Merci aussi à tous les colocs que j'ai connus : Jonathan, Valentin, Audrey, Ingwenog, Julia, Baptiste, Anne, Sébastien, Rémi. Je me suis fait une nouvelle famille avec vous. Pourtant je n'ai jamais eu besoin de remplacer ma famille, elle qui a toujours été incroyable et qui m'a toujours soutenu et surtout qui m'a permis d'en arriver là aujourd'hui. Je vous aime et j'espère pouvoir bientôt vous consacrer un peu plus de temps.

## REMERCIEMENTS AND ACKNOWLEDGMENTS

Enfin et sûrement la personne la plus importante de toutes à mes yeux, ma chère Azenor, celle qui partage ma vie depuis deux ans. Merci d'avoir été là dans les moments les plus difficiles, d'avoir su trouver les mots même si parfois cela était trop pour toi. Tu as supporté ce fardeau autant que moi, et ce travail tu y as participé beaucoup plus que ce que l'on pourrait croire, du remplissage des tableaux de données à partir de mon cahier de manips aux corrections orthographiques de toutes les conclusions en français, tu y es investie malgré toi. Tu es prête à tout pour moi, jusqu'à partir à l'autre bout du monde pour me suivre. J'espère que j'arriverai à équilibrer un peu plus mon temps par la suite pour passer un peu plus de temps auprès de toi et que j'arriverai à être à la hauteur. Une chose est sûre, je tiens à passer ma vie avec toi, mon amoureuse, ma future femme. Celle sans qui je n'envisage plus de faire ma vie.

# Table of Content

## TABLE OF CONTENT

# List of Figures

## LIST OF FIGURES

## LIST OF FIGURES

# List of Tables

# List of Abbreviations

| | |
|---|---|
| ± | "either side of" |
| ~ | approximately |
| µm | micrometers |
| µL | microliters |
| µM | micromolars |
| mm | milimeters |
| mL | mililiters |
| mM | milimolars |
| m | meters |
| km | kilometers |
| ‰ | parts per thousand |
| °C | degrees celsius |
| ♀ | female |
| ♂ | male |
| 16S | 16S subunit of the ribosomal RNA (gene) |
| AUV | Autonomous Underwater Vehicle |
| CBB | Cavin-Benson-Bashamm cycle |
| CIR | Central Indian Ridge |
| CL | Carapace lenght |
| COI | Cytochrome oxidase subunit I |
| CTmax | Critical thermal maximum |
| CT-scan | Computed Tomography scan |
| DIG | Dioxygenin |
| EPR | East Pacific Rise |

## LIST OF ABBREVIATIONS

| | |
|---|---|
| FISH | Fluoresecent in Situ Hybridization |
| HOV | Human Operated Vehicle |
| JdF | Juan de Fuca Ridge |
| MAR | Mid Atlantic RIdge |
| OTU | Operational Taxonomic Unit |
| PAR | Pacific-Antarctic Ridge |
| PCR | Polymerase Chain Reaction |
| PLD | Planktonic larval duration |
| ROV | Remotely Operated Vehicle |
| rTCA | reverse TriCarboxylicAcid cycle |
| SEIR | South East Indian Ridge |
| SEM | Scanning Electron Microscopy |
| SWIR | South West Indian Ridge |
| TEM | Transmission Electron Microscopy |

| | |
|---|---|
| $O_2$ | Dioxygen |
| $CO_2$ | Carbon dioxide |
| $H_2S$ | Hydrogen sulfur |
| $H_2$ | Dihydrogen |
| $CH_4$ | Methane |
| Fe | Iron |
| $Fe^{2+}$ | Ferrous iron |
| $Fe^{3+}$ | Ferric iron |

.

+

# Prologue: General introduction

Ce prologue sert à introduire au lecteur les différents aspects de la recherche abordés par les résultats de cette thèse. Ces résultats sont répartis en chapitres dans cet ouvrage, que l'on peut aussi voir comme certaines des étapes clés successives de la vie des crevettes étudiées, de leur naissance à leur reproduction.

Cette thèse s'intéresse au cycle de vie des espèces hydrothermales dans le contexte général de la compréhension des processus de colonisation des sites hydrothermaux. Elle prend pour modèle les crevettes *Rimicaris*, modèle aujourd'hui relativement bien étudié dans l'Unité Environnements Profonds de l'Ifremer mais dont le cycle de vie reste malgré tout peu compris. Comme beaucoup d'espèces de la faune hydrothermale visuellement dominantes, l'espèce principale dont il sera question abrite des microorganismes avec lesquels, elle forme une symbiose, indispensable à sa survie. La pérennité de cette association au cours du cycle de vie est donc un aspect fondamental pour la colonisation de ces milieux et est donc abordé de concert avec le cycle de vie de l'hôte

Ainsi, toute la première partie de cette introduction générale cherche à présenter leur écosystème pour en comprendre, à l'aune de nos connaissances actuelles, les principes généraux de leur fonctionnement et leurs particularités vis-à-vis des autres écosystèmes de notre planète. Premièrement, l'histoire de l'exploration des sources hydrothermales est détaillée permettant de faire un premier état général de leur distribution géographique mais aussi de mettre en avant les régions les moins considérées. Ensuite, et après avoir présenté le contexte géologique de leur formation, l'introduction met l'accent sur les caractéristiques chimiques particulières de ces environnements qui jouent un rôle majeur sur la distribution des espèces. En effet, comme le montre la suite, la vie dans ces écosystèmes se base non pas sur la photosynthèse, mais sur la chimiosynthèse utilisée par les bactéries. L'introduction se penche ainsi sur les différents microorganismes, leurs métabolismes, leur distribution et les facteurs environnementaux qui les affectent pour en venir ensuite à leurs interactions, d'abord entre eux puis avec la faune hydrothermale.

Ainsi le lecteur est amené progressivement vers la présentation des différentes symbioses qui ont pu être étudiées dans ces milieux en présentant à la fois les hôtes animaux et les adaptations qu'ils présentent, ainsi que la diversité de leurs bactéries symbiotiques. D'autres d'espèces sont ensuite brièvement présentées permettant d'aborder d'une part très rapidement le sujet des chaines trophiques de ces écosystèmes mais surtout la distribution inégale de toutes ces espèces sur le globe, réparties en différentes zones biogéographiques. Tout ce chemin permet ainsi de dresser un constat clair : celui du caractère éphémère et fragmenté des sources hydrothermales, ainsi que de la nécessité de dispersion entre différents sites, chez les espèces endémiques de ces écosystèmes pour maintenir leur existence dans le temps. Ceci amène ainsi pas à pas le lecteur vers la thématique principale de cette thèse : les cycles de vie et les étapes critiques influençant leurs capacités de colonisation et de survie. Parmi elles, on peut noter la reproduction, la dispersion et le recrutement ainsi que le maintien de la relation symbiotique pour ceux en possédant, qui sont ainsi toutes détaillées une à une.

Au-delà du cycle de vie d'une espèce modèle unique, *Rimicaris exoculata*, cette thèse s'intéresse à proposer une perspective élargie de la colonisation du milieu hydrothermal des autres espèces de la même famille, du stade œuf jusqu'à la reproduction. Un accent particulier est mis sur *Rimicaris chacei*, qui vit sur les mêmes sites, que *Rimicaris exoculata*. Leurs comportements trophiques, symbioses et adaptations sont respectivement comparées avant de finir sur les quelques connaissances existantes à l'heure actuelle sur leur cycle de vie, en mettant en avant les différentes lacunes les plus importantes. Ceci permet finalement d'aboutir aux buts généraux de cette étude et à la présentation des différents chapitres de l'histoire du cycle de vie de ces espèces.

.

*« Sur les rayons des bibliothèques je vis [tout] un monde surgir de l'horizon »*

*Martin Eden, Jack London*

# P.1. The hydrothermal vent ecosystems

## P.1.1 Geological context of hydrothermal vent systems

### P.1.1.1 Hydrothermal vents: a phenomenon hosted by the global ridge system

Hydrothermal vents are geological structures located on the ocean floor from which hot fluids geothermally heated are expelled. Consequence of plate tectonic movements, they are found in extension zones along mid-ocean ridges (MOR) where new oceanic crust is formed, as well as in volcanic arcs and back arc basins (BAB) formed behind subduction zones where a lithospheric plate sinks beneath another one. Some vent sites are also localized intraplate, such as the Lō'ihi seamount in the Hawaiian hotspot chain (Staudigel et al., 2006).

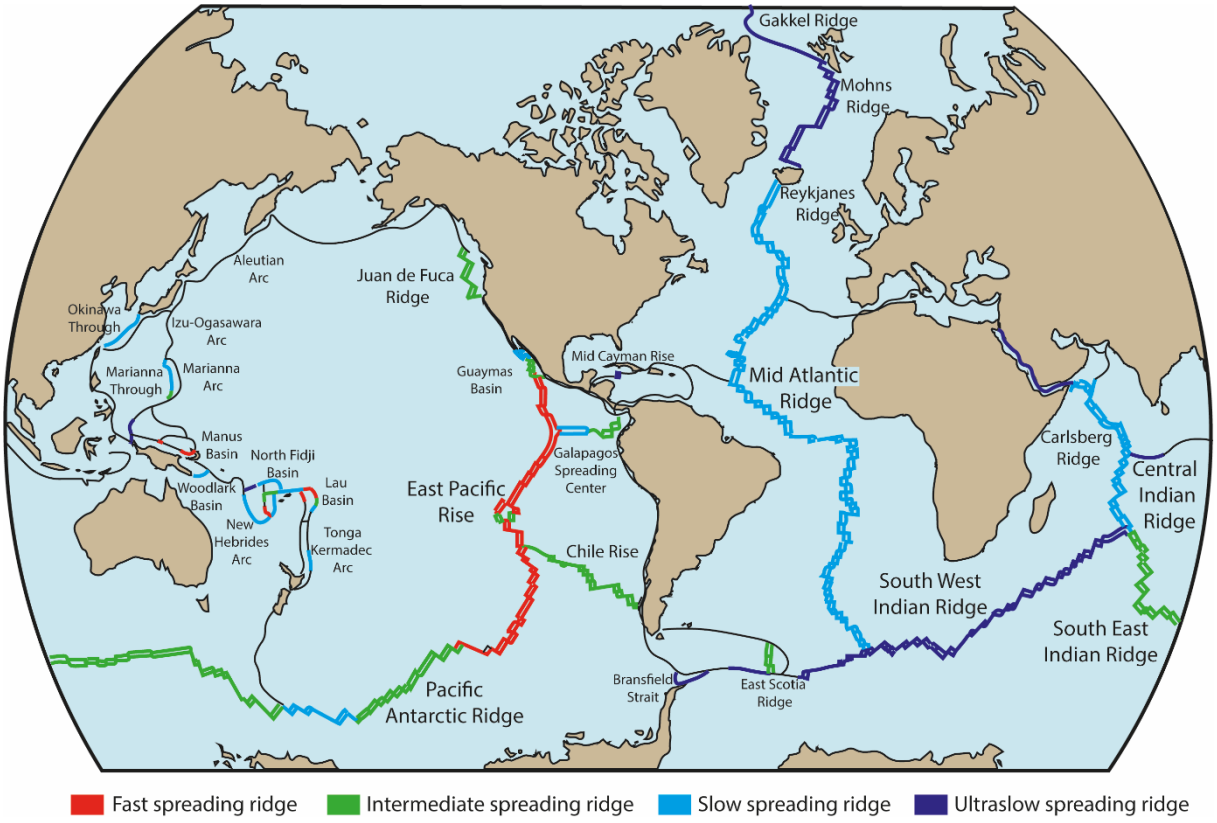


**Fig 1.** General map of spreading ridge rates around the globe. Adapted from Beaulieu et al. (2015) and Dick (2019).

Oceanic ridges are generally classified in four different categories (**Fig 1**.), depending on their spreading rate which influences greatly their topography (**Fig 2.**) and the presence of hydrothermal activity (Fouquet et al., 2010; Morgan and Chen, 1993):

- Fast spreading ridges (more than 80 mm/year) exhibit a morphology dominated by volcanic activity. Across its axis, the ridge presents an axial rise with a very narrow summit. Almost no evidence of faulting is found until the newly formed crust has moved few km away where some abyssal hills are sometimes observed. This category of ridge represents 25% of the global ridge system and mainly corresponds to the East Pacific Rise (EPR) region (**Fig 1.**) (Beaulieu et al., 2015).

- Ultraslow or slow spreading ridges (below 20 mm/year and between 20 and 55 mm/year respectively) are shaped by tectonic activity. This results in an important faulting of the ridge creating a broad axial rift valley of several km wide and approximately a km deep depending on the ridge. They are much more widespread than fast spreading ridges and represent 60% of the global ridge system (**Fig 1.**) (Beaulieu et al., 2015). Regions such as the Mid Atlantic Ridge (MAR), the Central and Southwest Indian Ridges, the Gakkel Ridge or the Mid Cayman Rise belong to this category.
- Intermediate spreading ridges (between 55 and 80 mm/year) exhibit transitional arrangements between slow and fast spreading ridge with an axial valley quite narrow and shallow compared to slow spreading ridges. They represent 15% of the global ridge system and include regions such as the Juan de Fuca Ridge, the South East Indian Ridge (SEIR) or the Lau Basin (**Fig 1.**) (Beaulieu et al., 2015).

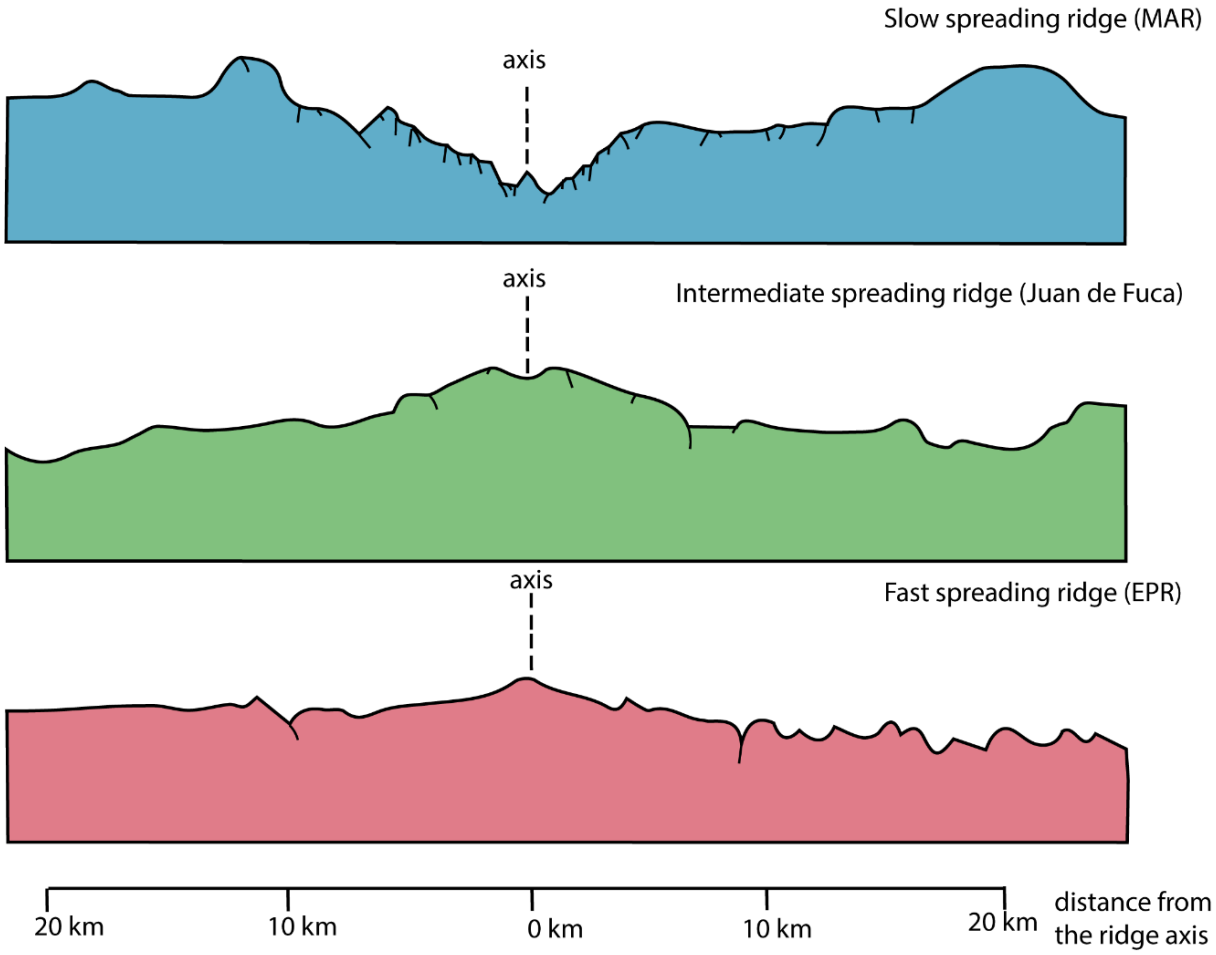


**Fig 2.** Different profiles of oceanic ridge morphology classified by spreading rate. Adapted from (Macdonald, 1982).

Both spreading rate and ridge topography result from local differences in magma supply beneath the oceanic crust as stated by the magmatic budget hypothesis. Fast spreading ridges are characterized by a much larger magma supply leading to more unstable and ephemeral vent sites, but closer to each other than vent sites hosted by slow spreading ridges. This was proposed according to the linear relationship observed between spreading rate and hydrothermal venting, with more frequent venting along fast spreading ridges. However, this tendency was largely based on

observations on the EPR and the Juan de Fuca Ridge only (Baker, 1996; Baker et al., 1994). The addition of results from hydrothermal plume surveys along three segments of the MAR nonetheless confirmed this relationship with an average distance of 130 km between each vents sites on this slow spreading ridge (German and Parson, 1998). Still, some variations can be expected from these observations as the more complex topologies of the slow spreading ridge could prevent detection of some hydrothermal plumes (German and Parson, 1998).

Accordingly, frequency of venting sites is supposed to be very low on ultraslow spreading ridges with average distances between sites around 200 km to 300 km. However, plume surveys along the Southwest Indian Ridge (SWIR) and the Gakkel Ridge revealed significant deviation from this expectation, with an average spacing of 100 km between potential vent sites (inferred from plume detection) (Snow and Edmonds, 2007). This seems to be related to the magmatic chamber, which is much shallower than usually observed (Snow and Edmonds, 2007). Current predictions on vent sites frequency and locations along ridges are likely to evolve as discoveries and advances are made in the exploration of our deep ocean.

## P.1.1.2 Exploration of deep sea hydrothermal vents: historic & current status

Exploration of mid oceanic ridges to demonstrate the plate tectonic theory started with the French American program FAMOUS in 1971. These pioneer expeditions revealed the presence of fossil hydrothermal deposits on the MAR (Ballard et al., 1975). The first proof of an active hydrothermal vent site was however made a few years later, in 1977, by the American deep submersible *Alvin* on the Galapagos spreading center (Corliss et al., 1979).

After that, active vent sites were found globally during the following decades. Their presence was first extended to fast spreading ridge regions such as the EPR (Haymon et al., 1991; Spiess et al., 1980) and the Juan de Fuca Ridge (Tunnicliffe et al., 1985). This was quickly followed by discoveries in the different back arc basins of the south west Pacific – Manus (Both et al., 1986), Lau (Cronan et al., 1984) and Fidji (Naganuma et al., 1989) – and the north west Pacific - Marianna (Hessler and Lonsdale, 1991) and Okinawa (Kimura et al., 1988). At the same period, active vent sites were finally discovered along the MAR, in 1985, with the TAG and Snake Pit vent fields (Kong et al., 1985; Rona et al., 1986). Today, 19 active vent fields have been confirmed on the MAR, the last one, Luso, having only been found last year in 2018 close to the Azores islands by a Portuguese expedition. Explorations in the late 90s led to the discovery of vents on the Central Indian Ridge with the Kairei and Edmond vent fields (Hashimoto et al., 2001; Van Dover, 2001), followed by the Dodo and Solitaire vent fields some years later (Nakamura et al., 2012).

Over the past 20 years, the most important discoveries of hydrothermal vents were probably made on the South MAR (Haase et al., 2007), the Arctic Ridge (Edmonds et al., 2003; Pedersen et al., 2010; Schander et al., 2010), the East Scotia Ridge (Rogers et al., 2012) and the Mid Cayman Rise (German et al., 2010), closing some of the previously identified gaps in vent global distribution (Ramirez-Llodra et al., 2007). Very recently, during the period of this thesis, the discoveries of five new vent sites were reported as well on the SWIR (Copley et al., 2016; Zhou et al., 2018), the SEIR (Gerdes et al., 2019) and the South MAR (Dong et al., 2019). In addition, new vent locations were reported in areas that had been extensively surveyed before, like the Okinawa Through (Miyazaki et al., 2017), the Guaymas Basin (Goffredi et al., 2017), the Marianna Through (Baker et al., 2017), and the Central Indian Ridge (CIR) (Ryu et al., 2019).

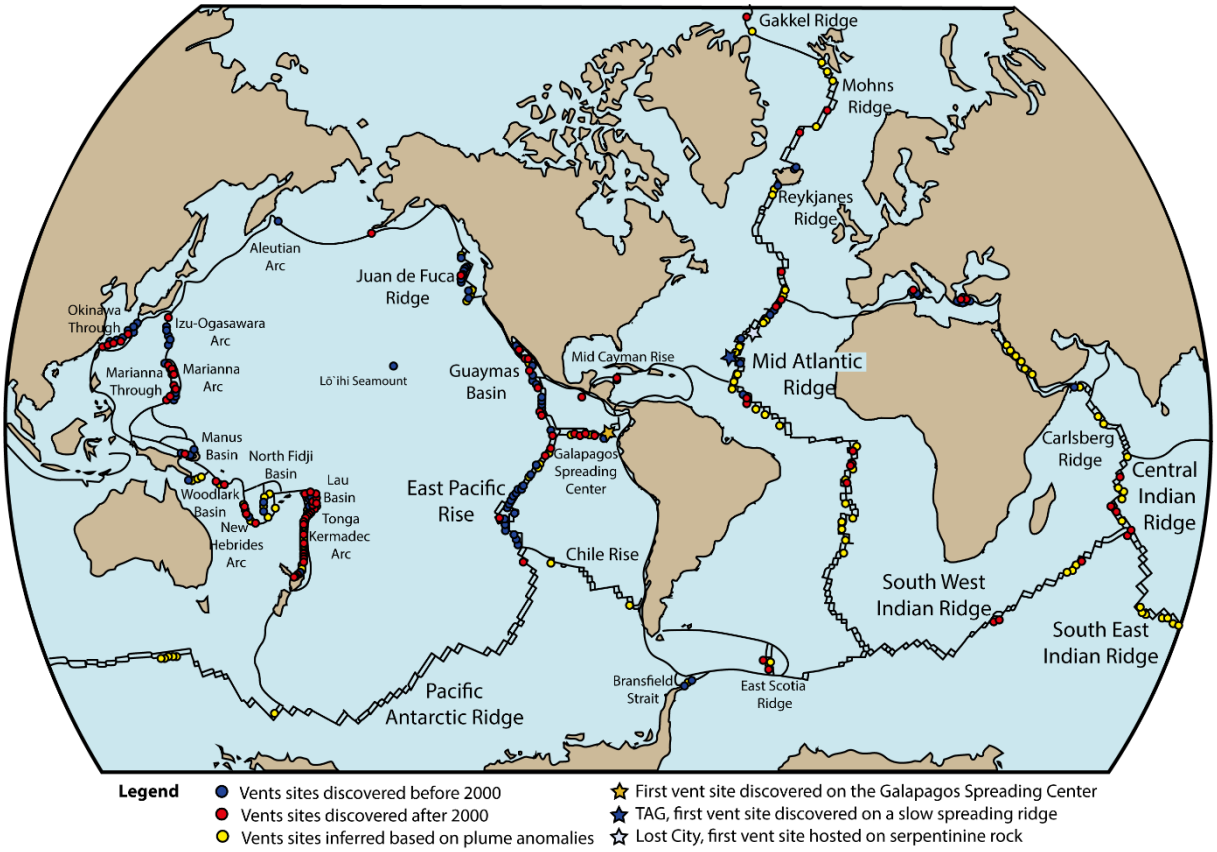


**Fig 3.** General state of confirmed and inferred hydrothermal vent site discoveries as in 2019. Adapted from Beaulieu et al. (2013) and the current InterRidge vent database v3.4

An overview of the distribution map of the currently known hydrothermal sites (**Fig 3.**) helps to highlight the largest gaps remaining today. Among them, despite some hypothetical vent locations already identified based on water column anomalies, the south MAR, the Chile rise and the global ridge system around Antarctica – Pacific Antarctic Ridge, SEIR and SWIR – are potentially the most critical parts of the globe that should be the subject of future explorations.

Besides insufficient exploration of the global ocean ridge system, technical issues have hampered the discovery of new vent fields. Most hydrothermal plumes are detected by heat or other physical or geochemical anomalies (turbidity, $CH_4$ or Mn for example) on vertical profiles made through the water column several kilometers below sea level. Such techniques are however not adapted to detect low temperature discharge of hydrothermal fluids, which could represent more than 25% of the global vent activity (Baker et al., 2016). Sites present on the flanks of axial valleys are also harder to detect from the surface. This could explain how many vent sites have been missed, even in repeatedly surveyed areas, such as the EPR and the Northern part of the MAR (Beaulieu et al., 2015). More exploration beyond surface ships, with AUVs (Autonomous Underwater Vehicle) coupled with other sensors like ORP (Oxidation-Reduction Potential sensors) will potentially drive the discovery of more of those particular vent fields (Baker, 2017). Ultimately, visual exploration with ROVs (Remotely Operated Vehicle) or HOV (Human Operated Vehicle) (**Fig 4.**) remains unavoidable to fully evaluate the extant, as well as the geochemical and biological properties of the newly discovered vents.

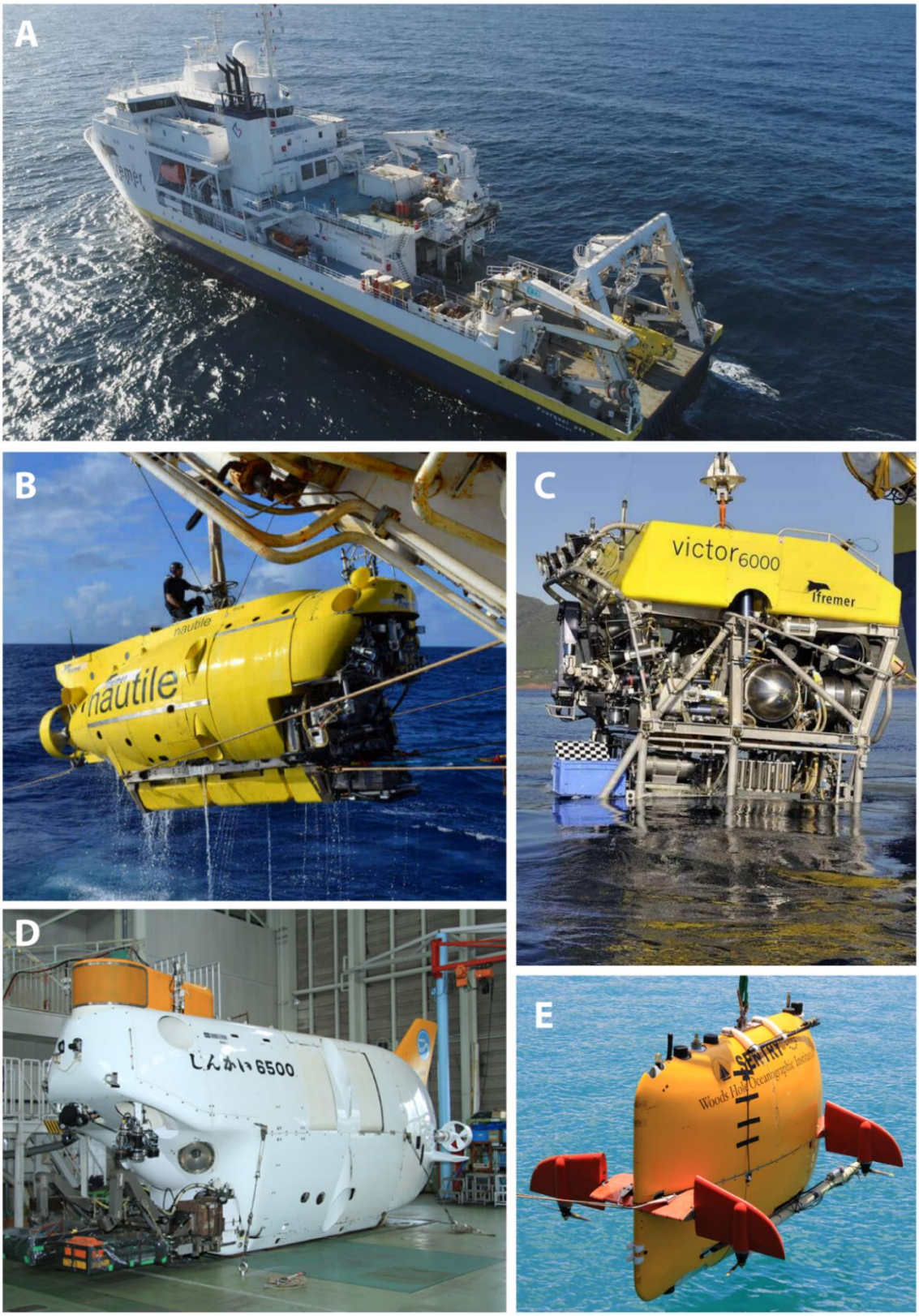


**Fig 4.** Examples of vehicles and Research Vessels (R/V) used for undersea operations and exploration. **A.** The R/V *Pourquoi pas?* operated by Ifremer. © Ifremer. **B.** The HOV *Nautile* operated by Ifremer (France). © Ifremer. **C.** The ROV *Victor6000* operated by Ifremer (France). © Ifremer. **D.** The HOV *Shinkai* operated by JAMSTEC (Japan). © JAMSTEC. **E.** The AUV *Sentry* of the Woods Hole Oceanographic Institute (WHOI; USA) equipped with different probes to locate and quantify hydrothermal fluxes. © WHOI.

## P.1.1.3 Formation of hydrothermal vent emissions

As described in part 1.1, ridge areas gather all the required conditions to host a hydrothermal activity namely the presence of a heat source – usually the magma chamber beneath the crust – and the presence of several fractures in the oceanic crust, resulting from the tectonic activity.

The first step of a hydrothermal vent formation starts in this important network of cracks and faults that allows the infiltration of cold and oxygenated seawater. Those areas are called recharge zones and extend through dozens of $km^2$ around the vent field (Tivey, 2007). During its way down, the water is submitted to increasing temperature and pressure, leaching and dissolving different compounds from the surrounding rocks. The fluid in formation progressively releases $Mg^{2+}$, becomes more acidic and gains other elements like $Ca^{2+}$, $Na^{+}$ until it reaches the reaction zone or "root zone" close to the magma chamber. There, the hot fluid is loaded with different metals, volatiles and reduced elements before it rises rapidly to the surface (Alt 1995; Tivey 2007). These four steps correspond to the currently accepted model for the formation of hydrothermal vent chimneys (**Fig 5.**).

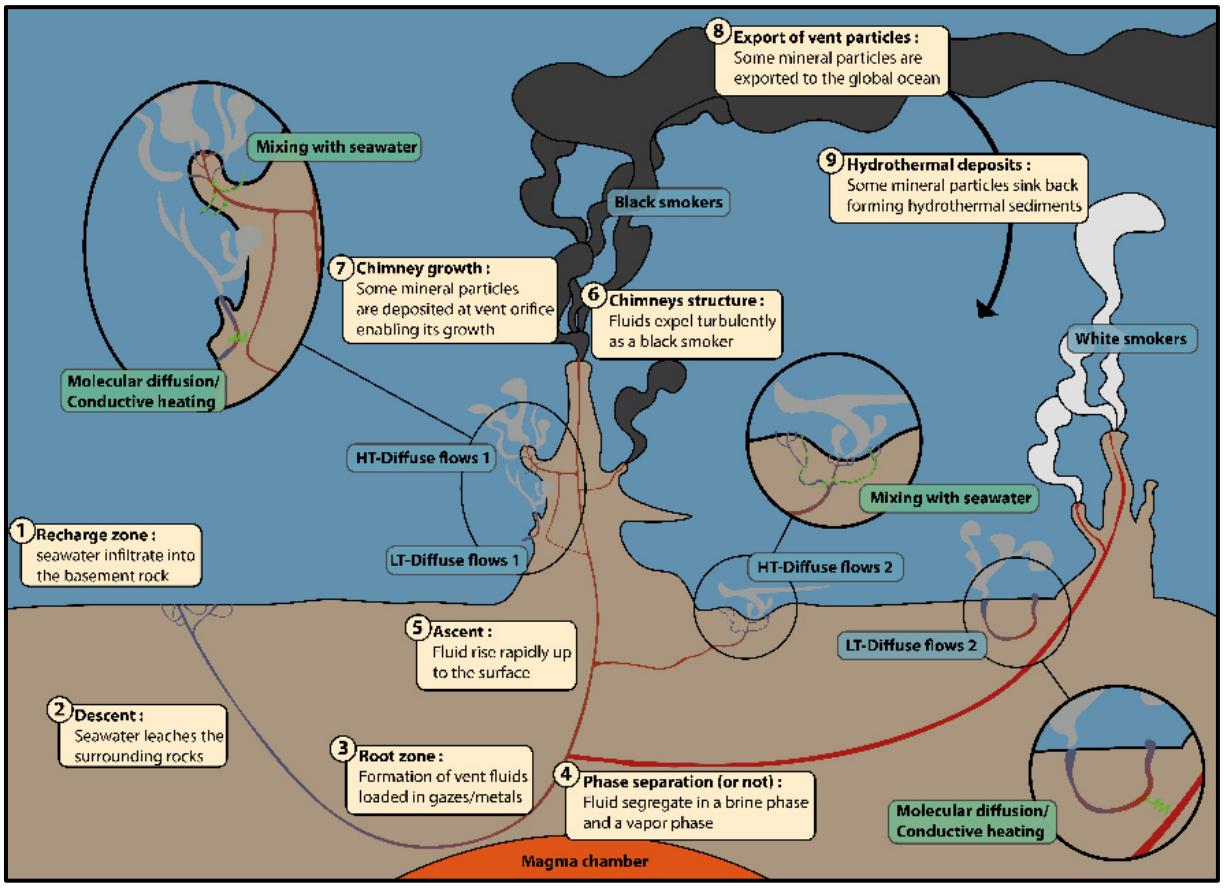


**Fig 5.** Schematic view of hydrothermal vent fluids formation. Adapted from Tivey et al. (2007) and Le Bris et al. (2019).

Within the "root zone", vent fluids can undergo a phase separation leading to the formation of a brine phase and a vapor phase (Foustoukos and Seyfried, 2007; Tivey, 2007). This phase separation is conditioned by the temperature but also the pressure conditions within the root zone – i.e. the depth of the vent field and that of the magmatic chamber – and has an important influence on vent fluid composition (Butterfield et al., 1994; Von Damm et al., 2003). Above specific conditions of very high pressure and very high temperature (reached for deeper vent fields and/or magmatic chambers), vent

fluids become supercritical as observed at the 5°S MAR vent site or at the Piccard vent site in the Cayman Rise (Koschinsky et al., 2008; Webber et al., 2015), and exhibit intermediate physical properties between fluids and gases.

When they exit the seafloor at the chimney orifice, the end member fluids – i.e. pure undiluted fluids – are "clear" and extremely hot (between 330°C and 405°C). Then, they rise rapidly with reported velocities of 0.1 $m.s^{-1}$ to 6.2 $m.s^{-1}$ (Ramondenc et al., 2006), and mix turbulently with the cold and oxygenated surrounding seawater. This provokes a drastic change in temperature, together with several chemical changes that lead to the precipitation of minerals from the fluids, especially sulfides, creating the typical black fluids observed in these environments (Tivey, 2014). Some of those mineral particles sink back to the ocean floor generating hydrothermal vent sediments, which will deposit around the vent field, whereas others are carried out upward by the vent plume several hundreds of meters above. When it reaches neutral buoyancy, the plume spreads out horizontally, dispersing metals and particles on several hundreds of kilometers away from its original source (Baker, 2014). Mineral particles that are not expelled by the vent are deposited at the vent orifices leading to the chimney growth (Fouquet et al., 1993; Tivey, 2014).

Some vent chimneys expel white fluids, reflecting at lower temperature (200°C to 300°C), compared to black smokers. For these chimneys a more important mineral precipitation on the subsurface lead to a clearer coloration of the exiting fluid. In addition, chimney openings are also narrower and fluids are usually enriched in zinc (Koski et al., 1994). Both black and white smokers are referred to as focused or discrete vent emissions (**Fig 6.**).

Hydrothermal fluids are also expelled as diffuse flow emissions, much cooler than black or white fluids expelled from focused emissions, with temperatures between 5 and 100°C (Bemis et al., 2012) (**Fig 6.**). Flow velocities are also much lower with an average speed ranging from 0.5 $mm.s^{-1}$ to 11 $cm.s^{-1}$ depending on vent sites (Mittelstaedt et al., 2012; Pruis and Johnson, 2004; Ramondenc et al., 2006; Scheirer et al., 2006). These secondary outflows are usually found on the wall of chimney structures or through cracks in the basement rocks (Bemis et al., 2012); (**Fig 5.**). This is the case of beehive diffusers, found for example at the Snake Pit vent field on the MAR. These structures do not have a central conduit like black or white smoker chimneys, but let seawater infiltrate through their porous walls, where it is mixed and heated with the vent fluid (Fouquet et al., 1993; Koski et al., 1994). Evidence of diffuse flow style can also be seen where white hydrothermal vents are surrounded with cracks on the seafloor such as around the ASHES vent field on the Juan de Fuca ridge (Pruis and Johnson, 2004) or around the TAG vent field on the MAR (Cambon-Bonavita, 2014; BICOSE 1 expedition).

Diffuse flow emissions are segregated in two types referred to as "high-temperature diffuse flows" or "HT-diffuse flows" and "low-temperature diffuse flows" or "LT-diffuse flows (Le Bris et al., 2019; Lowell et al., 2015) (**Fig 5.**). The HT-diffuse flows are the result of a mixing of end-member fluids with infiltrated seawater through cracks and faults or porous chimneys. Fluid is cooled down, changes in composition and discharges as shimmering water around the vent field. The LT-diffuse flows on the other hand derive from seawater infiltrated with no or limited mixing with the high temperature fluids. Warming and enrichment of these fluids in volatiles are mainly the result of molecular diffusion and conductive heating from distinct conduits of vent fluids nearby through the mineral layer (Lowell et al., 2015).

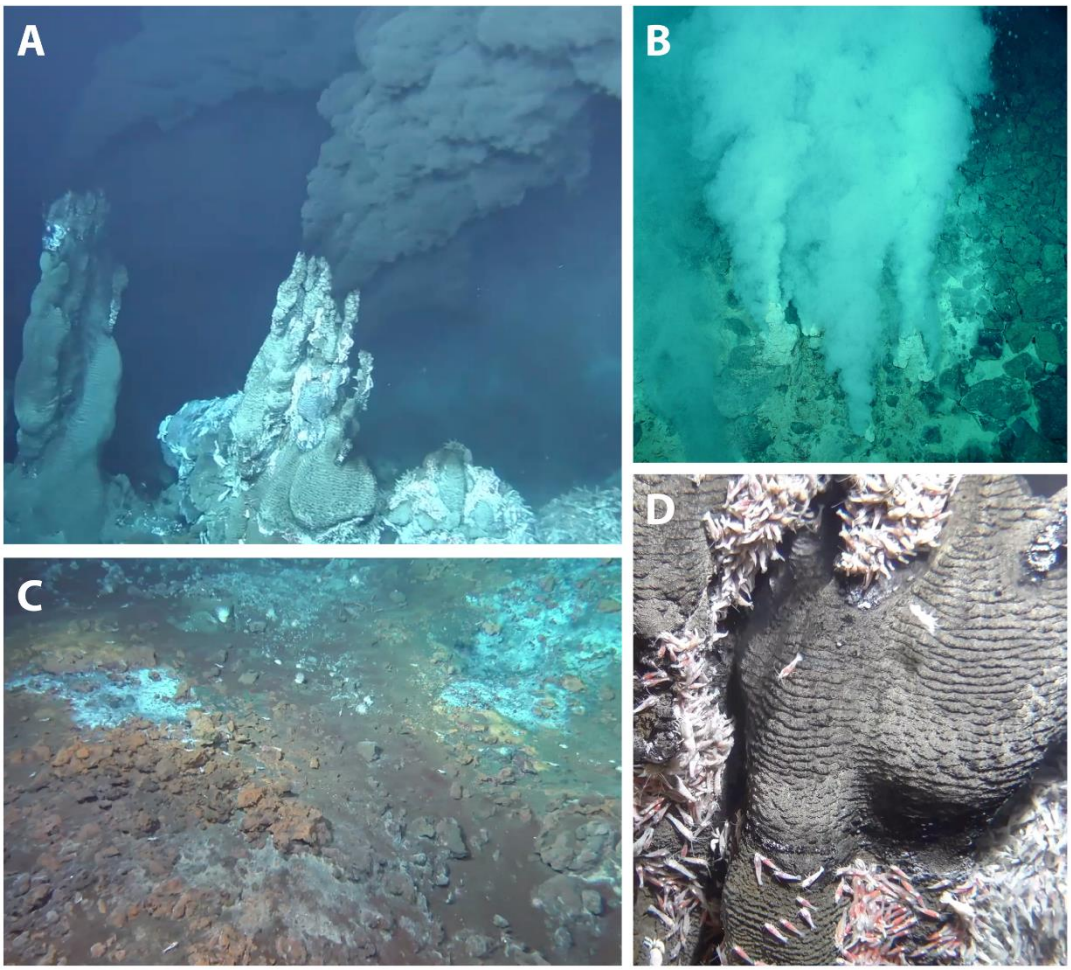


**Fig 6.** Different styles of hydrothermal venting. **A.** Black smokers at the Beehive edifice on the Snake Pit vent field (MAR). BICOSE2018-Nautile © Ifremer **B.** White smokers at the NW Eifuku seamount from the Marianna Arc. © Wikimedia commons. **C.** Diffuse emissions through cracks in the seafloor at the TAG vent field. Diffusions cannot be visualized on the picture but white marks on the seafloor are indicative of this type of emission. BICOSE2018-Nautile © Ifremer **D.** Beehive diffusers at the Beehive edifice on the Snake Pit vent field (MAR). Fluids are expelled through the darker lines on the wall of these particular edifices BICOSE2018-Nautile © Ifremer.

A significant part of the heat flux is emitted through diffuse emissions, varying from 50% to 90% of the total heat budget of the vent field (Barreyre et al., 2012; Ramondenc et al., 2006; Veirs et al., 2006). However, significant differences in the style of venting between edifices prevent accurate extrapolation at the scale a vent field (Mittelstaedt et al., 2012).

## P.1.1.4 Composition of hydrothermal vent fluids

All hydrothermal vents fluids are enriched in reduced elements and metals compared to the surrounding seawater. Nonetheless, concentrations of these elements are particularly variable between vent fields. On Mid Oceanic Ridges (MOR), $H_2S$ concentrations range between 0 and 19.5 mmol $kg^{-1}$ and they vary between 1 and 13.1 mmol.$kg^{-1}$ on back arc basins (BAB). Similar variability was reported for iron ($Fe^{2+}$) with concentrations between 0.007– 24 mmol.$kg^{-1}$ and between 0.01–13 mmol $kg^{-1}$ on MOR and BAB respectively (Charlou et al., 2010; Le Bris et al., 2019; Tivey, 2007). This variability between hydrothermal vent fields is governed by several factors shaping fluid composition.

Composition of end member fluids is generally greatly influenced by the basement rocks beneath the vent field (Holden et al., 2012). On MOR, fluids expelled by vent sites hosted on basaltic rocks are for example usually enriched in $H_2S$, silica and metals (Fouquet et al., 2010) **(Table 1.)**. On volcanic arcs, the aging oceanic crust close to convergent boundaries can harbor different types of rocks such as dacite and andesite. Hydrothermal vents hosted on these types of rocks tend to expel fluids with lower pH, low $H_2$ and $CH_4$ concentrations and higher dissolved metal concentrations, as seen for the Mariner vent filed in the Lau basin, the Brothers volcano on the Kermadec Arc or the PACMANUS vent fieldin the Manus basin (Mottl et al., 2011; Reeves et al., 2011; Takai et al., 2008b, 2009). On back arc spreading centers, just behind where new basaltic crust is formed, fields separated by only tens of kilometers, such as PACMANUS and Vienna Woods in the Manus Basin, can produce fluids with drastically different chemical compositions (Mottl et al., 2011; Reeves et al., 2011).

At slow spreading ridges, tectonic activity can create outcrops of ultramafic mantle rocks that are estimated to represent between 20 and 25% of the seafloor along these ridges (Cannat et al., 2010). Hydrothermal vents laying on these types of rocks are subjected to serpentinization reactions – i.e. the alteration of ultramafic minerals by seawater – producing end-member emissions with chemical signatures significantly different from those measured at basaltic hosted sites (Charlou et al., 2010; Fouquet et al., 2010; Kumagai et al., 2008). In these types of sites, hydrogen ($H_2$) usually reaches high concentrations ranging between 2.5 mM and 8.5 mM, like for example at the Kairei vent field on the CIR (Gamo et al., 2001; Kumagai et al., 2008) and up to 26 mM at the Rainbow vent field on the MAR (Charlou et al., 2002, 2010). Additionally, methane ($CH_4$) as a byproduct of the abiotic reaction between $H_2$ and $CO_2$ can also reach unusually high values. For example, $CH_4$ concentrations up to 3.5 mM have been recorded at the Logatchev vent field on the MAR (Schmidt et al., 2007), and 2.81 mM at the Von Damm vent field in the Mid Cayman Rise (Mcdermott et al., 2015). Conversely, methane concentrations in basaltic-hosted sites do not exceed 0.15 mM, except for the Main Endeavour vent field (MEF) for which high $CH_4$ concentrations have been attributed to a sedimentary context (Lilley et al., 1993) or for the Menez Gwen vent field (Charlou et al., 2010), which is located at a shallower depth than the other sites measured (**Table 1.**).

Vent depth also affects end member chemical concentrations as suggested for vent sites of the Mid Cayman Rise (MCR) (**Table 1.**). End member fluids of Piccard, the deepest known vent field hosted on a basaltic sublayer, exhibited slightly higher concentrations of $H_2$ than its shallower counterpart, Von Damm, an ultramafic vent field localized a few kilometers away (Mcdermott et al., 2015; McDermott et al., 2018). Authors have proposed that unusually high hydrogen concentrations for a basaltic site could be related to a higher pressure due to the great depth of Piccard that would modify conditions of the fluid phase separation. Temperature conditions of fluid-rock interactions in the root zone would then be unusually high leading to an increased uptake of hydrogen by the fluid when it leaches the basaltic rocks (McDermott et al., 2018).

Hydrothermal fluids may also exhibit variability between edifices of a same vent field (**Table 1.**). Although some vents display a remarkable homogeneity related to their single subsurface source such as the Rainbow vent field (Charlou et al., 2002), most vents discovered today exhibit differences in the end member fluid composition between edifices. This can result from a discontinuous magma chamber fueling different sub-seafloor plumbing systems such as for the 9°50'N EPR or the MEF vent field (Von Damm et al., 1995). For Lucky Strike vent field on the MAR, despite important variability of the chemistry of the end members of the different edifices, all fluids are fed by a single deep-rooted

source as for every vent fields on the MAR (Charlou et al., 2002; Fouquet et al., 2010). Variations in fluid composition are due to phase separation, which partitions the uprising fluid into brine and vapor (Chavagnac et al., 2018; Pester et al., 2012). Phase separation processes were even suspected to explain differences between fluids expelled from a single vent edifice, Brandon, at the Napa Nui vent site from the EPR (Von Damm et al., 2003).

Long-term studies have shown a great temporal stability of average temperature and vent fluid composition for periods between 3 to 6 years at the Lucky Strike vent field on the MAR (Barreyre et al., 2014; Campbell et al., 1988). Additionally, on shorter temporal scales, temperature oscillations correlated with tidal pressure, for high temperature fluids, and tidal currents, for low temperature emissions, were recorded at Lucky Strike (Barreyre et al., 2014). More generally, tidal influence was also identified on fluid characteristics at other vent sites such as MEF, the 9°50°N vent field on the EPR, or TAG (Lee et al., 2015; Scheirer et al., 2006; Sohn, 2007).

| LOCATIONS | Depth | RANGE OF CONCENTRATIONS | | | | | REFERENCES |
|---|---|---|---|---|---|---|---|
| | | pH | $H_2$ (mM) | $CH_4$ (mM) | $H_2S$ (mM) | Fe (mM) | |
| **MAFIC ROCKS (BASALTIC)** | | | | | | | |
| MEF, Juan de Fuca *(before eruption)* | 2200 m | 4.2–4.5 | 0.16–0.42 | 1.8–4.5 | 2.0–8.1 | 0.18–1.36 | Butterfield et al. (1994); Lilley et al. (1993,2003) |
| MEF, Juan de Fuca *(1 year after eruption)* | 2200 m | ND | 0.2–1.5 | 1–2 | 5–29 | 0.35–2.2 | Lilley et al. (2003); Seewald et al. (2003); Seyfried et al. (2004) |
| 9°50'N, EPR | 2520 m | 2.6–4.3 | 0.33–8.91 | 0.05–0.75 | 3.3–110 | 0.48–6.8 | Von Damm et al. (2004); Holden et al. (2012) |
| Menez Gwen, MAR | 840 m | 4.2–4.3 | 0.024–0.048 | 1.35–2.15 | 1.3–1.8 | 0.024–0.028 | Charlou et al. (2000) |
| Lucky Strike, MAR | 1740 m | 2.6–4.9 | 0.003–0.73 | 0.30–0.85 | 2.7–3.0 | 0.03–2.79 | Charlou et al. (2000); Chavagnac et al. (2018) |
| TAG, MAR | 3650 m | 3.1 | 0.37 | 0.15 | 6.7 | 5.17 | Charlou et al. (2010) |
| Snake Pit, MAR | 3500 m | 3 | 0.48 | 0.062 | 5.9 | 2.4 | Jean Baptiste et al. (1991) |
| Edmond, CIR | 3320 m | 3.1–3.4 | 0.05–0.11 | 0.23–0.31 | 1.1–3.9 | 0.012–0.014 | Kumagai et al. (2008) |
| Kilo Moana, Lau Basin | 2620 m | 2.9–4.0 | ND | ND | 5.4–6.4 | 0.87–0.095 | Mottl et al. (2011) |
| Vienna Woods, Manus Basin | 2500 m | 4.2–4.7 | 0.043–0.056 | 0.064–0.066 | 1.4–1.6 | 0.15–0.17 | Reeves et al. (2011) |
| Piccard (Beebe), Mid Cayman Rise | 4957 m | 3.0–3.2 | 18.9–20.7 | 0.12–0.13 | 11.8–12.3 | ND | Mcdermott et al. (2018) |
| **ULTRAMAFIC ROCKS** | | | | | | | |
| Rainbow, MAR | 2320 m | 2.8 | 16 | 2.5 | 1.2 | 24.1 | Charlou et al. (2002) |
| Logatchev, MAR | 3050 m | 3.3–3.9 | 12–19 | 2.1–3.5 | 0.8–2.5 | 2.4–2.5 | Schmidt et al. (2007) |
| Kairei, CIR | 2460 m | 3.4–3.6 | 7.9–8.2 | 0.08–0.20 | 4.0–6.4 | 0.0035–0.006 | Gamo et al. (2001); Kumagai et al. (2008) |
| Von Damm, Mid Cayman Rise | 2372 m | 5.56 | 18.2 | 2.81 | ND | ND | Mcdermott et al. (2015) |
| **DACITIC/ANDESITIC ROCKS** | | | | | | | |
| Mariner Field, Lau Basin | 1910 m | 1.9–4.2 | 0.45–0.96 | 0.008 | 4.2–9.3 | 10.5–13.0 | Takai et al. (2008); Mottl et al. (2011) |
| PACMANUS, Manus Basin | 1800 m | 2.3–2.7 | 0.018–0.306 | 0.014–0.062 | 2.8–20.8 | 1.22–11.7 | Reeves et al. (2011) |
| Brothers Volcano, Kermadec Arc | 1800 m | 2.8–3.0 | 0.01–0.02 | 0.002–0.007 | 2.3–7.9 | 4.2–7.3 | Takai et al. (2009) |
| **SEAWATER** | | | | | | | |
| Seawater | | 7.8 | 0.0004 | 0.00001 | 0 | 0.000061 | Turkekian et al. (1968) |

**Table 1.** Biologically relevant chemistry of end-member hydrothermal fluids from various sites and host-rock environments. ND = No data. Adapted from Holden et al. (2012) and references herein.

Volcanic eruptions and seismic episodes can also affect the apparent stability of end member fluids. Although they are rare, some of these events have been detected or directly observed in the MEF from the Juan de Fuca ridge in June 1999, and at the 9°50'N vent field on the EPR in 1991-1992 and 2005-2006 (Cowen et al., 2007; Fornari et al., 2012; Lilley et al., 2003; Von Damm et al., 1995). Each time, these eruptions lead to modifications of both temperature and fluid composition, with a strong initial increase – up to 110 mM of $H_2S$ at the 9°50N EPR vent field – followed by a stabilization phase to return to the pre-eruption fluid conditions within 2 to 3 years (Butterfield et al., 1994; Johnson et al., 2000; Lilley et al., 2003; Seewald et al., 2003; Seyfried et al., 2004; Von Damm, 2004; Von Damm et al., 1995; Yücel and Luther, 2013).

Owing to all these factors affecting its composition, each end-member fluid issuing from a black smoker edifice is truly unique in both space and time (Le Bris et al., 2019).

Once expelled from the chimney orifice, end-member fluids evolve by dilution or by reactions with other elements along a chemical gradient. With the permanent supply of fluid, a chemical disequilibrium is maintained in the mixing zone allowing the coexistence of both oxidized and reduced elements that should be mutually exclusive in stable conditions. Abiotic reactions between sulfur and oxygen for example form thiosulfate ($S_2O_3^{2-}$) or sulfate ($SO_4^{2-}$) along the dilution gradient but with a slow kinetic (Gartman et al., 2011). These elements can further react with metals such as iron (Fe), copper (Cu) and zinc (Zn) to form polymetallic sulfurs, which constitute most of the particles exported by hydrothermal plumes (Khripounoff et al., 2000; Klevenz et al., 2012; Le Bris et al., 2003). Abiotic iron oxidation also occurs within the mixing zone creating ferric oxides but with a much faster kinetic than sulfide oxidation. Some elements however do not react during the mixing with seawater, such as manganese (Mn) which is used as an accurate tracer of the dilution degree of hydrothermal fluid (Chin et al., 1994).

Concentrations of many elements from the fluids are positively or negatively correlated with temperature such as iron and sulfurs (Laes-Huon et al., 2014; Le Bris et al., 2006b): this is the so-called conservative dilution model. Diffuse fluids generally exhibit much more variable temperatures compared to focused emissions at both spatial and temporal scales (Barreyre et al., 2014; Scheirer et al., 2006; Sohn, 2007). It is usually admitted that reduced element concentrations within these fluids are fluctuating according to these temperature variations. Nonetheless, mismatches with the conservative dilution model have been repeatedly reported in diffuse fluids emissions (Ishibashi et al., 2014; Le Bris et al., 2006b, 2019; Nakamura and Takai, 2014), implying more *in situ* measurements to properly describe the habitat at small scales. Such “anomalies” have been attributed to the style of diffuse venting, whether it originated from seawater mixing or through conductive heating/molecular diffusion, or to consumption/production of reduced compound by microbial activities beneath the seafloor (Wankel et al., 2011).

## P.1.2 Hydrothermal vents – Unexpected oases of microbial life

### P.1.2.1 A chemosynthetic based ecosystem

Primary production of organic matter in hydrothermal vent biotopes is probably one of the most astonishing discoveries made in recent marine biology. Prior to early expeditions of the *Alvin* submarine on the Galapagos Rift in 1977, our deep ocean was seen as a cold biological desert (Forbes, 1843). Indeed, in absence of photosynthetically usable sunlight below 200 m (Ramirez-Llodra et al., 2010), no primary producers at first sight would survive. Most of deep sea species were then considered as dependent on surface primary production, using only sunken or advected food from the euphotic zone (Ramirez-Llodra et al., 2010). The presence of an environment teeming with life at 2.500 m depth, near active vent chimneys, was then highly unexpected (Corliss et al., 1979).

Even though suspension feeding had been considered at first (Lonsdale, 1977), interrogations remained about how such densely populated faunal communities could thrive only based on this type of nutrition. First clues of an explanation were given by the abundance of microbial mats and the rich quantities of sulfide emanating from vent chimneys. The use of chemosynthesis by microorganisms, a process known since 1867 but considered as playing a minor role on earth (Winogradsky, 1887), was

then proposed as being the main primary production source of those ecosystems (Cavanaugh, 1981; Felbeck, 1981).

For photosynthetic primary producers, light is used as an energy source to produce highly energetic molecules such as ATP or NADPH through electrolysis of water by photosynthetic pigments. On the other hand, chemosynthetic organisms exploit the chemical disequilibria resulting from the relatively slow inorganic reaction kinetics of many redox reactions to generate their energy. The mixing zone found at the interface between cold oxidized seawater and anaerobic hot vent fluids rich in reduced compounds, offers therefore suitable conditions for a diverse range of metabolisms, and so a huge variety of chemosynthetic prokaryotes (Fisher, Takai, and Le Bris 2007) (**Fig 7.**).

Due to the high concentrations of sulfur compounds found at vents, sulfur oxidation (also called thiotrophy) has been reported as one of the main chemosynthetic metabolism for archaea and bacteria in many sites (Akerman et al., 2013; Campbell et al., 2013; Fortunato et al., 2018; Huber et al., 2010). Mainly identified for bacteria affiliated to *Epsilonbacteraeota,* – novel phylum classified before in the *Proteobacteria* phylum as *Epsilonproteobacteria* (Waite et al., 2017) – *Gammaproteobacteria*, and *Aquificales*, oxidation of hydrogen sulfide ($H_2S$) in sulfate ($SO_4^{2-}$) can be performed through two different metabolic pathways: the Sox multienzyme system or the reverse sulfate reduction pathway (Yamamoto and Takai, 2011). The Sox multienzyme comprises seven genes (*sox*ABCD and *sox*XYZ) coding for periplasmic proteins but oftenly, *sox*CD genes are missing, such as in *Gammaproteobacteria*, allowing only partial oxidation of sulfur compounds. For the reverse sulfate reduction pathway, oxidation of $H_2S$ is performed with 3 key enzymes: AprA (adenosine 5'-phosphosulfate reductase), Dsr (dissimilatory sulfite reductase) and Sat (sulfate adenylyl transferase) (Yamamoto and Takai, 2011).

Hydrogen ($H_2$) can be also an important energy resource for chemosynthetic bacteria in hydrothermal vents. Oxidation of $H_2$ has been infered by the presence of several hydrogenase genes such as *hupL* in many groups of archaea or bacteria such as *Epsilonbacteraeota*, *Deferribacteres*, *Aquificales, Euryarchaeota and Crenarchaeota* called hydrogenotrophs. These hydrogenases sometimes co-exist with sulfur oxidation pathways and have therefore the capacity of using two different energy sources (Nakagawa and Takai, 2008). This offers to these organisms a strong versatility in a highly unstable environment such as the mixing gradient of hydrothermal vent fluids (Campbell et al., 2006).

Electrons produced by these oxidative metabolisms are usually coupled with respiratory proteins complex – cytochromes, NADH dehydrogenase – to create a proton gradient within the periplasm. As for the mechanism occurring in mitochondria, the gradient fuels an ATP synthase proton pump to produce more ATP for the cell. When available, oxygen is usually used as terminal electron acceptor in the respiratory chains of most chemoautotrophs (Sievert and Vetriani, 2012). Nonetheless, some *Epsilonbacteraeota* sulfur oxidizers are able to realize anaerobic respiration with nitrate ($NO^{3-}$) instead of $O_2$ and many hydrogenotrophic microorganisms can also breathe elemental sulfur (S°) (Campbell et al., 2006; Sievert and Vetriani, 2012). Less common, respiration with ferric iron ($Fe^{3+}$) or manganese ($Mn^{4+}$) coupled with hydrogen oxidation is found in some *Deferribacteres* (Slobodnika et al., 2009). Finally, methanogens corresponding to strictly anaerobic archaea, mostly hydrogenotrophs, are able to use $CO_2$ as electron acceptor, producing $CH_4$, as a byproduct of their energetic metabolism (Ferry, 2012).

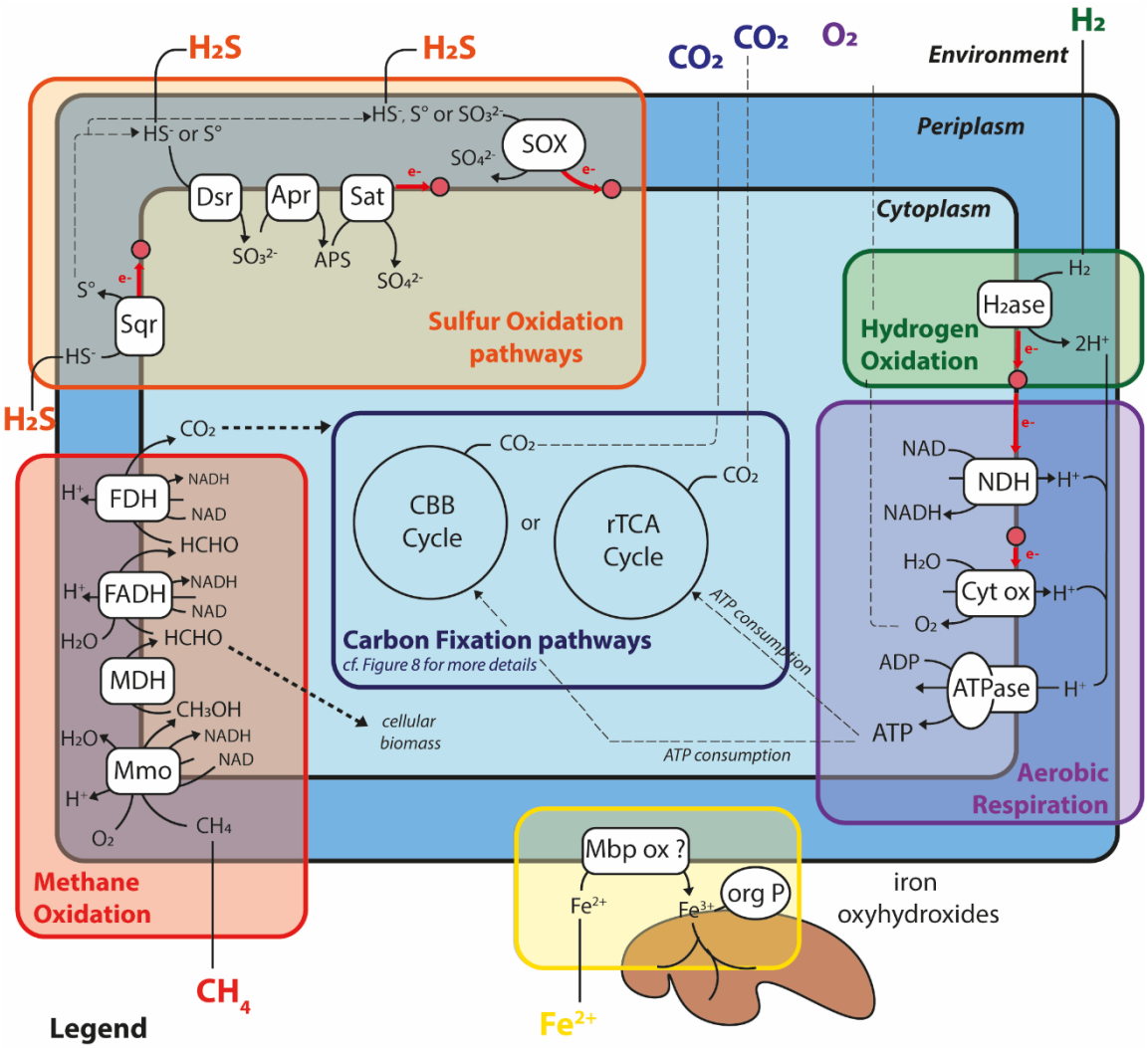


*NB : This figure does not represent the metabolism of a particular microorganism but a chimeric view of the main metabolic pathways used by different chemosynthetic bacteria from hydrothermal vents*

**Fig 7.** Potential energetic metabolisms used by some hydrothermal vent chemosynthetic bacteria. (Methou 2019).

Unlike sulfur and hydrogen, iron oxidation has been neglected for a long time as a major chemosynthetic metabolism in vent ecosystems. Competition with the spontaneous abiotic oxidation of ferrous iron ($Fe^{2+}$) at neutral pH, and the high quantities of dissolved $Fe^{2+}$ required for the reaction leading to poor energy production, were seen as critical obstacles for iron to be used by microorganisms. Additionally, iron-oxidizing microorganisms are also challenged by ferric iron ($Fe^{3+}$) instant precipitation into solid deposits of large size. These elements are therefore available with difficulty in a dissolved form. Moreover, due to the large iron atom size, iron oxidation has to occur externally outside the bacteria cell membranes, and uses transmembrane proteins. However, several

groups of bacteria, mainly represented by *Zetaproteobacteria* in hydrothermal vent ecosystems, have been recognized as iron oxidizers (Emerson et al., 2007; Fleming et al., 2013; Scott et al., 2015). To outcompete abiotic reaction, iron oxidation usually occurs in acidic or neutral pH microaerophilic conditions, as seen in freshwater isolates that were able to grow with oxygen concentrations up to 50 µM (Druschel et al., 2008). Although molecular mechanisms are not as clear as for sulfur oxidation, molybdopterin oxidoreductase genes, which could be involve in oxidation of $Fe^{2+}$ into $Fe^{3+}$, were identified in several, but not all, genomes of *Zetaproteobacteria* (Field et al., 2014). For their growth, *Zetaproteobacteria* typically excrete oxidized iron products outside their cells forming helical stalk of $Fe^{3+}$ bound to organic polymers. These organic molecules help to retard mineral growth, preventing encrustation of *Zetaproteobacteria* cells into the mineral matrice (Chan et al., 2011) leading to death. As for the other metabolisms, electrons formed by this oxidation are used by respiration pathways to produce more ATP.

At hydrothermal vents, methanotrophy, using $CH_4$ as electron and/or carbon donor, is mostly accomplished by some Archaea and *Gammaproteobacteria* even if other groups, such as *Alphaproteobacteria* and *Verrucomicrobia* could potentially perform this metabolism, as they were recognized as methanotrophs in other ecosystems (Op den Camp et al., 2009; Trotsenko and Murrell, 2008). The key enzyme of this metabolism is the methane monooxygenase (genes *pMMO* or *sMMO*) catalyzing the oxidation of $CH_4$ into methanol $CH_3OH$. Type I methanotrophs (*Gammaproteobacteria*) also exhibit particular morphologies with stacked internal membranes within their cytoplasm making them easily recognizable with microscopy techniques (Childress et al., 1986).

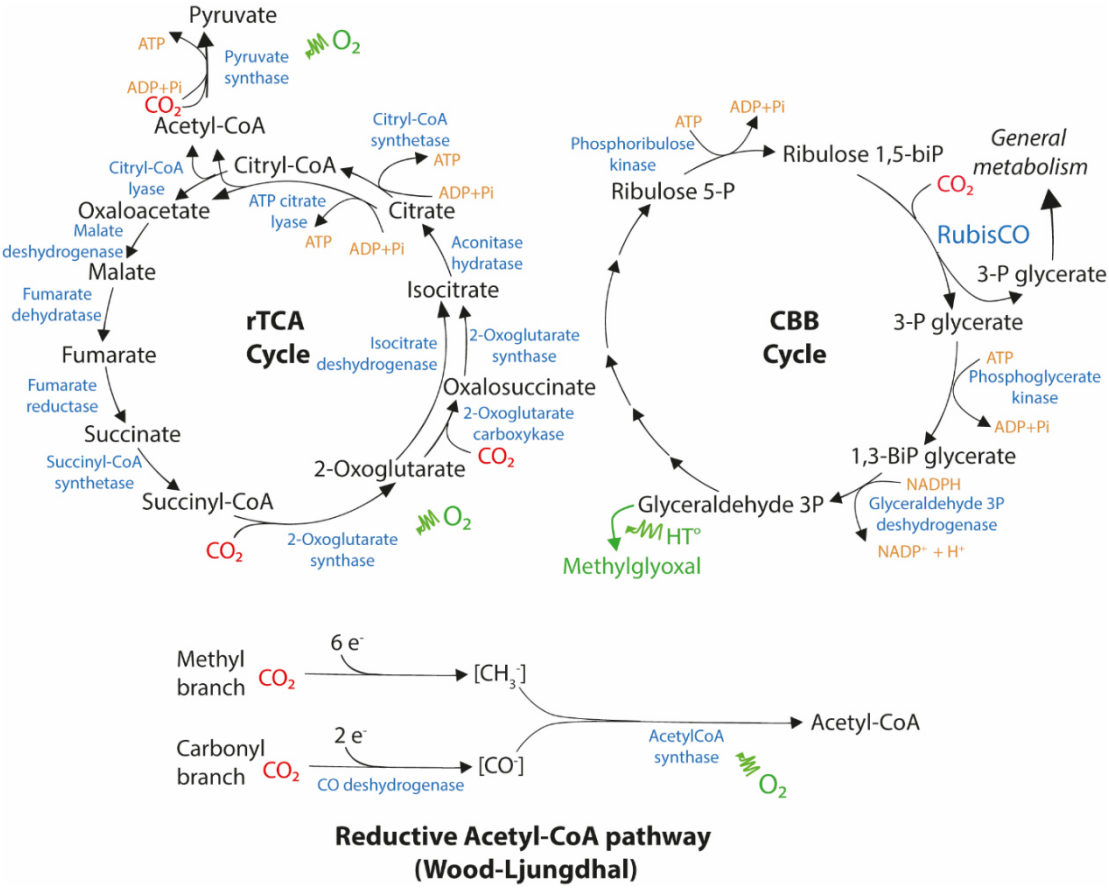


**Fig 8.** Major carbon fixation pathways in hydrothermal vents chemosynthetic bacteria. Adapted from Hügler and Sievert (2011).

Once ATP is formed by those different energetic pathways, a carbon source can be fixed to produce organic carbon. This source is usually dissolved $CO_2$ for chemoautotrophs even if chemoheterotrophs using organic carbon are also present. For methanotrophs, $CH_4$ can be used as both electron acceptor and carbon source. Carbon fixation can be achieved by six different metabolic pathways depending on species (Hügler and Sievert, 2011). The most commonly found in bacteria from hydrothermal vents is the Calvin Bensom-Bassham cycle (CBB) where $CO_2$ is fixed by the key enzyme RubisCO and the reductive Tricarboxylic Acid pathway (rTCA), known also as the reversed Krebs cycle (**Fig 8.**). Most of the enzymes of the rTCA are shared with Krebs cycle enzymes, since these reactions are reversible, and only three enzymes – the fumarate reductase, 2-oxoglutarate synthase and the citrate cleaving enzymes – are specific to the rTCA cycle (Campbell and Cary, 2004).

These two carbon fixation pathways differ by their ATP consumption with one ATP per molecule of fixed $CO_2$ for the rTCA cycle and three ATP per molecule of $CO_2$ for the CBB cycle (Hügler and Sievert, 2011). Additionally, with two major oxygen sensitive enzymes – the pyruvate synthase and 2-oxoglutarate synthase – rTCA can only function in microaerophilic or anaerobic conditions. On the other hand, thermal instability at high temperature of some products of the CBB cycle creates toxic compounds for the cell such as methylglyoxal narrowing its use in relatively low thermal conditions.

Less represented, the reductive acetyl CoA pathway – also called the Wood Ljungdahl (WL) pathway – is also found in hydrothermal vent microorganisms (Campbell and Cary, 2004; Nakagawa and Takai, 2008) (**Fig 8.**). It is the only carbon fixation pathway shared by bacteria and archaea, and was thus hypothesized to be the most ancient mechanism of autotrophic carbon fixation. Compared to the CBB and the rTCA cycles, the WL pathway is relatively simple and does not involve ATP consumption. However due to a very high sensitivity to oxygen of the main enzyme, the CO dehydrogenase, its use is restricted to strictly anaerobic conditions. Although absent from bacteria, the 3-Hydroxypropionate/4-Hydroxybutyrate cycle (3-HP/4-HB) and the Dicarboxylate/4-Hydroxybutyrate cycle (DC/4-HB) are two important pathways of carbon fixation in hydrothermal vents archaea (Hügler and Sievert, 2011).

## P.1.2.2 Microbial niche partitioning along the mixing gradient

Microorganisms are the main primary producers of hydrothermal vent ecosystems and are widely present in different environmental niches (Dick, 2019). Abundant in fluid flows, they are distributed along a thermal gradient between 2-3°C – the temperature of background seawater – to approximately 120°C, the currently known upper limit for microbial life (Takai et al., 2008a). Cultured microorganisms, and sometimes by extension their environmental relatives, are classified in hyperthermophilic (>80°C), thermophilic (55-80°C), mesophilic (20-55°C) and psychrophilic (<20°C) according to their optimal growth temperature (Alain et al., 2010; Inagaki et al., 2004; L'Haridon et al., 2003; Takai et al., 2003). Microorganisms with similar metabolisms thus further segregate according to their thermal niches, such as *Epsilonbacteraeota* and *Aquificales* sulfur oxidizers, respectively known as mesophilic and thermophilic (Campbell et al., 2006; Reysenbach and Shock, 2002; Sievert and Vetriani, 2012) (**Fig 9**.).

As stated previously (cf. part 1.1.4), this thermal gradient comes along with chemical fluctuations of reduced and oxidized compounds reflecting the dilution of the end member fluid with seawater. In addition to gradients created by the turbulent mixing, initial fluid composition specific to each vent also constrains the proliferation of chemosynthetic microorganisms according to their

respective metabolic capacities and growth optimum (**Fig 9.**). Methanotrophic species for example, like *Gammaproteobacteria* of the *Methylococcaceae* family or some archaea are more abundant at vent sites harboring higher $CH_4$ concentrations (Brazelton et al., 2006, 2011; Crépeau et al., 2011; Roussel et al., 2011; Zbinden et al., 2008).

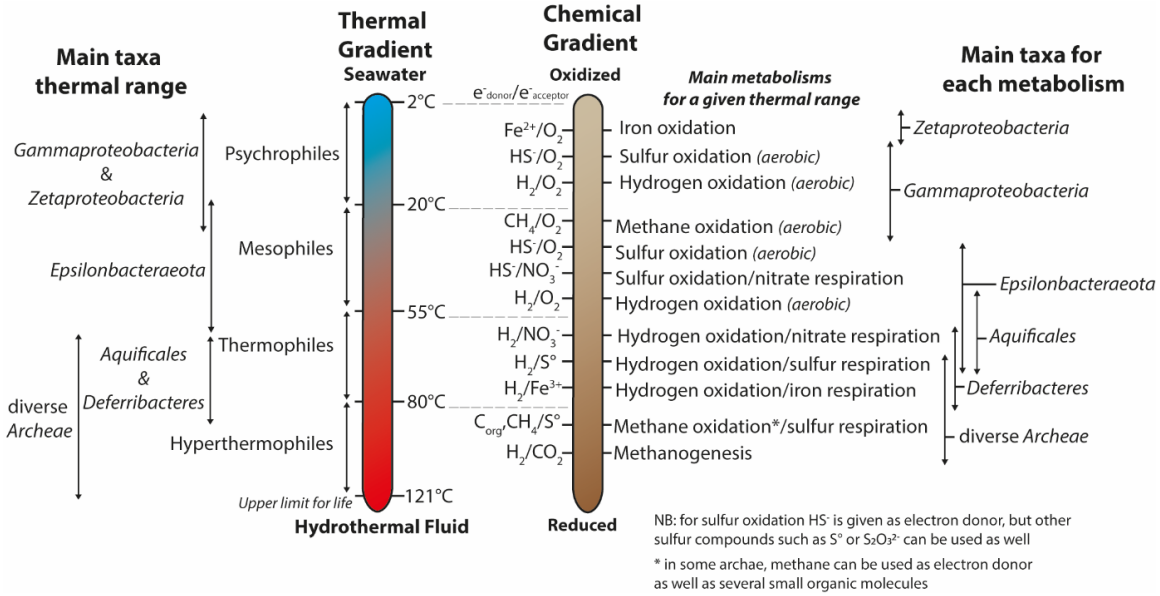


**Fig 9.** Schematic view of dominant metabolism along the mixing gradient. Adapted from Dick (2019).

Therefore, niche differentiation between microbial groups often results from a complex combination of thermal and fluid composition influences on their metabolism, as well illustrated by the example of co-occurring *Gammaproteobacteria* and *Epsilonbacteraeota* (Akerman et al., 2013; Fortunato et al., 2018; Jan et al., 2014; Meyer et al., 2013b; Perner et al., 2013a). Both sulfur oxidizers, they differ mainly by their carbon fixation pathways, the rTCA for *Epsilonbacteraeota* and the CBB for *Gammaproteobacteria*. *Epsilonbacteraeota* thrive in the less aerobic part of the gradient due the oxygen sensitivity of some of the rTCA enzymes, whereas *Gammaproteobacteria* grow in lower temperature areas due the thermal instability of the CBB byproduct and its lower efficiency compared to the rTCA. This is accentuated by the metabolic versatility of *Epsilonbacteraeota* to use alternative electron donors/acceptor, enabling them to grow in fully anaerobic conditions. This niche partitioning was observed or suggested by many studies (Akerman et al., 2013; Flores et al., 2011, 2012; Fortunato et al., 2018; Meyer et al., 2013b; Perner et al., 2013a; Sunamura et al., 2004); It was statistically supported by correlations between environmental fluid parameters and microbial composition of numerous samples (Meier et al., 2017).

Microbial communities are not restricted to fluid flows. They are found in many habitats such as hydrothermal plumes, within porous spaces in the wall of chimneys and in subseafloor conduits, or attached to diverse surfaces like rocks, sediments or even vent fauna (**Fig 10.**) (Campbell et al., 2006; Dick, 2019).

In microbial mat assemblages, many bacterial groups are organized in filamentous colonies reminding biofilms, such as *Thiotricales* (*Gammaproteobacteria*) or *Sulfurovum* (*Epsilonbacteraeota*) species. These communities also exhibit different diversity patterns than those found in fluid flows. Although some groups are highly abundant in both habitats, some others such as *Thiomicrospirales* (*Gammaproteobacteria*) seem to be restricted to only one of them. These differences of bacterial

lifestyle are expected to reflect genomic differences between these groups. Absence of pili, flagella or chemotaxis related genes were reported in genomes of fluid restricted groups compared to those found in mats, constraining them to a pelagic lifestyle (Meier et al., 2017).

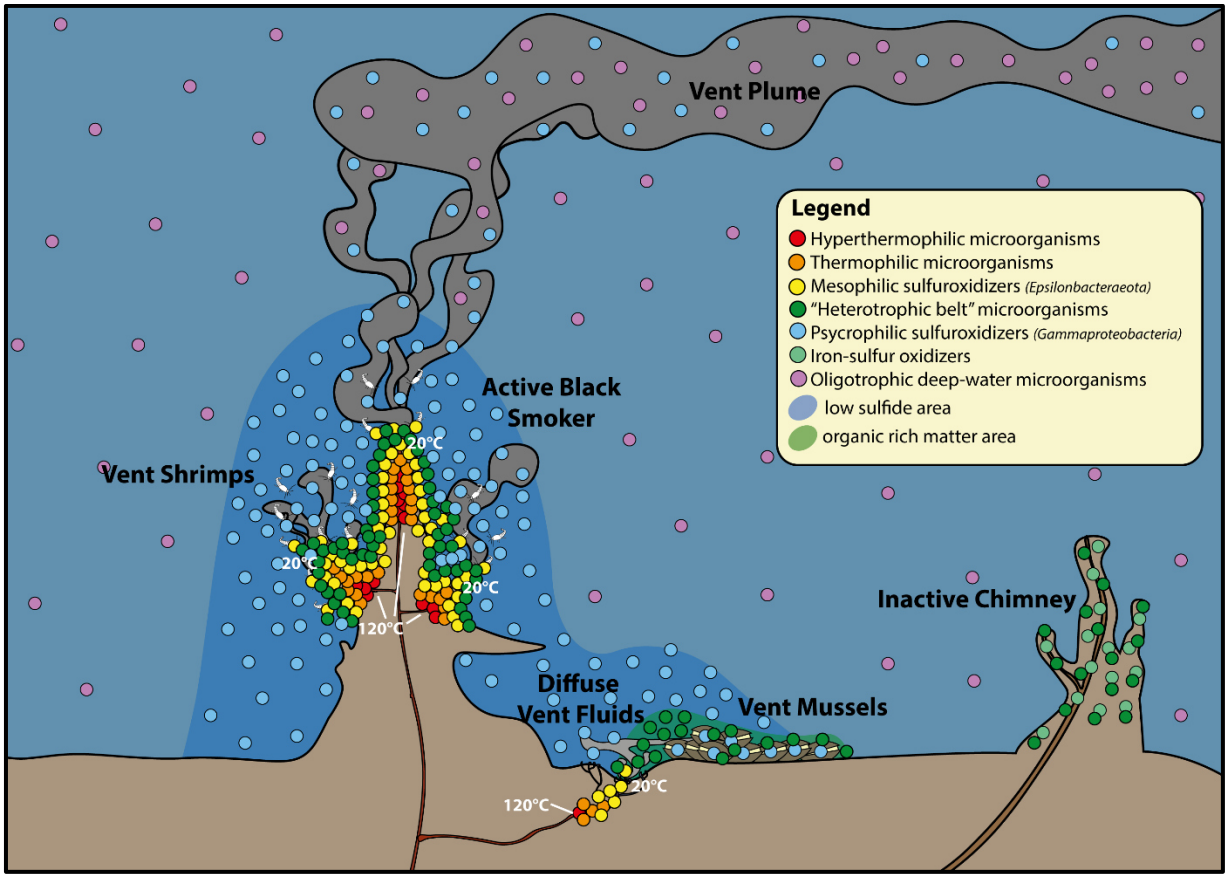


**Fig 10**. Schematic view of hydrothermal vent habitats occupied by microorganisms. Adapted from a scheme of the ph.D thesis of Meier (2016). (Meier, 2016).

Temperature and fluid composition are also key drivers of niche partitioning in these habitats (**Fig 10.**). Within chimney structures, studies generally showed that the cooler exterior regions contain a mix of bacteria and archaea, with a shift to predominantly hyperthermophilic archaea towards the hotter interior regions of the chimneys (Kormas et al., 2006; Pagé et al., 2008; Roussel et al., 2011). In mat communities as well, a strong influence of fluid compositions was reported or suggested for different locations (Hager et al., 2017; Meyer et al., 2013a; Scott et al., 2015). For example, Hager and collaborators showed that white mats near fluids rich in $H_2S$ were dominated by *Epsilonbacteraeota*, whereas orange mats with iron particles near fluids rich in iron were dominated or showed a much higher abundance of *Zetaproteobacteria* (Hager et al., 2017).

Nonetheless, in all these works, it is important to keep in mind that sampling technique can introduce important bias in the relative abundance of microbial groups within a sample. In a same study comparing microbial mats, two collection methods were used: some mats were sampled with a scoop scraping rocks and other mats with a syringe allowing a more targeted sampling. In one location with iron orange mats close to white mats, both tools were used in parallel. Comparison of communities revealed striking differences between the two samples with twice more *Zetaproteobacteria* in the one collected with the syringe than the one with the scoop scraper. This

second technique was less selective and had probably collected communities from different surrounding microhabitats (Hager et al., 2017).

This shed light on the concept of micro niche advanced by several studies stating that important changes can occur at very small scale from centimeters to millimeters especially in highly variable ecosystems such as hydrothermal vents (Meier et al., 2016, 2017; Perner et al., 2013b). Lack of stable conditions at small scale could also prevent adaptive equilibria, maintaining a high diversification of microorganisms in these environments.

### P.1.2.3 Spatial and temporal patterns of microbial niche repartition

At a local scale, microbial communities are mainly shaped by environmental factors such as temperature or fluid chemistry. Mineralogy can also have a great influence on microbial communities as proposed by some studies (Ferrera et al., 2014; Kormas et al., 2006; Lin et al., 2016; Pagé et al., 2008). Spatial repartition of *Aquificales* collected on chimneys from the Lau Basin for example revealed strong differences in OTU composition between samples with different geological context (Ferrera et al., 2014). Yet, as no fluid sampling had been performed in this study, it was difficult to assess which parameters between vent fluid chemistry, temperature and host rock composition was the most important determinant for microbial distribution. In microbial communities inhabiting rocks of inactive vent areas, the role of mineralogy has been more clearly identified. Although mainly composed of distinct populations from those found on venting structures – with the notable absence of thermophiles such as *Aquificales* and the low abundance of *Epsilonbacteraeota* (Sylvan et al., 2012) – strong link between host rock mineralogy and microbial communities has been pointed out (**Fig 10.**) (Sylvan et al., 2013; Toner et al., 2013).

At a global scale, apparent endemism of some vent taxa and large distances between vent sites led to the conclusion that geographical isolation and limited dispersal capacities could have a major role in shaping microbial communities from different vent sites (Akerman et al., 2013; Huber et al., 2010). Over a wide geographical range, important genetic differentiation was featured within the *Sulfurimonas* group – belonging to *Epsilonbacteraeota* – regardless of the environmental conditions at their locations (Mino et al., 2017). However, geographical patterns can sometimes reflect bias that could likewise be attributed to a lack of sampling. Previously described as restricted to vent sites from the Pacific in the Marianna Arc Basin or in the Lōʻihi Seamount, abundant communities of *Zetaproteobacteria* from iron mats have been now reported at three vent sites on the Mid Atlantic Ridge. This consequently enlarges their geographic repartition at a global scale. Moreover, the influence of geographical isolation and dispersal limitation in microbial distribution have been weakened by recent findings on open ocean samples, analyzed with a very high sequencing depth. Presence of "seed bank" populations formerly thought to be vent-specific was revealed in these samples, suggesting that vent exclusiveness of some taxa could be an artefact of low sequencing depth in most studies (Gonnella et al., 2016). If confirmed, through microbial activities analyses for example, this would advocate that vent microorganisms are able to survive and disperse in open oceans through oceanic circulation to colonize new vents field.

Such microbial signatures have driven recent research and exploration of hydrothermal plume communities. Mainly dominated by background ubiquitous seawater microorganisms such as *Pelagibacterales Alphaproteobacteria* (SAR11), they are also presenting mixture of diffuse vent fluid inhabitants consistent with the hypothesis of hydrothermal plumes as potential vectors for dispersal

of microorganisms linking vent site communities (Dick et al., 2013; Sheik et al., 2015). Less diverse than vent seafloor microbial populations, they are also much more stable in composition along rising plumes (Sheik et al., 2015). Despite highly diluted concentration of reduced compounds, chemosynthetic process seems to take place in vent plume communities where such metabolic capabilities have been detected (Anantharaman et al., 2016). The extent to how plume chemistry influences their microbial composition remains however unclear (Sheik et al., 2015).

While exploring these different spatial scales has been constantly at the heart of microbial distribution studies in hydrothermal vents, pushing for an always-higher resolution at a smaller scale, temporal variations of microbial communities have been overlooked too often. At short temporal scale, within ten to twenty minutes, small or drastic changes in microbial communities have been reported, in line with measured changes in thermal conditions and reduced compound concentrations (Perner et al., 2009, 2013a). Since no microorganism could react and grow in such brief periods, these variations more likely revealed entrainment of microorganisms by fluid flows from other locations. On the other hand, at larger temporal scale, despite some year to year fluctuations, individual fluids from similar locations maintained a distinct community structure for each sampled site (Fortunato et al., 2018; Opatkiewicz et al., 2009). To some extent, this suggests that despite short-term fluctuations, vent microbial communities can exhibit a certain stability over time.

These communities are also affected by discrete events such as eruptions or seismic activity. Generating important bursts of fluid supply, these events enable the development of visually dominant flocculent materials called “snowblower” emissions. Often described as “time zero” of successional patterns in vents communities, most of “snowblower” emissions are dominated by *Epsilonbacteraeota*. (Meyer et al., 2013a). Likewise, colonization experiments with artificial substrates have repeatedly reported *Epsilonbacteraeota* as pioneer colonizers in these environments, sometimes just few days after deployment (Alain et al., 2004; López-García et al., 2003; Szafranski et al., 2015a). Interestingly, artificial substrates deployed for more than a year exhibited higher diversity with no clear dominance of one taxonomical group compared to short term ones (Szafranski et al., 2015a). Such colonization experiments consistently reported a stronger influence of surrounding physicochemical properties than substrate type, both at hydrothermal vent and other deep sea ecosystems (Bellou et al., 2012; Lee et al., 2014; Szafranski et al., 2015a).

Even if a better understanding of the niche repartition of microbial communities present in hydrothermal vent ecosystems begins to take shape, strong gaps remain in determining the proportion of active populations (Sievert and Vetriani, 2012). Discrepancies between active and inactive portions of microbial communities emphasized by some studies, make clear that all microorganisms detected within a sample are not necessarily metabolically active (Fortunato et al., 2018; Lanzén et al., 2011; Li et al., 2016; Olins et al., 2017). For instance, in fluid samples from different vent sites at Axial Seamount (Juan de Fuca Ridge), one clear difference between taxonomy based on metagenomes and taxonomy based on metatranscriptomes, was that *Gammaproteobacteria* were on average more abundant in metagenomes compared to the metatranscriptomes with the opposite pattern for the *Epsilonbacteraeota* over the years (Fortunato et al., 2018). In the same way, some of the abundant groups such as *Verrucomicrobia* in hydrothermal plumes from the Guaymas Basin, were seen as weakly active (Li et al., 2016). Conversely, low abundance bacterial groups, usually carrying unique metabolic features, were much more highly active than previously assumed (Baker et al., 2013; Li et al., 2014).

This rehabilitates rare taxa as being unsuspected keystone players of their ecosystems where they may be well-adapted even if present at low concentrations.

## P.1.2.4 Microbial activities and interactions extend their potential niches

Niche partitioning of microbial communities is mainly driven by thermal influence and fluid chemistry at vents. These parameters further evolve on different spatial and temporal scale from the birth of nascent hydrothermal activity until emissions cease at the death of the vent edifice.

Some microorganisms appear to exert an influence on some of these parameters in return. For example, large proportion of hyperthermophilic and hydrogenotrophic methanogens in the hottest part of the gradient, especially in ultramafic vent fields with high $H_2$ concentrations, can significantly increase $CH_4$ and reduce $H_2$ within the subseafloor (Nercessian et al., 2005; Reveillaud et al., 2015; Wankel et al., 2011). Another example of this ecosystem engineer role of microorganisms can be observed with *Zetaproteobacteria*. Because of their particular metabolism, this group has the unusual capacity to form ironoxyhydroxides minerals, which alter microbial mats structure and likely affect fluid flow and potential energy source supply at a microscale. Thus, they are thought to provide new ecological niches enhancing local microbial diversity, as supported by the higher diversity observed in *Zetaproteobacteria* dominated mats compared to others (Hager et al., 2017).

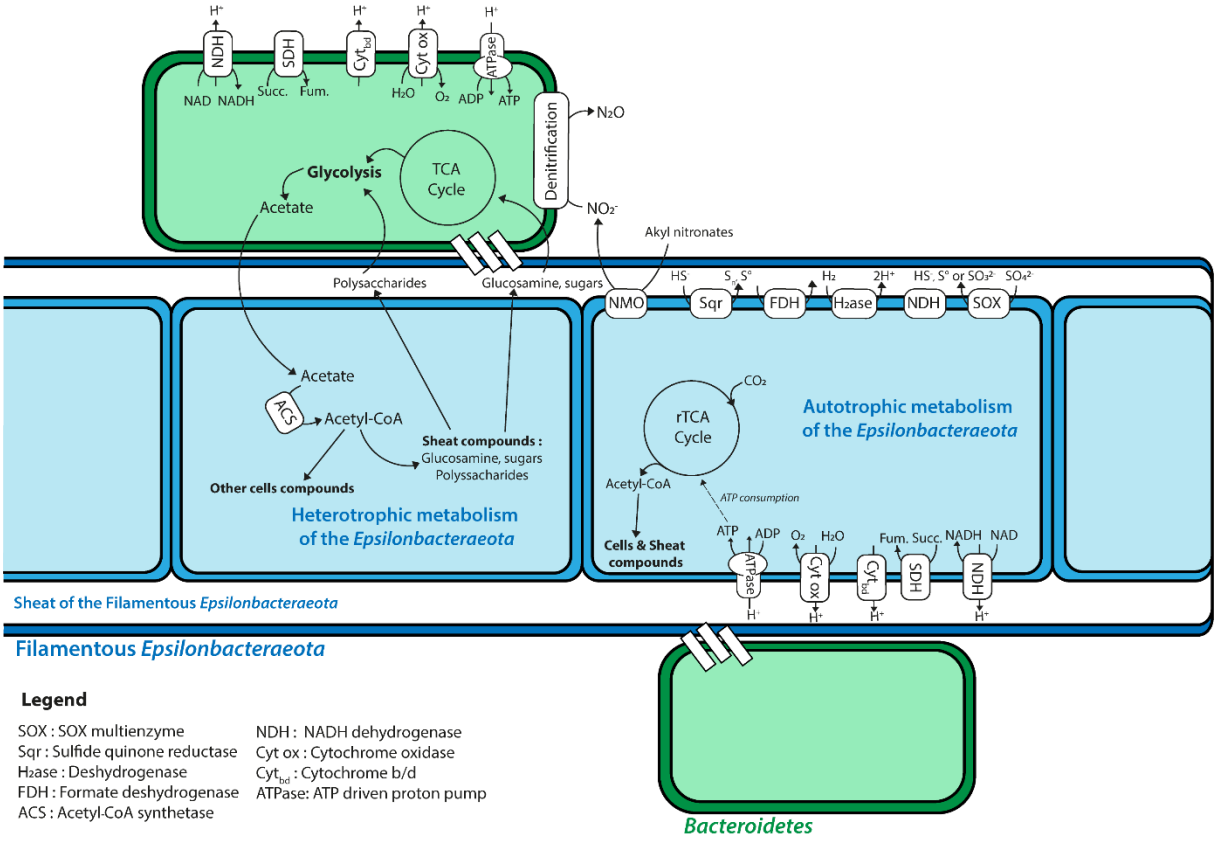


**Fig 11.** Example of syntrophic metabolisms between hydrothermal vent microorganisms. Adapted from Stokke et al. (2015).

Syntrophic interactions between microorganisms, as yet hampered by a lack of understanding (Sievert and Vetriani, 2012), have also been reported to affect their potential niche. For example, an interesting relation between sulfur oxidizing *Epsilonbacteraeota* and organotrophic *Bacteroidetes* has

been pointed out in mats from Loki Castle vent field (Stokke et al., 2015) (**Fig 11.**). Several *Epsilonbacteraeota* are known to create exopolysaccharide sheaths, forming filamentous structures surrounding their cells. These filaments provide both an attachment surface and a source of organic carbon offering a new niche to heterotrophic bacteria such as *Bacteroidetes*. With this food source, *Bacteroidetes* are able to fuel their heterotrophic metabolism to produce organic matter including acetate. This acetate can be metabolized by *Epsilonbacteraeota* in return, and used as a carbon source since they also have potential to grow heterotrophically by incorporating acetate with an Acetyl CoA synthetase (Stokke et al., 2015). This mixotrophic behavior of *Epsilonbacteraeota* allows them to be in this case, consumers of their own primary production. This emphasizes the versatile metabolic capabilities of some microorganisms and contrasts the traditional cut out between strict autotrophic primary producers and heterotrophic consumers. Moreover, the recent discovery of an *Aquificales* possessing a TCA cycle with fully reversible enzymes – unlike classical Krebs or rTCA cycle – and whose direction is controlled by the available carbon source, challenges also the necessity of classifying these organisms between autotrophs and heterotrophs (Nunoura et al., 2018).

Niche repartition of heterotrophic microorganisms remains even so, a poorly studied component of hydrothermal vent ecosystems, as these lineages were mostly studied for culturing purposes and biochemical properties. Often detected (Crépeau et al., 2011; Cruaud et al., 2017; Flores et al., 2011; Lanzén et al., 2011; Perner et al., 2013b), hydrothermal vent heterotrophs distribution has rarely been investigated in details, as the research on hydrothermal vent ecosystems was more oriented historically on chemolithoautotrophs. A recent finding from several samples collected at Menez Gwen vent field on the Mid Atlantic ridge has revealed abundant presence of heterotrophic bacteria in the immediate vicinity of diffuse vent fluids (Meier et al., 2016). Mainly composed of *Alphaproteobacteria* (*Rhodobacterales* such as *Sulfitobacter* or *Hyphomonas*) and *Gammaproteobacteria* (from *Oceanospirillales*, *Pseudomonales, Alteromonales* and *Vibrionales* family) groups, these communities were also different from those found in hydrothermally unaffected water nearby. Organic compounds produced by vent fauna or microbial mats can be used as carbon and energy source for these heterotrophic bacteria. Nonetheless, presence of genes related to unusual metabolic pathways showing ability to degrade organic compounds such as volatile fatty acids or hydrocarbons, suggest their use as an alternative energy source when present in vent fluids (Bertrand et al., 2013; Meier et al., 2016). This sketches out the existence of a "heterotrophic belt" surrounding zones of active primary production within vent fields.

Interactions with the vent fauna are also occurring with microbial mats covering sometimes visually dominant fauna such as tubeworms, crabs or mussels, but the nature of these interactions remain unclear (Crépeau et al., 2011; Giovannelli et al., 2016; O'Brien et al., 2015). In mussel assemblages for example, commensal relationships have been hypothesized where chemosynthetic bacteria would benefit from fluid dispersion by mussels and numerous heterotrophs could degrade organic material released by the animal (Crépeau et al., 2011).

By all means, symbiotic interactions between chemosynthetic bacteria and various hosts are at the core of ecosystem functioning in hydrothermal vents (Cavanaugh et al., 2013).

# P.1.3 Hydrothermal vents – Houses for an intriguing symbiotic life

## P.1.3.1 Clarification on the symbiosis definition

Since the beginning of hydrothermal vent biology research, symbiosis has always been considered as a fundamental characteristic driving ecosystems (Cavanaugh, 1981). For each vent field where dense faunal assemblages were observed, symbiotic interactions within the dominant megafaunal animals were discovered. With the increasing exploration and research of new vent fields (cf. part 1.1.2), many more are undoubtedly waiting to be unveiled. Recent focus on meiofauna, previously often overlook , could also be a large source of new discoveries (Bellec et al., 2018; Zeppilli et al., 2018).

However, giving a clear definition of what is a *symbiotic interaction* has proved to be a very difficult task, given that its exact meaning has evolved many times since the first definition proposed by Anton de Bary : "*Das Zusammenleben ungleichnamiger Organismen*" or "the together life of dissimilar organisms" (de Bary, 1879). Increased efforts to understand the roles of those intricate relationships between two (or even more) partners in the past century have led to confound *symbiosis* with *obligate mutualism* (*i.e.* reciprocal benefit) between two organisms. At that point, symbioses were integrated in a conceptual view of interspecies interactions, classified by the level of impact they have on each other. With this theoretical framework, interactions are divided between beneficial and detrimental relationships as summarized in (**Fig 12.**).

This concept of costs and benefits was closely linked to the notion of fitness, usually related to a measure of the reproductive success for each partner, both alone and together. To assess the nature of a given interaction, 'only' a measure of the number of offspring able to reach the reproductive age for each condition – with and without the interaction – was needed. Unfortunately, this has revealed to be nearly impossible to demonstrate in the case of obligate associations, since survival rates without the partner often reach zero by definition. In these cases, interdependency is so strong that speaking of benefits or costs does not make any sense, since no comparison with aposymbiotic individuals – i.e. without the symbiont – exists in nature (Duperron, 2017).

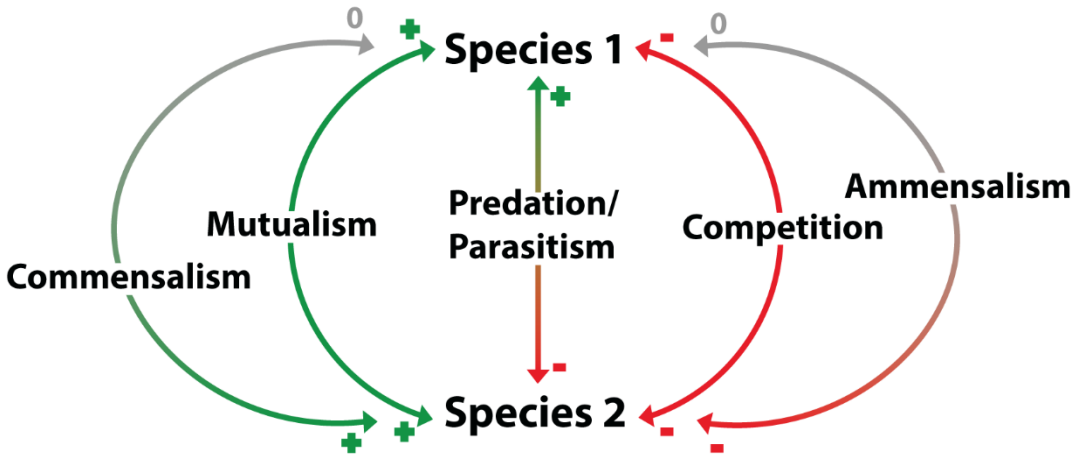


**Fig 12**. Schematic view of interspecies interactions. From Duperron (2017).

Owing to these issues, researchers have tried more recently to refine the concept of symbiosis without concealing the specificity of those interactions. Some have stressed the notion of *stability in time* with the idea of a *sustainable association*, including again parasitic interactions as well, like in the

first definition of Du Bary (Combes, 1995). This bridge between mutualistic symbioses and parasitic interactions, accentuated by this common notion of *long-term interactions*, suggests that one could have evolved from the other along the evolution. The similarity between mutualistic and parasitic interactions has found further support more recently with the discoveries of shared mechanisms for cell communication system and immune defense genes at the molecular level (Chu and Mazmanian, 2013; McFall-Ngai et al., 2012; Wippler et al., 2016). Others have insisted on the acquisition of new metabolic capabilities inherent to the interaction of the two partners, which joins the current of definition of *syntrophy* already discussed (cf. part 1.2.4) (Douglas, 1994). Each partner has the potential to realize only a part of a full metabolic pathway(s) and/or synthesis of some compounds, sometimes of high adaptive value. Then they are dependent on each other to fully realize complete metabolic pathways for growth.

Considerations on symbioses have progressively reshaped our perception of the evolution since our first understanding of their importance in "The Origin of Species" (Darwin, 1859). With the recent arise of the "holobiont" concept, a new postulate suggests that natural selection in some of those interactions could impact the chimeric entity formed by both partners – the holobiont – rather than each partner separately (Mindell, 1992). Holobiont entities, instead of species, would then correspond to the ecological units subjected to evolutionary processes. For a current definition of symbiosis, the rest of the manuscript will agree with the one given by (Zook, 2015), which summarizes all the advances made recently:

"Symbiosis is the acquisition of an organism(s) by another unlike organism(s) and through subsequent long-term integration, new structures and metabolism(s) emerge"

This can also be resumed by mathematical equations often used by Lynn Margulis (Margulis, 1971):

- **1 + 1 = 1** which implies one partner addition to one partner forming one unique entity
- **1 + 1 > 2** meaning that the whole entity potential is more than the sum of each partner capabilities, which joins the notion of emergence.

This definition has a significant advantage insofar as each of its part can be studied and tested. New structures can be observed with various microscopy techniques, and new metabolisms addressed with *in vivo* experiments and emerging meta-omics approaches. On the other hand, acquisition and subsequent long-term integration over the life cycle "only" require to have a global view of each partner's life cycle to follow their relationship at each life stage.

Although the world of symbiosis is extremely diverse, even in the restricted group of chemosynthetic symbioses which can be found in many ecosystems such as mangroves, coral reef or seagrass sediments, this manuscript will focus mainly on those found in hydrothermal vent ecosystems with some notes on other deep sea chemosynthetic based environments like cold seeps.

## P.1.3.2 Chemosynthetic symbioses: Variable hosting strategies

Symbiotic interactions have been identified in almost every metazoan phylum present in hydrothermal vents, including annelids, mollusks both bivalves and gastropods, arthropods, and nematodes (Bellec et al., 2018; Dubilier et al., 2008). To welcome their bacterial partners, a wide variety of morphological adaptions is displayed, as much between as within these different groups, reflecting a large adaptive flexibility from the hosts (**Fig 13.**). Depending on the symbiont locations,

symbioses are traditionally classified as endosymbioses when symbionts are housed internally and as ectosymbioses when they are external of the host cells/organs.

In siboglinids tubeworms (**Fig 14.**), symbionts are housed in a specialized organ, the trophosome, within cells called bacteriocytes. This trophosome originates from different embryonic tissues, depending on species, and exhibit different histo-anatomical characteristics. In vestimentiferan species – like *Riftia*, *Tevnia*, *Ridgea* or *Escarpia* –, this organ is massive, extending in the entire trunk region of the animal, and harbors a high bacterial density, up to 25% of the trophosome volume in *Riftia* (Bright and Sorgo, 2003). By contrast, the same organ in frenulates species only corresponds to the posterior part of the trunk, with much lower bacterial densities (less than 1% of the trophosome), but appears to have the same embryological origin (Katz et al., 2011). *Osedax* siboglinid bone-eating worms that colonize large carcasses falling on the seafloor, harbor a radically different trophosome that is hosted within root-like structures that invade and grow inside whalebones (Goffredi et al., 2005). However, it exhibits some convergence with the trophosome of large vestimentiferan species, being likewise derived from the mesoderm.

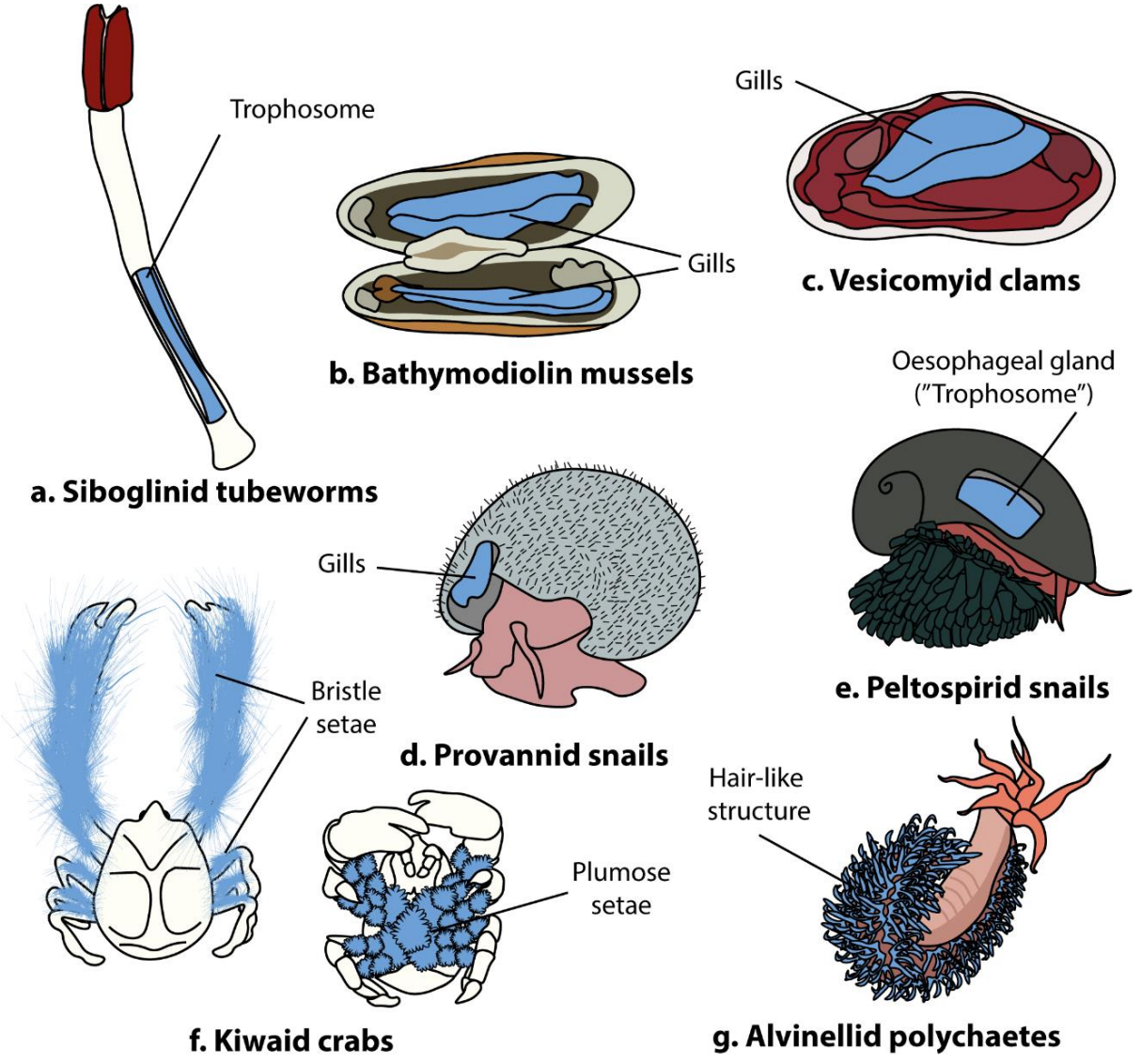


**Fig 13**. Some morphological adaptations displayed by hydrothermal vent species to house symbionts. *Blue*: hosting organs. Methou et al. (2019).

So far, the only other case of symbiont housed in an enclosed part of the body is found in gastropod species from the peltospirid family (**Fig 15.**): *Chrysomallon squamiferum* and the different *Gigantopelta* species (Chen et al., 2017). Their "trophosome" organs, derived from the esophageal gland in both cases but stem probably from two different and convergent evolutionary events to a symbiotic lifestyle (Chen et al., 2017). In these associations, reduced compounds and oxygen have to be brought by the hosts to the symbionts.

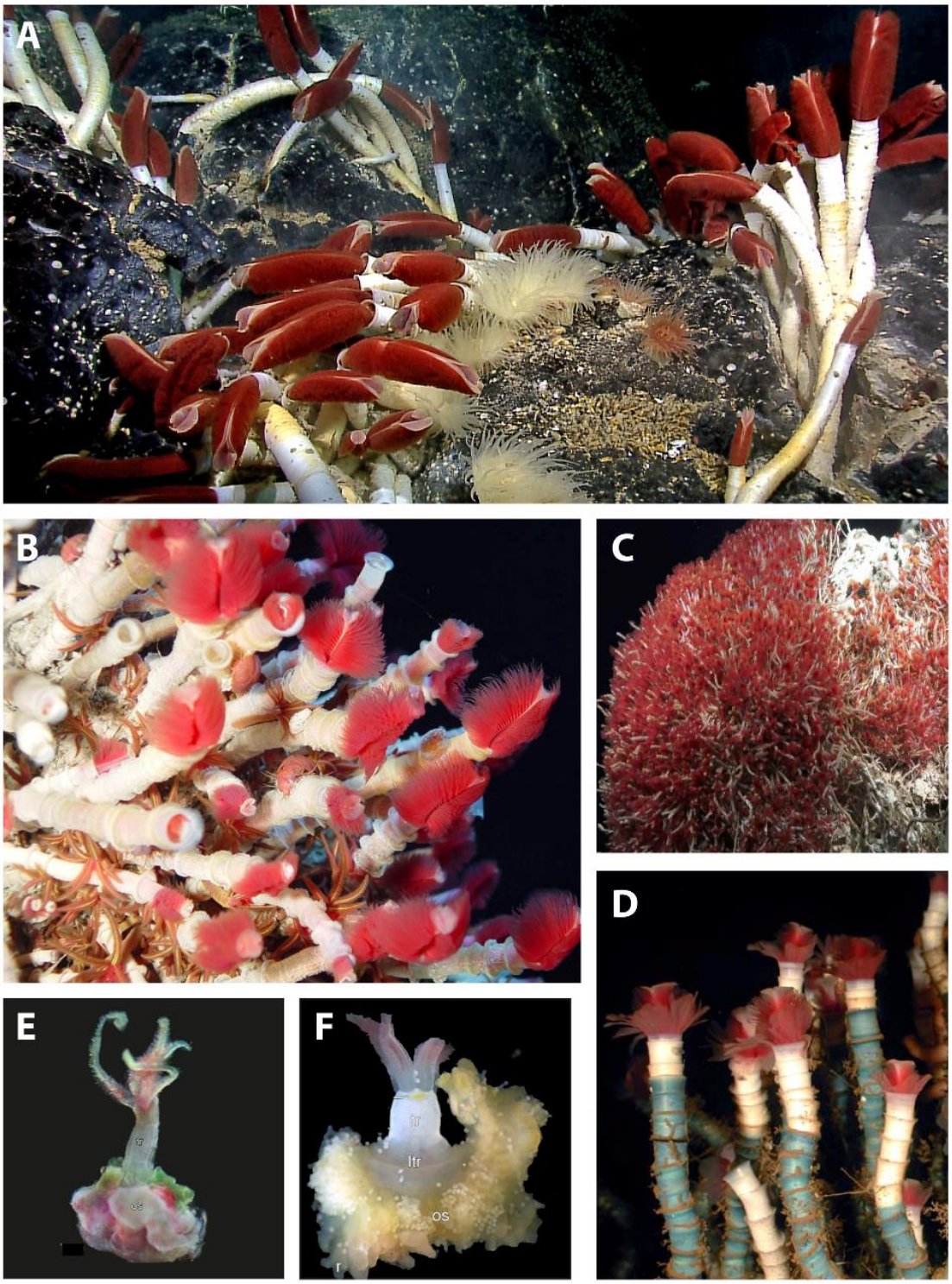


**Fig 14.** Overview of the siboglinid tubeworm diversity in hydrothermal vents and in other chemosynthetic ecosystems. **A.** *Riftia pachyptila* tubeworms from the Galapagos spreading center

where they have been first discovered. © Wikimedia commons. **B.** *Ridgea piscesae* tubeworms from the Juan de Fuca Ridge. © V. Tunicliffe and K. Juniper. **C.** *Oasisia alvinae* tubeworm colony usually associated with *Riftia pachyptila* and *Tevnia Jerichonana* in the EPR vent fields but observed alone in this vent field of the Pescadero Basin – i.e., the Junction between the EPR and the Guaymas Basin. © ROV Subastian/SOI (Schimdt Ocean Institute). **D.** *Lamellibrachia luymes*i individuals from the Gulf of Mexico. Blue color on the tube corresponds to artificial marking to follow their growth. © NOAA. **E.** *Osedax sigridae* specimen from whale falls in the Monterrey Canyon. © (Rouse et al., 2018). **F.** *Osedax talkovici* specimen from whale falls in the Monterrey Canyon. © (Rouse et al., 2018).

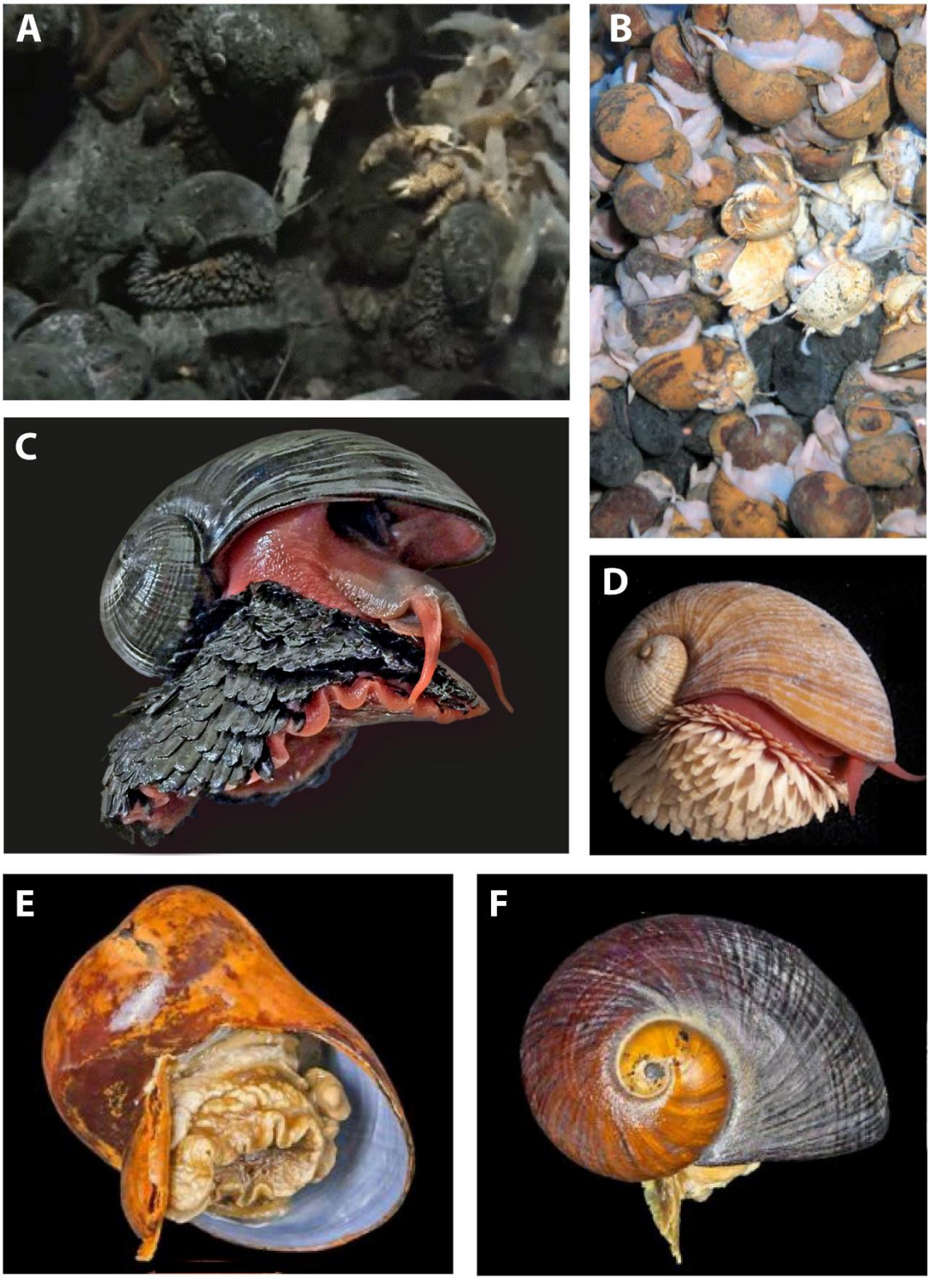

**Fig 15.** Overview of peltospirid snail diversity in hydrothermal vents **A.** Scaly foot gastropods (*C. squamiferum*) close to vent fluid emissions with vent crabs and vent shrimps at the Longqi vent field. © (Copley et al., 2016) **B.** *Chrysomallon squamiferum* and *Gigantopelta aegis* assemblages at Longqi vent field. © (Copley et al., 2016) **C.** Black morphotype of *Chrysomallon squamiferum* specimen from Kairei vent field. © Chong Chen; IUCN Red List **D.** White morphotype of *Chrysomallon squamiferum* specimen from Solitaire vent field. © (Nakamura et al., 2012). **E.** *Gigantopelta aegis* specimen from the South West Indian Ridge. © Chon Chen. **F.** *Gigantopelta chessoia* from the East Scotia Ridge. © Chong Chen.

In other gastropods from the provannid family, including *Ifremeria* and *Alviniconcha* species, endosymbionts are hosted inside gill cells and are more directly in contact with vent fluids (Suzuki et al., 2005a, 2005b; Urakawa et al., 2005; Windoffer and Giere, 1997). Moreover, for *Gigantopelta* snails, bacterial communities were observed in their gills in addition to "trophosome" ones (Heywood et al., 2017). Similar observations were made for many bivalves such as bathymodiolin mussels – *Bathymodiolus, Idas, Gigantidas and Benthomodiolus* – or vesicomyids clams – *Calyptogena, Phreagena* and *Issoporrodon* (**Fig 16.**) – with symbionts also located in their gills, inside vacuoles of bacteriocytes (Duperron, 2010; Duperron et al., 2013; Fiala-Médioni and Métivier, 1986). Surprisingly, the presence of symbionts nested extracellularly between gills microvilli was observed in some mytilid species such as *Idas washingtonia* and *Benthomodiolus erebus* in Juan de Fuca Ridge vent sites (Oliver, 2015; Southward, 2008).

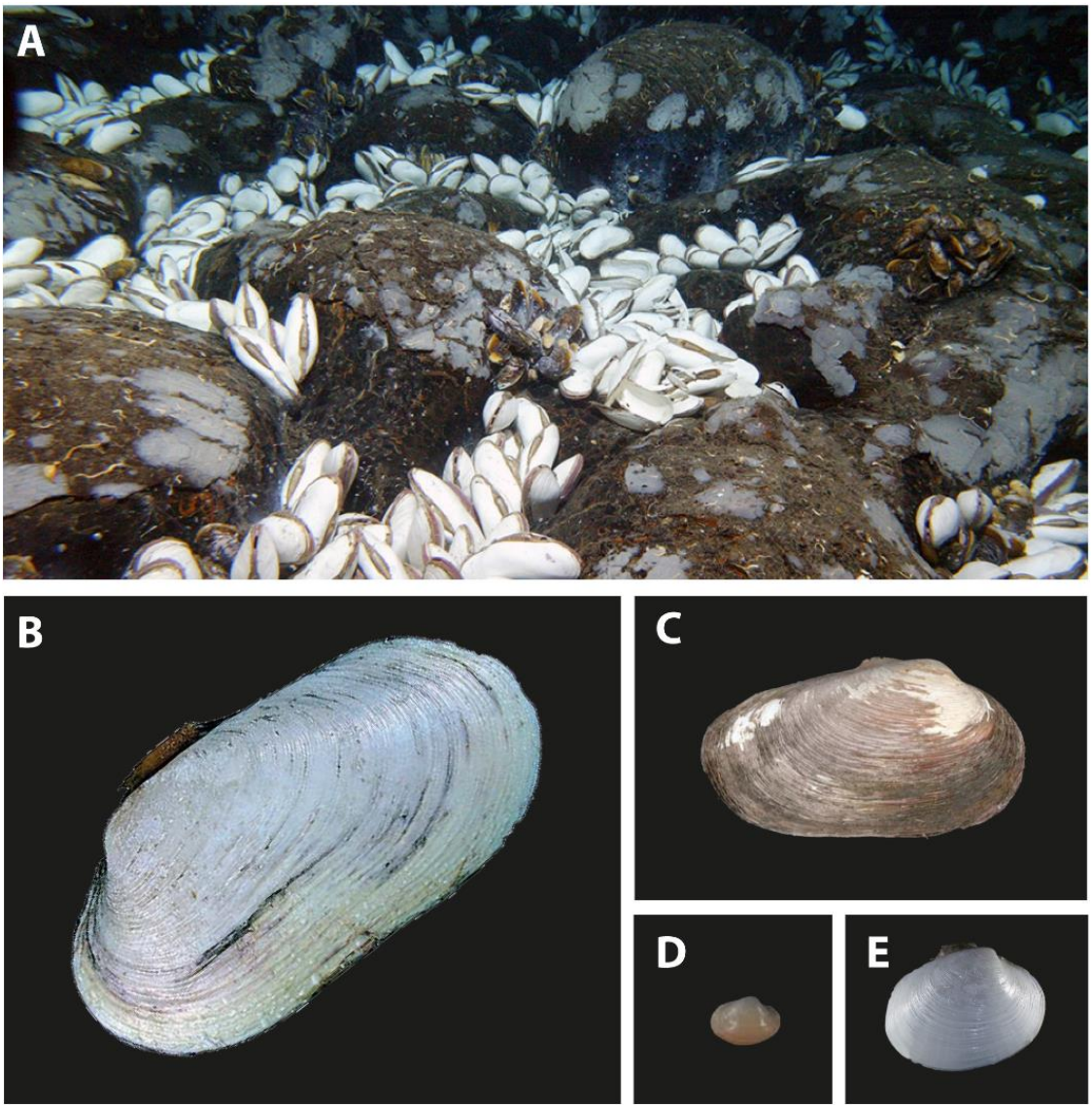


**Fig 16.** Overview of the vesicomyid clam diversity in hydrothermal vents and in other chemosynthetic ecosystems. **A.** *Calyptogena magnifica* clam beds from the EPR. © T. Shank (WHOI). **B.** *Phreagena okutanii* specimen from the Okinawa trough. © R. von Cosel (Chess). **C.** *Laubiericoncha chuni* specimen from the Gulf of Guinea cold seeps. © (Krylova and Sahling, 2010). **D.** *Isoporodon bigoti* specimen from the Gulf of Guinea cold seeps. © (Krylova and Sahling, 2010). **E.** *Isoporrodon megadesmus* specimen from the Gulf of Cadiz © (Oliver et al., 2011).

Ectosymbioses are observed in many other phyla. These types of symbiotic interactions exhibit different level of integration from "simply" fixed to body parts of the animal as for nematode worms (Bellec et al., 2018), to attached on specifically modified anatomical parts within the "branchial cavity" in Alvinocaridid shrimps (cf. part 2.1.2 for more details). In *Alvinella* spp. polychaetes for example, bacterial partners are localized on numerous hair-like structures present on the dorsal part of their body, which are absent in *Paralvinella*, their sister group species (Cary et al., 1997).

*Kiwa* crabs give another example of anatomical variation within the same family. Although spread all along their cuticular carapace, epibionts are preferentially associated to bristle setae of the enlarged arms – i.e. chelipeds – in *Kiwa puravida* (Thurber et al., 2011). Similarly, epibionts are more localized on dense plumose setae of the arms and on the ventral part of the legs in *Kiwa hirsuta*

(Macpherson et al., 2005), whereas they are restricted to ventral body parts in *Kiwa tyleri* (Thatje et al., 2015a). In the perspective of the evolutionary history of the group, the variation between plumose and bristle setae seems to correlate with a divergent event in the kiwaid family (Roterman et al., 2018). Interestingly, the hosting strategy of *K. tyleri* is more similar to the dense plumose setae also found on the ventral part of the body of *Shinkaia crosnieri* crabs, although both species belong to two different anomuran families (Tsuchida et al., 2011). This convergence denotes potentially a similar lifestyle to feed their symbionts in the two species.

## P.1.3.3 Chemosymbiosis: specificity and diversity of the bacterial partners

### P.1.3.3.1 Diversity of chemosynthetic endosymbioses

Chemosynthetic symbioses involve a wide diversity of bacterial partners in hydrothermal vents and other deep-sea ecosystems. Despite this diversity, thiotrophic *Gammaproteobacteria* have been identified as the main symbiont in most hydrothermal vent endosymbioses. Belonging to different bacterial lineages according to the host family, they have been reported as dominant in the gills of many bathymodiolin mussels, vesicomyid clams and provannid snails (Beinart et al., 2012; Duperron, 2010; Suzuki et al., 2006b) as well as in the trophosome of peltospirid gastropods and siboglinid tubeworms (Bright and Lallier, 2010; Goffredi et al., 2004; Heywood et al., 2017).

Whereas $H_2S$ consumption has been confirmed in early studies for many of these symbioses (Belkin et al., 1986; Childress et al., 1991; Fisher et al., 1987; Girguis and Childress, 2006), use of $H_2$ as alternative energy source by Gammaproteobacterial symbionts has only been acknowledged recently, offering some level of plasticity in vent fields with variable fluid geochemistry (Petersen et al., 2011a). Additionally, the use of partially oxidized sulfur compounds – like thiosulfate and polysulfide – more stable but less energetic than sulfide, appears to fuel their metabolism as well (Beinart et al., 2015). This ability to use different reduced states of sulfur compounds is believed to expand considerably the niche of Gammaproteobacterial symbionts to the cooler part of the mixing gradient, where sulfide species are completely oxidized but where other sulfur compounds are still available. Moreover, thiosulfate and polysulfide excretion by host animals under high sulfide conditions – most likely due to detoxification– stress their importance, animals closest to the fluids providing indirectly substrates for the ones behind (Beinart et al., 2015).

Metagenomic studies confirmed such plasticity of fueling sources highlighting that thiotrophic *Gammaproteobacteria* endosymbionts largely encompass metabolic capacities of their free-living relatives (Kuwahara et al., 2007; Nakagawa et al., 2014; Newton et al., 2007; Sayavedra et al., 2015). Still, one intriguing particularity found in genomes was the unexpected presence of both rTCA and CBB carbon fixation pathways co-occurring in *Riftia pachyptila* symbionts (Robidart et al., 2008) as well as in symbionts of other vestimentiferans species – but not frenulates (Gardebrecht et al., 2012; Li et al., 2018; Thiel et al., 2012). The rTCA cycle requiring less energy than the CBB cycle, the ability to switch between the two pathways has been suggested to be an adaptive advantage when energy sources are fluctuating. Correspondingly, symbionts thriving in high sulfur content environments express more CBB related proteins whereas those living within sulfur depleted habitats express more rTCA related proteins (Markert et al., 2007). Moreover, genes involved in heterotrophic metabolism, chemotaxis and motility were also retained in their genome, although not expressed as proteins in their hosts (Markert et al., 2007; Robidart et al., 2008). These genes are believed to correspond to the free-living

life style of those symbionts, consistent with the presence of these free-living stages in seawater outside the vent fluids influence (Harmer et al., 2008) .

Gammaproteobacterial symbionts from the *Chromatiales* order are highly conserved in siboglinid tubeworms, with a single phylotype per host species, based on 16S rRNA gene marker, in most studied individuals (Bright and Lallier, 2010). Furthermore, phylotypes were sometimes shared between co-occurring species of the same geographical region or between species of different ridge systems (Gardebrecht et al., 2012; Perez and Juniper, 2016). This homogeneity was further confirmed by metagenomics studies with a 90% conserved core genome, still, with some structuration according to geographic distance and/or host specificity. Variations, corresponding to different strains of the same symbiont species, between the different host genomes or according to their geographic regions were mainly attributed to genetic drift processes and adaptation to viral interactions (Perez and Juniper, 2016). The existence of several strains among *Riftia* tubeworms was confirmed also by recent studies (Perez and Juniper, 2018; Polzin et al., 2019).

On the other hand, different phylotypes of symbionts were reported within the same host species, between individuals from different geographical locations. For example, *Escarpia laminata* from two different areas of the Gulf of Mexico were harboring two different symbiont phylotypes (Nelson and Fisher, 2000). In addition, *Lamellibrachia anaximandri* tubeworms from Mediterranean vent sites and cold seeps harbored two closely related but different symbiont phylotypes within the same individual (Duperron et al., 2009; Zimmermann et al., 2014). These two symbionts were organized in regions all along the trophosome but without consistent pattern of distribution between individuals (Zimmermann et al., 2014). All these results highlight that different patterns of host specificity with bacterial partners can arise even from the same host group. In the first case, the presence of different symbionts according to the vent site could be related to a better fitness of this symbiont to the local environmental conditions or to the existence of two symbiont populations affected by dispersal barriers, unlike their host. In the second case, the presence of two symbionts within the same host could arise from hypervariable environmental conditions with one symbiont adapted to some parts of the environmental gradient and the second symbiont to the other parts. Indeed, even closely related microorganisms with apparently redundant metabolic capabilities can be adapted to subtly different environmental conditions as highlighted by several studies (Jaspers and Overmann, 2014; Johnson et al., 2006b; Meier et al., 2017). The same pattern could also come from a syntrophic relationship between the two symbionts, each performing partially some of their complete metabolic pathways.

Endosymbionts of bathymodiolin mussels (**Fig 17.**) were found to be even more diverse. The most abundant and widespread are belonging to another thiotrophic Gammaproteobacterial group, not endemic to hydrothermal vents ecosystems.

In rarer instances, methanotrophic Gammaproteobacterial symbionts were found to be the only symbiotic partner, such as for *Bathymodiolus childressi* (Childress et al., 1986; Duperron et al., 2007). In many cases, however, both symbionts were co-occurring within the same host, variations in their relative abundance being attributed to surrounding fluids composition rather than host species (Distel et al., 1995; Duperron et al., 2006, 2007, 2011) (**Fig 18.**).

Indeed, both *Bathymodiolus azoricus* and *Bathymodiolus puteoserpentis* from the MAR were dominated by methanotrophic symbionts in ultramafic vent sites presenting higher $CH_4$ concentrations

compared to basaltic vent sites (Duperron et al., 2006). This was further confirmed by several experiments performed using pressure chambers or at atmospheric pressure (**Fig 18.**). Changes in reduced compounds availability – induced by a sulfur or methane pulse – can drastically increase, or decrease symbionts relative abundance according to their preferential energy source (Duperron et al., 2016; Halary et al., 2008; Riou et al., 2008; Szafranski et al., 2015b), showing both plasticity and adaptability of symbioses in these cases.

Even more diverse associations were reported in *Bathymodiolin* mussels with up to 6 symbiont lineages in *Idas modiolaeformis* and an additional Gammaproteobacterial symbiont from the *Cycloclasticus* genus in *Bathymodiolus heckerae* (Duperron et al., 2008; Raggi et al., 2013). Potential to degrade and use short chain alkanes – such as butane or ethane – both as carbon and energy, was revealed in *Cycloclasticus* symbiont genomes. This metabolism was unlike the previously hypothesized use of polycyclic aromatic hydrocarbons (PAHs) that was based on the known metabolic capacities of the free living relatives (Rubin-Blum et al., 2017). All these studies emphasize the strong flexibility and large metabolic capacities of these associations, enabling their acclimatization to variable environmental conditions.

Like for siboglinid tubeworms, recent metagenomic studies uncovered an even larger diversity at the strain level of the sulfur-oxidizing endosymbionts with up to 16 different strains in four *Bathymodiolus* species of the MAR (Ansorge et al., 2019). These co-occuring strains differ in many key functions such as their use of energy and nutrient sources, viral defence genes and their electon acceptors. Such a large diversity results most likely from the important adaptability it brought to the holobiont. Nonetheless, the authors of this study also hypothetize that it could also be the consequence of a “low-cost” symbiosis (Ansorge et al., 2019). Indeed, unlike other symbioses, these mussels do not have to bear the cost of “feeding” their symbionts, as reduced compounds diffuse passively through the housing organ. Therefore, *Bathymodiolus* mussels may have a higher tolerance to maintain “less efficient” strains among “more efficient” ones as the cost for their maintenance is limited (Ansorge et al., 2019). These observations clearly contrasts with the other evolutionary theories existing so far that were based on “high costs” symbiosis where the nutritional exchanges were from the two sides (Frank, 1996).


**Fig 17.** Overview of the bathymodiolin mussel diversity in hydrothermal vents and in other chemosynthetic ecosystems. **A.** *Bathymodiolus puteoserpentis* mussel beds at Snake Pit (the Moose) in the MAR. BICOSE2018-Nautile © Ifremer. **B.** Open shell of *Bathymodiolus marsindica* from the SWIR with different organs and his commensal polynoid polychaete *Branchipolynoe longqiensis*. © (Copley et al., 2016). **C.** *Idas washingtoniana* specimen from the Juan de Fuca Ridge. © (Ritt et al., 2012). **D.** *Bathymodiolus thermophilus* specimen from the EPR. © S. Aiken. **E.** *Bathymodiolus securiformis* specimen from cold seeps off Yaeyema islands. © (Okutani et al., 2003). **F.** *Bathymodiolus childressi* specimen from cold seeps of the Gulf of Mexico. © S. Aiken. **G.** *Bathymodiolus heckerae* specimen from cold seeps of the Gulf of Mexico © (Raggi et al., 2013).

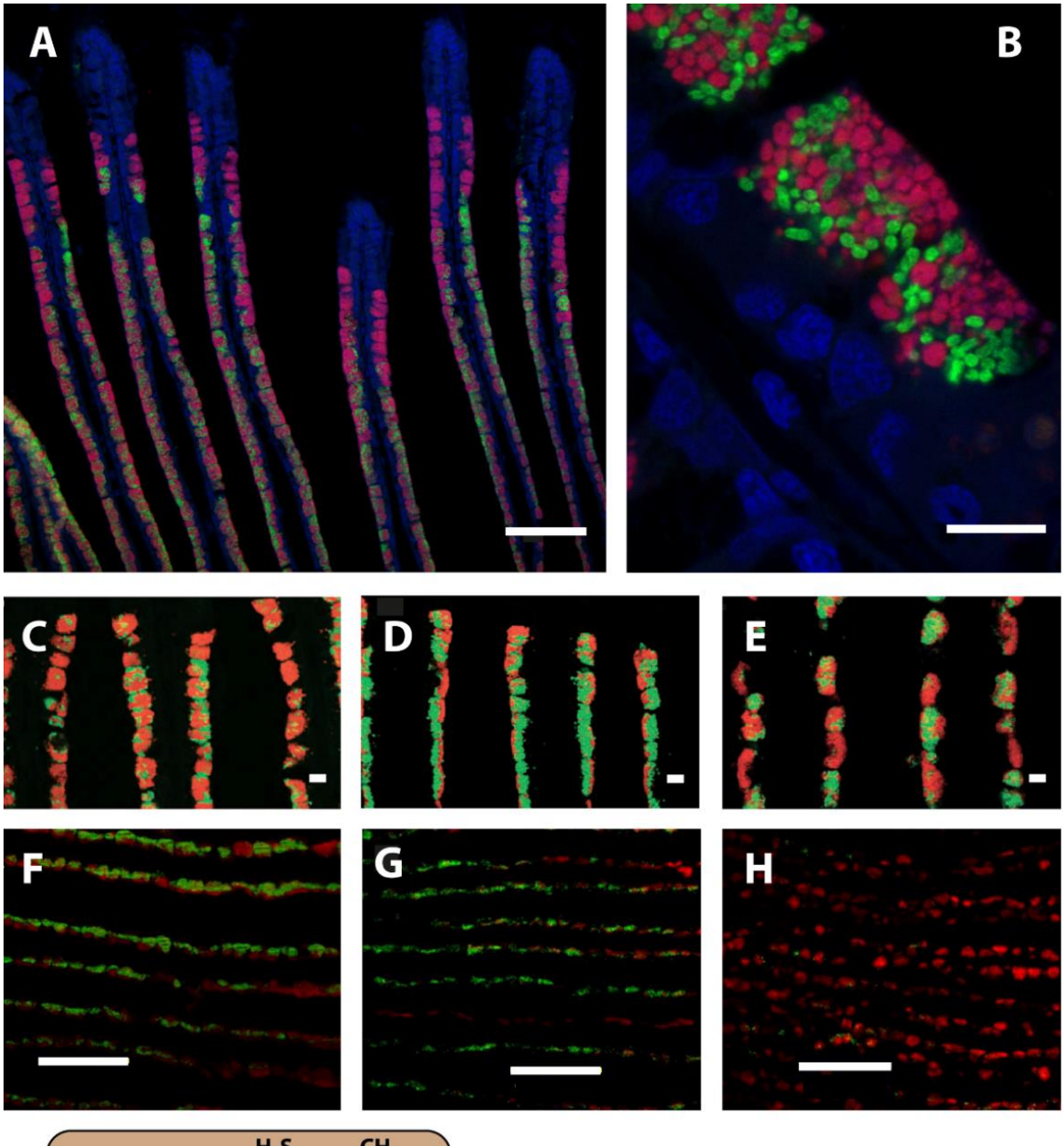


| | $H_2S$ | $CH_4$ |
|---|---|---|
| **Menez Gwen :** | 1.3-1.8 | 1.35-2.15 |
| **Lucky Strike :** | 2.7-3.0 | 0.30-0.85 |
| **Rainbow :** | 1.2* | 2.5 |
| **Logatchev :** | 0.8-2.5 | 2.1-3.5 |

* Not available for animal life, $H_2S$ react with Fe to form ironsulfides that cannot be used by the symbionts

**Fig 18.** Relative Abundance of bathymodiolin symbionts highlighted by Fluorescent in situ Hybridization (FISH) results. Red: thiotrophic symbionts. Green: methanotrophic symbionts. **A.** Gills of *B. azoricus* from Menez Gwen **B.** Close up from figure A. on thiotrophic and methanotrophic symbionts **C.** Gills of *B. azoricus* from Lucky Strike. **D.** Gills of *B. azoricus* from Lucky Strike. **E.** Gills of *B. puteoserpentis* from Logatchev. **F.** Gills of fresh *B. azoricus* specimen from Menez Gwen before treatment. **G.** Gills of *B. azoricus* after 5 days of incubation with $CH_4$. **H.** Gills of *B. azoricus* after 5 days of incubation with $H_2S$. Adapted from (Riou et al. 2008), (Duperron et al. 2006) and (Szafranski et al. 2015b).

A similar variability was observed in endosymbiotic associations of hydrothermal vents gastropods. In *Ifremeria* snails (**Fig 19.**), thiotrophic *Gammaproteobacteria* from another order – *Chromatiales* – are also found co-occurring with methanotrophic symbionts although the presence of this second partner was not always consistent between populations (Borowski et al., 2002; Seston et al., 2016; Suzuki et al., 2006a; Urakawa et al., 2005). In *Alviniconcha* gastropods (**Fig 19.**), a large variety of sulfur-oxidizing endosymbionts has been identified belonging to either *Gammaproteobacteria* from different order – closely related to *Ifremeria* thiotrophic symbionts or to the *Thiomicrospira* genus – or to *Epsilonbacteraeota*. *Alviniconcha* gastropods usually exhibit a preferential association with one symbiont species such as *Alviniconcha boucheti* or *Alviniconcha marsindicus,* always dominated by *Epsilonbacteraeota* symbionts, while *Alviniconcha kojimai or Alviniconcha hessleri* are dominated by *Gammaproteobacteria* (Beinart et al., 2012; Suzuki et al., 2005a, 2005b, 2006b). In the Lau Basin where three *Alviniconcha* species co-exist, a strong geographical pattern was observed with more *Alviniconcha* dominated by *Epsilonbacteraeota* in the northern sites and more *Alviniconcha* dominated by *Gammaproteobacteria* symbionts in the southern sites (Beinart et al., 2012). This was mainly attributed to differences in environmental conditions, the northern sites exhibiting higher $H_2S$ and $H_2$ concentrations. This was confirmed by transcriptomic studies in which *Epsilonbacteraeota* symbiont gene expressions were more suited for highly reduced and less oxygen-rich conditions, compared gene expression in *Gammaproteobacteria* symbionts (Sanders et al., 2013). Unlike *Bathymodiolus* mussels, potential flexibility of these associations between the different partners have still to be explored.

Infection by an additional *Oceanospirillales* was also reported in almost every *Alviniconcha* dominated by *Gammaproteobacteria* and seldom for *Alviniconcha* dominated by *Epsilonbacteraeota* (Beinart et al., 2014). Although this facultative partnership does not necessarily affect these symbioses, it could as well mitigate co-occurrence of different *Alviniconcha* species by offering a new metabolic capacity or acting as a parasite to only some of them. Such behavior was confirmed in the case of the facultative association between several bathymodiolins mussels and an endonuclear parasite – sharing 95% similarities with *Alviniconcha Oceanospirillales* – leading to nuclei burst and cells death in their gills (Zielinski et al., 2009).

Usually seen as highly integrated and highly specific with one or two symbiotic partners only, chemosynthetic endosymbioses generally hide a much more important diversity, as exemplified in many of the most recent studies presented here. This diversity lies in some cases, at the species level but in many other at the strain level. Such diversity contrasts with most evolutionary theories, which predict that a large genetic diversity can lead to competition between the different symbionts species/strains and destabilize the mutualistic relationship with their hosts. In chemosynthetic symbioses, however, these evolutionary conflicts can be counterbalanced by the plasticity brought by this diversity, which offers a larger adaptability and resilience, especially in environments with extremely variable conditions such as hydrothermal vents. “Low-cost” symbioses where the symbionts maintenance cost – feeding and upkeep – are limited could also have a higher tolerance to maintain a high symbiont diversity, as suggested in some recent evolutionary theories (Ansorge et al., 2019). In conclusion, the continuity in time of these symbiotic interactions results from a complex and fragile equilibria, whose balance is easily disturbed as seen in the few examples of "parasites" occasionally present, which can end the interaction with the other symbionts.

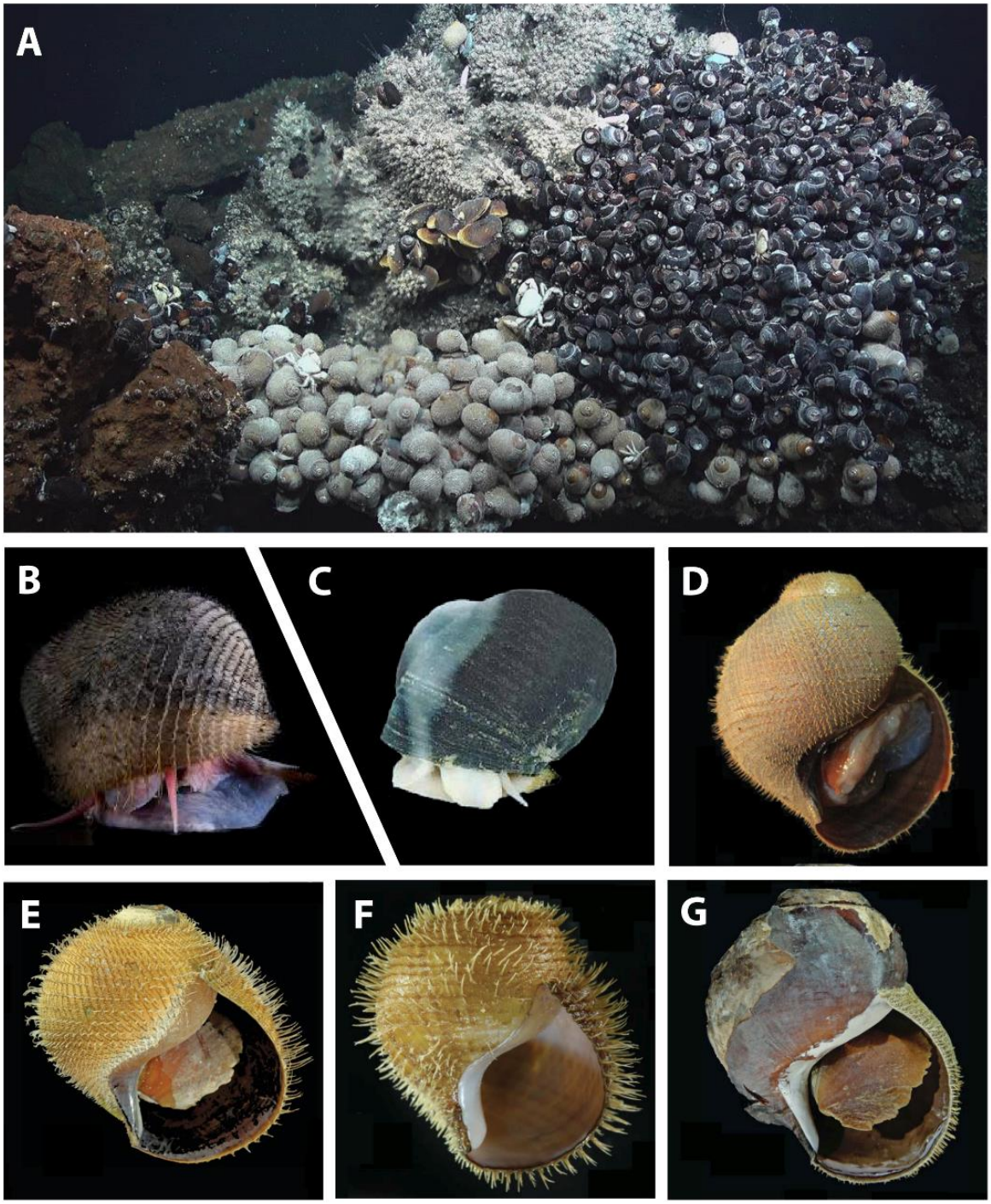


**Fig 19.** Overview of provannids snail diversity in hydrothermal vents. **A.** Colonies of *Ifremeria nautilei* (black gastropods) and different *Alviniconcha* species (white gastropods) from the North Fidji Basin © (Chubacarc expedition) **B.** *Alviniconcha marisindica* specimen from the Central and South Western Indian Ridge. © Yoshihiro & Fujikura, (JAMSTEC). **C.** *Ifremeria nautilei* specimen from the southwestern Pacific basins. © Maestrati (Chess). **D.** *Alviniconcha hessleri* specimen from the Marianna trough. © (Johnson et al., 2015). **E.** *Alviniconcha kojimai* specimen from the southwestern Pacific basins. © (Johnson et al., 2015). **F.** *Alviniconcha strummeri* specimen from the Lau basin**.** © (Johnson et al., 2015). **G.** *Alviniconcha boucheti* specimen from the southwestern Pacific basins. © (Johnson et al., 2015).

## P.1.3.3.2 Diversity of chemosynthetic ectosymbioses

As previously stated (cf. part 1.3.2), a significant part of the dominant vent megafauna also hosts ectosymbionts. More complex with the involvement, in general, of a wider range of partners, they are also less studied than endosymbiosis. In most vent ectosymbioses, hosts are associated with various thin and large filamentous morphotypes attached to a specific surface of their body even if small rod or cocci shaped individual bacteria can be also present. Moreover, whereas *Gammaproteobacteria* dominate endosymbiotic assemblages, *Epsilonbacteraeota* often prevail in ectosymbiotic microbial consortium (Cary et al., 1997; Goffredi, 2010; Goffredi et al., 2008; Tsuchida et al., 2011).

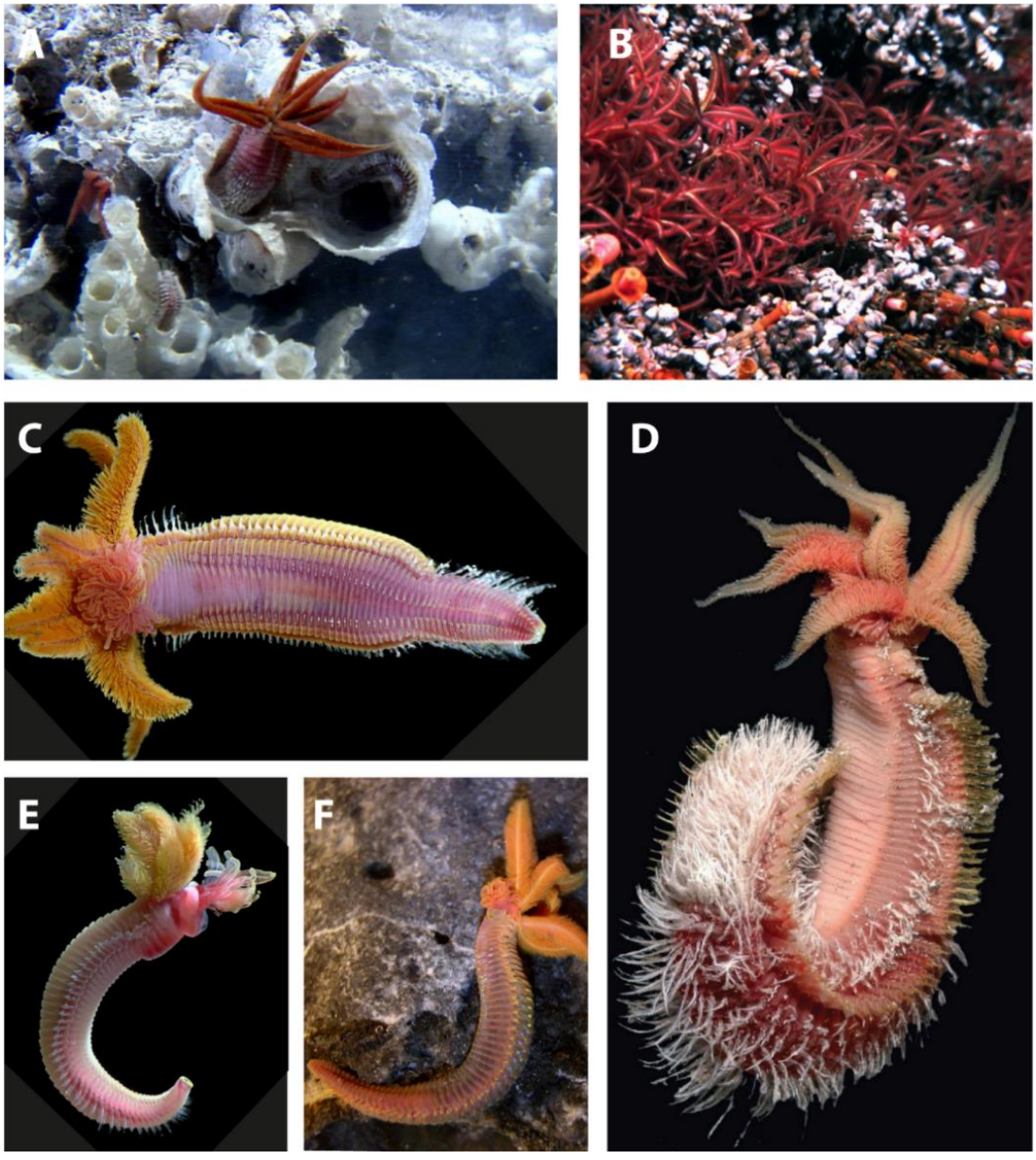


**Fig 20.** Overview of alvinellid polychaete worm diversity in hydrothermal vents. **A**. *Alvinella pompejana* in their tubes on the EPR. © Station Biologique de Roscoff. **B.** *Paralvinella palmiformis* assemblages at the Juan de Fuca Ridge. © Wikimedia commons. **C.** *Paralvinella fijensis* adult specimen (Fidji Basin). © Chess **D.** *Alvinella pompejana* adult specimen. © O. Dugornay (Ifremer). **E.** *Paralvinella fijensis* adult specimen. © Chess **F.** *Paralvinella sulfincola* on bare rock at the Juan de Fuca Ridge. © K. Onthank.

In *Alvinella pompejana* polychaetes (**Fig 20.**) for example, two phylotypes of filamentous *Epsilonbacteraeota* were found associated with the dorsal setae of their host (Cary et al., 1997). Knowledge of the symbiotic diversity was extended further by a metagenomic study reporting around 10 to 15 different phylotypes within the same host (Grzymski et al., 2008). Besides, this same study also revealed the very high plasticity of this relationship with the presence of several orthologous key proteins with different inferred thermal optimum in the episymbiotic core genome. This protein diversity provides most likely an adaptive advantage to a wider range of temperature, essential for *Alvinella* worms living very close to the fluid emissions in the most fluctuating part of these environments (Grzymski et al., 2008). However, it is still unclear whether these proteins correspond to an adaptation of each symbiont phylotype to a specific thermal range or if this offers to some – and maybe all – of them a large thermal tolerance.

Filamentous *Epsilonbacteraeota* are also predominant in communities associated with vent decapods like *Kiwa* and *Shinkaia* crabs (**Fig 21.**). Additionally, this dominant symbionts are always observed co-occurring with another sulfur-oxidizing epibionts – a *Gammaproteobacteria* from the *Thiotricaceae* family – and members of the CFB group including the *Bacteroidetes* (Goffredi et al., 2008; Tsuchida et al., 2011; Watsuji et al., 2010). The presence of this last group echoes the observations of Stokke and his collaborators discussed previously in this manuscript (cf. part 1.2.4). Although not highlighted by any studies so far, it is still plausible that similar syntrophic interactions between *Epsilonbacteraeota* and *Bacteroidetes* partners could take place in these symbiotic consortiums.

Methanotrophic *Gammaproteobacteria* were also detected in these associations, especially in individuals from methane rich environments such as *Kiwa puravida* from cold seeps off Costa Rica or *Shinkaia crosnieri* from the Iheya North vent site (Goffredi et al., 2014; Watsuji et al., 2010). For *S. crosnieri*, this symbiont was confirmed to be active using $CH_4$ as a sole energy and carbon source with radiolabeled $^{14}CH_4$ experiments (Watsuji et al., 2014). Moreover, long time rearing experiment – up to a year – with only methane as a feeding source, led to a shift in the ectosymbiotic community with a complete loss of the sulfur-oxidizing *Gammaproteobacteria* and *Epsilonbacteraeota* and a large dominance of the methanotrophic partners, still active and able to incorporate methane to feed their host (Watsuji et al., 2018).

In *Kiwa tyleri,* strong variations of the epibiotic communities were detected as well between crabs living in different vent fields (Zwirglmaier et al., 2015). As for *Alviniconcha* endosymbionts, *Epsilonbacteraeota* were the more abundant symbionts in crabs collected from vent sites with the highest $H_2S$ concentrations. *Kiwa* crabs from the other vent fields, enriched in Fe and unexpectedly highly concentrated in Mn, were exhibiting a more unusual relationship. In addition to a much higher abundance of *Thiotricaceae Gammaproteobacteria* as expected for low $H_2S$ conditions, *Gammaproteobacteria* affiliated to the *Marinobacter* family were highly abundant as well. Based on metabolic evidence from their free-living relatives (Edwards et al., 2003; Wang et al., 2012), authors have suggested that these newly described symbiotic partners would use Mn or Fe as energy source, consistent with the high abundance of these compounds in fluids from this vent field (Zwirglmaier et al., 2015). Although these hypotheses need confirmation with metagenomic studies and *in vivo* experiments with radiotracers, this underlines, once again, the strong versatility of these chemosynthetic symbioses, able to harness and make the better use of their symbiont metabolic potentials according to the environmental conditions.

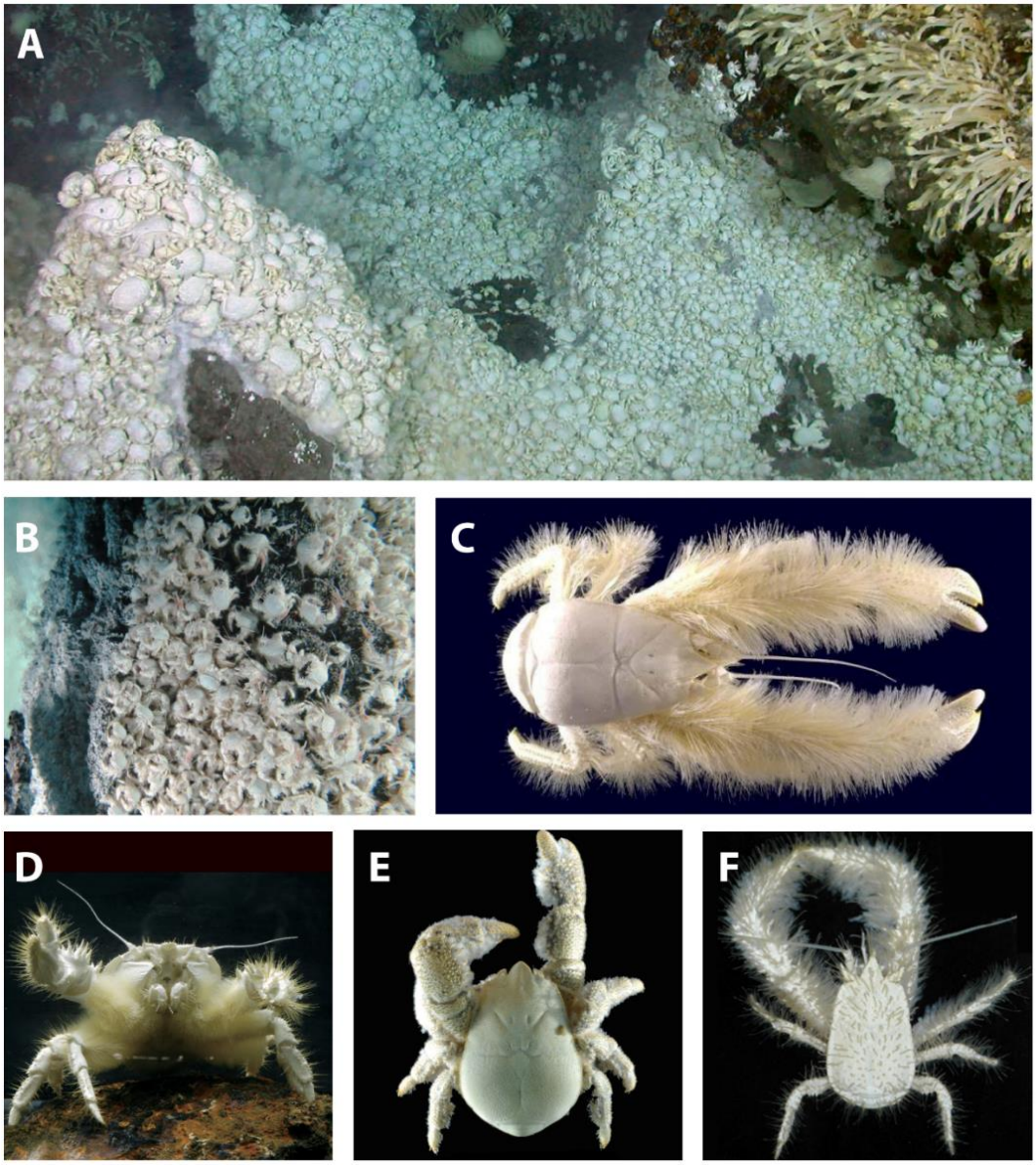


**Fig 21.** Overview of kiwaid crab diversity in hydrothermal vents and in other chemosynthetic ecosystems. **A.** *Kiwa tyleri* aggregates from the East Scotia Ridge. © (Rogers et al., 2012) **B.** *Shinkaia crosnieri* aggregates from the Okinawa trough. © (Yang et al., 2016). © **C.** *Kiwa hirsuta* specimen from the Pacific-Antarctic Ridge with bristle setae on its arms. © (Macpherson et al., 2005). **D**. *Shinkaia crosnieri* specimen with plumose setae on the ventral part of its body. **E.** *Kiwa tyleri* from the East Scotia Ridge (plumose setae on its ventral part). © (Thatje et al., 2015a). **F.** *Kiwa puravida* from cold seeps off Costa Rica with bristle setae © (Goffredi et al., 2014).

Metabolic abilities of symbiotic partners can also be counter intuitive as shown in the intriguinguing case of members of the *Candidatus Thiobarba* family (*Espilonbacteraeota*) occurring in epibiotic associations with bathymodiolin mussels (Assié et al., 2016). Found together with the gammaproteobacterial endobionts, these associations have only been described recently in several *Bathymodiolus* species such as *B. azoricus*, *B. childressi* or *B. manusensis*, but not in other species investigated such as in *B. puteoserpentis* or *B. thermophilus* (Assié et al., 2016). Unlike other *Espilonbacteraeota* that all posess a rTCA cycle (cf. part 1.2.1 and 1.2.2), *Ca. Thiobarba* ectosymbionts seem to have acquired a complete set of genes corresponding to a functional CBB cycle whereas many genes required for the rTCA cycle are lost (Assié et al., 2019). More surprisingly, the CBB genes of *Ca.*

*Thiobarba* appear to have been acquired horizontally from multiple co-occuring bacterial sources including the *Gammaproteobacteria* endosymbionts of their mussel host. This case highlights once again the predominant influence of the environmental conditions over phylogenetic relatedness on bacterial evolution and show the role that horizontal gene transfer can have on the metabolic modularity of bacteria (Assié et al., 2019). Still, the possible role of these epibionts for their host health and/or survival remains to be demonstrate.

In summary, ectosymbioses, although having varying degrees of integration with their host, remain always less integrated than any endosymbiotic interactions. This continuum of symbiont integration with their host, from ectosymbioses simply attached to the body surface to intracellular endosymbioses, does no reflect however the degree of intimacy and the evolutionarity stability of the relationship. Indeed, a comparison of two chemosynthetic symbioses from shallow water environments show more congruent topologies between the phylogenetic trees – and thus a larger level of cospeciation and evolutionary stability – of the host and its symbiont in the group harboring ectosymbioses – stilbonematine nematodes – than in the group harboring endosymbioses – phallodriline gutless annelids (Zimmermann et al., 2016). In general, deep-sea chemosynthetic ectosymbioses are more oftenly associated with *Epsilonbacteraeota* whereas endosymbioses are predominantly associated with *Gammaproteobacteria*. However, unlike chemosynthetic endosymbioses, chemosynthetic ectosymbioses diversity is not limited to these two bacterial groups and often involves a larger number of partners, and thus a wider metabolism diversity, using unusual energy sources such as Fe or Mn. Despite this fact, some studies on ectosymbiosis still presume bacterial metabolisms based solely on their taxonomy - 16S barcoding - without carrying out studies of their genomes, which can lead to innacurate interpretations.

## P.1.3.4 Host adaptation to a chemosymbiotic life style

Evaluating the degree of dependence of animal hosts on symbiotic nutrition has turned out to be quite challenging. Often, it is inferred from anatomical singularities that significantly depart from the typical body plan anatomy. Apart from a hypertrophied hosting organ, other anatomical traits, sometimes more specific to a taxonomical group, can also help to understand host-feeding mode. For example in gastropods, weak radula, a structure analogous to teeth, is probably of limited use for an active grazing or detritivorous feeding mode, and could denote a symbiotic based nutrition if associated bacteria are observed (Chen et al., 2015b; Goffredi, 2010). In general, total lack of digestive system such as for *Riftia* tubeworms, or at least its strong reduction as in vesycomyid clams, has been raised as undeniable evidence of a strong reliance of the host on its symbionts for nutrition (Fiala-Médioni and Métivier, 1986; Nussbaumer et al., 2006). However, nutritional transfer of the symbiont organic matter production is diverse, and the absence of digestive system reduction does not necessarily exclude a symbiotic lifestyle.

Indeed, *Kiwa* and *Shinkaia* crabs appear to harvest bacterial symbionts on their setae. As evidenced by behavioral observations and radiolabeled tracer experiments, crabs scrap off their epibionts and ingest them via their digestive organs (Miyake et al., 2007; Thurber, 2015; Watsuji et al., 2015). All digestive organs remain thus completely functional.

In other chemosynthetic symbioses, this nutritional transfer can be achieved by two different strategies: the leaking of small organic molecules from the symbionts, also called the “milking” strategy, or the complete digestion of the symbionts by the host, the “farming” strategy. In

*Bathymodiolus* mussels, the transfer of $^{14}C$ radiolabeled carbon to the host tissues takes days (Fisher and Childress, 1992; Riou et al., 2008) which supports other ultrastructural and enzymatic evidences that symbionts are killed and digested by their host in intracellular lysozymes (Fiala-Médioni et al., 1994, 2002; Streams et al., 1997). In *Riftia* tubeworms, the carbon transfer can be observed in incubations as short as 15 minutes, suggesting that an important part of the symbiont production is released in the form of organic molecules (Bright et al., 2000). Moreover, high apoptosis of bacteriocytes from the peripheral part of their trophosome indicates that both symbiont "farming" and "milking" contribute to their host nutrition (Bright et al., 2000; Pflugfelder et al., 2009). Similarly, enzymatic studies involving the detection of two different lysosomal vesicles in *Bathymodiolus* mussels with distinct enzymatic content and elemental composition indicate that these two strategies could co-occur in these animals as well (Kádár et al., 2008).

In addition to this symbiont-based nutrition, some host species can retain some ability for alternative nutrition modes, such as filter feeding in *Bathymodiolus* mussels (Page et al., 1991; Riou et al., 2010). Nonetheless, this feeding mechanism does not seem sufficient to sustain these mussels without the help of their symbionts, as suggested by the bad physiological state of mussels from waning vent sites, or transferred from fluid emissions to inactive habitats (Raulfs et al., 2004).

These nutritional strategies come along with physiological rearrangements and behavioral adaptations in the hosts to provide steadily both oxygen and reduced compounds to the symbionts (Childress and Girguis, 2011). For example, repeated observations of *Kiwa* crabs "dancing" by wavering their arms between seawater and reducing vent fluids have been interpreted as a behavior to increase their epibionts productivity (Thurber et al., 2011).

Symbiontic demand in oxygen and reduced compounds is especially critical if symbionts are located in enclosed organs with no access to the surrounding fluids. In many animals, $H_2S$ has been reported as a competitive inhibitor of oxygen for many respiratory pigments. *Riftia* tubeworms possess hemoglobins with an adapted protein structure presenting two different binding sites, one for sulfide and one for oxygen. The two compounds are fixed specifically and independently on the hemoglobin molecule in the red branchial plumes of *Riftia* (Zal et al., 1998). Then, these compounds are transported and released to the trophosome via the dense circulatory system of these animals to feed their symbionts (Childress and Girguis, 2011). A similar adaptation has been suggested to occur in *Chrysomallon* snails as well. These snails possess a giant heart – approximately 4% of their body volume – most likely to increase the oxygen supply to their endosymbionts (Chen et al., 2015b). In *Calyptogena* clams, the foot of the animal is wedged between vent cracks with diffuse emissions, whereas the siphon actively pumps the more oxygenated seawater. Thus, both sulfide and oxygen are provided independently to the symbionts with two transporters: one for sulfide within the foot and one for oxygen – a hemoglobin – through the circulatory system (Zal et al., 2000). Host proteins such as carbonic anhydrase (CA) can also facilitate $CO_2$ transport for its inorganic fixation by the symbionts (Goffredi et al., 1999). CA was found to be one of the most abundant proteins expressed in gills metaproteomes of *Bathymodiolus azoricus* where it could serve to preconcentrate $CO_2$ for carbon fixation by the sulfur-oxidizing symbionts or to transfer the waste products of the methanotrophic partners to the thiotrophic ones (Ponnudurai et al., 2016). This key role of CA for this symbiotic relationship was especially apparent when CA expression in the animal gills was compared to its lower expression in non-symbiotic tissues, like the foot. In *B. azoricus*, metabolic complements could also be brought by the host to replenish some crucial intermediates – like oxaloacetate or succinate – missing

from the thiotrophic symbiont Krebs cycle, unlike its free-living relative (Ponnudurai et al., 2016; Walsh et al., 2009). In return, symbionts have the possibility to compensate host's putative deficiency in some key amino acids and vitamins biosynthesis. This compensation of each partner auxotrophy – i.e. the inability to synthetize a vital compound – by the other one highlights the strong metabolic interdependencies observed in these symbioses.

In addition to their nutrition role, chemosynthetic symbionts are suspected in many cases to have a role of detoxification by transforming, with their metabolism, the toxic reduced compounds into less damaging byproducts (Auguste et al., 2016; Jan et al., 2014). The peltospirid snail, *Chrysomallon squamiferum*, present probably one of the most original ways of recycling these byproducts which are used to form the iron sulfide coating of its scales with iron from the fluids (Okada et al., 2019). These detoxifying process supported by the symbionts can act in addition to the own detoxifying mechanisms of their host or with those of species associated with their host (Bebianno et al., 2018; Zhou et al., 2018), such as the polynoid scale worms *Branchipolynoe seepensis*, living inside some vent mussels species. These polychaetes are probably detoxifying metals for their hosts as suggested by the lower metal concentrations and the lower enzymatic activity of antioxidant proteins in the mussels associated with these polychaetes in comparison to those without polychaetes (Bebianno et al., 2018). In addition to these adaptations related to the symbiotic life style, vent fauna exhibits also other specific adaptations to the particular environmental conditions of vent ecosystems.

## P.1.4 Hydrothermal vents - Adaptation and biogeography of fauna

### P.1.4.1 Adaptation to hydrothermal vents environmental conditions

In addition to the anatomical and physiological changes chemosymbiotic animals from hydrothermal vents have undergone to host their symbionts, they also have developed important adaptations allowing them to cope with the extreme conditions of these environments. Among the most important ones, the extremely high and variable temperatures, as well as the limited oxygen concentrations in the reduced part of the gradient, are probably the main limiting parameters that control the distribution of the vent fauna. Therefore, a strong zonation of the different vent species is frequently observed all along the environmental gradient (Cuvelier et al., 2009; Govenar et al., 2005; Luther et al., 2001; Marsh et al., 2012; Sarrazin and Juniper, 1999; Sen et al., 2013). Along the MAR, this zonation separates alvinocaridid shrimps, generally found at the hottest part of the inhabited gradient, from the bathymodiolin mussels living in the milder part and the predatory anemones – *Maractis rimicarivora* – at the periphery of the vent field in the colder part of the gradient (Copley et al., 1997; Cuvelier et al., 2009; Van Dover et al., 1997).

Thermal tolerance and respiratory adaptations have been studied mostly in species inhabiting the hottest part of the gradient such as *Alvinella pompejana* (Cary et al., 1998; Chevaldonné et al., 1992; Le Bris et al., 2005; Le Bris and Gaill, 2007; Ravaux et al., 2013) or *Rimicaris exoculata* (cf. part 2.1.3). Still today, *A. pompejana* is recognized as the metazoan with the highest thermal tolerance. Earlier studies have reported *in situ* temperature above 100°C in the close surroundings of these worms (Chevaldonné et al., 1992; Le Bris and Gaill, 2007). Additionally, temperature inside the tube they secrete, was in average between 60°C and 70°C according to other works (Cary et al., 1998; Le Bris et al., 2005). However, *in vivo* studies revealed that prolonged (2h) exposure to temperatures

between 50°C and 55°C is lethal or provokes important damages in *A. pompejana* individuals (Ravaux et al., 2013). Nevertheless, incubations at 42°C suggest that their upper thermal limit is above this temperature, confirming that this species ranks in the most thermotolerant metazoans (Ravaux et al., 2013). This tolerance to very high temperatures could be probably higher for shorter exposure times. The variability of the thermal conditions in these ecosystems being extremely high, prolonged exposures to these temperatures are probably never experienced by these worms. For instance, *Paralvinella sulfincola*, another alvinellid species, could survived to temperatures up to 55°C for 15 min exposure (Girguis and Childress, 2006). In many motile species, such as these worms, an avoidance behavior to high temperatures is observed, with thermal preferences usually lower than their maximal thermal tolerance (Bates et al., 2010; Girguis, 2006). *In vivo* incubations in pressure device with a thermal gradient revealed that many motile vent species actively seek cooler temperatures with thermal preference between 40°C and 50°C for *P. sulfincola* – which tolerate temperature up to 55°C – or below 5°C for the spider crab *Sericosura verenae* that tolerate temperatures up to 36°C (Bates et al., 2010; Girguis, 2006).

Hypoxia is also an important stress, especially for the chemosymbiotic vent fauna, which need to deal with their metabolic requirement, but also those of their symbionts, which are extremely demanding in oxygen, representing up to 80% of the total oxygen consumption of the holobionts (Childress and Girguis, 2011; Girguis and Childress, 2006). To increase their oxygen extraction, several species exhibit enlarged respiratory organs such as the branchial plume of the siboglinid tubeworms (Hourdez and Lallier, 2007). Similarly, the scale worms of the polynoid family from other environments are usually devoid of gills, whereas half of the hydrothermal vent polynoids possess well-develop gills (Hourdez and Lallier, 2007). Particular adaptation have also been observed on the oxygen transporters and oxygen storage proteins – the respiratory pigments– of vent species (Hourdez and Lallier, 2007; Hourdez and Weber, 2005). Among them, unusually high oxygen affinity ($P_{50}$) of the hemoglobins and hemocyanins of vent species have been reported as well as an absence of temperature effect on the $P_{50}$ of vent arthropod hemocyanins (Hourdez and Lallier, 2007; Hourdez and Weber, 2005).

## P.1.4.2 Diversity of "non-chemosymbiotic" vent fauna & trophic interactions

As suggested before along this introduction, not all hydrothermal vent species are necessarily chemosymbiotic *a priori*. Among them, the most well-known groups of "non chemosymbiotic" species are the different polynoid (scale-worm) and ampharetid polychaetes, bythograea crabs, dirivultid copepods, several amphipod families, and possibly some limpets such as *Shinkalepas briandi* (**Fig 22.**).

Although many small species from the macrofauna or the meiofauna have receive much less attention than the large megafaunal species. Among them, several species such as the limpet *Lepetodrilus fucensis* with a gammaproteobacterial symbiont or *Cyathermia naticoides* from the provannid family like the *Alviniconcha* correspond both both to gill episymbioses (Bates et al., 2011; Zbinden et al., 2014). In addition, epibiotic communities on both the cuticle and the digestive cavity of the nematode *Oncholaimus dyvae*, suggest the existence of a large potential of new symbioses discovery in meiofaunal species (Bellec et al., 2018; Zeppilli et al., 2019).

Nonetheless, it has to be kept in mind that future studies might reveal novel symbiotic relationships in some of these species, leading to reconsider them as part of the chemosymbiotic vent fauna. All these species constitutes complex food webs that are still poorly understood as today (Govenar, 2012; Portail et al., 2016, 2018).

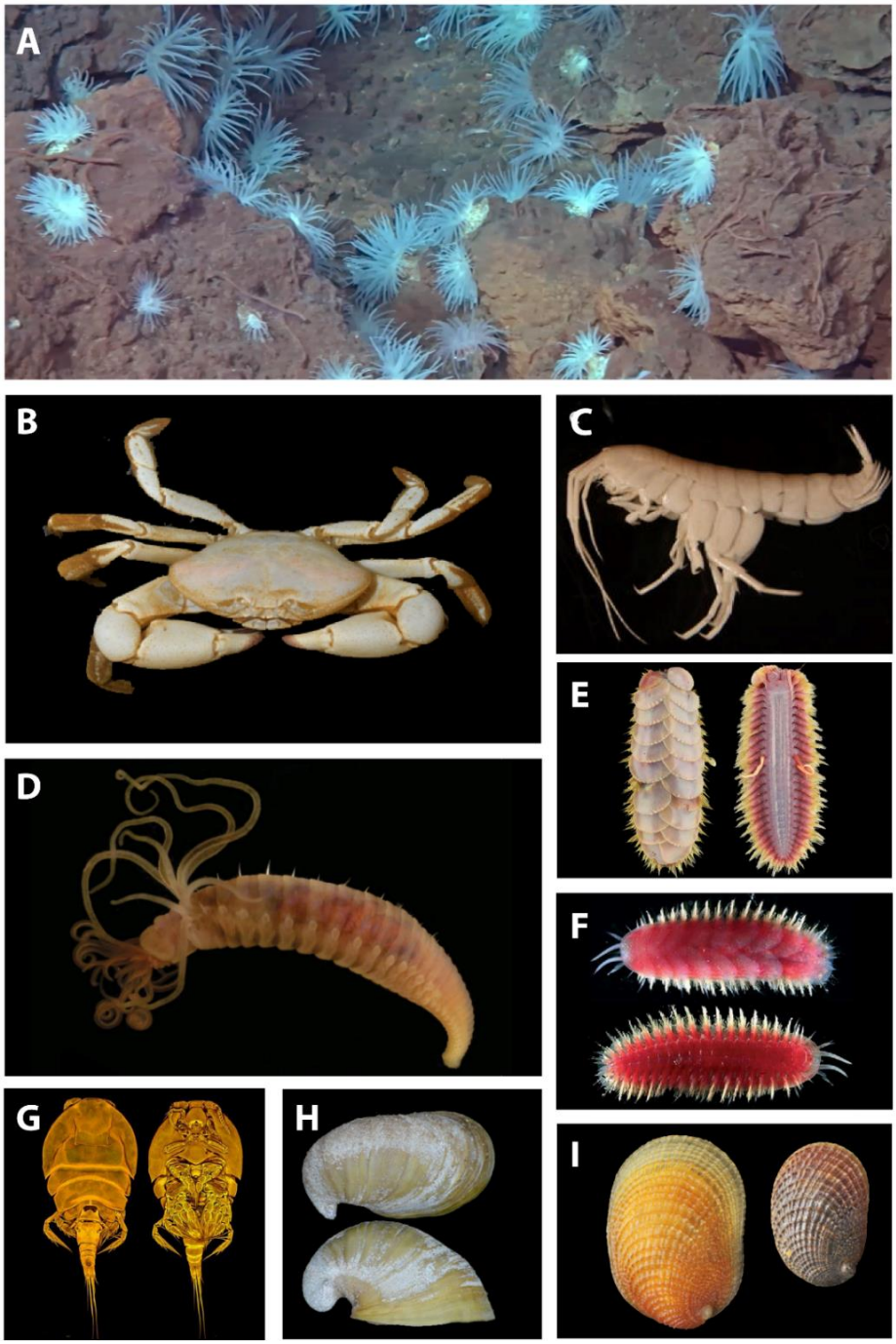


**Fig 22.** Others vent species including some "non chemosymbiotic" – according to our current knowledge on them, from hydrothermal vent ecosystems. **A.** *Maractis rimicarivora* anemone bed from the Mid Atlantic Ridge. Family: Kadosactinidae. BICOSE2018-Nautile © Ifremer. **B.** *Segonzacia mesatlantica* crab specimen from the Mid Atlantic Ridge. Family: Bythograeidae. © Océanopolis. **C.** *Exitomelita sigynae* amphipod specimen from the Loki Castle vent field (Mohn Ridge), potentially symbiotic with some evidences of gill epibionts. © (Tandberg et al., 2012). **D.** *Amphisamytha fauchaldi* polychaete specimen from the Guaymas Basin. Family: Ampharetidae. © (Stiller et al., 2013). **E.** *Levensteiniella manusensis* scale worm specimen from the Manus Basin. Family: Polynoidae. © (Wu and Xu, 2018). **F.** *Branchinotogluma trifurcus* scale worm specimen from the North Fidji Basin. Family: Polynoidae. © F. Pleijel (Chess). **G.** *Aphotopontius sp. nov.* copepod specimen from the Central Indian Ridge. Family: Dirivultidae. **H.** *Shinkailepas briandi* limpet specimen from the Mid Atlantic Ridge. Family: Phenacolepadidae. © (Yahagi et al., 2017a). **I.** *Lepetodrilus* fucensis limpet specimen from the Juan de Fuca Ridge. Family: Lepetodrilidae. © S. Aiken.

In addition to the species feeding on their symbionts, primary consumers are composed mostly of bacterivorous – grazing or filter feeding if they feed on microbial mats or free-living microorganisms from the fluid respectively – and detritivorous species – that can be secondary consumers as well if they feed on detritus of the fauna. Scavengers and predators are also commonly found in vents, although predation pressure is considered as generally low (Bergquist et al., 2007; Portail et al., 2015; Van Dover and Fry, 1994).

Moreover, many studies revealed that trophic flexibility of many heterotrophic species from hydrothermal vents is high which suggests a high degree of generalism (Bell et al., 2016; Levin et al., 2009; Portail et al., 2016, 2018) even if some vent consumers are more highly specialized (Govenar et al., 2015). One study on vent fields of the MAR also highlight the important trophic redundancy between co-occurring species, suggesting they might have the same role in the food-web (Portail et al., 2018). Therefore, the addition of species within a functional group does not necessarily lead to more complexity in the food-web (Portail et al., 2018).

Because of the limited possibility of long-term observations in these environments, trophic interactions are rarely observed and trophic behaviors are mostly studied using stables isotopes. Different stable isotopes are use in general for hydrothermal vents studies and provide different information on their feeding sources, according to the variation in their ratios. For example, differences in carbon isotopic ratios ($\delta^{13}C$) are attributed to carbon sources fixed with the reductive tricarboxylic acid (rTCA) cycle (2 ‰ to -14 ‰) or the Calvin-Benson-Bassham (CBB) cycle (-22 ‰ to -30 ‰) (Hügler and Sievert, 2011). On the other hand, nitrogen isotopic ratios ($\delta^{15}N$) are generally used in hydrothermal vents to infer the trophic position of a species within the food web (De Busserolles et al., 2009; Portail et al., 2018) but can also result also from the use of different inorganic nitrogen sources such as nitrates ($\delta^{15}N$ = 5-7 ‰) or ammonium ($\delta^{15}N$ <0 ‰) (Lee and Childress, 1994; Riekenberg et al., 2016). Additionally, the large difference in sulfur isotopic ratios ($\delta^{34}S$) that exists between seawater sulfate and vent fluid sulfides is used to discriminate organic matter of photosynthetic (approximately 16 ‰ to 21 ‰) and chemosynthetic origin (-9 ‰ to 10 ‰) (Fry et al., 1983; Reid et al., 2013). A recent study in hydrothermal vents of the Izu-Ogazawara Arc also revealed that natural-abundance of the radiocarbon content ($\Delta^{14}C$) clearly differed between nutrient from water-column planktonic origin and nutrient from vent- chimney fluids origin, and possibly from nutrient from bottom water origin as well (Nomaki et al., 2019).

## P.1.4.3 The biogeographical provinces of hydrothermal vent ecosystems

United by their shared dependence on chemosynthetic primary production, hydrothermal vent communities differ in the species they host based on their geographic location. In this way, each species encountered in these environments, present a more or less limited repartition, restricted to a single vent location in the most extreme cases, to a broader distribution in vent fields from an entire region of the globe.

With the discoveries of additional vent fields from different regions of the globe, several tentative have been conducted to classified vent communities in different biogeographic regions (Bachraty et al., 2009; Moalic et al., 2012; Ramirez-Llodra et al., 2007; Rogers et al., 2012; Thaler and Amon, 2019). All these studies identified between five to eleven different provinces with different degree of confidences for each province depending on the data available at their time. Moreover, their number have increase with discoveries of new regions harboring different faunal assemblages than

those encountered so far (Plouviez et al., 2015; Rogers et al., 2012). According to the more recent study (Thaler and Amon, 2019), compiling data from 262 expeditions in these environments, eight biogeographic provinces can be recognized today in hydrothermal vents (**Fig 23.**). These eight provinces correspond to the East Pacific Rise, the Mid Atlantic Ridge, the North East Pacific (Juan de Fuca Ridge), the North Western Pacific Basins (Okinawa Trough, Izu-Ogasawara Arc, Mariana Arc, and Mariana Trough), the South Western Pacific Basins, the Indian Ocean and the more recently discovered East Scotia Ridge and Mid Cayman Rise.

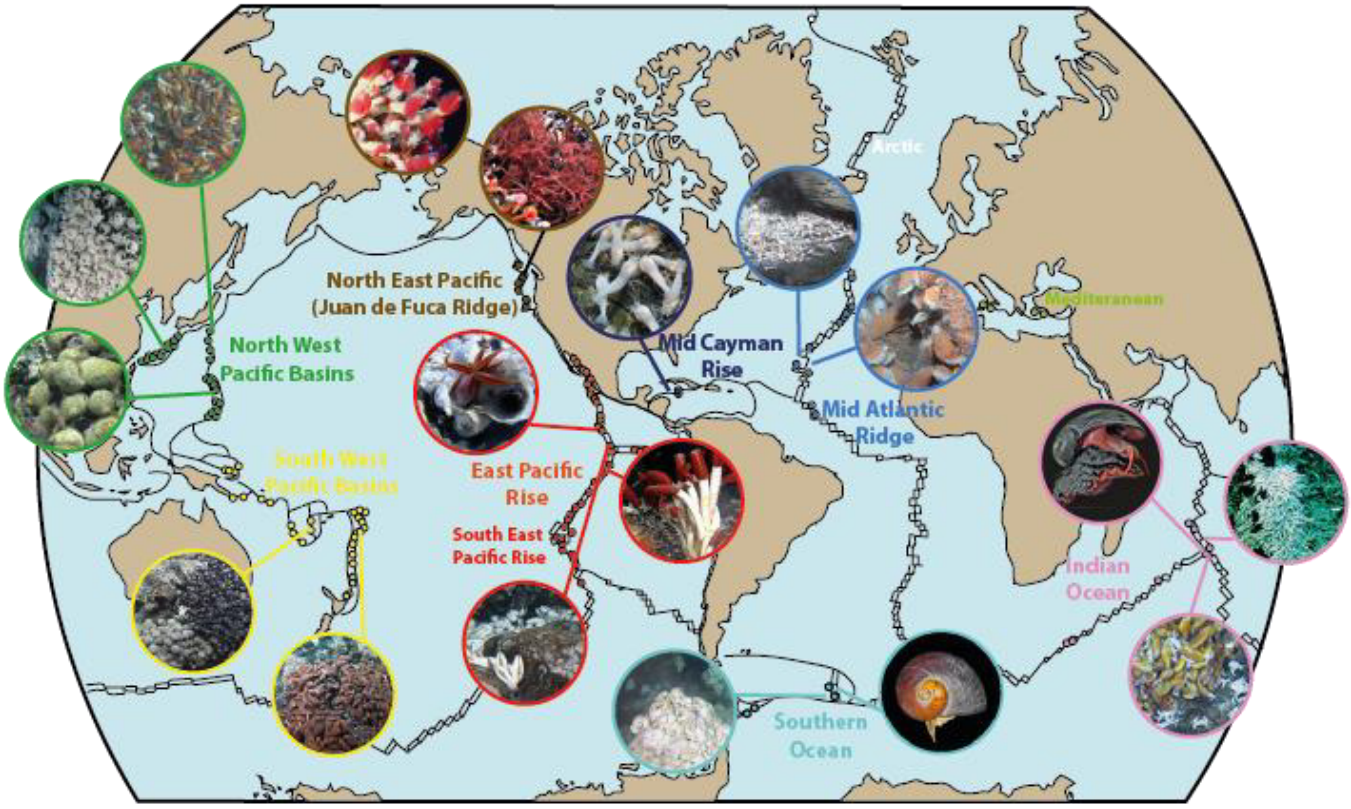


**Fig 23.** The eight biogeographic provinces of hydrothermal vent ecosystems. Adapted from Ramirez-Llodra et al. (2007) and Thaler and Amon (2019).

These biogeographic provinces are characterized by biomass dominant vent megafaunal taxa, which are in almost every cases, chemosymbiotic species. Communities of the East Pacific Rise and the North East Pacific are dominated by large tubeworms colonies (*R. pachyptila* and *R. piscesae*) by large aggregations of shrimps in the Mid Atlantic Ridge, the Mid Cayman Rise and the Indian Ocean (respectively *R. exoculata*, *R. hybisae* and *R. kairei*), by yeti crabs in the Southern Ocean (*K. tyleri*) or by large snail in the North and South West Pacific Basins (*Alviniconcha spp.* and *I. nautilei*) and to a lower extend in the Central Indian Ridge (*A. marsindicus*). Bathymodiolin mussels are also very abundant or dominant in some vent fields in many biogeographic provinces as well, including the Mid Atlantic Ridge (*B. azoricus and B*. puteoserpentis), Central Indian Ridge (*B. marsindica*) and the South West Pacific Basins (*B. septemdierum*, *B. platifrons*, *B. brevior, B. manusensis* and others). Peltospirid snails are also quite abundant in the East Scotia Ridge (*G. chessoia*) and in some vent fields of the Indian Ridges (*C. squamiferum* and *G. aegis*).

Among these different provinces, the Western Pacific Basins host probably the largest diversity of species, especially the Northern ones, followed by the Southern Ocean province (Thaler and Amon, 2019). This could be related to its geological diversity with both arc and back arcs settings. On the other hand, provinces of medium biodiversity – Mid Atlantic Ridge, East Pacific Rise, Juan de Fuca and Indian Ocean – all occurs on mid oceanic ridges. The Mid Cayman Rise, located on a transform fault from an old relic-spreading center, is by far the lowest diverse provinces, which could be related by its remoteness, far away from the other vents systems. Despite their extensive sampling, the regions with the highest expected diversity that remain to be discovered are within the West Pacific Basins. The Southern Ocean is also probably the poorest sampled biogeographic provinces and host as well one of the highest expected diversity. On the contrary, the Mid Cayman Rise, discovered approximately at the same period, is expected to have almost reach its unity, in term of diversity at the family level (Thaler and Amon, 2019).

In addition, three expected new provinces could complete this biogeographic dataset. The East Pacific Rise have been recognized as two different provinces, one for the Northern part and one for the Southern part – including the Pacific Antarctic ridge – by some authors, whereas others classified it as a single province. Today, data are probably insufficient from the southern part to clearly separate the two (Thaler and Amon, 2019). The Mediterranean vent fields could also constitute their own province, although with the exception of some tubeworms they did not appear to have their own characteristic chemoautotrophic macrofaunal communities (Danovaro et al., 2010). This is likely due to their remoteness from the other vents as well as the relatively shallow depth of the vent fields discovered so far. At last, the Arctic offer a promising new province with the discovery of the endemic amphipod *Exitomelita sigynae* as well as some methane seep associated tubeworms (Schander et al., 2010). Unfortunately, most of the work in this region were conducted with commercial resource exploration companies and data from the fauna of these areas are not publicly available (Thaler and Amon, 2019).

These geographic patterns of distribution for a given species are governed by two principal factors acting at different time scales (Ramirez-Llodra et al., 2007). First, the historical events that have shaped its geographical range which act on geological/evolutionary time scales. Then, the dispersal potential of the species determined by the life-history patterns of their lifecycle – reproduction, larval ecology, recruitment abilities, symbiont availability – as well as the current topography and hydrography – ridge topology, water-currents – which act on ecological time scales (Ramirez-Llodra et al., 2007; Tunnicliffe and Fowler, 1996).

## P.1.5 Life-cycle ecology in hydrothermal vent ecosystems

Beyond their singular physicochemical conditions, hydrothermal vent ecosystems are fragmented, separated by tens to thousands of kilometers, but also ephemeral owing to their geological instability. Some catastrophic events such as magmatic eruption have been exceptionally observed, mainly in the most active parts of the ridge system, leading to the collapse of entire faunal populations (Fornari et al., 2012). Such events have also been inferred from the regular observations of extinct vent sites with indications of dead or dying vent communities.

Therefore, it has been supposed that vent species would develop life cycles with particular life-history adaptations to the insular, ephemeral and dynamic nature of vent ecosystems, such as asynchronous reproduction, high dispersal, and high fecundities. However, this prediction was quickly refuted by the large variety of reproduction patterns, developmental modes and dispersal strategies observed in vent species suggesting that a single vent life cycle model cannot be raised for all species (Tyler and Young, 1999).

Among the main steps that vent organisms, like many marine organisms, undergo along a series of changes to give birth to a new generation of the same species: the reproduction, the dispersal phase and the settlement and recruitment back to a vent fields are probably the most critical ones (**Fig 24.**). In addition, the acquisition of symbionts, trough maternal inheritance (vertical mode) or environmental encounter (horizontal mode) is also crucial for chemosymbiotic species, as these relationships are obligatory for their survival (cf. part 1.4.) (**Fig 24.**).

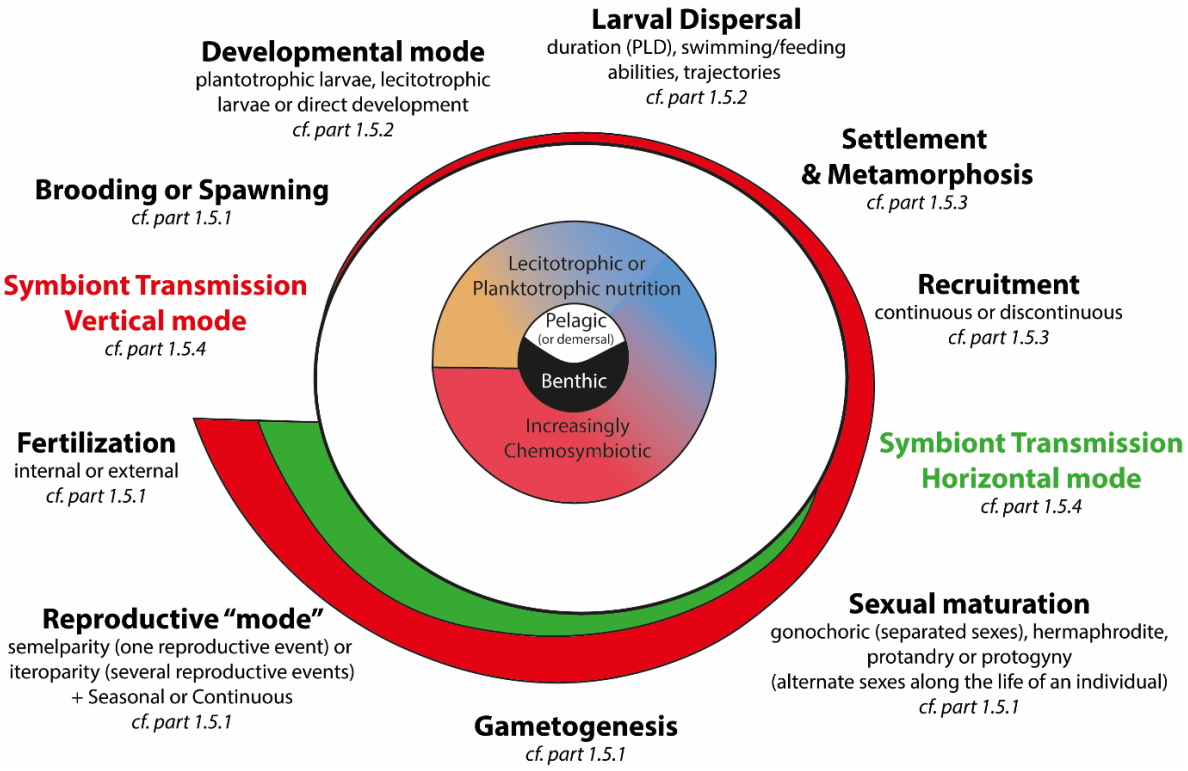


**Fig 24.** Critical steps in the lifecycle of a hydrothermal vent species. Methou (2019)

## P.1.5.1 Reproductive patterns in hydrothermal vent species

### P.1.5.1.1 Gametogenesis and sexual determination

In general, reproductive processes appear to be rather conserved phylogenetically with no specific adaptation to deep-sea hydrothermal vents (Young, 2003). Consequently, gametogenesis generally follows the patterns described in related species from shallow waters (Laming et al., 2018; Ramirez-Llodra et al., 2000). Gamete production can occur freely in the coelomic cavity, as it is the case in many polychaetes (Tyler and Young, 1999). In siboglinids tubeworms, gametogenesis is located within the trunk, starting at its anterior end, closely associated and surrounded by the trophosome tissue (Hilario et al., 2005). In other vent species – including some polychaetes like *B. seepensis* (Jollivet et al., 2000) – this process takes place in specialized tissues: the gonads, also called ovaries for females. In vent mussels, the gonad proliferates from the mantle and is not present all the time during their adult life as for their shallow water counterparts. Nutrient reserves are stored in the mantle during some periods of the year, whereas the mantle is the site for gamete production at other times, at the expense of the reserve storage (Gabbott and Peek, 1991). In crustaceans, the gonads are present during all the adult life and are located dorsally within the abdomen for peracarids – isopods and amphipods – or within the cephalothorax for decapods – caridean shrimps, anomurans and brachyuran crabs. The female gametogenesis – also called oogenesis – comprises three major steps with a proliferative phase of oogonia production followed by a differentiation phase of oogonia (diploidic cells) into previtellogenic oocyte (haploid cells), which then undergo vitellogenesis. This last step corresponds to the yolk formation by synthesis and storage of energetic reserves within the oocytes that significantly grow in size. Once mature, oocytes are not stored in ovaries but transferred to the pleopods before their fertilization.

Many vent species are strictly gonochoric with separated sexes such as most polychaetes, gastropods and nearly all crustaceans (Tyler and Young, 1999). However some exceptions exist such as hermaphroditism in the snail *Chrysomallon squamiferum* whereas every other peltospirid species, even a closely related one like *Gigantopelta chessoia,* have been recognized as gonochoristic (Chen et al., 2017). In bathymodiolin mussels, protandry appears to be the norm in small sized species – *Idas* and *Adipicola* – while both gonochorism and simultaneous hermaphrodism have been identified in the larger *Bathymodiolus* mussels (Gaudron et al., 2012; Laming et al., 2018; Tyler et al., 2009). Therefore, sex determination in vent mussels appears to be related to the body size of the species rather than to the phylogeny of the group, as *Bathymodiolus* and *Idas* genus are paraphyletic (Thubaut et al., 2013). More recently, rare protogynous specimens in the predominantly gonochoric species *Bathymodiolus septemdierum* were reported reflecting the complexity of sex determination in these species (Rossi and Tunnicliffe, 2017). Although no occurrence of hermaphroditic crustaceans has been reported at hydrothermal vents yet, the example of pandalid shrimps from other deep sea ecosystems underlines that complex sex determination could also arise within this group (Chiba, 2007).

### P.1.5.1.2 Fertilization, spawning or brooding and fecundity

In vent mussels and clams, fertilization occurs externally after the spawning of gametes from both males and females within the populations. Even if these spawning events have never been observed in the field, they have been induced experimentally – by injection of serotonin in the mantle tissue – in few vent mussel species such as *Bathymodiolus childressi*, *Idas simpsoni* and *Idas modiolaeformis* (Arellano and Young, 2009; Laming et al., 2018). However, these artificial spawning

failed to accurately estimate their fecundity since induction with serotonin can be unreliable and often induce spawning of immature oocytes (Arellano and Young, 2009). Information is then often limited to egg size or maximum oocyte size, which are generally rather small, like in shallow water mussels, between 50 µm and 80 µm (Arellano and Young, 2009; Berg, 1985; Colaço et al., 2006; Laming et al., 2018; Le Pennec and Beninger, 2000; Tyler et al., 2009). On the contrary, egg size of vesicomyid clams, the other group of bivalve commonly found at vents, is much larger with estimated size between 160 µm and 660 µm (Beninger and Le Pennec, 1997; Berg, 1985; Endow and Ohta, 1990; Fiala-Medioni and Pennec, 1989; Le Pennec and Beninger, 2000). Based on the small size of their eggs, high fecundity has been inferred in vent mussels (Tyler and Young, 1999). However, direct measurement of egg number are limited to few *Idas* species ranging between approximately 400 eggs in *I. simpsoni* and *I. modiolaeformis* to 3000 eggs – based on one individual – in *I. argenteus* (Dean, 1993; Laming et al., 2018).

In tubeworms, spawning of *Riftia pachyptila* has been observed in December at the 9°50 EPR vent field during an hour (Van Dover, 1994). This spawning was intermittent and involved only few individuals out of a colony of hundreds of tubeworms (Van Dover, 1994). However, *R. pachyptila* spawns fertilized eggs and not gametes like mussels do. Indeed fertilization has been confirmed to occur internally in females of *R. pachyptila* as well as in other siboglinid species including *Ridgeia piscesae*, *Tevnia jerichonana*, *Seepiophila jonesi* and *Lamellibrachia luymesi* (Hilario et al., 2005). In all these species, sperm storage was observed at the posterior end of the oviducts and only fertilized eggs were collected in the spawn around colonies of *R. pachyptila* and *L. luymesi*. Yet, most of these eggs were uncleaved suggesting that the first division is only completed after the egg release in those species. The embryonic period is then entirely included during the dispersal phase (Hilario et al., 2005).

In crustaceans, fertilization occurs through copulation. Although this copulatory behavior remains to be observed within vent habitats, observations of non-motile aflagellate spermatozoa in some alvinocaridid specimens are indicative of the transfer of a spermatophore through copulation, as in shallow-water species (Ramirez-Llodra and Segonzac, 2006). Copulation behavior was observed in *Gandalfus yunohana* crabs maintained in aquarium, subsequently after molting (Miyake et al., 2007). Moreover, mate guarding before molting was also seen in these same individuals (Miyake et al., 2007). Females lay their eggs and keep their brood during embryonic development under the abdomen in decapods, attached to the tail in an ovisac for copepods or enclosed in the marsupium pouch in peracarids. Because of this brooding behavior, direct measures of termed fecundity are easier to obtain and are reported for more crustacean species comparatively to other hydrothermal vent groups.

Although gametogenesis appears phylogenetically conserved (cf. part 1.5.1.1), important variations in terms of allocated resources during the vitellogenesis can be observed between species, which affects in consequence their fecundity. For instance, hydrothermal vent amphipods exhibit higher brood and egg sizes than typical deep-sea species (Johnson et al., 2001; Sheader et al., 2000, 2004; Sheader and Van Dover, 2007). This might be related to the higher food availability at vents and could serve as a strategy to increase the number of offsprings to that will colonize new vents (Sheader and Van Dover, 2007). Widely variable strategies are observed in vent species, even in the sole range of crustaceans, with a high fecundity and small egg size in *Bythograea* crabs, whereas *Munidopsis* squat lobsters spawn few very large eggs (Dittel et al., 2008; Van Dover et al., 1985). This trade-off between fecundity and egg size was also reported among alvinocaridid species, the ones with the lowest

fecundity – like *Alvinocaris stactophila*, *Mirocaris fortunata* – presenting also larger eggs than species with higher fecundity like *Alvinocaris muricola* (Copley and Young, 2006; Ramirez-Llodra et al., 2000; Ramirez-Llodra and Segonzac, 2006). Important reproductive investment was also reported for *Kiwa tyleri* with few large yolky eggs relatively to their size (Marsh et al., 2015). In every alvinocaridid shrimps and kiwaid crabs studied to date, a positive relationship between fecundity – estimated by the egg number per brood – and female size – estimated by carapace length (CL), the standard measure for crustacean – was observed with a higher fecundity for the biggest females (Copley and Young, 2006; Marsh et al., 2015; Nye et al., 2013; Ramirez-Llodra et al., 2000; Ramirez-Llodra and Segonzac, 2006).

Information about brooding length is lacking in almost every vent crustaceans but could be as variable as that of shallow water relatives. Incubation experiments with eggs of *Shinkaicaris leurokolos* and *Alvinocaris longirostris* revealed an important influence of temperature on brooding duration ranging from a maximum of 250 days at 5°C to less than a month above 15°C (Watanabe et al., 2016). In *Kiwa tyleri*, evidence of necrosis and important deposition of hydrothermal particles on carapace of brooding females supported a considerably extended brooding period (Marsh et al., 2015), putatively above 18 months according to values reported in other crab species (Reid et al., 2007).

#### P.1.5.1.3 Seasonality and spatial patterns of reproduction

Timing of the reproductive activity in shallow-water ecosystems is generally constrained by the seasonal variability of the photosynthetic primary production in response to temperature or daylight length variations. In the absence of these environmental cues, deep-sea species were once considered isolated from the driving processes influencing reproductive seasonality. Accordingly, observations of asynchronous oocyte development between individuals of the same population and/or between individuals from different sampling periods have suggested continuous or semi-continuous reproduction in many vent species such as in the polychaetes *Alvinella pompejana* (Faure et al., 2007), *Paralvinella palmiformis* (Copley et al., 2003), *Riftia pachyptila* (Hilario et al., 2005) and many gastropods (Matabos and Thiebaut, 2010; Tyler et al., 2008).

However, a seasonal pattern was observed in the gametogenesis of some species. In *Bathymodiolus azoricus* from the Lucky Strike vent field, gametes develop in the mantle inform July until a spawning event in next January (Dixon et al., 2006). This pattern correlates well with the surface photosynthetic production, *B. azoricus* spawning period preceding the peak of primary production in the euphotic zone (Dixon et al., 2006). Similarly, reproductive seasonality was found in *Bathymodiolus childressi* from cold seeps in the Gulf of Mexico with the initiation of gametogenesis from December to March, and a spawning period from October to February (Tyler et al., 2007). In crustaceans as well, evidences of reproductive seasonality were observed. *Bythograea thermydron* crabs from the 9°50 EPR vent sites exhibited a peak in egg hatching in April/May, and ovarian development also appeared to be synchronized, suggesting seasonal spawninglinked to variations in the supply of photosynthetic material from the euphotic zone (Perovich et al., 2003). In contrast, a lack of synchrony was found for the gametogenesis of the bythograean crabs *B. laubieri* and *B. vrijenhoeki*, two species co-occurring in Pacific Antarctic Ridge (PAR) vent sites (Hilário et al., 2009). This lack of synchrony might result from the lack of environmental cues owing to their geographical locations under oligotrophic surface waters, unlike *B. thermydron*. Variable strategies were reported also in alvinocaridid shrimps from cold seeps with a continuous egg production for *Alvinocaris muricola* and a seasonal brooding period between late November and March for *Alvinocaris stactophila* (Copley and Young, 2006; Ramirez-Llodra and Segonzac, 2006). Intriguingly, presence of ovigerous females in winter samples but not in summer ones

would suggest a seasonal brooding period for *Rimicaris hybisae* as well, despite the absence of synchrony in their gamete production (Nye et al., 2013). Therefore, absence of seasonal sampling in *A. muricola* should preclude any inference on the seasonality of the brooding period of this species.

Spatial reproductive patterns with a migration of brooding females towards the vent periphery were also reported in many crustacean species, especially anomuran crabs such as *Kiwa Tyleri* (**Fig 25.**) or bythograeid crabs such as *Bythograea thermydron* (Marsh et al., 2015; Perovich et al., 2003) but also in *Ventiella sulfuris* amphipods (Sheader and Van Dover, 2007). Similar brooding migration were proposed to occur in *Bythograea laubieri* and *B. vrijenhoeki* when no ovigerous females could be collected despite evidences of continuous reproduction (Hilário et al., 2009). Current hypothesis suggests that females actively seek to avoid hypoxic and damaging conditions of active vent emissions to protect their embryos especially for species with extended brooding periods. This was supported by observations of *Alvinocaris stactophila* brooding females gathering towards the inner part of cold seeps mussel beds, which is less hypoxic and sulfidic than the outer part (Copley and Young, 2006). However, the opposite zonation was found in *Rimicaris hybisae* where brooding females were absent from the periphery and abundant within the dense aggregates directly in contact with the active vent fluid emissions (Nye et al., 2013).

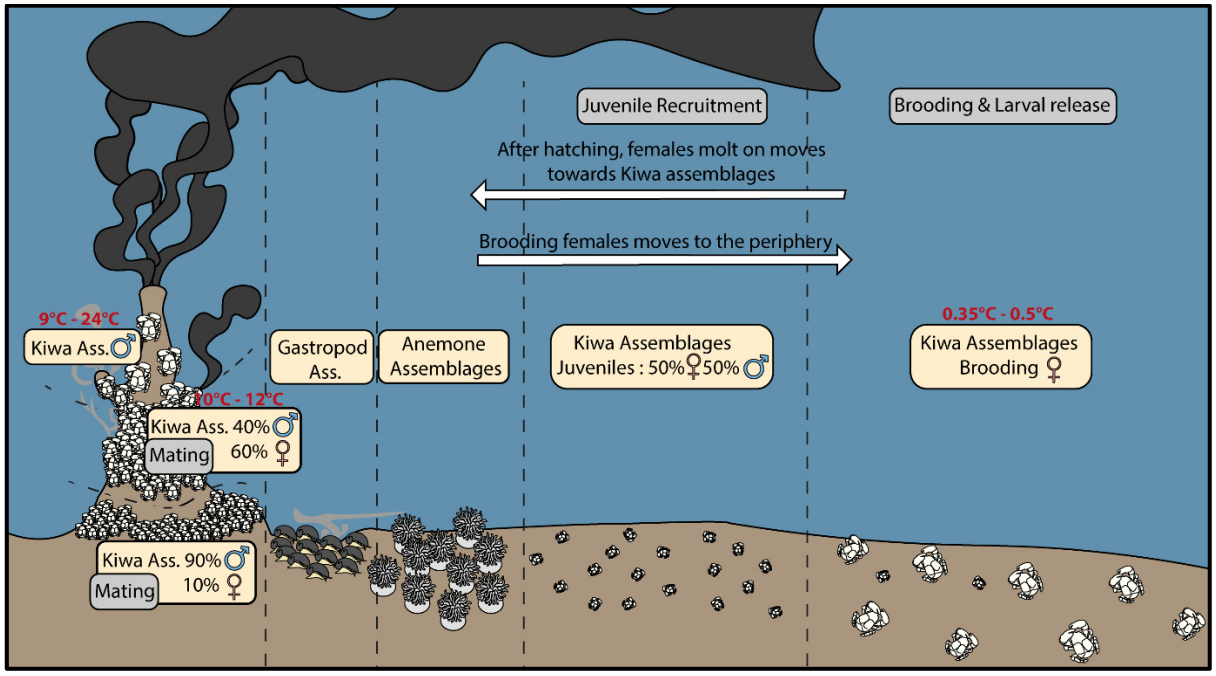


**Fig 25**. Spatial distribution of *Kiwa tyleri* crabs population. Adapted from Marsh et al. (2015)

## P.1.5.2 Larval phase and dispersal in hydrothermal vent species

### P.1.5.2.1 Larval biology: anatomy, nutrition and behavior

Subsequently after spawning – or hatching in brooding species – eggs (in spawning species) or larvae (in brooding species) are released in the water column, with the exception of larval brooding species like peracarids (amphipods, cumaceans, isopods, tanaidaceans and mysidaceans). The theory of Haeckel (Haeckel, 1866) suggesting that "Ontogeny recapitulates evolution" has been dismissed long ago. Nonetheless, embryonic morphologies – and by extension larval ones – are strongly shaped by their phylogenetic position rather than selective pressures during the earlier periods of

development. However, this is only because they resemble other taxa at that stage – and not because they correspond to ancestral adults as stated by Haeckel (Kalinka and Tomancak, 2012). Similar morphologies can thus be observed within species of the same phyla with a trochophore larva developing into metatrochophore in annelids, or a typical trochophore morphology rapidly followed by a veliger larva – with a forming shell – in molluscs (**Fig 26.**), (Mills et al., 2009). At a higher taxonomical level, this veliger larva usually develops into a protodissoconch larva in bivalves and a protoconch larva in gastropods (**Fig 26.**), (Mills et al., 2009).

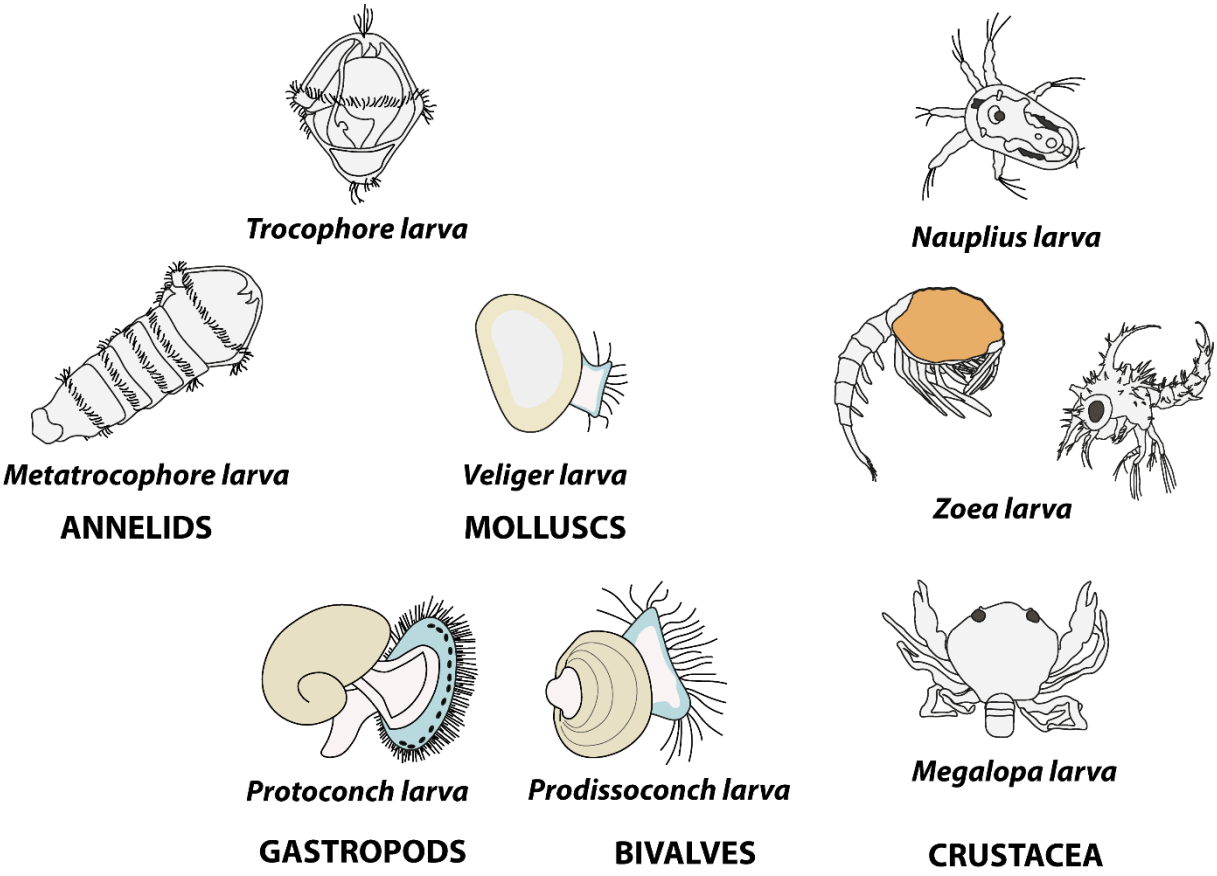


**Fig 26**. Example of larval forms observed in hydrothermal vents species. (Methou, 2019). Inspired by specimens reported by Miyake et al. (2010), Nakajima et al. (2010), Thatje et al. (2015), Laming et al. (2018) and Mills et al. (2009).

In crustacean a wide diversity of larval forms have been found between the different groups (**Fig 26.**). In general, nauplius larvae are considered as the most universal and ancestral form in crustacean (Anger, 2006). It is characterized by an ovoid shape, three cephalic natatory appendages and a single eye. This larva corresponds to the hatching form in many taxa such as cirripeds (barnacles), copepods or in the phylogenetically basal decapods (dendrobranchiate shrimps) (Anger, 2006). Other decapods like caridean shrimps also pass through this nauplius phase but encapsulated in the egg membrane during the brooding and hatch as zoeal larvae. General morphology of the zoeal larva is closer to adult morphologies, with paired compound eyes and thoracic appendages for swimming instead of cephalic ones that are involved in perception and processing of food at that stage. Pleopods – abdominal appendages – are in general not developed until the next larval stage (Anger, 2001). Later larval stages are often referred as post larvae in crustaceans but this term is considered misleading in the view of some authors (Anger, 2001). Indeed, “post larva” implies a non-larval nature but is

currently used in the literature for both early juveniles and late larval stages. To prevent more confusion, megalopa (in crabs) or decapodid (other crustaceans) already used in other studies should be preferred for designation of late crustacean larval stages (Anger, 2001).

Since many adult stages of hydrothermal vent species exhibit no (like vent tubeworms) or very low (like clams, mussels or gastropods) motility capacities, larval stages are recognized as the major dispersal form in the lifecycle of most vent organisms. This may be questionable in species like shrimps with high swimming capacities at juvenile and adult stages that could enable them to travel between close-by vent fields. However, no evidence of dispersal at these stages has been found so far. Larval transport and survival between vent sites are therefore key factors influencing the dispersal potential of a species in these particular marine ecosystems (Pineda et al., 2007). Potentially, larval transport could also be facilitate for some species by the mean of migrant species, not endemic to hydrothermal vents, with a wider distribution to all the deep sea floor for instance, but that would make regular incursions in these ecosystems. This transport, attached to the body of another species, is called zoochory and have been hypothethized for the alvinellid *P. palmiformis* that have been observed on the legs of the non-vent endemic crabs *Macroregonia macrochira* at the Juan de Fuca Ridge (Tunnicliffe and Jensen, 1987).

Although they should be corroborated by other approaches, morphological observations of both external and internal anatomy can provide essential information on larval life such as their potential feeding or natatory capacity at a given stage. Rearing experiment of *Riftia pachyptila* embryos revealed for example that ciliated bands of trocophore larva, enabling low but active swimming, only appears after 34 days of development, at which point mouth is still not developed for feeding (Marsh et al., 2001). Therefore, *Riftia* larvae are, for a long period, unable to feed or to swim in the water column, their moves being dictated only by their buoyancy and the hydrodynamics of water currents. In the same way, inferences about larval duration and dispersal potential can also be derived from morphological observations. For instance, hatching larvae of *Kiwa tyleri* exhibit developed pleopods, suggesting an abbreviated planktonic larval phase and low dispersal with a hatched larva morphology close to a recruited stage (Thatje et al., 2015b).

However, real estimations of the planktonic larval duration (PLD), defined as the period between eggs/larvae spawning/hatching in the water column and the arrival of larvae at the settlement location, are scarce despite being of prime importance to understand larval transport potential. This is partially explained by the difficulty to rear deep-sea larvae that often require pressure equipments to develop normally in experimental conditions (Marsh et al., 2001; Pradillon et al., 2001). Still, some species from relatively shallow hydrothermal vents – between 100m and 450m depth – have successfully developed into latter larval stages at atmospheric pressures such as *Lamellibrachia satsuma* tubeworms (Miyake et al., 2006) or *Gandalfus yunohana* crabs (Hamasaki et al., 2010). In other cases, most species maintained at atmospheric pressure did not show any sign of development and some specimens hatched in the same conditions even exhibited abnormal morphologies (Brooke and Young, 2009; Miyake et al., 2007; Watanabe et al., 2016). To skirt these issues, other methods have been employed to provide indirect estimates of the full PLD period. In species with a seasonal reproduction for example, PLD have been estimated indirectly by comparing spawning/hatching and settlement time. In *Bathymodiolus childressi*, a PLD of 9 to 16 months has been infered using this method (Arellano and Young, 2009). When larval metabolic consumption rates and available energy storages can be measured, PLD can also be computed but only for non-feeding larva relying only on

their own energy storage. In *Riftia pachyptila*, larval duration (if no feeding ability develops in later larval stages) has been estimated to be 38 days with this method (Marsh et al., 2001).

Commonly, larval nutrition is classified as planktotrophic or lecithotrophic, the former actively feeding in the water column whereas the latter is mostly relying on maternally derived yolk reserves. In general planktotrophic larvae are associated to a higher fecundity and lower maternal investment – in energetic storages – compared to lecithotrophic larvae (Strathmann, 1985). Both larval modes are represented in hydrothermal vents with planktotrophic larvae for bathymodiolin mussels and bythograeid crabs (Hamasaki et al., 2010; Laming et al., 2018; Van Dover et al., 1985) and with lecithotrophic larvae for vestimentiferan tubeworms and vesicomyid clams (Le Pennec and Beninger, 2000). In most examples, these developmental modes have been inferred from egg size data (Thorson, 1950), although the validity of such inferences is subject to debate. In *Kiwa tyleri*, elemental analysis of egg content has provided more direct evidence of lecithotrophic feeding with an exceptionally high C:N ratio – current record in anomuran crabs – reflecting a high lipid content in their first larval stage (Thatje et al., 2015b). However, more complex larval modes are possible with primary lecithotrophy in earlier stage before planktotrophic feeding (Hernández-Ávila et al., 2015). Additionally, facultative lecithotrophy could also exist in hydrothermal vent species, as observed in some freshwater crabs with zoeal larvae capable to develop into megalopa in the presence or not of a feeding source (Anger et al., 2005). However, unfed megalopa that are sustained only by their maternal reserves during the larval phase are significantly smaller and could be inferior competitors for food and space than the fed ones (Anger et al., 2005).

Due to their feeding ability, planktotrophic larvae are believed to have higher PLDs than lecithotrophic larvae, and thus higher dispersal capacity, but also higher mortality. However, these traditional views of relationships between developmental mode and dispersal potential may not always hold true in hydrothermal vents and more generally in the deep sea (Tyler and Young, 1999). Increased temperature have been recognized to have an universal impact on larval stages, increasing their development rate, and lowering their duration, presumably in relation to an increased metabolism (O'Connor et al., 2007). Hydrothermal vent organisms are no exception as seen for *Shinkaia leurokolos* or *Alvinocaris longirostris* shrimps (Watanabe et al., 2016), or the crab *Gandalfus yunohana* (Hamasaki et al., 2010). Thus, larval dispersion in cold waters of the deep ocean could significantly extend PLDs even for lecitotrophic larvae, which could also be a more advantageous strategy in poor-nutrient waters. Moreover, arrest in development in cold waters were seen in *Alvinella pompejana* embryos which could constitute a mechanism to delay their development until warmer waters are encountered and significantly affect PLD and dispersal potential of this species (Pradillon et al., 2001).

Despite being poor swimmers in front of many oceanic currents – horizontal position –, many larvae can still alter their vertical position actively through vertical swimming behavior or passively with differential buoyancy between stages (Adams et al., 2012). This active mediation of transport by the larvae themselves has a broad impact on their dispersal potential since it affects the water mass into which they will be carried (cf. part 1.5.2.2). Nonetheless, very limited information is available on swimming behavior of vent species. Fast swimming was reported for megalopa larvae of *Bythograea thermydron* with an average swimming speed of 4 $cm.s^{-1}$, which is similar to tidal currents speed and twice as great as the speed of near bottom tidal currents (Epifanio et al., 1999; Kim and Mullineaux, 1998). With increased metabolic rate at higher temperature, this swimming speed could increase up

to 10 cm.s$^{-1}$ at 25°C (Epifanio et al., 1999). Interesting swimming behavior was also observed in early larva of *Shinkailepas myojinensis* with a constant migration upwards – and a gravitationally sinking when obstacles are encountered – at a speed of 16 mm.min$^{-1}$ at 5°C (and 44.2 mm.min$^{-1}$ at 25°C) suggesting they could reach the photic zone in 4 to 10 days (Yahagi et al., 2017c). In vent polychaetes, both downwards and upwards swimming behavior were observed with in general a faster swimming speed downwards (0.6 and 0.8 mm.s$^{-1}$ in average for each species respectively) compared to upwards swimming (between 0.2 and 0.6 mm.s$^{-1}$ in average for each species respectively) (Beaulieu et al., 2014).

### P.1.5.2.2 Where are the larva?

Based on currently available data, different models of dispersal trajectories have been hypothesized for hydrothermal vent larvae. Larval transport could occur near the seafloor following bottom currents, or several hundreds of meters above seafloor in the water column in ridge-controlled currents, or far above the vent fields, up to the photic zone, in stronger oceanic currents (**Fig 27**).

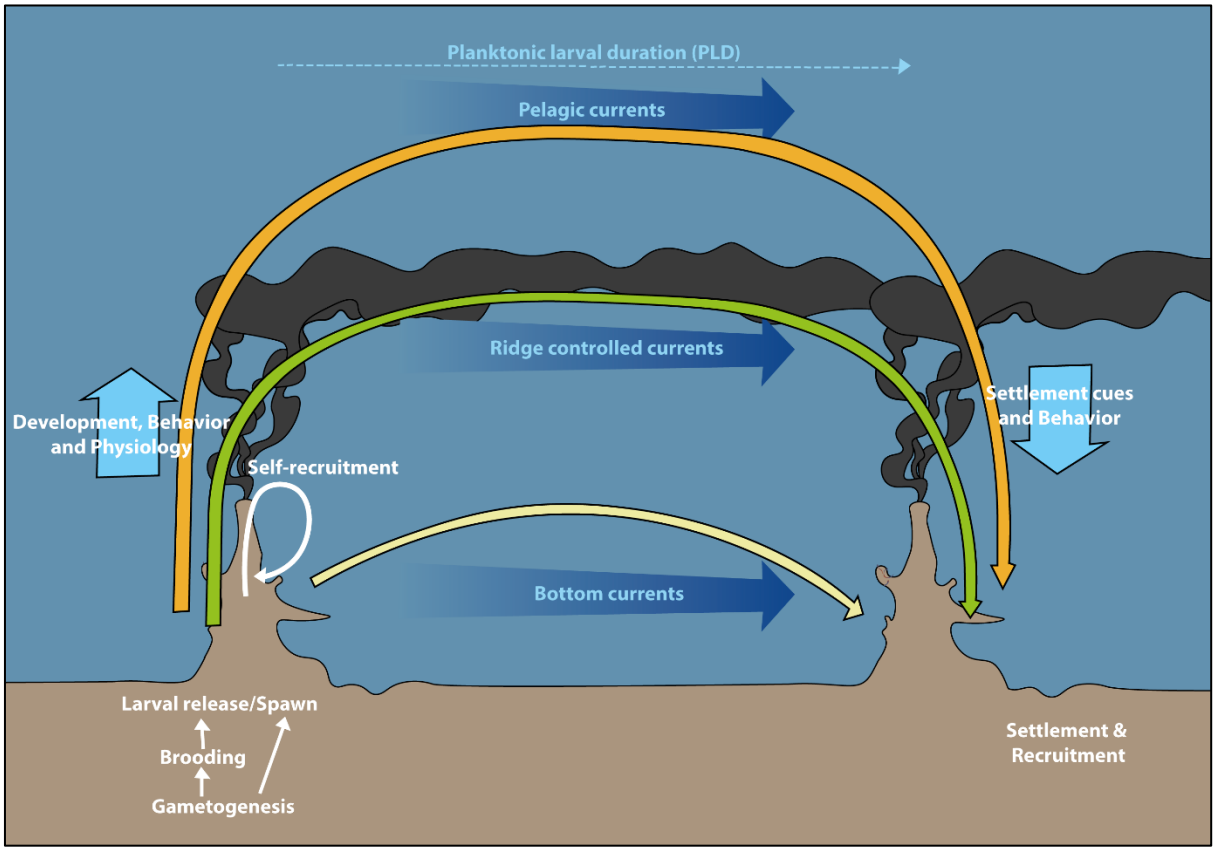


**Fig 27**. Model of larva trajectories. Adapted from Adams et al. (2012).

Unfortunately, finding larvae directly in the pelagic environment to confirm these hypotheses has turned out to be an extremely challenging task, even with great sampling efforts. Recent development of new sampling tools such as high volume plankton pumps, sediment traps, or high throughput sampling system mounted on AUV (Autonomous underwater vehicles) are encouraging for the future but still come with their own limitations (Beaulieu et al., 2009; Billings et al., 2017; Hernández-Ávila et al., 2015) (**Fig 28**). Larvae with escape behavior can avoid sediment traps which catch more easily larvae with downward or "sinking" trajectories – in general those that come back to settle in the vent field – whereas larval pumps are in general still limited by the volume screened. Thus,

sediment traps and larval pump do not catch the same species and so have some level of selectivity (Beaulieu et al., 2009; Kersten et al., 2017). Coupling complementary sampling strategies is therefore suited to have a more accurate representation of the larval pool.

This challenge is further increased when it comes to species identification of each individual from a mixed larval pool, especially for larva from closely related species that can have extremely similar morphologies. Molecular techniques such as barcoding are very useful tools but require a robust sequence database based on adult sequences (Vrijenhoek, 2009). Other nondestructive techniques such as the use of FISH probes are a good compromise for accurate identification while preserving morphology of the specimen (Pradillon et al., 2007). However, this technique is only suited for targeting specific larvae.

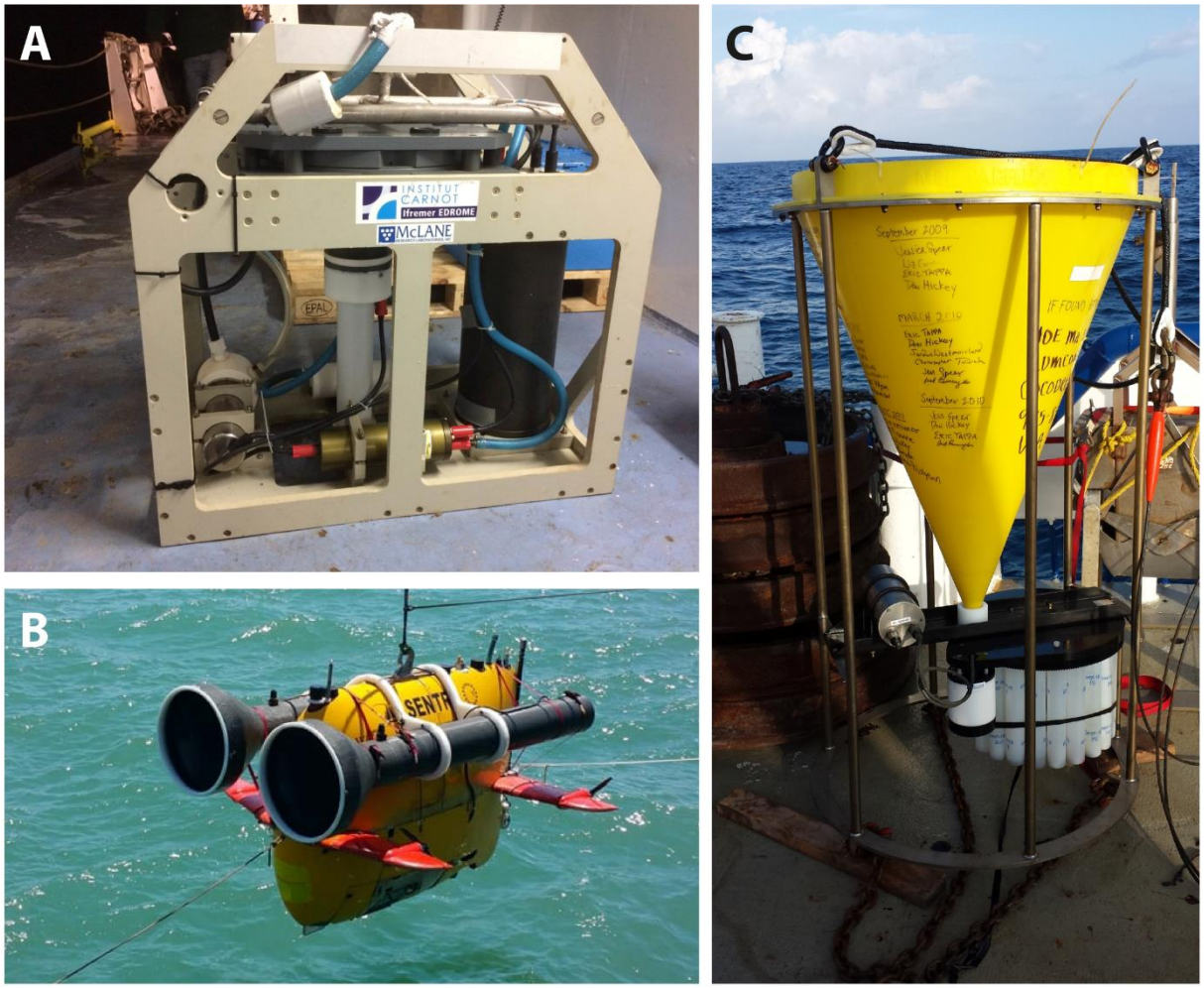


**Fig 28**. Examples of sampling devices for deep-sea larval collection. **A.** SALSA (Serial Autonomous Larval Sampler) larval pump developed by the Ifremer to collected larvae. Conception: F. Pradillon and L. Bignon © Ifremer **B.** SyPRID (*Sentry* Precision Robotic Impeller Driven) larval sampler mounted on the AUV Sentry of the WHOI. © WHOI **C.** Sediment trap deployed on a mooring in the water column above vent fields. © Monterrey Bay Aquarium Research Insitute (MBARI).

For now, few larval specimens have been collected *in situ*. Sampling above the EPR vent fields, revealed a clear decrease in the abundance of several gastropod larvae with increasing distances from the source both vertically (1, 20 and 175 meters above) and horizontally (on and off vent) (Mullineaux et al., 2005). This suggests that a large proportion of the newly hatched larvae could be retained at

their natal vent site, with low dispersion towards neighboring vent fields. Although vent plume were suggested to be "larval highway" for many species, overall larval abundance were much higher in near bottom currents than in the upper layer sof the water column (Metaxas, 2004; Mullineaux et al., 2005). By today, vertical migrations in the photic zone have been seen in only two species from cold seeps – *Bathymodiolus childressi* mussels and *Thalassonerita naticoidea* gastropods – (Arellano et al., 2014), and remain to be confirmed for other vent species. Moreover, marked changes in larval supply and colonist species before and after a volcanic eruption that erased local populations and therefore local sources of larvae on the EPR, suggest long range dispersal for some larvae originating from distant sites (Mullineaux et al., 2010).

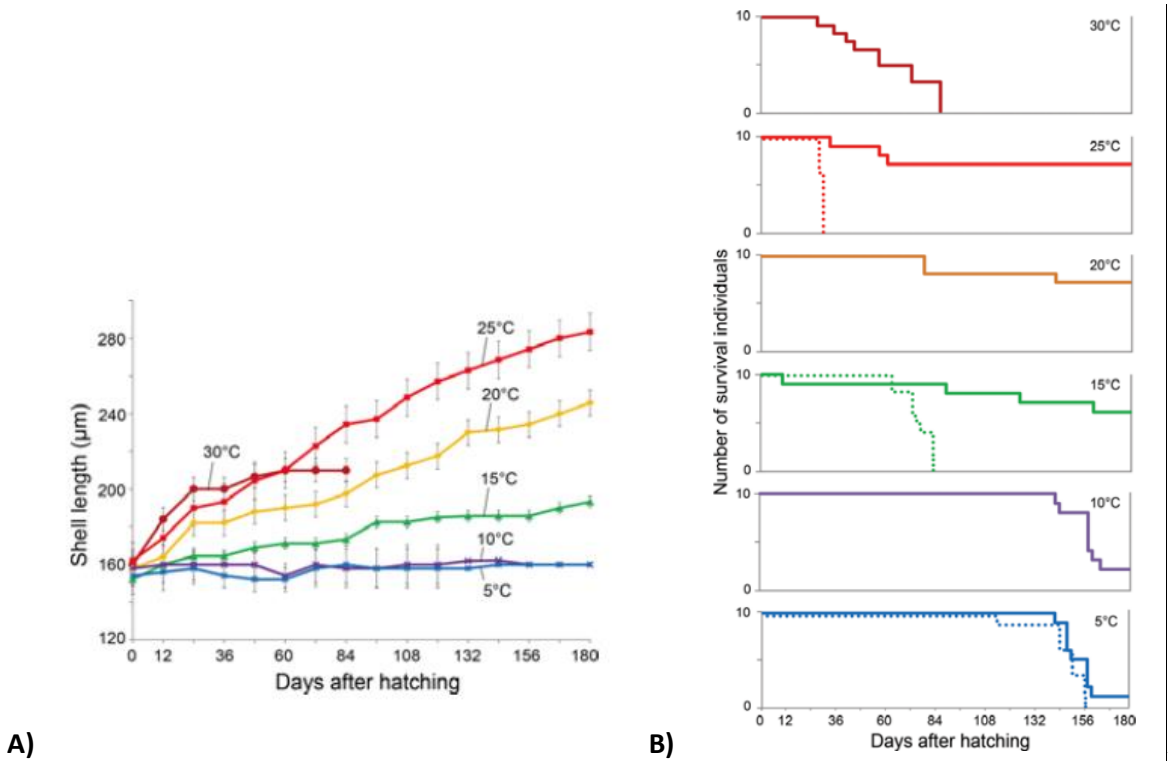


**Fig 29**. Physiological tolerance of vent larvae exemplified by the Yahagi et al. (2017) study **A.** Comparative growth of fed larvae of *Shinkailepas myojinensis* at six temperature conditions. Each data point represents mean for surviving larvae **B.** Comparative survival analysis of larvae of *Shinkailepas myojinensis*. Solid lines: survival of fed larvae at six temperature conditions; dotted lines: survival of starved larvae.

Physiological tolerance of the larvae – especially thermal tolerance – can also be particularly informative on their vertical migration potential. As for many organisms, Yahagi and his colleagues (Yahagi et al., 2017c) reported a shorter survival after hatching with increased temperature for starved larva of *Shinkailepas myojinensis* limpets. However, fed larvae survived and grew best at 25°C and 20°C, which corresponds approximately to the sea surface temperature of their geographic area (**Fig 29**). More surprisingly, larvae of *S. myojinensis* could not ultimately tolerate temperatures of the adult surrounding environment – lower than 15°C – excluding their retention in the vent field and supporting further a vertical migration in the upper layer in accordance with their swimming behavior (Yahagi et al., 2017c). On the contrary, many larvae of other vent species like *Riftia pachyptila*, *Alvinella pompejana* or vent barnacles could not tolerate temperature above 20°C making their presence in the near surface water layers unlikely (Brooke and Young, 2009; Pradillon et al., 2001; Watanabe et al., 2006). In the same way, high temperatures surrounding *Riftia* adult tubes would also inhibit early

embryonic development of their larva suggesting that they must not be retained in the vent environment but disperse in the cold deep sea waters (Brooke and Young, 2009). Other techniques, less experimentally constraining, such as the use of oxygen isotopes and trace elements (Mn, Ba) composition in calcareous tissues of newly recruited individual can provide another clue for such vertical migration (T. Yahagi, 15th DSBS, talk presentation).

#### P.1.5.2.3 Studying connectivity: inferences from biophysical models & populations gene flow

Faced with logistical difficulties to measure larval dispersal directly, it is often inferred with two techniques: biophysical models, which inform on the dispersal potential of a species, and genetic connectivity between different vent populations, which integrate both their dispersal ability and their ability to recruit successfully in the vent field (Cowen and Sponaugle, 2009). Therefore, absence of connectivity could result either from a limited dispersal, from a saturation of the reached vent – resulting from intra or interspecific competition for space between individuals – or from unsuitable conditions for larval settlement like in areas of declining activity where some adults still survive but where conditions are not attractive anymore to larvae.

Biophysical models are based on lagrangian particles tracking methods simulating larval release and trajectories within the hydrodynamic flow field simulated from oceanic circulation models that incorporate surface forcing to predict flow fields through the entire water column. In most published studies, passive particles are used to represent theoretical larvae (Hilario et al., 2015). To better constrain the model parameters, many data derived from biological traits, such as number of particles released – i.e. the fecundity –, the particles release depth (spawning location), their vertical position (swimming behavior and physiological tolerance) and the particles tracking time (planktonic larval duration : PLD) are generally required, highlighting the importance of background knowledge on reproductive and larval biology (Hilario et al., 2015; Metaxas and Saunders, 2009). In general, longer PLD are associated with larger dispersal distance potential both in hydrothermal vents and other marine ecosystems – but some exceptions exist (Mitarai et al., 2016; Young et al., 2012). Considering larval position, many models have shown that larval transport through near bottom circulation is relatively slow and strongly influenced by topographic features of the ridge (Adams et al., 2012; McGillicuddy Jr. et al., 2010; Thomson et al., 2003, 2009). On the other hand, larvae able to reach higher position in the water column are transported by faster currents increasing the potential dispersal distance traveled by the larva for a given PLD (Mitarai et al., 2016; Young et al., 2012). Considerations on larval physiology and seawater temperature at each depth remain needed as counteracting effects can be observed with a shorter PLD due to higher temperature at lower depth (Mitarai et al., 2016).

Studying molecular gene flow between vent site populations can help to highlight potential dispersal barriers for a particular species. For example, the genetic divergence between *Lepetodrilus* sp. populations of the Juan de Fuca ridge and of the Gorda Ridge suggests that fractures in the axial valley such as the Blanco transform fault could inhibit exchange of larvae between the two locations (Johnson et al., 2006a). In general, large distances hamper exchanges of migrants such as between *Chrysomallon squamiferum* populations of the SWIR that diverge genetically from the two others populations of the CIR (Chen et al., 2015a). Comparison between species from the same geographical areas enable to confirm and support the existence of different dispersal strategies such as for *Ifremeria nautilei* gastropods which were genetically subdivided between North Fiji/Lau and Manus basins populations, whereas populations of the shrimp *Rimicaris variabilis* in the same area did not exhibit

genetic structure with the same genetic markers (Thaler et al., 2011, 2014). Similarly, in the East Pacific, *Alvinella pompejana* populations were genetically separated between the North and South segments of the EPR when *Branchipolynoe symmytilda* populations from the Galapagos vents diverged from the ones found all along the EPR (Hurtado et al., 2004). On the other hand populations of *Riftia pachyptila* and *Bathymodiolus thermophilus* from the EPR and the Galapagos were relatively homogenous until vent sites above the Eastern Microplate (Hurtado et al., 2004; Won et al., 2003). In many cases, no genetic structuration could be observed on the entire geographic distribution of these species (Beedessee et al., 2013; Roterman et al., 2016; Teixeira et al., 2013; Yahagi et al., 2015, 2017c).

Nonetheless, both methods have their limitations (Breusing et al., 2016; Cowen and Sponaugle, 2009). Chosen genetic markers in molecular studies might not sufficiently resolve contemporary dispersal between vent field populations and therefore fail to detect direct connectivity, especially if intermediate vent site habitats have not been integrated. Conversely, these genetic markers could also fail to detect current absence of connectivity because populations once connected still maintain a relatively homogeneous genetic structure while they do not exchange larvae anymore. On the other hand, biophysical model simulations can easily lead to inaccurate assumption due to under parametrization, especially in the "bio" components of the model, which are poorly constrained usually (Hilario et al., 2015; Metaxas and Saunders, 2009). Combination of both types of approaches is then recommended to provide accurate hypothesis on larval dispersal. Incongruences between connectivity inferred from the genetic structure of bathymodiolin mussel populations from the MAR, and dispersal trajectories that failed to connect some populations as predicted from a biophysical model in the northern section of the ridge were reconciled by suggesting the existence of "phantom" stepping-stones vent fields (Breusing et al., 2016). However, improvement of hydrodynamic models, using higher spatial resolution of the flow fields in the deep-sea including sub-mesoscale turbulences as well as tidal effects, significantly enhanced predicted dispersal distances of mussel larvae in the northern part of the MAR (Vic et al., 2018). Without denying the existence of undiscovered vent fields acting as stepping stone, model refinements both the their physical/hydrodynamics and biological components, as well as the use of new genetic markers at genome scale may ultimately led to converge towards realistic estimates of larval dispersal in the deep-sea.

### P.1.5.3 Settlement cues and recruitment into hydrothermal populations

If larvae survive sufficiently long enough during the dispersal phase, they will ultimately become competent for settlement and will need to encounter suitable places to colonize, whether it corresponds to their natal or a new vent site. While some species may simply settle after they reach a certain stage, larvae of other species are supposedly guided by environmental cues back to hydrothermal vent fields (Adams et al., 2012).

Many studies from other ecosystems have suggested an influence of substrate type through characteristics like surface energy and vibrations perceived by mechanoreceptor cells in several marine species (reviewed in Rittschof et al., 1998). Influence of substrate remains however elusive in hydrothermal vents. Pilot experiments of substrate colonization on the MAR revealed little effect of the substrate type on macrofaunal or meiofaunal settlement between organic (wood) and inorganic (plate) substrate (Cuvelier et al., 2014). On the other hand, following experiments focused on some specific taxa – copepods and nematodes – acknowledged a wider weight of substrate type on their colonization than previously addressed (Plum et al., 2017; Zeppilli et al., 2015). Moreover, a study conducted at another vent field on the MAR reported stronger effect of the different types of organic

substrate on macrofaunal colonization (Gaudron et al., 2010). According to the authors, this could be attributed to substrate 3D structures, some providing more niches for the colonists in term of space, or to the production of nutrients fueling food webs in the form of sulfide produced by bacterial degradation of the wood in long-term deployment (Gaudron et al., 2010). In any of these studies, influence of temperature or vent fluid chemistry was stronger than the substrate effect (Cuvelier et al., 2014; Gaudron et al., 2010; Plum et al., 2017; Zeppilli et al., 2015). However, in all these experiments, colonization comes both from recruited larvae and from immigration of adults and juveniles of surrounding populations. It is therefore difficult to separate the two processes to assess exactly which part correspond truly to the recruited individuals.

Detection of chemical cues from the vent fluid by the larvae, such as sulfide has rarely been tested experimentally for these ecosystems (Renninger et al., 1995; Rittschof et al., 1998; Zbinden et al., 2017). Among the few studies, colonization experiments with alginate gels impregnated or not with sulfide and deployed in vent sites from the Juan de Fuca Ridge are headed in this direction for some species of polychaetes with a colonization on gels impregnated with sulfide but not on control gels (Rittschof et al., 1998). These chemical signals from the fluids can be completed by a cocktail of other chemical cues from conspecifics, predators or any other species that could have a strong impact on larva post-settlement success. For instance, *Bathymodiolus childressi* mussel beds provide habitat for *Thalassonerita naticoidea* gastropods and the two species are commonly associated together. Y-maze experiments revealed that *T. naticoidea* adults were always choosing preferentially maze arms with *Bathymodiolus childressi* chemical exudates over maze arms with controlled seawater conditions or chemical exudates of shallow water mussels (Dattagupta et al., 2007). This detection capability has been hypothesized for their larval stage as well but remains to be tested (Dattagupta et al., 2007). Similar mechanisms could also occur in tubeworms from the EPR as suggested by observed successional patterns where *Tevnia jerichonana* colonization on vent substrate always precede installation of *Riftia pachyptila*, which ultimately outcompete *Tevnia* tubeworms (Mullineaux et al., 2000). For some authors, this succession would result from differential tolerances and nutritional requirements of the two species, to progressive changes in fluid as the vent ages (Shank et al., 1998a). However, other experiments give more support to the existence of chemical signals produced by *Tevnia jerichonana* required for *Riftia pachyptila* larval settlement (Mullineaux et al., 2000).

In other ecosystems like shallow water coral reefs, such settlement cues from biotic interactions have been recognized of prime importance for habitat choice of fish and crustaceans larvae (Dixson et al., 2014; Lecchini et al., 2010; Lecchini and Nakamura, 2013). Settling fish larvae are even capable of olfactory discrimination among reefs, preferring the water-borne odors of their natal reefs compared to neighboring reef habitats (Gerlach et al., 2007). Moreover, investigations of chemical anthropogenic disturbances have revealed a strong deleterious effect of various pollutant on larval recruitment of fish and crustaceans larvae (Lecchini et al., 2017). Understanding the mechanisms of such settlement cues is therefore essential in the context of deep-sea mining, since larvae in the water column are likely to be the first impacted if the extractions are held in the peripheral inactive sites (Van Dover, 2014; Van Dover et al., 2017).

Additionally and given the importance of symbiotic interactions in hydrothermal vents, presence of microbial partners could be a major condition as well for settlement and growth of chemosymbiotic species into juveniles (discussed in part 1.5.4). In other marine ecosystems, biofilm have been highlighted as major cues for larval settlement of several species such as coral, barnacles,

polychaetes, echinoderms, bivalves or crabs (Hadfield, 2011; Huang and Hadfield, 2003; Ritson-Williams et al., 2016; Watson et al., 2016). For example, the presence of bacteria from the *Pseudalteromonas* genus within the biofilm is required for larvae of the polychaete *Hydroides elegans* to settle (Huang and Hadfield, 2003). On the other hand, presence of several protozoan ciliates in the microbial biofilm inhibits completely the settlement of *Galeolaria caespitosa* polychaete larva (Watson et al., 2016).

In some cases, absence of satisfying environmental cues for settlement can lead to a delay of metamorphosis – also referred as retention of the larval state, which is not to be confounded with the retention of larval individuals next to the hatching site during the dispersal phase (cf. part 1.5.2.2) – until appropriate conditions would be encountered by the larvae (Bishop et al., 2006) (**Fig 30.**). Depending on species, this retention of competency for settlement will either be absolute, lasting until larval death or be modulate by a decreased discrimination for the chosen habitat as a function of time (Bishop et al., 2006) (**Fig 30.**).

Once settlement site is selected, larvae undergo their metamorphosis into juveniles, a critical life-cycle step characterized by more or less drastic morphological changes, sometimes nutritional as well (see 1.5.4) and a high mortality rate. This transitional process between the pelagic environment and a benthic life in the vent represents a key period in the ontogeny of an organism and participates greatly in the recruitment, namely the addition of new individuals within the population. Ecological models focused on hydrothermal vents have indeed highlighted that variations in recruitment have greater incidence on population growth than adult survival or even fecundity (Kelly and Metaxas, 2010).

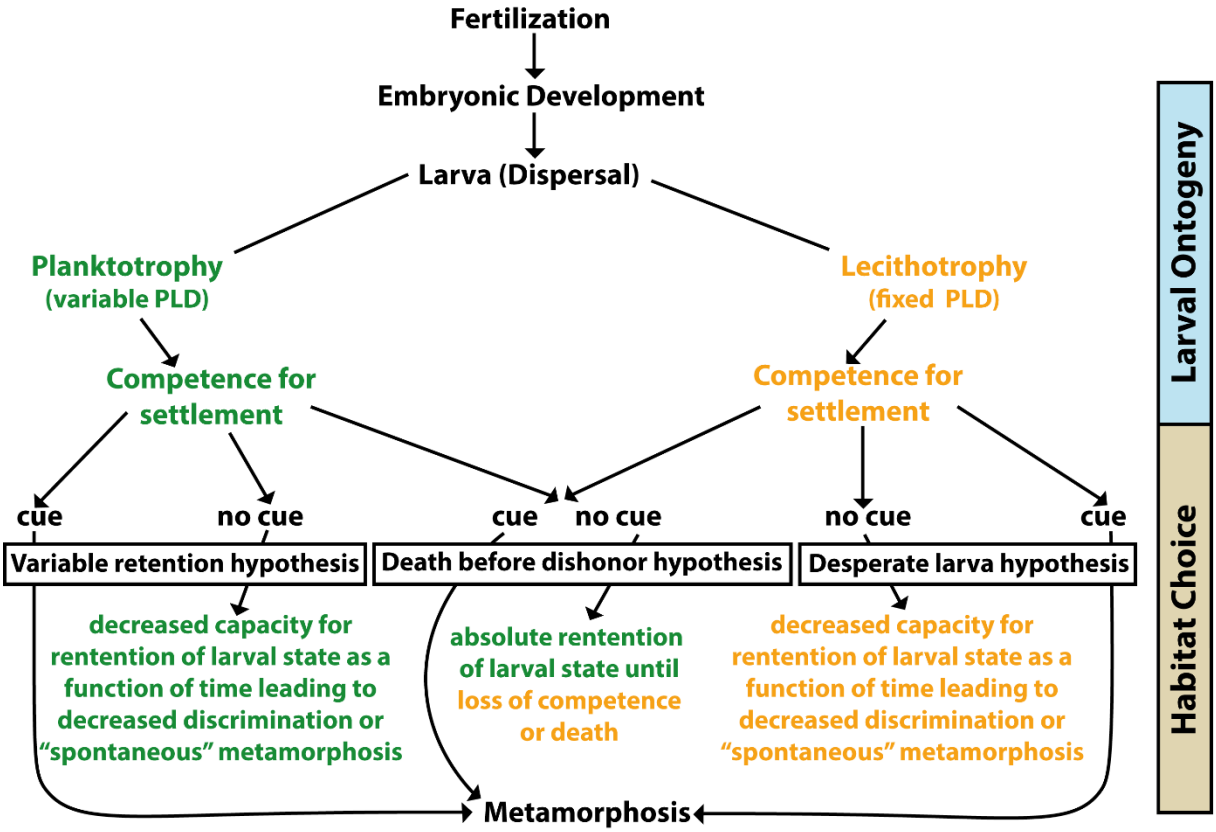


**Fig 30**. Theoretical framework of environmental cues influencing habitat choice and metamorphosis delay of larva in hydrothermal vent ecosystem. Adapted from Bishop et al. 2006.

Many species in hydrothermal vents are distributed in more or less dense assemblages of adult individuals, yet it is not clear whether this results from a gregarious settlement of larvae attracted by similar environmental cues, or if it derives from post settlement dynamics in the population (Laming et al., 2018). Variations in population demographics of any species are therefore a function of variations in specific factors including the larva supply - i.e., the number of competent larva reaching the vent site –, the probability of successful settlement for the new recruits and the mortality rates of each successive life stages (Kelly and Metaxas, 2008; Menge, 1991). For that reason, many studies have explored recruitment processes through size-frequency distribution within populations of different species, the size being used as a proxy for the age of each individuals.

In most cases studied to date in hydrothermal vents, modal decomposition of animal size frequency distribution revealed several cohorts with distinct peaks visible in the distribution (**Fig 31.**). Therefore a discontinuous recruitment has been suggested in approximately every hydrothermal vent genus including vent tubeworms (Thiébaut et al., 2002), alvinellid polychaetes (Faure et al., 2007; McHugh, 1989; Zal et al., 1995), bathymodiolin mussels (Comtet and Desbruyères, 1998) and several gastropods (Kelly and Metaxas, 2008; Matabos and Thiebaut, 2010; Sadosky et al., 2002). In some species like *Bathymodiolus azoricus*, the presence of these multiple size cohorts suggest a periodicity in the recruitment with punctual events of massive recruitment that could possibly be linked with the periodicity in their reproduction discussed above (cf. part 1.5.1) (Comtet and Desbruyères, 1998; Tyler et al., 2007).

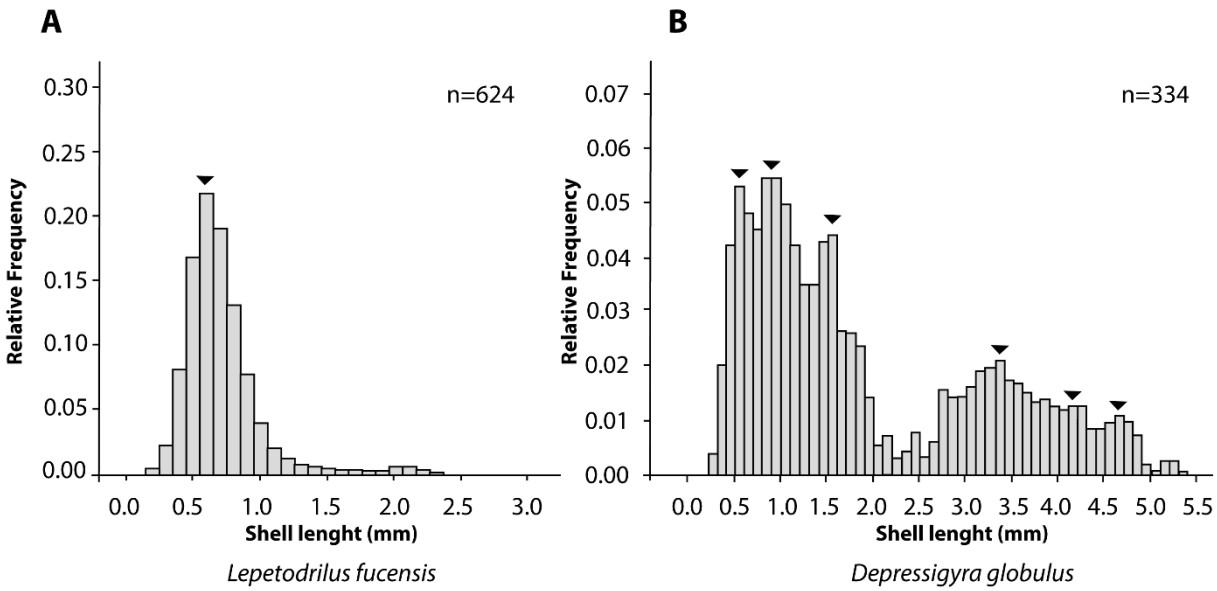


**Fig 31**. Characteristic population structures reflecting **A.** Continuous recruitment (*Lepetodrilus fucensis*) and **B.** Discontinuous recruitment (*Depressigyra globulus*). From Kelly and Metaxas (2008).

Nonetheless, rare examples of unimodal distribution or absence of distinct peaks at defined interval in the distribution have suggested that continuous recruitment are also observed in some species like *Lepetodrilus fucensis* or *Paralvinella pandorae* (Kelly and Metaxas, 2008; McHugh, 1989) (**Fig 31.**). This highlights that distinct recruitment strategies can exist between species settling on the same surface location like *Lepetodrilus fucensis* and *Depressigyra globulus* (Kelly and Metaxas, 2008) or between species of the same genus – even those co-occurring in the same vent site – such as in *Paralvinella* (McHugh, 1989; Zal et al., 1995).

However, limitations of size-frequency distribution studies can arise from variation in growth between individuals due to the variability of venting conditions for adults or variability in size at settlement between individuals – outcome itself of variable larval life (Mullineaux et al., 1998). This can result in broad size ranges for similarly aged individuals, which may thus obscure history of settlement and recruitment within the population (Mullineaux et al., 1998). Other methods for age assessment such as repeated image records, skeletal or shell staining are therefore recommended to be used in parallel to give stronger support to such results (Lutz et al., 1994; Nedoncelle et al., 2013; Urcuyo et al., 2007). Proper age assessment in some metazoan groups is however challenging, especially in crustaceans in reason of their molting cycle and their high motility, and the validity of the methods used today still remains debated (Becker et al., 2018). In such cases, other means of life stage identifications should be used instead to limit bias in population analyses.

## P.1.5.4 General mechanisms of symbiont acquisition

For vent holobionts, the continuity of the association between host and symbionts through their life-cycle, including the acquisition of symbiotic partners, is a key prossess for the survival of the following generation and completion of the life cycle. Depending on species, two main modes of transmission are possible: vertical transmission and horizontal transmission (Bright and Bulgheresi, 2010). In vertical transmission, symbionts are acquired by the offsprings directly from their parents, in general from the mother, and the symbiotic association is maintained during the entire life cycle of the host species. In horizontal transmission however, offsprings experience an aposymbiotic phase during their early life and symbionts are acquired from the environment at some point(s) (one or several) of their life cycle. In this last case, symbiotic life is considered facultative, from the symbiont point of view, which is supposed to thrive as well in the environment as within the host (Bright and Bulgheresi, 2010). However, microorganisms are also able to remain in dormancy for very long periods, up to several millions years (Imachi et al., 2019; Jones and Lennon, 2010). In such way, horizontally transmitted symbionts could then survive but not develop until the meet with their host. This could explain why no chemosynthetic symbiont from hydrothermal vents have been cultivated singly despite numerous tentatives over the past in different laboratory (Sievert and Vetriani, 2012).

In hydrothermal vents and other chemosynthetic ecosystems, vesicomyid clams are the only recognized case so far of vertically transmitted symbionts from the mother to the offsprings (**Fig 32.**). First described in *Phreagena soyoae* (Endow and Ohta, 1990), the presence of symbionts in ovarian tissues has been found since in many other vesicomyid species from different genera including *Phreagena okutanii*, *Calyptogena magnifica*, *Abyssogena phaseoliformis* and *Isoropoddon bigoti* (Cary and Giovannoni, 1993; Ikuta et al., 2016; Szafranski et al., 2014). However, the localization of symbionts associated with spawned eggs has only been observed recently in *Phreagena okutanii* with a small population of 400 symbiotic cells on average, that was only found on the outer surface of the plasma membrane at the vegetal pole of the eggs (Ikuta et al., 2016).

This transmission mode is in line with the strongly reduced symbiont genomes of the family (Kuwahara et al., 2007; Newton et al., 2007). Reduced symbiont genomes could result from a combined effect of lower selective pressures to maintain genes essential for an extracellular lifestyle, and a severe genetic drift by bottleneck effect during transmission with small symbiont populations transmitted to eggs at each generation. Moreover, vertical inheritance of symbionts is supported as well by congruent branching patterns between the vesicomyid hosts and their symbiont phylogenies (Peek et al., 1998). Whereas a true co-speciation was observed in more than six vesicomyid species,

incongruent topologies were also reported in some lineages with occasional host switching events between host species (Ozawa et al., 2017). This host switching could be promoted by a physical proximity, as suggested for the geographically close but phylogenetically distinct, *Cristineconcha regab* and *Laubiericoncha juni* vesicomyids. When the two vesicomyid hosts co-occur within the same clam beds, each of the two clam species possesses a small population of the symbiont from the other respective species, along with its own symbiont (Decker et al., 2013). With an external symbiont location on egg membrane, an alternative horizontal transmission could then be possible as well in this group, by egg-to-egg contact (**Fig 32.**). *Update:* However, a very recent study showed that the explanation of this switch was completely different (Breusing et al., 2019). Indeed, a more detailed molecular analysis – not only limited to the COI – of two clams from the Gulf of California, *Phreagena soyoae* and *Archivesica gigas*, revealed the existence of hybrid specimens between the two host species with individual possessing the COI mitochondrial gene from a different genetic origin than nuclear genes. More interestingly, the symbiont specific of *P. soyoae* were only present in hybrids possessing mitochondrial genes of *A. gigas* but the nuclear genes of *P. soyae* (Breusing et al., 2019). This revealed an unidirectional hybridization, suggesting therefore a role of the symbionts in a hybrid incompatibility, and thus in the reinforcement of the speciation processes, as suggested by others (Brucker and Bordenstein, 2012).

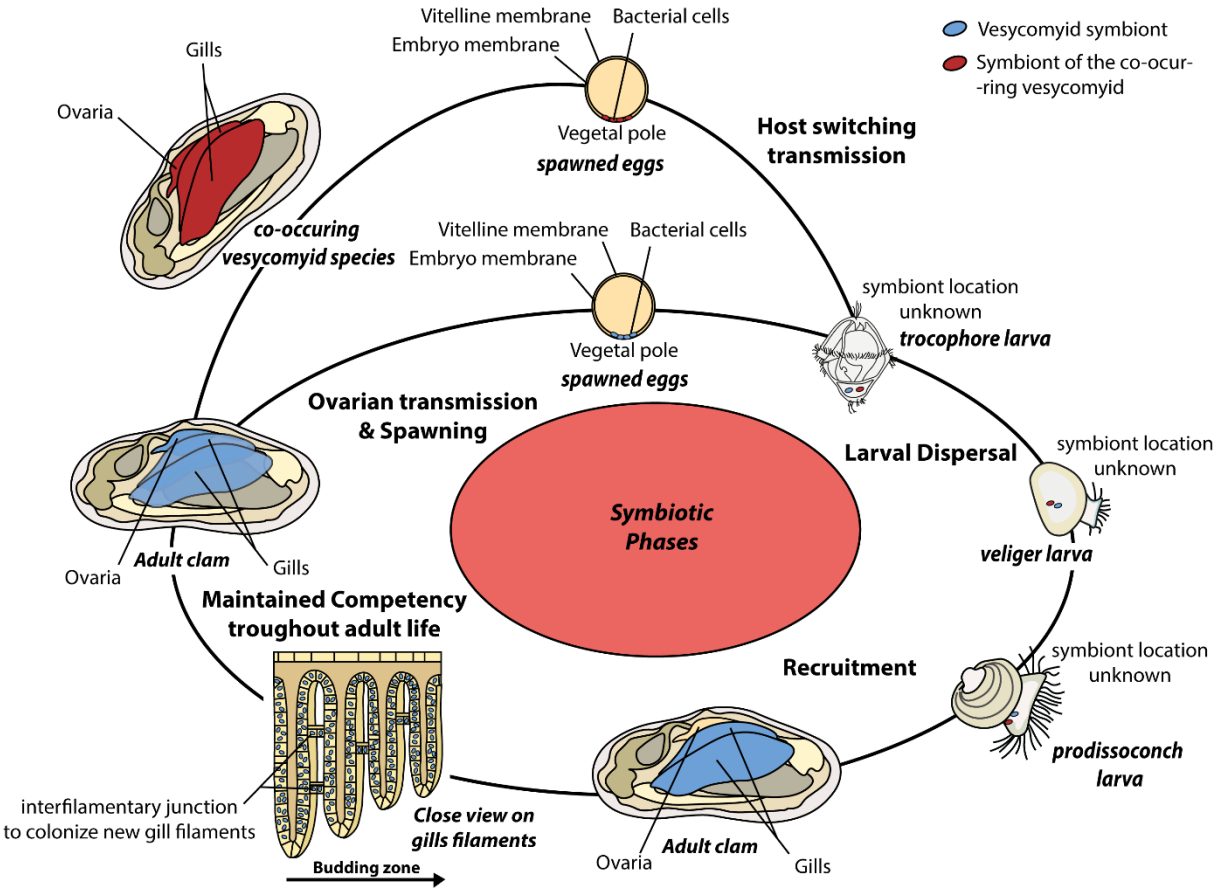


**Fig 32.** Hypothetical life cycle in vesicomyid clams showingsymbiont transmission pathways. Methou (2019). Inspired from the research of Decker et al. (2013), Wentrup (2014), Ikuta et al. (2016) and Ozawa et al. (2017).

Moreover, even if vertically transmitted symbionts are exclusively of maternal inheritance in vesicomyids, alternative pathways should also be considered for other species in which symbiont transmission mode remains undescribed. Indeed, examples of paternally inherited or biparental transmission have been retrieved in other ecosystems for some insect and sponge species with symbionts housed in male sperm cells (Moran and Dunbar, 2006; Usher et al., 2005).

Similarly, in social insects like termites, ants or bees, intriguing mode of vertical transmission have been reported. In these species, infections by different microorganisms can occur during social interactions between young and adults through coprophagic behavior, stomodeal trophollaxis with regurgitation of gut microbiome or proctodeal trophollaxis with contact anus-mouth exchanges of gut fluids between adults and post larvae (Salem et al., 2015). In termites, this behavior is reproduced at each molt cycle to allow the recovery of the microbiome that has been lost with the exuvia, favoring close contacts between individuals and the social structure of those species (Duarte et al., 2017; Nalepa, 2015). In those cases, symbionts are indeed transmitted from parents but hosts are aposymbiotic for a part of their life cycle like in horizontal transmission.

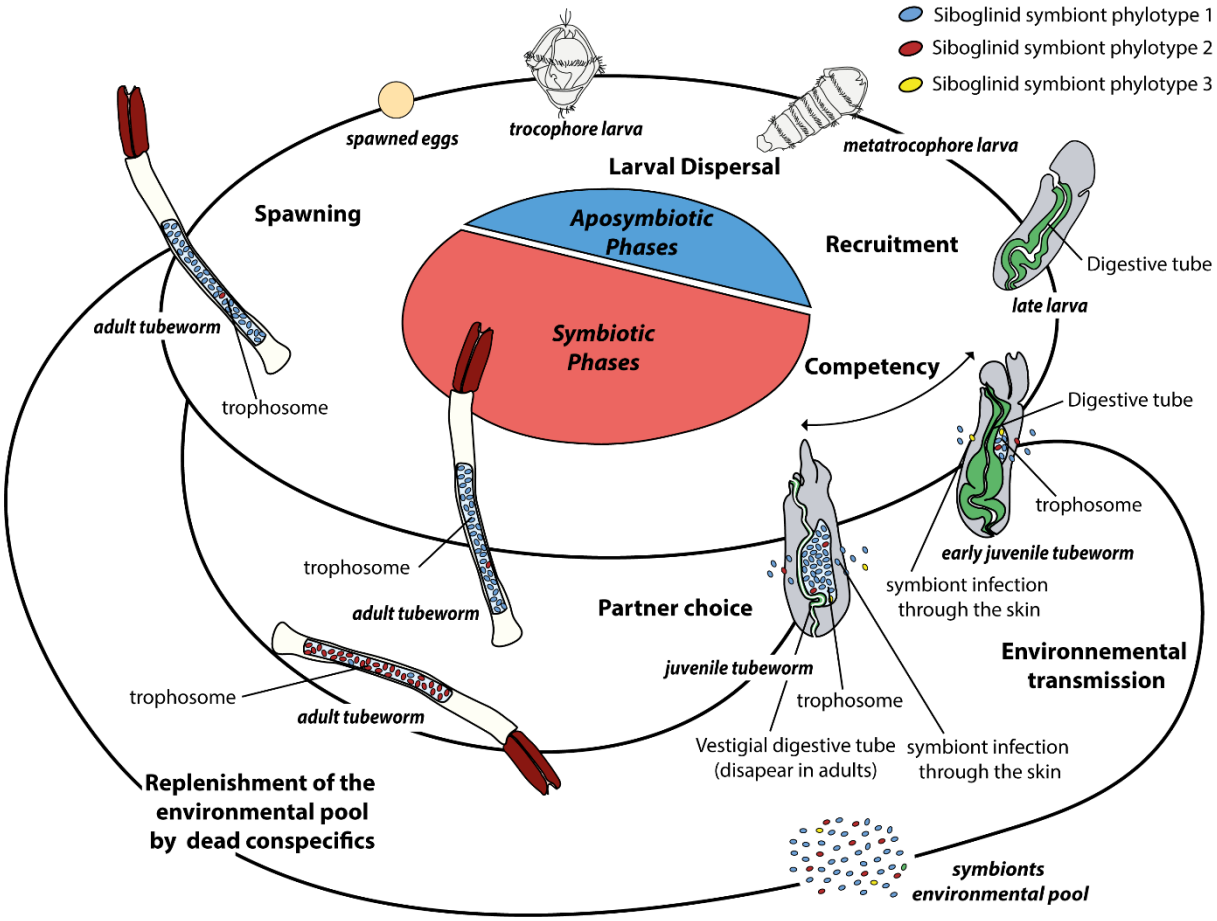


**Fig 33.** Hypothetical model of symbiont transmission through the lifecycle of siboglinid tubeworms. Methou (2019). Inspired from the research of Marsh et al. (2001), Nussbaumer et al. (2006) and Polzin et al. (2019).

Nevertheless, in every other hydrothermal vent organisms currently documented, the mode of symbiont transmission is horizontal. Among them, transmission in *Riftia pachyptila* tubeworms is probably the best understood case at present (**Fig 33.**). As in many species from other ecosystems, symbiont acquisition in *R. pachyptila* occurs upon settlement in a specific and restricted period of

"competency" after which acquisition of new symbionts is no longer possible (Nussbaumer et al., 2006). New partners of *Riftia* tubeworms do not enter the host through the mouth and the digestive system but through the skin to colonize the trophosome organ in formation. This colonization extends until the late juvenile stage after which the acquisition of bacteria ceases and a massive apoptosis of the colonized cells from the epidermis ensues, restricting thus the symbiont population location strictly within the trophosome (Nussbaumer et al., 2006). Although hypothesized as monoclonal for a long time (Gardebrecht et al., 2012; Robidart et al., 2008), high coverage metagenomics of symbionts of *R. pachyptila* as well *Ridgeia piscesae* tubeworms have recently revealed the existence of several genetic variants in their symbiont populations with a clear dominance of a single variant strain (Perez and Juniper, 2018; Polzin et al., 2019).

The dominant *Endoriftia* strain was variable between adult tubeworms even between individuals of the same clump, but the exact parameters that could have led to this differential selection of a specific symbiotic strain are still unknown. Among the potential valid hypotheses, variable environmental conditions upon settlement of each tubeworm individual or genetic interactions between a specific *Endoriftia* strain and a host genotype are currently considered (Polzin et al., 2019). In any case, the variant diversity found within all the tubeworms investigated – 16 individual tubeworms in total – was still much lower than the one observed in the free-living *Endoriftia* metagenomes (Polzin et al., 2019).

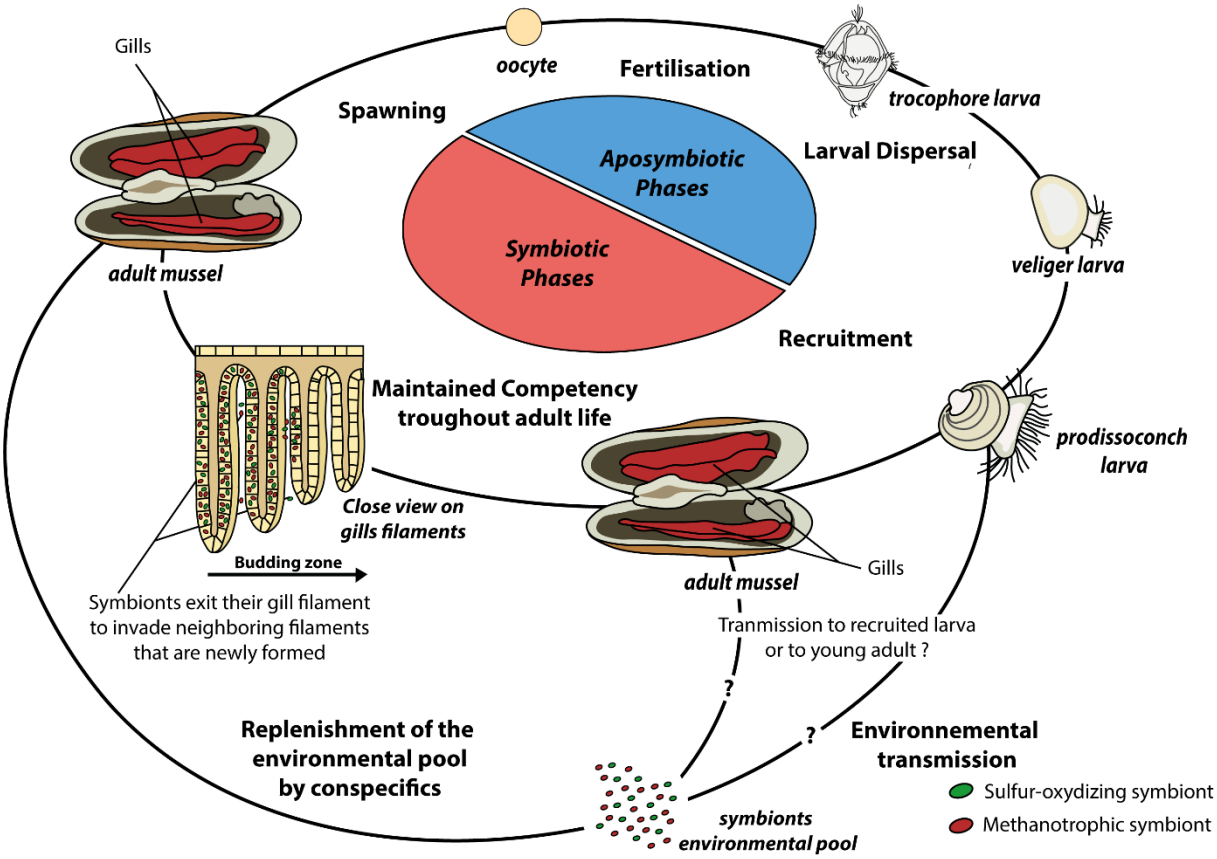


**Fig 34.** Hypothetical model of symbiont transmission through the lifecycle of bathymodiolin mussels Methou (2019). Inspired from the research of Wentrup (2014).

"Competency" for the acquisition of new symbionts in hydrothermal vent species is nonetheless not always restricted for every species to a short period of their life cycle. In

*Bathymodiolus* for example, gills containing symbionts are growing during the whole individual life span and colonization by symbionts is a continuous process in the new tissues after their differentiation throughout the host life (Wentrup et al., 2014) (**Fig 34.**). Still, it remains unclear if the new symbionts are transferred in the newly formed gill tissues from the surrounding environment, by self-infection from older gill tissues that have already been colonized or by both pathways (Wentrup et al., 2014). However, first acquisition and colonization of symbionts in a young juvenile host is radically different from further potential acquisition in adults by being not restricted to the gill host organ. Indeed, colonization of symbionts in juveniles of *Bathymodiolus azoricus* or *Bathymodiolus puteoserpentis*, have been detected in epithelial cells of the foot, the refractor mantle or the mantle but not in every organs either, and start to be limited to gills tissues when they become larger (Wentrup et al., 2013). Nevertheless, since no aposymbiotic juvenile individuals have ever been collected in any bathymodiolin specimens so far – unlike for *Riftia* tubeworms –, the exact timing for the onset of symbiont acquisition is still unresolved for any species of this family (Laming et al., 2018).

In any case, whether symbiont acquisition is limited to a specific life stage window or occurs all along the host lifetime, both *Bathymodiolus* mussels and siboglinid tubeworms rely on the existence of an environmental pool of their symbionts that must be encountered at some point of their life cycle. This acquisition can be facilitated in *Bathymodiolus* by adult conspecifics that have the ability to release some of their bacterial partners and, in this way, replenish the environmental pool (Kádár et al., 2005; Salerno et al., 2005). Similarly in *Riftia* tubeworms, evidences brought by pressurized incubation experiments have shown that symbiont released by dead worms from the adult population retain their ability to colonize new surfaces – artificial glass coverslip in the experiment – and thus potentially newly recruited tubeworm larvae (Klose et al., 2015). Considering the tubeworm densities found in the vent fields as well as the symbiont densities within the trophosome, these authors have estimated a number of released symbionts from a few million up to 1.5 billion upon the death of a single tubeworm clump (Klose et al., 2015).

Apart from these three families, symbiont acquisition in other vent species is extremely poorly understood. Nonetheless, recent evidences on the peltospirid gastropod *Gigantopelta chessoia* have revealed an absence of symbionts in the oesophageal gland (the symbiont-housing organ), of small juveniles in comparison to adult specimens (Chen et al., 2018). Moreover, and despite the absence of any change in their external morphology, the symbiont acquisition is accompanied by drastic changes in the internal anatomy of the host with a progressive increase of the oesophageal gland volume and a decrease of the rest of the digestive system along their growth towards adult stage size (Chen et al., 2018). These observations suggest therefore the existence of a trophic shift from unclear nutrition mode, potentially grazing, in juveniles to a symbiotic based nutrition in adults. This is also supported by stable isotopic analyses, which exhibit a length-based trend in $\delta^{13}C$ and $\delta^{15}N$ for *G. chessoia* at each vent site, although the smaller sized individuals were lacking compared to the previous study (Chen et al., 2018; Reid et al., 2016). On the other hand, symbionts were found in all the early life stages available for *Chrysomallon squamiferum*, another symbiont housing peltospirid snail and no drastic anatomical changes were observed along its ontogeny (Chen et al. 2017). Indeed, the eosophageal gland appears to increase isometrically all along the size growth of this species. These differences in symbiotic acquisition and proliferation patterns suggest that the oesophageal gland in *Gigantopelta* and *Chrysomallon* may represent parallel adaptive evolution (Chen et al., 2017, 2018). For vent species hosting epibiotic symbiotic communities, understanding of the symbiotic partner transmission mode between host generations is also very limited. Whereas many studies have suggested a horizontal

transmission mode based on the presence of sequences closely related to symbiotic lineages in the surrounding environment (Petersen et al., 2010; Szafranski et al., 2015a; Thurber et al., 2011), the degree of specificity of those epibiotic communities compared to the environmental ones and the related selection mechanisms and/or environmental factors are far from being understood. In *Kiwa puravida* crabs, a presence of bacterial communities have been observed in all known life stages with a colonization on egg surfaces as well as on many body parts of juveniles and adults (Goffredi et al., 2014). Change in bacterial dominance – from a *Gammaproteobacteria* dominated assemblage in eggs to *Epsilonbacteraeota* in juveniles/adults – as well as a higher bacterial diversity in earlier life stages – i.e. eggs and juveniles – compared to adults suggest a variation in these selection mechanisms along the ontogeny of those animals (Goffredi et al., 2014). Additionally, maternal transmission of epibionts during egg brooding is still possible and has been suggested for the freshwater cave amphipod *Niphargus ictus* living in symbiosis with filamentous *Gammaproteobacteria* affiliated to the *Thiotrix* clade (Dattagupta et al., 2009). These chemoautotrophic epibionts were specific to the amphipod and distinct from the free-living relative in their surrounding environment. Additionally, when kept in aquarium for more than 3 months, these amphipods were still maintaining a large coverage of epibionts, despite a regular molting. Given the particular reproductive characteristic of those animals (cf. part 1.5.1), the transmission between host generations could occur from the mother to juveniles when brooded in her pouch (Dattagupta et al., 2009).

In summary, traditionally divided in two symbiont transmission modes, vertical or horizontal, this simplification hides the complexity of the symbiont acquisition processes usually mixing both pathways. These transmission modes can be affected indeed by many biological contraints and processes. For example, species hybridization can provoke host switch in vertically transmitted symbionts. Social transmission between congenerics, between adults or with larvae/juveniles, may imply trophallaxy or symbiont release in the surrounding environemnt without being really aposymbiotic. Molt cycle in arthropods imply a renewal of the ectosymbiotic communities at each molt during adult stage, and so regular symbiont acquisition, being then limited not only to offspring. With only three detailed examples of tranmission models in chemosynthetic species – vesicomyid clams, siboglinid tubeworms and bathymodiolin mussels –, it appears quite clearly that generalizations cannot be establish, with for each, a particular case that differs sometime drastically from the others.

# P.2 *Rimicaris* species as model organisms to study lifecycles in hydrothermal vents

## P.2.1 Geographic distribution and current phylogenetic state

Alvinocarididae are a monophyletic family of caridean shrimps, endemic to chemosynthetic ecosystems and comprising currently nine genera and 35 species distributed worldwide (**Fig 35.** to **38.**). Yet, new species are still found oftenly with three new alvinocaridids that have been described since the beginning of this work in 2016 – including *Alvinocaris kexueae* (Wang and Sha, 2017), *A. costaricensis* (Martin et al., 2018) and *Rimicaris falkorae* (Komai and Giguère, 2019). Additionally, some remain to be described (Stevens et al., 2008; Yahagi et al., 2015) (*updated 20/12/19:* described as *Alvinocaris marimonte* (Hiraoka et al., 2019)) and potentially several more are to be discovered.

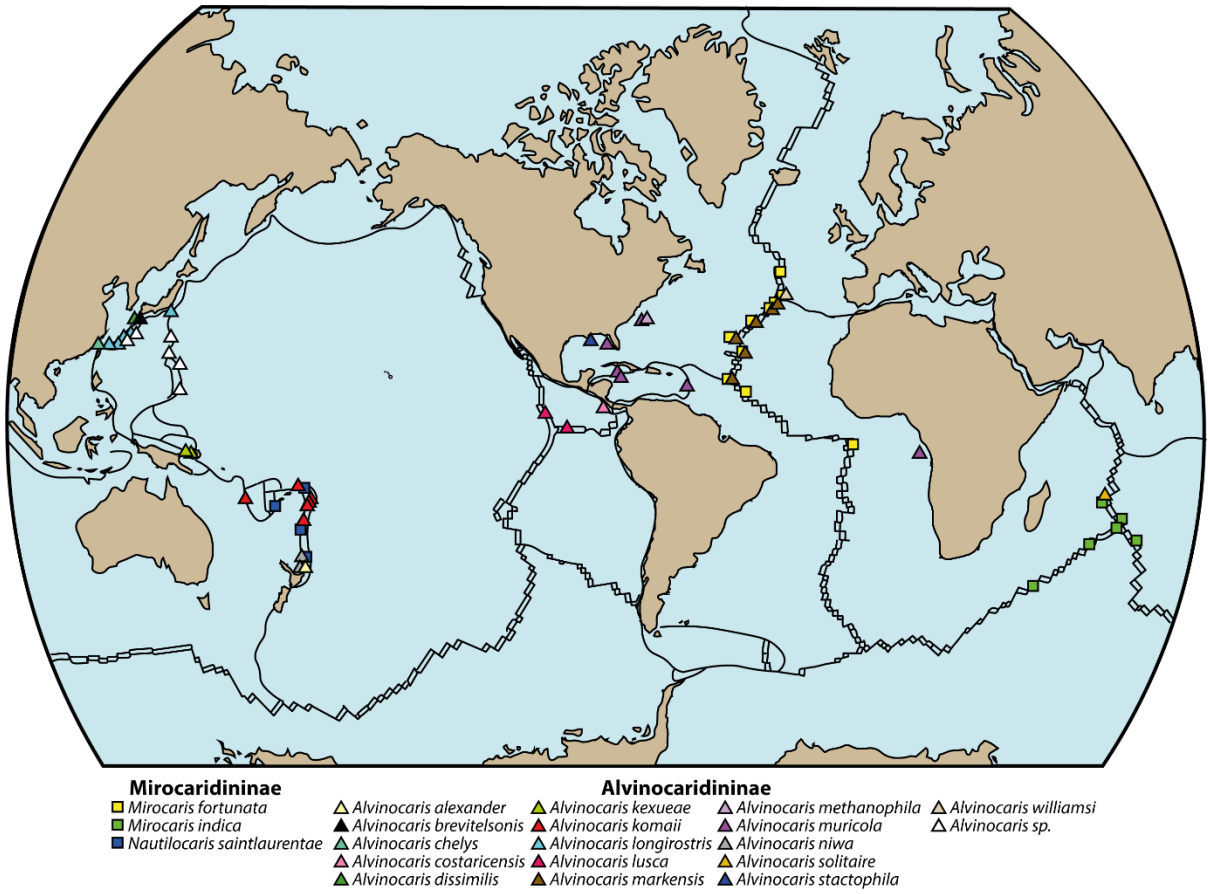


**Fig 35.** Geographic distribution of *Mirocaridininae* (*Mirocaris* + *Nautilocaris*) and *Alvinocaridinae* (*Alvinocaris*) subfamilies as in 2019. Adapted from Lunina and Vereshchaka (2014).

The *Rimicaris* genus is the second largest within this family with 10 described species distributed in four different biogeographical areas (**Fig 36.**): the Western Pacific basins for *Rimicaris variabilis*, *R. parva*, *R. vandoverae* and *R. falkorae*; the Eastern Pacific with *R. paulexa*; the Indian Ocean with *R. kairei*, and the Atlantic Ocean/Caribbean Sea for *R. susannae*, *R. chacei*, *R. exoculata* and *R. hybisae* (Komai and Giguère, 2019; Lunina and Vereshchaka, 2014). Among them, *Rimicaris exoculata* (Williams and Rona, 1986) is currently the more widely distributed species with the widest known

distribution, populations being observed from the Rainbow vent field at 36°N – and potentially up to the Moytirra vent field at 45°N – to the Deyin vent field at 15°S along the MAR (Dong et al., 2019; Lunina and Vereshchaka, 2014; Wheeler et al., 2013). *R. exoculata* shrimps are co-occurring with two other alvinocaridid species, *Rimicaris susannae* and *Mirocaris fortunata*, in at least some of the southern MAR vent fields (Komai et al., 2007), and with three species in the northern MAR vent fields: *Rimicaris chacei*, *Mirocaris fortunata* and *Alvinocaris markensis*. These species however appear to live in different ecological niches (Segonzac et al., 1993).

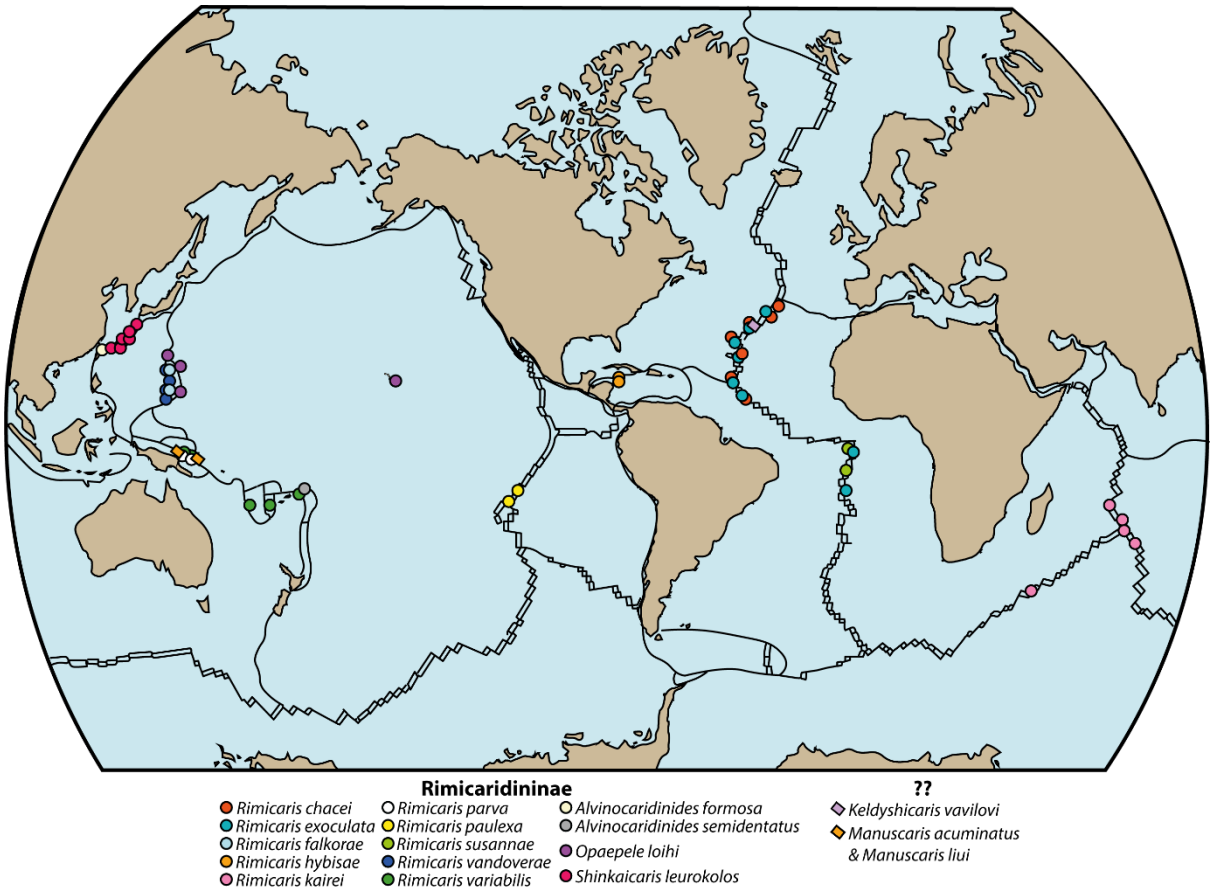


**Fig 36.** Geographic distribution of *Rimicaridinae* subfamily as in 2019. Adapted from Lunina and Vereshchaka (2014).

The current *Rimicaris* genus was previously divided in two, based on morphological characteristic of the cephalothorax: the *Rimicaris* genus comprising species with a strongly inflated cephalothorax – *Rimicaris exoculata* and *Rimicaris kairei* – and the *Chorocaris* genus with a straight cephalothorax comprising the others (Komai and Segonzac, 2008). However, the discovery of *Rimicaris hybisae* in the Mid Cayman Rise (Nye et al., 2012), morphologically similar to a "big head" *Rimicaris* but genetically closer to a *Chorocaris* – *"Chorocaris" chacei* – has led to the reclassification of the genus which includes now both *Rimicaris* and the previously known *Chorocaris*, as well as one *Opaepele* species, *Opaepele susannae* (Komai and Tsuchida, 2015; Vereshchaka et al., 2015). All belong to one of the three alvinocaridid subfamilies: the *Rimicaridinae,* forming a monophyletic group with four other genera – *Alvinocaridinides*, *Manuscaris*, *Opaepele* and *Shinkaicaris* – each comprising one or two species at most, many of which having a phylogenetic position still debated within the group (Vereshchaka et al., 2015) (**Fig 37.**).

## P.2 RIMICARIS SPECIES AS MODEL ORGANISMS TO STUDY LIFECYCLES IN HYDROTHERMAL VENTS

Recently, it has been hypothesized that alvinocaridids began to colonize hydrothermal vent ecosystems about 35 million years ago (Mya), in the early Oligocene, rather than during the late Cretaceous, 59 to 70 Mya, as previously assumed (Sun et al., 2018; Yang et al., 2013). This colonization would have started from the Western Pacific area, before reaching other geographical regions, the Indian Ocean acting as a transition for the colonization of the MAR (Sun et al., 2018). However, caution should be exercised with respect to the conclusions of this study, above the inherent bias of molecular clock methods. In addition to some inaccuracies such as the affiliation of some species to the incorrect location – i.e. *Rimicaris paulexa* in the Western Pacific instead of the Eastern Pacific – the used dataset was clearly biased in favor of the Western Pacific region with 10 species out of 13, making the origin of the group from another region very unlikely, even randomly.

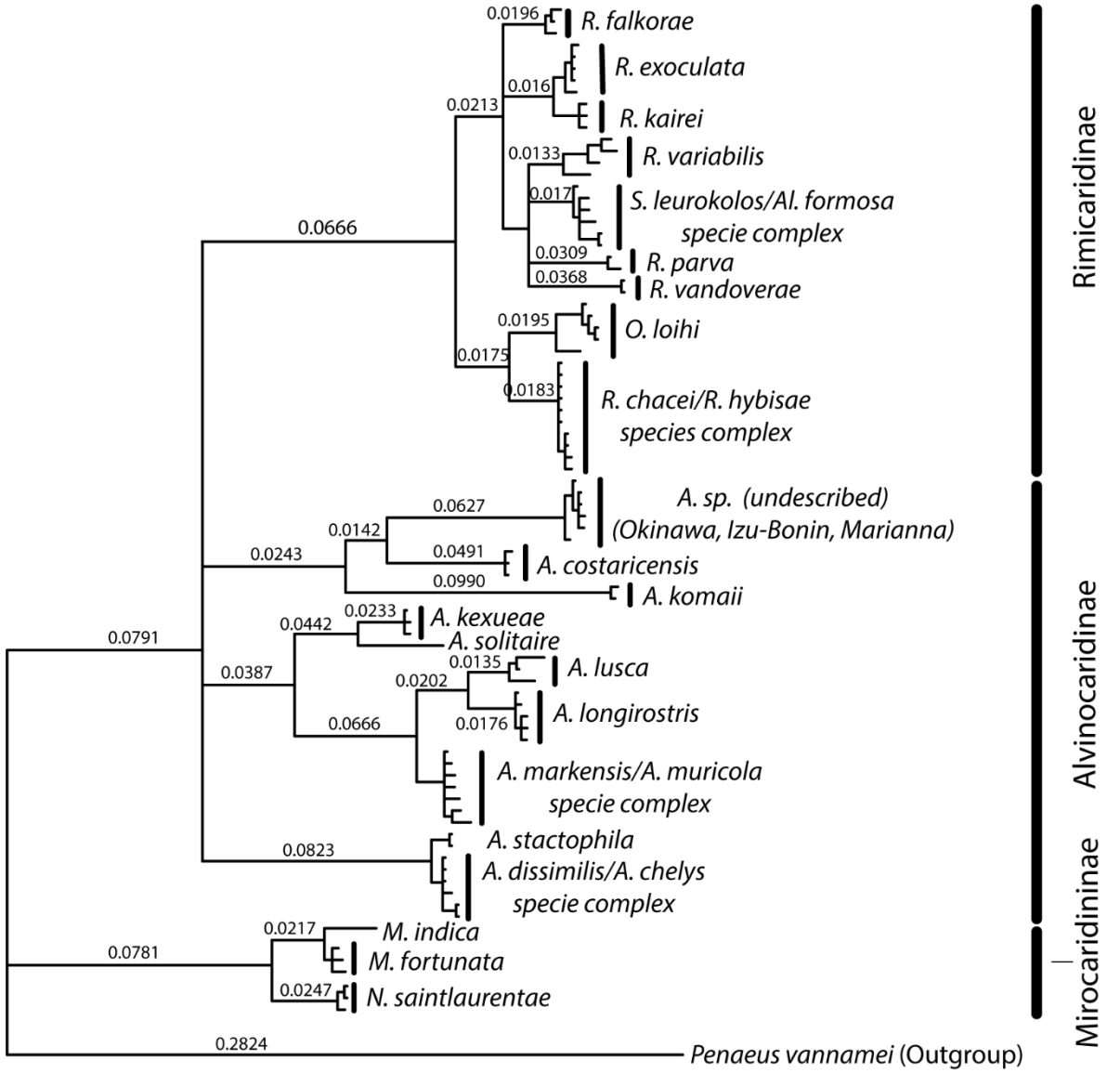


**Fig 37.**Bayesianphylogenetic tree based on COI sequences of all alvinocaridid species for which genetic data have been acquired. Currently, genetic confirmations are still missing for 10 species within the family. This includes *Alvinocaris alexander*, *Alvinocaris brevitelsonis*, *Alvinocaris niwa*, *Alvinocaris williamsi*, *Alvinocaridinides semidentatus*, *Rimicaris paulexa*, *Rimicaris susannae*, *Manuscaris liui*, *Manuscaris acuminatus* and *Keldyshicaris vavilovi*. Methou (2019).

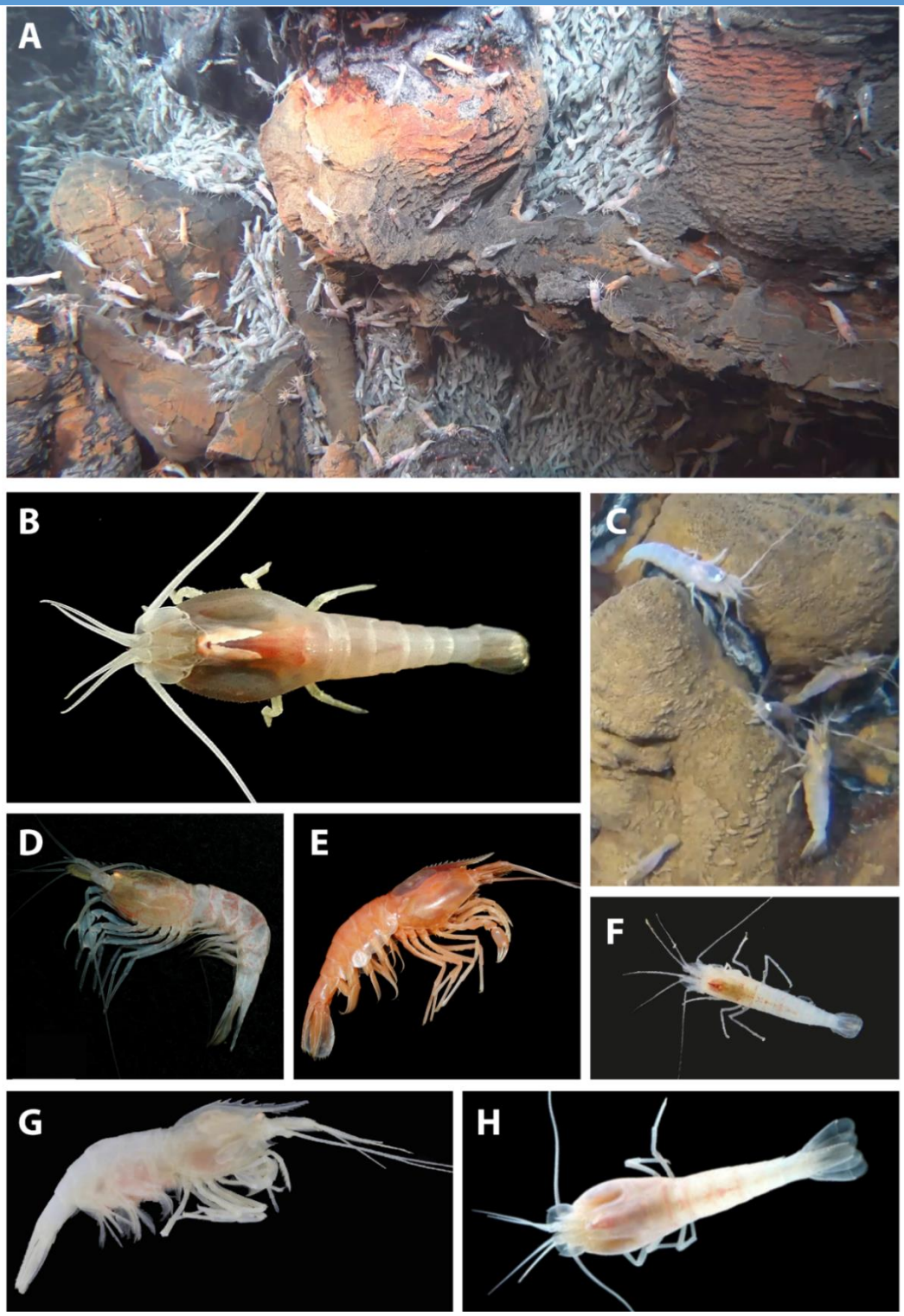


**Fig 38**. Overview of the alvinocaridid shrimp diversity in hydrothermal vents and other chemosynthetic ecosystems. **A.** *Rimicaris exoculata* aggregates with some scattered *Rimicaris chacei* individuals at the Moose Edifice from the Snake Pit vent fields. BICOSE2018-Nautile © Ifremer. **B.** *Rimicaris exoculata* specimen from the MAR. © M. Zbinden. **C.** *Rimicaris chacei* individuals at the TAG vent fields. BICOSE2018-Nautile © Ifremer. **D.** *Alvinocaris costaricensis* specimen from cold seeps off Costa Rica. (Martin et al., 2018) **E.** *Alvinocaris markensis* specimen from the MAR. BICOSE2018-Nautile © Ifremer. **F.** *Mirocaris fortunata* specimen from the MAR. © J. Machon. **G.** *Alvinocaris kexueae* specimen from the Manus Basin. (Wang and Sha, 2017). **H.** *Rimicaris hybisae* specimen from the Cayman Rise. © L. Marsh.

Moreover, given the current geographical range and the phylogenetic position of the subgroup *Opaepele loihi* – *Rimicaris hybisae* – *Rimicaris chacei* (**Fig 36. and 37.**), a colonization of the MAR from the Eastern Pacific through the Caribbean Sea by the Panama isthmus before its closing rather than through the Indian Ocean, should still be considered as an alternative hypothesis for some species (Shank et al., 1999). Therefore, the use of additional alvinocaridid shrimps from other regions than the Western Pacific, especially the more phylogenetically basal ones like *Mirocaris indica*, could have drawn some slightly different conclusions than those proposed by (Sun et al., 2018).

## P.2.2 Trophic ecology & symbiotic interactions in *Rimicaris* shrimps

### P.2.2.1 One shrimp host, two different communities of symbiotic partners

In many vent fields, *Rimicaris* shrimps such as *R. exoculata*, *R. kairei* or *R. hybisae* constitute one of the dominant species living mostly in very dense aggregates close to the active vent emissions (Nye et al., 2013; Segonzac et al., 1993; Van Dover, 2001). These three alvinocaridids stand out from the others by several morphological differences that could explain their apparent evolutionary success. Indeed these three shrimps present a strongly inflated cephalothorax, that significantly increases the volume of their cephalothoracic cavity (Komai and Segonzac, 2008; Nye et al., 2012; Watabe and Hashimoto, 2002). Moreover, two particular mouthparts internalized within this cavity, the scaphognathite and the exopodite, are significantly enlarged and largely covered by abundant plumose setae that further increase the surface of these appendages (Komai and Segonzac, 2008; Nye et al., 2012; Watabe and Hashimoto, 2002).

These morphological modifications offer colonization space to very dense communities of filamentous bacteria that were observed attached to the mouthparts and the branchiostegites – i.e. the membranes covering the inner parts of the cephalothoracic cavity – of these animals (Casanova et al., 1993; Nye et al., 2012; Van Dover et al., 1988; Zbinden et al., 2004) (**Fig 39.**). These bacteria were found in association with mineral depositions (sulfur and iron oxides) that accumulate to form a crust embedding the bacteria at the end of the molt cycle (Corbari et al., 2008a).

Whereas few studies have focused on the bacterial communities of *R. kairei* and *R. hybisae* (Assié, 2016), many others have investigated the composition and the metabolic capacities of bacterial communities hosted by *R. exoculata* (Guri et al., 2012; Hügler et al., 2011; Jan et al., 2014; Petersen et al., 2010; Polz and Cavanaugh, 1995; Zbinden et al., 2008). These are mainly dominated by thick and thin filamentous *Epsilonbacteraeota* – affiliated to *Sulfurovum* free-living bacteria – with thin filamentous thiotrophic *Gammaproteobacteria* – affiliated to *Thiotrix* free-living bacteria – in a lower proportion (Petersen et al., 2010; Polz and Cavanaugh, 1995; Zbinden et al., 2008). Other bacterial partners were also found in those communities including *Zetaproteobacteria*, *Deltaproteobacteria* and methanotrophic *Gammaproteobacteria* in lower relative abundance (Guri et al., 2012; Hügler et al., 2011; Jan et al., 2014; Zbinden et al., 2008). Bacteria from the *Alphaproteobacteria* and the *Bacteroidetes* group were also regularly detected through sequencing approaches, but their presence in *R. exoculata* symbiotic communities was never visually confirmed with FISH observations (Guri et al., 2012; Hügler et al., 2011; Jan et al., 2014; Petersen et al., 2010; Zbinden et al., 2008).

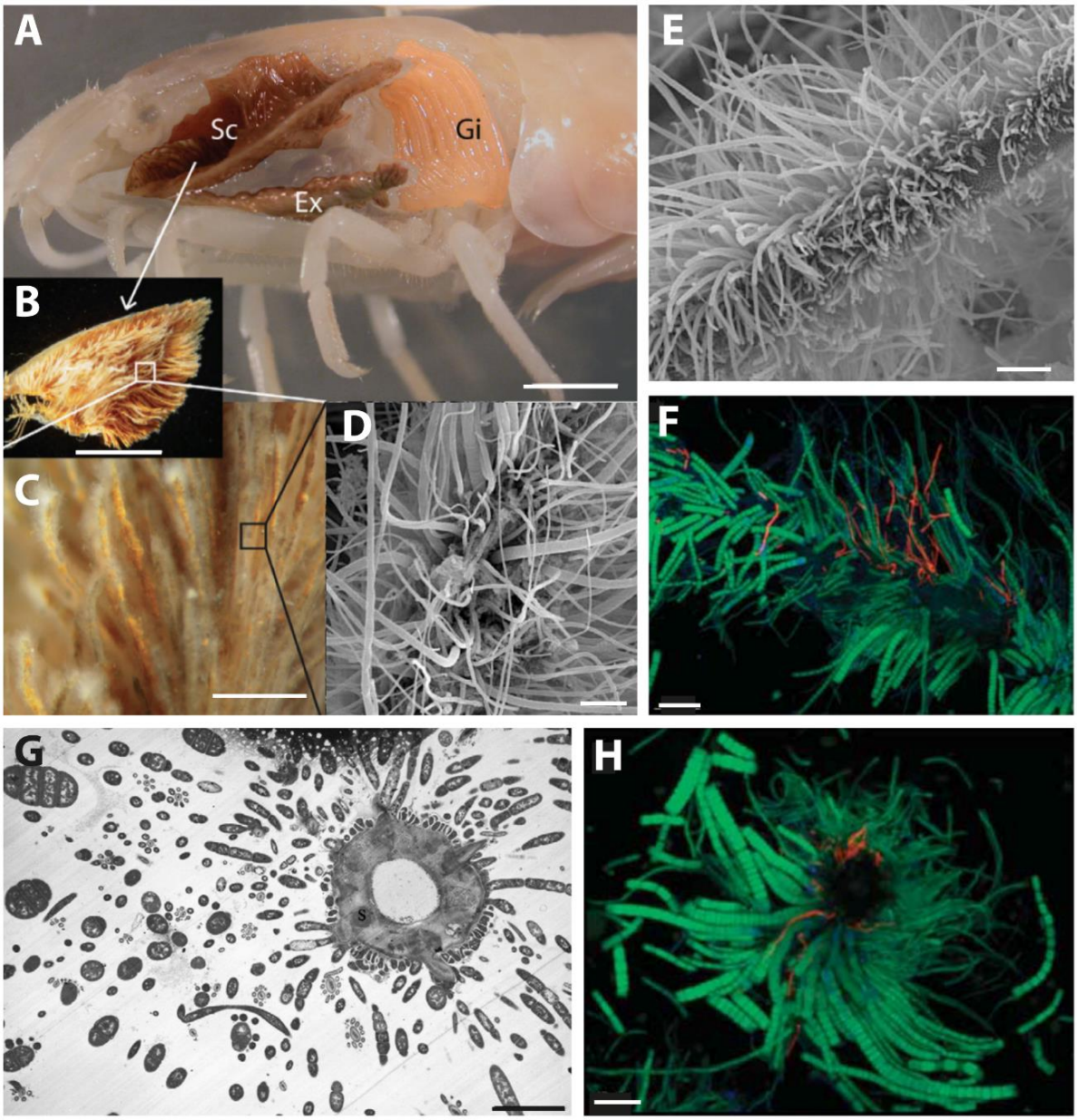


**Fig 39**. Different views of the cephalothoracic cavity of *Rimicaris exoculata*. Images taken from either Zbinden et al. (2004), Zbinden et al. (2008), Petersen et al. (2010) or Guri et al. (2012). **A.** The *R. exoculata* gill chamber with carapace removed, showing the mouthparts (Sc and Ex) to which the shrimp epibionts are attached. Sc: scaphognathite; Ex: exopodite; Gi: gill. Scale bar = 5 mm. **B.** Scaphognathite dissected out of the shrimp. Scale bar = 5 mm. **C.** Closer view of the scaphognathite setae. The filamentous epibiotic bacteria can be seen as a white fuzzy material. **D.** Scanning Electron Microscopy (SEM) observations of bacterial mats and mineral deposits on setae of the scaphognathite of a shrimp from Rainbow. Scale bar = 10 µm **E.** SEM observations of bacterial mats and mineral deposits on setae of the scaphognathite of a shrimp from Rainbow. Scale bar = 10 µm **F.** FISH observations of scaphognathite setae (longitudinal view) with epibionts of a shrimp from Logatchev hybridized with specific probe targeting *Epsilonbacteraeota* (green) and *Gammaproteobacteria* (red) symbionts. Scale bar = 10 µm. **G.** Transmission Electron Microscopy (TEM) observations of bacterial mats and mineral deposits on setae of the scaphognathite of a shrimp from Rainbow. Scale bar = 5 µm **H.** FISH observations of scaphognathite setae (tranversal view) with epibionts of a shrimp from Logatchev with specific probe targeting *Epsilonbacteraeota* (green) and *Gammaproteobacteria* (red) symbionts Scale bar = 10 µm.

Metabolic capabilities of three of these bacteria were also revealed using metagenomic analyses. These approaches showed potential for oxidation of sulfur, iron and hydrogen as energy source coupled with autotrophic carbon fixed through the CBB cycle – for the *Gammaproteobacteria* and *Zetaproteobacteria* – or the rTCA cycle – for the *Epsilonbacteraeota* (Jan et al., 2014) (**Fig 40.**).

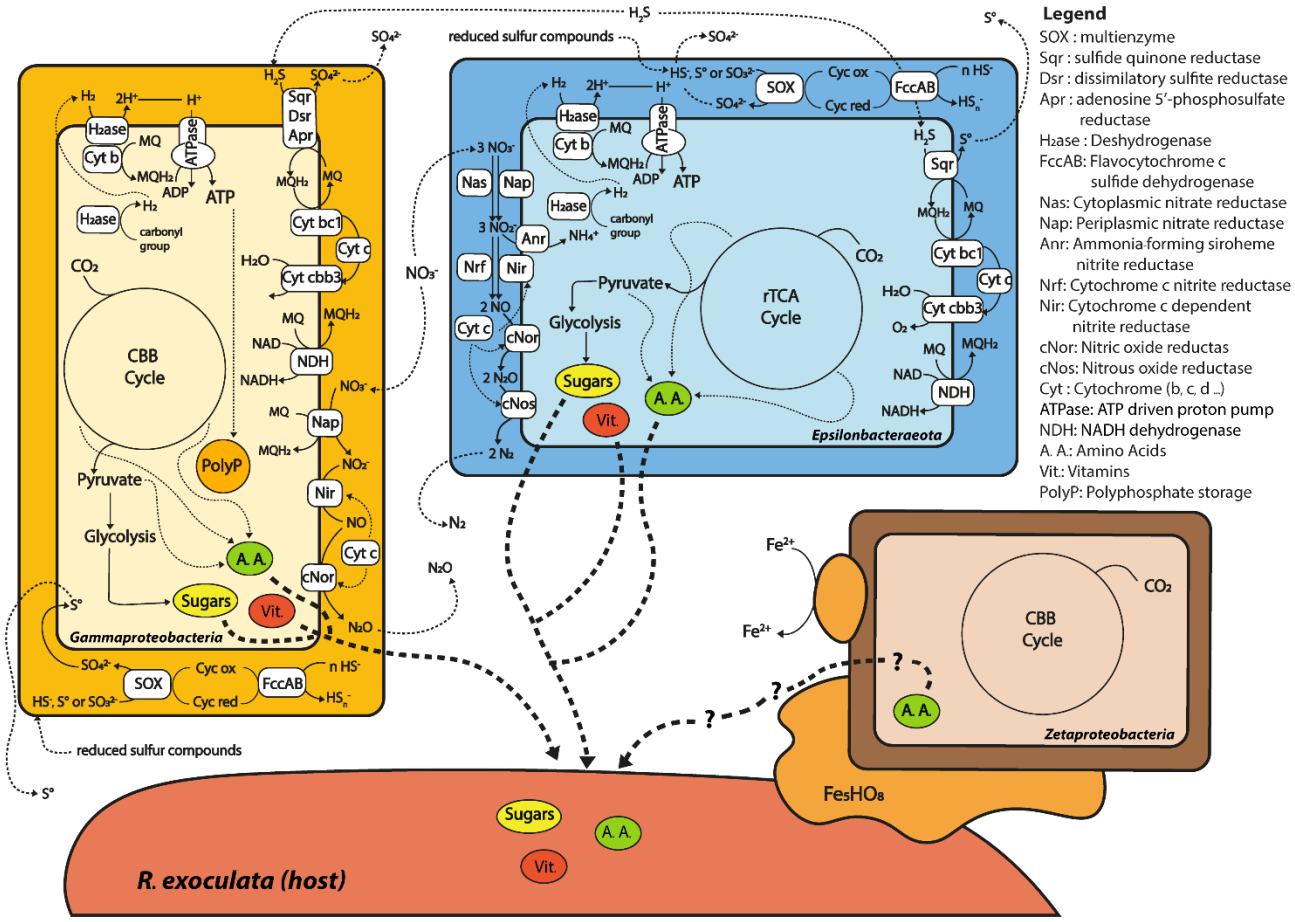


**Fig 40**. Metabolic pathways of *Epsilonbacteraeota*, *Gammaproteobacteria* and *Zetaproteobacteria* symbionts of *R. exoculata* according to their partial metagenomes. Adapted from Jan et al. (2014)

These symbionts provide most of their host nutrition, particularly the dominant *Epsilonbacteraeota*, as suggested by isotopic composition of *R. exoculata* shrimp muscles that are in agreement with a diet mostly derived from a rTCA-fixed carbon source (Colaço et al., 2002; Gebruk et al., 2000; Polz et al., 1998; Van Dover et al., 1988). In addition, analysis of *R. exoculata* digestive system revealed a strongly reduced gut and stomach compared to other co-occurring species and a gut content mostly composed of mineral particles, thus suggesting a minor role of these digestive organs for the shrimp nutrition (Segonzac et al., 1993). Moreover, this nutritional role of epibionts was confirmed with *in vivo* experiments using radiolabeled carbon tracers (Ponsard et al., 2013). First, symbionts of the cephalothorax were confirmed to be chemosynthetically active, able to incorporate inorganic carbon – as well as small organic molecules like acetate – with different electron donors including thiosulfate and reduced iron. Additionally, a transfer of the incorporated carbon by the symbionts to the host was also observed in shrimps incubated with the radiotracers for a duration as short as 1h (Ponsard et al., 2013). In this experiment also, the digestive tract was almost not labeled with the radiotracers, indicating that nutrients are poorly absorbed by this organ (Ponsard et al., 2013). These observations support more strongly the hypothesis of a direct transcuticular transfer of

nutriments from the symbionts to the host rather than a bacterial "farming" and further ingestion through the digestive system, an alternative hypothesis previously weakened by the absence of scraping or grazing marks in the branchial cavity (Corbari *et al.*, 2008; Zbinden *et al.*, 2008).

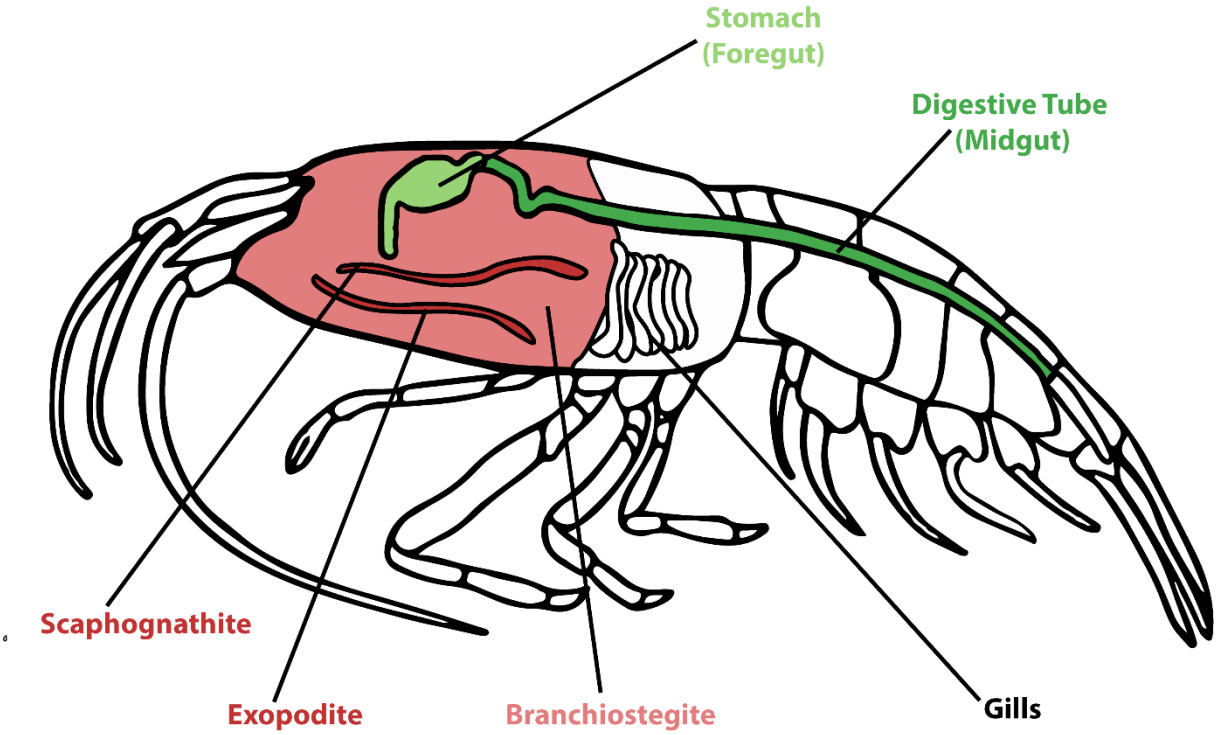


**Fig 41**. Different hosting organs of the *Rimicaris exoculata* dual symbiosis.

A second symbiotic community of resident bacteria has been observed in the digestive tract of *R. exoculata*, inserted between microvilli of the epithelial cells of the midgut,and mainly composed of Mollicutes and Deferribacteres but also of *Epsilonproteobacteria* and *Gammaproteobacteria* (Durand et al., 2010, 2015; Zbinden and Cambon-Bonavita, 2003) (**Fig 41.**). Similar bacterial communities are found as well in the stomach (Cowart et al., 2017). However, recent studies revealed a slight distinction with more Mollicutes in the stomach and more Deferribacteres inside the midgut (Cueff-Gauchard et al. in prep, Velo-Suárez et al. in prep). Yet, the exact location of each of those partners remain to be confirmed with FISH experiments. Furthermore, their potential role in the symbiotic relationship is still unknown, but metabolic capacities of these bacteria are currently under investigation (Velo-Suárez et al. in prep). Nonetheless, some hypotheses can be made by comparison with metabolisms found in free-living bacterial relatives. These include iron-reduction or sulfur-reduction metabolisms for Deferribacteres (Slobodnika et al., 2009; Takaki et al., 2010), suggesting a complementary role for the host nutrition.

*Rimicaris chacei*, a species lacking the symbiont-related enlargement of the cephalothorax, constitutes an interesting case to study the evolution of symbiosis within the alvinocaridid family (**Fig 42.**). Co-occurring with *R. exoculata* in many vent fields of the MAR (cf. par 2.1.1), this shrimp does not exhibit most of the morphological adaptations to host symbionts, including the enlarged mouthparts and the inflated cephalothorax (Komai and Segonzac, 2008). Nonetheless, *R. chacei* shrimps bear important plumose setae on the mouthparts, unlike all the other *Rimicaris* species (Komai and Giguère, 2019; Komai and Segonzac, 2008; Komai and Tsuchida, 2015). Moreover, its phylogenetic position within the family is extremely close to *R. hybisae*, to the extent that the two species share same COI

haplotypes and cannot be distinguished based on genetic only – according to the genetic markers used so far – despite their strong morphological and ecological differences and their distinct geographical range (Hernández-Ávila, 2016).

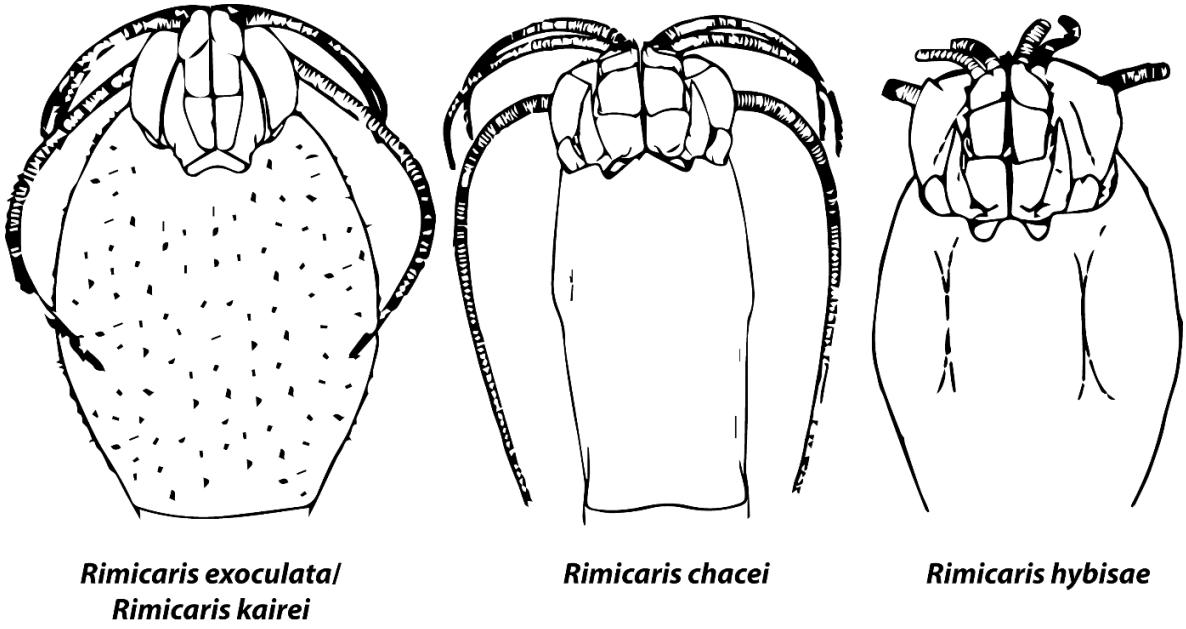


**Fig 42**. Comparative morphology of the cephalothorax between *Rimicaris exoculata*, *Rimicaris kairei*, *Rimicaris chacei* and *Rimicaris hybisae*. Adapted from Williams and Rona (1986) and Nye et al. (2012)

It has been hypothesized that *R. chacei* would have a mixotrophic diet based on symbiosis and complementary feeding sources as suggested by their isotopic composition (Colaço et al., 2002; Gebruk et al., 2000). This is supported by observations of dissected *R. chacei* individuals that revealed a larger stomach and gut than *R. exoculata,* and a gut content containing a mix of organic materials and mineral particles which both suggest a larger implication of the digestive system in the shrimp nutrition (Segonzac et al., 1993). Recent work also showed that *R. chacei* shrimps host symbiotic communities with similar lineages to those found in *R. exoculata,* both within their cephalothoracic cavity and their digestive tract (Apremont et al., 2018). This has led the authors to hypothesize that *R. chacei* could maintain a mixed trophic strategy due to its niche competition with *R. exoculata*, in contrast with *R. hybisae* that has full access to vent fluid emissions to fuel its symbiotic bacteria, lacking yet any known competitor in its environment (Apremont et al., 2018).

## P.2.2.2 Dynamic of symbiotic relationship along molt stages and life stages

One of the particularity of the *Rimicaris* symbiosis is that mouthparts and branchiostegites are recolonized several times during the adult life (Corbari et al., 2008b) (**Fig 43.**). As for any arthropods, growth is limited to the ecdysis period after molting that renew the entire cuticle of the animal. Bacterial communities and mineral deposits present on the cuticle are therefore discarded at each molt cycle. New cuticle is recolonized probably from selected free living bacteria or from ingestion/contact with the old cuticle (Corbari et al., 2008b). This colonization also appears to be heavily controlled, since bacteria do not proliferate on the gills neither on the branchiostegites parts that faces those gills both for *R. exoculata* and for *R. chacei* (Apremont et al., 2018; Zbinden et al., 2004). However, this molting process does not concern the gut community since the midgut is not

covered with cuticle. Bacterial symbionts from this compartment are then kept at least during the entire adult life – and possibly in other life stages – and might by acquired differently (Durand et al., 2010, 2015).

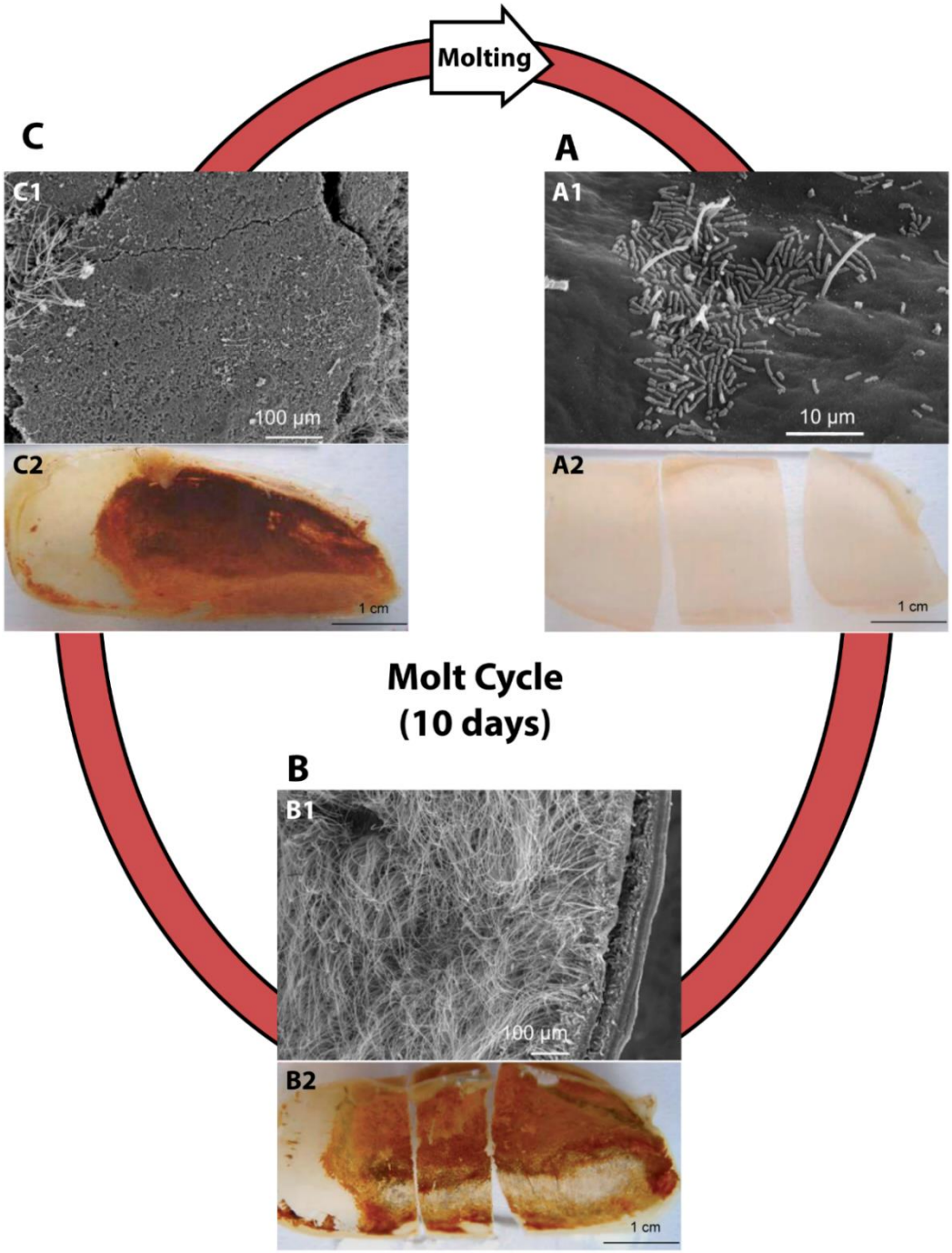


**Fig 43**. *Rimicaris exoculata* cephalothoracic symbiotic community throughout the host molt cycle. Adapted from Corbari et al. (2008b). Inner view of the branchiostegites of shrimps from the Rainbow vent field at different phases of the molt cycle A. Postecdysis molt stage, white. B. Early preecdysis molt stage, light red. C. Late preecdysis molt stage, dark red. Observations are made by in SEM (**A1, B1, C1**) and with a stereomicroscope (**A2, B2, C2**)

Since molt cycle imposes a frequent and complete renewal of the cephalothoracic bacterial community, symbionts of the cephalothoracic cavity are supposed to be primarily acquired

horizontally from the environment where some of them have been identified. Partial 16S rDNA sequences of *Epsilonbacteraeota*, *Gammaproteobacteria* and *Zetaproteobacteria* symbionts were indeed detected in seawater, vent chimneys and artificial colonization devices at both TAG and Rainbow vent fields where *R. exoculata* are abundant (Durand et al., 2015; Szafranski et al., 2015a). This is further supported by the geographic distribution of bacterial OTUs for *Epsilonproteobacteria* symbionts – and *Gammaproteobacteria* ones to a lower extend – which showed differentiation between vent sites, favoring the hypothesis of horizontal transmission (Cowart et al., 2017; Durand et al., 2015; Petersen et al., 2010). However, neither the Mollicutes nor the Deferribacteres *Rimicaris* symbionts have been found in the shrimp environment yet, and no clear segregation between vent sites has been shown, which may be in favor of a vertical transmission for those symbionts (Cowart et al., 2017; Durand et al., 2015). A more precise comprehension could be brought by the utilization of other geographic markers. Thus, the use of *Lux* genes for instance, has proved to resolve more clearly the biogeographic distribution of *Gammaproteobacteria* (*LuxR*) with a clear distinction according to vent site, where 16S markers gene showed little discrimination previously (Le Bloa et al., 2017).

Along *R. exoculata* life cycle, bacterial communities have been observed both in juveniles and on egg surfaces (Cowart et al., 2017; Guri et al., 2012). Composition of juvenile bacterial communities were similar in all aspects to those of adults, but egg communities differed by a significantly higher proportion of *Gammaproteobacteria* suggesting a shift from a *Gammaproteobacteria* dominated community in those early life stages to a dominance of *Epsilonbacteraeota* in later ones (Cowart et al., 2017; Guri et al., 2012). However, it is still unclear when the onset for this bacterial colonization along the embryonic development is, since the previous study did not precisely identified the developmental stage of the observed egg broods (Guri et al., 2012). More work is also required to conclude if this colonization on the eggs is opportunistic, corresponding to a simple bacterial fouling on a newly available surface, or if there is a specificity of the egg bacterial assemblage, suggesting a possible bacterial selection – but not necessarily – by the host. Uncertainties remain also concerning the larval phase to confirm if this life stage is aposymbiotic indeed, or if some of the symbionts could have been transmitted during the brooding phase. In the end, more studies will be required to assess if first colonization in juveniles follows the same patterns than colonization at each molt in adults, or if some differences can be observed with for example a bacterial proliferation in other parts of the cephalothoracic cavity such as gills.

In addition, the underlying mechanisms controlling the regulation of the symbionts growth and proliferation as well as the bacterial selection from the microbial environmental pool are still poorly understood. A recent study has highlighted the potential role of a C-type lectin, a recognized microbe-pattern recognition receptor in other species (Boutet et al., 2011; Chaston and Goodrich-Blair, 2010; Kvennefors et al., 2008; Wippler et al., 2016), which was found highly expressed in a scaphognathite transcriptome of *R. exoculata* (Liu et al., 2019). The expression level of this particular lectin was correlated with the *Epsilonbacteraeota* and *Gammaproteobacteria* symbionts, but not the *Deltaproteobacteria*, with a higher expression when symbionts were more abundant (Liu et al., 2019). This lectin could be part of a cocktail of molecules produced by the shrimp, acting synergistically to shape the symbiont community and/or to prevent the colonization of the gills. In this way, antimicrobial peptides (AMPs) such as Crustine, could be good candidates, as high levels of Crustine expression were observed in several parts of the cephalothoracic cavity – but were very low in the digestive system – of *R. exoculata* (Le Bloa et al. in prep; in Annex of this manuscript). Molecular conversations between the different symbiont partners could also occur to control the development

of each member of the microbial biofilms, such as with quorum-sensing genes, that were found to be expressed in *Gammaproteobacteria* (*LuxR*) and *Epsilonbacteraeota* (*LuxS*) symbionts (Le Bloa et al., 2017).

## P.2.3 Physiological and sensorial adaptations of *Rimicaris* shrimps

Besides their symbiotic relationship with chemosynthetic bacteria, which enable them to feed in these ecosystems, *Rimicaris* shrimps exhibit many other adaptations to the hydrothermal vent particular environmental conditions.

By living close to the active vent emissions, *R. exoculata* shrimps are directly exposed to the hot vent fluids and they face both high concentrations of potentially toxic compounds and highly variable temperatures in very short temporal – of the order of seconds – and spatial – of the order of cm – scales. These animals are typically described as living in the hottest part of the thermal gradient with reported living temperature from 10°C up to 40°C according to some authors (Gebruk et al., 1993, 2000; Van Dover et al., 1988). However, these early records were not carried out directly around the shrimp aggregates and a more accurate view of the shrimp environment has been brought by other studies, reporting associated *in situ* temperature measurements between 4.6°C and 16°C in average within the shrimp aggregates (Desbruyères et al., 2001; Geret et al., 2002; Schmidt et al., 2008; Segonzac et al., 1993; Zbinden et al., 2004).

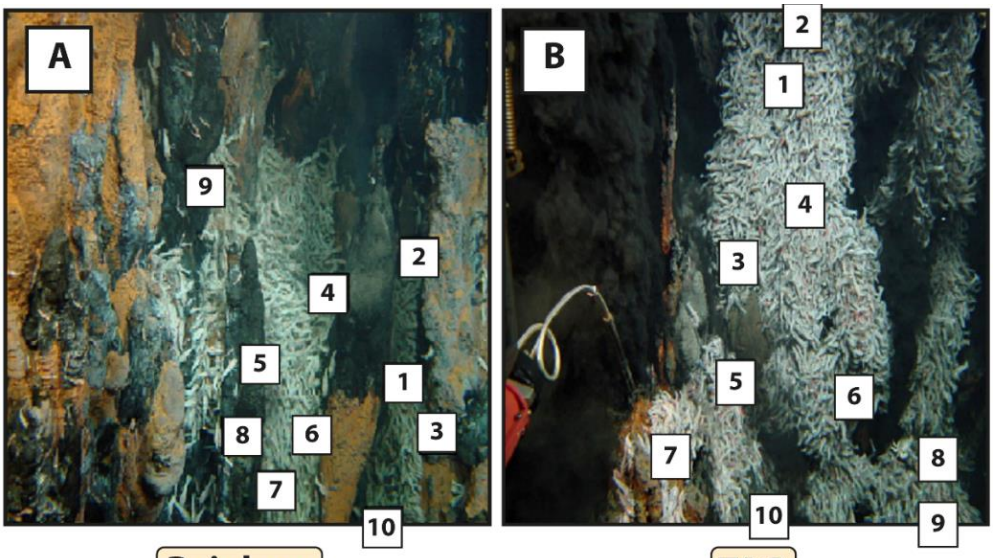


**Rainbow**

| | $T_{min}$ | $T_{mean}$ | $T_{max}$ | SD |
|---|---|---|---|---|
| 1 | 5.3 | 6.2 | 6.7 | 0.4 |
| 2 | 5.3 | 6.2 | 7.1 | 0.4 |
| 3 | 6.4 | 7.7 | 9 | 0.6 |
| 4 | 9.7 | 11.9 | 14.5 | 1.3 |
| 5 | 6.8 | 8.5 | 11.3 | 1 |
| 6 | 7.3 | 10.9 | 15.8 | 2.2 |
| 7 | 7.2 | 12.3 | 18.2 | 2.2 |
| 8 | 9.3 | 10.6 | 14.6 | 1.2 |
| 9 | 7.4 | 9.3 | 12.7 | 1.2 |
| 10 | 11.4 | 16 | 17.3 | 1.3 |

**TAG**

| | $T_{min}$ | $T_{mean}$ | $T_{max}$ | SD |
|---|---|---|---|---|
| 1 | 5.3 | 7.2 | 11.9 | 1.2 |
| 2 | 2.8 | 5.3 | 7.9 | 1.2 |
| 3 | 3.3 | 5.9 | 9.1 | 1.3 |
| 4 | 4 | 7.1 | 13.3 | 1.7 |
| 5 | 5.1 | 6.4 | 8.2 | 0.7 |
| 6 | 4 | 7.5 | 12.6 | 1.6 |
| 7 | 3.6 | 6 | 8.5 | 1.1 |
| 8 | 4.1 | 9 | 17.4 | 2.5 |
| 9 | 4 | 10.2 | 16.6 | 3.2 |
| 10 | 3.6 | 4.6 | 5.4 | 0.4 |

*All temperature values are in degree celsius (°C)*

**Fig 44**. Variability of the thermal environment of *Rimicaris exoculata* shrimps at TAG and Rainbow. Adapted from Schmidt et al. (2008).

Given the dynamic gradient bathing them, *Rimicaris* shrimps are regularly exposed to variable temperatures from 2°C to 25°C according to the maximum temperatures reported by those same studies (Geret et al., 2002; Schmidt et al., 2008; Zbinden et al., 2004). These temperatures can significantly vary between and within the same aggregate as evidenced by Schmidt and colleagues (Schmidt et al., 2008). They indeed reported *in situ* measurements at 10 different sampling points of a same aggregate that varied between 6.2°C and 16°C in average – maximum between 6.7°C and 18.2°C – at Rainbow and between 4.6°C and 10.2°C in average – maximum between 5.4°C and 17.4°C – at TAG (Schmidt et al., 2008) (**Fig 44**).

Thermal tolerance of some alvinocaridids was studied with *in vivo* physiological experiments using pressure devices to avoid other stress bias by maintaining their environmental pressure conditions on board or throughout the sampling process (Cottin et al., 2010a, 2010b; Matabos et al., 2015; Ravaux et al., 2003, 2009, 2019; Shillito et al., 2006). Earlier work revealed that *R. exoculata* does not tolerate sustained exposures (1h) to temperatures in the 33-38.5°C range and that the critical thermal maximum ($CT_{max}$) might be observed at lower temperature (Ravaux et al., 2003). Moreover, two hsp70 proteins, recognized as universal heat inducible stress proteins among metazoans (Ravaux et al., 2003), were identified in *R. exoculata* –with a synthesis threshold lower than 25°C (1h exposure) (Cottin et al., 2010b; Ravaux et al., 2003). Additional experiments on *Mirocaris fortunata*, a species living in a cooler part of the thermal gradient, suggested a similar thermal tolerance with a $CT_{max}$ of approximately 36°C (Shillito et al., 2006) and the presence of heat shock proteins, although their expression threshold remain unknown (Ravaux et al., 2007). These heat shock proteins were highly expressed in *R. exoculata* after an exposure of 1h at 30°C, especially in comparison to coastal shrimp (*Palaemonetes varians*) – 400 fold versus 15 fold of increase respectively – (Cottin et al., 2010b). However, natural populations always displayed very low level of expression of these proteins at Rainbow, TAG or Snake Pit (Ravaux et al., 2009, 2019).

Recently, the thermal tolerance of *R. exoculata* was redefined by assessing the effect of the duration time of the heat shock on the molecular and the behavioral response of those shrimps (Ravaux et al., 2019) (**Fig 45.**). Indeed heat shock of 30°C conducted for 10 min and 30 min did not revealed any up regulation of hsp70 proteins unlike experiments carried for 60 min. Their expression was found to be higher compared to control expression levels only at 35°C and 39°C for a 10 min heat shock. Additionally, the shrimp mortality at 39°C was only of 35% for the 10 min experiments whereas all individuals were found dead when exposed to only 33°C for 60 min (Ravaux et al., 2003, 2019). This revealed that *R. exoculata* are able to tolerate easily high temperatures, above 35°C, but for short periods only, few minutes of exposure. With this redefinition of the thermal tolerance, a more satisfying explanation of the low expression level of heat-shock proteins in natural populations can be brought. As shrimps are always swimming, they probably never experience temperature above 40°C for more than few seconds/minutes (**Fig 45.** and discussion above.)

Behavior of *R. exoculata* was also strongly affected by the heat treatment in the pressure vessels. At temperatures above 30°C, a higher proportion of actively swimming shrimps and a lower number of shrimps packed in aggregates were observed (Ravaux et al., 2019). This was suggested to be an escape response to avoid cellular damages by the thermal stress with an onset of 30°C that coincides with the onset of the molecular response for prolonged exposure over 10 min. Moreover, observations of a "maintained aggregate" behavior in the pressure vessels in absence to any environmental cues suggest as well that *R. exoculata* shrimps form active and social "self-organize"

swarms – by analogy with bee swarms – of individuals. This cohesion would therefore be maintained because of the many derived benefits – protection from predators, location of ressources more effectively, facilitation of mate finding and reproduction … (Ritz et al., 2011) – of the cohesion itself for the individual, rather than being the result of a collective response of individuals seeking similar resources and/or temperature conditions within their habitat (Ravaux et al., 2019).

Acquisition of thermal tolerance in early life stages remains to be explored in *R. exoculata*. It might likely differ from adult thermal tolerance, as suggested for *Palaemonetes elegans*, a coastal caridean shrimp often used as a comparative model in alvinocaridid physiological studies. Adults of this species exhibited a higher $CT_{max}$ – about 32°C – than larvae – between 25°C and 29°C according to developmental stages (Ravaux et al., 2016). No hsp70 expression could be observed before the juvenile metamorphosis and this late acquisition of the thermal tolerance was hypothesized to be an adaptive response to the environmental change from the open ocean habitat where larvae experience rather constant temperatures, to the highly variable intertidal habitat where adults live (Ravaux et al., 2016). Similar patterns could therefore be expected between *Rimicaris* larvae and juvenile stages upon their recruitment in the hydrothermal vent field.

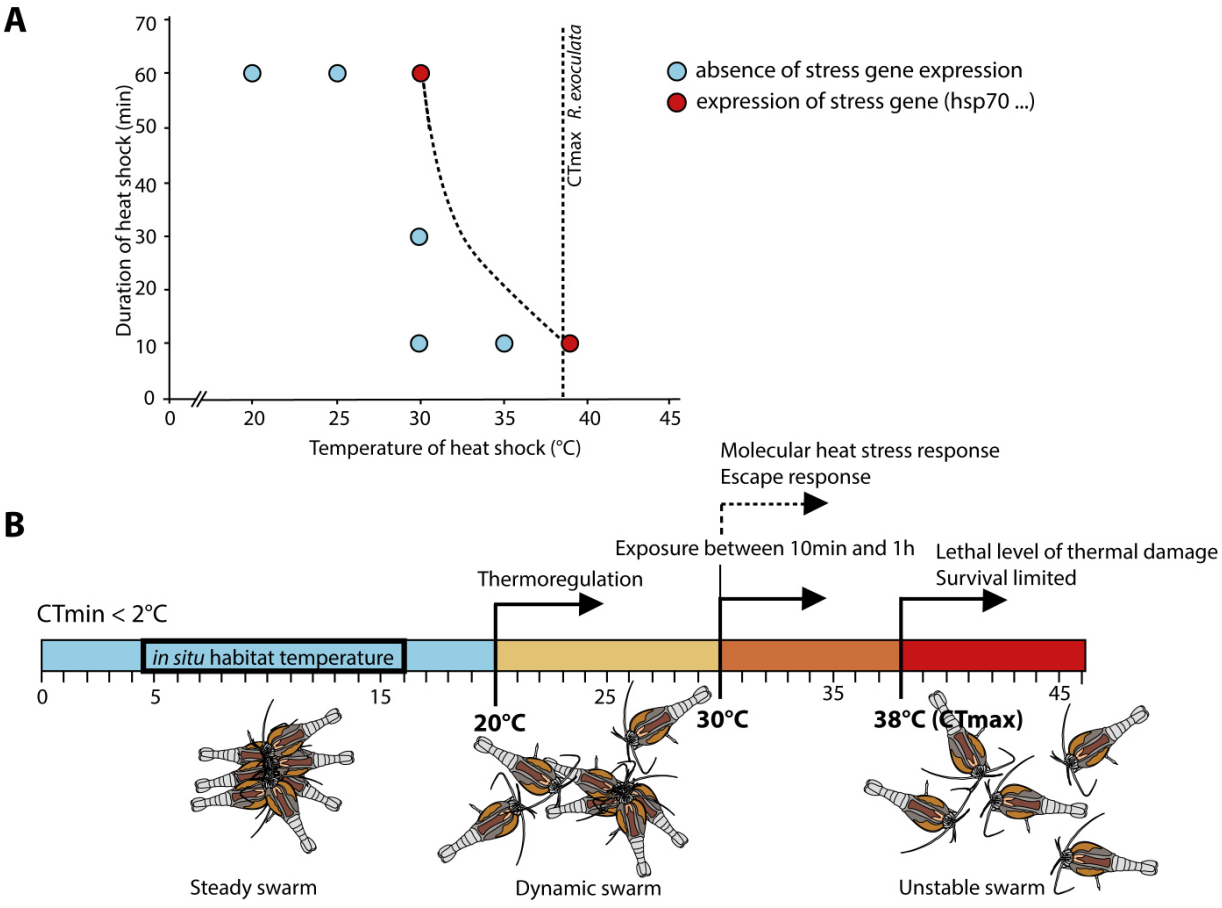


**Fig 45**. Thermal tolerance of *Rimicaris exoculata* shrimps. From Ravaux et al. (2019).

Sensorial abilities of *Rimicaris* shrimps, although essential in ecological studies to understand how these animals perceive and interact with their environment, have only been explored by few studies on their potential visual and olfactory capacities, some of which still remaining speculative.

## P.2 RIMICARIS SPECIES AS MODEL ORGANISMS TO STUDY LIFECYCLES IN HYDROTHERMAL VENTS

One of the very particular characteristic of *Rimicaris exoculata* is its visual organ, – from which comes its species name: *exoculata* – an ocular plate that extends to the middle of the cephalothorax in a large bilobed organ connected by large nerve tracts to the brain (Van Dover et al., 1989). This organ is formed by the fusion of the eyes, separated in juveniles, and corresponds to one of the major morphological changes occurring during their metamorphosis into adult (Gaten et al., 1998; Komai and Segonzac, 2008). Although no image-forming optic structures could be observed, the implication of this particular organ in the vision of the shrimp is supported by the presence of rhodopsin and photoreceptors, potentially detecting low-level illumination (Van Dover et al., 1989). A more detailed study of the organization of this organ revealed photoreceptor cells with greatly hypertrophied rhabdom segment – a central tube to optimize the light transport to the photoreceptor cells – that occupies 70% to 80% of the volume of this retinal region which greatly differ from shallow water shrimp species (Jinks et al., 1998). In *Rimicaris chacei* and *Mirocaris fortunata*, the structural organization of the ocular plate was similar although the eyes of these species are not completely fused like *R. exoculata*. Eyes of *Alvinocaris markensis* differ strongly, being separated but also atrophied with degenerated and disorganized photoreceptors cells (Jinks et al., 1998). Observations of early life stages revealed a more typical crustacean eye organization, with the presence of cone cells in prezoea larvae of *Mirocaris fortunata* and in the oldest eye tissue part of *Rimicaris* juveniles,suggesting a change of their visual abilities along their life cycle (Gaten et al., 1998; Komai and Segonzac, 2008).

According to the spectral sensitivity of their rhodopsin pigments, as well as their high concentrations, eyes of *R. exoculata* were hypothesized to potentially detect the black body radiation emitted by the hot vent fluids (Pelli and Chamberlain, 1989). Although being an interesting hypothesis, caution is required with this statement since it is only based on theoretical physics calculations of the emission and absorption wavelengths (Pelli and Chamberlain, 1989). Therefore, further behavioral studies on light-responses of *Rimicaris* shrimps, which have failed to trigger any response so far (Jinks et al., 1998), need to be conducted to confirm this. Moreover, even if it is tempting to infer a visual role for this intriguing organ based on the presence of a photoreceptor pigment, it is not necessarily this function that rhodopsin perform *in situ* in this animal. As stated by the concept of “Molecular Tinkering” (Jacob, 1977), similar proteins can have different role in different species as it has been widely showed in symbiotic interactions where partner selection mechanisms arise from proteins of the immune system and have even been attributed to respiratory pigments (Coates and Decker, 2016; Kremer et al., 2014; McFall-Ngai et al., 2012).

Chemoreception in alvinocaridid shrimps is mediated by chemosensory sensilla mainly localized on antennae and antennules like in other crustaceans (Zbinden et al., 2017). Some specialized sensilla, the aesthetascs, house olfactory receptor neurons that carry the chemical signal to the central nervous system. No specific adaptation regarding the size or number of aesthetascs could be observed in alvinocaridids in comparison to coastal shrimp species (Zbinden et al., 2017). Nonetheless, a dense coat of filamentous bacteria mainly affiliated to the shrimp symbiotic community was observed on the surfaces of those appendages (Zbinden et al., 2018). Such bacterial coat is absent from coastal shrimp species whose antennae and antennule surfaces were almost clear of epibionts. Bacteria on alvinocaridid antennae and antennules could protect them from the harsh vent chemicals but could also alter the chemical cues reaching the animal or isolate and filter other information (thermal isolation, shock absorption …) (Zbinden et al., 2018).

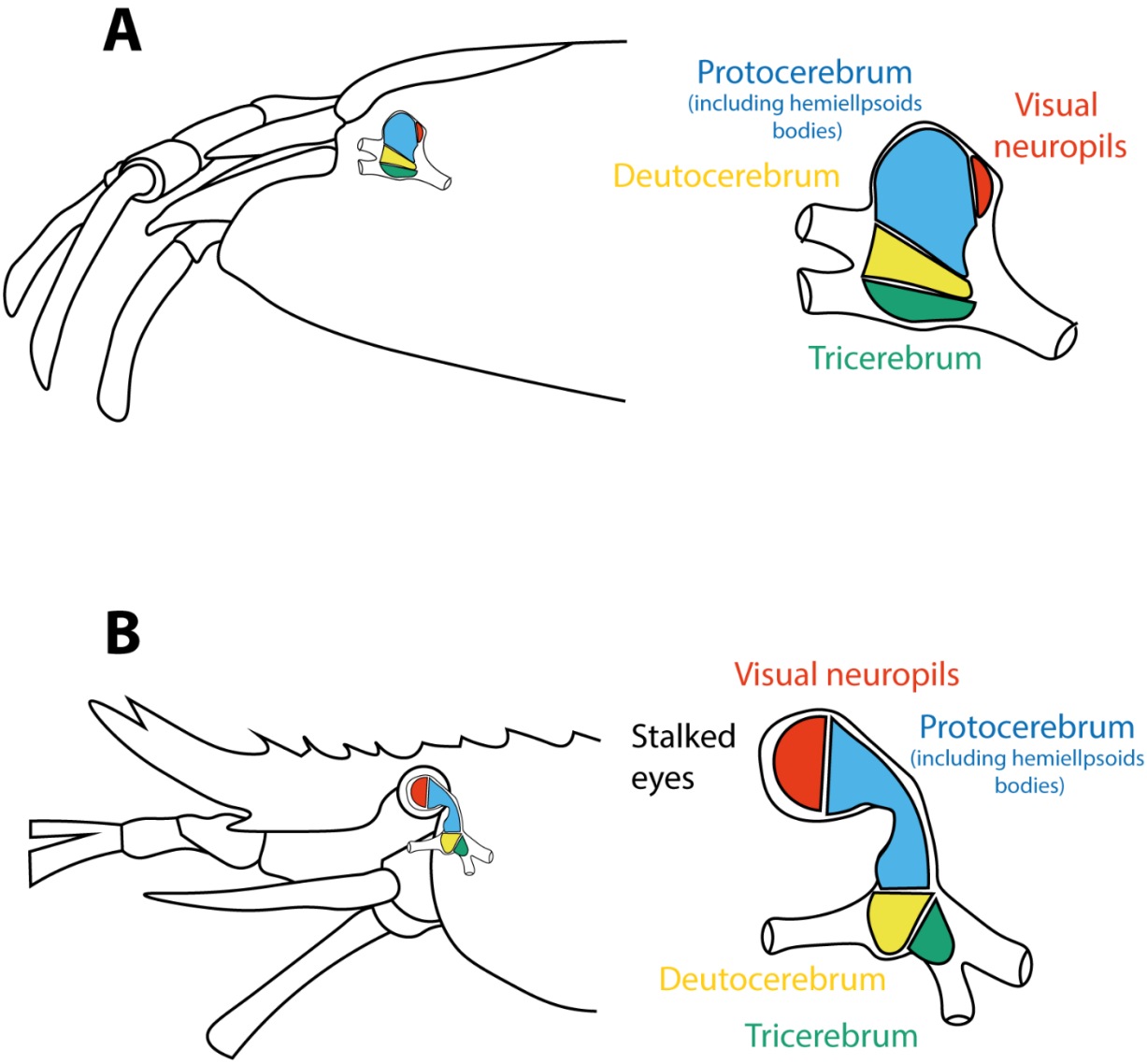


**Fig 46**. Neuroanatomy of **A.** *R. exoculata* compared to **B.** the one of coastal shrimp, *Palaemonetes elegans* with the overall organization of their brains. Simplified from (Machon et al. 2019)

Earlier work revealed that *R. exoculata* shrimps were able to detect sulfide with their antennae (Jinks et al., 1998; Renninger et al., 1995). With the development of a new electrophysiological approach adapted to crustaceans, detection capacities of these organs were tested as well for *Mirocaris fortunata* (Machon et al., 2016). Both sulfide and food extracts – that could correspond to short distance vent fluid signals – could be detected by the shrimps, but not iron or manganese – that could correspond to long distance vent fluid signals (Machon et al., 2018). However, electroantenography (EAG) responses were obtained for both *R. exoculata* and *M. fortunata* but at sulfide concentrations much higher than those encountered in their natural habitat (Machon et al., 2018; Renninger et al., 1995). Moreover, no clear specific behavioral answer could be observed at those sulfide concentrations for any of the two species, leaving a doubt on the ecological relevance of this detection ability *in situ* (Machon et al., 2018; Machon and Ravaux, personal communication in Zbinden et al., 2018). Extending these recent works on alvinocaridids olfaction to their early life stage would be of key importance to understand how larval stages could find their way back to the vent

fields after the dispersal phase and how they are able to interact with their own environment during these life stages. More behavioral observations on their exact visual abilities should be conducted as well.

Olfactory and visual informations are integrated by their higher integrative centers – i.e. the brain (Machon et al., 2019). This organ presents a particular anatomy in these animals with very small visual and olfactory neuropils and well-developed hemiellipsoids bodies (**Fig 47.**). Combined with observations of their olfactory abilities, it seems that olfaction is probably not a dominant sensory ability in *R. exoculata* (Machon et al., 2019), unlike what has been proposed so far (Renninger et al., 1995). On the other hand, despite their reduction, visual neuropils are maintained, unlike some other crustaceans living in dim-light conditions or complete darkness (Brenneis and Richter, 2010; Fanenbruck et al., 2004; Ramm and Scholtz, 2017; Stegner et al., 2015). The existence of a functional visual system in these animals may mean that there is "light" to exploit in their environment. At last, the large hemiellipsoids bodies have been proposed to play a role in place memory for their navigation strategies, as suggested previously by (Wolff et al., 2017). Although this hypothesis remains speculative, it is further supported by the presence of serotonergic tracts within this part of the brain (Machon et al., 2019), since serotonin has a function for place memory and learning in insects (Sitaraman et al., 2008). This would also explain the exploratory behavior of these shrimps, observed by many researchers during dives with ROV or HOV (including personal observations), moving around and touching the submersible and every instruments they encountered. Since organization of the visual organs dramatically changes between juveniles and adults of *R. exoculata*, it would be particularly interesting to compare the organization of the brain with the size of its different areas – in particular the hemiellipsoids bodies and the visual neuropils –along the ontogeny of the animal.

## P.2.4 The hypothesized lifecycle of *Rimicaris* shrimps

### P.2.4.1 Reproduction and population structure of *Rimicaris* shrimps

Research efforts on *Rimicaris* shrimp have focused at first on the trophic behavior and on the physiological abilities of those animals (Van Dover et al., 1988, 1989) (cf. part 2.1.2 and 2.1.3) whereas less attention has been paid on the main characteristics of their lifecycle such as their reproduction and their larval life. This can be partially explained by the recurrent absence of collected specimens for those specific life stages.

Indeed, the earlier work on reproduction of the alvinocaridids from the MAR – *Rimicaris exoculata*, *Rimicaris chacei* and *Mirocaris fortunata* – where faced with a paradox (Ramirez-Llodra et al., 2000). Oocyte-size-frequency analyses revealed an absence of synchronicity in the gametogenesis within the population of these species suggesting a continuous reproduction for all of these species (Copley et al., 2007; Ramirez-Llodra et al., 2000). However, brooding female individuals were absent or limited to one or two individuals in sample of *R. exoculata* and one individual in total for *R. chacei* in all the sampling periods – mostly between June and November – conducted so far at that time. Conversely, *Mirocaris fortunata* brooding females were regularly collected in large numbers, relatively to the total population size, in almost every sampling expeditions (Ramirez-Llodra et al., 2000). The polymodal population structure observed for *R. exoculata*, which suggests discrete recruitment events for this species, was also contrasting with this asynchronous reproduction for which a continuous

reproductive output and a continuous recruitment would be usually expected (Copley, 1998). Rather than a seasonal pattern, the absence of brooding females for *R. exoculata* and *R. chacei* was explained by their migration in the periphery of the active vent sites – a hypothesis which has proved to be valid for *Kiwa tyleri* (Marsh et al., 2015) – to protect their embryos from the harsh vent fluids (Ramirez-Llodra et al., 2000).

First evidence of seasonality in alvinocaridids was brought by a study on *Alvinocaris stactophila* living in cold seeps of the Gulf of Mexico. Analyses of oocyte-size frequency distributions revealed an important synchrony within the population with only small previtellogenic oocytes in females collected in spring and only large oocytes in females collected in summer and later, the largest being found during the autumn (Copley and Young, 2006). Additionally, brooding females could only be collected between November and March, with mostly early embryos in November and many broods ready to hatch in March. As for many other studies on deep-sea species where seasonal patterns were observed, this study proposed that photosynthetic surface production falling down to the cold seep could explain this seasonal pattern, the larval release in early spring timing with the peak of surface productivity (Copley and Young, 2006).

| SPECIE | *Alvinocaris muricola* (n = 9) | *Alvinocaris stactophila* (n= 55) | *Alvinocaris stactophila* (n= 65) | *Mirocaris fortunata* (n= 30) | *Rimicaris exoculata* (n= 47) | *Rimicaris exoculata* (n= 45) | *Rimicaris hybisae* (n= 562) | *Rimicaris hybisae* (n= 397) |
|---|---|---|---|---|---|---|---|---|
| **SITE** | **Congo Basin (seep)** | **Gulf Mexico: Brine Pool IMB (seep)** | **Gulf Mexico: Brine Pool MMB (seep)** | **MAR: Lucky Strike (vent)** | **MAR: TAG (vent)** | **MAR: Snake Pit (vent)** | **MCSC: Piccard (vent)** | **MCSC: Von Damm (vent)** |
| Depth (m) | 3113-3150 | 500 | | 1690 | 3650 | 3500 | 4972 | 2294 |
| **SIZE & FECUNDITY** | | | | | | | | |
| CL (mm) Mean ± SD | 20.7 ± 2.3 | 3.77 | 3.91 | 7.17 ± 0.18 | 15.7 ± 1.43 | 17.5 ± 1.37 | 10.2 ± 1.5 | 13.9 ± 2.3 |
| Realized Fecundity Mean ± SD | 3130 ± 1180.9 | 147 | 98 | 174.7 ± 22.8 | 591 ± 205 | 1045 ± 287 | 341.7 ± 146.2 | 1054.2 ± 229.8 |
| Size-Specific Fecundity Mean ± SD | 149.1 ± 48.0 | 39 | 25 | 24.3 | 37.3 ± 11.4 | 59.3 ± 13.4 | 30.6 ± 11.8 | 68.0 ± 13.2 |
| **EGG SIZE** | | | | | | | | |
| Mean all stage embryo size (mm) | 0.66 x 0.55 | 0.80 | 0.79 x 0.57 | 0.70 x 0.49 | 0.78 x 0.62 | 0.80 x 0.64 | 0.64 x 0.48 | 0.63 x 0.48 |
| Mean early stage embryo size (mm) | - | - | - | - | 0.70 x 0.60 | 0.73 x 0.63 | - | - |
| Mean mid stage embryo size (mm) | - | - | - | - | 0.80 x 0.62 | 0.82 x 0.64 | - | - |
| Mean late stage embryo size (mm) | - | - | - | - | 0.87 x 0.65 | 0.85 x 0.66 | - | - |
| **TEMPORAL & SPATIAL PATTERNS** | | | | | | | | |
| Spatial location | Periphery of fluids | Periphery of fluids | Periphery of fluids | Close to fluids | Close to fluids | Close to fluids | Close to fluids | Close to fluids |
| Periodicity | - | Seasonal | Seasonal | Continuous | Seasonal | Seasonal | Seasonal | Seasonal |
| References | Ramirez-Llodra & Segonzac (2006) | Copley & Young (2006) | Copley & Young (2006) | Ramirez-Llodra et al. (2000) | Hernández-Ávila et al. (in prep) | Hernández-Ávila et al. (in prep) | Nye et al. (2013) | Nye et al. (2013) |

**Table 2.** Summary of the documented alvinocaridids reproductive characteristics. Adapted from Nye et al. (2013).

However, it was not until later that a seasonal reproduction was suggested for an alvinocaridid inhabiting hydrothermal vents (**Fig 47.** and **Table 1.**). In *R. hybisae*, a large number of brooding females were collected in January and February whereas a complete absence of those females was reported in July and August (Watanabe personnal communication; Nye, 2013; Nye et al., 2013). Oocyte-size frequency distribution was asynchronous and variable between females from different samples although with a greater degree of synchrony than what was reported for *R. exoculata* (Nye et al., 2013). Embryonic development of *Rimicaris hybisae* was also clearly asynchronous between females collected at the same time, suggesting an asynchronous larval release with several larval pools (Nye et al., 2013).

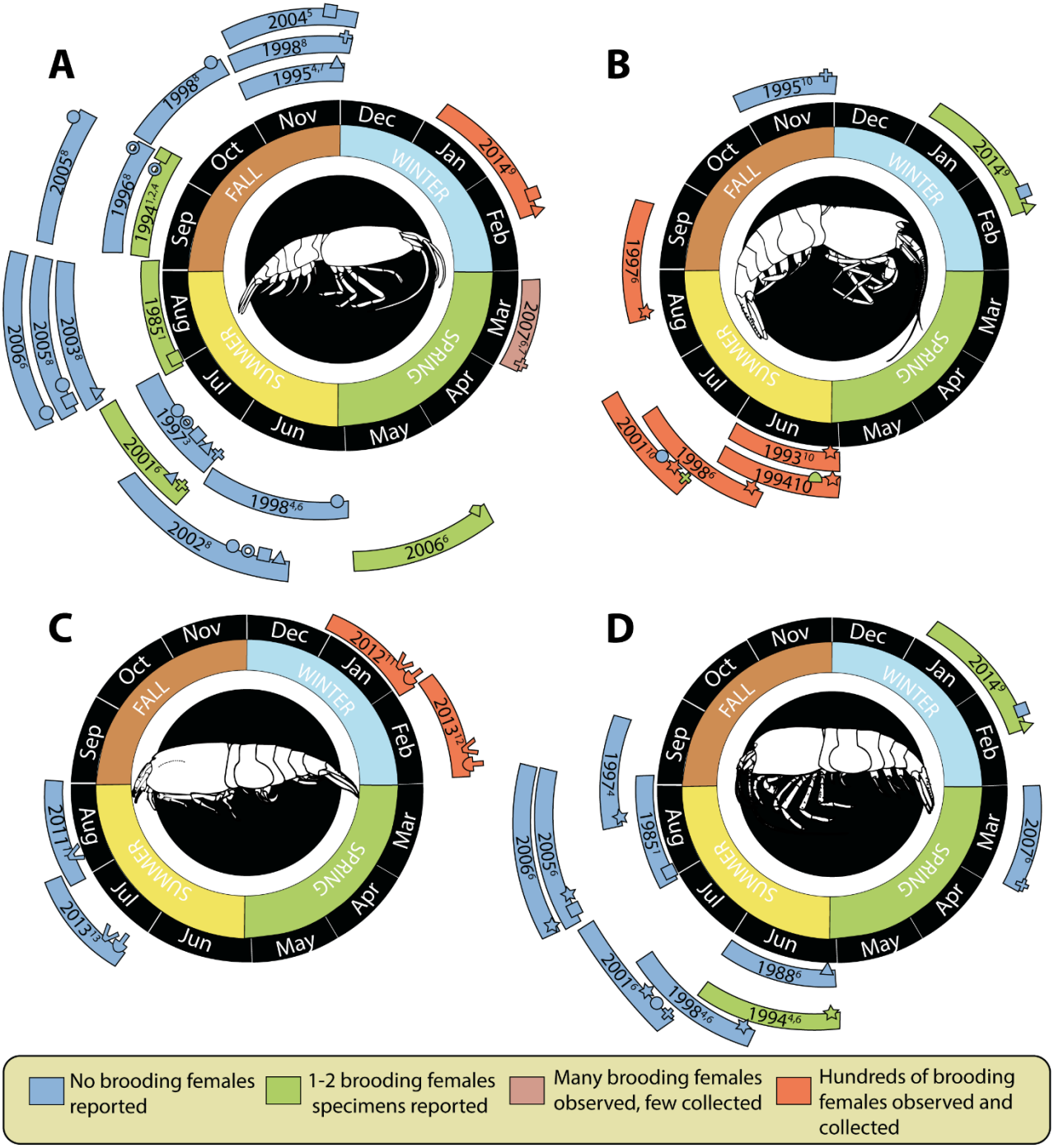


[1]Williams and Rona (1986), [2]Vereshchaka (1997), [3]Shank et al. (1998), [4]Ramirez-Llodra et al. (2000), [5]Copley et al. (2007), [6]Komai and Segonzac (2008), [7]Gebruk et al. (2010), Guri et al. (2012), [8]Lunina & Vereshchaka (2014), [9]Hernández-Ávila Thesis (2016) & Cruise Repport BICOSE (2014), [10]Komai and Segonzac (2003), [11]Nye et al. (2013),[12]Nye Ph.D. Thesis (2013) [13]Watanabe *personnal communication*

**Fig 48.** Current knowledge on the occurrence of brooding females in hydrothermal vent alvinocaridids at different periods of the year. **A.** *Rimicaris exoculata*. **B.** *Mirocaris fortunata*. **C.** *Rimicaris hybisae*. **D.** *Rimicaris chacei*.

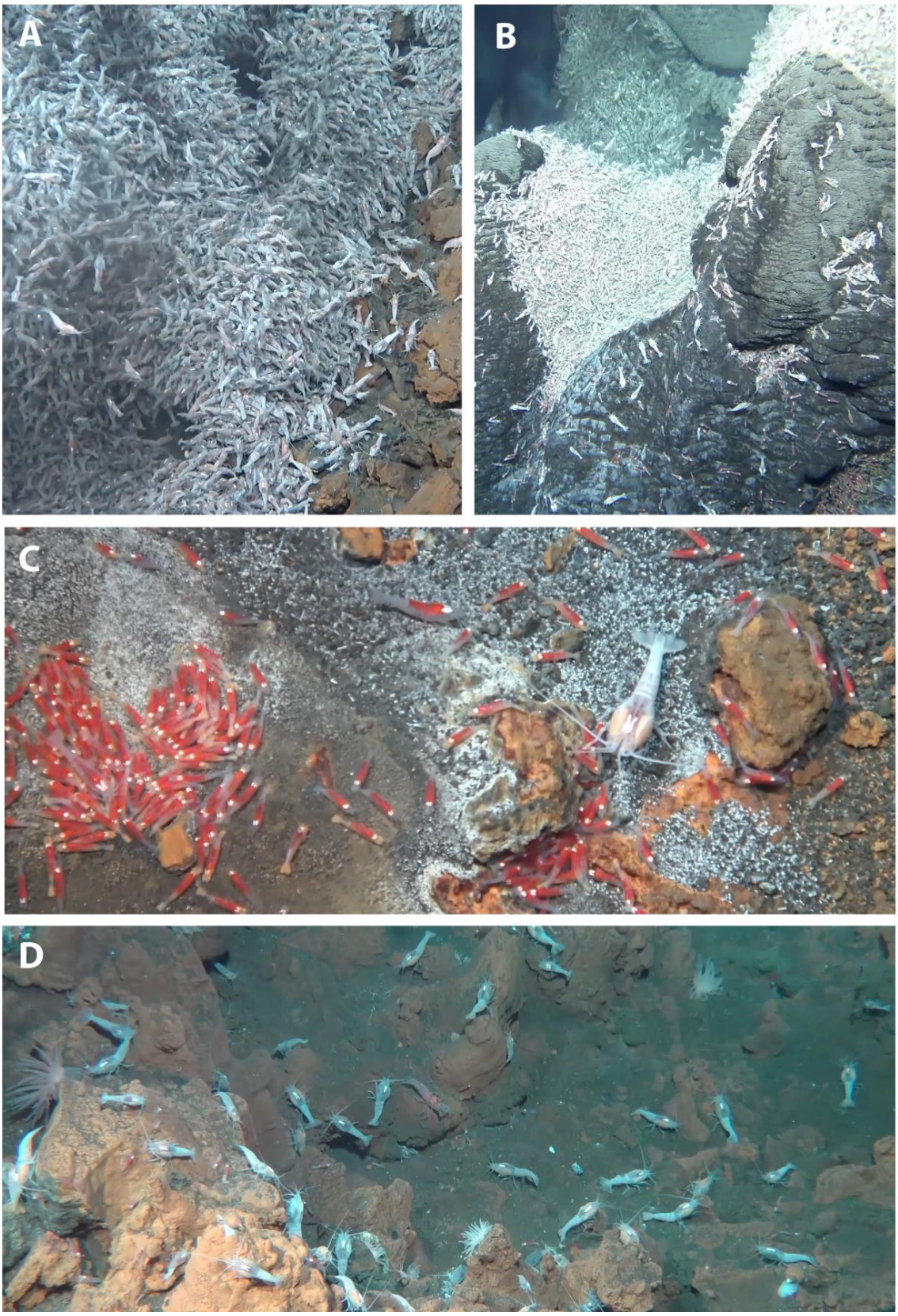


**Fig 49**. Local distribution of *Rimicaris* shrimps in different types of assemblages at the TAG and Snake Pit vent fields. **A.** Dense aggregates of *R. exoculata* adults from TAG. **B.** Dense aggregates of *R. exoculata* adults from Snake Pit. **C.** "Nurseries" of small alvinocaridid juveniles at TAG **D**. Scattered shrimps sparsely distributed at the periphery of the aggregates at TAG. Assemblages defined by Hernández-Ávila (2016).

In addition to these observations in *R. hybisae*, the brooding migration hypothesis in *R. exoculata* was also severely weaken by the presence of some brooding females within the aggregates close to the vent emissions in March 2007 at the Logatchev vent field (Gebruk et al., 2010; Guri et al., 2012). This hypothesis was definitely discarded more recently in January 2014 –BICOSE expedition – when a complete absence of those brooding females in shrimp samples collected from the periphery was reported. Indeed, large numbers of brooding females were collected at the same period within the dense aggregates both at TAG and Snake Pit vent fields (Hernández-Ávila, 2016) (**Fig 47.**). This same study also revealed an interesting spatial pattern between the *R. exoculata* collected within aggregations close to the vent fluids – at TAG and Snake Pit – and the *R. exoculata* individuals distributed sparsely at the periphery – only at TAG – (**Fig 48.**). In aggregates, sex ratio was strongly biased toward females, these ones representing between 61 and 97% of the sexed specimens, whereas the opposite was found for those at the periphery with a large dominance of males (Hernández-Ávila, 2016). These locally biased sex ratios in *R. exoculata* were not as pronounced in the case *R. hybisae*, although they seemed to share a similar ecology with an organization in dense aggregates close to the vent emissions (cf. part 2.1.1).

Large aggregations of small alvinocaridid juveniles were also discovered close to shimmering vent emissions at TAG during the BICOSE expedition (Hernández-Ávila, 2016). These juveniles were similar to *R. exoculata* earlier juvenile stages but COI barcoding of these individuals surprisingly identified them as *R. chacei* juveniles. Given the extended repartition of these nurseries harboring high densities of juveniles, it appeared that *R. chacei* is probably more abundant than expected in these MAR vent fields, at least for their juvenile stages, and likely constitute a more important component in these ecosystems than previously thought (Hernández-Ávila, 2016).

Since earlier *R. exoculata* juveniles – stage A juveniles – and *R. chacei* juveniles were described as very similar, only distinguishable by few characters that required a careful examination of the specimens (Komai and Segonzac, 2008), it is still unclear if there is a misidentification of their juveniles in the current taxonomy, or if *R. exoculata* stage A juveniles were simply absent from these nurseries. Therefore, a proper taxonomic reassessment of the *Rimicaris* juveniles from the MAR coupled with individual barcoding is required to settle this issue. Once this juvenile identification will be properly assessed, population structure of *Rimicaris chacei* should be explored and compared with other documented alvinocaridids, as well as its reproductive characteristics, if a sufficient number of brooding females can be sampled.

### 2.1.4.1 Larval dispersal and recruitment in *Rimicaris* shrimps

Larval stages of *Rimicaris* shrimps remain a true black box and are undoubtedly one of the major locks that prevents from a more comprehensive and global understanding of the life cycle of these species.

Whereas many hydrothermal vent species have populations that reflect genetic structure and limited migrant exchanges (Chen et al., 2015a; Hurtado et al., 2004; Won et al., 2003), all alvinocaridid species investigated so far exhibit a high connectivity and a lack of genetic structure between populations. For example, COI haplotype networks of *R. kairei* and *R. variabilis* exhibited no genetic structure between populations of Solitaire and Kairei vent fields or between populations of the Manus and the Fidji basin respectively (Beedessee et al., 2013; Thaler et al., 2014). Similarly, populations of *Shinkaicaris leurokolos*, *Alvinocaris longirostris* or *Alvinocaris marimonte* did not show any genetic

structure all along their distribution area in the Okinawa through, neither between the Okinawa and Sagami bay populations for *A. longirostris* or between the Okinawa and Izu Bonin arc populations for *Alvinocaris marimonte* (Yahagi et al., 2015). This absence of genetic structure with COI haplotypes could be related to the apparent low mutation rates of this gene in alvinocaridids (Shank et al., 1999; Teixeira et al., 2011) in comparison to other crustacean species (Knowlton and Weigt, 1998; Schubart et al., 1998). Therefore, studies using a single marker gene like the COI might not represent the current dispersal occurring between the different populations. Yet, studies using several microsatellites loci were still congruent with large scale gene flows between the different *R. exoculata* populations from Rainbow to 5°S MAR vent fields, and even between the species complex *A. markensis*/*A. muricola* of the Gulf of Mexico cold seeps, the Congo pockmarks and the hydrothermal vents of the MAR (Teixeira et al., 2012, 2013).

Because of this extensive connectivity, a very large potential for dispersal is expected in alvinocaridid shrimps. Unfortunately, sampling of those life stages is limited to early hatched individuals or few early zoeal stages collected close to the vent field for some species (Hernández-Ávila et al., 2015; Miyake et al., 2010). Information about their larval life has also been inferred from $\delta^{13}C$ isotopes and lipids composition of their early juvenile stages. Indeed, several "typical photosynthetic" lipids markers – like C20:4n6 or C22:6n3 fatty acids – were retrieved abundantly in the juveniles stages of several alvinocaridid species identified as *R. exoculata*, *R. chacei, A. markensis*, *M. fortunata*, *O. loihi* and *A. marimonte* (Pond et al., 1997b, 1997a, 2000; Stevens et al., 2008). These lipids and isotopic compositions also varied along ontogeny of those shrimps, showing "chemosynthetic" signatures in adults and "photosynthetic" signatures in juveniles (Pond et al., 1997b, 1997a, 2000; Stevens et al., 2008). This has led some authors to suggest a vertical migration of alvinocaridid larvae that would inhabit the upper part of the water column for at least a part of their larval life (Copley et al., 1998; Dixon et al., 1998b). Since surface currents are stronger, enabling larval transport on larger distances, this hypothesis would also be congruent with the large connectivity observed in alvinocaridids. However, similar "photosynthetic" signatures were also found in bathypelagic shrimps and in the surrounding micronekton collected above the MAR axial valley at 2000 m depth (Pond et al., 1999). Therefore, vertical migration of alvinocaridid larvae does not necessarily extend up to the photic zone. Additionally, recent findings highlighted that biosynthesis of some of these typical photosynthetic lipid markers could also be performed by deep-sea bacteria (Fang et al., 2006). Therefore, these lipid markers could also be potentially produced by *Rimicaris exoculata* digestive symbionts – Mollicutes and *Deferribacteres* – whose metabolisms are still unknown (Durand et al., 2010) or by other environmental bacteria within the hydrothermal vent field. Furthermore, reared larvae of *M. fortunata* – obtained from hatched broods – were active and survived at different pressures, between 1 and 300 atm at 10°C, but not in low pressure conditions (1 atm) at 20°C (Tyler and Dixon, 2000). This suggests that at least some alvinocaridid species cannot tolerate the environmental conditions of the photic zone. To date, sample records of early alvinocaridid juveniles outside the vent field are limited to a maximum of 100 km further the closest vent field, between 2000 m and 3000 m depth in the water column above the MAR and between 1500 m and 3000 m depth above the CIR (Herring, 2006; Herring and Dixon, 1998).

Athough isotopic values of juvenile stages suggest a planktotrophic larval life in alvinocaridids, detailed examination of the morphology of early zoea larvae revealed a primary lecithotrophic phase. Indeed, pleopod appendages were absent and their mouthparts were clearly undeveloped (Hernández-Ávila et al., 2015). Without feeding capacity and with the presence of large lipid storages,

this suggests a primary lecitotrophic larval phase as well as an extended larval development in alvinocaridids larvae (**Fig 49.**). In addition, without their appendages, swimming capacities of these larvae are limited and their vertical migration might be postponed to latter larval stages – although a vertical transport through the vent plume is still possible.

The length of this lecitotrophic phase is however unknown and should be explored with *in vivo* rearing of alvinocaridid larvae and observations of the external and internal anatomy – by coupling different techniques such as electron microscopy, traditional dissections and CT-scan with 3D tomography – at different rearing length. Other characteristics of these larvae such as their exact lipid storage content – that could be obtained with elemental analysis as in *K. tyleri* (Thatje et al., 2015b) – or their behavior – swimming speed, level of activity, survival – at different environmental conditions could provide valuable information to better estimate their PLD and potential larval trajectories with biophysical models.

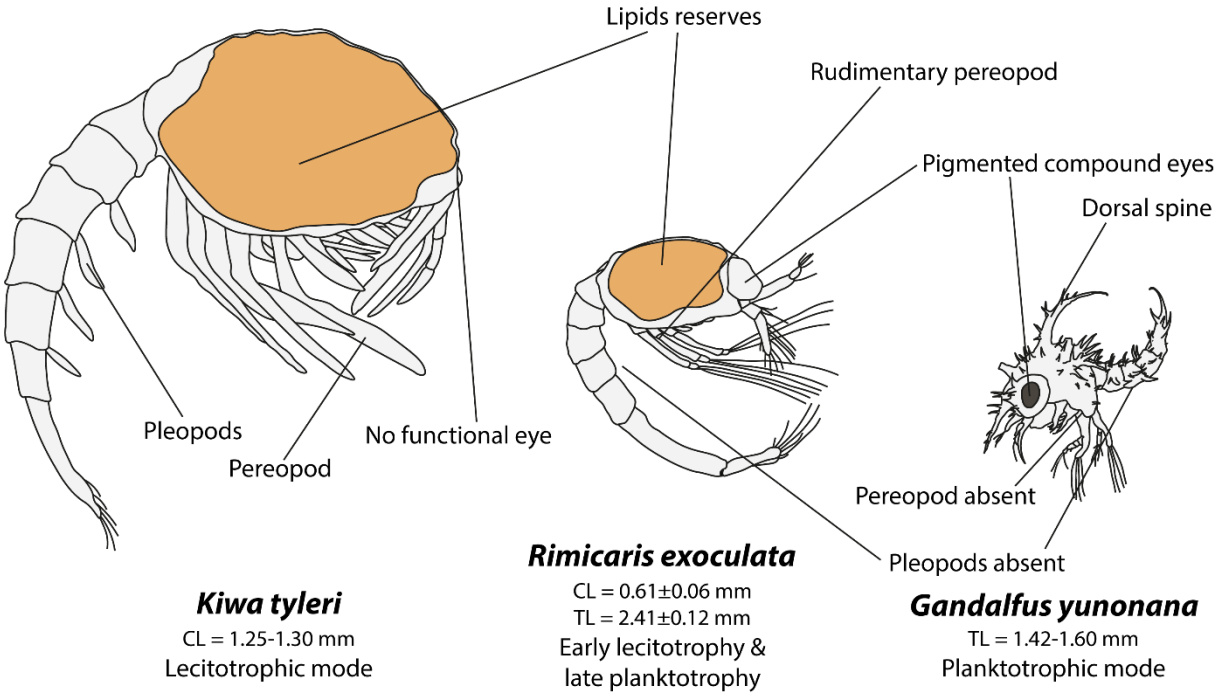


**Fig 50**. Morphological comparison between first zoeal larval stages of alvinocaridids and first zoeal stages of others hydrothermal vent crustaceans. Adapted from Nakajima et al. (2010), Thatje et al. (2015) and Hernández-Ávila et al. (2015).

However, rearing these early life stages remain a challenging task as the transition to certain development stages could only be triggered by specific conditions – temperature as seen in alvinellids (Pradillon et al., 2001) or pressure for instance – that correspond to the transition experienced in their environment, an environment that is still unknown. Attempts to rear larvae of *S. leurokolos* and *A. longirostris* inhabiting relatively shallow vent fields – between 200 m and 2200 m depth – were conducted at atmospheric pressure with broods incubated until hatching (Watanabe et al., 2016). In this experiment, larvae were further maintained without feeding up to 150 days. No apparent morphological changes in their external anatomy were noted although modifications of their internal anatomy might have occurred. However, many individuals presented abnormal morphologies after hatching with shortened abdomen, the proportion of abnormal individuals increasing with higher

brooding temperature. Larval survival was also correlated to their rearing temperature with a lower survival at higher temperatures, which probably reflected the effect of an increased metabolism at higher temperatures (Watanabe et al., 2016). Additional rearing experiments following the scheme used for gastropods (Yahagi et al., 2017c) (cf. part 1.4.2.2. and **Fig 31.**), with fed and starved larva coupled with explorations of their internal anatomy at different time point should provide a more accurate view of their larval life. Similar experiments in *Rimicaris* from the MAR should also be conducted. They might however require the use of pressure tanks since those species have only been reported in much deeper vent fields – between 1500 m and 4000 m. Additionally, regarding the results of Watanabe and her colleagues (Watanabe et al., 2016) these under pressure experiments will probably have to be extended for periods exceeding possible durations on board during the expeditions.

# P.2 RIMICARIS SPECIES AS MODEL ORGANISMS TO STUDY LIFECYCLES IN HYDROTHERMAL VENTS

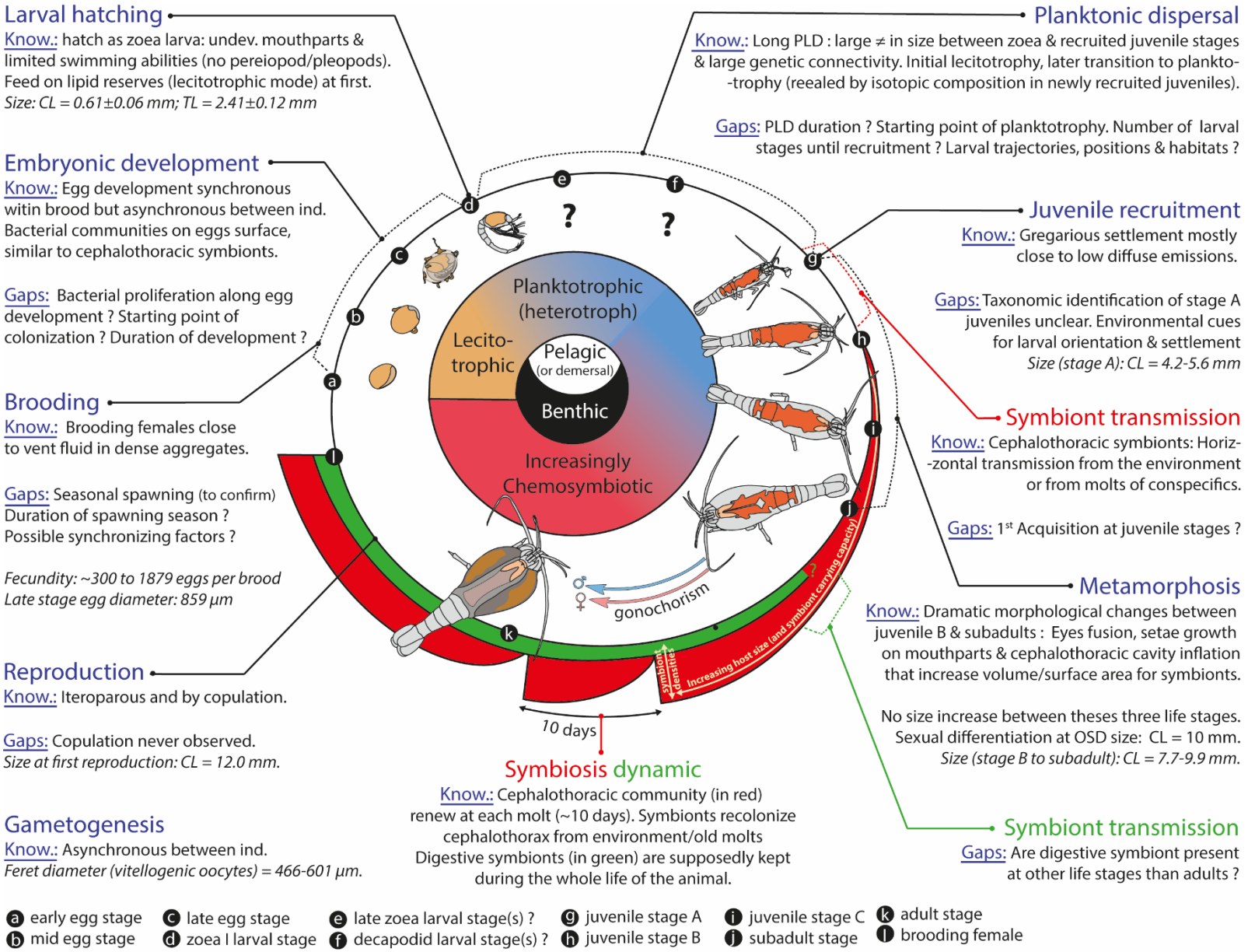


**Fig 51.** Diagram displaying of the alvinocaridid lifecycle indicating current knowledge and gaps in their reproductive characteristics, ontogenic development, larval transport, settlement and recruitment, symbiont acquisition pathways and habitat characteristics per life stages. Largely inspired from the diagram depicting the life cycles of bathymodiolin mussels of Laming et al. (2018)

# P.3 Aim of this study

Throughout the presentation of the *Rimicaris* model given in the introduction (part 2.1), current knowledge as well as persistent gaps in the understanding of the life cycle of these species have been highlighted (summarized by **Fig 50.**). The diagram presented in **Fig 50.** clearly points at several striking facts. First, the pelagic phase that corresponds to the dispersal period is basically unknown and constitutes probably the major gap. Despite this fact, many fundamental parts of the benthic phase, such as the brooding period, the embryonic development or the juvenile recruitment are also poorly understood. If we consider the holobiont, the two symbioses are relatively well described at adult stages, but their dynamic of acquisition and colonization along the rest of the lifecycle needs to be investigated. However, the most noticeable point is probably the fact that most of our knowledge on *Rimicaris* lifecycles have been acquired only from a single model: *Rimicaris exoculata*. The study of other *Rimicaris* species - or even other alvinocaridids – from different regions of the world is therefore a prerequisite to establish general rules that are representative of the whole shrimp family.

From this statement, the aim of this study is twofold: first, to characterize and compare the life history traits of certain critical life steps of these shrimps and secondly, to put the *Rimicaris* species symbioses into the temporal framework of their cycle of life. Precisely, the interspecific comparison will be done on three fundamental aspects: the fecundity and the brooding period, the demographic structure detailed per life stages as well as the ecological niche characterization for each of these stages, and finally the morphological and trophic transitions of the juvenile stages along their metamorphosis and recruitment.

These fundamental questions will be explored by using a taxon-focused approach, whose final purpose – beyond the scope of this single study – would be to propose, with all the informations gathered, a model of conservation for these species (Glover et al., 2018). Two species will receive a particular focus in this work: *Rimicaris exoculata* and *Rimicaris chacei* two co-occuring species of the Mid Atlantic Ridge, as they represent the two main “morphotypes” within the *Rimicaris* genus, which correspond to different degree of symbiosis dependence and of morphological modifications that result from it.

This work fits into the framework of the mineral exploration license of the seafloor massive sulfides (SMS) deposits of the MAR granted by the International Seabed Authority (ISA) to France (2014-2029) with a view for future exploitation (Dunn et al., 2018; Van Dover et al., 2018) (**Fig 51.**). The area covered by this licence comprises the TAG and Snake Pit vent fields, both hosting communities dominated by large populations *R. exoculata* shrimps and that served as study area for this work.

Given the extent of knowledge shortcoming currently existing on the life cycle of these species, this thesis focuses on some specific aspects divided in four different research axes:

The first research axis aims to explore the bacterial assemblages associated to *Rimicaris* early life stages with a focus on eggs of *R. exoculata* (cf. part 3.). This first study seeks to extend the preliminary observations made by (Guri et al., 2012) that found bacterial communities associated with the envelope of *Rimicaris* eggs. This work is articulated around two main questions: *i)* What are the

temporal - along the embryonic developpment - and spatial dynamics - within the brood - of bacterial colonization on *Rimicaris exoculata* eggs? *ii)* Are these bacterial communities specific to egg surfaces, thus suggesting a possible selection by the host, or similar to any body surface of these shrimps, then suggesting a simple fouling? The first question is explored with microscopic approaches – SEM and FISH – whereas the second one involves molecular techniques and bioinformatic anlyses – 16S metabarcoding. To attest the specificity of the egg bacterial assemblages, egg brood samples are compared with pleopod samples of the same mother, a body surface subjected to the same environmental conditions. This work also explores, in the light of the results obtained, new hypotheses of symbiont transmission along the *Rimicaris exoculata* lifecycle.

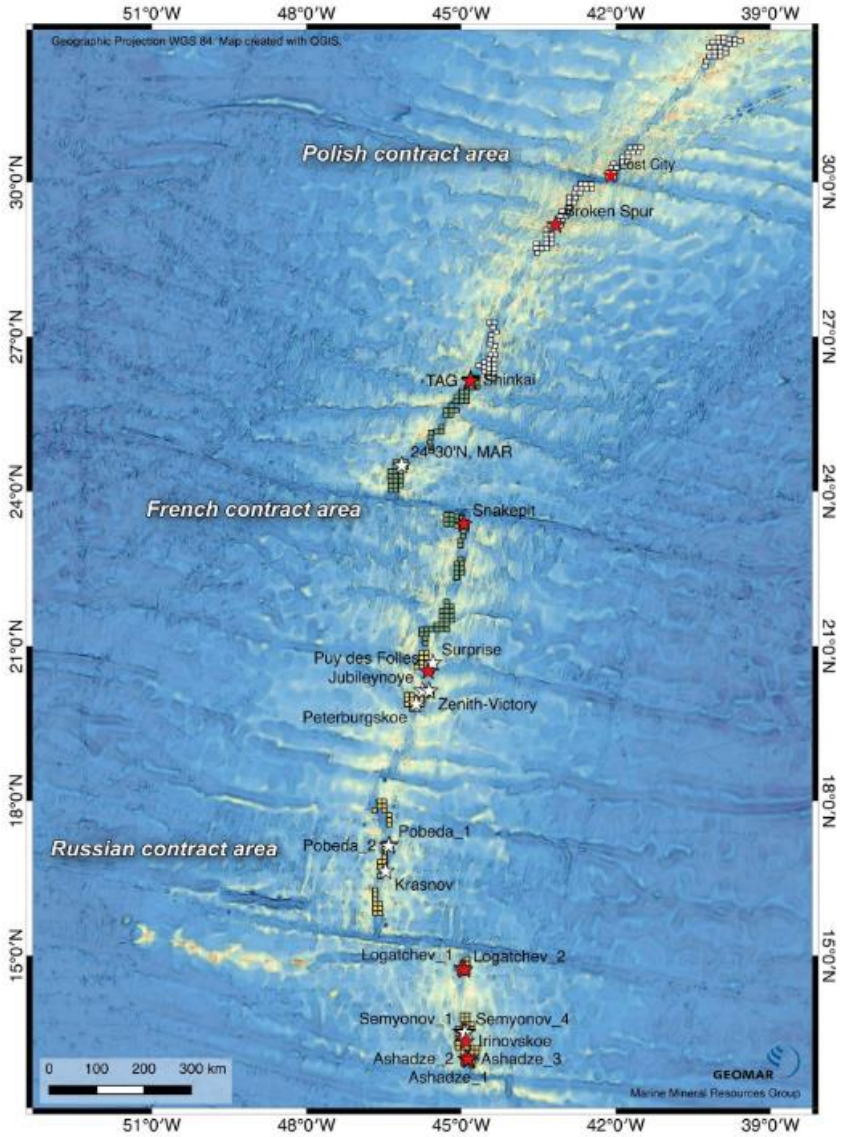


**Fig 52.** Contracted areas approved for exploration by the ISA in the Mid Atlantic Ridge, with the locations of known active vent ecosystems and inactive sulfide mounds. From Van Dover et al. (2018).

The second research axis seeks to solve the potential taxonomic issues in the identification of *Rimicaris* juveniles from the MAR that continue to persist today (cf. part 4.). This is be done by careful examination of morphological characters given by Komai & Segonzac (2008) to distinguish juveniles of *R. chacei* and *R. exoculata* coupled with individual barcode of each specimen. With this clarification,

the main purpose of this work is to see if the different degree of metamorphosis between the two species reflected the evolution of their trophic transition. This hypothesis is tested by using a stable isotopes approach using carbon and nitrogen, but also for the first time on these species, sulfur, to establish if the origin of their nutritional sources derived from a chemosynthetic or a photosynthetic primary production. By using an isotopic niche approach, this axis also compares the habitat use of each *Rimicaris* species and deciphers the potential competition existing between *R. exoculata* and *R. chacei*.

The third research axis aims to describe the population structure of *Rimicaris exoculata* and *Rimicaris chacei* (cf. part 5.). The main question of this part is to assess if all the differences observed previously in the second axis between the two species juveniles – recruitment size, trophic differences … - have an influence on their recruitment strategies. For that, a cohort analysis is applied to both compare recruitment process and mortality rate after this critical lifecycle step. With the clarification obtained in the second axis, another goal was to precisely assess the habitat of the different life stages, distributed in assemblages as seen before (Hernández-Ávila, 2016), and to characterize the ecological niche of these life stages, using thermal conditions as a proxy. Separated and repeated samples of different shrimps from different habitats defined visually constitute the base of this work. Using these data, a modelling approach to define the thermal niche – obtained by environmental measurement associated with each shrimp sample – of each species and each life stage per species, is used to assess the potential effect of temperature on the shrimp distribution. Although more limited, some samples of *M. fortunata* co-occurring with the two *Rimicaris* are added to compare their characteristics with the others species.

The fourth research axis is articulated around two main questions: *i)* Can we observe different reproductive strategies in species from the same genus and co-occuring in the same locations? *ii)* What are the temporal dynamics of *Rimicaris exoculata* reproduction? The first question is explored by the comparison of different life history traits related to the shrimp reproduction between three different MAR species. The temporal dynamics is observed from two different angles to test the current hypothesis of a seasonal reproduction in *R. exoculata* between January and February (Hernández-Ávila, 2016). First, an interranual comparison of *R. exoculata* reproductive traits between sampling years is conducted. Secondly, data obtained for *R. exoculata* are compared with samples of its sister species *R. kairei* inhabiting areas of the globe at opposite latitude. This second part seeks to observe if opposite reproductive patterns exist between closely related species inhabiting regions where seasons are inverted.

*« Il y a trop de spécialités, pour qu'un seul homme puisse, en une seule existence, en posséder à fond une seule miette »*

*Martin Eden, Jack London*

# Chapter 1

# The Birth

The aim of this study was to continue the work obtained previously on the bacterial assemblages associated to the earlier life stages of *R. exoculata* shrimp, initiated first by (Guri et al., 2012) who described the bacterial diversity associated to eggs, in order to extend it to a larger number from different sites, throughout the embryonic development. Preliminary results to this aim were obtained by Ivan Hernández-Ávila during his thesis (Hernández-Ávila, 2016), where he explored the evolution of this bacterial colonization along the embryonic development. He realized most of the SEM observations kept in the following article as well as bacterial diversity analyses obtained by PCR cloning (unpublished data).

The work realized during this thesis concern therefore only the 16S barcoding (NGS sequencing) for the bacterial diversity, the FISH observations and some of the SEM observations (pleopods mainly). Sampling of the animals was an integral part of this Ph.D. work and was realized during the BICOSE 2 expedition in 2018 to be used for most of the 16S barcoding analyses and several FISH observations. Other samples were collected by different people during the BICOSE expedition. With different egg stages, we compared the assemblages at different point providing a general view of the bacterial colonization evolution along the embryonic development. All these samples were collected from two different vent fields, TAG and Snake Pit, to evaluate the influence of the surrounding environmental conditions – temperature, vent fluid chemistry for instance. Additionally, both egg and pleopods – two body surfaces exposed to similar environmental conditions – for each brooding females were taken to characterize the potential specificity of the bacterial communities associated to eggs. Put back in the context of the vent shrimp life cycle, this study sought to propose new hypotheses – or to reassess previous in the light of our results – on the symbiont acquisition pathways and on the potential role of the bacterial assemblages associated to eggs.

# 1.1. Diversity and variation in microbial communities colonizing broods of the vent shrimp *Rimicaris exoculata* during the egg development

## Article Methou et al. (2019) *published in Frontiers in Microbiology*

frontiers in Microbiology

ORIGINAL RESEARCH
published: 17 April 2019
doi: 10.3389/fmicb.2019.00808

# Is It First the Egg or the Shrimp? – Diversity and Variation in Microbial Communities Colonizing Broods of the Vent Shrimp *Rimicaris exoculata* During Embryonic Development

*Pierre Methou[1,2], Ivan Hernández-Ávila[1,2†], Johanne Aube[1], Valérie Cueff-Gauchard[1], Nicolas Gayet[2], Louis Amand[3], Bruce Shillito[3], Florence Pradillon[2] and Marie-Anne Cambon-Bonavita[1]**

[1] Univ Brest, CNRS, Ifremer, Laboratoire de Microbiologie des Environnements Extrêmes, Plouzané, France, [2] Ifremer, Laboratoire Environnement Profond (REM/EEP/LEP), Plouzané, France, [3] Unité Biologie des Organismes et Ecosystèmes Aquatiques, Muséum National d'Histoire Naturelle, Eq. Adaptations aux Milieux Extrêmes (BOREA), CNRS, IRD, Sorbonne Université, Université de Caen Normandie, Université des Antilles, Paris, France

*Rimicaris exoculata* is one of the most well-known and emblematic species of endemic vent fauna. Like many other species from these ecosystems, *Rimicaris* shrimps host important communities of chemosynthetic bacteria living in symbiosis with their host inside the cephalothorax and gut. For many of these symbiotic partners, the mode of transmission remains to be elucidated and the starting point of the symbiotic relationship is not yet defined, but could begin with the egg. In this study, we explored the proliferation of microbial communities on *R. exoculata* broods through embryonic development using a combination of NGS sequencing and microscopy approaches. Variations in abundance and diversity of egg microbial communities were analyzed in broods at different developmental stages and collected from mothers at two distinct vent fields on the Mid-Atlantic Ridge (TAG and Snake Pit). We also assessed the specificity of the egg microbiome by comparing communities developing on egg surfaces with those developing on the cuticle of pleopods, which are thought to be exposed to similar environmental conditions because the brood is held under the female's abdomen. In terms of abundance, bacterial colonization clearly increases with both egg developmental stage and the position of the egg within the brood: those closest to the exterior having a higher bacterial coverage. Bacterial biomass increase also accompanies an increase of mineral precipitations and thus clearly relates to the degree of exposure to vent fluids. In terms of diversity, most bacterial lineages were found in all samples and were also those found in the cephalothorax of adults. However, significant variation occurs in the relative abundance of these lineages, most of this variation being explained by body surface (egg vs. pleopod),

OPEN ACCESS

**Edited by:**
*Zhiyong Li,*
*Shanghai Jiao Tong University, China*

**Reviewed by:**
*Craig Lee Moyer,*
*Western Washington University, United States*
*Spencer V. Nyholm,*
*University of Connecticut, United States*

***Correspondence:**
*Marie-Anne Cambon-Bonavita*
*marie.anne.cambon@ifremer.fr*

**†Present address:**
*Ivan Hernández-Ávila,*
*Laboratorio de Biodiversidad Marina y Cambio Climático, Campeche, Mexico*

**Specialty section:**
*This article was submitted to Microbial Symbioses, a section of the journal Frontiers in Microbiology*

**Received:** *10 December 2018*
**Accepted:** *29 March 2019*
**Published:** *17 April 2019*

**Citation:**
*Methou P, Hernández-Ávila I, Aube J, Cueff-Gauchard V, Gayet N, Amand L, Shillito B, Pradillon F and Cambon-Bonavita M-A (2019) Is It First the Egg or the Shrimp? – Diversity and Variation in Microbial Communities Colonizing Broods of the Vent Shrimp Rimicaris exoculata During Embryonic Development. Front. Microbiol. 10:808. doi: 10.3389/fmicb.2019.00808*

vent field, and developmental stage. The occurrence of symbiont-related lineages of *Epsilonbacteraeota*, *Gammaproteobacteria*, *Zetaproteobacteria*, and Mollicutes provide a basis for discussion on both the acquisition of symbionts and the potential roles of these bacterial communities during egg development.

**Keywords: hydrothermal, shrimp, microbial colonization, Alvinocarididae, egg development**

## INTRODUCTION

Deep-sea hydrothermal vents are oases of life, mainly sustained by primary microbial chemosynthetic production. In these ecosystems, microbial life thrives in several microhabitats from water fluids to rock or sediment surfaces (Campbell et al., 2006). As in other aquatic environments, the bodies of vent fauna also offer suitable surfaces for bacterial communities to establish themselves and have never been observed without microorganisms (López-García et al., 2002; Duperron et al., 2009; Goffredi, 2010). More intricate and specific, relationships formed by chemosynthetic symbioses, where symbionts provide most of their host's nutrition, are also widespread in several dominant vent megafauna taxa (Dubilier et al., 2008). Among these, the alvinocaridid shrimp *Rimicaris exoculata* (Williams and Rona, 1986) is found in several vent fields on the Mid-Atlantic Ridge (MAR), like TAG and Snake Pit, where it forms dense aggregates of thousands of shrimps per $m^2$ close to hydrothermal vents (Segonzac et al., 1993; Copley et al., 2007).

Adult stages of *R. exoculata* host episymbiotic bacteria in their cephalothorax (or branchial chamber) and on mouthparts, which are modified and adapted to the colonization and growth of the symbiotic bacteria (Segonzac et al., 1993; Zbinden et al., 2004). Moreover, shrimps host a distinct epibiotic microbial community in their gut (Zbinden and Cambon-Bonavita, 2003; Durand et al., 2010, 2015). The bacterial assemblage in the cephalothorax provides nutrition to the shrimp by direct transfer of organic carbon generated by chemosynthesis (Ponsard et al., 2013). In addition, the metabolic activity of the bacteria could also protect the shrimp from harmful vent fluids by facilitating detoxification processes (Zbinden et al., 2008; Ponsard et al., 2013; Jan et al., 2014).

The microbial community hosted in the cephalothorax is particularly dynamic due to the short molting cycle of the shrimp (roughly 10 days). Because bacteria colonize the inner surface of the cephalothorax and mouthparts, these episymbionts are eliminated after each molt (Corbari et al., 2008b). The molting cycle of the shrimp generates a constant cycle of production of new body surfaces followed by symbiont recolonization, development, and accumulation of mineral deposits (Corbari et al., 2008a,b). In contrast, as the gut has no cuticle layer and is thus not subjected to surface renewal during molting, symbionts in this part of the body are supposedly maintained throughout the life of the animal following their acquisition (Durand et al., 2010).

The symbiotic bacterial assemblages are diverse in both cephalothorax and gut compartments, but are usually dominated by *Epsilonbacteraeota* and *Gammaproteobacteria* in the cephalothorax (Zbinden et al., 2008; Petersen et al., 2010; Jan et al., 2014) and by *Deferribacteres*, *Entomoplamatales*, and *Epsilonbacteraeota* in the gut (Durand et al., 2010, 2015; Cowart et al., 2017). Whereas *Epsilonbacteraeota*- and *Gammaproteobacteria*-related lineages have been found in abundance in the surrounding fluids (Petersen et al., 2010), *Deferribacteres* and *Entomoplamatales* symbionts have not yet been detected in the shrimp environment.

In caridean shrimps, females molt just before mating and extruding eggs. During this molt, pleopods become modified, with more developed setae, which is related to their role in holding the eggs during the brooding period (Correa and Thiel, 2003; Bauer, 2013). After mating, the eggs are extruded, mixed with sperm and covered with a mucus layer that ensures they remain adhered together and to the pleopods (Fisher and Clark, 1983). Since ovigerous females remain in dense populations crawling on the walls of active chimneys during the entire brooding period (Hernández-Ávila, 2016), their eggs experience environmental conditions found in the adult aggregations. They are thus exposed to the dynamic mixing between seawater and warm vent fluids and may provide attachment surfaces for microorganisms with chemoautotrophic metabolism.

Colonization of eggs of this species by epibiotic bacteria was recently described, and the lineages of *Gammaproteobacteria* and *Epsilonbacteraeota* found were the same as those retrieved within the cephalothorax of adults (Guri et al., 2012). This finding indicates that the bacteria-host relationship could start after the extrusion of the eggs by the female, during embryonic development (brooding phase).

Here we expand on Guri's study by assessing variations in bacterial communities associated with broods of *R. exoculata* across different geographic locations, and at different stages through embryonic development. We also aimed to test the hypothesis of an establishment of the symbiotic relationship very soon after egg extrusion, by comparing bacterial communities developing on eggs with those developing on the pleopods holding the brood. Surfaces of both structures are co-localized on the female body and are thus assumed to be exposed to the same environmental conditions. If an opportunistic unspecific colonization (fouling) occurs on both structures, then we would expect similar bacterial assemblages. In such a case, a lack of specificity in egg-associated microorganisms would not support the hypothesis of the development of a symbiotic relationship at this stage. If egg surfaces trigger the attachment of specific microorganisms, then bacterial assemblages on pleopods would be expected to be significantly different from those developing on eggs. Such a pattern would be in favor of a selective mechanism, which could help establish symbiotic relationships very early in a shrimp's life cycle.

In our study, bacterial assemblages that colonize the surfaces of eggs and of pleopods were analyzed in females holding broods at different stages of embryonic development collected from two different vent fields: Snake Pit (3460 m depth) and TAG (3630 m depth). The goals of this study were (i) to compare the bacterial assemblages found on the surface of the eggs and pleopods of brooding females; (ii) to assess variations in bacterial assemblages through embryonic development, and (iii) to compare the colonization of bacterial communities on eggs and pleopods from two different vent fields.

# MATERIALS AND METHODS

## Sample Collection

*Rimicaris exoculata* brooding females were collected at two vent fields on the MAR (**Figure 1A**), Snake Pit (23°22′N; 44°57′W, 3460 m depth) and TAG (26°08′N; 44°49.5′W, 3630 m depth), during the BICOSE (January 11 – February 10 2014) and BICOSE 2 cruises (January 26 2018 – March 10 2018). Specimens were collected in large aggregates inhabiting active emission habitats (**Figure 1B**), using a suction sampler manipulated by the Remote Operated Vehicle (ROV) Victor 6000 (BICOSE) or Human Operated Vehicle (HOV) Nautile (BICOSE 2).

Sampling at such depths implies that the collected organisms spend more than 1 h of ascent through the water column, before they are made available to scientists on board the oceanographic ship. Uncontrolled decompression during this ascent may considerably impair the physiological state of sampled fauna, leading to significant levels of mortality upon final recovery on board the ship. In order to improve the sampling conditions, pressurized recoveries of the specimens were performed using the PERISCOP®device: 18 such samplings were undertaken, 6 and 12 at the Snake Pit and TAG sites respectively (**Supplementary Table S1**). The specimens were collected inside a PVC sampling cell, which was connected to the slurp gun of the ROV or HOV. This sampling cell was further transferred to the isobaric chamber PERISCOP®before starting the ascent to the surface (Shillito et al., 2008). On board of the ship (R/V *Pourquoi pas?*) samples were rapidly decompressed in a controlled manner and processed for dissection and fixation. Survival rates were then close to 100%, as witnessed by the intense activity of the shrimp following the opening of the PERISCOP device.

Brooding females (**Figure 1C**) were selected from each site according to the developmental stage of the embryos in their brood. The eggs were classified into three developmental stages (**Figures 1E–G**):

- Early stage from one-cell embryos to fully segmented embryos (blastula);
- Middle stage includes embryos at the gastrulation (a clear area starts to be visible at one pole of the egg) to embryos showing early differentiation of larval structures;
- Late stage includes embryos with advanced development of larval structures and eyespots visible through the egg envelope.

For each female, the full brood was removed and two pleopods (**Figure 1D**) were dissected. A pleopod and a small number of eggs were fixed in 3% formalin for 3 h, rinsed with phosphate-buffered saline (PBS)/sterile seawater buffer (1:1) and stored in PBS/Alcohol at −20°C for FISH analyses (1:1) (Durand et al., 2010), while another pleopod and the rest of the brood were frozen at −80°C for DNA analyses.

In all, 40 *R. exoculata* samples were selected covering all combinations of body structure (brood vs. pleopod), developmental stage (early, middle, or late), and vent field (Snake Pit or TAG), each combination being replicated at least three times (**Supplementary Table S1**).

Other samples were also collected for complementary experiments (**Supplementary Table S1**) using scanning electron microscopy (SEM) and Fluorescent *In Situ* Hybridization (FISH). Samples were formalin-fixed as described above for the FISH analyses, or fixed in 2.5% glutaraldehyde in seawater, rinsed after 12 h of fixation and kept at 4°C in seawater for SEM analyses (Zbinden et al., 2004). For illustrative purpose (**Figures 1**, **2**), images of egg broods, individual eggs and pleopods were taken under a stereomicroscope (Leica MS125, Leica Microsystems).

## DNA Extraction, Sequencing Method, and Sequence Processing

DNA from eggs and pleopods was extracted using a NucleoSpin®Soil Kit (Macherey-Nagel, Germany) following manufacturer's instructions. The extracted DNA samples were then sent to the MR DNA laboratory (Molecular Research LP, Shallowater, TX, United States) for amplification and sequencing of prokaryotic diversity. This was performed on a 450 bp fragment of the 16S rRNA gene (16S) using Illumina's MiSeq technology with the 2 × 300 bp chemistry. Briefly, the 16S V3-V4 variable region (Fadrosh et al., 2014) [341/785 primers, with barcode on the forward primer (Herlemann et al., 2011)] was amplified in a 28-cycle PCR using the HotStarTaq Plus Master Mix Kit (Qiagen, United States) under the following conditions: 94°C for 3 min, followed by 28 cycles of 94°C for 30 s, 53°C for 40 s and 72°C for 1 min, after which a final elongation step was performed at 72°C for 5 min. PCR products were then purified using calibrated Ampure XP beads and used to prepare a DNA library following the Illumina TruSeq DNA library preparation protocol. Blank DNA extraction controls were sequenced to verify there was no contamination, which was confirmed as these gave no amplification.

Prokaryotic 16S rRNA paired-end reads were merged using USEARCH (Edgar and Flyvbjerg, 2015) after q25 trimming of the ends. The resulting 16S reads were processed using FROGS, implemented on the Galaxy platform (Escudié et al., 2018), multifasta files were parsed, checked for quality, and trimmed by length (expected value of 455b ± 35b). Sequences were then clustered with SWARM (Mahé et al., 2014) using a distance threshold of three, chimeras were removed using the UCHIME algorithm (Edgar et al., 2011) implemented in VSEARCH (Rognes et al., 2016), and taxonomic affiliation was performed for each OTU by NCBI Blast+(Camacho et al., 2009) using the Silva

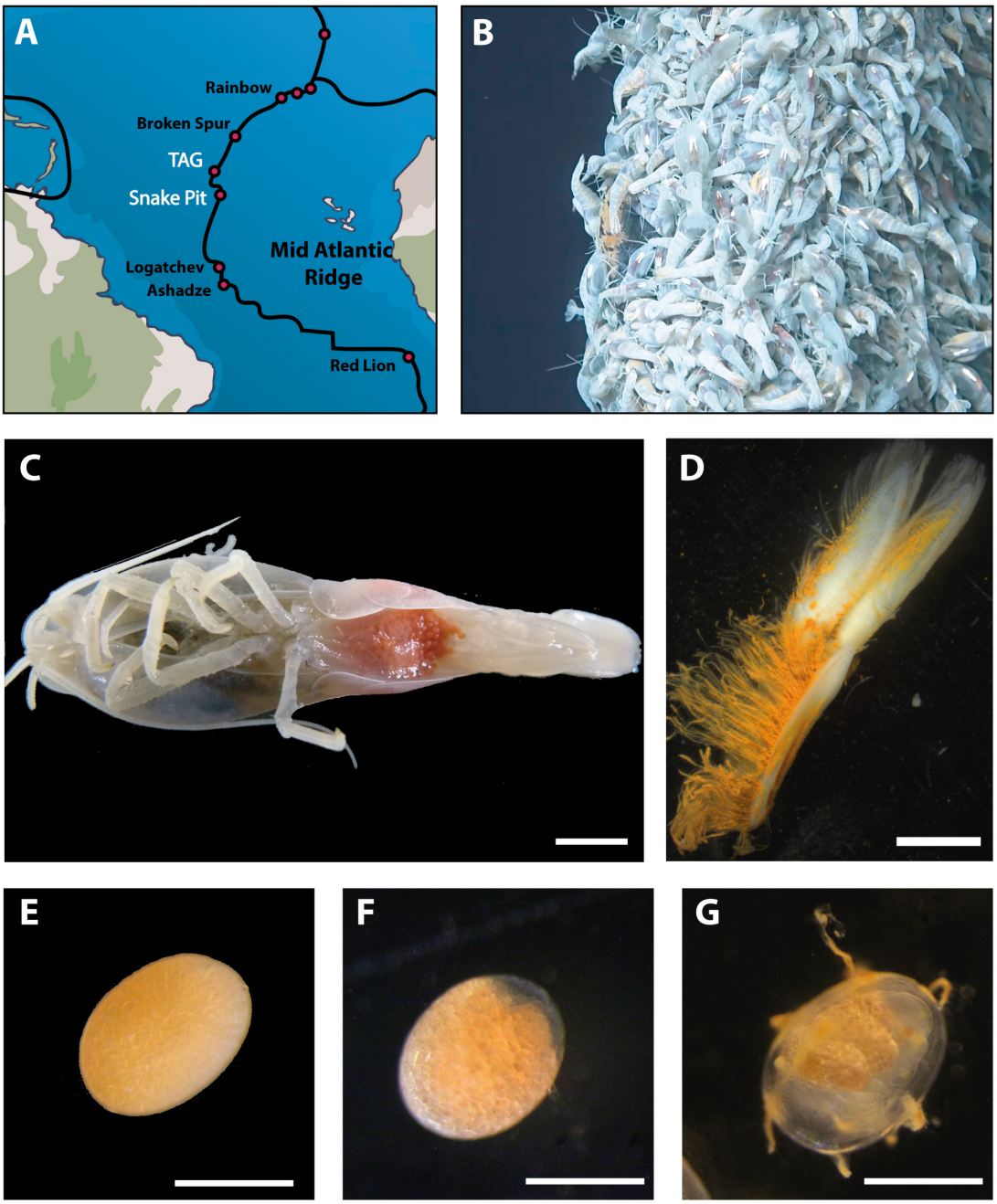


**FIGURE 1 |** Sampling and dissection procedures. **(A)** Geographic location of hydrothermal vent sites where *Rimicaris exoculata* are present (black) and where brooding females were sampled (white). **(B)** Example of a shrimp aggregate where brooding females were collected at TAG vent field. **(C)** *Rimicaris exoculata* brooding female holding eggs between pleopods under the abdomen; scale bar = 5 mm. **(D)** First pleopod with modified setae dissected from a brooding female; scale bar = 2 mm. Single eggs **(E)** at early stage **(F)** middle stage **(G),** and late stage of development; scale bars = 0.5 mm.

132 16S gene database (Quast et al., 2013). Additional filtering on abundance at the threshold of 0.005% (Bokulich et al., 2013) and on BLAST at 95% minimum coverage and 80% minimum identity was also performed to remove non-biologically relevant OTU sequences. Two OTUs affiliated to plant chloroplast and mitochondria (260 and 144 sequences of the total dataset, respectively) were manually removed from the dataset. The 16S rRNA data are available in the NCBI SRA repository (SubmissionID SUB4881289, BioProjectID PRJNA509116).

## Statistical Analysis

Alpha diversity within the 40 samples was estimated with OTU number and Inverse Simpson index (Simpson, 1949). Difference in the alpha diversity indexes among body structure and vent

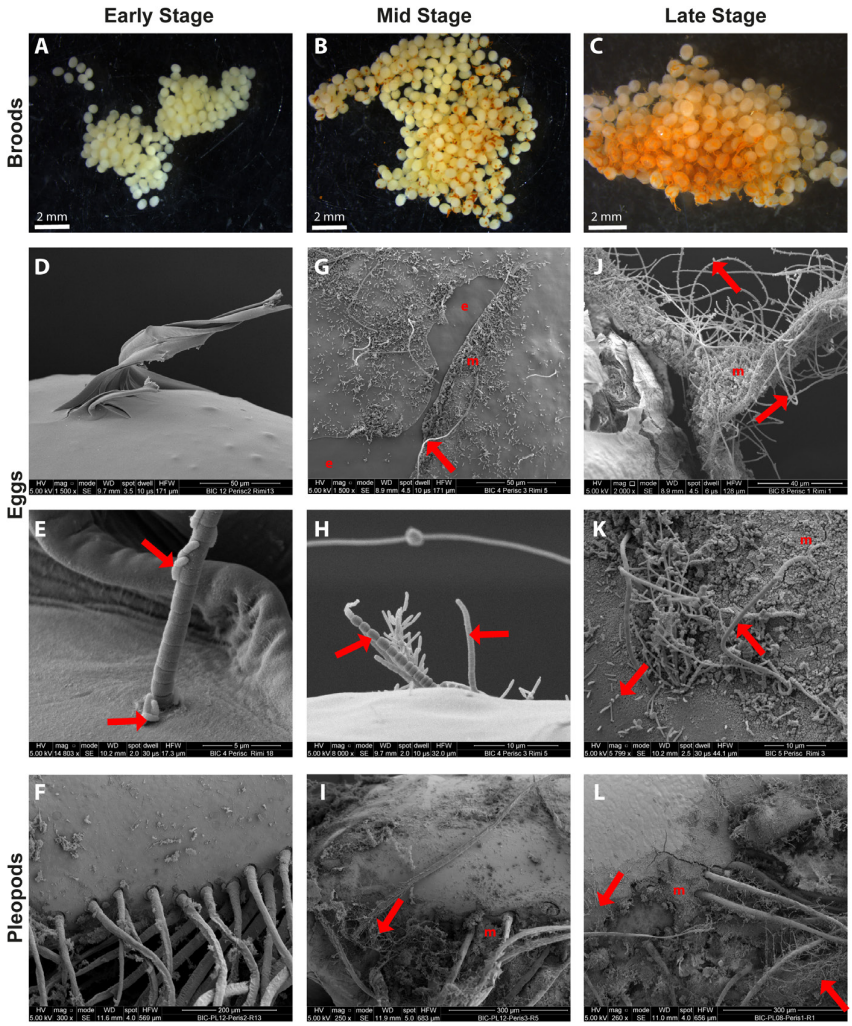


**FIGURE 2 |** SEM observations of epibiotic bacteria on the surface of *R. exoculata* eggs and pleopods. *Rimicaris exoculata* egg broods observed under a stereomicroscope with eggs at **(A)** early stage, **(B)** mid stage, **(C)** and late stage. Individual eggs observed under a scanning electron microscope with eggs at **(D,E)** early stage, **(G,H)** mid stage **(J,K)** and late stage. Pleopods observed under a scanning electron microscope holding broods at **(F)** early stage, **(I)** mid stage, **(L)** and late stage. The crusts observed in the close-ups both on eggs **(K)** and pleopods **(L)** in SEM are deposits of ferric oxide, which correspond to the orange coloration observed under stereomicroscope on egg broods **(B,C)**. Red arrows are targeting some of the rod shaped and filamentous bacteria observed in these pictures. e, bare egg envelope areas where mucus layer have been removed and m, egg envelope areas covered by mineral crusts.

field categories were tested using Mann-Whitney tests and the difference between developmental stages, by Kruskal–Wallis followed by pairwise Wilcox tests; $p < 0.05$ was considered the threshold of significance for a difference between samples.

For further statistical analysis, the sequence dataset was normalized by cumulative sum scaling to minimize the effect of different sequence numbers obtained with each sample (Paulson et al., 2013). Beta diversity was analyzed by hierarchical clustering using the complete method based on Bray-Curtis dissimilarity matrices. The homogeneity between categories was tested with the betadisper function of the *Vegan* R package, and significant differences between categories were tested for by Permutational Analysis of Variance (PERMANOVA, 9999 permutations) with the adonis function of the same package (Oksanen et al., 2008). Multilevel comparisons for the developmental stage condition were also performed with the pairwise adonis function (Arbizu, 2017).

Taxonomic composition and diversity results were visualized using the R package *Phyloseq v.1.14.0* (McMurdie and Holmes, 2013). The linear discriminant analysis (LDA) effect size (LefSE) method (Segata et al., 2011) was used to characterize and highlight microorganisms specific to each of the different conditions. Results were shown both with a plot of LDA score for each bacterial group and with a cladogram, each concentric circle representing a taxonomic level, the innermost being the phylum and the outermost the genus.

## Scanning Electron Microscopy

Eggs and pleopods were dehydrated with an ethanol series (30, 50, 70, 95, and 100% ethanol) and then for 5 h in a critical point dryer

CPD 020 (Balzers Union, Balzers, Liechtenstein). Finally, samples were gold-coated with an SCD 040 (Balzers Union). Observations and imaging were performed using a Quanta 200 microscope (FEI-Thermo Fisher, Hillsboro, OR, United States). The chemical composition of the mineral crust present on egg and pleopod surfaces was also analyzed with an X-ray Energy Dispersive Spectrometer (EDX) using an X-Max 80 (Oxford Instruments, Oxford, United Kingdom) and displayed with AZtec software (Oxford Instruments, Oxford, United Kingdom).

## Fluorescent *in situ* Hybridization

Eggs were dehydrated with a PBS-Ethanol series (from 50:50 to pure ethanol with a 10% increase for each bath, 10 min each) and progressively transferred to LR-white resin in an Ethanol-Resin series (2:1, 1:1, and 1:2 Ethanol/Resin ratio; 30 min each). After three baths of 30 min in pure LR-white resin to remove any trace of ethanol, samples were placed in gelatin capsules filled with LR-white and left for 48h for further impregnation at room temperature. The LR-white resin was polymerized in the gelatin capsules at 50°C for 24 h. Before sectioning, the gelatin was removed with hot water and the LR-white blocks were cut into 2-μm sections in series through the entire egg or half of it using an ultramicrotome Ultracut UCT (Leica).

Sections were mounted on glass slides, and hybridized in a reaction mixture containing 0.5 mM of each probe in a 30% formamide hybridization buffer [0.9M NaCl, 0.02M Tris-HCl, 0.01% sodium dodecyl sulfate (SDS), and 30% deionized formamide] for 6 h at 46°C. Different concentrations of formamide (10, 20, 30, 40, and 50%) were initially tested, but 30% formamide always gave the best results. Hybridization temperature was chosen according to Guri et al. (2012). Sections were washed at 48°C for 30 min in a washing buffer (0.102M NaCl, 0.02M Tris-HCl, 0.005M EDTA, 0.01% SDS) and rinsed briefly with water. Sections were covered with Slow Fades Gold antifade reagent containing 40-6-diamidino-2-phenylindole (DAPI) (Invitrogen), and a cover slip. The probes used in this study (Eurofins) were Eub338, targeting most of the *Eubacteria* (Amann et al., 1990); GAM42a, targeting the *Gammaproteobacteria* (Manz et al., 1992); Epsy914, targeting *Epsilonbacteraeota* (Loy et al., 2003); and Zeta123, targeting *Zetaproteobacteria* (Kato et al., 2009); and labeled with Cyanine 3 or Cyanine 5 (**Supplementary Table S2**).

Observations were made on a Zeiss AxioImager.Z2 microscope equipped with Apotome, an AxioCam, and a Colibri LED light source with three light-emitting diodes (UV-emitting LED, 365 ± 4.5 nm for DAPI; green emitting LED, 550 ± 14 nm for Cyanine3; red-emitting LED, 590 ± 17.5 nm for Cy5) (Carl Zeiss MicroImaging GmbH, Göttingen, Germany). Micrographs were analyzed using Zen (Zeiss) software.

# RESULTS

## Electron Microscopy Analysis

Observed under a light microscope, early stage broods were almost devoid of mineral deposits, except for some thin and scattered mineral deposits found on some eggs (**Figure 2A**). Conversely, middle stage broods had small patches of mineral deposits (**Figure 2B**). Mineral deposits were even greater on late stage broods, some of which were almost half covered with a thick mineral crust (**Figure 2C**). Eggs in these late broods showed high variation in mineral coverage, with more minerals covering eggs of the external part of the brood (**Figure 2C**).

As shown in the SEM images, the surface of early stage eggs was colonized by only a few scattered bacteria (**Figure 2D**). The morphotypes identified at this stage were small isolated rod-shaped bacteria, mostly attached laterally, and 1-μm thick filaments with a proximal attachment to the eggs, measuring 10 s to 100 s μm (**Figure 2E**). The surface of pleopods holding these early stage broods was also colonized by a few rod-shaped and filamentous bacteria (**Figure 2F**).

At the middle stage, the broods showed different degrees of bacterial colonization, usually with patches of bacteria over the eggs and on the connective mucus. In general, the bacterial coverage was denser than on early stage broods, with more bacterial filaments, including thin (<1 μm) and thick (>1 μm) filaments and erect rod-shaped bacteria (**Figures 2G,H**). In sections where the mucus coat was broken, allowing observation of the egg envelope itself, mostly, no bacteria directly attached to the egg envelope were observed (**Figure 2G**). In addition, in some areas, the bacteria were found with crusts of mineral deposits of different thickness (up to 5 μm). Spectrophotometric analysis of this mineral crust showed that the deposits were mainly composed of ferric oxides for both eggs and pleopods (**Supplementary Figures S1D,E**). Similar bacterial colonization was also observed on pleopod surfaces (**Figure 2I**).

On broods in the late stage of embryonic development, bacteria covered the eggs almost entirely. The morphotypes identified were the same as those found on middle stage eggs (**Figures 2J,K**). However, the distribution was more uniform over the eggs and connective mucus. Similarly, there were more mineral deposits, which tended to form thick crusts (5–7 μm thick), covering even the connective mucus. In some spots with mineral deposits, it seemed that the crust covered a part of the bacterial biofilm, but there were still bacterial cells visible over the crust. The surface of pleopods holding late stage broods were also covered by a thick crust of mineral deposits and colonized by several thick and thin filaments similar to those found on eggs (**Figure 2L**). Bacterial colonization on the eggs or pleopods during embryonic development showed similar patterns in the TAG and Snake Pit vent fields. As for middle stages, spectrophotometric analysis of the thick mineral crust confirmed presence of ferric oxides on both late stage egg and pleopod surfaces (**Supplementary Figures S1A–C**).

## Microbial Diversity Analysis

Our metabarcoding of the bacterial communities associated with eggs or pleopods of *R. exoculata* generated a total of 3,361,475 sequences. After sequence filtering, there remained a total of 2,269,630 partial 16S RNA (V3-V4 regions) sequences clustered in 228 OTUs to assess bacterial diversity. Most sequences were identified on both body structures, with only one OTU and one bacterial order of Mollicutes specific to eggs, namely the *Entomoplasmatales* (**Supplementary Figure S2**). In the same way,

two OTUs were specific to Snake Pit and one order of Mollicutes specific to TAG, namely the *Mycoplasmatales*, the rest being common to both vent fields (**Supplementary Figure S2**). All OTUs except one, absent from late stage samples, were present at every developmental stage (**Supplementary Figure S2**).

None of our samples had difference in average bacterial OTU number according to surface type (egg vs. pleopod), vent site or developmental stage (**Supplementary Figure S3**). However, Inverse Simpson values indicated a greater mean evenness in egg samples compared with pleopod samples ($p$ = 0.001041; **Supplementary Figure S3A**). Pleopods were dominated by fewer OTUs whereas eggs had more even microbial communities in comparison. Interestingly, a shift could be observed through the developmental stages with a significantly higher evenness for late stage pleopods compared with middle and early stages ($p$ = 0.003; **Supplementary Figure S3E**). Similar variation was observed for eggs with a slight increase in average Inverse Simpson values for late stages compared to early and middle stages, although supported by a marginal $p$-value ($p$ = 0.052; **Supplementary Figure S3D**). No significant differences were found between TAG and Snake Pit samples for eggs or pleopods (**Supplementary Figures S3B,C**).

Regardless of the vent site, egg, and pleopod communities were significantly different from each other (PERMANOVA $R^2$ = 0.233, $p < 0.001$, **Supplementary Table S3**). Body surface (egg vs. pleopod) was also the main factor structuring our dataset, followed by vent site effect ($R^2$ = 0.195) and developmental stage effect ($R^2$ = 0.148, **Supplementary Table S3**). Taken separately, both egg and pleopod surfaces, showed a strong vent site effect on bacterial community composition, with significant differences between TAG and Snake Pit assemblages (PERMANOVA $R^2$ 0.291 and 0.316 $p < 0.001$ for both eggs and pleopods).

In addition, significant variations in bacterial communities were detected through the egg development stages (PERMANOVA $R^2$ 0.263 and 0.308, $p$ = 0.004 for both eggs and pleopods). These variations were mainly observed between early stages and late stages for both surfaces (Pairwise PERMANOVA $R^2$ 0.299 and 0.379, $p$ = 0.013 and 0.009 for eggs and pleopods, respectively). Indeed, no significant differences were found between middle and late stage for either surface, or between early and middle stages for pleopods. Only slightly significant variations were found between early stages and middle stages for eggs (Pairwise PERMANOVA, **Supplementary Table S3**).

These results were further supported by hierarchical clustering, which separated most Snake Pit eggs from all other samples and then most TAG eggs from the rest, most of which were pleopod samples (**Figure 3**). Only some early stage egg samples (from both sites) clustered together with early stage pleopods in a separate cluster (**Figure 3**). In any case, body surface samples (i.e., eggs vs. pleopods) or vent site origin, were more closely related to each other than were samples originating from the same brooding female.

## Microbial Taxonomic Comparison

Based on rDNA 16S sequence affiliation according to the Silva 132 database, nine phyla could be identified in our samples, with just four phyla accounting for more than 99% of the sequences obtained (**Figure 3**). The most abundant taxa were *Epsilonbacteraeota*, representing in 39% of the total dataset in relative abundance, followed by *Proteobacteria* (36%), *Patescibacteria* (13%), and *Bacteroidetes* (11%). Among *Proteobacteria*, three major classes were present with a clear dominance of *Gammaproteobacteria* (63.7%), followed by *Zetaproteobacteria* and *Alphaproteobacteria* (17.7% each). Sequences affiliated to *Rothia* sp. from the *Actinobacteria* phylum (0.007%), *Streptococcus* sp., and *Enterococcus* sp. from the *Firmicutes* phylum (0.013%) were only present in a few samples and most likely correspond to potential contaminants. In the same way, two other phyla, *Tenericutes* (0.025%) and *Deinococcus–Thermus* (0.32%) were present in only a few samples.

One of the major differences between bacterial communities on eggs and pleopods was the relative proportion of the different *Epsilonbacteraeota* families. As shown by LDA analysis (**Figure 4** and **Supplementary Figure S4**), *Epsilonbacteraeota* were significantly more abundant in pleopod than in egg communities (49 and 36%, respectively). Additionally, among this phylum, members of the *Sulfurovaceae* family were much more abundant in pleopod (97.8% of the relative abundance of all *Epsilonbacteraeota*) than in egg communities (57.5% of all *Epsilonbacteraeota*). Conversely, members of the *Arcobacteraceae* and *Campylobacteraceae* families were much more abundant in egg (22.1 and 18% of all *Epsilonbacteraeota*, respectively) than in pleopod communities (less than 1% for both). The relative abundance of *Zetaproteobacteria* (8% in eggs compared with 3% in pleopods) also contributed to the difference between egg and pleopod communities (**Figure 4**). Despite their relatively high abundance, *Gammaproteobacteria* show similar relative abundance with no significant differences in both eggs and pleopod communities (24 and 19%, respectively). Only one *Gammaproteobacteria* genus, *Colwellia*, was shown by the LDA analysis to be significantly more abundant in eggs. This result was the effect of a single brooding female – Rimi185 – on whose eggs the *Colwellia* family accounted for 50% of the total *Gammaproteobacteria* class. In other samples, including the pleopods of Rimi185, *Colwellia* were always present in low abundance and the *Gammaproteobacteria* class was mainly dominated by *Thiotricaceae*. Interestingly, as illustrated by Venn diagrams (**Supplementary Figure S2**), our LDA analysis confirms Mollicutes from the *Entomoplasmatales* order as an egg-specific group present only in some of our egg samples.

Regarding vent site influence, LDA analysis (**Figure 5** and **Supplementary Figure S5**) revealed that *Zetaproteobacteria* (13 and 3% for TAG and Snake Pit, respectively) *Campylobacteraceae* (2 and 11% for TAG and Snake Pit, respectively), and the JGI_00000069_P22 order of the *Gracilibacteria* family (6 and 13% for TAG and Snake Pit, respectively), were the main lineages responsible for the difference between the two vent fields in egg communities (**Figure 5A**). By contrast, *Alphaproteobacteria*, mainly from the *Rhodobacterales* order (8 and 3% for TAG and Snake Pit, respectively), *Zetaproteobacteria* (8 and 2% for TAG and Snake Pit, respectively), and the *Bacteroidetes* family of *Saprospiraceae* (9 and 6% for TAG and Snake Pit, respectively) were the main lineages responsible for the difference between the two vent fields in pleopod communities (**Figure 5B**).

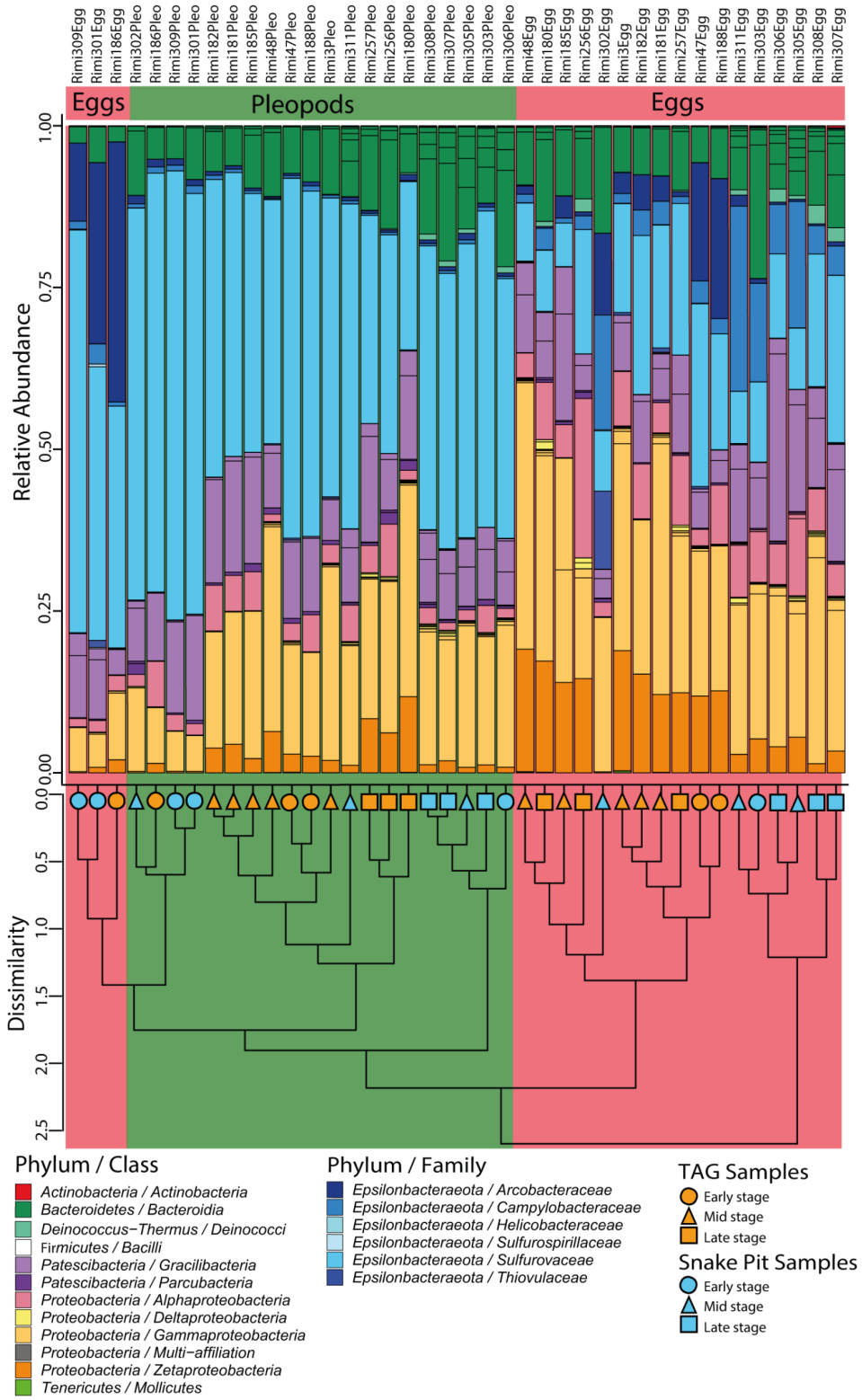


**FIGURE 3 |** Relative abundances of 16S rRNA gene sequence reads from egg and pleopod samples according to their classification (Silva 132 database). Groups are at the family level for the *Epsilonbacteraeota* phylum and at the class level for other phyla. The cluster dendrogram depicts the average linkage hierarchical clustering based on a Bray-Curtis dissimilarity matrix of community compositions resolved down to OTU level.

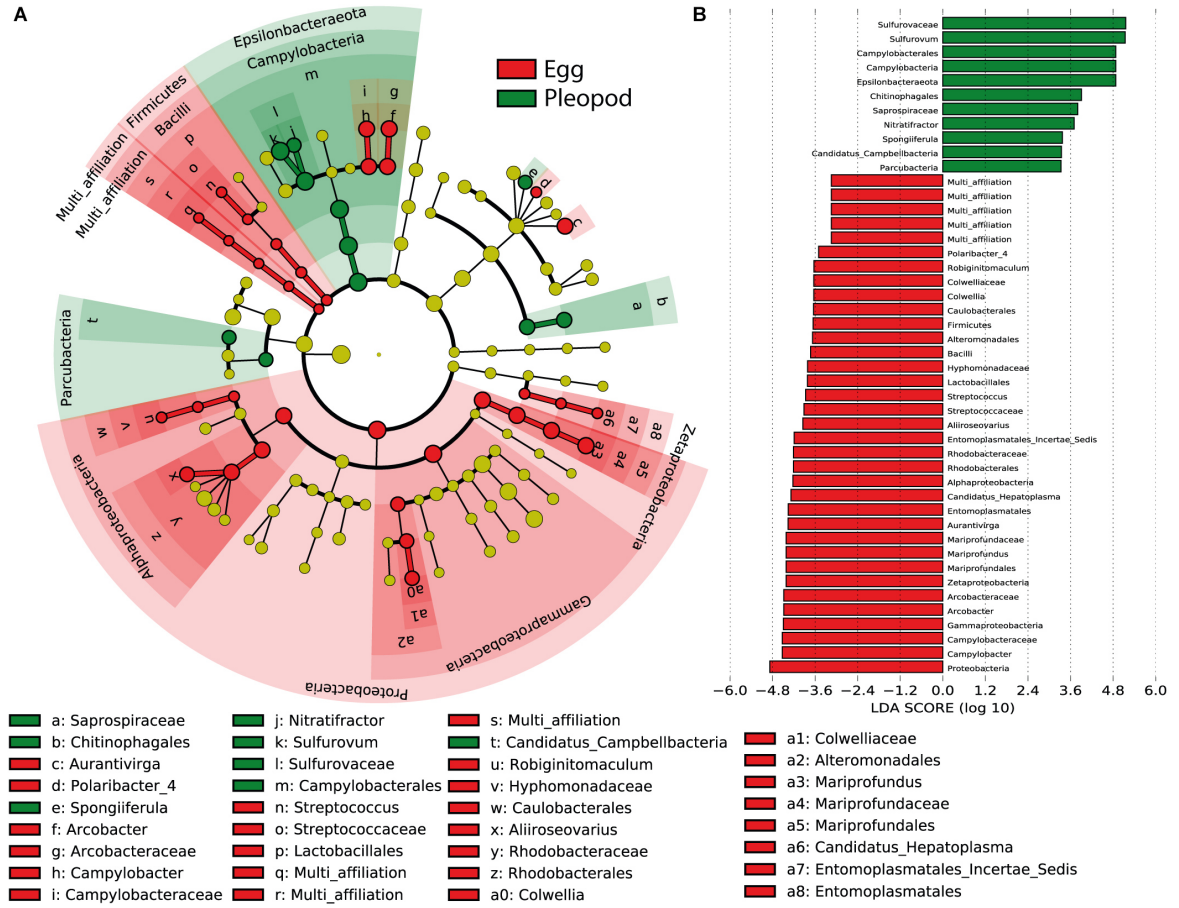


**FIGURE 4 |** Most differentially abundant bacterial taxa between eggs (red) and pleopods (green). **(A)** Cladogram representing taxonomic distribution of the differentially abundant bacterial taxa. The dots represent the specific bacterial taxa, with colors corresponding to the surface (eggs or pleopods) where these are relatively more abundant, yellow-greenish color denoting taxa with no significant difference in relative abundance between eggs and pleopods. The size of dots is proportional to the relative abundance. **(B)** Ranked LDA scores of the differentially abundant bacterial taxa, with taxa with highest relative abundance in pleopods in green, and taxa with highest relative abundance in eggs in red.

During egg development, an important shift between *Epsilonbacteraeota* and *Gammaproteobacteria* was observed, *Epsilonbacteraeota* being more abundant at early stages (from 58 to 23% for eggs and from 56 to 33% for pleopods) and *Gammaproteobacteria,* more abundant at late stages (from 15 to 26% for eggs and from 15 to 24% for pleopods) (**Figures 6A,B** and **Supplementary Figure S6**). Increased abundance at late stages for *Deinoccocus–Thermus* (from less than 0.1 to 2% for both eggs and pleopods), *Bacteroidetes* family *Saprospiraceae* (from less than 0.1–4% for eggs; 6% for pleopods), and *Deltaproteobacteria* (from less than 0.1–1% for both eggs and pleopods) lineages were also highlighted by LDA analysis (**Figures 6A,B** and **Supplementary Figure S6**).

## Fluorescent *in situ* Hybridization Observations

On the hybridized sections, a positive signal with the *Eubacteria* probe was obtained on the envelope of all late stage eggs covered with mineral deposits, showing thin filaments and rod-shaped structures (**Figure 7A**). By contrast, no positive signal was obtained with the *Eubacteria* probe on most hybridized sections of early stage eggs (**Supplementary Figure S7**), confirming SEM observations that bacterial assemblages are hardly present at all at this stage.

At the late stage, however, eggs from the same brood showed high variation in terms of bacterial coverage, showing some eggs with abundant mineral deposits, and others without any mineral deposit on their envelope. The first type had a large number of filamentous bacteria and rod-shaped bacteria (**Figures 7A,C,D**), whereas those without mineral deposits had less bacteria, more similar to the early stage, with only a few rod-shaped erected bacteria revealed by a weak Eub338 signal (**Figure 7B**). Differences in the abundance of mineral deposits on the eggs were associated with egg position in the brood. The egg with many mineral deposits being the most external and the most exposed to the hydrothermal fluids.

Positive signals were obtained with the *Epsilonbacteraeota* probe on the thick filaments and with the *Gammaproteobacteria* probe on thin filaments for late stage eggs, confirming their status

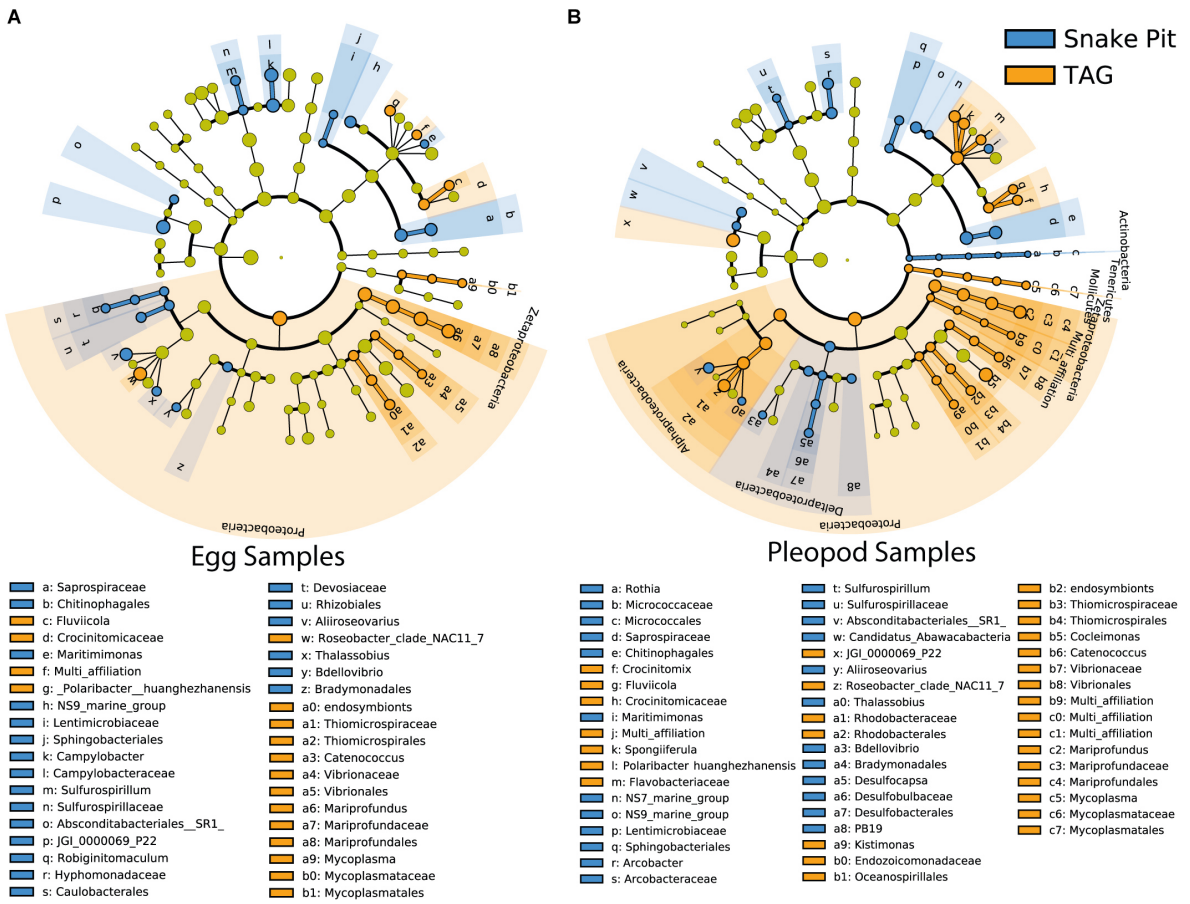


**FIGURE 5 |** Most differentially abundant taxa of egg communities **(A)** and pleopod communities **(B)** between TAG (orange) and Snake Pit (blue) vent fields. The dots represent the specific bacterial taxa, with colors corresponding to the vent field where these are relatively more abundant, yellow-greenish color denoting taxa with no significant difference in relative abundance between vent fields. The size of dots is proportional to the relative abundance.

as active bacteria on egg surfaces (**Figures 8A,B**). Positive signal with the *Zetaproteobacteria* probe was also obtained for bacteria entangled within the mineral crust for late stage eggs (**Figure 8C**). Moreover, the *Gammaproteobacteria* signal matched with most of the thin filamentous bacteria and the small-rod bacteria observed with DAPI, corroborating their high abundance at these stages (**Supplementary Figure S7**). This was further supported by co-hybridization with *Gammaproteobacteria* and *Eubacteria* probes, which showed that a *Gammaproteobacteria* signal co-localized with most of the *Eubacteria* signals (**Supplementary Figure S7**). Considering the low bacterial coverage at the early stage, no consistent signal could be observed with specific probes (*Gammaproteobacteria* or *Epsilonbacteraeota*). For each of these groups, no signal with specific probes was reported inside the eggs or elsewhere than on the surface of egg envelopes (**Figure 8** and **Supplementary Figure S7**).

## DISCUSSION

When the bacterial association with eggs of *R. exoculata* was first described, in Guri et al. (2012), lineages of *Gammaproteobacteria*, *Epsilonbacteraeota*, *Alphaproteobacteria,* and *Bacteroidetes* similar to those retrieved within the cephalothorax of adults were reported. In our present study, in addition to the previous ones, symbiont-related lineages of *Zetaproteobacteria* or *Entomoplasmatales* previously reported in *R. exoculata*, cephalothorax or gut were also retrieved (Zbinden and Cambon-Bonavita, 2003; Jan et al., 2014). For three of these, namely the *Gammaproteobacteria*, *Zetaproteobacteria*, and *Epsilonbacteraeota*, localization on the egg surface close to mineral deposits was confirmed here by FISH (**Figure 8**). Our results also highlight significant differences between the bacterial assemblages found on eggs and on pleopods, as well as a significant effect of the mother's vent of origin and the developmental stage of the brood.

### Variation in Bacterial Assemblages Through *Rimicaris exoculata* Embryonic Development

At the early stage, egg and pleopod surfaces have low bacterial coverage, with only a few rod-shaped and filamentous bacteria shown by SEM images, and no positive signal with FISH

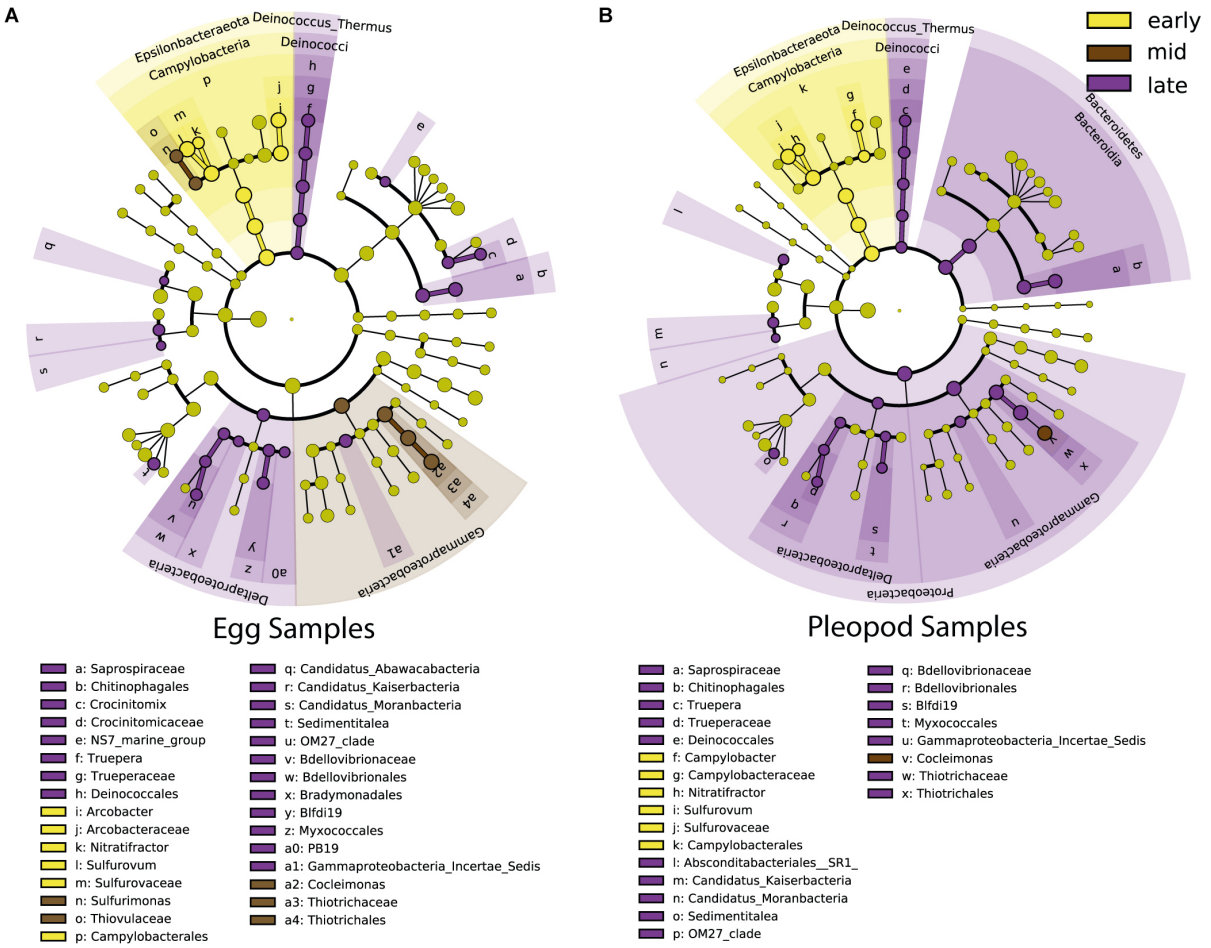


**FIGURE 6 |** Most differentially abundant taxa of egg communities **(A)** and pleopod communities **(B)** between early stages (yellow), middle stages (brown) and late stages (purple). The dots represent the specific bacterial taxa, with colors corresponding to the stage where these are relatively more abundant, yellow-greenish color denoting taxa with no significant difference in relative abundance between stages. The size of dots is proportional to the relative abundance

bacteria-specific probes. These small assemblages already include almost every bacteria found throughout embryonic development. Nonetheless, most assemblages are mainly dominated by *Epsilonbacteraeota*, other phyla being present only in low relative abundance at this developmental stage. High abundance of this group on newly available surfaces, i.e., freshly laid eggs and recently molted pleopods, is in good agreement with previous studies reporting *Epsilonbacteraeota* as pioneer colonizers on several types of substratum available at vents after just a few days of colonization (López-García et al., 2003; Alain et al., 2004; Szafranski et al., 2015a).

As embryonic development progresses, bacterial coverage and mineral deposits both appear to follow a gradual progression on eggs and pleopods, clearly reminiscent of what is observed inside the cephalothorax after molting (Zbinden et al., 2004; Corbari et al., 2008b). This increase of bacterial coverage at later stages is accompanied by important changes in community composition. For both types of body surface, higher Inverse Simpson index suggests a more even distribution and a higher diversity in bacterial assemblages at the late stage than at the early or middle stages. Although *Epsilonbacteraeota* may be more abundant in late stage communities than in small early stage assemblages, relative abundance clearly decreases in favor of other groups. Among these, *Gammaproteobacteria*, *Deltaproteobacteria*, and *Deinococcus–Thermus* were significantly more abundant on late stage surfaces, resembling the most complex communities found on long-term colonized surfaces of the MAR (Szafranski et al., 2015a).

Molting of caridean brooding females can be postponed in some cases until the end of embryonic development and hatching of the larvae, but not in every species and never for more than a few days (Hess, 1941; Pandian et al., 1982; Bauer and Abdalla, 2000; Raviv et al., 2008). In *R. exoculata*, the time period between two successive molts in non-reproductive individuals has been estimated to be rather short, around 10 days (Corbari et al., 2008b). Egg hatching in the Alvinocaridid shrimp *Shinkaicaris leurokolos* incubated experimentally at temperatures representative of the adult habitat (around 20°C) occurred within a month (Watanabe et al., 2016), and the brooding period in *R. exoculata* likely has similar duration, thus extending their

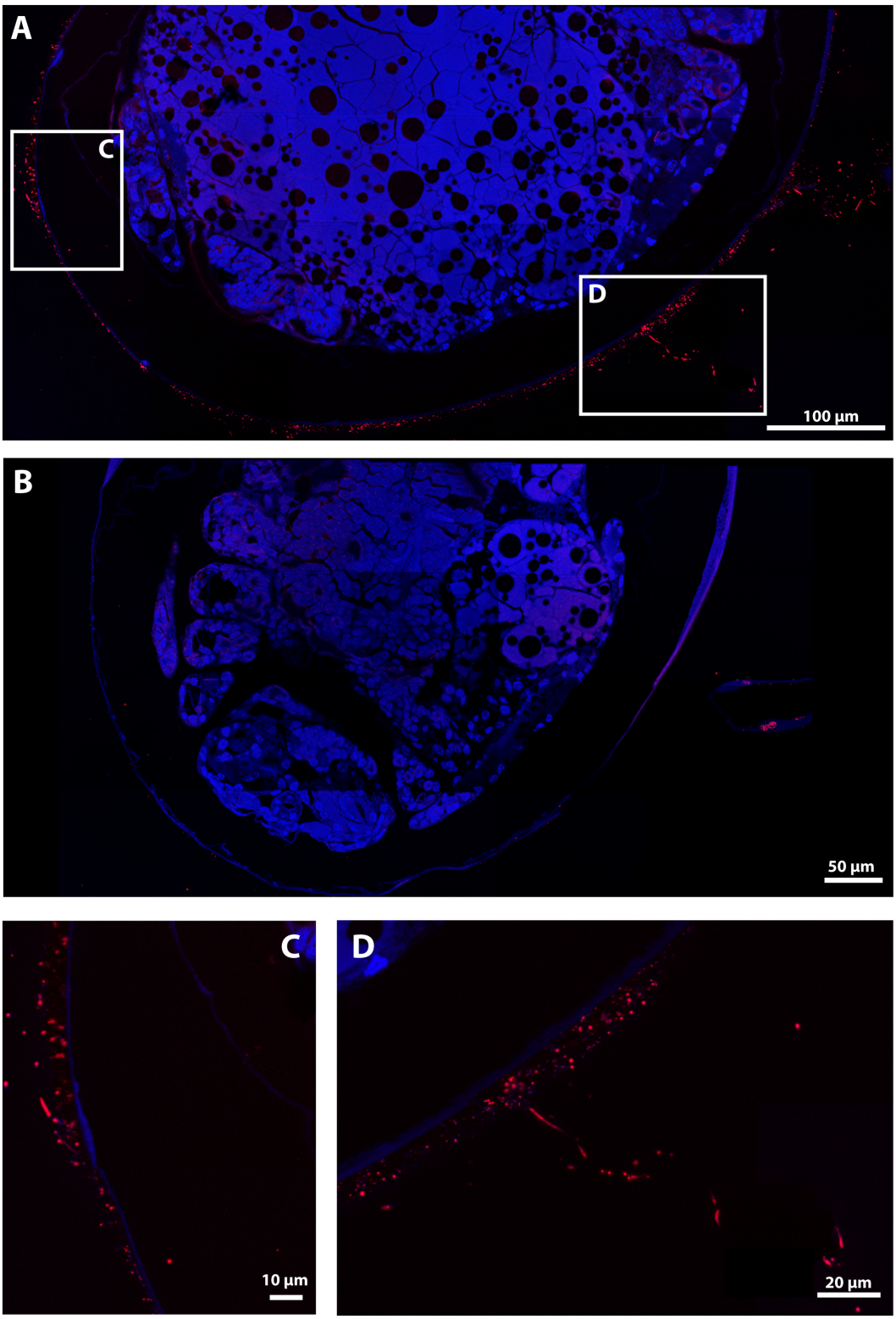


**FIGURE 7 |** FISH Observations of *Rimicaris exoculata* late stage eggs with universal bacteria probes. Observations were performed on semi-thin sections (2 µm) stained with DAPI (blue) and hybridized with Eub338-Cy5. **(A,C,D)** Egg from the external part of the brood with abundant mineral deposits, **(B)** Egg from the internal part of the brood without mineral deposits, Colors = Red (*Eubacteria*).

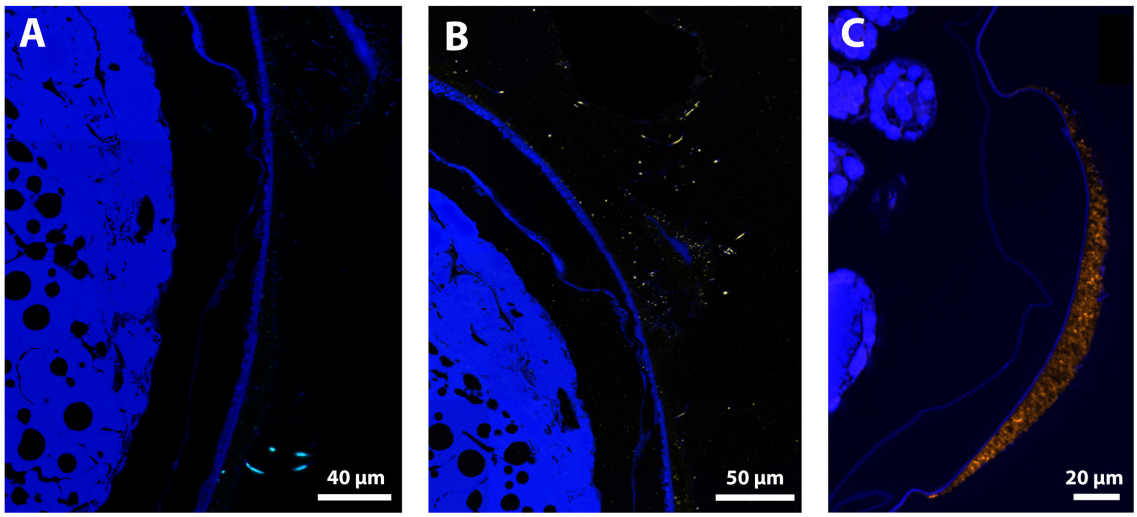


**FIGURE 8 |** FISH Observations of *Rimicaris exoculata* late stage eggs with specific probes. Observations were performed on semi-thin sections (2 µm) stained with DAPI (blue) with eggs from the external part of the brood with abundant mineral deposits, hybridized **(A)** with Epsi914-Cy5, **(B)** with Gam42a-Cy5, and **(C)** with Zeta123-Cy3. Colors = Light Blue (*Epsilonbacteraeota*), Yellow (*Gammaproteobacteria*), and Orange (*Zetaproteobacteria*).

usual intermolt period to a few weeks at most. Therefore, it is interesting to observe that colonization patterns in our samples are different from those observed in studies with a similar exposure period – approximately 2 weeks – both for experimental colonization devices and for other cuticular surfaces of the same species (Guri et al., 2012; Szafranski et al., 2015a; Zbinden et al., 2018). Rather than being dominated by *Epsilonbacteraeota*, our late stage samples, especially the eggs, show bacterial assemblages with higher evenness that are closer to those of long-term colonized surfaces deployed for about a year on MAR vent sites (Szafranski et al., 2015a).

Although a full understanding of all the drivers influencing colonization over egg development phases is not provided here, we can propose an explanation of colonization by some bacterial groups, arising from a combination of environmental influences and female behavior. *Epsilonbacteraeota* and thiotrophic *Gammaproteobacteria* are often described as sulfur oxidizers thriving in close but differing environmental niches due to their metabolic capacities (Petersen et al., 2010; Meier et al., 2017). Members of the first group, which predominantly use the rTCA cycle, are described as anaerobic or microaerophilic sulfur oxidizers, whereas members of the second group use the CBB cycle and are able to grow at higher $O_2$ concentration (Nakagawa and Takai, 2008). Additionally, many caridean shrimps and other decapods actively ventilate their egg mass by moving the pleopods frequently and quickly, with the frequency of this ventilation behavior increasing as the embryos mature (Fernández et al., 2002; Reinsel et al., 2014). A faster ventilation on late stage broods of *R. exoculata* could therefore result in a boost of oxygen supply to both egg and pleopod surfaces, promoting the growth of *Gammaproteobacteria* at the expense of *Epsilonbacteraeota*. *Zetaproteobacteria* are iron oxidizers that also use the CBB cycle (Field et al., 2014; Jan et al., 2014). However, they do not show significant abundance increase in response to increased mother ventilation with brood development. The increased oxygen supply could favor abiotic iron oxidation rather than bacterial metabolism, thus counterbalancing *Zetaproteobacteria* growth which remains approximately stable during egg development.

With microscopy, finer-scale observations revealed another level of variation when different eggs from the same brood were compared. As highlighted by FISH results (**Figure 7**), late stage eggs from the outer part of the brood have more mineral deposits and are colonized by more bacteria than late stage eggs from the inner part of the brood, for which bacterial coverage on the envelope is almost non-existent. Arguably, bacterial coverage on the egg envelope seems to be driven by both the position of the egg within the brood and the egg developmental stage, which ultimately reflects the degree of exposure of an egg to vent fluids. Therefore, not all eggs of *R. exoculata* are found to have a close association with bacterial assemblages on their envelope. Bacterial association at this stage of the animal life cycle should therefore perhaps be considered at the scale of the mother for the entire brood rather than at an individual scale for each embryo. The way in which this relationship evolves after hatching of *Rimicaris* larvae cannot be clarified with currently available data.

## Bacterial Assemblages of *Rimicaris exoculata* Eggs Are Influenced by Vent Fluid Chemistry

A sharp contrast between the bacterial communities in TAG and Snake Pit vent sites also underlines the importance of environmental influences on these assemblages. Geographical isolation has been proposed in some studies to explain the existence of distinct bacterial communities between different vent sites (Huber et al., 2010; Akerman et al., 2013). It is more

likely, however, that variations in vent fluid chemistry could explain the differences between TAG and Snake Pit assemblages. Indeed, with the exception of *Mycoplasmatales*, an order found only in TAG samples, or some *Cand. Campbellbacteria* OTUs present only at Snake Pit (**Supplementary Figure S2**), every other OTU was shared between communities from both vent sites, invalidating the hypothesis of a geographical exclusion. In addition the absence of these two groups in either TAG or Snake Pit samples could also be related to an insufficient sequencing depth since they were present in low abundance in our dataset.

A striking case supporting the major influence of vent fluid chemistry is that of *Zetaproteobacteria*, a group of iron-oxidizing bacteria that were significantly more abundant in TAG than in Snake Pit samples, both on egg and pleopod surfaces. Vent fluids from TAG are described as having much higher concentrations of Fe, Cu, and Mn than Snake Pit, which are richer in Cd and Pb (Jean-Baptiste et al., 1991; Tivey et al., 1995; Fouquet et al., 2010). Thus, a higher relative abundance of *Zetaproteobacteria* on both surfaces at TAG could result from a higher concentration of the energy source that fuels their metabolism. This is mirrored by observations made by Guri et al. (2012) on egg broods from Logatchev. In this vent site, fluids are enriched in $CH_4$ compared with TAG and Snake Pit, where $CH_4$ concentrations are very low (Charlou et al., 2002; Fouquet et al., 2010). Whereas no sequences of methanotrophic *Gammaproteobacteria* were found in our samples, a high number of sequences of this particular group were retrieved from clone libraries from Logatchev egg broods. Similar variations according to vent fluid composition were also described for symbiont communities within the cephalothorax of adult *R. exoculata* (Guri et al., 2012; Jan et al., 2014) and are not uncommon even in endosymbiotic communities of other vent species. Bathymodiolin species of the MAR, for example, show high flexibility in their relationship with two *Gammaproteobacteria* partners with distinct metabolic capacities. Variations in relative abundance of methane or sulfur-oxidizing symbionts were observed according to the fluid chemistry of their vent site of origin, but also according to the availability of these chemical substrates when mussels were incubated experimentally in pressure vessels (Duperron et al., 2006; Szafranski et al., 2015b). Such cases emphasize the important effect of vent fluid chemistry on the diversity observed in bacterial assemblages from specific vent sites.

Positive interactions between two or more of the bacterial partners could also explain the difference in relative abundance between TAG and Snake Pit communities in some lineages that are apparently not favored by local geochemistry. In such cases, if one of the partners is found to be more abundant in response to favorable vent fluid composition, the other partner could also be more abundant but not as a direct impact of the vent fluid chemistry. Such an interaction was previously observed between *Epsilonbacteraeota* and *Bacteroidetes* (Stokke et al., 2015), and could explain the higher abundance of some *Bacteroidetes* lineages in Snake Pit samples compared with those from TAG. Additional samples of brooding females and comparison of egg and pleopod assemblages from other vent sites with a greater difference in fluid composition, such as the ultramafic vent sites of Rainbow or Logatchev, would provide more evidence on the relative influence of vent fluid and body surface factors on the microbial community composition.

## Is There a Specific Bacterial Assemblage Associated With *Rimicaris exoculata* Egg Broods?

Despite of the importance of vent fluid chemistry, bacterial assemblages developing on eggs and pleopods were significantly different whatever their vent site of origin or developmental stage. Surprisingly, although they have been reported as the dominant symbionts within the *R. exoculata* cephalothorax in many studies (Petersen et al., 2010; Hügler et al., 2011; Guri et al., 2012), establishment of *Epsilonbacteraeota* from the *Sulfurovaceae* family was not as favored on egg envelopes as it was on pleopods. On the other hand, other families from this phylum, namely the *Arcobacteraceae* and the *Campylobacteraceae* had higher abundances on egg envelopes. Likewise, *Thiotricaceae* from the *Gammaproteobacteria* phylum, another important group retrieved within the cephalothorax, was not specifically associated with egg broods, being as abundant on their surfaces as on pleopods.

By contrast and despite their higher abundance in TAG bacterial assemblages, *Zetaproteobacteria* were always relatively more abundant on egg broods than on pleopod surfaces. *Zetaproteobacteria* have already been reported in close association with *R. exoculata* but never in such high relative abundance (Jan et al., 2014). They are often described as ecosystem engineers due to their capacity to shape the local environment by producing iron oxyhydroxide sheaths and stalks (Chan et al., 2011; Fleming et al., 2013; Scott et al., 2015). These structures provide architecture for the mats, which can alter local geochemistry, enhancing microbial diversity. For example, *Zetaproteobacteria*-dominated mats showed significantly higher diversity, both in terms of OTU numbers and evenness, than other bacterial mats (Hager et al., 2017). A significantly higher evenness of egg surfaces compared to pleopods could also result from the higher abundance of *Zetaproteobacteria* observed in our egg brood samples. All these results indicated a clear difference between egg and pleopod bacterial communities, supporting the existence of a specific brood microbial assemblage that differs from a simple opportunistic colonization on the egg surface but also from the symbiotic community within the adult cephalothorax.

This divergence between egg and pleopod microbial communities could be linked to distinct physical properties such as surface energy, hydrophobicity, and roughness between the hard exoskeleton cuticle of pleopods and the soft envelope of *R. exoculata* eggs. These factors have indeed been observed in laboratory experiments as playing an important role in determining which microorganisms could successfully attach to a specific substrate (Cooksey and Wigglesworth-Cooksey, 1995). Nonetheless, several studies with colonization devices conducted on deep sea ecosystems, noted little impact of substrate type on the microbial community composition compared with other environmental factors (Bellou et al., 2012; Lee et al., 2014; Szafranski et al., 2015a). Other characteristics of *R. exoculata* eggs

could therefore offer another explanation for this divergence between bacterial assemblages of different host surfaces. As stated in a previous study (Guri et al., 2012), our SEM observations confirmed the presence of a mucus-like material surrounding the eggs at every developmental stage (**Figure 2G**). This mucus coat seems to allow bacteria to attach since in areas where this mucus coat was lacerated bacteria were absent. Several studies have shown the importance of mucus for inter-partner recognition and for microorganism selection by many symbiotic metazoan hosts (Nyholm and McFall-Ngai, 2004; Nussbaumer et al., 2006; Bright and Bulgheresi, 2010). This selection usually implies tight chemical communication involving many molecules produced by the host, such as surface sugars, sugar-binding proteins or antimicrobial peptides (AMPs), all of which are important components of host mucus matrices (Bright and Bulgheresi, 2010; Rosa and Barracco, 2010). Such chemical communication molecules, the *luxS* and *luxR* genes, were already reported for *Epsilonbacteraeota* and *Gammaproteobacteria* symbionts of *R. exoculata* and are likely to be involved in the regulation of the symbiont population (Le Bloa et al., 2017). We hypothesize that similar mechanisms exist in *R. exoculata* during embryonic development and that a differential and regulated positive selection between host surfaces could explain differences observed between egg and pleopod bacterial communities. Future investigations on potential mechanisms, such as production and localization of potential AMPs within the brood or other aspects of shrimp maternal immunity are needed to understand these processes of selection more clearly.

## Perspectives on Roles and Acquisition of Bacteria Through the *Rimicaris* Life Cycle: What Gets Colonized First, the Egg or the Shrimp?

Our results provide first insights about bacterial colonization on different body surfaces of *R. exoculata*, which might be a host-controlled process. If such a selection exists, there must be an associated cost for the animal, counterbalanced by a potential role enhancing its fitness. The production of a cocktail of molecules by the mother or developing eggs to select specific bacteria could be one of these processes, and maternal behavioral responses, such as increased ventilation along egg development could be another. For adult shrimps, a nutritional role is now established for the symbiosis within the cephalothorax, which harbors bacterial lineages similar to those found in our work (Ponsard et al., 2013). However, absence of direct association for some eggs within the brood – those of the inner area – and high abundance of lipid reserves maintained even after hatching in *Rimicaris* larvae (Hernández-Ávila et al., 2015) suggest that a similar role is quite unlikely for eggs. If bacterial assemblages on the surface of eggs have a role for their host, it is certainly different from that observed in the cephalothorax of adults. As *R. exoculata* brooding females are found in dense aggregates close to hydrothermal emissions, bacterial assemblages could potentially offer protection against toxic compounds. This hypothesis has already been proposed for adults (Jan et al., 2014), and is supported in our results by the increased bacterial coverage observed on eggs more exposed to hydrothermal fluids and by a high sensitivity of egg brood bacterial assemblages to vent fluid composition. Protection against potential pathogens could be another role. Such anti-pathogen protection was suggested for epibiotic bacteria associated with *Homarus americanus* or *Palaemon macrodactylus* embryos, which produce substances inhibiting growth of pathogenic fungi (Gil-Turnes et al., 1989; Gil-Turnes and Fenical, 1992). Bacterial partners producing potent toxins protecting their hosts are also often described on egg surfaces of several species of terrestrial arthropods. These bacteria play an antipredator role for their insect hosts, as demonstrated by laboratory induced aposymbiotic eggs, which appear to experience more fungal infestation or more predation from spiders than eggs with bacterial symbionts (Kellner and Dettner, 1996; Flórez et al., 2017). All these examples stress the protective role of symbiosis in early life stages of arthropods and suggest that similar processes could be taking place in *R. exoculata*.

*Epsilonbacteraeota*, *Gammaproteobacteria,* and *Zetaproteobacteria* symbiont-related lineages appear able to colonize different surfaces of their host, such as eggs, pleopods (this study) or antennae (Zbinden et al., 2018). This observation resembles the case of *Kiwa puravida* yeti crabs from cold seeps, which have bacterial coverage on several body parts with closely related lineages (Goffredi et al., 2014). This capacity to settle quickly on different types of surfaces shows a strong ability for colonization in deep sea vent for these groups especially for *Epsilonbacteraeota* for which a highly conserved quorum sensing machinery enabling biofilm formation has been retrieved in every lineages (Pérez-Rodriguez et al., 2015). This machinery, in addition to LuxR genes for the *Gammaproteobacteria*, has furthermore been found in *Rimicaris exoculata* cephalothorax epibionts lineages (Le Bloa et al., 2017). Occurrence of *Epsilonbacteraeota*, *Gammaproteobacteria* and *Zetaproteobacteria* symbiont-related lineages in vent fluids and microbial mats of vent sites where *R. exoculata* also lives (Petersen et al., 2010; Scott et al., 2015) supports the hypothesis of a horizontal transmission mode for these three groups. More information on larval life of *R. exoculata* is needed to assess whether these bacterial lineages maintain a continuous presence or not throughout their host's life cycle. Intriguingly, a symbiont-related lineage of *Entomoplasmatales* was the sole bacterial group present on egg samples alone. Despite their very low abundance, our metabarcoding results provide a second report of this group on the eggs of *R. exoculata* with a different sequencing technique: Illumina MiSeq versus 454 Pyrosequencing used in Cowart et al. (2017). Considering technical limitations for detecting bacteria occurring at very low abundance with standard FISH, and the absence of a specific probe for this group, our observations failed to localize them precisely. Potential locations could be the egg surface, as for *Gammaproteobacteria* or *Epsilonbacteraeota,* inside eggs and directly associated with the embryos, or only in the mucus matrix. However, *Entomoplasmatales*-related sequences were not detected in any of our egg brood samples, which could be related to insufficient sequencing depth. Occasional contamination of this group on mucus embedded eggs by maternal anal excretion cannot be eliminated, whether or not this corresponds to a true transmission pathway for *Rimicaris*

shrimps. Whereas the presence of *Entomoplasmatales* on eggs is not completely confirmed by our work, we do not exclude the possibility of a vertical transmission for this group, especially since *Entomoplasmatales* have never been retrieved from the surrounding environment. This might occur during embryonic development by release of bacteria from the gut of the mother in the mucus coat during or after oviposition, by infection of ovaries during vitellogenesis as proposed by Durand et al. (2015), or later on by trophallaxis between juveniles and adults (Durand et al., 2015). To improve understanding of symbiont acquisition during the life cycle of *R. exoculata*, targeted FISH experiments with specific *Entomoplasmatales* probes are now needed to precisely locate them, first in the adult digestive system and then in other life stages. More investigations on the internal anatomy of *Rimicaris* larvae could also help to determine the possible existence of a hosting organ for this group at this life stage.

## AUTHOR CONTRIBUTIONS

PM contributed to data acquisition and analysis, wrote the first draft of the manuscript, review and editing of this manuscript. IH-A contributed for electron microscopy data acquisition and conception and design of the study, review and editing of this manuscript. JA contributed for analysis of sequencing data and review corresponding sections of this manuscript. VC-G contributed for data acquisition and methodology for molecular biology work. NG contributed for electron microscopy data acquisition. BS and LA designed, provided, and serviced the PERISCOP device, and supervised the corresponding *in situ* sampling operations. FP and M-AC-B contributed to conception and design of the study, review and editing of the manuscript, and supervision of the project.

## FUNDING

This work was supported by the Ifremer REMIMA program. Pressure equipments used in this study were funded by the European Community programs EXOCET/D (FP6-GOCE-CT-2003-505342), and MIDAS (FP7/2007-2013-603418) and by the CNRS project "Defi Instrumentation aux limites" (2016).

## ACKNOWLEDGMENTS

We would like to thank the chief scientists of the BICOSE 2014 (http://dx.doi.org/10.17600/14000100) and BICOSE 2 (http://dx.doi.org/10.17600/18000004) cruises (M-AC-B), the captains and crews of the R/V *Pourquoi pas?*, the ROV Victor 6000 and Nautile submersible teams for their efficiency. We would like to thank G. Hamel for his implication in the design of the pressurized-recovery device. We would like to thank P. Elies and the PIMM platform of Université de Bretagne Occidentale for the use of the ultramicrotome for thin sectioning used for FISH experiments. We would like to thank Dr. S. Laming for his help and knowledge about microscopy, from sectioning to image capturing for FISH experiments. We would also like to thank H. Mc Combie-Boudry of the Bureau de Traduction of Université de Bretagne Occidentale for English edition.

## SUPPLEMENTARY MATERIAL

The Supplementary Material for this article can be found online at: https://www.frontiersin.org/articles/10.3389/fmicb.2019.00808/full#supplementary-material

**FIGURE S1 |** X-Ray Spectrophotometric analysis (EDX) showing SEM analyzed areas of mineral crusts or mineral deposits for each sample with the corresponding spectrum. For some samples, bare surface areas clear of minerals were also analyzed as control. Analyzed were performed on **(A,B)** late stage eggs, **(C)** late stage pleopods, **(D)** mid stage eggs, **(E)** and mid stage pleopods.

**FIGURE S2 |** Venn diagrams representing the numbers of shared OTUs across all samples. Affiliations of taxa representative of a body structure, vent field, or developmental stage are indicated.

**FIGURE S3 |** Alpha diversity measures of OTU number (Richness) and Inverse Simpson index (Evenness) compared **(A)** between eggs and pleopods, **(B)** between TAG and Snake Pit egg samples, **(C)** between TAG and Snake Pit pleopod samples, **(D)** between developmental stages of egg samples, and **(E)** between developmental stages of the corresponding eggs for pleopod samples. * mean that significant differences were statistically supported.

**FIGURE S4 |** Mean relative abundances per categories of 16S rRNA gene sequence reads according to their classification (Silva 132 database). Groups are at the family level for the *Epsilonbacteraeota* phylum and at the class level for other phyla.

**FIGURE S5 |** Ranked LDA scores of the differentially abundant bacterial taxa, with taxa with highest relative abundance at TAG in orange, and taxa with highest relative abundance at Snake Pit in blue for bacterial communities covering **(A)** eggs and **(B)** pleopods of ovigerous *R. exoculata*.

**FIGURE S6 |** Ranked LDA scores of the differentially abundant bacterial taxa, with taxa with highest relative abundance at early stage in yellow, at mid stage in brown and at late stage in purple for bacterial communities covering **(A)** eggs and **(B)** pleopods of ovigerous *R. exoculata.*

**FIGURE S7 |** Additional FISH observations of *Rimicaris exoculata* eggs. Observations were performed on semi-thin sections (2 μm) stained with DAPI (blue) **(A)** Early stage egg hybridized with Eub338-Cy5 and **(B)** Late stage egg co-hybridized with Eub338-Cy5 and Gam42a-Cy5. Colors, Green (*Eubacteria*), Red (*Gammaproteobacteria*), and Yellow (Co-*hybridized probes*).

**TABLE S1 |** List of samples used in this study.

**TABLE S2 |** List of FISH probes used in this study.

**TABLE S3 |** PERMANOVA analysis.

## REFERENCES

Akerman, N. H., Butterfield, D. A., and Huber, J. A. (2013). Phylogenetic diversity and functional gene patterns of sulfur-oxidizing subseafloor Epsilonproteobacteria in diffuse hydrothermal vent fluids. *Front. Microbiol.* 4:185. doi: 10.3389/fmicb.2013.00185

Alain, K., Zbinden, M., Le, Bris N, Lesongeur, F., Quérellou, J., Gaill, F., et al. (2004). Early steps in microbial colonization processes at deep-sea hydrothermal vents. *Environ. Microbiol.* 6, 227–241. doi: 10.1111/j.1462-2920.2004.00557.x

Amann, R. I., Krumholz, L., and Stahl, D. A. (1990). Fluorescent-oligonucleotide probing of whole cells for determinative, phylogenetic, and environmental

studies in microbiology. *J. Bacteriol.* 172, 762–770. doi: 10.1128/JB.172.2.762-770.1990

Arbizu, M. (2017). *Pairwiseadonis: Pairwise Multilevel Comparison Using Adonis. R Packag. Version 0.0 1* Available at: https://github.com/pmartinezarbizu/pairwiseAdonis. doi: 10.1128/jb.172.2.762-770.1990

Bauer, R. T. (2013). "Adaptive modification of appendages for grooming (cleaning, antifouling) and reproduction in the crustacea," in *Functional Morphology Crustacea* eds L. Walting, and M. theil (NewYork, NY: Oxford University Press), 327–364. doi: 10.1093/acprof:osobl/9780195398038.003.0013

Bauer, R. T., and Abdalla, J. H. (2000). Patterns of brood production in the grass shrimp Palaemonetes pugio ( Decapoda: Caridea ). *Invertebr. Reprod. Dev.* 38, 107–113. doi: 10.1080/07924259.2000.9652445

Bellou, N., Papathanassiou, E., Dobretsov, S., Lykousis, V., and Colijn, F. (2012). The effect of substratum type, orientation and depth on the development of bacterial deep-sea biofilm communities grown on artificial substrata deployed in the Eastern Mediterranean. *Biofouling* 28, 199–213. doi: 10.1080/08927014.2012.662675

Bokulich, N. A., Subramanian, S., Faith, J. J., Gevers, D., Gordon, I., Knight, R., et al. (2013). Quality-filtering vastly improves diversity estimates from Illumina amplicon sequencing. *Nat. Methods* 10, 57–59. doi: 10.1038/nmeth.2276.Quality-filtering

Bright, M., and Bulgheresi, S. (2010). A complex journey: transmission of microbial symbionts. *Nat. Rev. Microbiol.* 8, 218–230. doi: 10.1038/nrmicro2262

Camacho, C., Coulouris, G., Avagyan, V., Ma, N., Papadopoulos, J., Bealer, K., et al. (2009). BLAST+: architecture and applications. *BMC Bioinformatics* 10:421. doi: 10.1186/1471-2105-10-421

Campbell, B. J., Engel, A. S., Porter, M. L., and Takai, K. (2006). The versatile ?-*proteobacteria*: key players in sulphidic habitats. *Nat. Rev. Microbiol.* 4, 458–468. doi: 10.1038/nrmicro1414

Chan, C. S., Fakra, S. C., Emerson, D., Fleming, E. J., and Edwards, K. J. (2011). Lithotrophic iron-oxidizing bacteria produce organic stalks to control mineral growth: implications for biosignature formation. *ISME J.* 5, 717–727. doi: 10.1038/ismej.2010.173

Charlou, J. L., Donval, J. P., Fouquet, Y., Jean-Baptiste, P., and Holm, N. (2002). Geochemistry of high H2 and CH4 vent fluids issuing from ultramafic rocks at the Rainbow hydrothermal field (36°14'N,MAR). *Chem. Geol.* 191, 345–359. doi: 10.1016/S0009-2541(02)00134-1

Cooksey, K. E., and Wigglesworth-Cooksey, B. (1995). Adhesion of bacteria and diatoms to surfaces in the sea: a review. *Aquat. Microb. Ecol.* 9, 87–96. doi: 10.3354/ame009087

Copley, J. T., Jorgensen, P. B. K., and Sohn, R. A. (2007). Assessment of decadal-scale ecological change at a deep Mid-Atlantic hydrothermal vent and reproductive time-series in the shrimp *Rimicaris exoculata*. *J. Mar. Biol. Assoc.* 87, 859–867. doi: 10.1017/S0025315407056512

Corbari, L., Cambon-Bonavita, M. A., Long, G. J., Grandjean, F., Zbinden, M., Gaill, F., et al. (2008a). Iron oxide deposits associated with the ectosymbiotic bacteria in the hydrothermal vent shrimp *Rimicaris exoculata*. *Biogeosciences Discuss.* 5, 1825–1865. doi: 10.5194/bgd-5-1825-2008

Corbari, L., Zbinden, M., Cambon-Bonavita, M. A., Gaill, F., and Compère, P. (2008b). Bacterial symbionts and mineral deposits in the branchial chamber of the hydrothermal vent shrimp *Rimicaris exoculata*: relationship to moult cycle. *Aquat. Biol.* 1, 225–238. doi: 10.3354/ab00024

Correa, C., and Thiel, M. (2003). Mating systems in caridean shrimp (Decapoda: Caridea) and their evolutionary consequences for sexual dimorphism and reproductive biology Sistemas de apareamiento en camarones carideos (Decapoda: Caridea) y sus consecuencias evolutivas en el dimorfismo sex. *Rev. Chil. Hist. Nat.* 76, 187–203. doi: 10.4067/S0716-078X2003000200006

Cowart, D. A., Durand, L., Cambon-Bonavita, M. A., and Arnaud-Haond, S. (2017). Investigation of bacterial communities within the digestive organs of the hydrothermal vent shrimp *Rimicaris exoculata* provide insights into holobiont geographic clustering. *PLoS One* 12:e0172543. doi: 10.1371/journal.pone.0172543

Dubilier, N., Bergin, C., and Lott, C. (2008). Symbiotic diversity in marine animals: the art of harnessing chemosynthesis. *Nat. Rev. Microbiol.* 6, 725–740. doi: 10.1038/nrmicro1992

Duperron, S., Bergin, C., Zielinski, F., Blazejak, A., Pernthaler, A., McKiness, Z. P., et al. (2006). A dual symbiosis shared by two mussel species, Bathymodiolus azoricus and Bathymodiolus puteoserpentis (Bivalvia: Mytilidae), from hydrothermal vents along the northern Mid-Atlantic Ridge. *Environ. Microbiol.* 8, 1441–1447. doi: 10.1111/j.1462-2920.2006.01038.x

Duperron, S., De Beer, D., Zbinden, M., Boetius, A., Schipani, V., Kahil, N., et al. (2009). Molecular characterization of bacteria associated with the trophosome and the tube of *Lamellibrachia* sp., a siboglinid annelid from cold seeps in the eastern Mediterranean. *FEMS Microbiol. Ecol.* 69, 395–409. doi: 10.1111/j.1574-6941.2009.00724.x

Durand, L., Roumagnac, M., Cueff-Gauchard, V., Jan, C., Guri, M., Tessier, C., et al. (2015). Biogeographical distribution of *Rimicaris exoculata* resident gut epibiont communities along the Mid-Atlantic Ridge hydrothermal vent sites. *FEMS Microbiol. Ecol.* 91, 1–15. doi: 10.1093/femsec/fiv101

Durand, L., Zbinden, M., Cueff-Gauchard, V., Duperron, S., Roussel, E. G., Shillito, B., et al. (2010). Microbial diversity associated with the hydrothermal shrimp *Rimicaris exoculata* gut and occurrence of a resident microbial community. *FEMS Microbiol. Ecol.* 71, 291–303. doi: 10.1111/j.1574-6941.2009.00806.x

Edgar, R. C., and Flyvbjerg, H. (2015). Error filtering, pair assembly and error correction for next-generation sequencing reads. *Bioinformatics* 31, 3476–3482. doi: 10.1093/bioinformatics/btv401

Edgar, R. C., Haas, B. J., Clemente, J. C., Quince, C., and Knight, R. (2011). UCHIME improves sensitivity and speed of chimera detection. *Bioinformatics* 27, 2194–2200. doi: 10.1093/bioinformatics/btr381

Escudié, F., Auer, L., Bernard, M., Mariadassou, M., Cauquil, L., Vidal, K., et al. (2018). FROGS: find, Rapidly, OTUs with Galaxy Solution. *Bioinformatics* 34, 1287–1294. doi: 10.1093/bioinformatics/btx791

Fadrosh, D. W., Ma, B., Gajer, P., Sengamalay, N., Ott, S., Brotman, R. M., et al. (2014). An improved dual-indexing approach for multiplexed 16S rRNA gene sequencing on the Illumina MiSeqplatform. *Microbiome* 2:6. doi: 10.1186/2049-2618-2-6

Fernández, M., Pardo, L. M., and Baeza, J. A. (2002). Patterns of oxygen supply in embryo masses of brachyuran crabs throughout development: the effect of oxygen availability and chemical cues in determining female brooding behavior. *Mar. Ecol. Prog. Ser.* 245, 181–190. doi: 10.3354/meps245181

Field, E. K., Sczyrba, A., Lyman, A. E., Harris, C. C., Woyke, T., Stepanauskas, R., et al. (2014). Genomic insights into the uncultivated marine Zeta*proteobacteria* at Loihi Seamount. *ISME J.* 9, 857–870. doi: 10.1038/ismej.2014.183

Fisher, W. S., and Clark, W. H. J. (1983). Eggs of Palaemon macrodactylus: I. Attachment to the pleopods and formation of the outer investment coat. *Biol. Bull.* 164, 189–200. doi: 10.2307/1541140

Fleming, E. J., Davis, R. E., Mcallister, S. M., Chan, C. S., Moyer, C. L., Tebo, B. M., et al. (2013). Hidden in plain sight: discovery of sheath-forming, iron-oxidizing Zetaproteobacteria at Loihi Seamount, Hawaii, USA. *FEMS Microbiol. Ecol.* 85, 116–127. doi: 10.1111/1574-6941.12104

Flórez, L. V., Scherlach, K., Gaube, P., Ross, C., Sitte, E., Hermes, C., et al. (2017). Antibiotic-producing symbionts dynamically transition between plant pathogenicity and insect-defensive mutualism. *Nat. Commun.* 8:15172. doi: 10.1038/ncomms15172

Fouquet, Y., Cambon, P., Etoubleau, J., Charlou, J. L., Ondréas, H., Barriga, F. J. A. S., et al. (2010). "Geodiversity of Hydrothermal Processes Along the Mid-Atlantic Ridge and Ultramafic-Hosted Mineralization: a New Type of Oceanic Cu-Zn-Co-Au Volcanogenic Massive Sulfide Deposit," in *Diversity of Hydrothermal Systems on Slow Spreading Ocean Ridges*, eds P. A. Rona, and C. W. Devey (Washington,DC: AGU), 321–367. doi: 10.1029/2008GM000746

Gil-Turnes, M. S., and Fenical, W. (1992). Embryos of Homarus americanus are protected by epibiotic bacteria. *Biol. Bull.* 182, 105–108. doi: 10.2307/1542184

Gil-Turnes, M. S., Hay, M., and Fenical, W. (1989). Symbiotic marine bacteria chemically defend crustacean embryos from a pathogenic fungus. *Science* 246, 116–118. doi: 10.1126/science.2781297

Goffredi, S. K. (2010). Indigenous ectosymbiotic bacteria associated with diverse hydrothermal vent invertebrates. *Environ. Microbiol. Rep.* 2, 479–488. doi: 10.1111/j.1758-2229.2010.00136.x

Goffredi, S. K., Gregory, A., Jones, W. J., Morella, N. M., and Sakamoto, R. I. (2014). Ontogenetic variation in epibiont community structure in the deep-sea yeti crab, *Kiwa puravida*: convergence among crustaceans. *Mol. Ecol.* 23, 1457–1472. doi: 10.1111/mec.12439

Guri, M., Durand, L., Cueff-Gauchard, V., Zbinden, M., Crassous, P., Shillito, B., et al. (2012). Acquisition of epibiotic bacteria along the life cycle of the

hydrothermal shrimp *Rimicaris exoculata*. *ISME J.* 6, 597–609. doi: 10.1038/ismej.2011.133

Hager, K. W., Fullerton, H., Butterfield, D. A., and Moyer, C. L. (2017). Community structure of lithotrophically-driven hydrothermal microbial mats from the Mariana Arc and back-arc. *Front. Microbiol.* 8:1578. doi: 10.3389/fmicb.2017.01578

Herlemann, D. P. R., Labrenz, M., Jürgens, K., Bertilsson, S., Waniek, J. J., and Andersson, A. F. (2011). Transitions in bacterial communities along the 2000 km salinity gradient of the Baltic Sea. *ISME J.* 5, 1571–1579. doi: 10.1038/ismej.2011.41

Hernández-Ávila, I. (2016). *Larval Dispersal and Life Cycle in deep-water hydrothermal vents: The case of Rimicaris exoculata and related species*. Available at: https://tel.archives-ouvertes.fr/tel-01612011 doi: 10.1038/ismej.2011.41

Hernández-Ávila, I., Cambon-Bonavita, M. A., and Pradillon, F. (2015). Morphology of first zoeal stage of four genera of alvinocaridid shrimps from hydrothermal vents and cold seeps: Implications for ecology, larval biology and phylogeny. *PLoS One* 10:e0144657. doi: 10.1371/journal.pone.0144657

Hess, W. N. (1941). Factors influencing moulting in the crustacean, *Crangon armillatus*. *Biol. Bull. Mar. Biol. Lab.* 81, 215–220. doi: 10.2307/1537788

Huber, J. A., Cantin, H. V., Huse, S. M., Mark Welch, D. B., Sogin, M. L., and Butterfield, D. A. (2010). Isolated communities of Epsilon*proteobacteria* in hydrothermal vent fluids of the Mariana Arc seamounts. *FEMS Microbiol. Ecol.* 73, 538–549. doi: 10.1111/j.1574-6941.2010.00910.x

Hügler, M., Petersen, J. M., Dubilier, N., Imhoff, J. F., and Sievert, S. M. (2011). Pathways of carbon and energy metabolism of the epibiotic community associated with the deep-sea hydrothermal vent shrimp *Rimicaris exoculata*. *PLoS One* 6:e16018. doi: 10.1371/journal.pone.0016018

Jan, C., Petersen, J. M., Werner, J., Teeling, H., Huang, S., Glöckner, F. O., et al. (2014). The gill chamber epibiosis of deep-sea shrimp *Rimicaris exoculata*: an in-depth metagenomic investigation and discovery of Zetaproteobacteria. *Environ. Microbiol.* 16, 2723–2738. doi: 10.1111/1462-2920.12406

Jean-Baptiste, P., Charlou, J. L., Stievenard, M., Donval, J. P., Bougault, H., and Mevel, C. (1991). Helium and methane measurements in hydrothermal fluids from the mid-Atlantic ridge: the Snake Pit site at 23°N. *Earth Planet. Sci. Lett.* 106, 17–28. doi: 10.1016/0012-821X(91)90060-U

Kato, S., Yanagawa, K., Sunamura, M., Takano, Y., Ishibashi, J. I., Kakegawa, T., et al. (2009). Abundance of Zeta*proteobacteria* within crustal fluids in back-arc hydrothermal fields of the Southern Mariana Trough. *Environ. Microbiol.* 11, 3210–3222. doi: 10.1111/j.1462-2920.2009.02031.x

Kellner, R. L. L., and Dettner, K. (1996). Differential efficacy of toxic pederin in deterring potential arthropod predators of Paederus (Coleoptera: Staphylinidae) offspring. *Oecologia* 107, 293–300. doi: 10.1007/BF00328445

Le Bloa, S., Durand, L., Cueff-Gauchard, V., Le Bars, J., Taupin, L., Marteau, C., et al. (2017). Highlighting of quorum sensing lux genes and their expression in the hydrothermal vent shrimp *Rimicaris exoculata* ectosymbiontic community. Possible use as biogeographic markers. *PLoS One* 12:e0174338. doi: 10.1371/journal.pone.0174338

Lee, O. O., Wang, Y., Tian, R., Zhang, W., Shek, C. S., Bougouffa, S., et al. (2014). In situ environment rather than substrate type dictates microbial community structure of biofilms in a cold seep system. *Sci. Rep.* 4, 1–10. doi: 10.1038/srep03587

López-García, P., Duperron, S., Philippot, P., Foriel, J., Susini, J., and Moreira, D. (2003). Bacterial diversity in hydrothermal sediment and epsilonproteobacterial dominance in experimental microcolonizers at the Mid-Atlantic Ridge. *Environ. Microbiol.* 5, 961–976. doi: 10.1046/j.1462-2920.2003.00495.x

López-García, P., Gaill, F., and Moreira, D. (2002). Wide bacterial diversity associated with tubes of the vent worm *Riftia pachyptila*. *Environ. Microbiol.* 4, 204–215. doi: 10.1046/j.1462-2920.2002.00286.x

Loy, A., Horn, M., and Wagner, M. (2003). probeBase: an online ressource for rRNA-targeted oligonucleotide probes. *Nucleic Acids Res.* 31, 514–516. doi: 10.1093/nar/gkg015

Mahé, F., Rognes, T., Quince, C., de Vargas, C., and Dunthorn, M. (2014). Swarm: robust and fast clustering method for amplicon-based studies. *PeerJ* 2:e593. doi: 10.7717/peerj.593

Manz, W., Amann, R., Ludwig, W., Wagner, M., and Schleifer, K. H. (1992). Phylogenetic Oligodeoxynucleotide Probes for the Major Subclasses of *Proteobacteria*: problems and Solutions. *Syst. Appl. Microbiol.* 15, 593–600. doi: 10.1016/S0723-2020(11)80121-9

McMurdie, P. J., and Holmes, S. (2013). Phyloseq: an R Package for reproducible interactive analysis and graphics of microbiome census data. *PLoS One* 8:e61217. doi: 10.1371/journal.pone.0061217

Meier, D. V., Pjevac, P., Bach, W., Hourdez, S., Girguis, P. R., Vidoudez, C., et al. (2017). Niche partitioning of diverse sulfur-oxidizing bacteria at hydrothermal vents. *ISME J.* 11, 1545–1558. doi: 10.1038/ismej.2017.37

Nakagawa, S., and Takai, K. (2008). Deep-sea vent chemoautotrophs: diversity, biochemistry and ecological significance. *FEMS Microbiol. Ecol.* 65, 1–14. doi: 10.1111/j.1574-6941.2008.00502.x

Nussbaumer, A. D., Fisher, C. R., and Bright, M. (2006). Horizontal endosymbiont transmission in hydrothermal vent tubeworms. *Nature* 441, 345–348. doi: 10.1038/nature04793

Nyholm, S. V., and McFall-Ngai, M. (2004). The winnowing: establishing the squid–vibrio symbiosis. *Nat. Rev. Microbiol.* 2, 632–642. doi: 10.1038/nrmicro957

Oksanen, J., Kindt, R., Legendre, P., O'Hara, B., Simpson, G. L., Solymos, P. M., et al. (2008). The vegan package. *Community Ecol. Packag.* 190:254. doi: 10.4135/9781412971874.n145

Pandian, T. J., Balasundaram, C., and Kamaraj, M. (1982). Moulting and spawning cycles in *Macrobrachium nobilii* ( Henderson and Mathai ). *Int. J. Invertebr. Reprod.* 5, 21–30. doi: 10.1080/01651269.1982.10553451

Paulson, J. N., Stile, C. O., Bravo, H. C., and Pop, M. (2013). Robust methods for differential abundance analysis in marker gene surveys. *Nat. Methods* 10, 1200–1202. doi: 10.1038/nmeth.2658.Robust

Pérez-Rodriguez, I., Bolognini, M., Ricci, J., Bini, E., and Vetriani, C. (2015). From deep-sea volcanoes to human pathogens: a conserved quorum-sensing signal in Epsilon *proteobacteria*. *ISME J.* 9, 1222–1234. doi: 10.1038/ismej.2014.214

Petersen, J. M., Ramette, A., Lott, C., Cambon-Bonavita, M. A., Zbinden, M., and Dubilier, N. (2010). Dual symbiosis of the vent shrimp *Rimicaris exoculata* with filamentous gamma- and epsilonproteobacteria at four mid-atlantic ridge hydrothermal vent fields. *Environ. Microbiol.* 12, 2204–2218. doi: 10.1111/j.1462-2920.2009.02129.x

Ponsard, J., Cambon-Bonavita, M. A., Zbinden, M., Lepoint, G., Joassin, A., Corbari, L., et al. (2013). Inorganic carbon fixation by chemosynthetic ectosymbionts and nutritional transfers to the hydrothermal vent host-shrimp *Rimicaris exoculata*. *ISME J.* 7, 96–109. doi: 10.1038/ismej.2012.87

Quast, C., Pruesse, E., Yilmaz, P., Gerken, J., Schweer, T., Yarza, P., et al. (2013). The SILVA ribosomal RNA gene database project: improved data processing and web-based tools. *Nucleic Acids Res.* 41, 590–596. doi: 10.1093/nar/gks1219

Raviv, S., Parnes, S., and Sagi, A. (2008). "Coordination of Reproduction and Molt in Decapods," in *Reproductive Biology of Crustaceans*, ed. E. Mente (Enfield, NH: Science Publishers), 365–390. doi: 10.1201/9781439843345-c9

Reinsel, K. A., Pagel, K., Kissel, M., Foran, E., Clare, A. S., and Rittschof, D. (2014). Egg mass ventilation by caridean shrimp: Similarities to other decapods and insight into pheromone receptor location. *J. Mar. Biol. Assoc. U. K.* 94, 1009–1017. doi: 10.1017/S0025315414000332

Rognes, T., Flouri, T., Nichols, B., Quince, C., and Mahé, F. (2016). VSEARCH: a versatile open source tool for metagenomics. *PeerJ* 4:e2584. doi: 10.7717/peerj.2584

Rosa, R. D., and Barracco, M. A. (2010). Antimicrobial peptides in crustaceans. *ISJ* 7, 262–284. doi: 10.1016/j.jip.2010.09.012

Scott, J. J., Breier, J. A., Luther, G. W., and Emerson, D. (2015). Microbial iron mats at the mid-atlantic ridge and evidence that zetaproteobacteria may be restricted to iron-oxidizing marine systems. *PLoS One* 10:e119284. doi: 10.1371/journal.pone.0119284

Segata, N., Izard, J., Waldron, L., Gevers, D., Miropolsky, L., Garrett, W. S., et al. (2011). Metagenomic biomarker discovery and explanation. *Genome Biol.* 12:R60. doi: 10.1186/gb-2011-12-6-r60

Segonzac, M., de Saint Laurent, M., and Casanova, B. (1993). L'enigme du comportement trophique des crevettes Alvinocarididae des sites hydrothermaux de la dorsale medio-atlantique. *Cah. Biol. Mar.* 34, 535–571.

Shillito, B., Hamel, G., Duchi, C., Cottin, D., Sarrazin, J., Sarradin, P. M., et al. (2008). Live capture of megafauna from 2300 m depth, using a newly designed Pressurized Recovery Device. *Deep Res. Part I Oceanogr. Res. Pap.* 55, 881–889. doi: 10.1016/j.dsr.2008.03.010

Simpson, E. H. (1949). Measurement of diversity. *Nature* 163:688. doi: 10.1038/163688a0

Stokke, R., Dahle, H., Roalkvam, I., Wissuwa, J., Daae, F. L., Tooming-Klunderud, A., et al. (2015). Functional interactions among filamentous Epsilon*proteobacteria* and Bacteroidetes in a deep-sea hydrothermal vent biofilm. *Environ. Microbiol.* 17, 4063–4077. doi: 10.1111/1462-2920.12970

Szafranski, K. M., Deschamps, P., Cunha, M. R., Gaudron, S. M., and Duperron, S. (2015a). Colonization of plant substrates at hydrothermal vents and cold seeps in the northeast Atlantic and Mediterranean and occurrence of symbiont-related bacteria. *Front. Microbiol.* 6:162. doi: 10.3389/fmicb.2015.00162

Szafranski, K. M., Piquet, B., Shillito, B., Lallier, F. H., and Duperron, S. (2015b). Relative abundances of methane- and sulfur-oxidizing symbionts in gills of the deep-sea hydrothermal vent mussel *Bathymodiolus azoricus* under pressure. *Deep Res. Part I Oceanogr. Res. Pap.* 101, 7–13. doi: 10.1016/j.dsr.2015.03.003

Tivey, M. K., Humphris, S. E., Thompson, G., Hannington, M. D., and Rona, P. A. (1995). Deducing patterns of fluid flow and mixing within the TAG active hydrothermal mound using mineralogical and geochemical data. *J. Geophys. Res. Solid Earth* 100, 12527–12555. doi: 10.1029/95JB00610

Watanabe, H., Yahagi, T., Nagai, Y., Seo, M., Kojima, S., Ishibashi, J., et al. (2016). Different thermal preferences for brooding and larval dispersal of two neighboring shrimps in deep-sea hydrothermal vent fields. *Mar. Ecol.* 37, 1–8. doi: 10.1111/maec.12318

Williams, A. B., and Rona, P. A. (1986). Two new caridean shrimps from a hydrothermal field on the mid Atlantic Ridge. *J. Crustac. Biol.* 6, 446–462. doi: 10.1163/193724086x00299

Zbinden, M., and Cambon-Bonavita, M. A. (2003). Occurrence of Deferribacterales and Entomoplasmatales in the deep-sea Alvinocarid shrimp *Rimicaris exoculata* gut. *FEMS Microbiol. Ecol.* 46, 23–30. doi: 10.1016/S0168-6496(03)00176-4

Zbinden, M., Gallet, A., Szafranski, K. M., Machon, J., Ravaux, J., Léger, N., et al. (2018). Blow your nose, shrimp! unexpectedly dense bacterial communities occur on the antennae and antennules of hydrothermal vent shrimp. *Front. Mar. Sci.* 5:357. doi: 10.3389/fmars.2018.00357

Zbinden, M., Le Bris, N., Gaill, F., and Compère, P. (2004). Distribution of bacteria and associated minerals in the gill chamber of the vent shrimp *Rimicaris exoculata* and related biogeochemical processes. *Mar. Ecol. Prog. Ser.* 284, 237–251. doi: 10.3354/meps284237

Zbinden, M., Shillito, B., Le Bris, N., de Villardi, de Montlaur, C., Roussel, E., et al. (2008). New insigths on the metabolic diversity among the epibiotic microbial communitiy of the hydrothermal shrimp *Rimicaris exoculata*. *J. Exp. Mar. Bio. Ecol.* 359, 131–140. doi: 10.1016/j.jembe.2008.03.009

**Conflict of Interest Statement:** The authors declare that the research was conducted in the absence of any commercial or financial relationships that could be construed as a potential conflict of interest.

# Article Supplementary materials

## A) BIC-PL10-Peris3-Rimi8: Late stage egg

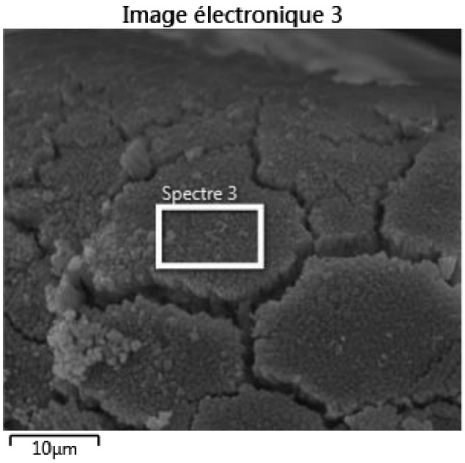


***SEM image analyzed by EDX***

**Spectre 3: Mineral crust area analyzed for this egg**

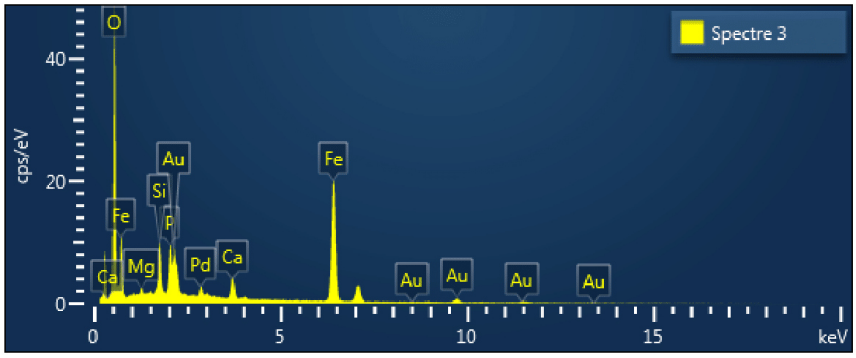

# B) BIC-PL08-Peris1-R1: Late stage egg

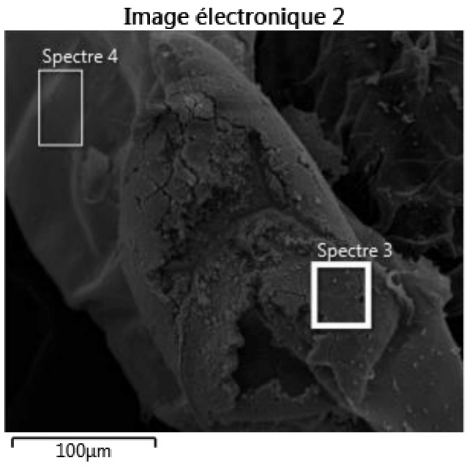


***SEM image analyzed by EDX***

**<u>Spectre 3</u>: Mineral crust area analyzed for this egg**

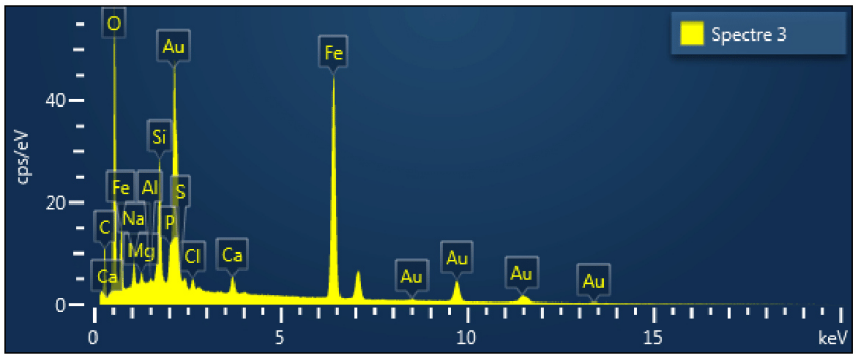


**<u>Spectre 4</u>: Bare egg envelope area analyzed for this egg as control**

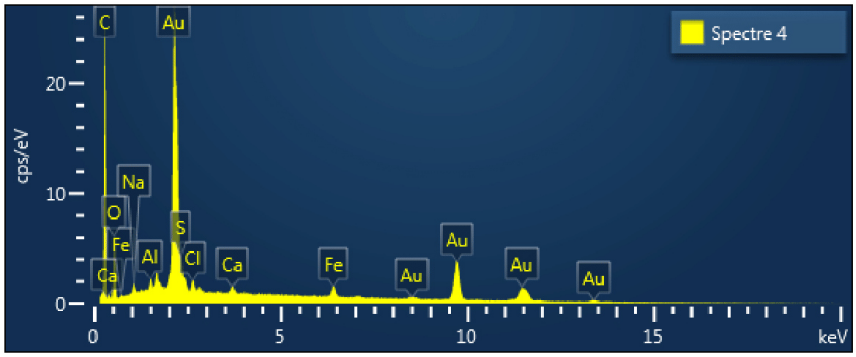

# C) BIC-PL08-Peris1-R1: Late stage pleopod

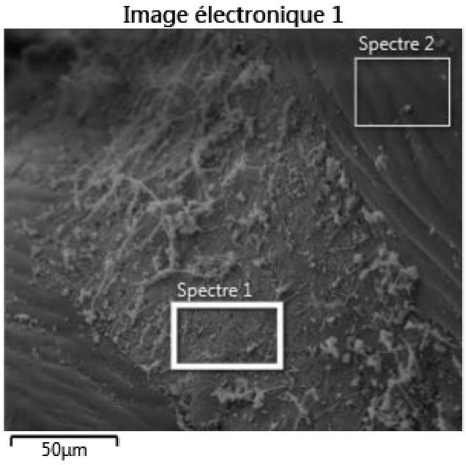


***SEM image analyzed by EDX***

**<u>Spectre 1</u>: Mineral crust area analyzed for this pleopod**

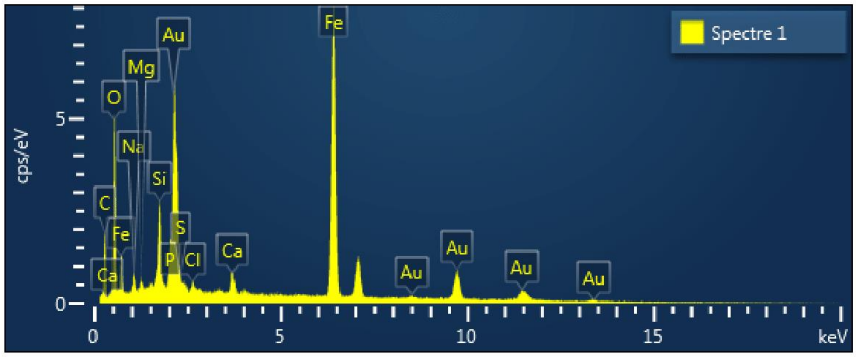


**<u>Spectre 2</u>: Bare pleopod surface area analyzed for this pleopod as control**

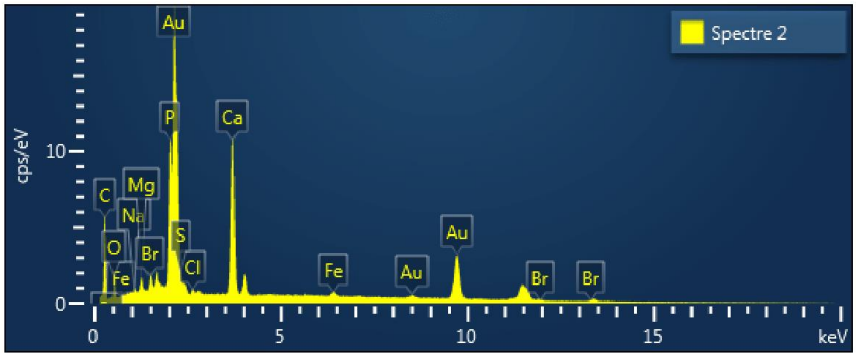

# D) BIC-PL12-Peris3-R5: Mid stage egg

Image électronique 4

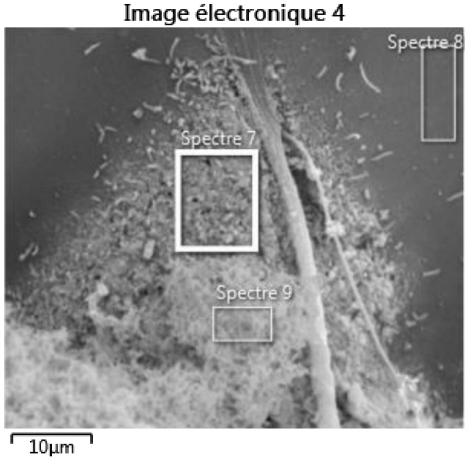


***SEM image analyzed by EDX***

**<u>Spectre 7</u>: Mineral deposit area analyzed for this egg**

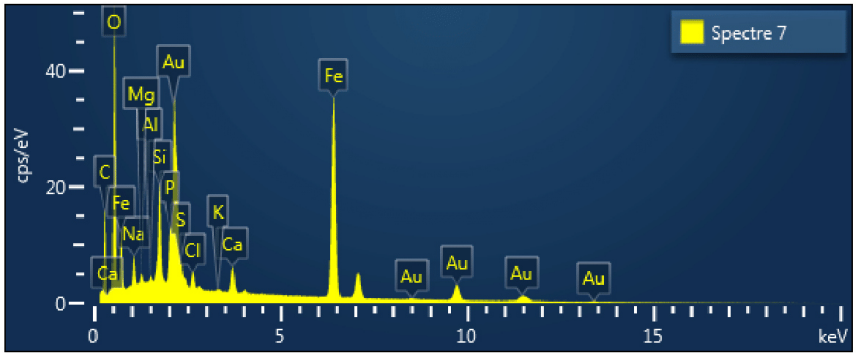


**<u>Spectre 8</u>: Bare egg envelope area analyzed for this egg as control**

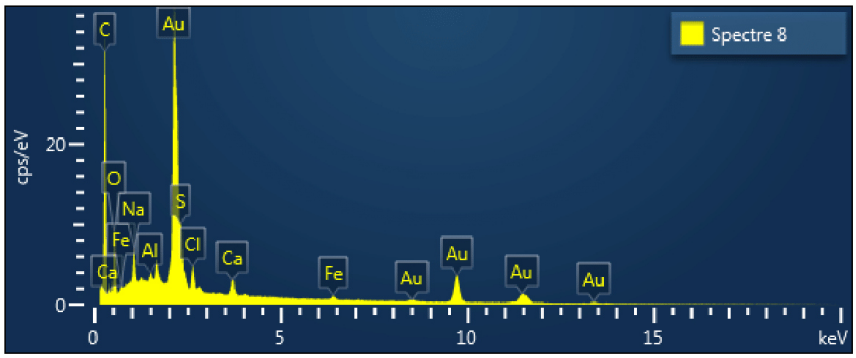

**Spectre 9: Additional mineral deposits area analyzed for this egg**

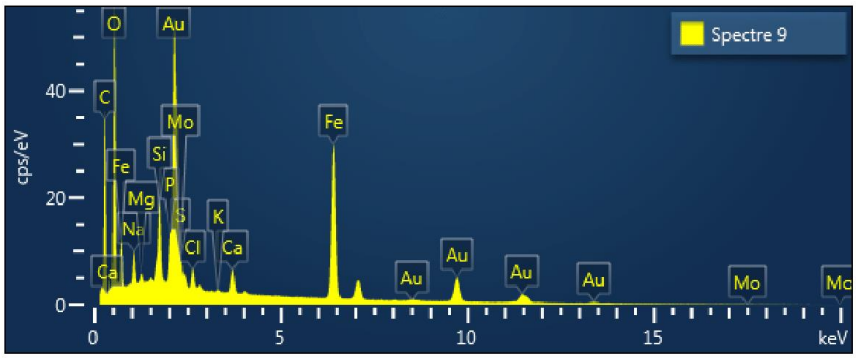


## E) BIC-PL12-Peris3-R5: Mid stage pleopod

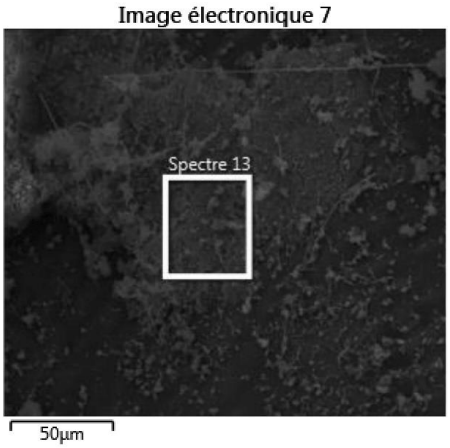


***SEM image analyzed by EDX***

**Spectre 13: Mineral crust area analyzed for this pleopod**

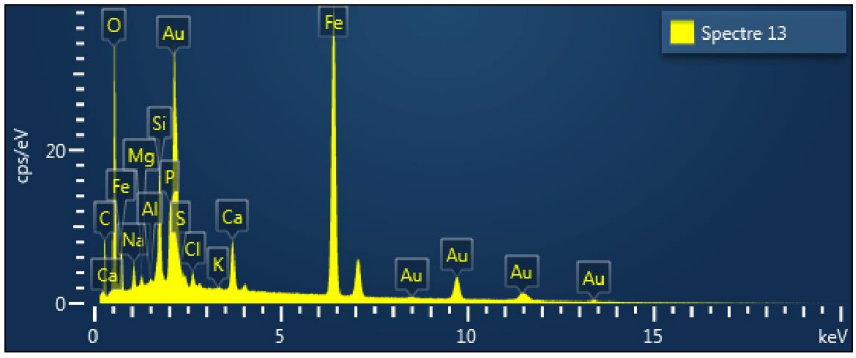


**FIGURE S1 |** X-Ray Spectrophotometric analysis (EDX) showing SEM analyzed areas of mineral crusts or mineral deposits for each sample with the corresponding spectrum. For some samples, bare surface areas clear of minerals were also analyzed as control. Analyzed were performed on **(A,B)** late stage

eggs, **(C)** late stage pleopods, **(D)** mid stage eggs, **(E)** and mid stage pleopods. Article Egg Symbiosis Supplementary materials

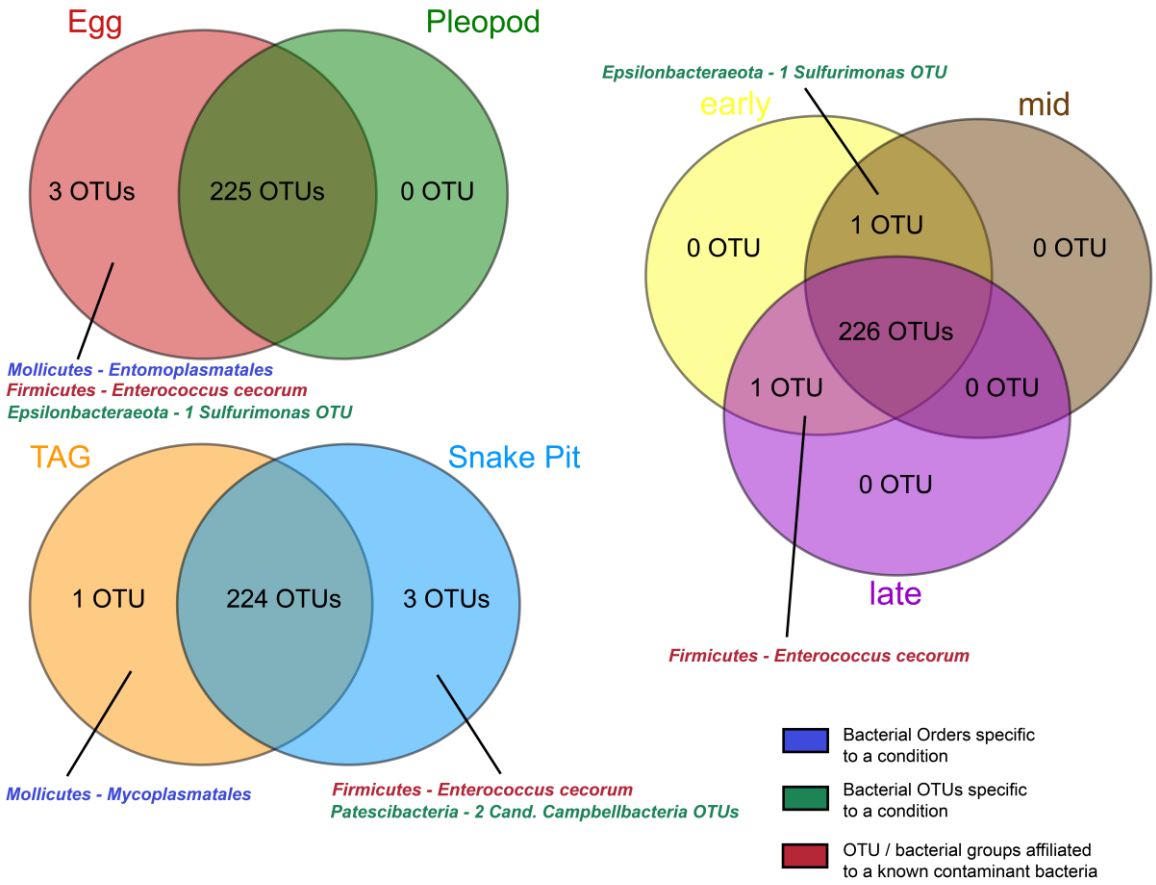


**FIGURE S2 |** Venn diagrams representing the numbers of shared OTUs across all samples. Affiliations of taxa representative of a body structure, vent field, or developmental stage are indicated.

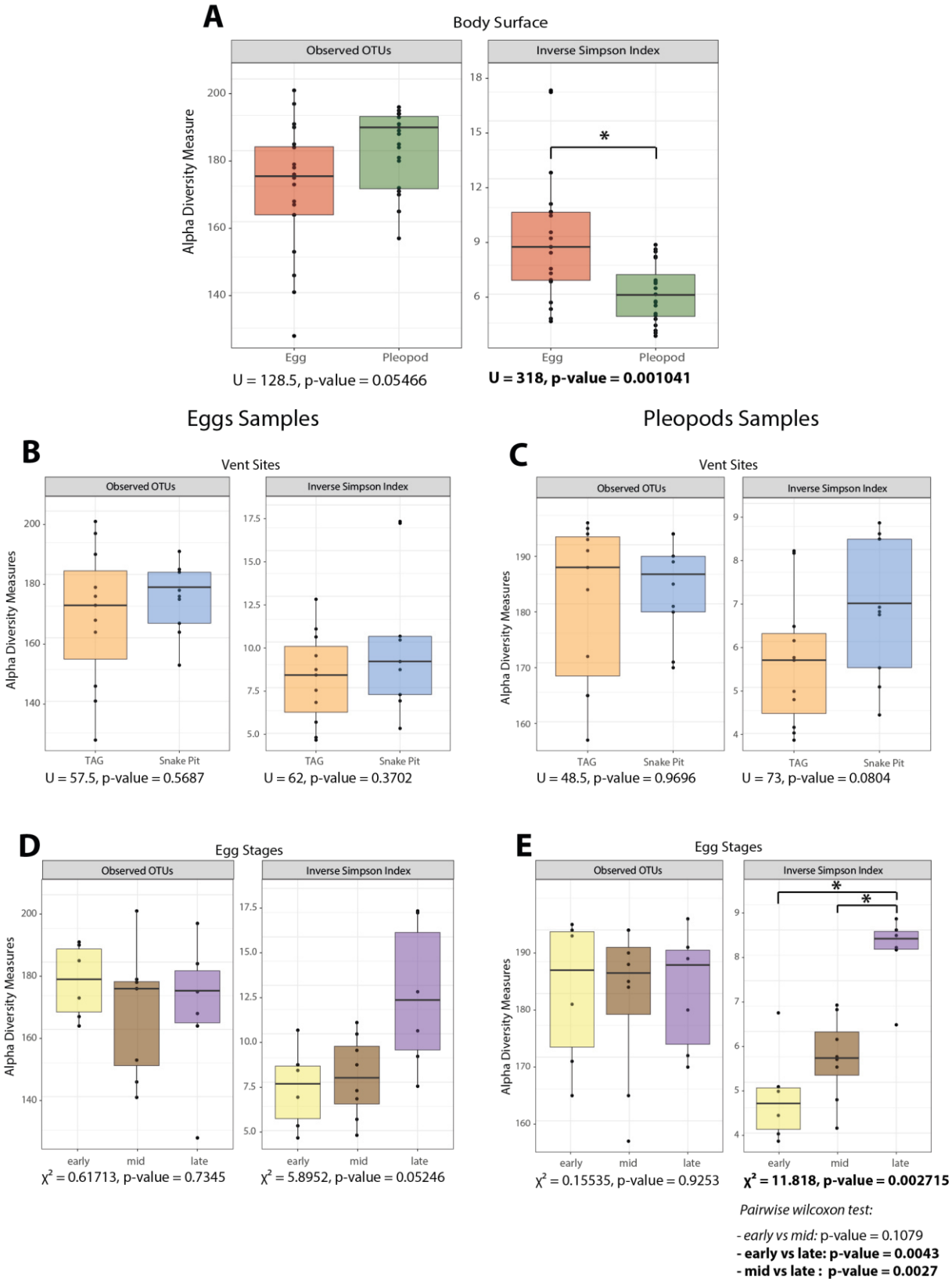


**FIGURE S3 |** Alpha diversity measures of OTU number (Richness) and Inverse Simpson index (Evenness) compared **(A)** between eggs and pleopods, **(B)** between TAG and Snake Pit egg samples, **(C)** between TAG and Snake Pit pleopod samples, **(D)** between developmental stages of egg samples, and **(E)** between developmental stages of the corresponding eggs for pleopod samples. * mean that significant differences were statistically supported.

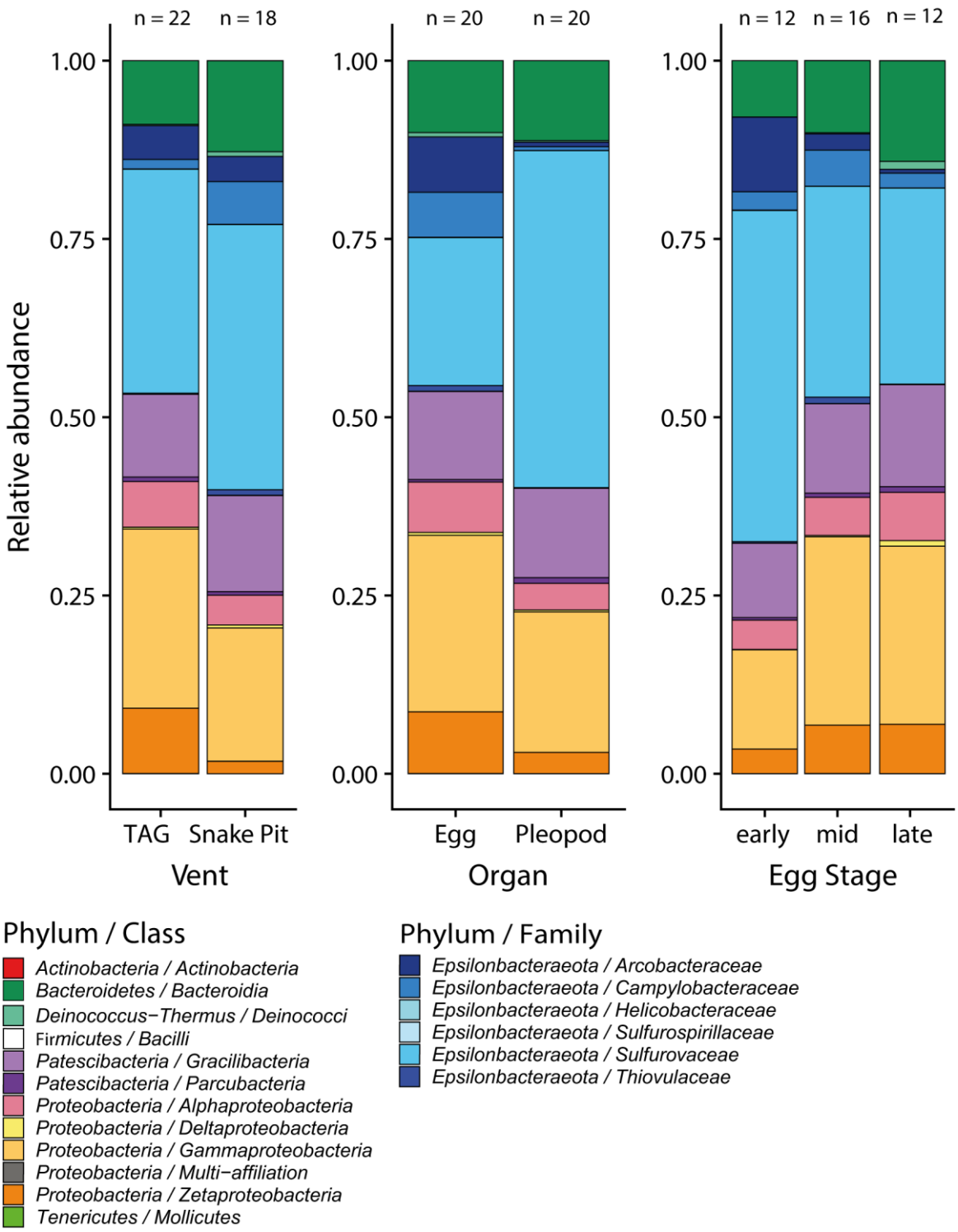


**FIGURE S4 |** Mean relative abundances per categories of 16S rRNA gene sequence reads according to their classification (Silva 132 database). Groups are at the family level for *Epsilonbacteraeota* phylum and at the class level for other phyla.

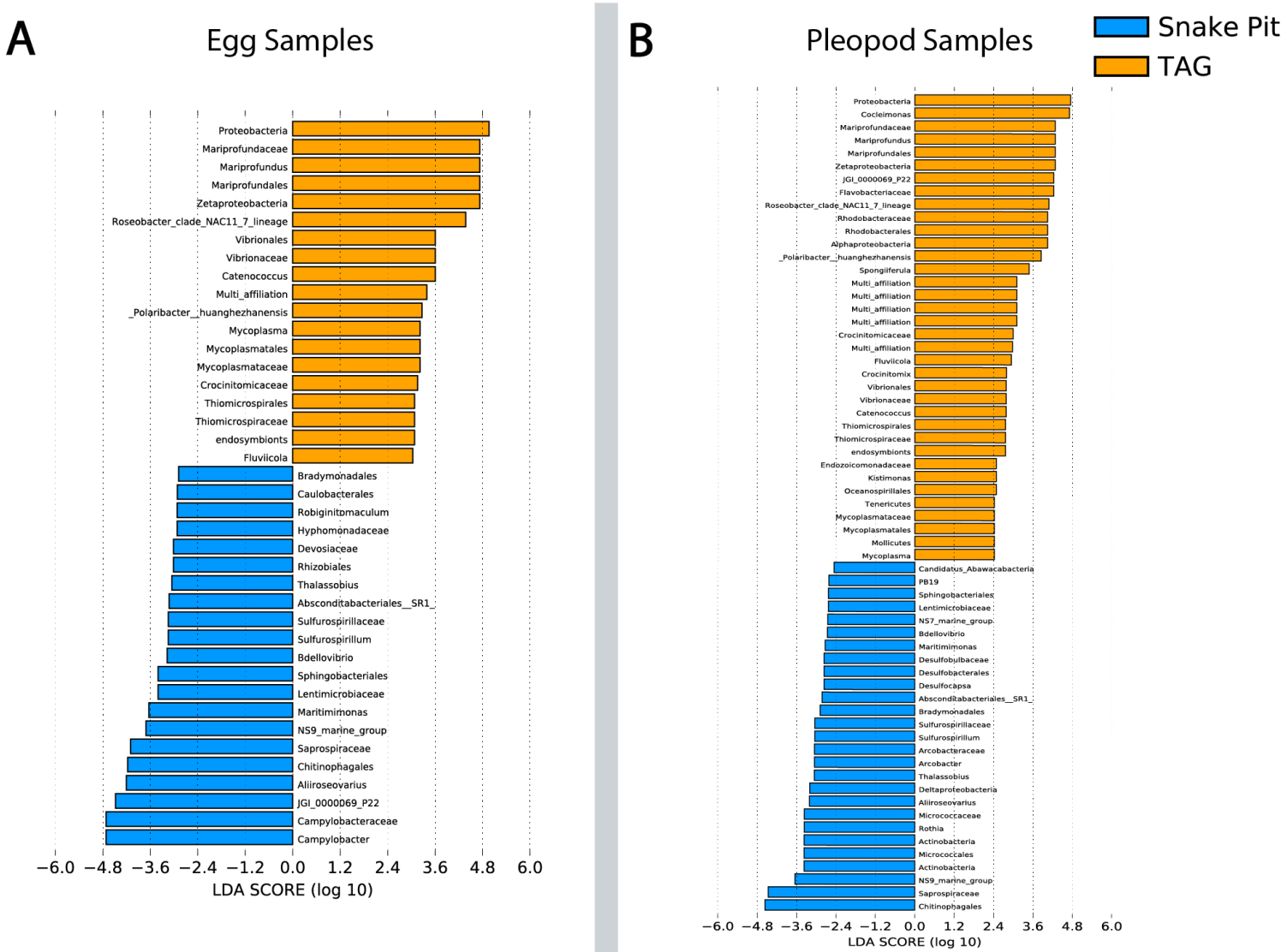


**FIGURE S5 |** Ranked LDA scores of the differentially abundant bacterial taxa, with taxa with highest relative abundance at TAG in orange, and taxa with highest relative abundance at Snake Pit in blue for bacterial communities covering **(A)** eggs and **(B)** pleopods of ovigerous *R. exoculata*.

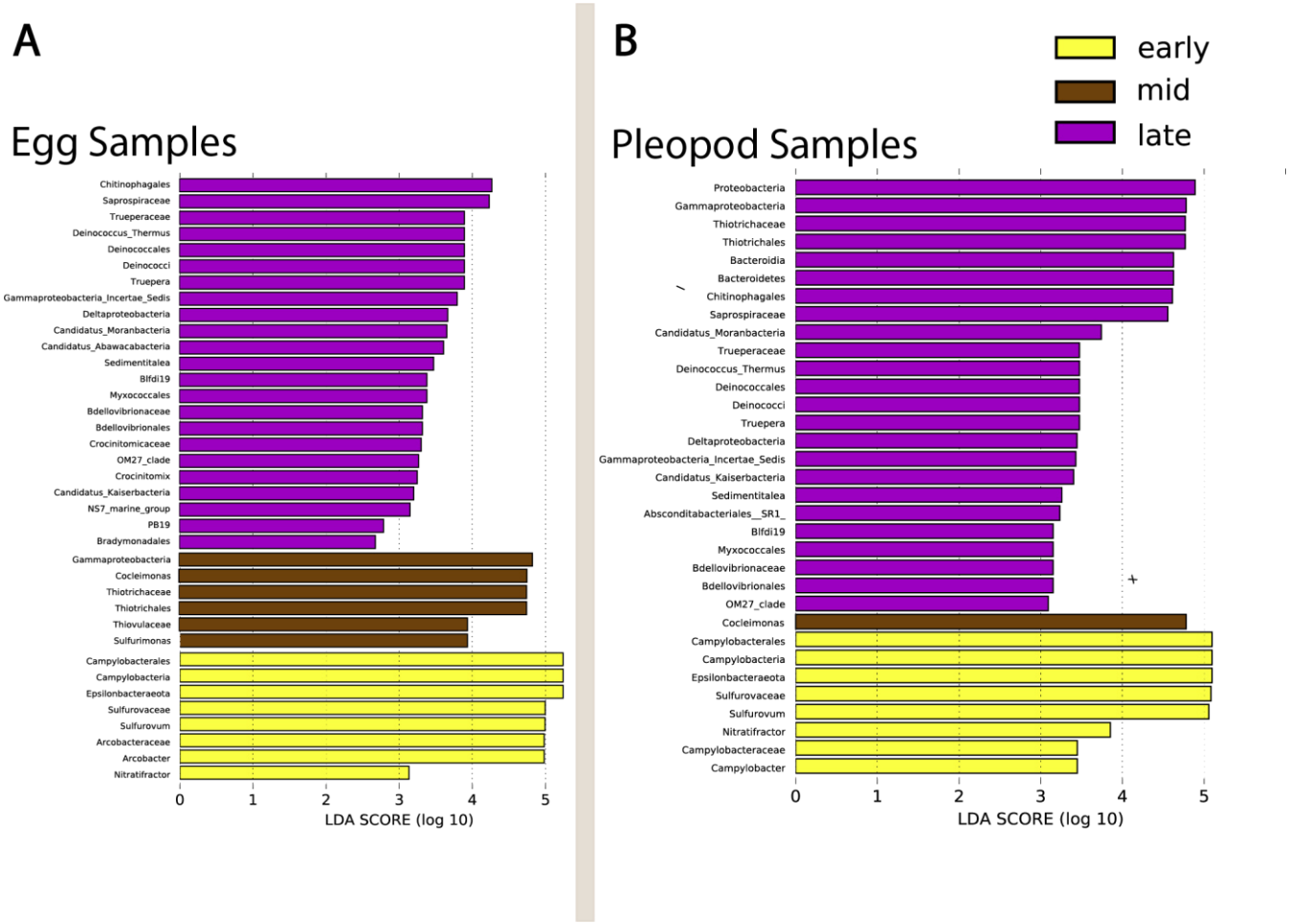


**FIGURE S6 |** Ranked LDA scores of the differentially abundant bacterial taxa, with taxa with highest relative abundance at early stage in yellow, at mid stage in brown and at late stage in purple for bacterial communities covering **(A)** eggs and **(B)** pleopods of ovigerous *R. exoculata.*

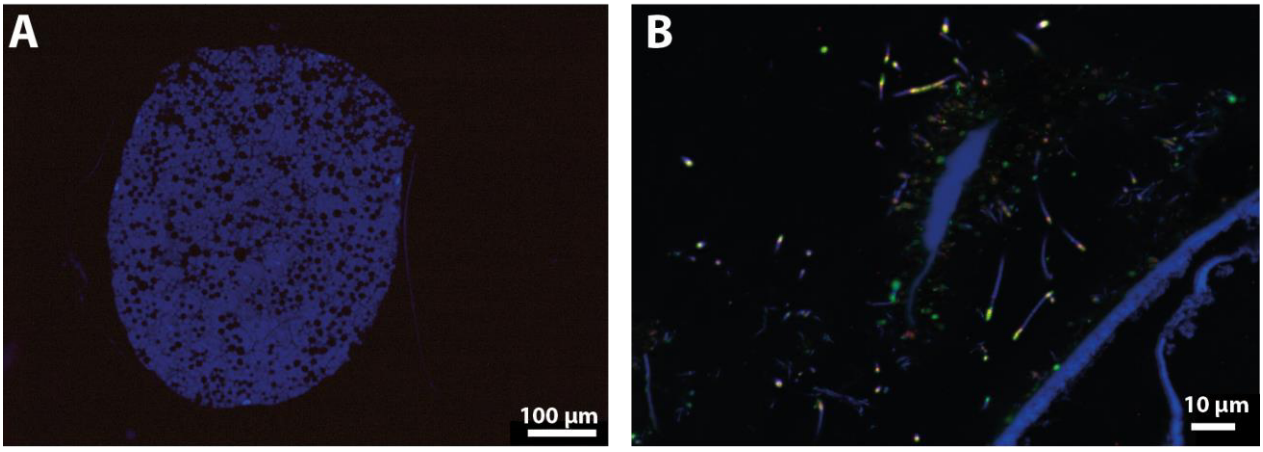


**FIGURE S7 |** Additional FISH observations of *Rimicaris exoculata* eggs. Observations were performed on semi-thin sections (2 µm) stained with DAPI (blue) **(A)** Early stage egg hybridized with Eub338-Cy5 and **(B)** Late stage egg co-hybridized with Eub338-Cy5 and Gam42a-Cy5. Colors, Green (*Eubacteria*), Red (*Gammaproteobacteria*), and Yellow (Co-*hybridized probes*).

# 1.2 Additionnal results

In addition to the 16S barcoding results from egg broods and pleopods of *R. exoculata*, one brood and one pleopod of a *R. chacei* female were sequenced as well. Interrestingly, egg brood and pleopod bacterial communities of *R. chacei* from TAG were different from those of *R. exoculata* clustering together with all the egg broods of R. exoculata from Snake Pit (**Fig 52.**). This specifity could be related to the environmental conditions along the brood if R. exoculata and R. chacei occupied different environmental niches – even if, this *R. chacei* female were collected together with two of the sequenced *R. exoculata*, since they are very motile. Another non-excluding hypothesis would be a difference related to the differences in the immunity of the two species. In any cases, with only one R. chacei female, nothing can be concluded from these results (**Fig 52.**). *More discussion on part 7.*

Internal anatomy of *R. exoculata* hatched larva from late broods was also investigated with serial sectionning and Eosine-Hematoxylin staining. Lipid reserves are still important in these life stages. Oesophagus could be identified in saggital and frontal view. Although, it appear to end, not too far after its opening with no clear link with a stomach (All sections between the slides 19 and 24 in saggital view were observed to follow the digestive system (**Fig 53.**)). A stomach could have been identified close to lipid reserves, although it might be something completely different (**Fig 53.**). If a stomach was indeed present, in remain in development, with among other no link with the posterior or anterior part of the digestive system (**Fig 53.**). A small part of digestive tube was also observed as well, but again, end up in a dead end according to our observations (**Fig 53.**). Eyes were well developped and easy to observe in these larvae. The existence of a developed central nervous system is also supposed in these observations (**Fig 53.**).

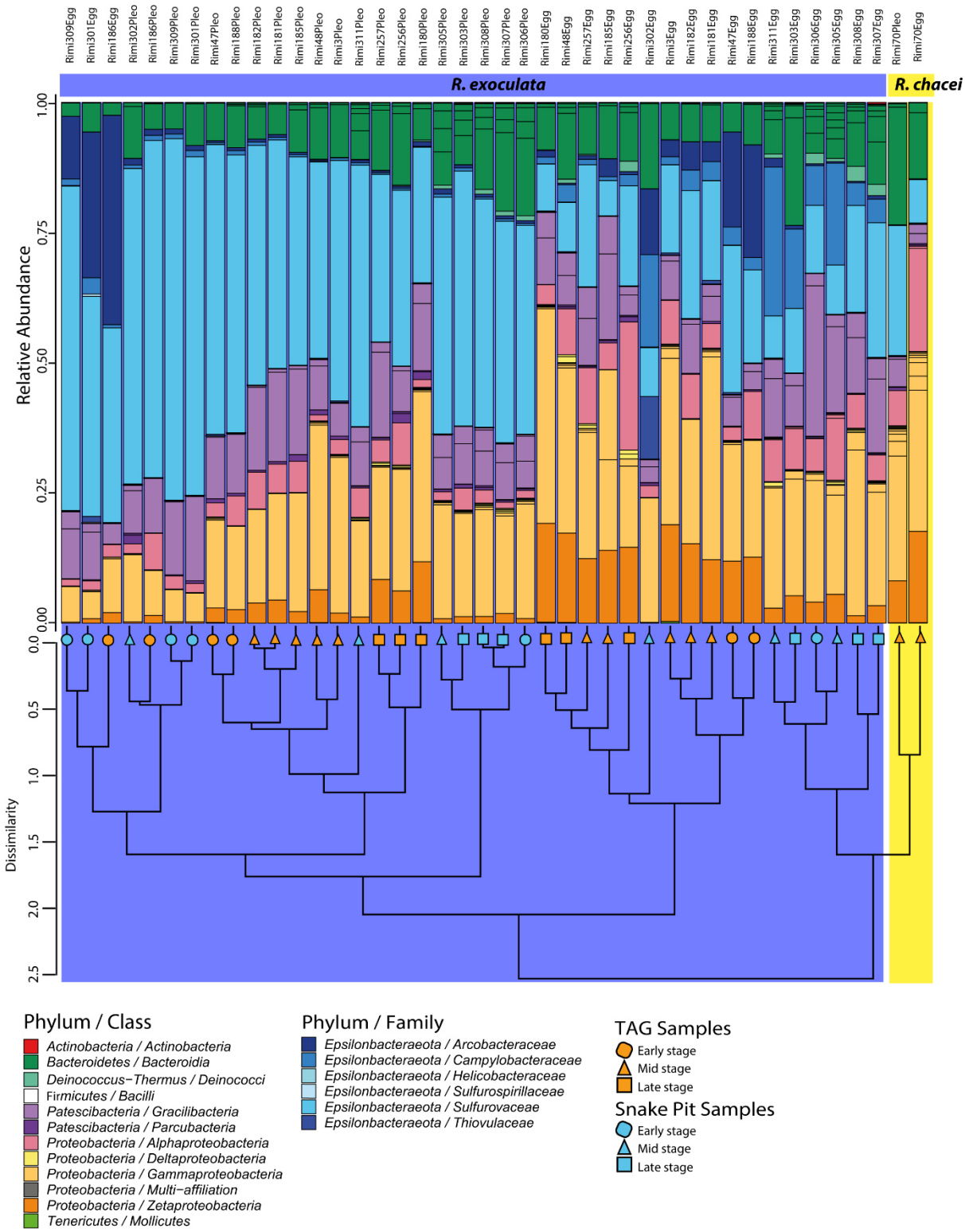


**Fig 53.** Relative abundances of 16S rRNA gene sequence reads from egg and pleopod samples of *R. exoculata* at different developmental stage and one *R. chacei* according to their classification (Silva 132 database). Groups are at the family level for the Epsilonbacteraeota phylum and at the class level for other phyla. The cluster dendrogram depicts the average linkage hierarchical clustering based on a Bray-Curtis dissimilarity matrix of community compositions resolved down to OTU level.

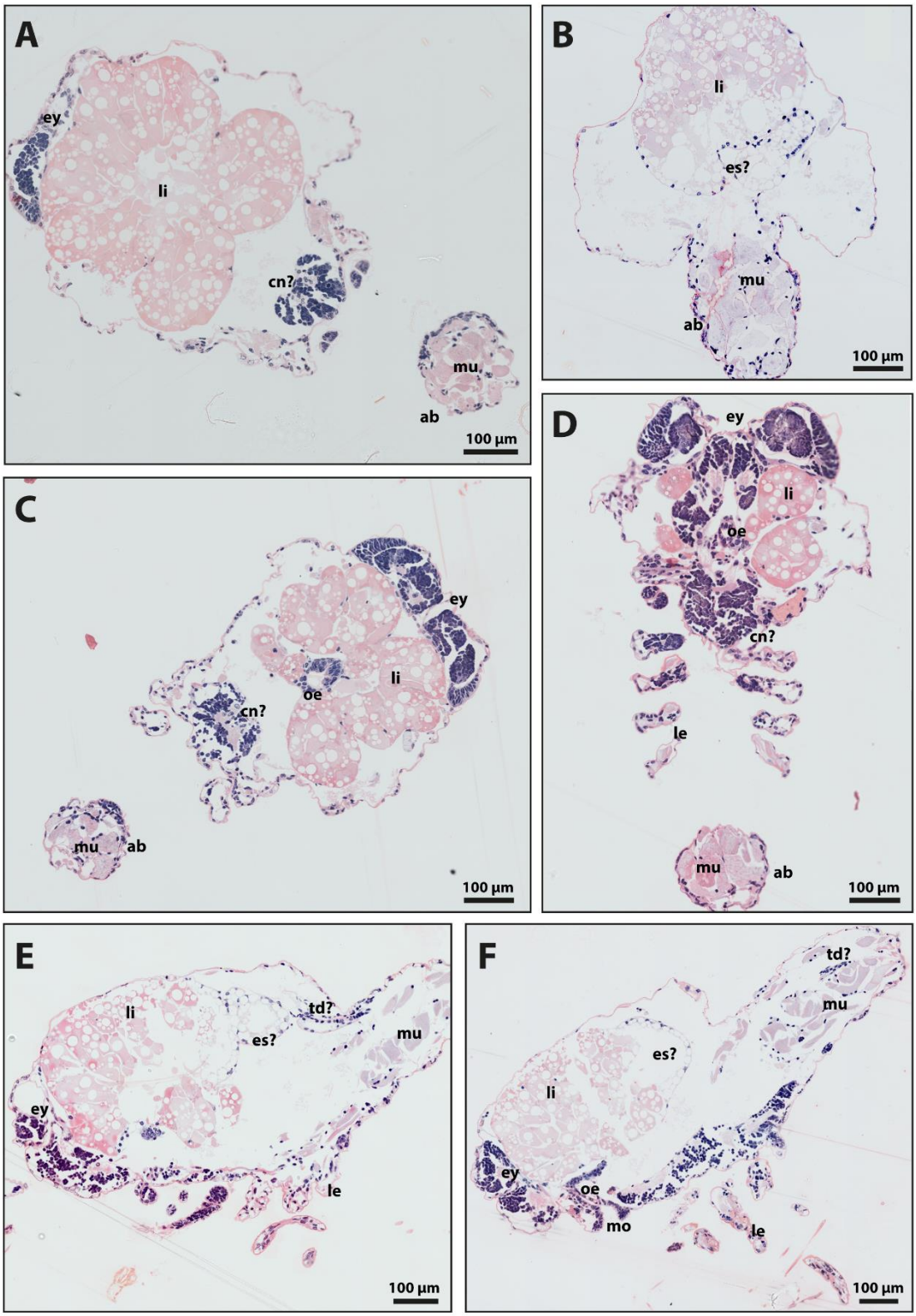


**Fig 54.** Haematoxylin & Eosin stained section – 2 µm thick – of *R. exoculata* hatched larva, from broods hatched on board. Serial sectionning of two individuals in frontal view (A-D) and sagittal view (E-F) with 10 sections per slide; no more than 1 to 2 sections were lost between each section. **A.** Slide 24. **B.** Slide 7. **C.** Slide 29. **D.** Slide 34. **E.** Slide 19. **F.** Slide 24. **Ab:** abdomen; **cn:** central nervous system; **es:** stomach; **le:** legs; **li:** lipid reserves; **mu:** muscles; **oe:** oesophagus; **td:** digestive tube.

# Growing up and

# Chapter 2

# Reach a new home

The aim of this study was to continue the work on early life stages started in Chapter 1 with a focus on the juvenile stages. Previous work from the thesis of Ivan Hernández-Ávila have suggested the existence of misendifications in the current taxonomy of alvinocaridid juveniles between *R. chacei* and *R. exoculata* (Hernández-Ávila, 2016). The main goal of this work was then to properly reassess the taxonomic identifications of *Rimicaris exoculata* and *Rimicaris chacei* juvenile stages with a coupled approach combining detailed morphological identifications and barcoding for each individual. The second purpose of this work was to revisit the trophic shifts occurring along *R. exoculata* metamorphosis according to our taxonomic reexamination and assess if such shifts also occurs for *R. chacei*. This work also proposes new hypotheses concerning the larval and recruitment histories in the life cycle of these species that will be further explored in the next chapter.

# 2.1 Trophic shifts and distinct larval histories between two co-occurring *Rimicaris* species from the Mid-Atlantic Ridge

## Authors and Affiliations

Pierre Methou[1,2], Loïc N. Michel[2], Michel Segonzac[3], Marie-Anne Cambon-Bonavita[1], Florence Pradillon[2*]

[1] : Ifremer, Univ Brest, CNRS, Laboratoire de Microbiologie des Environnements Extrêmes, UMR6197, 29280 Plouzané, France
[2] : Ifremer, Centre Brest, Laboratoire Environnements Profonds (REM/EEP/LEP), ZI de la pointe du diable, 29280 Plouzané, France
[3] : Institut de Systématique, Évolution, Biodiversité (ISYEB), Muséum national d'Histoire naturelle, CNRS, Sorbonne Université, EPHE, case postale 53, 57 rue Cuvier, F-75231 Paris cedex 05 (France)

**Keywords:** hydrothermal vent, stable isotopes, taxonomy, crustaceans, life history, ontogeny

## Abstract

Among hydrothermal vent species, *Rimicaris exoculata* is one of the most emblematic, hosting a well-developed ectosymbiosis. Living in dense aggregates, they co-occur with the less abundant *Rimicaris chacei* in the Mid Atlantic Ridge. Previous work have described a trophic shift along the *R. exoculata* lifecycle from a photosynthetic-derived based nutrition in juveniles to a chemosymbiotic feeding mode in adults. However, recent observations have suggested potential taxonomic misidentifications of *R. exoculata* earlier juveniles that could correspond to *R. chacei* juveniles. Our work confirms this misidentification and proposes a reassessment of the current taxonomy of these species. It also confirms the trophic shift between adults and juveniles for both *R. exoculata* and *R. chacei*. Nonetheless, it revealed distinct larval/recruitment histories that would have been interpreted as ontogenetic variations without our taxonomic reexamination. Interestingly, our nitrogen isotopic values of *R. exoculata,* in the light of their symbiont metagenomes, led us to propose an unusual interpretation that should be considered more often in studies dealing with stable isotopes in chemosynthetic ecosystems. Our results provide here a good illustration of the taxonomic issues persisting in deep-sea ecosystems and the importance of taxonomy to provide an accurate view of fundamental aspects of the biology/ecology of species inhabiting these environments.

## 2.1.1 Introduction

Most of the deep Ocean – defined as all marine waters below 200 m depth – remains unexplored, and certainly contains the biggest reservoir of undescribed species of our planet. While it was initially considered unsuitable for life (Forbes, 1843), existence of several biological hotspots biodiversity such as hydrothermal vents, cold seeps, canyons and seamount ecosystems is now established (Ramirez-Llodra et al., 2010). Without endogenous photosynthesis, their high productivity

is supported by other mechanisms, like chemosynthesis, or through physical processes enhancing transport and deposition of particles sinking from the surface. In hydrothermal vents, it is mainly the chemical disequilibria generated by the mixing of cold oxygenated seawater and hot reduced fluid emissions that sustain a wide range of chemosynthetic microorganisms that in turn support food webs (Sievert and Vetriani, 2012). Impact of photosynthesis-derived sunken organic matter is therefore usually considered a minor subsidy in deep vent fields.

However, insufficient sampling in these remote places often fails to capture the full range of spatial and temporal biological variability, even for the most well-known species (Vrijenhoek, 2009). Often disregarded, developmental plasticity in response to a variable environmental context can have major influence on some organisms' morphology. This has led to many taxonomic controversies. For example, in the northeast Pacific vent fields, short fat or long skinny morphotypes of *Ridgeia piscesae* tubeworms were first attributed to discrete co-occurring species and only the advances of molecular biology have allowed to recognize these two morphotypes as the same species (Southward et al., 1995; Tunnicliffe et al., 2014; Vrijenhoek, 2009).

Ontogenic morphological variability is also a great source of taxonomical biases. Small orange/reddish alvinocaridid shrimps found in hydrothermal vents close to dense swarms of *Rimicaris exoculata* (Williams and Rona, 1986) are one of the most emblematic example of such variations between life stages. Simultaneously described as *Iorania concordia* and *R. aurantiaca* by two concomitant studies (Martin et al., 1997; Vereshchaka, 1996), confusion about their taxonomic status was dispelled by molecular investigations of these specimens (Shank et al., 1998b). These shrimps were revealed to be, in fact juvenile stages of *R. exoculata*, which was further supported by the absence of sexually mature individuals in these small orange morphotypes (Shank et al., 1998b). These juveniles were latter described by Komai and Segonzac (Komai and Segonzac, 2008) as four distinct stages corresponding to the different ontogenic transitions of *R. exoculata*, from smaller stage A juveniles to stage D subadults, morphologically similar to adult individuals but not yet sexually mature.

Beyond the taxonomic field, this redescription of *R. exoculata* life stages had a drastic impact on the understanding of life history and trophic ecology of this species. In hydrothermal vent ecosystems, food web structure and trophic interactions have often been inferred based on stable isotope markers. Different stable isotope ratios can provide complementary ecological information. For example, the large difference in sulfur isotopic ratios ($\delta^{34}S$) that exists between seawater sulfate and vent fluid sulfides has been used to discriminate organic matter of photosynthetic (approximately 16 ‰ to 21 ‰) and chemosynthetic origin (-9 ‰ to 10 ‰) (Fry et al., 1983; Reid et al., 2013). On the other hand, differences in carbon isotopic ratios ($\delta^{13}C$) are attributed to carbon sources fixed through the reductive tricarboxylic acid (rTCA) cycle (2 ‰ to -14 ‰) or the Calvin-Benson-Bassham (CBB) cycle (-22 ‰ to -30 ‰) (Hügler and Sievert, 2011). Additionally, nitrogen isotopic ratios ($\delta^{15}N$) are generally used to infer the trophic position of a species within the food web (Minagawa and Wada, 1984).

*R. exoculata* adults depend on the dense chemosynthetic episymbiotic communities hosted in their enlarged cephalothorax cavity for their nutrition (Guri et al., 2012; Jan et al., 2014; Petersen et al., 2010). Despite unusually high $\delta^{15}N$ values for an animal feeding directly on chemosynthetic bacteria, $\delta^{13}C$ composition of *R. exoculata* adults is congruent with a nutrition mainly based on primary producers using the rTCA carbon fixation pathway (Gebruk et al., 2000; Rieley et al., 1999; Van Dover

et al., 1988). Moreover, a clear trophic link was assessed between the host and its symbionts (Rieley et al., 1999) with a direct nutritional transfer of light organic carbon compounds (Ponsard et al., 2013). On the other hand, several evidences from lipid and isotope compositions have suggested a photosynthetic origin diet in the small orange shrimps (Gebruk et al., 2000; Pond et al., 2000). Thus, rather than two species with distinct feeding habits, this redescription has highlighted an ontogenic trophic shift from a photosynthesis-based nutrition outside the vent field to a feeding mode dependent on chemosynthetic symbionts. This argues for the hypothesis of a long larval dispersion of *R. exoculata*, involving feeding in the water column at some point of their development, before they settle as juveniles to an hydrothermal vent field and transition to a chemosynthetic feeding mode (Dixon et al., 1998a).

Recently, small alvinocaridid juveniles living in dense patchy aggregations were collected close to diffuse emissions arising from cracks at the TAG vent field (Hernández-Ávila, 2016). These juveniles were harboring red/orange lipid storages and were alike *R. exoculata* stage A juveniles in terms of size and global morphology. Surprisingly, through genetic identification, all these specimens were clearly affiliated to *R. chacei,* a co-occurring species (Segonzac et al., 1993; Williams and Rona, 1986). This suggested that the earliest stage of *R. exoculata* juveniles could have been misidentified and confounded with juveniles of *R. chacei,* but detailed morphological information was lacking to confirm this assumption.

Trophic ecology of *R. chacei* is an interesting case among alvinocaridids as it is hypothesized as having a mixotrophic diet, halfway through symbiotrophy and bacterivore/scavenger feeding (Apremont et al., 2018; Segonzac et al., 1993). This feeding behavior is supported by both anatomical characteristics and examination of their symbiotic communities, closely related to those found with *R. exoculata,* but less developed. Moreover, this mixotrophy could be the result of a competition for space with *R. exoculata* that would maintain *R. chacei* at a distance from the vent fluids, essential to fuel their symbionts (Apremont et al., 2018). Still, a better understanding of how symbiosis and trophic behavior of this species evolve between juveniles and adults in comparison to *R. exoculata* is required to test this hypothesis.

Here, we aimed 1) to clarify, through coupled morphological analyses and DNA barcoding, the taxonomical status of small alvinocaridid juveniles collected from nursery habitats; 2) to compare, using stable isotopes, ontogenic trophic shifts and feeding habits of *R. exoculata* and *R. chacei*; and 3) to understand how these results influence our current knowledge of these two species' life cycles, which ultimately conditions their role in hydrothermal ecosystems.

## 2.1.2 Materials and Methods

### 2.1.2.1 Sample Collection

Alvinocaridid shrimps were collected from the Snake Pit (23°22'N; 44°57'W, 3460 m depth) and TAG (26°08' N; 44°49.5' W, 3630 m depth) vent fields on the Mid-Atlantic Ridge (MAR) using a suction sampler manipulated by the Human Operated Vehicle (HOV) Nautile. Carapace length (CL) of each individual was measured with Vernier calipers from the posterior margin of the ocular shield (or

eye socket) to the mid-point of the posterior margin of the carapace, with an estimated precision of 0.1 mm. Small alvinocaridid juveniles collected from nurseries or *R. exoculata* dense aggregates during the HERMINE cruise (March 16 – April 27 2017) were stored in 80 % ethanol for later detailed morphological analysis and individual barcode (**Table S1**.).

*Rimicaris* shrimps of both species and at all life stages were collected during the BICOSE 2 cruise (January 206-March 10 2018). This second collection was used to assess onset of sexual differenciation (OSD) in *R. chacei*, on formalin fixed individuals, and to perform isotopic analyses using -80°C frozen tissues (**Table S1**.).

### 2.1.2.2 Morphological Analysis

Juvenile specimens were examined in details under a stereomicroscope (Leica MS80) to assess their individual stage and/or species according to morphological descriptions of stage A juveniles of *R. exoculata* and juveniles of *R. chacei* (Komai and Segonzac, 2008), (**Fig S1.**). Since doubt has been raised by earlier sequencing on the species identity of the former (Komai and Segonzac, 2008) here we first ascribe specimens to two morphological types without species or stage reference. These morphotypes are expected to be distinct on each of 5 morphological characters (**Fig 54. and S1.**) selected from published taxonomical description (Komai and Segonzac, 2008):

- Morphotype 1 has a dorsally triangular produced rostrum, pterygostomial angle of the carapace straight or very slightly produced, no or small and partially obscured distolateral tooth on the first segment of the antennular peduncle, spiniform setae on the posterior margin of the telson, and meri of second and third pereopods armed with spines.
- Morphotype 2 has a rounded and only slightly produced rostrum, pterygostomial angle of the carapace produced anteriorly, a conspicuous distolateral tooth on the first segment of the antennular peduncle, plumose setae on the posterior margin of the telson and meri of second and third pereopods unarmed.

### 2.1.2.3 Genetic Identifications

Juveniles selected from the 2017 collection, and representing all morphological types identified, were individually characterized genetically (Table S1). DNA was extracted from pieces of telson or muscle with the DNeasy Blood & Tissue kit (Quiagen) following manufacturer's instructions. To avoid amplification of potential mitochondrial pseudogenes, new primers Cari-COI-1F (5'-GCAGTCTRGYGTCTTAATTTCCAC-3') and Cari-COI-1R (5'-GCTTCTTTTTTACC RGATTCTTGTC-3') were designed based on an alignment of the mitochondrial genome of six alvinocaridid species (Hernández-Ávila/Pradillon in prep). These primers amplified a 891 bp fragment in the 5' region of the COI gene, including the section amplified by the universal LCOI1490 and HCOI2198 primers (Folmer et al., 1994). Amplicons were sequenced (Sanger) on both strands (Macrogen). To confirm taxonomical assignation, each individual sequence was blasted against the NCBI database. The haplotype network was obtained and edited with PopART(Leigh and Bryant, 2015) with a Median Joining approach (Bandelt et al., 1999) using *R. exoculata* (KP759507.1, HM125956.1), *R. chacei* (KC840930.1, KT210445.1) and *M. fortunata* (KP759434.1, KT210455.1) as reference sequences.

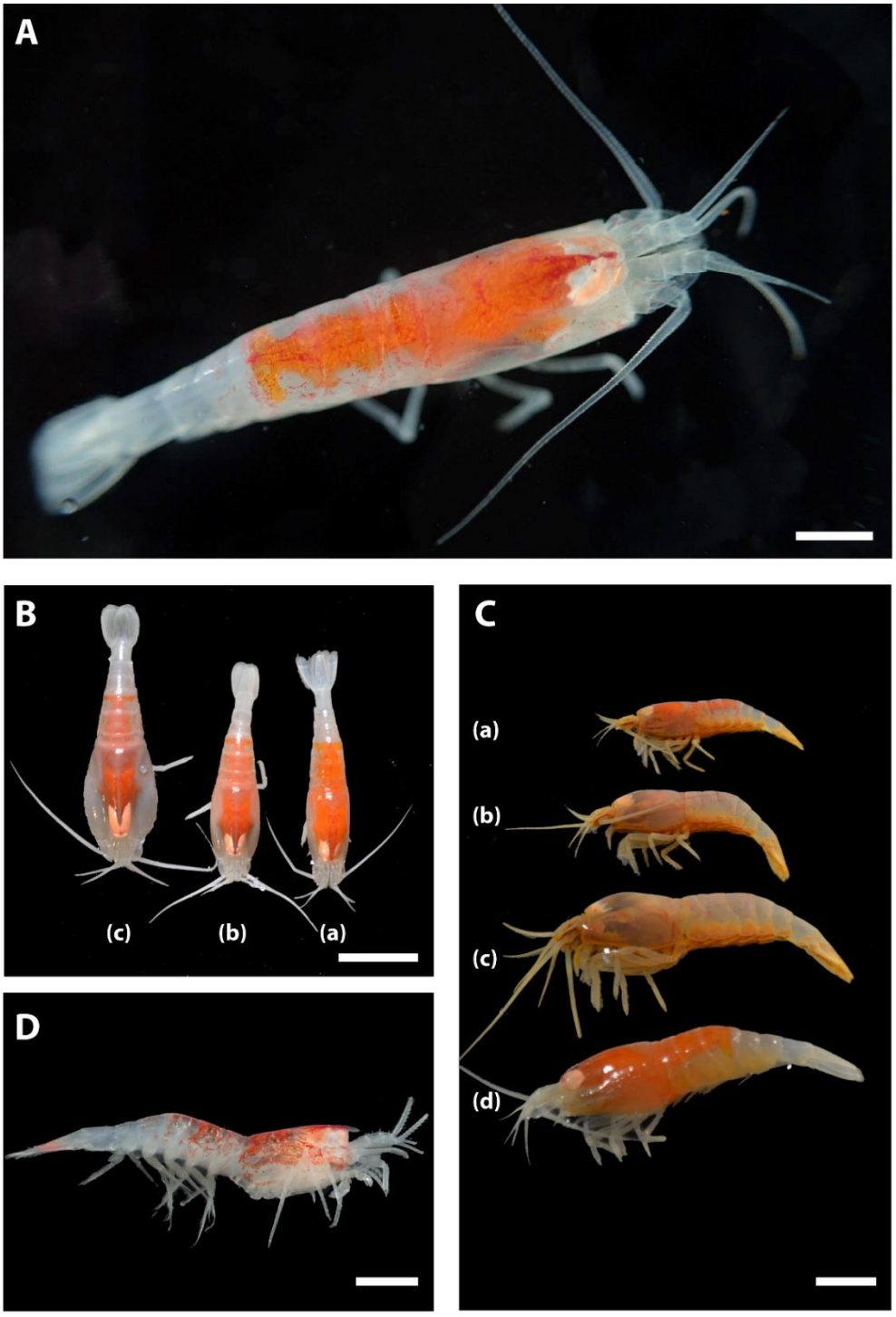


**Fig 55.** Revised juveniles stage of alvinocaridids from the Mid Atlantic ridge. **A.** Small alvinocaridid juvenile from the MAR previously identified as *R. exoculata* stage A juvenile but reassigned as *R. chacei* stage A juvenile by this work. Scale bar = 2 mm. **B.** Different juvenile stages of *R. exoculata* **(a)** stage A juvenile (previously stage B), **(b)** stage B juvenile (previously stage C), **(c)** stage C/ subadult (previously stage D). Scale bar = 5 mm. **C.** Different life stages of *R. chacei* **(a)** stage A juvenile as the individual on Fig 54A., **(b)** stage B juvenile/ subadult, **(c)** small adult, **(d)** compared with an early stage A juvenile of *R. exoculata* (previously stage B). Scale bar = 10 mm. **D.** *Mirocaris fortunata* juvenile that closely resemble morphologically to stage A juvenile of *R. chacei* and that can be found in the same locations. Scale bar = 2 mm.

### 2.1.2.4 Stable Isotopes Analysis

Abdominal muscle samples were oven-dried to constant mass at 50 °C (> 48 h) before being ground into a homogeneous powder using a mortar and pestle. Stable isotope ratio measurements were performed via continuous flow - elemental analysis - isotope ratio mass spectrometry (CF-EA-IRMS) at University of Liège (Belgium), using a vario MICRO cube C-N-S elemental analyser (Elementar Analysensysteme GMBH, Hanau, Germany) coupled to an IsoPrime100 isotope ratio mass spectrometer (Isoprime, Cheadle, United Kingdom). Isotopic ratios were expressed using the widespread δ notation (Coplen, 2011), in ‰ and relative to the international references Vienna Pee Dee Belemnite (for carbon), Atmospheric Air (for nitrogen) and Vienna Canyon Diablo Troilite (for sulfur). Sucrose (IAEA-C-6; $\delta^{13}C$ = -10.8 ± 0.5 ‰; mean ± SD), ammonium sulphate (IAEA-N-1; $\delta^{15}N$ = 0.4 ± 0.2 ‰; mean ± SD) and silver sulfide (IAEA-S-1; $\delta^{34}S$ = -0.3 ‰) were used as primary analytical standards. Sulfanilic acid (Sigma-Aldrich; $\delta^{13}C$ = -25.6 ± 0.4 ‰; $\delta^{15}N$ = -0.13 ± 0.4 ‰; $\delta^{34}S$ = 5.9 ± 0.5 ‰; means ± SD) was used as secondary analytical standard. Standard deviations on multi-batch replicate measurements of secondary and internal laboratory standards (seabass muscle) analysed interspersed with samples (one replicate of each standard every 15 analyses) were 0.2 ‰ for $\delta^{13}C$, 0.3 ‰ for $\delta^{15}N$ and 0.4 ‰ for $\delta^{34}S$.

### 2.1.2.5 Statistical analysis and data processing

All analyses were performed in the R 3.5.1 statistical environment (R Core Team 2015). Alvinocaridid shrimps were clustered according to species, life stage and vent field origin (**Table S1.**). Visual examination of our dataset and Shapiro-Wilk normality tests revealed that none of the three isotopic ratio ($\delta^{13}C$, $\delta^{15}N$ and $\delta^{34}S$) followed a Gaussian distribution. Therefore, non-parametric tests were used for intergroup comparison (Wilcoxon test when two groups were compared, Kruskal-Wallis test followed by post-hoc pairwise Wilcoxon test when three or four groups were compared) (**Table S2.**). Ecological niches were explored using the SIBER (Stable Isotope Bayesian Ellipses in R) version 2.1.4 package (Jackson et al., 2011). Two separate sets of standard ellipses were constructed: one using $\delta^{13}C$ and $\delta^{15}N$ data and another using $\delta^{13}C$ and $\delta^{34}S$ data.

## 2.1.3 Results

### 2.1.3.1 Taxonomic identification

According to the literature, two very similar but distinct morphotypes of small alvinocaridid juveniles coexist in the MAR (Komai and Segonzac, 2008). These two morphotypes can be distinguished on the base of 4 characters as the stage A juvenile of *R. exoculata* (morphotype 1 in this article) and the juvenile stage of *R. chacei* (morphotype 2 in this article).

Our reexamination of these morphological characters based on of 202 small alvinocaridid juveniles observations from TAG and Snake Pit have revealed the existence of an important number of chimeric morphotypes, sharing characters of both morphotypes 1 and 2, whatever the number of characters observed (**Fig S1.**). These observations indicate the existence of undescribed intermediate juvenile stages or invalidate at least some characters that would correspond to intraspecific rather than interspecific variations. Barcoding of a subsample of 68 individuals revealed that all these

morphotypes correspond to *R. chacei,* as illustrated on haplotype network (**Fig 55.**). Several haplotypes (circle) were shared both by morphotype 1 and 2 confirming their affiliation to the same species. This invalidates the previous taxonomic identification of these life stages. The analysis of sexual differentiation – *i.e*. the proportion of individuals with differentiated gonads – shows that it occurs early in *R. chacei* with only one juvenile stage and an onset of sexual differentiation (OSD) at 5.98 mm compared to an OSD at 10 mm for *R. exoculata* (**Fig S2.**). These results have led to propose a revised taxonomy with two juvenile stages and one subadult stage for *R. exoculata*, and one juvenile stage and one subadult stage for *R. chacei* (**Table 3.**).

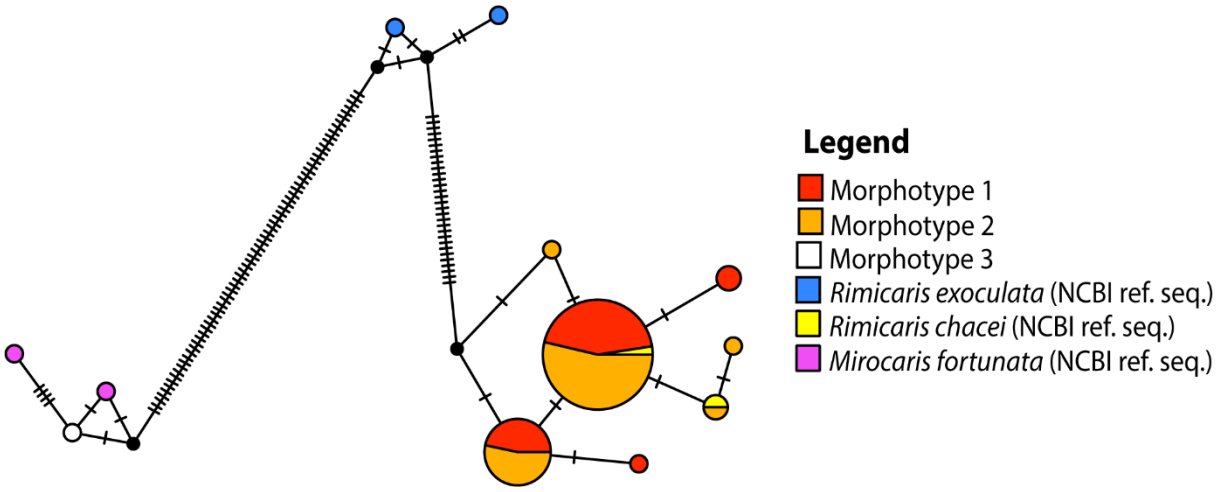


**Fig 56.** Haplotypes network obtained with a Median-Joining method in PopART for COI sequences (n = 62) of the different small alvinocaridid juvenile morphotypes that have been analyzed morphologically with additional COI reference sequences of alvinocaridid adults from the MAR (n=6). Sizes of colored circles indicate relative allelic frequencies. Tick marks indicate the mutational steps between species.

In addition to these two morphotypes, a third one, smaller than the others (CL= 3.8 mm), was also observed in TAG nursery (**Fig 54D.**). Whereas some red pigmentation on its cuticle could be observed on freshly collected specimens, this juvenile did not possessed the internal red/orange lipid storages typically observed in *Rimicaris sp.* juveniles (**Fig 54A. to 54C.**). This third morphotype also had a carapace with a straight pterygostomial angle and a spine shape under the eye as in *Mirocaris fortunata*. COI sequence of this particular juvenile was identical to a sequence of a *M. fortunata* adult from the NCBI database, confirming this identification (**Fig 55.**).

### 2.1.3.2 Stable isotope ratios of carbon, nitrogen, and sulfur along *Rimicaris* shrimps life stages

The $\delta^{13}C$ data of *R. exoculata* and *R. chacei* indicated a general trend of $^{13}C$-enrichment in later life stages both for TAG and Snake Pit populations (Kruskal-Wallis, $p<0.05$) (**Fig 56A.**). Moreover, these enrichments in $^{13}C$ were progressive, with significant differences between almost all successive life stages of each species for a given vent field (pairwise Wilcoxon test, $p<0.05$) (**Fig 56A.**). Only $\delta^{13}C$ values between stage A juveniles and stage B juveniles or stage B juveniles and subadults of *R. exoculata* from TAG and between subadults and adults of *R. chacei* from Snake Pit were not significantly different (pairwise Wilcoxon test, $p>0.05$) (**Fig 56A.**).

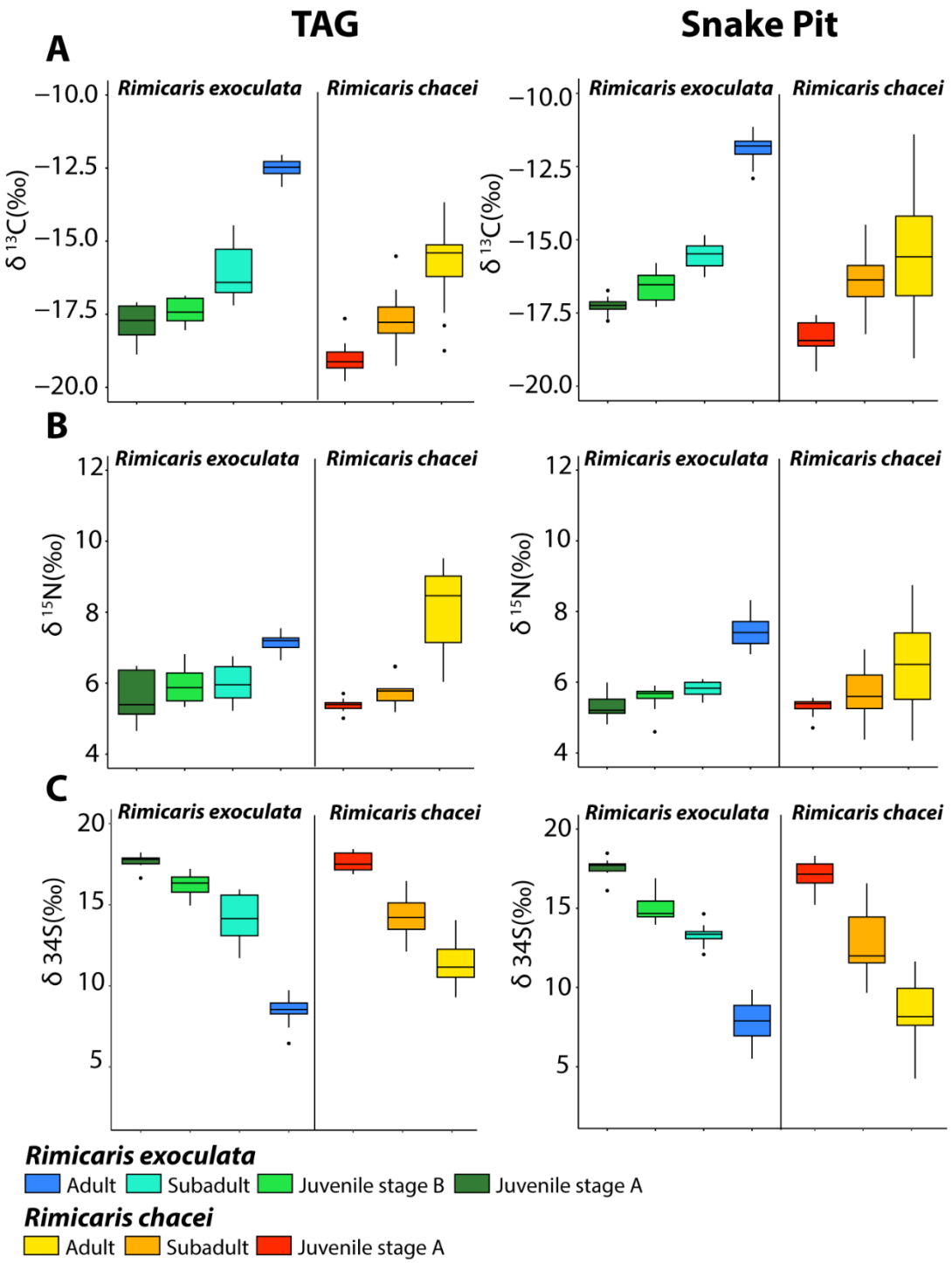


**Fig 57.** Isotopic ratios of *R. exoculata* and *R. chacei* from TAG and Snake Pit at different life stages for **A.** Carbon, **B.** Nitrogen, **C.** and Sulfur isotopes.

Differences could also be observed when similar life stages were compared between species. Stage A juveniles of *R. exoculata* exhibited significantly higher $\delta^{13}C$ values than *R. chacei* stage A juveniles both at TAG (*R. exoculata*: $\delta^{13}C$ = -17.8 ± 0.6 ‰; *R. chacei*: $\delta^{13}C$ = -19.0 ± 0.6 ‰; Wilcoxon test, $p<0.05$) and Snake Pit (*R. exoculata*: $\delta^{13}C$ = -17.3 ± 0.3 ‰; *R. chacei*: $\delta^{13}C$ = -18.6 ± 0.8 ‰; Wilcoxon test, $p<0.05$) (**Fig 56A.**). The same patterns of $^{13}C$-enrichment were observed in adults from TAG (*R.*

*exoculata*: $\delta^{13}C$ = -12.5 ± 0.3 ‰; *R. chacei*: $\delta^{13}C$ = -15.7 ± 1.1 ‰; Wilcoxon test, p<0.05) or Snake Pit (*R. exoculata*: $\delta^{13}C$ = -11.8 ± 0.4 ‰; *R. chacei*: $\delta^{13}C$ = -15.7 ± 2.1 ‰; Wilcoxon test, p<0.05) (**Fig 56A.**).

No significant $\delta^{15}N$ variations were found between any subadult and juvenile stages inside a species or vent site (Wilcoxon test, p>0.05) (**Fig 56B.**). Significant $^{15}N$-enrichment were only observed between adults and earlier life stages for both species (pairwise Wilcoxon test, p<0.05) and between stage A juvenile and subadult of *R. exoculata* from Snake Pit (pairwise Wilcoxon test, p<0.05) (**Fig 56B.**).

Adults of *R. exoculata* and *R. chacei* from each vent field were strongly depleted in $^{34}S$ compared to their earlier life stages (Kruskal-Wallis, p<0.05) (**Fig 56C.**). As with $\delta^{13}C$ values, these depletions in $^{34}S$ were progressive, with significant differences between *R. exoculata* and *R. chacei* successive life stages of each vent field (pairwise Wilcoxon test, p>0.05) (**Fig 56C.**). Interestingly, inter species comparison of $\delta^{34}S$ values between similar life stages did not show any significant differences at either TAG or Snake Pit, except between *R. exoculata* and *R. chacei* adults from TAG (*R. exoculata*: $\delta^{34}S$ = 8.5 ± 0.7‰ *R. chacei*: $\delta^{34}S$ = 11.3 ± 1.2 ‰; Wilcoxon test, p<0.05) (**Fig 56C.**).

### 2.1.3.3 Stable isotope ellipses: variation between *Rimicaris* life stages.

SIBER analysis revealed that core isotopic niches of *R. exoculata* juveniles were markedly separated from that of adults when looking either at carbon and sulfur ellipses (**Fig 57A. and 57B.**) or carbon and nitrogen ellipses (**Fig 57C. and 57D.**). Isotopic niche segregation could be seen also to some extent between juvenile stages with, in most cases, absolutely no overlap between successive stages from the same vent site for carbon and sulfur ellipses (**Fig 57A. and 57B.**). The only exception was at TAG where a very low overlap of 0.02 $‰^2$ (i.e. 2.6 % of the smaller ellipse area) was found between subadults (turquoise, **Fig 57A.**) and stage B juveniles (light green, **Fig 57A**.). A similar pattern could be observed using carbon and nitrogen ellipses, for which overlap was more frequent but always low (**Fig 57C. and 57D.**). At TAG, ellipses of stage A and stage B juveniles were overlapping for less than 0.06 $‰^2$ (i.e. 7.9 % of smaller ellipse area), and stage B juveniles and subadults ellipses' overlap was 0.04 $‰^2$ (i.e., 5.8 % of smaller ellipse area; **Fig 57C.**). In the same way, at Snake Pit, ellipses of stage A and stage B juveniles were overlapping for only 0.05 $‰^2$ (i.e., 11.6 % of smaller ellipse area), and no overlap could be observed between ellipses of stage B juveniles and subadults (**Fig 57D.**).

For *R. chacei*, the same pattern of a clear isotopic niche segregation was observed between each life stage, except between subadults and adults at Snake Pit (**Fig 57.**). The overlap between these two life stages was quite low when carbon and sulfur ellipses were examined (0.24 $‰^2$, i.e. 0.3 % of the smaller ellipse area; **Fig 57B.**) but more important with carbon and nitrogen ellipses (1.97 $‰^2$, i.e. 76.2 % of the smaller ellipse area; **Fig 57D.**).

Interspecies comparisons of *Rimicaris* life stages with SIBER analysis revealed a strong isotopic niche segregation between species for carbon and sulfur ellipses (**Fig 57A. and 57B.**). Therefore, no overlap could be observed between species at TAG except between *R. exoculata* and *R. chacei* stage A juveniles with an overlap of 0.02 $‰^2$ (i.e. 3.1% of the *R. exoculata* ellipse area) (**Fig 57A.**). Similarly, few overlaps could be observed between species at Snake Pit with an overlap of 0.45 $‰^2$ (i.e. 41.3 % of the *R. exoculata* ellipse area) between *R. chacei* subadults and *R. exoculata* juvenile B and an overlap of 0.36 $‰^2$ (i.e. 39.6 % of the *R. exoculata* ellipse area) between *R. chacei* and *R. exoculata* subadults (**Fig 57B.**). On the other hand, more overlaps were observed for carbon and nitrogen

ellipses (**Fig 57C. and 57D.**). Despite this, no overlap could be observed between the stage A juveniles or the adults of the two species both at TAG and Snake Pit.

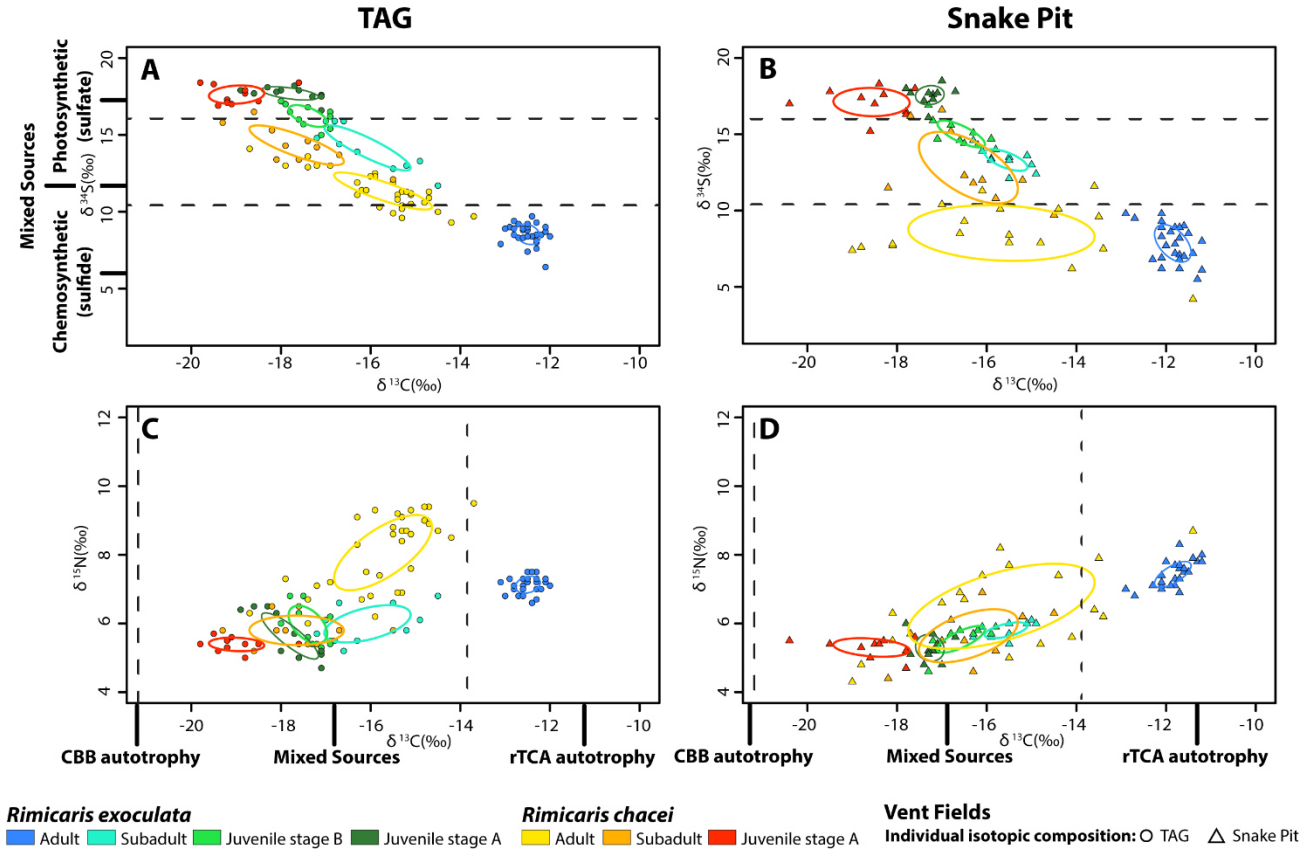


**Fig 58**. Isotopic niches of **A.** *Rimicaris* life stages from TAG for carbon and sulfur, B. *Rimicaris* life stages from Snake Pit for carbon and sulfur, **C.** *R. Rimicaris* life stages from TAG for carbon and nitrogen, **D.** *Rimicaris* life stages from Snake Pit for carbon and nitrogen

## 2.1.4 Discussion

### 2.1.4.1 Taxonomic revision of *Rimicaris exoculata* and *Rimicaris chacei* juveniles

Our results, coupling detailed morphological analysis and individual barcoding, confirm that small alvinocaridid juveniles previously assigned as stage A juveniles of *R. exoculata* correspond in fact to juveniles of *R. chacei*. We therefore suggest that specimens previously described as *R. chacei* juveniles are in fact a more advanced stage of development of this species: the subadult stage. Accordingly, juveniles of *R. chacei* were classified in this study in two different stages according to two characters only – the shape of their pterygostomial angle and the expansion of their rostrum –, their size and the presence of lipid reserves. Specimens with a straight pterygostomial angle and a more pronounced rostrum were classified as stage A juveniles of *R. chacei* and specimens with a rounded pterygostomial angle and a reduced rostrum as subadults of *R. chacei* (**Fig 54B and Table 3.**).

| This Study | After Komai et Segonzac (2008) | Before Shank et al. (1998) | Size range (CL in mm) | Lipid reserves | Morphological characteristics* | Corresponding Figure |
|---|---|---|---|---|---|---|
| ***Rimicaris chacei* stage A (juvenile)** | *Rimicaris exoculata* stage A (juvenile) | | 3.7 - 5.4 | yes | pterygostomial angle straight, pronounced rostrum, rounded eyes | Figure 1A & 1C (a) |
| ***Rimicaris chacei* stage B (subadult)** | *Rimicaris chacei* (juvenile) | | 4 - 5.98 | reduced | pterygostomial angle rounded, reduced rostrum, oval shaped eyes | Figure 1C (b) |
| ***Rimicaris chacei* (adult)** | *Rimicaris chacei* (adult) | *Rimicaris chacei* (adult) | 5.98 - 21.7 | no | pterygostomial angle rounded, reduced rostrum, oval shaped eyes | Figure 1C (c) |
| ***Rimicaris exoculata* stage A (juvenile)** | *Rimicaris exoculata* stage B (juvenile) | *Iorania concordia* / *Rimicaris aurantiaca* | 5.7 - 9.7 | yes | carapace not inflated, oval shaped eyes clearly separated, pronounced rostrum | Figure 1B (c) & 1C (d) |
| ***Rimicaris exoculata* stage B (juvenile)** | *Rimicaris exoculata* stage C (juvenile) | | 6.2 - 9.9 | yes | carapace more inflated, eyes closer to each other's, in fusion, rostrum extremely reduced | Figure 1B (b) |
| ***Rimicaris exoculata* stage C (subadult)** | *Rimicaris exoculata* stage D (subadult) | | 7.6 - 9.9 | reduced | carapace strongly inflated, ocular plate formed, rostrum absent | Figure 1B (a) |
| ***Rimicaris exoculata* (adult)** | *Rimicaris exoculata (adult)* | *Rimicaris exoculata* (adult) | 9.9 - 24.4 | no | carapace strongly inflated, ocular plate formed, rostrum absent | |
| ***Mirocaris fortunata* juvenile** | | | 3.5 - 4.9** | no | pterygostomial angle straight, small spine on the carapace under the eye, pronounced rostrum | Figure 1D |

*Listed characteristics correspond here to key morphological traits to be used for taxonomical identification to identify each life stage rather than an exhaustive list of all their characteristics

**Maximum juvenile size determined according to size of the smaller male of our HERMINE and BICOSE 2 samples. A more clear estimation of the OSD is still needed for this species.

**Table 3**. Revised classification of alvinocaridids juveniles. Figure 1 = Fig 54.

Taking into account these changes, we propose to rename juvenile stages of *R. exoculata* previously categorized by Komai and Segonzac (Komai and Segonzac, 2008). In this way, stage B juveniles of *R. exoculata* from the previous classification are now corresponding to stage A juveniles of *R. exoculata* and stage C juveniles to stage B of *R. exoculata* (**Fig 54C. and Table 3.**). Despite their larger size than the juveniles of *R. chacei*, we still think that the stage A juveniles of *R. exoculata* are earliest life stage of this species encountered in hydrothermal vents, which is supported by their sulfur isotopic composition similar to that of the earliest *R. chacei* juveniles.

Still, caution about alvinocaridid juveniles from the MAR identification should be exercised for futures studies. Indeed, juveniles of *M. fortunata* (morphotype 3 in this study) were also found at TAG, in the same samples, as slightly larger but morphologically very similar to *R. chacei* juveniles. In freshly collected specimens, red/orange lipid storage proved a reliable criterion to discriminate juveniles of the two species. However, this coloration of lipids quickly faded after a few weeks of ethanol storage, being then misleading. The front part of the carapace, which features a straight pterygostomial angle in both cases, but bears a prominent spine below the eye in *M. fortunata*, could be an additional criterion for morphological distinction. For a proper identification, we recommend the use of COI barcoding whenever doubt subsists.

## 2.1.4.2 Isotopic niches suggest contrasting resource use and ontogenic trophic shifts in R. *exoculata* and *R. chacei*

Since animals isotopic composition is partially driven by their habitat use (Flaherty and Ben-David, 2010; Newsome et al., 2008), analyzing stable isotope ratios of recent immigrants can provide a record of their migratory history if the encountered environments exhibit sufficiently distinct isotopic

sources (Pizzochero et al., 2017). In hydrothermal vents, the large difference in $\delta^{34}S$ existing between seawater sulfate and vent fluid sulfides has been used to discriminate organic matter of photosynthetic origin (approximately 16 ‰ to 19 ‰) or generated by local chemosynthetic production (sulfide oxidation; -9 ‰ to 10 ‰) (Fry et al., 1983; Reid et al., 2013).

In our study, most alvinocaridid adults had $\delta^{34}S$ values under the 10-‰ threshold, indicating a strong reliance on the sulfur oxidizing microbial production. Conversely, almost every earlier stages of *Rimicaris* juveniles showed $\delta^{34}S$ values higher than 16 ‰, consistent with a nutrition directly or indirectly based on epipelagic photosynthetic production. Previous work on storage lipids of *R. exoculata* juveniles from the MAR already suggested an important influence of photosynthesis-derived carbon source on their diet (Pond et al., 2000). These studies were based on typical photosynthetic lipid markers – like C20:4n6 or C22:6n3 fatty acids – and $\delta^{13}C$ isotopic composition. However, recent findings showed that biosynthesis of some of these lipid markers could also be performed by deep-sea bacteria (Fang et al., 2006). This bacterial origin was also proposed for the carotenoid pigments – giving the red/orange lipids storage color – in *R. exoculata* (Nègre-Sadargues et al., 2000). Therefore, the possibility that these lipid markers could be produced by *R. exoculata* digestive symbionts – Mollicutes and *Deferribacteres* – whose metabolisms are still unknown (Durand et al., 2010) or by environmental bacteria cannot be completely ruled out.

In any case, the use of sulfur isotopes confirmed the existence of such trophic shift between ontogenic stages of *R. exoculata* and provided additional evidence to support the hypothesis of a bathypelagic life outside the vent field before juvenile recruitment. Moreover, ontogenic $\delta^{34}S$ variations for *R. chacei* also highlighted a similar trophic shift between photosynthesis-based nutrition in juveniles, to mostly thiotrophy in adults. Gradual increase in $\delta^{13}C$, and, to a lesser extent, in $\delta^{15}N$ from juveniles to adults further strengthen the hypothesis of an ontogenetic nutritional shift. Overall, isotopic compositions of intermediate stages (juvenile B and subadults) are compatible with feeding on a mixture of both photosynthetic and chemosynthetic sources. This could be caused by the progressive accumulation in the growing juveniles of tissue newly synthesized from organic matter of hydrothermal origin that progressively take over tissues built from photosynthesis-derived production during larval life outside the vent field. Still, without information on the spatial foraging behavior of these animals, the hypothesis of a mixed diet maintaining photosynthetic uptake in addition to chemosynthesis remains valid, as these shrimp life stages might come and go outside the vent fields and feed in contrasted habitats. At TAG, their $\delta^{34}S$ values accordingly suggested that their diet might not exclusively made of chemosynthetic items.

Despite these similarities in their trophic shifts along life stages, adult stages of each species exhibited distinct isotopic niches suggesting a different use of the resources offered by vents. This absence of overlap was largely related to a significant $^{13}C$-enrichement for *R. exoculata*. According to several studies (Apremont et al., 2018; Guri et al., 2012; Jan et al., 2014; Petersen et al., 2010), both rTCA and CBB-fixing symbionts – respectively affiliated to *Epsilonbacteraeota* for the rTCA and *Gammaproteobacteria* or *Zetaproteobacteria* for the CBB – are hosted within *R. exoculata* and *R. chacei* cephalothorax. Given their $\delta^{13}C$ values clearly in the range of carbon sources fixed with the rTCA, *R. exoculata* adults appear to be mainly supplied with nutrients from their dominant *Epsilonbacteraeota* symbionts, the other symbionts having a minor contribution to their diet. On the other hand, $\delta^{13}C$ values of *R. chacei* adults suggest a mixed diet, based on multiple carbon sources.

This could be related to a larger contribution of the *Gammaproteobacteria* or other CBB-fixing symbionts over the *Epsilonbacteraeota* in comparison to *R. exoculata*. However, they could also depend on food items other than their symbionts (see above). Previous observations of organic matter in the stomach contents of *R. chacei* also support a mixotrophic nutrition (Segonzac et al., 1993).

In general, high $\delta^{15}N$ values are associated with a high trophic position, consumers presenting stepwise $^{15}N$ enrichment with each trophic level (Minagawa and Wada, 1984). However, variations of $\delta^{15}N$ in producers can also be related to different inorganic nitrogen sources such as nitrates ($\delta^{15}N$ = 5-7 ‰) and ammonium ($\delta^{15}N$ <0 ‰) (Lee and Childress, 1994; Riekenberg et al., 2016). According to our results and previous studies, $\delta^{15}N$ values of *R. exoculata* are higher than those of other chemosymbiotic species from hydrothermal vents (Van Dover et al., 1988). Metagenomics studies on the cephalothorax of *R. exoculata* revealed that *Epsilonbacteraeota* possess nitrogen fixation pathways to use nitrate as a nitrogen source to produce ammonium, unlike the other symbionts (Jan et al., 2014). Therefore, the relatively high $\delta^{15}N$ values of *R. exoculata* adults could also be attributed to a higher supply from the *Epsilonbacteraeota* than from other symbionts. These results highlight that, in hydrothermal vent ecosystems, variations in inorganic nitrogen use at the base of food webs should be taken into account when trying to estimate trophic position of animals. Indeed, even if many free-living *Epsilonbacteraeota* do not have this ability to use nitrate as a nitrogen source (Nakagawa et al., 2007; Sievert et al., 2008), others, such as the mat-forming *Sulfurovum sp.* (Stokke et al., 2015), do. Moreover, sequences close to *R. exoculata Epsilonbacteraeota* symbionts have been retrieved in the environment in several MAR vent sites (Petersen et al., 2010; Szafranski et al., 2015b), where they could be an important food source for the vent fauna.

### 2.1.4.3 What can we learn about the *Rimicaris* life cycle?

Our results confirmed that both *R. exoculata* and *R. chacei* juveniles rely or have relied during their larval phase on food sources derived from photosynthetic production, while adults gain most or all of their energy through chemosynthesis. Still, up to now, no conclusion can be drawn about where exactly in the water column the larvae may live. They may stay close to the seafloor with other deep-sea epibenthic fauna, or live several meters above vent fields, while consuming, in both scenarios, organic carbon sinking from the surface. In any case, they most likely reach the pelagic environment early, before the end of their dispersal, as *Rimicaris* "post-larvae" – no precise species identification – have been collected between 1990-3060 m depth above the MAR (Herring and Dixon, 1998). Because of the higher productivity and larger food availability in surface waters, combined with the fact that crustacean larvae are in general strong swimmers in comparison to other faunal groups (Adams et al., 2012), it is tempting to hypothesize a larval migration up to the photic zone. However, it is unclear if these larvae could support the low pressure and higher temperatures in these areas. *M. fortunata* hatched larvae, collected from a shallower vent field, could survive in a good physiological state at atmospheric pressure and 10 °C but were found dead at 20 °C in the same pressure conditions (Tyler and Dixon, 2000). Therefore, it appears that the upper distribution limit in the water column for this species could be determined by temperature below the photic area. Similar experiments could be conducted to confirm if *R. exoculata* and *R. chacei* larvae share the same physiological limitations. At adult stages, two of them exhibit rather similar thermal tolerances with a thermal limit of 36 °C for *M. fortunata* (Shillito et al., 2006) and of 38.5 ± 2 °C for *R. exoculata* (Ravaux et al., 2003, 2019). Recently, Nomaki and colleagues revealed that natural-abundance radiocarbon content ($\Delta^{14}C$) clearly shifted

from lower ratio in bottom water or vent- chimney fluids from vent fields to higher ratio in water-column plankton in the area of the Izu-Ogasawara Arc (Nomaki et al., 2019). In this context, use of $\Delta^{14}C$ as an ecological tracer could provide more information on the *Rimicaris* larvae habitat during their dispersal phase.

While few assumptions could be made concerning the exact location of *Rimicaris* juveniles during their previous life outside the vent field influence, a clear segregation could be observed between isotopic niches of *R. exoculata* and *R. chacei* stage A juveniles, with more $^{13-}$C-depleted values for *R. chacei* (**Fig 57.**). This segregation between the two species at juvenile stage could arise from $\delta^{13}C$ variations linked to bionomic (resource-related) or scenopoetic (habitat-related) factors during their post-larval life (Flaherty and Ben-David, 2010; Newsome et al., 2008). In either case, this suggests that *R. exoculata* and *R. chacei* could present different larval life histories, with different spatial distributions and/or different feeding habits. Our results indicate that the two species recruit at different size class, unlike indicated previously (Komai and Segonzac, 2008), with a minimal carapace length size of 5.7 mm and 4.3 mm for the earliest juveniles of *R. exoculata* and *R. chacei*, respectively (**Table 3.**). This also supports the hypothesis of distinct larval dispersal histories between the two species.

The large abundance of small *R. chacei* juveniles in dense aggregations close to diffuse fluids (Hernández-Ávila, 2016) is surprising considering the recognized low abundance of *R. chacei* adults (Segonzac et al., 1993). Such difference between juvenile and adult abundances was not observed in *R. exoculata* (Hernández-Ávila, 2016). This could arise from a lower survival after recruitment, a more important adult population than previously stated for *R. chacei,* or both. A proper characterization of the comparative population structures of *R. exoculata* and *R. chacei* at different vent fields should be conducted to properly assess if these differences in the abundance of their different life stages is related to different recruitment strategy.

Overall, our results provide a good illustration of the taxonomic issues that still persist in deep-sea ecosystems, even in the most well-known species of these environments, like *R. exoculata*. As exemplified by this study, these misidentifications are not only small details of interest for expert taxonomists. The interspecific differences we highlighted would have been, through confusion between the two congeneric species' juveniles, interpreted as ontogenic variations of *R. exoculata* otherwise. This could be an important source of bias when attempting to understand fundamental aspects of the ecology and the biology of these species, including but not limited to their nutrition and life history traits. These issues also preclude from an accurate overview of the biodiversity of these ecosystems, and of our planet in general. We reiterate here the recent call by Glover *et al.* (Glover et al., 2018) for an integrative taxonomy, maintaining traditional taxonomic procedures but coupling them to other insights about the biology of a given species, and keeping in mind that previous identifications should be considered as a current hypothesis, open to reassessment when necessary, like any other scientific result.

## Acknowledgements

This work was supported by the Ifremer REMIMA program. The authors thank the captains and crews of the R/V *Pourquoi pas*? and the Nautile submersible team for their efficiency. We also thank the chief scientists of the HERMINE 2017 (http://dx.doi.org/10.17600/17000200) expedition, Dr. Yves Fouquet and Dr. Ewan Pelleter, as well as the chief scientist of the BICOSE 2 (http://dx.doi.org/10.17600/18000004) expedition, Dr. Marie-Anne Cambon- Bonavita. We are also grateful to Dr. Laure Corbari and the artist Lowick MNR for the pictures of the alvinocaridids juveniles they took on board of the BICOSE 2 expedition which were used for the first figure of this article.

# References


Adams, D. K., Arellano, S. M., and Govenar, B. (2012). Larval dispersal : vent life in the water column. *Oceanography* 25, 256–268. doi:10.5670/oceanog.2012.24.

Apremont, V., Cambon-Bonavita, M. A., Cueff-Gauchard, V., François, D., Pradillon, F., Corbari, L., et al. (2018). Gill chamber and gut microbial communities of the hydrothermal shrimp Rimicaris chacei Williams and Rona 1986: A possible symbiosis. *PLoS One* 13, e0206084. doi:10.1371/journal.pone.0206084.

Bandelt, H.-J., Forster, P., and Röhl, A. (1999). Median-Joining Networks for Inferring Intraspecific Phylogenies. *Mol. Biol. Evol.* 16, 37–48.

Coplen, T. B. (2011). Guidelines and recommended terms for expression of stable-isotope-ratio and gas-ratio measurement results. *Rapid Commun. Mass Spectrom.* 25, 2538–2560. doi:10.1002/rcm.5129.

Dixon, D. R., Dixon, L. R. J., and Pond, D. W. (1998). Recent advances in our understanding of the life history of bresilid vent shrimps on the MAR. *Cah. Biol. Mar.* 39, 383–386.

Durand, L., Zbinden, M., Cueff-Gauchard, V., Duperron, S., Roussel, E. G., Shillito, B., et al. (2010). Microbial diversity associated with the hydrothermal shrimp Rimicaris exoculata gut and occurrence of a resident microbial community. *FEMS Microbiol. Ecol.* 71, 291–303. doi:10.1111/j.1574-6941.2009.00806.x.

Fang, J., Uhle, M., Billmark, K., Bartlett, D. H., and Kato, C. (2006). Fractionation of carbon isotopes in biosynthesis of fatty acids by a piezophilic bacterium Moritella japonica strain DSK1. *Geochim. Cosmochim. Acta* 70, 1753–1760. doi:10.1016/j.gca.2005.12.011.

Flaherty, E. A., and Ben-David, M. (2010). Overlap and partitioning of the ecological and isotopic niches. *Oikos* 119, 1409–1416. doi:10.1111/j.1600-0706.2010.18259.x.

Folmer, O., Black, M., Hoeh, W., Lutz, R., and Vrijenhoek, R. (1994). DNA primers for amplification of mitochondrial cytochrome c oxidase subunit I from diverse metazoan invertebrates. *Mol. Mar. Biol. Biotechnol.* 3, 294–299. doi:10.1371/journal.pone.0013102.

Forbes, E. (1843). *Report on the Mollusca and Radiata of the Aegean Sea: And on Their Distribution, Considered as Bearing on Geology*.

Fry, B., Gest, H., and Hayes, J. M. (1983). Sulphur isotopic compositions of deep-sea hydrothermal vent animals. *Nature* 306.

Gebruk, A. V., Southward, E. C., Kennedy, H., and Southward, A. J. (2000). Food sources, behaviour, and distribution of hydrothermal vent shrimps at the Mid-Atlantic Ridge. *J. Mar. Biol. Assoc. United Kingdom* 80, 485–499. doi:10.1017/S0025315400002186.

Glover, A. G., Wiklund, H., Chen, C., and Thomas, G. (2018). Managing a sustainable deep- sea ‘ blue economy ’ requires knowledge of what actually lives there. *Elife* 7, 1–7.

Guri, M., Durand, L., Cueff-Gauchard, V., Zbinden, M., Crassous, P., Shillito, B., et al. (2012). Acquisition of epibiotic bacteria along the life cycle of the hydrothermal shrimp Rimicaris exoculata. *ISME J.* 6, 597–609. doi:10.1038/ismej.2011.133.

Hernández-Ávila, I. (2016). Larval dispersal and life cycle in deep-water hydrothermal vents : The caseof Rimicaris exoculata and related species.

Herring, P. J., and Dixon, D. R. (1998). Extensive deep-sea dispersal of postlarval shrimp from a

hydrothermal vent. *Deep. Res. Part I Oceanogr. Res. Pap.* 45, 2105–2118. doi:10.1016/S0967-0637(98)00050-8.

Hügler, M., and Sievert, S. M. (2011). Beyond the Calvin Cycle : Autotrophic Carbon Fixation in the Ocean. *Ann. Rev. Mar. Sci.* doi:10.1146/annurev-marine-120709-142712.

Jackson, A. L., Inger, R., Parnell, A. C., and Bearhop, S. (2011). Comparing isotopic niche widths among and within communities: SIBER - Stable Isotope Bayesian Ellipses in R. *J. Anim. Ecol.* 80, 595–602. doi:10.1111/j.1365-2656.2011.01806.x.

Jan, C., Petersen, J. M., Werner, J., Teeling, H., Huang, S., Glöckner, F. O., et al. (2014). The gill chamber epibiosis of deep-sea shrimp Rimicaris exoculata: An in-depth metagenomic investigation and discovery of Zetaproteobacteria. *Environ. Microbiol.* 16, 2723–2738. doi:10.1111/1462-2920.12406.

Komai, T., and Segonzac, M. (2008). Taxonomic Review of the Hydrothermal Vent Shrimp Genera Rimicaris Williams & Rona and Chorocaris Martin & Hessler (Crustacea: Decapoda: Caridea: Alvinocarididae). *J. Shellfish Res.* 27, 21–41. doi:10.2983/0730-8000(2008)27[21:TROTHV]2.0.CO;2.

Lee, R. W., and Childress, J. J. (1994). Assimilation of Inorganic Nitrogen by Marine Invertebrates and Their Chemoautotrophic and Methanotrophic Symbionts. *Appl. Environ. Microbiol.* 60, 1852–1858.

Leigh, J. W., and Bryant, D. (2015). POPART : full-feature software for haplotype network construction. *Methods Ecol. Evol.* 6, 1110–1116. doi:10.1111/2041-210X.12410.

Martin, J. W., Signorovitch, J., and Patel, H. (1997). A new species of Rimicaris (Crustacea: Decapoda: Bresiliidae) from the Snake Pit hydrothermal vent field on the Mid-Atlantic Ridge. *Proc. Biol. Soc. Washingt.* 110, 399–411.

Minagawa, M., and Wada, E. (1984). Stepwise enrichment of 15N along food chains : Further evidence and the relation between 615N and animal age. *Geochim. Cosmochim. Acta* 48, 1135–1140.

Nakagawa, S., Takaki, Y., Shimamura, S., Reysenbach, A., and Takai, K. (2007). Deep-sea vent epsilonproteobacterial genomes provide insight into emergence of pathogens. *Proc. Natl. Acad. Sci. U. S. A.* 104, 12146–12150.

Nègre-Sadargues, G., Castillo, R., and Segonzac, M. (2000). Carotenoid pigments and trophic behaviour of deep-sea shrimps (Crustacea, Decapoda, Alvinocarididae) from a hydrothermal area of the Mid-Atlantic Ridge. *Comp. Biochem. Physiol. - A Mol. Integr. Physiol.* 127, 293–300. doi:10.1016/S1095-6433(00)00258-0.

Newsome, S. D., Martinez del Rio, C., Bearhop, S., and Phillips, D. L. (2008). A niche for isotopic ecology. *J. Physiol. Pharmacol.* 59, 123–134. doi:10.1890/060150.01.

Nomaki, H., Uejima, Y., Ogawa, N. O., Yamane, M., Watanabe, H. K., Senokuchi, R., et al. (2019). Nutritional sources of meio- and macrofauna at hydrothermal vents and adjacent areas : natural- abundance radiocarbon and stable isotope analyses. *Mar. Ecol. Prog. Ser.* 622, 49–65.

Petersen, J. M., Ramette, A., Lott, C., Cambon-Bonavita, M. A., Zbinden, M., and Dubilier, N. (2010). Dual symbiosis of the vent shrimp Rimicaris exoculata with filamentous gamma- and epsilonproteobacteria at four mid-atlantic ridge hydrothermal vent fields. *Environ. Microbiol.* 12, 2204–2218. doi:10.1111/j.1462-2920.2009.02129.x.

Pizzochero, A. C., Michel, L. N., Chenery, S. R., McCarthy, I. D., Vianna, M., Malm, O., et al. (2017). Use of multielement stable isotope ratios to investigate ontogenetic movements of Micropogonias furnieri in a tropical Brazilian estuary . *Can. J. Fish. Aquat. Sci.* 373, 1–10. doi:10.1139/cjfas-2017-0148.

Pond, D. W., Gebruk, A., Southward, E. C., Southward, A. J., Fallick, A. E., Bell, M. V., et al. (2000). Unusual fatty acid composition of storage lipids in the bresilioid shrimp Rimicaris exoculata couples the photic zone with MAR hydrothermal vent sites. *Mar. Ecol. Prog. Ser.* 198, 171–179. doi:10.3354/meps198171.

Ponsard, J., Cambon-Bonavita, M. A., Zbinden, M., Lepoint, G., Joassin, A., Corbari, L., et al. (2013). Inorganic carbon fixation by chemosynthetic ectosymbionts and nutritional transfers to the hydrothermal vent host-shrimp Rimicaris exoculata. *ISME J.* 7, 96–109. doi:10.1038/ismej.2012.87.

Ramirez-Llodra, E., Brandt, A., Danovaro, R., De Mol, B., Escobar, E., German, C. R., et al. (2010). Deep, diverse and definitely different: Unique attributes of the world's largest ecosystem. *Biogeosciences* 7, 2851–2899. doi:10.5194/bg-7-2851-2010.

Ravaux, J., Gaill, F., Le Bris, N., Sarradin, P., Jollivet, D., and Shillito, B. (2003). Heat-shock response and temperature resistance in the deep-sea vent shrimp Rimicaris exoculata. *J. Exp. Biol.* 206, 2345–54. doi:10.1242/jeb.00419.

Ravaux, J., Léger, N., Hamel, G., and Shillito, B. (2019). Assessing a species thermal tolerance through a multiparameter approach: the case study of the deep-sea hydrothermal vent shrimp Rimicaris exoculata. *Cell Stress Chaperones* 24, 647–659. doi:10.1007/s12192-019-01003-0.

Reid, W. D. K., Sweeting, C. J., Wigham, B. D., Zwirglmaier, K., Hawkes, J. A., McGill, R. A. R., et al. (2013). Spatial Differences in East Scotia Ridge Hydrothermal Vent Food Webs: Influences of Chemistry, Microbiology and Predation on Trophodynamics. *PLoS One* 8, 1–11. doi:10.1371/journal.pone.0065553.

Riekenberg, P. M., Carney, R. S., and Fry, B. (2016). Trophic plasticity of the methanotrophic mussel Bathymodiolus childressi in the Gulf of Mexico. *Mar. Ecol. Prog. Ser.* 547, 91–106. doi:10.3354/meps11645.

Rieley, G., Van Dover, C. L., Hedrick, D. B., and Eglinton, G. (1999). Trophic ecology of Rimicaris exoculata: A combined lipid abundance/stable isotope approach. *Mar. Biol.* 133, 495–499. doi:10.1007/s002270050489.

Segonzac, M., de Saint Laurent, M., and Casanova, B. (1993). L'enigme du comportement trophique des crevettes Alvinocarididae des sites hydrothermaux de la dorsale medio-atlantique. *Cah.Biol.Mar.* 34, 535–571.

Shank, T. M., Lutz, R. a, and Vrijenhoek, R. C. (1998). Molecular systematics of shrimp (Decapoda: Bresiliidae) from deep-sea hydrothermal vents, I: Enigmatic "small orange" shrimp from the Mid-Atlantic Ridge are juvenile Rimicaris exoculata. *Mol. Mar. Biol. Biotechnol.* 7, 88–96.

Shillito, B., Le Bris, N., Hourdez, S. M., Ravaux, J., Cottin, D., Caprais, J. C., et al. (2006). Temperature resistance studies on the deep-sea vent shrimp Mirocaris fortunata. *J. Exp. Biol.* 209, 945–955. doi:10.1242/jeb.02102.

Sievert, S. M., Scott, K. M., Klotz, M. G., Chain, P. S. G., Hauser, L. J., Hemp, J., et al. (2008). Genome of the Epsilonproteobacterial Chemolithoautotroph Sulfurimonas denitrificans. *Appl. Environ. Microbiol.* 74, 1145–1156. doi:10.1128/aem.01844-07.

Sievert, S., and Vetriani, C. (2012). Chemoautotrophy at Deep-Sea Vents: Past, Present, and Future. *Oceanography* 25, 218–233. doi:10.5670/oceanog.2012.21.

Southward, E. C., Tunnicliffe, V., and Black, M. (1995). Revision of the species of Ridgeia from northeast Pacific hydrothermal vents, with a redescription of Ridgeia piscesae Jones (Pogonophora: Obturata = Vestimentifera). *Can. J. Zool.* 73, 282–295. doi:10.1139/z95-033.

Stokke, R., Dahle, H., Roalkvam, I., Wissuwa, J., Daae, F. L., Tooming-Klunderud, A., et al. (2015). Functional interactions among filamentous Epsilonproteobacteria and Bacteroidetes in a deep-sea hydrothermal vent biofilm. *Environ. Microbiol.* 17, 4063–4077. doi:10.1111/1462-2920.12970.

Szafranski, K. M., Piquet, B., Shillito, B., Lallier, F. H., and Duperron, S. (2015). Relative abundances of methane- and sulfur-oxidizing symbionts in gills of the deep-sea hydrothermal vent mussel Bathymodiolus azoricus under pressure. *Deep. Res. Part I Oceanogr. Res. Pap.* 101, 7–13. doi:10.1016/j.dsr.2015.03.003.

Tyler, P. A., and Dixon, D. R. (2000). Temperature/pressure tolerance of the first larval stage of Mirocaris fortunata from Lucky Strike hydrothermal vent field. *J. Mar. Biol. Assoc. United Kingdom* 80, 739–740. doi:10.1017/S0025315400002605.

Van Dover, C. L., Fry, B., Grassle, J. F., Humphris, S., and Rona, P. A. (1988). Feeding biology of the shrimp Rimicaris exoculata at hydrothermal vents on the Mid-Atlantic Ridge. *Mar. Biol.* 98, 209–216. doi:10.1007/BF00391196.

Vereshchaka, A. L. (1996). Comparative analysis of taxonomic composition of shrimps as edificators of hydrothermal communities in the Mid-Atlantic Ridge. in *Doklady Biological Sciences* (New York: Consultants Bureau, c1965-1992.), 576–578.

Vrijenhoek, R. C. (2009). Cryptic species, phenotypic plasticity, and complex life histories: Assessing deep-sea faunal diversity with molecular markers. *Deep. Res. Part II Top. Stud. Oceanogr.* 56, 1713–1723. doi:10.1016/j.dsr2.2009.05.016.

Williams, A. B., and Rona, P. A. (1986). Two New Caridean Shrimps from a Hydrothermal Field on the Mid Atlantic Ridge. *J. Crustac. Biol.* 6, 446–462.

## 2.1.5 Supplementary Materials and Methods

### 2.1.5.1 Morphological analysis: Determination of the *R. chacei* Onset of Sexual Differentiation (OSD)

Since subadult shrimps are morphologically similar to small females – i.e. lack of male appendices – dissection procedures to assess the lack of gonadal tissue are needed to separate sexually mature females from subadults. To differentiate the two in our dataset, an average shrimp size for onset of sexual differentiation (OSD) was defined as a proxy. For *R. exoculata*, this size was  10 mm as estimated by a previous study from the same vent sites and year period (Hernández-Ávila, 2016). To have a similar estimation for *R. chacei*, a subsample of 10 to 20 shrimps per size class – ranging from 4 mm to 12 mm in CL – were collected during BICOSE 2 cruise – 130 individuals in total – and dissected to verify macroscopic evidence of gonadal tissue. OSD was then calculated according to (Hernández-Ávila, 2016; Wenner et al., 1974).

### 2.1.5.2 Genetic Identifications: PCR Amplification protocol

PCR Amplifications were conducted with 1 µl of template DNA in a 50 µL solution of 1X reaction buffer, 2 mM MgCl2, 0.4 µM dNTP, 0.6 units of Taq polymerase and 0.6mM of each primer. They were performed as following: initial denaturation (5 min at 94°C), 35 cycles including denaturation (1 min at 94°C), annealing (1 min at 50 °C) and elongation (2 min at 72 °C), followed by a final elongation of 7 min at 72°C. All PCR amplifications were conducted on a GeneAmp PCR system 9700 (Applied Biosystems). PCR products that produced light bands after electrophoresis on 1% agarose gel were sent to the MacroGen Europe Laboratory in Amsterdam (The Netherlands) to obtain sequences, using the same set of primers as used for the PCR. Overlapping sequence (forward and reverse) fragments were merged into consensus sequences using Geneious Pro 8.1.9 (Biomatters Ltd). The minimal length of all COI sequences coverage was 597 bp.

### 2.1.5.3 Statistical analysis and data processing: The isotopic niche analysis

The SIBER approach involves the use of ellipses (Jackson et al., 2011) to define isotopic niches, i.e., the space occupied by an animal population in a bivariate isotopic space. Since variation in the isotopic composition of animals (i.e., position of points in the isotopic space) is driven by both consumed prey items (Jackson et al., 2011; McCutchan et al., 2003) and habitat use (Flaherty and Ben-David, 2010), this isotopic niche can be used as a proxy of the realized ecological niche. Overlap between ellipses associated with different populations suggests that these groups partly exploit the same food and/or habitat resources. The bigger the overlap, the more resources are shared by the two populations. Here, we used standard ellipses (bivariate equivalent of standard deviations). These standard ellipses contains only the “typical” members of a population (but may not encompass outlier individuals in isotopic space). For this reason, they have been termed “core isotopic niches”, as it can be used as a proxy of the trophic and habitat resources most commonly used by populations (Layman and Allgeier, 2012)

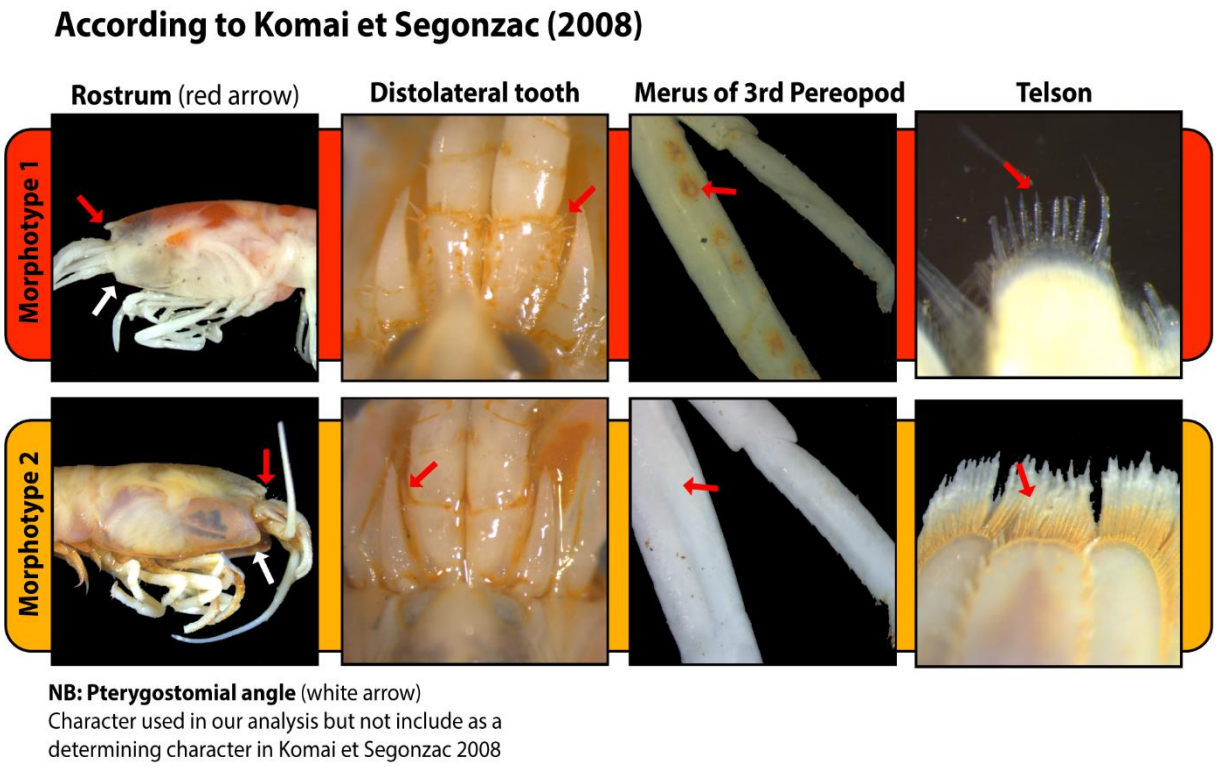


**Fig S1.** Detailed morphological analysis coupled with genetic identification of small alvinocaridids juveniles collected during the HERMINE expedition from TAG and Snake Pit. based on 5 criteria according to (Komai and Segonzac, 2008) + 1 additional ones.

| Size Class | Non Gonadal Tissues | Gonadal Tissues |
|---|---|---|
| 4 | 11 | 0 |
| 5 | 17 | 3 |
| 6 | 11 | 15 |
| 7 | 2 | 9 |
| 8 | 0 | 15 |
| 9 | 0 | 12 |
| 10 | 0 | 18 |
| 11 | 0 | 10 |
| 12 | 0 | 6 |

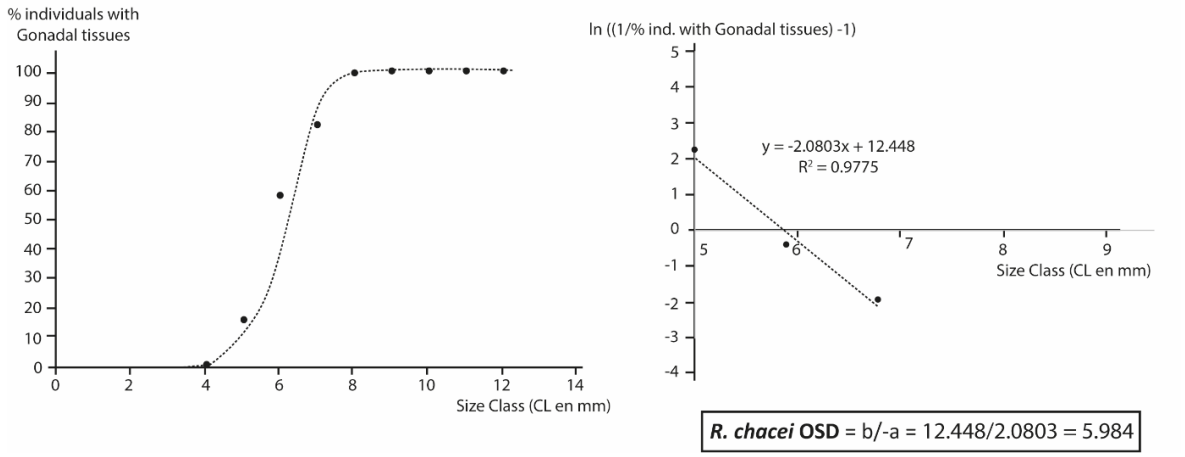


**Fig S2.** Estimation of *R. chacei* sexual maturity to determine its OSD. **A.** Table presenting the number of indidividuals with absent/undeveloped gonad tissues and those with developed gonad tissues per size class. **B.** Proportion of individuals with developed gonadal tissues per size class. **C.** Log-transformed proportion of individuals with developed gonadal tissues per size class per size class.

**Morphological analysis (203 individual from the HERMINE expedition):**

| | Vent Field | |
|---|---|---|
| **Morphotype** | TAG | Snake Pit |
| Morphotype 1 | 10 | 100 |
| Morphotype 2 | 90 | 2 |
| Morphotype 3 | 1 | 0 |

**Individual barcoding (64 ind. subsample from those of the morphological analysis):**

| | Vent Field | |
|---|---|---|
| **Morphotype** | TAG | Snake Pit |
| Morphotype 1 | 10 | 18 |
| Morphotype 2 | 33 | 2 |
| Morphotype 3 | 1 | 0 |

**Stable Isotopes analysis (208 individuals from the BICOSE 2 expedition):**

| | | Vent Field | |
|---|---|---|---|
| **Specie** | **Life Stage*** | TAG | Snake Pit |
| *Rimicaris chacei* | Stage A juvenile | 10 | 10 |
| | Subadult (stage B) | 10 | 10 |
| | Adult | 33 | 18 |
| *Rimicaris exoculata* | Stage A juvenile | 11 | 10 |
| | Stage B juvenile | 10 | 10 |
| | Subadult (stage C) | 10 | 10 |
| | Adult | 30 | 26 |

*according to taxonomic revision summarized in Table 1

**Table S1.** Number of specimens per species, life stages and vent field for taxonomical, barcoding and isotopic analysis.

## Statistical p-value of the pairwise Wilcoxon tests:

***R. exoculata* from TAG:**

| $\delta^{13}C$ | Stage A juvenile | Stage B juvenile | Subadult |
|---|---|---|---|
| Stage B juvenile | 5,1843E-01 | | |
| Subadult | 5,1588E-02 | 1,8124E-01 | |
| Adult | **1,3535E-08** | **1,7369E-06** | **2,3947E-03** |

| $\delta^{15}N$ | Stage A juvenile | Stage B juvenile | Subadult |
|---|---|---|---|
| Stage B juvenile | 3,0000E-01 | | |
| Subadult | 1,7000E-01 | 9,1000E-01 | |
| Adult | **3,8000E-09** | **1,4000E-07** | **2,8000E-08** |

| $\delta^{34}S$ | Stage A juvenile | Stage B juvenile | Subadult |
|---|---|---|---|
| Stage B juvenile | **4,8000E-05** | | |
| Subadult | **8,5000E-06** | **1,1000E-03** | |
| Adult | **3,8000E-09** | **4,7000E-09** | **4,7000E-09** |

***R. exoculata* from Snake Pit:**

| $\delta^{13}C$ | Stage A juvenile | Stage B juvenile | Subadult |
|---|---|---|---|
| Stage B juvenile | **5,2000E-03** | | |
| Subadult | **1,6000E-05** | **5,8000E-04** | |
| Adult | **1,6000E-08** | **1,6000E-08** | **1,6000E-08** |

| $\delta^{15}N$ | Stage A juvenile | Stage B juvenile | Subadult |
|---|---|---|---|
| Stage B juvenile | 1,2300E-01 | | |
| Subadult | **3,1000E-03** | 9,0300E-02 | |
| Adult | **1,6000E-08** | **1,6000E-08** | **1,6000E-08** |

| $\delta^{34}S$ | Stage A juvenile | Stage B juvenile | Subadult |
|---|---|---|---|
| Stage B juvenile | **2,6000E-05** | | |
| Subadult | **2,6000E-05** | **1,3000E-04** | |
| Adult | **1,6000E-08** | **1,6000E-08** | **1,6000E-08** |

## Statistical p-value of the pairwise Wilcoxon tests:

***R. chacei* from TAG:**

| $\delta^{13}C$ | Stage A juvenile | Subadult |
|---|---|---|
| Subadult | **2,9000E-03** | |
| Adult | **2,2000E-08** | **7,9000E-05** |

| $\delta^{15}N$ | Stage A juvenile | Subadult |
|---|---|---|
| Subadult | **1,5000E-02** | |
| Adult | **3,1000E-09** | **4,7000E-08** |

| $\delta^{34}S$ | Stage A juvenile | Subadult |
|---|---|---|
| Subadult | **1,1000E-05** | |
| Adult | **3,1000E-09** | **7,7000E-07** |

***R. chacei* from Snake Pit:**

| $\delta^{13}C$ | Stage A juvenile | Subadult |
|---|---|---|
| Subadult | **3,9000E-04** | |
| Adult | **7,0000E-04** | 3,3180E-01 |

| $\delta^{15}N$ | Stage A juvenile | Subadult |
|---|---|---|
| Subadult | 1,9000E-01 | |
| Adult | **2,2000E-02** | 1,0800E-01 |

| $\delta^{34}S$ | Stage A juvenile | Subadult |
|---|---|---|
| Subadult | **1,3000E-04** | |
| Adult | **4,6000E-07** | **1,5000E-05** |

**Table S2.** P-values of the statistical pairwise Wilcoxon comparisons for the stable isotopes ratios of *R. exoculata* and *R. chacei* life stages. Numbers highlighted in bold are considered as statistically significant.

# 2.Z Additional results

*In situ* hybridization on *R. exoculata* juveniles with specific probes for Epsilonbacteraeota or Gammaproteobacteria revealed that the two symbionts are present in the earlier juvenile stages of *R. exoculata* with a similar location on scaphognathite and branchiostegites (**Fig 58B.** and **58B.**) (Photos made by M. Gueganton). Hybridization on the entire section of a *R. chacei* juvenile with Eubacteria probes, revealed a large bacterial colonization on scaphognathite and branchiostegites (**Fig 58C.**) (result of this thesis). However, this juvenile was collected and stored before the revision of the taxonomy and it is unclear if it is a subadult or a stage A juvenile. Further FISH examination on properly identified specimen should be realized on these life stages (M. Gueganton Thesis). *More discussion in part 7.*

Isotopic ratio and isotopic niches of *R. exoculata* females or males from aggregate or from the periphery did not exhibit any variations in $\delta^{13}C$ (**Fig 59A.**), $\delta^{15}N$ (**Fig 59B.**) or $\delta^{34}S$ (**Fig 59C.**). Moreover, very important overlap are observed between their niches either for carbon and sulfur (**Fig 59D.**) or for carbon and nitrogen (**Fig 59E.**), especially for TAG specimens (more differentiation for those from Snake Pit). *More discussion in part 7.*

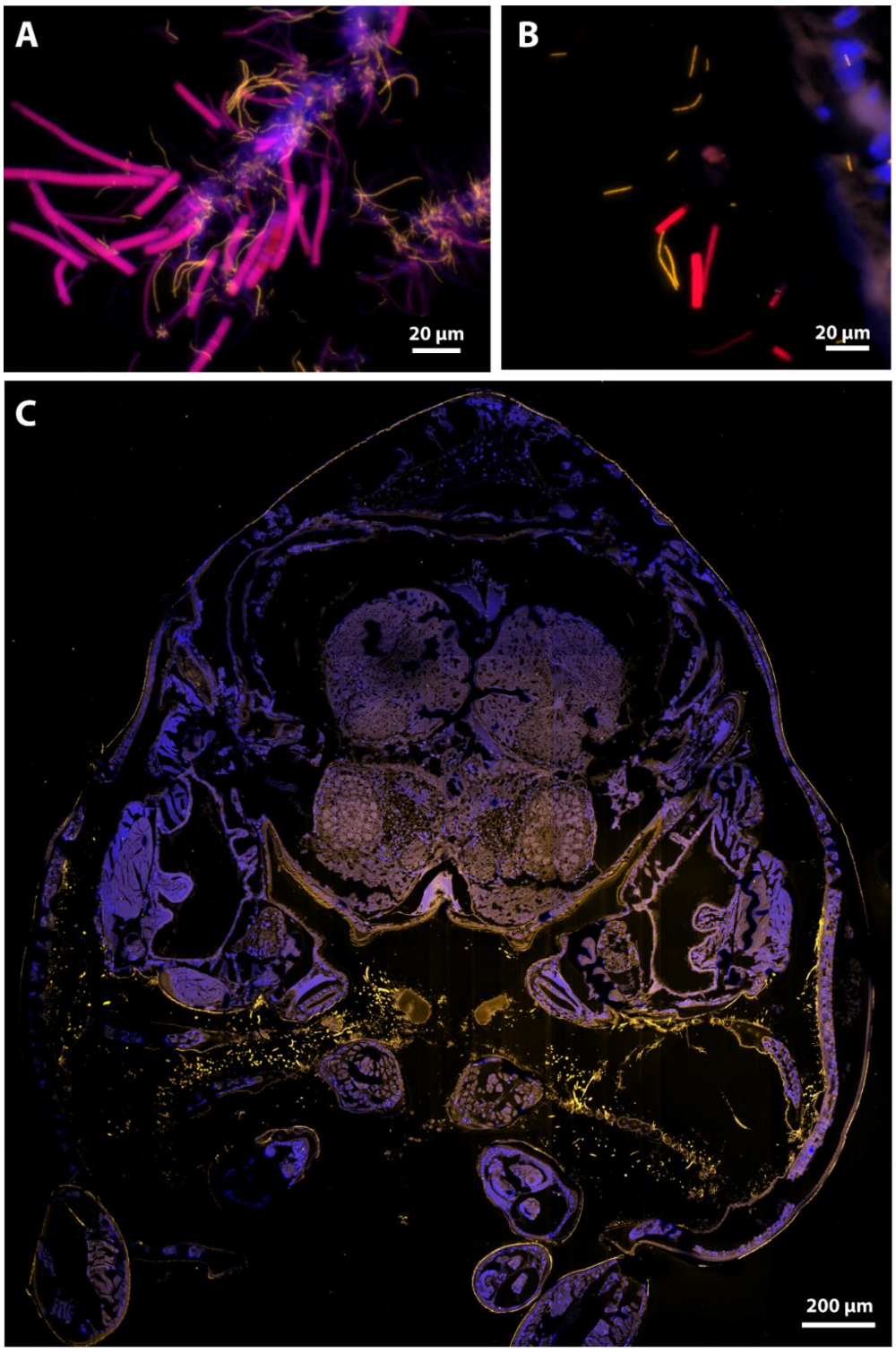


**Fig 59.** FISH Observations of Rimicaris juveniles collected during the HERMINE expedition with specific probes. The first two images (**A.** and **B.**) were made by Marion Gueganton during her 6 months internship. Observations were performed on semi-thin sections – **A.** and **B.** 10µm or **C.** 2 µm – stained with DAPI (blue) **A.** Scaphognathite of *R. exoculata* stage A juvenile hybridzed with Epsy914 (red) and Gam42a (yellow). **B.** Branchiostegite of *R. exoculata* stage A juvenile hybridzed with Epsy914 (red) and Gam42a yellow). **C.** Entire *R. chacei* juvenile – stage A or subadult, not identified precisely – hybridzed with Eub338 (yellow).

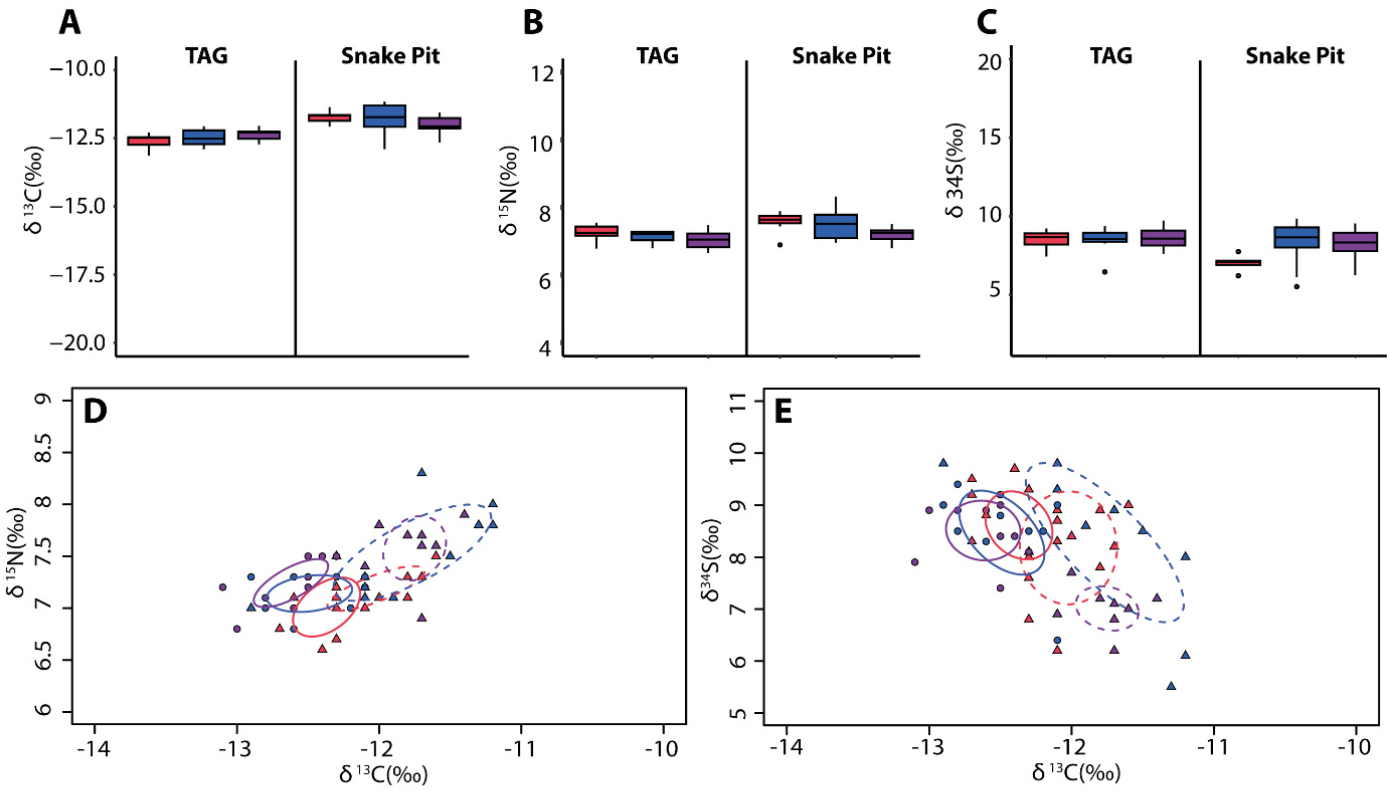


**Fig 60.** Isotopic ratios and isotopic niches of *R. exoculata* adults from TAG (filled colors) and Snake Pit (contoured colors) at different life stages for **A.** Carbon, **B.** Nitrogen, **C.** and Sulfur isotopes. **D.** isotopic niche for carbon and azote ellipses. **E.** isotopic niche for carbon and azote ellipses.

# Chapter 3

# Finding a place in the society

The aim of this study was to assess comparatively the similarities and the divergences of the global population structures of *R. exoculata*, *R. chacei* and *M. fortunata* in terms of sex ratio, juvenile proportions and proportions of reproductive individuals. In addition, a cohort analysis was performed to compare the dynamics of recruitment between these three species. Spatial variations of their respective population structures were also examined between different assemblages for each life stages of each species. Temperature measurements on different assemblages were used to reconstruct the thermal niches of the three species as well as the niches of *R. exoculata* and *R. chacei* life stages. A major part of the samples used in this study was collected during the BICOSE 2 expedition, during which all the fieldwork of this thesis was performed.

This part of the thesis is probably the less advanced one with part of the analyses that remains to be done, including the inter-annual comparison between BICOSE 2 dataset (2018) with those from the BICOSE expedition in 2014 (Hernández-Ávila, 2016) and those from the HERMINE expedition in 2017 (around 3500 individuals, sorted during this thesis). Short scale temporal comparison should also be conducted between assemblages that were collected at the same place with several days of differences (summarized in a supplementary table in this chapter). An integration of the chemical composition data – $Fe^{2+}$ concentration, total iron and total $H_2S$ concentration – obtained for some assemblages could also be considered. Moreover, most of the introduction and the discussion part are still work in progress and should be completed later.

# 3.1 Population structure and thermal niches of alvinocaridids from the Mid Atlantic Ridge

## Authors and Affiliations

Pierre Methou[1,2], Ivan Hernández-Ávila[1,2†], Cécile Cathalot[3], Marie-Anne Cambon-Bonavita[1], Florence Pradillon[2*]

[1] : Ifremer, Univ Brest, CNRS, Laboratoire de Microbiologie des Environnements Extrêmes, UMR6197, 29280 Plouzané, France

[2] : Ifremer, Centre Brest, Laboratoire Environnements Profonds (REM/EEP/LEP), ZI de la pointe du diable, 29280 Plouzané, France

[3:] Ifremer, Centre de Bretagne, REM/GM, Laboratoire Cycles Géochimiques et Ressources, F-29280 Plouzané, France

[†]Current address: Postdoctoral fellow, Laboratorio de Biodiversidad Marina y Cambio Climático, El Colegio de la Frontera Sur, Campeche, México.

## 3.1.1 Introduction

The concept of niche, as defined by Hutchinson, is a fundamental principle of ecology. The niche of a given species can be summarized as an *n*-dimensional hypervolume within which this species can survive indefinitely (Hutchinson, 1957). Therefore, tolerance of this species to different environmental gradients and the functional interactions it has with other species, delineate the boundaries of its niche. In hydrothermal vent ecosystems, hot fluids, rich in reduced elements, are expelled rapidly to collide turbulently with the cold and oxygenated seawater. This creates a mixing gradient of highly variable thermal and chemical conditions that can drastically change on small spatial scales from the order of the cm. This gradient strongly structures vent species distribution and strong zonation of the faunal assemblages is frequently observed all along this environmental gradient in many vent fields (Cuvelier et al., 2009; Govenar et al., 2005; Luther et al., 2001; Marsh et al., 2012; Sarrazin and Juniper, 1999; Sen et al., 2013). Thermal conditions are one the main drivers of this zonation, in particular the variability rather than the average temperatures (Cuvelier et al., 2011; Podowski et al., 2010). Many species from these environments exhibit thermal adaptations to cope with the "extreme" conditions they encounter. Indeed, some of the most eurythermal species in the world, are inhabiting these ecosystems such as the alvinellid polychaete, *Alvinella pompejana*, that can cope with temperatures beyond 42°C for more than 2 hours (Ravaux et al., 2013). Nonetheless, many motile species rather escape the high thermal conditions and actively seek cooler temperatures than their maximal thermal tolerance (Bates et al., 2010; Shillito et al., 2001). Other environmental factors have also a strong influence on the distribution of species along the gradient, such as oxygen or reduced compounds concentrations. However, given that temperature is correlated to the dilution of the vent fluid in the seawater, thermal conditions can give a good proxy of the chemical concentrations, if chemical compositions of non-dilute fluids are known (Le Bris et al., 2006b).

Several vent taxa are therefore characteristic of particular parts of the gradient. For instance, vent fields of the Mid Atlantic Ridge are characterized by a dominance of alvinocaridid shrimp in the hottest part of the gradient, either *R. exoculata* or *M. fortunata*, a large presence of Bathymodiolin mussels in the cooler part and *Maractis rimicarivora* anemones, in the colder part at the periphery (Cuvelier et al., 2011; Desbruyères et al., 2000; Fabri et al., 2011). Nonetheless, this zonation is not limited to species distribution as segregation can be observed between the different life stages of a species along the thermal gradient, like for *Kiwa tyleri* crabs from East Scotia Ridge (Marsh et al., 2015). Male individuals are distributed mostly in the hot part of the mixing gradient between 9°C and 24°C whereas females and juvenile were restricted to colder habitats. Moreover, brooding migration of *K. tyleri* females was observed at the periphery of the vent field (Marsh et al., 2015). Differences between thermal niches of the different size classes of *B. azoricus* mussels from Lucky Strike were also found with small mussels in the colder areas and large ones at higher temperature (Husson et al., 2017). These changes of their thermal niche were gradual, each size class niche overlapping the niches of its neighboring size categories (Husson et al., 2017).

In *R. exoculata*, distinct distribution of male and female individuals was reported at TAG, with females being mostly present in the dense aggregates close to the active vent emissions whereas males were distributed mostly at the periphery where no vent fluids could be observed (Hernández-Ávila, 2016). Moreover, a nursery of small alvinocaridid was also observed suggesting the existence of a third assemblage for these life stages. However, genetic identification of these small individuals affiliated them to *R. chacei*.

With the reexamination of the juvenile taxonomy realized in the previous chapter, our aim was to reassess the population structure of *R. exoculata* and *R. chacei*, and to a lower extent *M. fortunata*, as well as their spatial variation in different types of assemblages. Moreover, with the measurement of the thermal condition surrounding these different assemblages, we attempted to compare the thermal niches of each species as well as those of each life stages for both *R. exoculata* and *R. chacei*.

## 3.1.2 Materials & Methods

### 3.1.2.1 Field Sampling

Alvinocaridid shrimps were collected during the BICOSE 2 expedition on board of the R/V *Pourquoi Pas?*, between February and early March 2018 at the TAG (26°08.2'N, 44°49.5'W, 3620 m depth) and the Snake Pit (23°22.1'N 44°57.1'W, 3470 m depth) hydrothermal vent fields (**Fig 60.**) using the suction sampler of the French HOV *Nautile*. Three different edifices were sampled at the Snake Pit vent field: The Beehive, the Moose and the Nail (**Fig 60.**). In total, 3945 *R. exoculata* shrimps (1533 from TAG and 2413 from Snake Pit), 1235 *R. chacei* shrimps (884 from TAG and 351 from Snake Pit) and 195 *M. fortunata* shrimps (21 from TAG and 174 from Snake Pit) were collected.

Discrete spatial samples were targeted to explore the fine scale variations in the population of each species with 13 different spatial samples at TAG and 17 at Snake Pit (8 from the Beehive edifice, 6 from the Moose edifice and 4 from the Nail edifice). During the dives, spatial samples were kept separate using the different chambers of the suction sampler carousel and the closeable bioboxes of the French HOV *Nautile*. For 21 of these sampling points, discrete temperature measurements prior to sampling using the HOV temperature probe at several points in the assemblage, during at least 5 min.

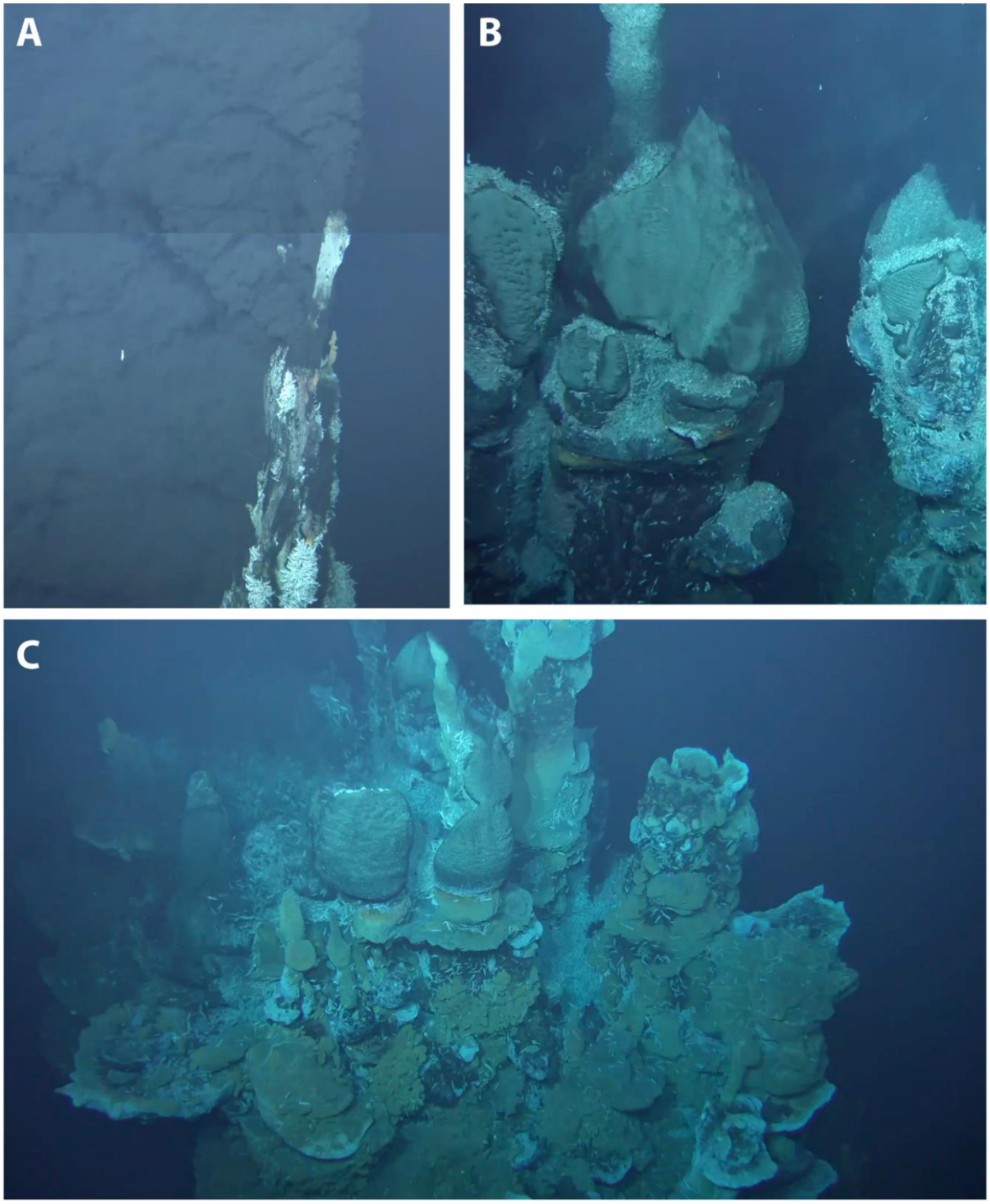


**Fig 61.** Vent fields of the study with their edifices observed during the BICOSE 2 expedition. **A.** Top part of the chimney of the Main Mound of the TAG vent field. **B.** Two chimney of the Beehive edifice at the Snake Pit vent field. **C.** Top view of the Moose edifice with its complex topography edifice at the Snake Pit vent field.

### 3.1.2.2 Life stage identifications and measurements

Once on board the ship, ovigerous females and females with developed gonads were identified, separated from the rest of the sample preserved in formalin and stored individually. All the other shrimps were stored in 80% EtOH. For each alvinocaridid shrimp, the standard measure of body

size for carideans, carapace length (CL), was determined to the nearest 0.1 mm by Vernier calipers from the rear of the eye socket to the rear of the carapace on the mid-dorsal line. Each shrimp was identified and sorted by life stages, sex and by their reproductive condition. Sex was identified for adults by the occurrence of the appendix masculina on the second pleopod in males, and by the shape of the endopod of the first pleopod (Komai and Segonzac, 2008) (**Fig S3A., Fig S3B.**). Since these sexual characters appear only at the adult stage, sex of juvenile specimens could not be determined.

Juvenile stages of *R. exoculata* and *R. chacei* were identified according to the revised taxonomy presented in a previous study (Chapter 2). Pleopod morphologies are identical between subadults and small females, which cannot be distinguished on their morphology. Separation was made between these two stages according to the Onset of Sexual Differentiation (OSD) size (size at which more than 50% of the individuals have developed gonads) defined previously for *R. exoculata* and *R. chacei*.. OSD size is respectively CL =10 mm and CL = 5.98 mm for *R. exoculata* and *R. chacei* (Hernández-Ávila, 2016; Chapter 2). Subadults and juvenile stages were sometimes grouped in the analysis as immature life stages. All the individuals with a higher size than the OSD, and showing female external morphology (ie lacking appendix masculina, and male first pleopod) were sorted as females, and all the individuals with a size below OSD, as subadults. Since the number of *M. fortunata* was too limited to define the OSD size for this specie, the distinction between adults and subadults was made according to the size of the smallest male retrieved in our samples, with a CL of 4.9 mm.

Females were further sorted according to their reproductive status. Those with developed gonads were characterized on board by the marked pink color of their gonads under their cephalothorax (**Fig S3C.**) and ovigerous females by the presence of modified pleopods bearing setae that help to maintain the brood – including brooding females and females with hatched or lost broods (**Fig S3D.**). Females with developed gonads and ovigerous females were considered as reproductively active females. All the other females were classified as non-reproductive individuals.

### 3.1.2.3 Statistical analysis of the population structure

Alvinocaridid shrimps were grouped first by species and then, by life stages for each vent field, or, within Snake Pit, for each vent edifice. Visual examination of our dataset and Shapiro-Wilk normality tests revealed that the size of the alvinocaridid shrimps collected during the BICOSE 2 expedition were not following a Gaussian distribution. Therefore, non-parametric tests were used for intergroup comparisons, with a Mann Whitney test when two groups were compared and a Kruskal-Wallis test followed by post-hoc Dunn tests when three or more groups were compared. Frequencies of males and females in samples were tested for significant variation from a 1:1 sex ratio using $\chi 2$ tests with Yate's correction for one degree of freedom. Similarly, frequencies of adults and immatures, of reproductively active females and non-reproductive females and frequencies of the different juvenile stages were tested for a significant variation from a 1:1 sex ratio using the same statistical test. All tests were performed using R version 3.6.1.

### 3.1.2.4 Cohort analysis of the population structures

Histograms of the size frequency distributions were analyzed as mixtures of statistical distributions for samples containing at least 40 individuals. Size-frequency histograms were plotted using a 1 mm size class interval. This interval was chosen to meet the following criteria described by (Jollivet et al., 2000): (1) most size-classes have at least five individuals each, (2) adjacent empty size-

classes have been minimized and (3) an interval clearly larger than the estimated error rates on measurements. We determined the overlapping component distribution that gives the best fit to the histogram with the "mixdist" package (Macdonald and Du, 2012; Macdonald and Pitcher, 1979) in R version 3.6.1. Our modal decompositions were considered as valid according to the test from the "mixdist" package, which is based on the $\chi 2$ approximation to the likelihood ratio statistic. This allowed the identification of gamma components and their parameters – mean, sigma, estimated and proportion – each corresponding respectively to the mean CL size, the standard deviation on the CL size and the proportion of a defined cohort.

### 3.1.2.5 Environmental Characterization & Niche analysis

Four temperature descriptors were calculated from the 21 assemblages where thermal conditions were measured (**Table S3.**): the mean (Avg.T), the minimum (Min.T), the maximum (Max.T) and the standard deviation (Std.T). Pearson's correlation was used to select non-redundant variables.

Like for the *B. azoricus* mussels and the community of the Lucky Strike vent fields (Husson et al., 2017), the niche of a set of species was studied using the outlier mean index (OMI) created by (Doledec et al., 2000), and computed using the "niche" function of R package ade4 (Dray and Dufour, 2007). On a PCA of environmental parameters, sampling points – i.e., the different assemblages collected – are weighted by the $\log_e$-transformed specie's number. The center of gravity of these weighted points is the species average position in the scatterplot defined by the PCA, i.e. the average thermal conditions in which the species thrive. This method is particularly efficient for describing species niches because, unlike other univariate or multivariate analyses, it does not make the assumption of a linear or unimodal response of faunal descriptors to environmental drivers.

Different indexes are given by the OMI analysis. The OMI index, also called "marginality", is a parameter that gives the squared distance between the species center of gravity and the PCA center. The higher this distance is, the more different the species niche thermal conditions are from the average conditions of the study (i.e. the center of the PCA). A permutation test is used to check the significance of this index, indicating if species marginality is significantly higher than expected by chance. If this test is not significant, this test means that the species distribution is independent of the thermal conditions and dependent from these conditions if the test is significant. The OMI analysis also gives a measure of the niche breath: the tolerance index (Tol), which corresponds to the variance around the centroid. Associated to the tolerance (Tol), the residual tolerance (RTol) index, is defined as the part of the variance that is not explained by the environmental variables used in the PCA. Thus, the RTol index indicates whether the chosen variables are suitable for the niche analysis. These three index (OMI, Tol and RTol) constitute total inertia of the niche, and each can be expressed as a percentage of this inertia.

At the same time, OMI analysis also identified the thermal variables of the PCA that best differentiate the thermal niches of the studied species. Graphic representation of the OMI analysis is a deformation of the PCA plot. Three PCA were conducted: PCA-shrimps to describe the thermal niches of the three different alvinocaridid shrimps sampled in this study, as well as PCA-Rexoculata and PCA-Rchacei to describe the thermal niches of each life stages of *R. exoculata* and *R. chacei* respectively.

## 3.1.3 Results

### 3.1.3.1 Population structure of alvinocaridid shrimps at TAG & Snake Pit in February-March 2018

As in 2014 (Hernández-Ávila, 2016), sex ratio of *R. exoculata* collected in 2018 from TAG and Snake Pit were strongly biased towards females (**Table 4.**). Of the 1168 adult specimens of *R. exoculata* collected at TAG, only 135 were identified as male resulting in an overall sex ratio that deviated significantly from 1:1 ($\chi^2$ = 690.41, p < 0.05) (**Fig 61A.**).

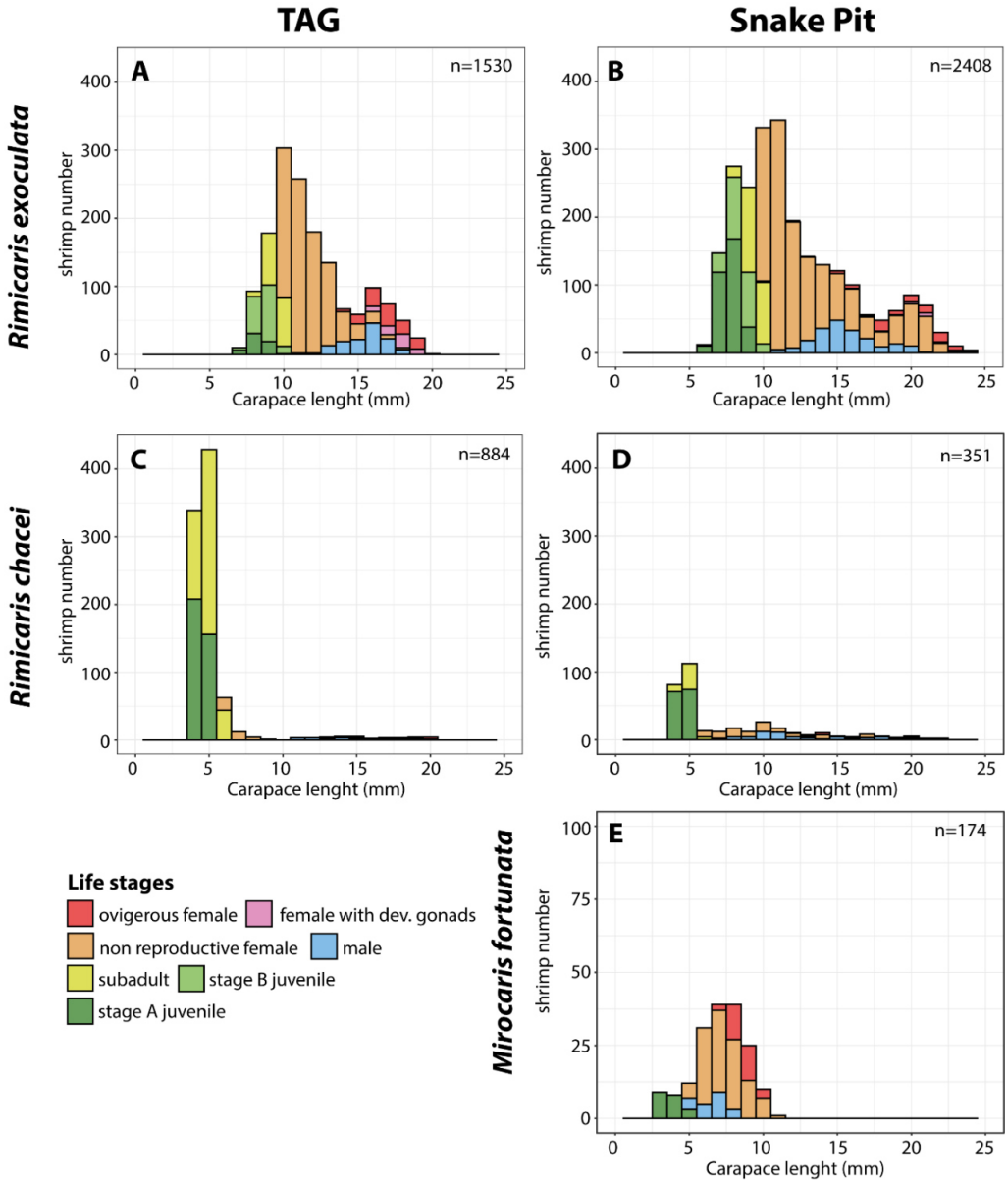


**Fig 62.** Population structure of alvinocaridid shrimps per life stages from TAG and Snake Pit denoting life stages and reproductive status of females. **A.** Population structure of *R. exoculata* from TAG. **B.** Population structure of *R. exoculata* from Snake Pit. **C.** Population structure of *R. chacei* from TAG. **D.** Population structure of *R. chacei* from Snake Pit. **E.** Population structure of *M. fortunata* from Snake Pit.

| Species | Vent field/ edifice | Total n. specimens | Adult | Female | | | Male | Immature | | | |
|---|---|---|---|---|---|---|---|---|---|---|---|
| | | | Total (TA) | Total (TF) | Ovigerous | Dev. Gonads | Non Reproductive | Total (TM) | Total (TI) | Subadult | stage B juvenile | stage A juvenile |
| *Rimicaris exoculata* | TAG | 1533 | 1168 | 1033 | 114 | 50 | 869 | 135 | 365 | 155 | 153 | 57 |
| | Snake Pit | 2413 | 1628 | 1425 | 80 | 16 | 1329 | 203 | 787 | 232 | 216 | 339 |
| | The Beehive | 1275 | 747 | 622 | 14 | 1 | 607 | 125 | 528 | 94 | 166 | 268 |
| | The Moose | 725 | 634 | 598 | 65 | 13 | 520 | 36 | 91 | 22 | 15 | 54 |
| | The Nail | 413 | 247 | 205 | 1 | 2 | 202 | 42 | 166 | 116 | 35 | 15 |
| *Rimicaris chacei* | TAG | 884 | 72 | 53 | 12 | 1 | 40 | 19 | 812 | 448 | - | 364 |
| | Snake Pit | 351 | 154 | 98 | 11 | 1 | 86 | 56 | 197 | 52 | - | 145 |
| | The Beehive | 158 | 11 | 9 | 0 | 0 | 9 | 2 | 147 | 29 | - | 118 |
| | The Moose | 142 | 110 | 66 | 11 | 1 | 54 | 44 | 32 | 11 | - | 21 |
| | The Nail | 51 | 33 | 23 | 0 | 0 | 23 | 10 | 18 | 12 | - | 6 |
| *Mirocaris fortunata* | TAG | 21 | 21 | 17 | 2 | - | 15 | 4 | 0 | - | - | 0 |
| | Snake Pit | 174 | 154 | 133 | 29 | - | 104 | 21 | 20 | - | - | 20 |
| | The Beehive | 26 | 12 | 10 | 0 | - | 10 | 2 | 14 | - | - | 14 |
| | The Moose | 15 | 14 | 11 | 1 | - | 10 | 3 | 1 | - | - | 1 |
| | The Nail | 133 | 128 | 112 | 28 | - | 84 | 16 | 5 | - | - | 5 |

| Species | Vent field/ edifice | Sex Ratio | | | Juvenile Ratio | | | Reproductive Ratio | | |
|---|---|---|---|---|---|---|---|---|---|---|
| | | TM:TF | χ2 (1 df) | Significance | TI:TA | χ2 (1 df) | Significance | TR:TNR | χ2 (1 df) | Significance |
| *Rimicaris exoculata* | TAG | 0.13:1 | 690.41 | *** | 0.31:1 | 420.62 | *** | 0.19:1 | 481.15 | *** |
| | Snake Pit | 0.14:1 | 917.25 | *** | 0.48:1 | 292.87 | *** | 0.07:1 | 1064 | *** |
| | The Beehive | 0.20:1 | 330.67 | *** | 0.71:1 | 37.61 | *** | 0.02:1 | 568.79 | *** |
| | The Moose | 0.06:1 | 498.18 | *** | 0.13:1 | 406.69 | *** | 0.15:1 | 320.81 | *** |
| | The Nail | 0.21:1 | 104.92 | *** | 0.17:1 | 15.89 | *** | 0.01:1 | 187.02 | *** |
| *Rimicaris chacei* | TAG | 0.36:1 | 16.06 | *** | 11.3:1 | 619.46 | *** | 0.32:1 | 13.75 | *** |
| | Snake Pit | 0.57:1 | 11.46 | *** | 1.3:1 | 5.27 | * | 0.14:1 | 53.06 | *** |
| | The Beehive | 0.22:1 | 4.45 | * | 13.4:1 | 117.06 | *** | - | - | - |
| | The Moose | 0.67:1 | 4.40 | * | 0.29:1 | 42.85 | *** | 0.22:1 | 26.72 | *** |
| | The Nail | 0.43:1 | 5.12 | * | 0.55:1 | 1.79 | NS | - | - | - |
| *Mirocaris fortunata* | TAG | 0.24:1 | 8.48 | ** | - | - | - | 0.09:1 | 8.33 | *** |
| | Snake Pit | 0.16:1 | 81.46 | *** | 0.13:1 | 103.2 | *** | 0.28:1 | 42.29 | ** |
| | The Beehive | 0.20:1 | 5.33 | * | 1.2:1 | 0.15 | NS | - | - | - |
| | The Moose | 0.27:1 | 4.57 | * | 0.07:1 | 11.27 | *** | 0.1:1 | 7.36 | *** |
| | The Nail | 0.14:1 | 72.0 | *** | 0.04:1 | 113.75 | *** | 0:1 | 28 | *** |

**Table 4.** Sample and population data of alvinocaridid used in this study per vent field and per edifice for the TAG and Snake Pit vent fields.

Similarly, only 203 males were collected at Snake Pit out of the 1628 adult specimens retrieved at this vent field ($\chi^2$ = 917.25, p < 0.05) (**Fig 61B.**). Overall sex ratio of the *R. chacei* collected at these same vent sites also deviated significantly from 1:1 (**Table 4.**), with 19 males out of the 72 adult specimens collected at TAG ($\chi^2$ = 16.06, p < 0.05) and 53 males out of the 154 adults collected at Snake Pit ($\chi^2$ = 11.46, p < 0.05) (**Fig 61C. and 61D.**). However, proportions of males in TAG and Snake Pit adult populations were higher for *R. chacei* (TAG: 26.4% Snake Pit: 36.4%) compared to *R. exoculata* (TAG: 11.6% Snake Pit: 12.5%) with a less important deviation from a 1:1 sex ratio for *R. chacei* (TAG: $\chi^2$ = 19.67, p < 0.05; Snake Pit: $\chi^2$ = 116.53, p < 0.05). *M. fortunata* populations of TAG and Snake Pit both presented an overall sex ratio that deviated significantly from 1:1, as well (TAG: $\chi^2$ = 8.05, p < 0.05; Snake Pit: $\chi^2$ = 81.46, p < 0.05), (**Fig 61E.**), (**Table 4.**). These deviations in their sex ratio were rather similar to those of *R. exoculata* with similar proportions of males at Snake Pit compared to *R. exoculata* (Snake Pit: 12.5%)

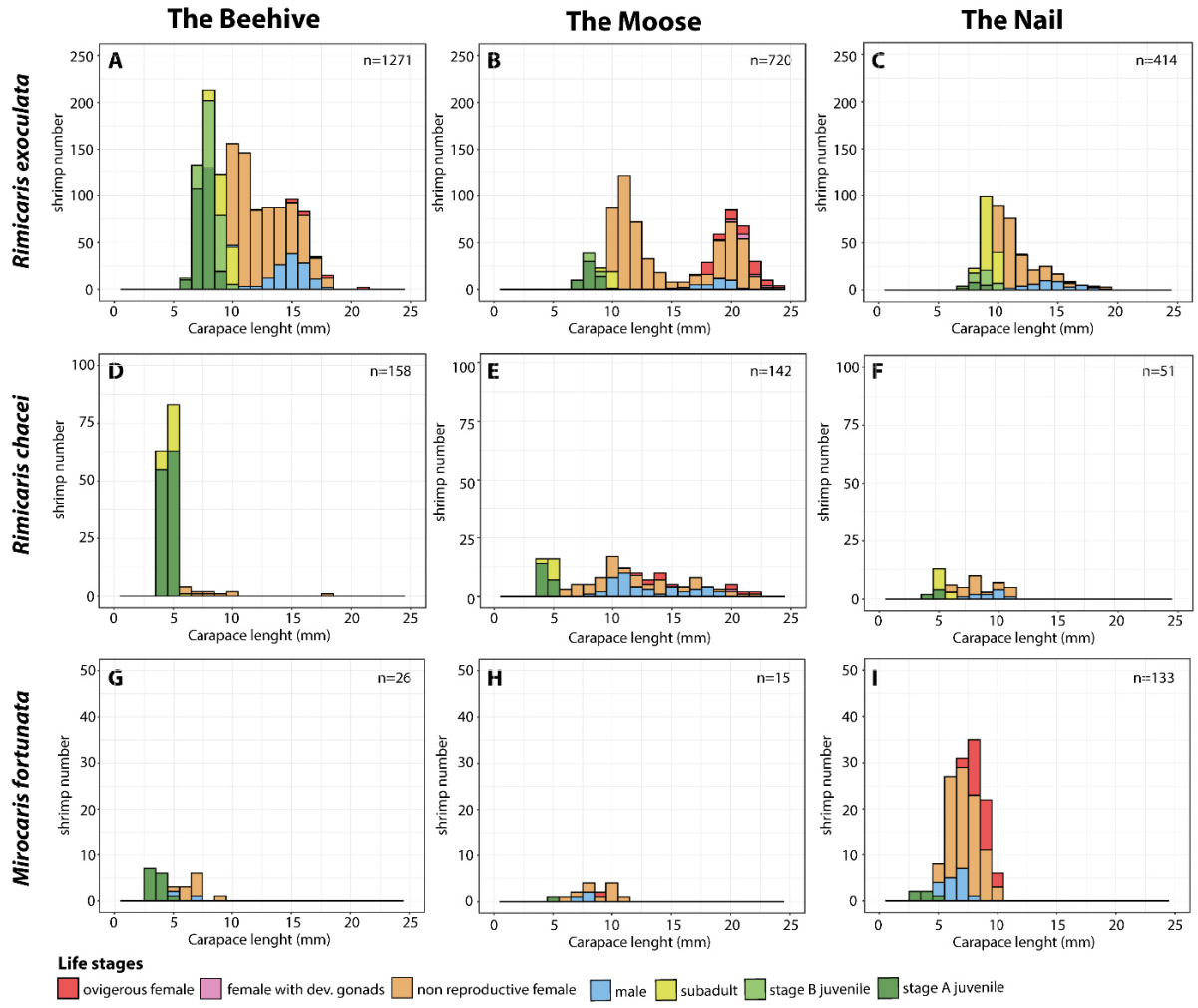


**Fig 63.** Population structure of alvinocaridid shrimps from the different edifices of Snake Pit denoting life stages and reproductive status of females. **A.** Population structure of *R. exoculata* from the Beehive. **B.** Population structure of *R. exoculata* from the Moose. **C.** Population structure of *R. exoculata* from the Nail. **D.** Population structure of *R. chacei* from the Beehive. E. Population structure of *R. chacei* from the Moose. **F.** Population structure of *R. chacei* from the Nail. **G.** Population structure of *M. fortunata* from the Beehive. **H.** Population structure of *M. fortunata* from the Moose. I. Population structure of *M. fortunata* from the Nail.

In details, for each vent edifice of Snake Pit, sex ratio of *R. exoculata* and *M. fortunata* were biased towards females as well ($\chi^2$ tests, $p < 0.05$) (**Fig 62A.** to **3C.** and **3G.** to **3I.**). On the other hand, *R. chacei* presented distinct sex ratio between the different edifices of Snake Pit, with a sex ratio slightly biased towards females at the Beehive and the Nail edifices (The Beehive: $\chi^2 = 4.45$, $p < 0.05$; The Nail: $\chi^2 = 56.12$, $p < 0.05$), but biased towards males at the Moose edifice ($\chi^2 = 4.4$, $p < 0.05$) (**Fig 62D. to 62F.**).

A large proportion of the females were at a reproductive stage for the three different species (**Fig 61.** and **Table 4.**). With 164 reproductively active females of *R. exoculata* at TAG and 94 at Snake Pit, they represented respectively 15.9 % and 6.6 % of all females from TAG or from Snake Pit (TAG: $\chi^2 = 19.67$, $p < 0.05$; Snake Pit: $\chi^2 = 116.53$, $p < 0.05$). Although, their number were much lower, respectively 13 and 12 for TAG and for Snake Pit, reproductively active females of *R. chacei* represented a higher proportion of all females compared to *R. exoculata*, representing 24.5 % of all females at TAG and 12.6 % at Snake Pit (TAG: $\chi^2 = 19.67$, $p < 0.05$; Snake Pit: $\chi^2 = 116.53$, $p < 0.05$). For *M. fortunata*, reproductively active females also represented an important part of all females, respectively 8.3 % and 21.8 % at TAG and Snake Pit (TAG: $\chi^2 = 19.67$, $p < 0.05$; Snake Pit: $\chi^2 = 116.53$, $p < 0.05$).

With 365 immatures individuals – subadults and juveniles – collected at TAG and 787 at Snake Pit, the proportions of *R. exoculata* adults (TAG: 76.2% Snake Pit: 67.4%) were always much higher than the proportions of immature individuals (TAG: 23.8% Snake Pit: 32.6%) in these vent fields (TAG: $\chi^2 = 420.6$, $p < 0.05$; Snake Pit: $\chi^2 = 292.9$, $p < 0.05$) (**Fig 61A.** and **61B.**). Similarly, the proportion of *M. fortunata* adults from Snake Pit (88.5%) was higher than the proportion of immature individuals (11.5%), ($\chi^2 = 103.2$, $p < 0.05$). On the other hand, proportions of *R. chacei* adults (TAG: 8.1% Snake Pit: 43.9%) were always lower than the proportions of immature individuals (TAG: 91.9% Snake Pit: 56.1%), especially at TAG (TAG: $\chi^2 = 519.5$, $p < 0.05$; Snake Pit: $\chi^2 = 5.3$, $p < 0.05$) (**Fig 61C.** and **61D.**). Interestingly, distinct patterns in the proportions of adult and immature shrimps were found between vent edifices of Snake Pit for *R. chacei* and, to some extent, for *R. exoculata* as well (**Fig 62.**). Whereas the proportion of immatures individuals of *R. chacei* was higher at the Beehive edifice ($\chi^2 = 117.06$, $p < 0.05$), than for the entire vent field, it was lower at the Moose edifice ($\chi^2 = 42.85$, $p < 0.05$) (**Fig 62D.** and **62E.**). Additionally, proportions of adult and immature *R. chacei* were balanced at the Nail edifice ($\chi^2 = 1.79$, $p > 0.05$), (**Fig 62F.**). For *R. exoculata*, proportions of adults were always higher at any vent edifice ($\chi^2$ tests, $p < 0.05$), although they were always lower at the Beehive and the Nail edifices compared to the Moose edifice ($\chi^2$ tests, $p < 0.05$), (**Fig 62A.** to **62C.**).

The size-frequency distributions of *R. exoculata* populations from TAG and Snake Pit were rather similar with a very slightly higher average size for the Snake Pit population (TAG: 12.0 ± 2.8 mm; Snake Pit: 12.2 ± 4.0 mm; Mann-Whitney U-test, W= 1909204, $p = 0.046$). Overall, their CL size ranged from 7 mm at TAG and 5.7 mm at Snake Pit for the smallest juveniles, to 20.1 mm at TAG and 24.4 mm at Snake Pit for the biggest adults collected in this study. MIX analysis detected four cohorts in the population of *R. exoculata* from TAG and from Snake Pit overall, the most frequently represented (respectively, 92.5% and 54%) having mean CL of 11.8 mm and 13.8 mm, respectively (**Fig 63A.** and **63B.**).

On the other hand, size-frequency distributions of *R. chacei* populations from TAG and Snake Pit were clearly different (Mann-Whitney U-test, W= 105454, $p < 0.05$) with a higher mean CL size for the Snake

Pit population (TAG: 5.2 ± 2.3 mm; Snake Pit: 7.7 ± 4.4 mm). Their CL size ranged from 3.8 mm at TAG and 3.7 mm at Snake Pit for the smallest juveniles, to 20.5 mm at TAG and 21.8 mm at Snake Pit for the biggest adults collected in this study. MIX analysis detected three cohorts overall in the population of *R. chacei* from TAG and four cohorts for the population from Snake Pit, the most frequently represented (respectively, 39.6% and 33.9%) having mean CL of 4.6 mm and 4.7 mm, respectively (**Fig 63C.** and **63D.**).

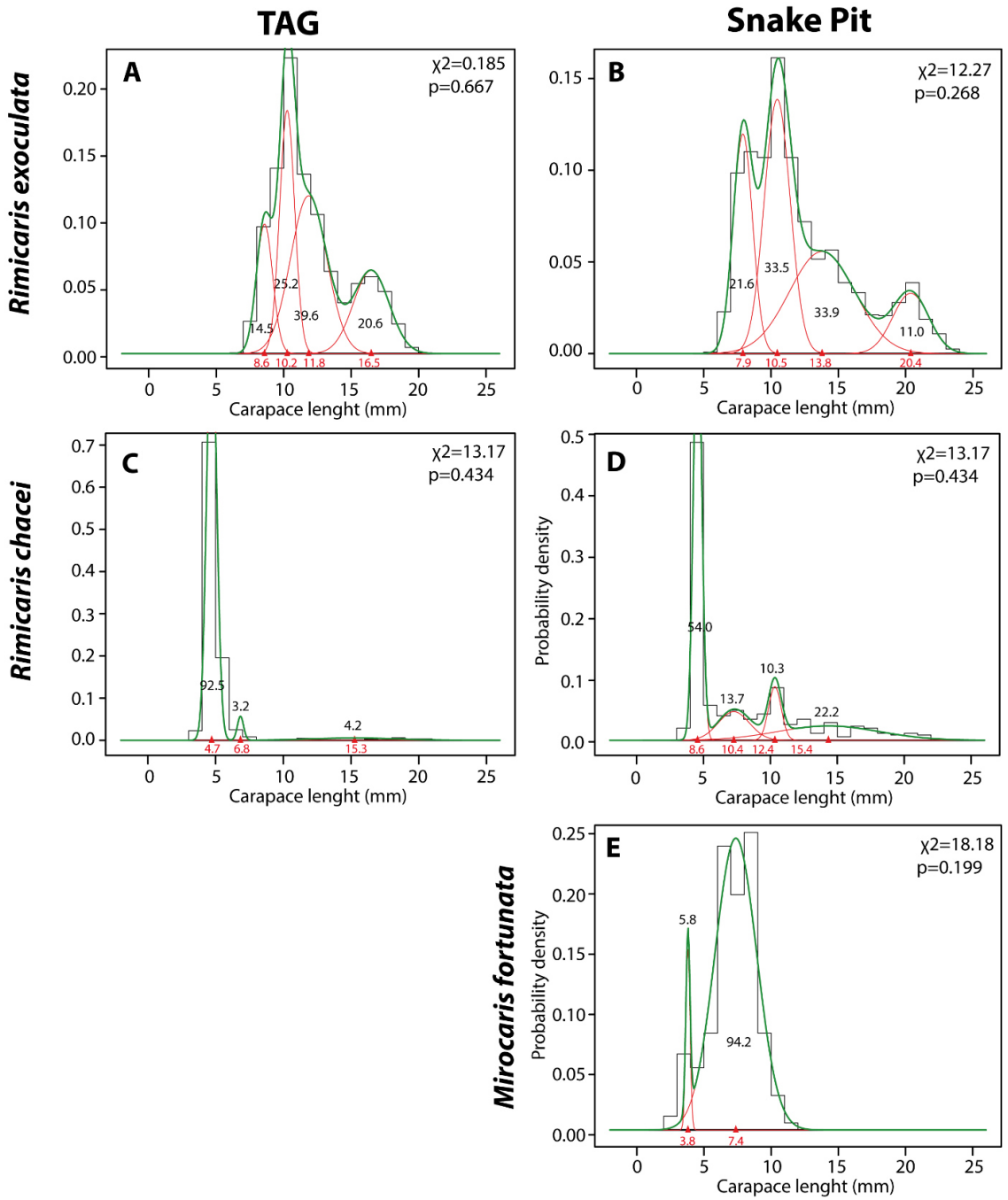


**Fig 64.** Cohort analysis of alvinocaridid shrimps per life stages from TAG and Snake Pit. **A.** Cohort analysis of *R. exoculata* from TAG. **B.** Cohort analysis of *R. exoculata* from Snake Pit. **C.** Cohort analysis of *R. chacei* from TAG. **D.** Cohort analysis of *R. chacei* from Snake Pit. **E.** Cohort analysis of *M. fortunata* from Snake Pit.

| Species | Vent field/ edifice | Ovigerous Females | | | | Females with Dev. Gonads | | | | Non Reproductive Females | | | | Male | | | |
|---|---|---|---|---|---|---|---|---|---|---|---|---|---|---|---|---|---|
| | | mean | sd | max | min | mean | sd | max | min | mean | sd | max | min | mean | sd | max | min |
| *Rimicaris exoculata* | TAG | 17 | 1.32 | 20.1 | 14.1 | 17.6 | 0.86 | 19.2 | 16 | 11.7 | 1.50 | 18.4 | 10 | 15.5 | 1.55 | 18.2 | 10.5 |
| | Snake Pit | 19.9 | 2.36 | 23.8 | 14.6 | 20.3 | 2.15 | 23 | 15.6 | 13.4 | 3.36 | 24.4 | 10 | 15.5 | 2.17 | 20.6 | 10.5 |
| | The Beehive | 17 | 2.01 | 21.4 | 14.6 | - | - | - | - | 12.7 | 2.15 | 18.5 | 10 | 14.9 | 1.49 | 18.2 | 10.5 |
| | The Moose | 20.6 | 1.85 | 23.8 | 17.3 | 21.2 | 1.25 | 23 | 18.6 | 14.8 | 4.32 | 24.4 | 10 | 18.8 | 1.29 | 20.6 | 15.2 |
| | The Nail | - | - | - | - | 16.8 | 1.70 | 18 | 15.6 | 11.7 | 1.67 | 19.3 | 10 | 14.6 | 1.82 | 18.8 | 10.8 |
| *Rimicaris chacei* | TAG | 17.3 | 2.50 | 20.2 | 12.9 | - | - | - | - | 7.6 | 2.77 | 18.7 | 6 | 14.3 | 2.62 | 19.1 | 10.9 |
| | Snake Pit | 16.2 | 3.66 | 21.8 | 11.8 | - | - | - | - | 10.7 | 3.95 | 21.7 | 6.2 | 12.1 | 3.28 | 19 | 7 |
| | The Beehive | - | - | - | - | - | - | - | - | 8.9 | 3.59 | 17.6 | 6.3 | 7.7 | 0.92 | 8.3 | 7 |
| | The Moose | 16.2 | 3.66 | 21.8 | 11.8 | - | - | - | - | 12 | 4.19 | 21.7 | 6.2 | 13 | 3.17 | 19 | 8 |
| | The Nail | - | - | - | - | - | - | - | - | 8.5 | 1.65 | 11.3 | 6.3 | 9.4 | 1.09 | 10.8 | 7.4 |
| *Mirocaris fortunata* | TAG | 7.9 | 0.50 | 8.2 | 7.5 | - | - | - | - | 6.8 | 0.99 | 9 | 5.2 | 6.7 | 0.21 | 6.9 | 6.5 |
| | Snake Pit | 8.6 | 0.74 | 10.2 | 7.1 | - | - | - | - | 7.5 | 1.29 | 11.2 | 5 | 6.7 | 0.90 | 8.5 | 4.9 |
| | The Beehive | - | - | - | - | - | - | - | - | 6.9 | 1.11 | 9.5 | 5.2 | 5.8 | 1.27 | 6.7 | 4.9 |
| | The Moose | - | - | - | - | - | - | - | - | 8.9 | 1.66 | 11.2 | 5.8 | 7.8 | 0.70 | 8.5 | 7.1 |
| | The Nail | 8.6 | 0.75 | 10.2 | 7.1 | - | - | - | - | 7.3 | 1.16 | 10.1 | 5 | 6.6 | 0.74 | 8.2 | 5.5 |

**Table 5.** Body size (CL) of adult alvinocaridids denoting reproductive status of females.

| Species | Vent field/ edifice | Subadult | | | | Stage B juveniles (*R. exoculata* only) | | | | Stage A juveniles | | | |
|---|---|---|---|---|---|---|---|---|---|---|---|---|---|
| | | mean | sd | max | min | mean | sd | max | min | mean | sd | max | min |
| *Rimicaris exoculata* | TAG | 9.4 | 0.43 | 9.9 | 7.7 | 8.8 | 0.57 | 10 | 7.2 | 8.3 | 0.63 | 9.7 | 7 |
| | Snake Pit | 9. | 0.46 | 9.9 | 7.6 | 8.4 | 0.75 | 10.2 | 6.2 | 7.8 | 0.36 | 9.5 | 5.7 |
| | The Beehive | 9.3 | 0.53 | 9.9 | 7.6 | 8.3 | 0.74 | 9.7 | 6.2 | 7.7 | 0.61 | 9.1 | 5.7 |
| | The Moose | 9.6 | 0.34 | 9.9 | 8.6 | 8.7 | 0.54 | 9.6 | 8 | 8.2 | 0.59 | 9.5 | 6.8 |
| | The Nail | 9.3 | 0.39 | 9.9 | 8.3 | 8.8 | 0.71 | 10.2 | 7.5 | 8.3 | 0.66 | 9.4 | 7.3 |
| *Rimicaris chacei* | TAG | 4.9 | 0.45 | 5.9 | 4 | - | - | - | - | 4.5 | 0.29 | 5.4 | 3.8 |
| | Snake Pit | 4.9 | 0.43 | 5.9 | 4.1 | - | - | - | - | 4.5 | 0.32 | 5.4 | 3.7 |
| | The Beehive | 4.8 | 0.37 | 5.7 | 4.1 | - | - | - | - | 4.6 | 0.32 | 5.4 | 3.7 |
| | The Moose | 4.8 | 0.31 | 5.3 | 4.2 | - | - | - | - | 4.4 | 0.26 | 5.3 | 4 |
| | The Nail | 5.3 | 0.44 | 5.9 | 4.6 | - | - | - | - | 4.7 | 0.46 | 5.1 | 4 |
| *Mirocaris fortunata* | TAG | - | - | - | - | - | - | - | - | - | - | - | - |
| | Snake Pit | - | - | - | - | - | - | - | - | 3.8 | 0.58 | 4.8 | 3 |
| | The Beehive | - | - | - | - | - | - | - | - | 3.7 | 0.53 | 4.8 | 3 |
| | The Moose | - | - | - | - | - | - | - | - | - | - | - | - |
| | The Nail | - | - | - | - | - | - | - | - | 4 | 0.61 | 4.8 | 3.3 |

**Table 6.** Body size (CL) of immatures alvinocaridids denoting life stages.

Surprisingly, MIX analysis of *M. fortunata* population from Snake Pit detected only two cohorts overall in the population of *M. fortunata* from Snake Pit, the most frequently represented (94.2% of the population) having mean CL of 7.4 mm and the second, with a mean CL of 3.8 mm, representing only 5.8% of the population (**Fig 63E**.). In detail, average sizes of *R. exoculata* and *R. chacei* were always significantly higher at the Moose edifice (*R. exoculata*: 14.8 ± 4.8 mm; *R. chacei*: 11.0 ± 4.9 mm) compared to the other sites including TAG (Kruskal-Wallis, *R. exoculata*: H= 308.27, $p < 0.05$; *R. chacei*: H= 147.5, $p < 0.05$; Dunn's Multiple Comparison Test, $p < 0.05$). Averages sizes of *R. exoculata* were similar between the Beehive and the Nail edifices (The Beehive: 11.1 ± 3.1 mm; The Nail: 11.0 ± 2.3 mm; Dunn's Multiple Comparison Test, $p > 0.05$) whereas they were higher at the Nail edifice for *R. chacei* (*T*he Beehive: 4.9 ± 1.4 mm; The Nail: 7.5 ± 2.2 mm; Dunn's Multiple Comparison Test, $p < 0.05$).

Concerning *R. exoculata* life stages, average sizes of males and all the different females stages were significantly distinct at the two vent fields (Kruskal-Wallis, TAG: H= 594.1, $p < 0.05$; Snake Pit: H= 296.9, $p < 0.05$) (**Table 5. and 6.**). Nonetheless, whereas male were significantly bigger than non-reproductive females (Dunn's Multiple Comparison Test, $p < 0.05$), they were significantly smaller than reproductively active females (Dunn's Multiple Comparison Test, $p < 0.05$) (**Table 5.**). The average sizes of females with developed gonads and ovigerous females were similar (Dunn's Multiple Comparison Test, $p > 0.05$), (**Table 5.**). Unlike previously reported (Komai and Segonzac, 2008), average sizes of *R. exoculata* juveniles and subadults were also significantly different (Kruskal-Wallis, TAG: H= 144.8, $p < 0.05$; Snake Pit: H= 426.0, $p < 0.05$), with a size increase between each stages along the juvenile ontogeny at the two vent fields (Dunn's Multiple Comparison Test, $p < 0.05$), (**Table 6.**). Average sizes of males and females (reproductive and non-reproductive) of *R. chacei* were also significantly different at the two vent fields (Kruskal-Wallis, TAG: H= 46.03, $p < 0.05$; Snake Pit: H= 24.54, $p < 0.05$) (**Table 5.**). These size differences were mainly related to the smaller size of non-reproductive females compared to the size of male and ovigerous females at both vent fields (Dunn's Multiple Comparison Test, $p < 0.05$ (**Table 5.**). Males had similar size to ovigerous females at TAG (Dunn's Multiple Comparison Test, $p > 0.05$) but slightly smaller at Snake Pit (Dunn's Multiple Comparison Test, $p < 0.05$), (**Table 5.**). Average sizes were also significantly different between subadults and juvenile stages with a size increase for subadult stages (Mann-Whitney U-test, TAG: W= 120073, $p < 0.05$; Snake Pit: W= 5507.5, $p < 0.05$), (**Table 6.**).

### 3.1.3.2 Spatial variation in the population structure of alvinocaridid shrimps from TAG & Snake Pit

Discrete spatial variations in the population structure of the different alvinocaridid shrimp species were explored among 31 discrete samples collected from seven different types of assemblages (**Fig 64.**). These assemblages were first distinguished based on *in situ* visual characteristics including shrimp densities, size of individuals, and closeness to active venting. Proportion of dominant species (alvinocaridid shrimps constitute the vast majority if not the totality of each sample) were further used following on board sorting to refine characterization of assemblages into distinct types. *R. exoculata* was present in all of the samples collected although only 25 of them exhibited more than 10 individuals. *R. chacei* were totally absent from 8 samples and only 14 out of the 31 samples exhibited more than 10 individuals. *M. fortunata* were by far the less abundant alvinocaridids, completely absent from 18 samples present in only 4 assemblages with more than 10 individuals. However, sampling was

targeted for the two *Rimicaris* species, which inevitably introduced a bias for the abundance of *M. fortunata*, although, it still reflect qualitatively the lower abundances of this species at this vent fields.

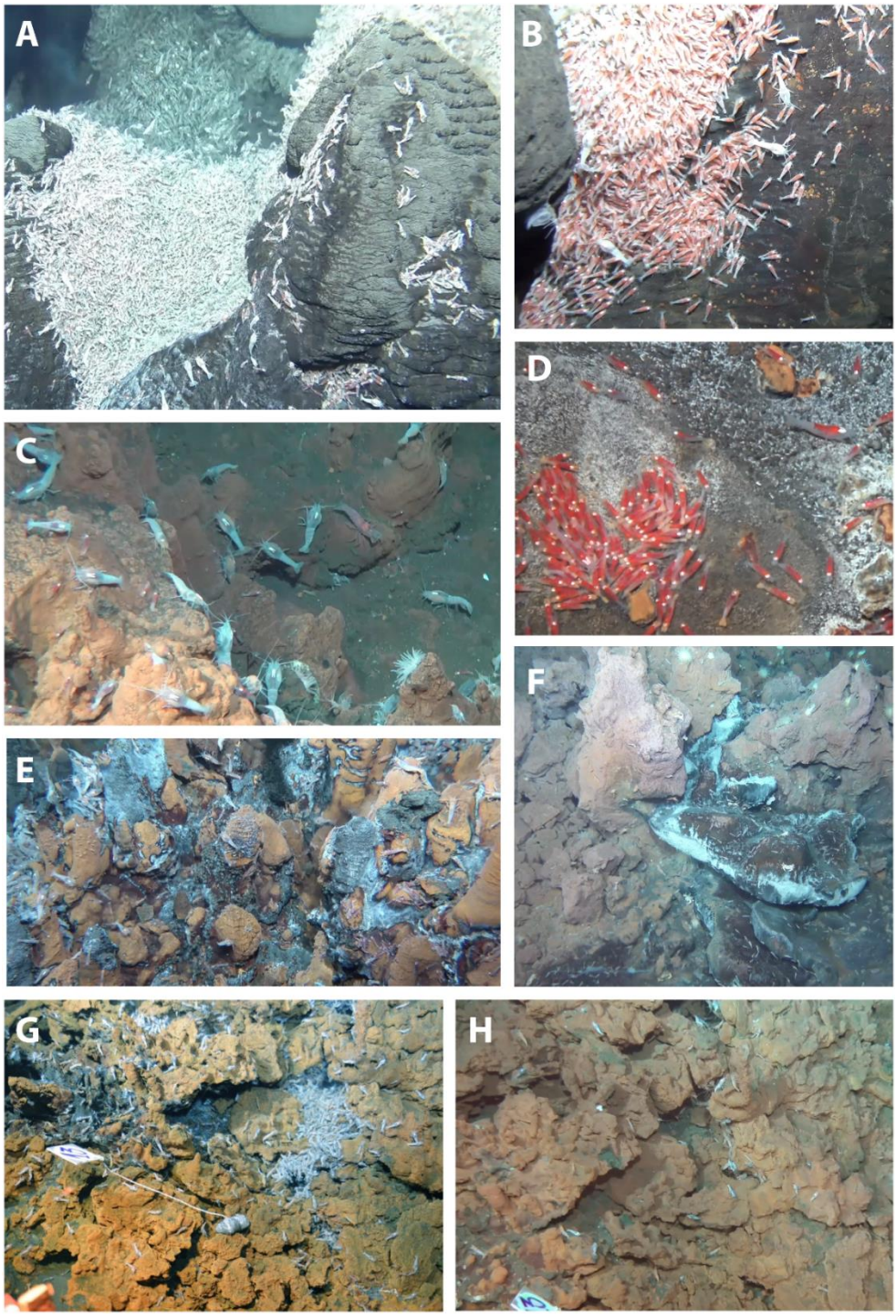


**Fig 65.** Overview of the different assemblage types collected at TAG and Snake Pit in 2018 during the BICOSE 2 expedition. **A.** Dense aggregates of *R. exoculata* shrimps. **B.** *R. exoculata* nurseries on the flank of the Beehive edifice. **C.** Peripheral areas of scattered individuals. **D.** *R. chacei* nurseries close to diffuse emissions. **E.** Alvinocaridids in the vicinity of dense aggregates. **F.** Peripheral areas close to diffuse emissions dominated by *M. fortunata* at the Nail edifice. **G.** Dense aggregate of *R. exoculata* between rocks, replaced 10 days later by **H.** Hidden aggregate of *R. chacei* adults.

## 3.1 POPULATION STRUCTURE AND THERMAL NICHES OF ALVINOCARIDIDS FROM THE MID ATLANTIC RIDGE

The first type of assemblage was the most visually dominant in the studied vent fields: the dense aggregates (**Fig 64A.**, **Fig 65A.**) also called ('active emission habitats' in (Hernández-Ávila, 2016)). Dense aggregates were largely dominated by *R. exoculata* shrimps ($\chi^2$ = 110.99 – 834, $p < 0.05$) with occasional occurrence of *R. chacei* individuals (1 to 12 per sample of 'dense aggregates'), especially at the Moose edifice, and on rarer instances, one or two *M. fortunata* individuals (**Table 7.**). At the highest, proportions of *R. chacei* represented 10.4% % of all the alvinocaridid shrimps from these samples whereas *M. fortunata* never exceeded 0.01 %. Samples of 'dense aggregate' were mostly constituted of *R. exoculata* adults, representing between 64.7% and 94.2% of all the *R. exoculata* from these assemblages ($\chi^2$ = 24.26 – 250.3, $p < 0.05$), with only one dense aggregate from the Nail edifice showing an equilibrated proportion of adults and immature individuals ($\chi^2$ = 0.316, $p > 0.05$), (**Table 7.**). As observed in 2014 (Hernández-Ávila, 2016), for nearly all the 'dense aggregates' samples, sex ratio of *R. exoculata* strongly deviated from 1:1 ($\chi^2$ = 31.15 – 311.01, $p < 0.05$), with a large bias towards females (**Table 7.**). One exception though, was found in a sample from TAG that presented a balanced sex ratio for *R. exoculata* ($\chi^2$ = 0.695, $p > 0.05$), (**Table 7.**). Still, even without this particular sample, proportions of *R. exoculata* females were variable among 'dense aggregate' samples, from 81.8% to 99.7% of all adults. Moreover, most of the reproductively active females of *R. exoculata* were found in 'dense aggregate' samples with 250 individuals out of the 258 collected overall. For nearly all of the 'dense aggregate' samples, proportions of reproductively active and non-reproductive females of *R. exoculata* significantly deviated from 1:1 ($\chi^2$ = 4.96 – 262.87, $p < 0.05$), except one aggregate from Snake Pit ($\chi^2$ = 3.07, $p > 0.05$), (**Table 8.**). In most cases, proportions of reproductively active females were lower than of non-reproductive ones (between 0.8% and 38.2% of all females), although the first two aggregates collected during the cruise exhibited a higher proportion of reproductively active females (74% and 61.8% of all females). None of the 'dense aggregate' samples presented a sufficient number of *R. chacei* individuals to conclude about sex ratio or proportions of immature individuals in these type of assemblages.

Another type of assemblage called 'juvenile aggregate from chimneys' clearly dominated by *R. exoculata* was retrieved too, but only at Snake Pit on the flank of the main chimneys of the Beehive edifice (**Fig 64B.**, **Fig 65B.**). Unlike dense aggregates of *R. exoculata* adults, these assemblages mostly consisted of immature individuals representing around 90.4% and 91.3% of all the *R. exoculata* from these assemblages ($\chi^2$ = 102.73 and 117.23, $p < 0.05$), (**Table 7.**). These immature individuals were clearly stage A juveniles in majority, representing 70.4% and 74.5% of all the immature individuals from these assemblages ($\chi^2$ = 306.15 and 344, $p < 0.05$). On the other hand, stage B juveniles were representing 21% and 22.5% of all the immature individuals, and subadults only 4.5% and 7%. Although the number of adults was limited, sex ratio of these assemblages could be estimated. Unlike dense aggregates, this sex ratio did not significantly deviated from 1:1 or only slightly towards females ($\chi^2$ = 5.4, $p < 0.05$; 3.27, $p > 0.05$), (**Table 7.**). Apart from these *R. exoculata*, only two *R. chacei* subadults in one of the two samples collected were found. These nurseries of *R. exoculata* were associated with the gastropods *Peltospira smaragdina*.

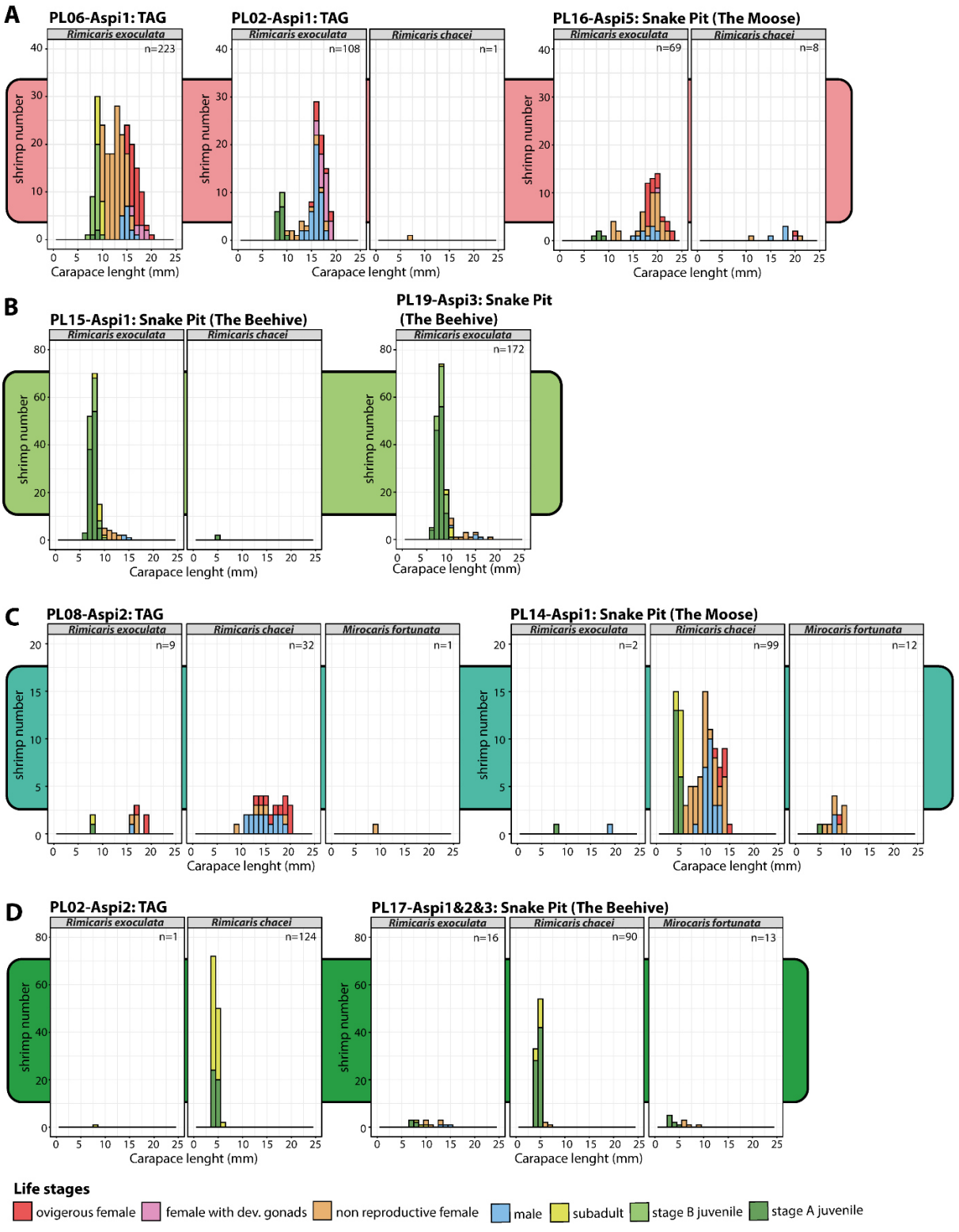


**Fig 66.** Size-frequency distributions of three alvinocaridid species in assemblages dominated by *R. exoculata* (A and B) or by *R. chacei* (C and D). **A.** Dense aggregates of *R. exoculata* adults close to active vent fluids. **B.** Nursery of *R. exoculata* at Snake Pit on the flank of the chimneys with diffuse emissions, close to dense aggregates. Assemblage associated with *P. smaragdina* gastropods. **C.** Hidden aggregates of *R. chacei* found behind rocks at TAG or behind mussel beds at Snake Pit, near diffuse vent fluid emissions. **D.** *R. chacei* nursery associated with low temperature diffusions. Additional histogram are presented in **Fig S4**.

A third type of assemblage, not evidenced before our 2018 expedition, was clearly dominated by *R. chacei* (**Fig 64G.**, **Fig 65C.**). These were dense but limited aggregates, hidden between rocks at TAG or in holes between *B. puteoserpentis* mussels at Snake Pit. *R. chacei* represented most of the alvinocaridid shrimps (**Fig 65C.**) in this type of assemblage called 'hidden aggregates'. Accounting for 76.2% and 87.6% of all shrimps at TAG and Snake Pit respectively ($\chi^2$ = 4.96 – 262.87, p < 0.05) (**Table 7.**). In these assemblages, *R. chacei* were mostly represented by adults, accounting for all the *R. chacei* individuals from these samples at TAG and 71.7% of those from Snake Pit (TAG: $\chi^2$ = 32, p < 0.05; Snake Pit: $\chi^2$ = 18.68, p < 0.05), (**Table 7.**). *R. chacei* sex ratio in 'hidden aggregate' samples was balanced at TAG ($\chi^2$ = 0, p > 0.05) but biased towards females at Snake Pit ($\chi^2$ = 7.45 p > 0.05), (**Table 7.**). These assemblages were also the location where the largest concentrations of reproductively active *R. chacei* were retrieved with 11 individuals at TAG out of the 13 collected and 7 at Snake Pit out of the 12 collected, the others being distributed sparsely in the different dense aggregates of *R. exoculata*. Ratio of reproductively active females among all females significantly deviated from a 1:1 (TAG: $\chi^2$ = 2.25, p < 0.05; Snake Pit: $\chi^2$ = 23.17, p < 0.05) with an equilibrated proportion of reproductively active and non-reproductive females at TAG (68.75% of all the females) and a lower proportion of reproductively active females at Snake Pit (17.5% of all the females), (**Table 8.**). Other species were too scarce to estimate sex and juvenile ratios for them in these assemblages.

Similarly to '*R. chacei* nurseries' observed in 2014 at TAG (also called 'diffuse emission habitat') (Hernández-Ávila, 2016), assemblages of very small alvinocaridids were observed again in 2018, not only at TAG, but also at Snake Pit (**Fig 64D.**, **Fig 65D.**). Again, these small juveniles all belong to *R. chacei* (see chapter 2). These stage A *R. chacei* juveniles represented between 66.7% and 99.5% of all alvinocaridids from these assemblages ($\chi^2$ = 4.96 – 262.87, p < 0.05), (**Table 7.**). The rest of the shrimps in these samples were *R. chacei* subadults; immature stages of *R. chacei* thus representing between 95.8% and 99.1% of all the *R. chacei* individuals from these assemblages ($\chi^2$ = 20.17 – 436.14, p < 0.05), (**Table 7.**). None of the samples from '*R. chacei* nurseries' had a sufficient number of *R. chacei* adults to conclude about the sex ratio of this species in these assemblages. Interestingly, the proportions of stage A juveniles and subadults differed widely between the different nurseries. Three of them – two from Snake Pit and one from TAG – were dominated by stage A juveniles (between 70% and 83% of stage A, $\chi^2$ = 9.78 – 70.72, p < 0.05) whereas one from TAG was largely dominated by subadult stages (65% of subadult, $\chi^2$ = 10.45, p < 0.05). The numbers of *R. exoculata* and *M. fortunata* were also in general too low to evaluate their sex ratio as well as the proportions of their immatures, except in one nursery from Snake Pit. In this nursery, the proportions of immatures and adults were similar both for *R. exoculata* and for M. *fortunata* (*R. exoculata*: $\chi^2$ = 0, p < 0.05; M. *fortunata*: $\chi^2$ = 0.692, p < 0.05), (**Table 7.**). No *P. smaragdina* gastropods were observed in the vicinity of these *R. chacei* nurseries.

In addition to these four different types of alvinocaridid assemblages, three other types have been identified, exhibiting mixtures of at least two of the three alvinocaridid species reported here (**Fig 66.**). Among them, the peripheral areas consisted of scattered individuals laying at distance from any visible diffusion, but still close enough to be considered under vent field influence (also called 'inactive emission habitat' in (Hernández-Ávila, 2016)), presented in some cases mixed populations of the three alvinocaridids (**Fig 64C.**, **Fig 66.A.**). In one 'periphery' sample from TAG, proportions of each species were well balanced, representing 47.5%, 33.9% and 18.6% respectively for *R. exoculata*, *R. chacei* and *M. fortunata* ($\chi^2$ 2.18, p > 0.05), (**Table 7.**).

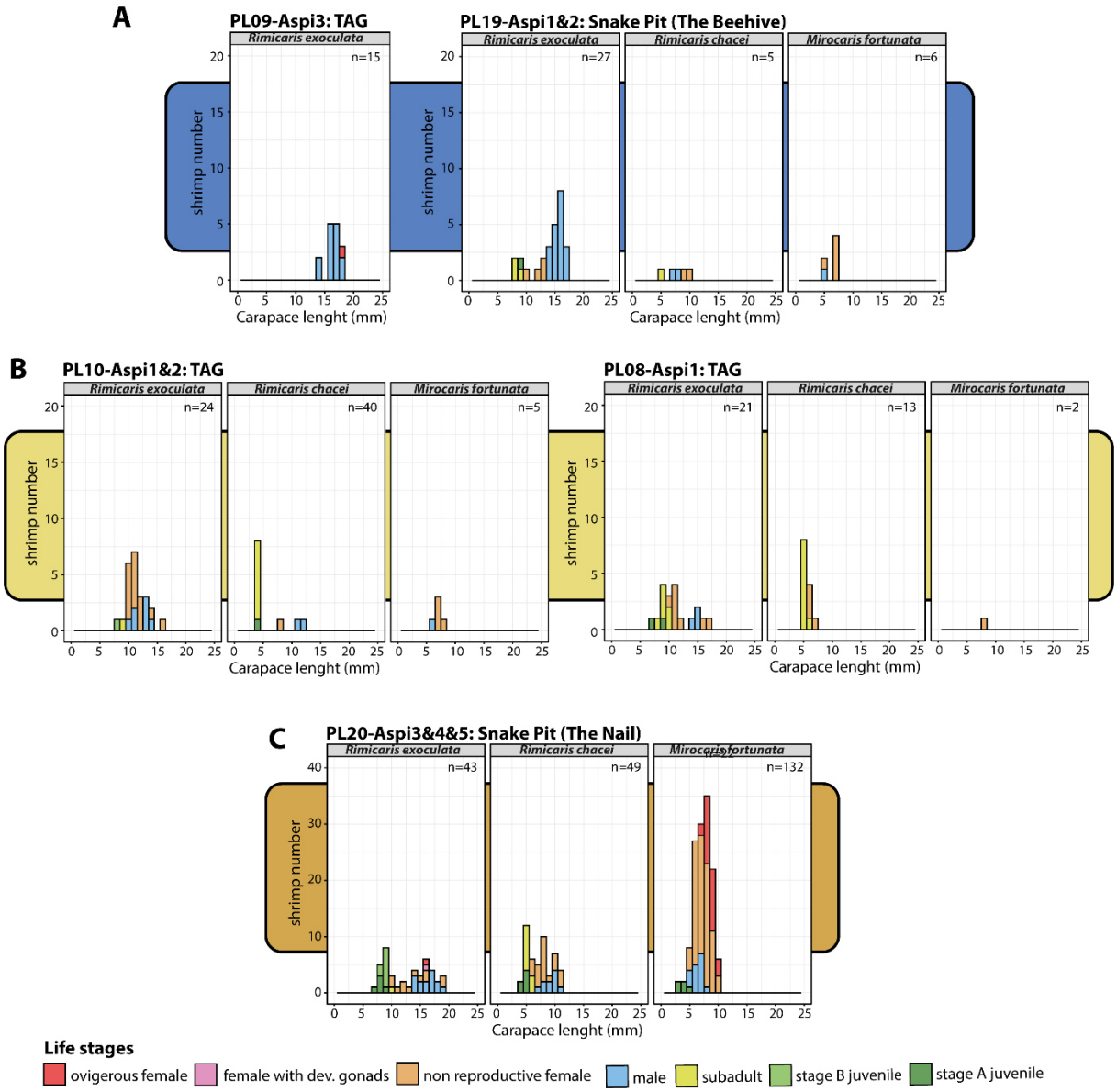


**Fig 67.** Size-frequency distributions of three alvinocaridid species in mixt assemblages from peripheral areas at TAG and Snake Pit. **A.** Peripheral assemblages of scattered individuals, found in areas without visible vent diffusion but still under the hydrothermal vent field influence. **B.** Assemblages of scattered individuals in close vicinity (<1m) of the dense aggregates of *R. exoculata* around high temperature fluid emissions at TAG. Assemblage associated with *P. smaragdina* gastropods. **C.** Assemblage of scattered individuals in a diffuse fluid area at the Nail edifice with a dominance of *M. fortunata*. Additional histogram are presented in **Fig S5**.

In the samples from Snake Pit, two species were usually dominant, one sample being dominated by balanced proportions of *R. exoculata* and *R. chacei* ($\chi^2 = 2.18$, $p > 0.05$) in the absence of *M. fortunata*, and the other sample being dominated by *R. exoculata* with lower but balanced proportions of *R. chacei* and *M. fortunata* ($\chi^2 = 0.09$, $p > 0.05$), (**Table 7.**).

| Vent Field / Edifice | Assemblage Type | Sample ID | *Rimicaris exoculata* | | | | | | | *Rimicaris chacei* | | | | | | | *Mirocaris fortunat* | | | | | | | All Alvinocaridid Species Ratio | |
|---|---|---|---|---|---|---|---|---|---|---|---|---|---|---|---|---|---|---|---|---|---|---|---|---|---|
| | | | Total n. specimens | Sex Ratio TM:TF | Sex Ratio χ2 (1 df) | Sex Ratio Signif. | Juvenile Ratio TI:TA | Juvenile Ratio χ2 (1 df) | Juvenile Ratio Signif. | Total n. specimens | Sex Ratio TM:TF | Sex Ratio χ2 (1 df) | Sex Ratio Signif. | Juvenile Ratio TI:TA | Juvenile Ratio χ2 (1 df) | Juvenile Ratio Signif. | Total n. specimens | Sex Ratio TM:TF | Sex Ratio χ2 (1 df) | Sex Ratio Signif. | Juvenile Ratio TI:TA | Juvenile Ratio χ2 (1 df) | Juvenile Ratio Signif. | χ2 (1 df) | Signif. |
| TAG | Dense Aggregate | PL02-A1 | 109 | 0.84:1 | 0.695 | NS | 0.18:1 | 51.6 | *** | 1 | - | - | - | - | - | - | 0 | - | - | - | - | - | - | 212.06 | *** |
| TAG | Dense Aggregate | PL02-A3 | 111 | 0.07:1 | 72.516 | *** | 0.17:1 | 56.22 | *** | 8 | - | - | - | - | - | - | 0 | - | - | - | - | - | - | 193.3 | *** |
| TAG | Dense Aggregate | PL06-A1 | 223 | 0.09:1 | 120.14 | *** | 0.27:1 | 72.33 | *** | 0 | - | - | - | - | - | - | 0 | - | - | - | - | - | - | 458.1 | *** |
| TAG | Dense Aggregate | PL07-A2 | 339 | 0.02:1 | 251.52 | *** | 0.23:1 | 131.33 | *** | 0 | - | - | - | - | - | - | 0 | - | - | - | - | - | - | 678 | *** |
| TAG | Dense Aggregate | PL08-A3 | 417 | 0.03:1 | 268.07 | *** | 0.38:1 | 85.66 | *** | 0 | - | - | - | - | - | - | 0 | - | - | - | - | - | - | 834 | *** |
| TAG | Hidden Aggregate | PL08-A2 | 9 | - | - | - | - | - | - | 32 | 1:1 | 0 | *** | 0:1 | 32 | *** | 1 | - | - | - | - | - | - | 34.37 | *** |
| TAG | *R. chacei* Nursery | PL02-A2 | 1 | - | - | - | - | - | - | 124 | - | - | - | - | 124 | *** | 0 | - | - | - | - | - | - | 244.05 | *** |
| TAG | *R. chacei* Nursery | PL09-A1&2 | 2 | - | - | - | - | - | - | 452 | - | - | - | 112:1 | 436.14 | *** | 0 | - | - | - | - | - | - | 896.05 | *** |
| TAG | Periphery | PL09-A3 | 15 | 14:1 | 11.27 | *** | 0:1 | 15 | *** | 0 | - | - | - | - | - | - | 0 | - | - | - | - | - | - | 30 | *** |
| TAG | Periphery | PL10-A3&4 | 28 | 8:1 | 16.33 | *** | 0.04:1 | 24.14 | *** | 20 | - | - | - | 19:1 | 16.2 | *** | 11 | 0.38:1 | 2.27 | NS | 0:1 | 11 | *** | 2.18 | NS |
| TAG | Vicinity of Aggregates | PL05-A1&2&3 | 234 | 0.05:1 | 117.36 | *** | 0.63:1 | 12.46 | *** | 193 | 0:1 | 25 | *** | 6.72:1 | 105.95 | *** | 2 | - | - | - | - | - | - | 3.94 | * |
| TAG | Vicinity of Aggregates | PL08-A1 | 21 | 0.33:1 | 3 | NS | 0.75:1 | 0.428 | NS | 13 | - | - | - | 2.25:1 | 1.92 | NS | 1 | - | - | - | - | - | - | 1.88 | NS |
| TAG | Vicinity of Aggregates | PL10-A1&2 | 24 | 0.47:1 | 2.91 | NS | 0.09:1 | 16.67 | *** | 41 | - | - | - | 12.67:1 | 29.8 | *** | 5 | - | - | - | - | - | - | 3.88 | * |
| Snake Pit / The Beehive | Dense Aggregate | PL15-A2 | 185 | 0.22:1 | 50.79 | *** | 0.47:1 | 24.26 | *** | 0 | - | - | - | - | - | - | 0 | - | - | - | - | - | - | 370 | *** |
| Snake Pit / The Beehive | Dense Aggregate | PL15-A3 | 326 | 0.10:1 | 181.19 | *** | 0.2:1 | 145.78 | *** | 0 | - | - | - | - | - | - | 0 | - | - | - | - | - | - | 652 | *** |
| Snake Pit / The Beehive | Dense Aggregate | PL19-A4&5 | 362 | 0.17:1 | 131.96 | *** | 0.37:1 | 77.97 | *** | 1 | - | - | - | - | - | - | 0 | - | - | - | - | - | - | 720.02 | *** |
| Snake Pit / The Moose | Dense Aggregate | PL14-A3 | 338 | 0.003:1 | 311.01 | *** | 0.07:1 | 250.3 | *** | 12 | 3:1 | | | 0.5:1 | | | 2 | - | - | - | - | - | - | 622.93 | *** |
| Snake Pit / The Moose | Dense Aggregate | PL16-A5 | 69 | 0.18:1 | 31.15 | *** | 0.06:1 | 53.93 | *** | 8 | - | - | - | - | - | - | 0 | - | - | - | - | - | - | 110.99 | *** |
| Snake Pit / The Moose | Dense Aggregate | PL18-A1&2 | 160 | 0.06:1 | 91.12 | *** | 0.31:1 | 70.42 | *** | 8 | - | - | - | - | - | - | 0 | - | - | - | - | - | - | 247.95 | *** |
| Snake Pit / The Moose | Dense Aggregate | PL20-P1 | 142 | 0.07:1 | 95.61 | *** | 0.17:1 | 44.1 | *** | 10 | 0.11:1 | | | 0:1 | | | 0 | - | - | - | - | - | - | 290.29 | *** |
| Snake Pit / The Nail | Dense Aggregate | PL20-A1 | 215 | 0.19:1 | 67.59 | *** | 0.48:1 | 26.16 | *** | 0 | - | - | - | - | - | - | 0 | - | - | - | - | - | - | 430 | *** |
| Snake Pit / The Nail | Dense Aggregate | PL20-A2 | 155 | 0.07:1 | 55.35 | *** | 1.09:1 | 0.316 | NS | 2 | - | - | - | - | - | - | 1 | - | - | - | - | - | - | 298.27 | *** |
| Snake Pit / The Moose | Hidden Aggregate | PL14-A1 | 2 | - | - | - | - | - | - | 99 | 0.51:1 | 7.45 | ** | 0.39:1 | 18.68 | *** | 12 | 0.22:1 | | | 0.09:1 | | | 129.95 | *** |
| Snake Pit / The Beehive | *R. chacei* Nursery | PL15-A4 | 7 | - | - | - | - | - | - | 24 | - | - | - | 23:1 | 20.17 | *** | 5 | - | - | - | - | - | - | 18.17 | *** |
| Snake Pit / The Beehive | *R. chacei* Nursery | PL17-A1&2&3 | 16 | - | - | - | 1:1 | 0 | NS | 90 | - | - | - | 29:1 | 78.4 | *** | 13 | 0:1 | | | 1.6:1 | 0.692 | NS | 86 | *** |
| Snake Pit / The Beehive | *R. exoculata* Nursery | PL15-A1 | 157 | 0.25:1 | 5.4 | * | 9.47:1 | 102.73 | *** | 2 | - | - | - | - | - | - | 0 | - | - | - | - | - | - | 11.27 | *** |
| Snake Pit / The Beehive | *R. exoculata* Nursery | PL19-A3 | 172 | 0.36:1 | 3.27 | NS | 10.47:1 | 117.23 | *** | 0 | - | - | - | - | - | - | 0 | - | - | - | - | - | - | 31 | *** |
| Snake Pit / The Beehive | Periphery | PL19-A1&2 | 31 | 4.75:1 | 6.4 | ** | 0.35:1 | 7.26 | ** | 5 | - | - | - | - | - | - | 6 | - | - | - | - | - | - | 31 | *** |
| Snake Pit / The Moose | Periphery | PL14-A2 | 10 | 9:1 | 9.78 | ** | 0:1 | 10 | ** | 12 | 3:1 | 3 | NS | 0:1 | 12 | *** | 0 | - | - | - | - | - | - | 11.27 | ** |
| Snake Pit / The Nail | Periphery - *Mirocaris* | PL20-A3&4&5 | 43 | 1:1 | 0 | NS | 0.54:1 | 3.93 | * | 49 | 0.45:1 | 4.5 | * | 0.53:1 | 4.59 | * | 132 | 0.14:1 | 71.06 | *** | 0.04:1 | 112.76 | *** | 66.27 | *** |

**Table 7.** Sex and stage distributions in alvinocaridid shrimps from the different assemblages.

Unlike the others, the second "periphery" sample from TAG consisted only of *R. exoculata* shrimps (**Table 7.**). In all 'periphery' samples, *R. exoculata* shrimps were mostly adults ($\chi^2$ = 7.26 – 24.14, $p < 0.05$) with a maximum of 25.8% of immature individuals in one sample from Snake Pit. On the other hand, in samples with a sufficiently large number of *R. chacei* to perform statistical tests (2 samples), this species was mostly represented by immature individuals at TAG ($\chi^2$ = 16.2, $p < 0.05$), and by adults at Snake Pit ($\chi^2$ = 12, $p < 0.05$), (**Table 7.**).

All *M. fortunata* from "periphery" samples were adults. As observed in 2014 at TAG (Hernández-Ávila, 2016), sex ratios of *R. exoculata* in 'periphery' samples were strongly biased towards males ($\chi^2$ = 6.4 – 16.33, $p < 0.05$) (**Table 7.**). On the other hand, sex ratios of *R. chacei* and *M. fortunata* from the 'periphery' did not significantly deviated from 1:1 (*R. chacei*: $\chi^2$ = 3, $p < 0.05$; *M. fortunata*: $\chi^2$ = 2.27, $p < 0.05$), (**Table 7.**).

The two last types of assemblages were retrieved in only one of the two vent fields. The first one, at the vicinity of some of the dense aggregates at TAG, presented a rather equilibrated proportion of *R. exoculata* and of *R. chacei* (**Fig 64E.**, **Fig 66A.**) in the three sampling points ($\chi^2$ = 3.94, p = 0.047; $\chi^2$ = 1.88, p = 0.17; $\chi^2$ = 3.88, p = 0.049) with a very low number or a total absence of *M. fortunata* (**Table 7.**).

| | | | RF | NRF | χ2 | Signif. |
|---|---|---|---|---|---|---|
| ***R. exoculata*** | | | | | | |
| TAG | Dense Aggregate | PL02-A1 | 37 | 13 | 11.52 | *** |
| TAG | Dense Aggregate | PL02-A3 | 55 | 34 | 4.96 | * |
| TAG | Dense Aggregate | PL06-A1 | 49 | 111 | 24.06 | *** |
| TAG | Dense Aggregate | PL07-A2 | 9 | 260 | 234.2 | *** |
| TAG | Dense Aggregate | PL08-A3 | 8 | 286 | 262.87 | *** |
| Snake Pit / The Beehive | Dense Aggregate | PL15-A2 | 2 | 101 | 95.16 | *** |
| Snake Pit / The Beehive | Dense Aggregate | PL15-A3 | 2 | 245 | 239.06 | *** |
| Snake Pit / The Beehive | Dense Aggregate | PL19-A4&5 | 7 | 219 | 198.87 | *** |
| Snake Pit / The Moose | Dense Aggregate | PL14-A3 | 0 | 314 | 314 | *** |
| Snake Pit / The Moose | Dense Aggregate | PL16-A5 | 21 | 34 | 3.07 | NS |
| Snake Pit / The Moose | Dense Aggregate | PL18-A1&2 | 36 | 79 | 39.72 | *** |
| Snake Pit / The Moose | Dense Aggregate | PL20-P1 | 23 | 90 | 16.08 | *** |
| Snake Pit / The Nail | Dense Aggregate | PL20-A1 | 1 | 121 | 118.03 | *** |
| Snake Pit / The Nail | Dense Aggregate | PL20-A2 | 0 | 69 | 69 | *** |
| ***R. chacei*** | | | | | | |
| TAG | Hidden Aggregate | PL08-A2 | 11 | 5 | 2.25 | NS |
| Snake Pit / The Moose | Hidden Aggregate | PL14-A1 | 7 | 40 | 23.17 | *** |
| ***M. fortunata*** | | | | | | |
| Snake Pit / The Nail | Periphery - Mirocaris | PL20-A3&4&5 | 28 | 83 | 27.25 | *** |

**Table 8.** Proportions of reproductively active alvinocaridid females from the different assemblages (**RF:** reproductive females including ovigerous females and females with developed gonads; **NRF:** non-reproductive females).

For both *R. exoculata* and *R. chacei*, these 'vicinity of aggregate' samples exhibited proportions of immature individuals in agreement with the general tendency of their global populations, with a significant dominance of adults for *R. exoculata* ($\chi^2$ = 12.46 – 16.67, $p < 0.05$) and a significant

dominance of immature individuals for *R. chacei* ($\chi^2$ = 29.8 – 105.95, p < 0.05), (**Table 7.**). In one case at TAG however, proportions of adults and immatures were rather similar for the two species (*R. exoculata*: $\chi^2$ = 0.428, p < 0.05; *R. chacei*: $\chi^2$ = 1.92, p < 0.05), (**Table 7.**). *R. exoculata* sex ratios did not significantly deviated from 1:1 in general ($\chi^2$ = 2.91– 3, p > 0.05), except in one sample exhibiting a strongly female biased sex ratio ($\chi^2$ = 117.36, p < 0.05), (**Table 7.**). *R. chacei* adult numbers were too limited to estimate their sex ratio in these assemblages, except in one case were all adults were females only. Like the nurseries of *R. exoculata* from Snake Pit, these assemblages from TAG were associated with the peltospirid snails, *P. smaragdina*.

The last assemblage was only observed at Snake Pit around the Nail edifice and consisted of the three alvinocaridid species, but was dominated by *M. fortunata*, which accounted for51.9% of the alvinocaridids of the sample ($\chi^2$ = 66.27, p < 0.05). *R. exoculata* and *R. chacei* accounted respectively for 19.2% and 21.9% of the alvinocaridids (**Fig 64C.**, **Fig 66.A.**). This assemblage resembles strongly to the peripheral assemblages, although active diffuse emissions could be observed around the shrimps. *In situ*, it is also located close to the 'vicinity of dense aggregates' assemblages, but differed from them by its position, clearly separated from the dense aggregates assemblages of the Nail. For both *R. exoculata* and *R. chacei*, proportions of immature individuals were only slightly lower than the proportions of adults (*R. exoculata*: $\chi^2$ = 3.93, p < 0.05; *R. chacei*: $\chi^2$ = 4.59, p < 0.05), (**Table 7.**). Moreover, their sex ratio did not significantly deviated from 1:1 or only slightly towards females for *R. chacei* (*R. exoculata*: $\chi^2$ = 0, p > 0.05; *R. chacei*: $\chi^2$ = 4.5, p < 0.05), (**Table 7.**). *M. fortunata* was mostly represented by adults in this assemblage (97% of all *M. fortunata*; $\chi^2$ = 112.76, p > 0.05), with a strongly female biased sex ratio ($\chi^2$ = 71.06, p > 0.05), (**Table 7.**). This assemblage was also the one where most reproductively active females of *M. fortunata* were collected – 28 out of the 31 collected at Snake Pit – representing 25% of all the females from this assemblage (**Table 8.**).

### 3.1.3.3 Thermal niches of alvinocaridid shrimps and their life stages from TAG & Snake Pit

Average temperatures around alvinocaridid assemblages were comprised between 3.4°C and 22.5°C, with maximum peaks of temperature reaching up to 38.1°C punctually, and minimum ones down to 3.1°C (**Table 9.**). Standard deviations that can be considered as the thermal variability around the assemblages varied from 0.3°C to 7.6°C. As the minimal temperatures were strongly correlated with the average temperatures ($r^2$=0.98, p, < 0.05), only Avg.T, Std.T and Max.T were used in PCA-shrimp, PCA-Rexoculata and PCA-Rchacei. All the three variables were very well represented in the PCA (∑cos2 = 0.99, 0.99 and 0.98 for Avg.T, Std.T and Max.T respectively) and were strongly correlated with the first axis especially for the Max.T (85%, 84.5% and 98% for Avg.T, Std.T and Max.T respectively) but less with the second axis (15% and 14.5% for Avg.T and Std.T respectively). Avg.T, Std.T and Max.T almost contributed equally to the construction of the first axis (contribution = 31.8%, 31.6% and 36.7% respectively). Similarly, Avg.T and Std.T also contributed equally to the construction of the first axis (contribution = 49.1% and 50.8% respectively).

The PCA-shrimps of the different alvinocaridid shrimp species explained only 36% of the variance with 35.5% on the first axis (**Fig 67**.). As depicted by the PCA-shrimp, each alvinocaridid species occupied a different thermal niche that changed in overall position and in breadth (**Fig 67A.**). Both *R. chacei* and *M. fortunata* were mostly restricted on the left side of the niche plot with lower maximum and mean temperatures compared to *R. exoculata* (**Table 9.**) that was situated on both side

of the niche plot (**Fig 67A.**). Mean position along the first axis was closer to warmer habitats for *R. exoculata* in comparison to *R. chacei*, and for *R. chacei* in comparison to *M. fortunata* (**Fig 67B.**). Similarly, standard deviation was wider for *R. exoculata* in comparison to *R. chacei* and for *R. chacei* in comparison to *M. fortunata* as well (**Fig 67B.**). Tolerance, i.e. the niche breath, was comprised between 85.4% and 11% of the total inertia with *R. exoculata* having the largest niche breath and *M. fortunata* the lowest.

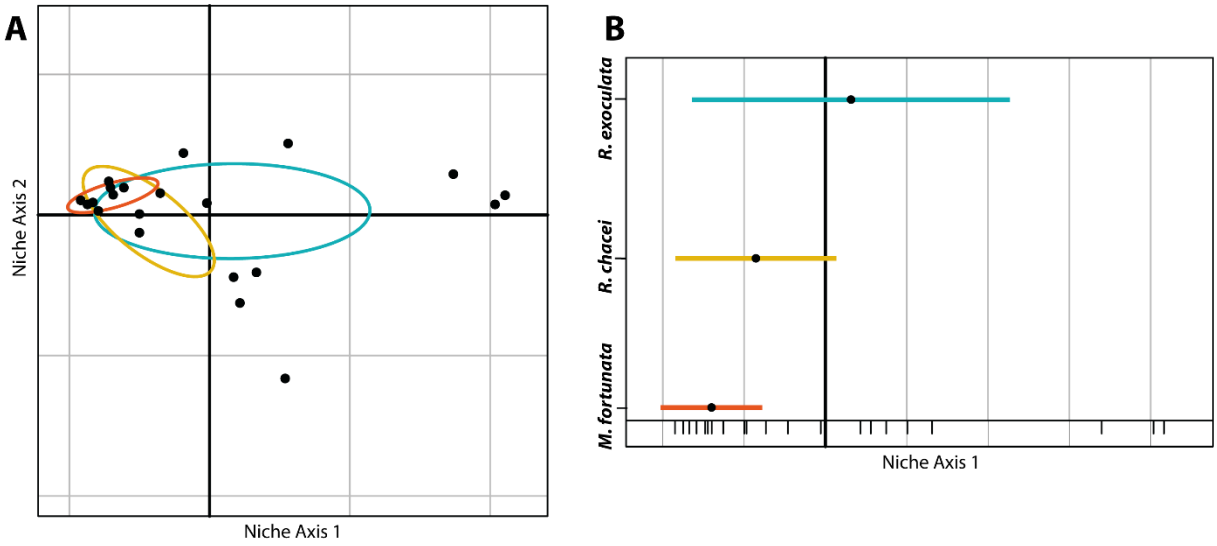


**Fig 68.** Thermal niches of alvinocaridid species **A.** OMI analysis two-dimensional plot. **B.** Mean position of the different alvinocaridid species + k standard deviation along the first axis of the niche analysis. Red: *Mirocaris fortunata*, Yellow: *Rimicaris chacei*, Blue: *Rimicaris exoculata.*

| | Average temperatures (°C) | | | Thermal range (°C) | | OMI analysis | | | | | | | Permutation test |
|---|---|---|---|---|---|---|---|---|---|---|---|---|---|
| | mean | min | max | min | max | inertia | OMI | Tol | Rtol | *omi* | *tol* | *rtol* | *p.value* |
| **Niche of Alvinocaridids species** | | | | | | | | | | | | | |
| ***Rimicaris exoculata*** | 11.3 | 3.4 | 22.5 | 3.1 | 38.1 | 3.22 | 0.07 | 2.75 | 0.40 | 2.1 | 85.4 | 12.4 | 0.0669 |
| ***Rimicaris chacei*** | 4.5 | 3.4 | 14.5 | 3.1 | 25.2 | 2.03 | 0.55 | 1.01 | 0.48 | 26.9 | 49.6 | 23.5 | 0.0529 |
| ***Mirocaris fortunata*** | 4.6 | 3.4 | 14.5 | 3.1 | 25.2 | 2.14 | 1.83 | 0.23 | 0.07 | 85.7 | 11,0 | 3.3 | 0.0729 |
| **Niche of *Rimicaris exoculata* life stage** | | | | | | | | | | | | | |
| **Ovigerous Female** | 12.3 | 4.4 | 20.3 | 3.7 | 38.1 | 2.72 | 0.24 | 2.28 | 0.20 | 8.9 | 83.8 | 7.3 | 0.3147 |
| **Females with dev. Gonads** | 10.4 | 4.4 | 22.5 | 3.7 | 33 | 3.01 | 0.68 | 2.01 | 0.32 | 22.8 | 66.7 | 10.6 | 0.2717 |
| **Non Reproductive Female** | 12.7 | 3.4 | 22.5 | 3.1 | 38.1 | 3.47 | 0.29 | 2.83 | 0.35 | 8.4 | 81.5 | 10.1 | 0.0110* |
| **Male** | 10 | 3.4 | 22.5 | 3.1 | 38.1 | 3.24 | 0.05 | 2.78 | 0.40 | 1.6 | 85.9 | 12.5 | 0.2827 |
| **Subadults** | 13.5 | 3.4 | 22.5 | 3.2 | 38.1 | 4.05 | 0.52 | 3.06 | 0.46 | 13,0 | 75.7 | 11.4 | 0.0260* |
| **Stage B juvenile** | 10.7 | 3.4 | 22.5 | 3.2 | 38.1 | 3.69 | 0.20 | 2.9 | 0.59 | 5.3 | 78.8 | 15.9 | 0.1678 |
| **Stage A juvenile** | 5.9 | 3.4 | 22.5 | 3.1 | 38.1 | 2.6 | 0.02 | 2.13 | 0.45 | 0.8 | 81.8 | 17.4 | 0.6893 |
| **Niche of *Rimicaris chacei* life stage** | | | | | | | | | | | | | |
| **Ovigerous Female** | 5.4 | 4.9 | 7.1 | 3.9 | 9.6 | 1.0 | 0.72 | 0.25 | 0.03 | 72.2 | 24.8 | 2.9 | 0.4945 |
| **Non Reproductive Female** | 5.3 | 3.6 | 14.5 | 3.3 | 25.2 | 1.64 | 0.47 | 0.89 | 0.28 | 28.5 | 54.4 | 17.1 | 0.1658 |
| **Male** | 5 | 3.4 | 8.2 | 3.1 | 20.7 | 1.48 | 0.99 | 0.44 | 0.05 | 67.1 | 29.8 | 3.1 | 0.1039 |
| **Subadults** | 4.8 | 3.4 | 14.5 | 3.1 | 25.2 | 2.26 | 0.72 | 1.10 | 0.44 | 31.7 | 48.8 | 19.5 | 0.1309 |
| **Stage A juvenile** | 4.1 | 3.4 | 8.2 | 3.1 | 25.2 | 2.71 | 0.78 | 1.02 | 0.91 | 28.7 | 37.7 | 33.6 | 0.1828 |

**Table 9.** Thermal range and parameters of the OMI analysis for the different alvinocaridid species and their life stages. *slightly significant.

Marginality (OMI index) was extremely low for *R. exoculata* representing only 2.1% of the total inertia which means that the thermal conditions, in which this species was found, were similar to the average conditions measured among all samples (the center of the PCA); (**Table 9.**). On the other hand, *R. chacei* and *M. fortunata* showed preference for more marginal habitats, especially for *M. fortunata* that exhibited the highest values between the three species (85.7% of the total inertia), whereas intermediate values between the two were found for *R. chacei* (26.9% of the total inertia); (**Table 9.**). However, permutation tests did not gave any significant *p* values for the different alvinocaridid species indicating that none of these species appear to select their habitat based on temperature (or related factors).

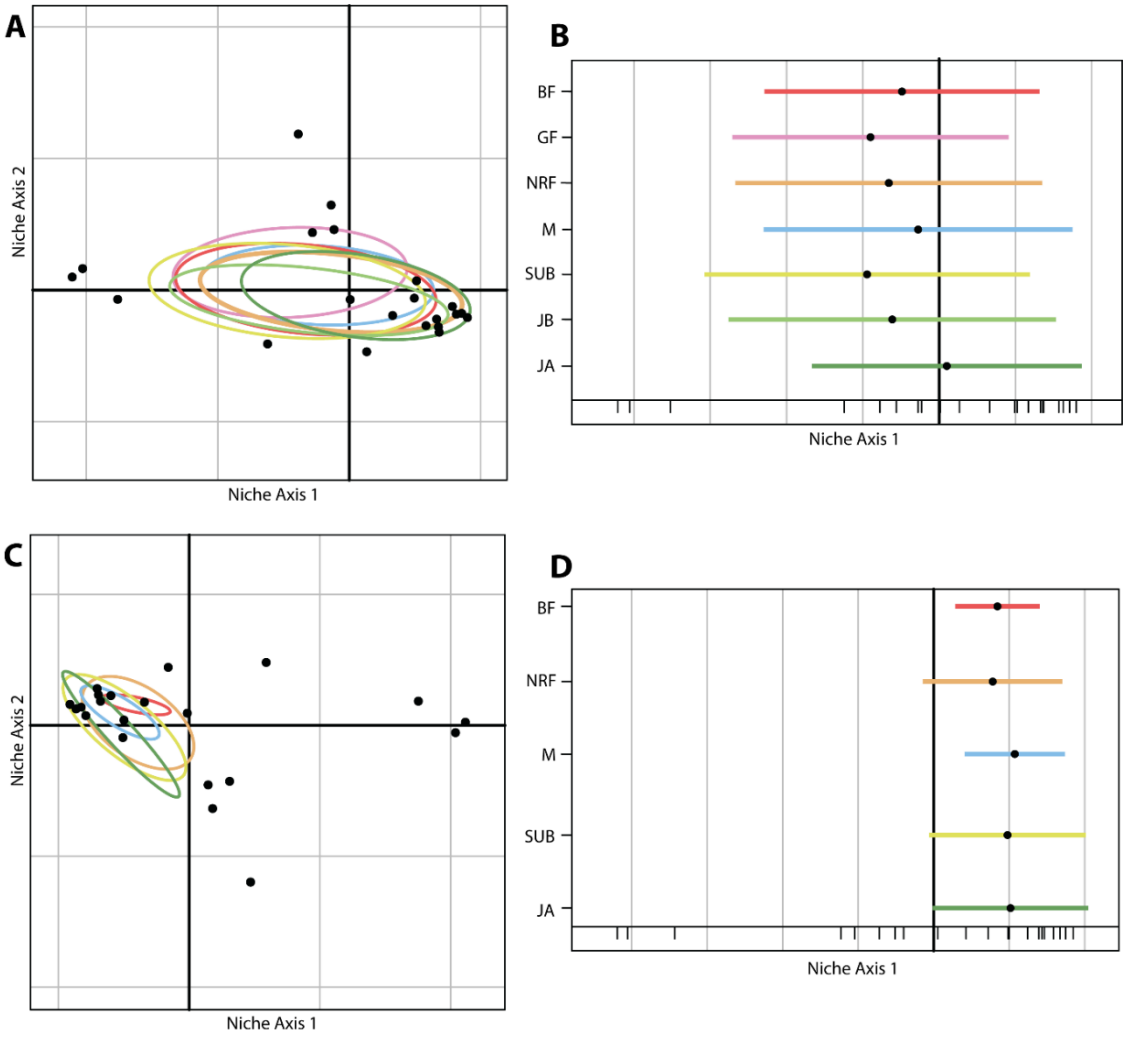


**Fig 69.** Thermal niches of *R. exoculata* and *R. chacei* life stages. **A.** OMI analysis of *R. exoculata* life stages in two-dimensional plot. **B.** Mean position of the different *R. exoculata* life stages + k standard deviation along the first axis of the niche analysis. **C.** OMI analysis of *R. chacei* life stages in two-dimensional plot. **D.** Mean position of the different *R. chacei* life stages + k standard deviation along the first axis of the niche analysis. Red: ovigerous females, Pink: Females with developed gonads, Orange: Non-reproductive females, Blue: males, Yellow: subadults, Light green: stage B juveniles; Dark green: stage A juveniles.

PCA-Rexoculata and PCA-Rchacei of the different life stages of *R. exoculata* and *R. chacei* explained 23.5% and 72.5% of the variance for *R. exoculata* and *R. chacei* respectively, with respectively 23% and 71.5% on the first axis (**Fig 68.**). As depicted by these two PCA, each life stages of *R. exoculata* and each life stages of *R. chacei* occupied rather similar thermal niches, with limited changes in their overall position and few variations of their breath (Fig **68A.** and **68B.**). Indeed all life stages of *R. chacei* were restricted to the left side of the niche plot and all life stages of *R. exoculata* were situated on both side of the niche plot (**Fig 68A.** and **68B.**). Moreover, overlaps between the niches of different life stages of *R. exoculata* or between those of the different life stages of *R. chacei* were very important, no life stages having a completely distinct thermal niche than the others for both species (**Fig 68.**). Mean position along the first axis were more far from the warmer habitats for stage A juveniles and males of *R. exoculata* compared to its other stages that all exhibited a similar position, although slightly closer to the warmer habitats for subadults and females with developed gonads (**Fig 68C.**).

Position along the first axis were approximately similar between all life stages of *R. chacei*, except for the non-reproductive females that were slightly farer from the warmer habitats (Fig 68D). Residual tolerance ranged from 7.3% to 17.4% of total inertia for *R. exoculata* and from 2.9% to 33.6% for *R. chacei*; thus the variables used to describe the niches, at each sampling site explained 82.6% to 92.7% of niche distribution of *R. exoculata* and 66.4% to 97.1% of niche distribution of *R. chacei* (**Table 9.**). Tolerance of *R. exoculata* life stages was comprised between 66.7% and 85.9% of the total inertia, with slightly smaller niche breath for stage A juveniles and the different reproductive female stages compared to the other life stages (**Table 9.**). Similarly, tolerance of *R. chacei* life stages was comprised between 24.8% and 54.4% of the total inertia, with clearly smaller niche breath for ovigerous females and to a lower extent for the males as well (**Table 9.**).

Marginality of *R. exoculata* life stages was extremely low for stage A juveniles and males, slightly higher for stage B juveniles, non-reproductive females and ovigerous females, and even higher for subadults and females with developed gonads, although they all remained comprised between 0.02 and 0.68, representing between 0.8% and 22.8% of the total inertia (**Table 9.**). Marginality of *R. chacei* life stages were all rather similar ranging from 28.5% to 72.2% (**Table 9.**). Again, permutation tests did not give any significant *p* values for the different life stages of *R. chacei* indicating that none of them appears to select their habitat based on temperature. For most of *R. exoculata* life stages, permutation tests gave similar results as well. Still, they gave significant *p* values for two of them: the non-reproductive females and the subadults.

## 3.1.4 Directions for future discussion

Our results confirmed the general bias in the sex ratios, with significantly higher proportions of females in *R. exoculata* populations from TAG and Snake Pit, like in 2014. Sex ratios of the two other alvinocaridid species were also biased towards females, although this bias was more limited for *R. chacei*. Reproductively active females of each alvinocaridid species were quite abundant, representing between 6.6% and 24.5% – respectively for *R. exoculata* from Snake Pit and *R. chacei* from TAG– of all the females collected depending on the species. These reproductive females were mostly distributed within the type of assemblages where their species were the dominant alvinocaridid.

## 3.1 POPULATION STRUCTURE AND THERMAL NICHES OF ALVINOCARIDIDS FROM THE MID ATLANTIC RIDGE

Analysis of the population structure of the three co-occurring alvinocaridid species revealed distinct dynamics of recruitment between each of them. Between three and four cohorts were found for *R. exoculata* and *R. chacei* but only two for *M. fortunata* with a large majority in a single cohort. This suggests a continuous or semi-continuous recruitment for *M. fortunata* and a discontinuous recruitment for the two others. Additionally most of the collected individuals were at an immature stage for *R. chacei* whereas the majority were at adult stages for *R. exoculata*. With the shape of their size-class distribution, it appears that post-settlement survival differs between the two species with a higher mortality for *R. chacei* juveniles, especially at TAG. Potentially, these differences could be related to a higher predator pressure on *R. chacei* juvenile and subadult stages, which are more accessible to them than *R. exoculata* ones, as observed several times in 2014 and 2018 with macrourid fishes feeding within the *R. chacei* nursery.

Interestingly these dynamics of recruitment diverged between the different edifices of Snake Pit, in a similar way for the three alvinocaridid species. A higher proportion of immature individuals was always observed at the Beehive whereas adult stages were much more abundant at the Moose, with an intermediate position between the two edifices for the shrimps from the Nail edifice.

Seven types of alvinocaridid assemblages were identified in our samples at both vent fields for four of them, the three other being only retrieved at one location and so were potentially specific to either TAG or Snake Pit. The '*R. chacei* nurseries' sampled only at TAG in 2014 (Hernández-Ávila, 2016), were retrieved in both vent fields in 2018. Two assemblages, the 'dense aggregate' and the 'nursery of *R. exoculata*', were largely dominated by *R. exoculata* with only few individuals of the other species. Two other assemblages, the 'hidden aggregates' and 'the nursery of *R. chacei*' were clearly dominated by *R. chacei*. On the other hand, the three last assemblages, the 'periphery' assemblage the 'vicinity of dense aggregates' assemblage and the *Mirocaris* assemblage all exhibited relatively mixed proportions of the two species.

An important segregation in the distribution of the different life stages of *R. exoculata* could be clearly observed between the different types of alvinocaridid assemblages. Dense aggregates of *R. exoculata* were mostly composed of the different reproductive female stages with some subadults and juvenile individuals. On the other hand, scattered *R. exoculata* shrimps distributed at the periphery were mostly composed of male individuals in both vent fields. This segregation between sexes was not observed for *R. chacei*. However, adults were clearly living mostly in different assemblages, the hidden aggregates, than their juvenile and subadult stages found in a large majority in the nursery assemblages. Interestingly, mixed population of both *R. chacei* and *R. exoculata* were only found in the more scattered assemblages whereas assemblages dominated by one of the two species were much denser.

Thermal niche of *R. exoculata* was clearly larger and almost entirely overlapped the niches of *R. chacei* or of *M. fortunata*. This confirms that this species is not restricted to some part of the environmental gradient but occupies most of the available thermal niches in its environment, with temperatures between 3.1°C and 38.1°C. These conditions do not exceed the upper thermal tolerance threshold (CTmax) of this species that was experimentally estimated at 38°C - its $CT_{max}$, i.e. the critical thermal maximum – for long duration exposure (1 hour), and above 38°C for shorter exposure (10 min) (Ravaux et al., 2019). *R. chacei* and *M. fortunata* are restricted to cooler parts of the thermal gradient between 3.1°C and 25.2°C for both of them. Unfortunately, *R. chacei* thermal physiology has not been

examined experimentally yet. The thermal range observed here for *M. fortunata* is much lower than its thermal upper limit, experimentally estimated to be around 36°C (Shillito et al., 2006). The narrower niches of *R. chacei* and *M. fortunata* could result from a competition for space with *R. exoculata* that restricts their thermal niches to cooler temperatures, although they would be physiologically able to cope with higher temperatures. However, thermal niches of *M. fortunata* from Lucky Strike, where no competition could exist with *R. exoculata* that is absent from this vent field, were not very different from the ones we found in our study, with an even narrower thermal range between 3.7°C and 14.2° (Husson et al., 2017). Therefore, the hypothesis of a competitive exclusion of *M. fortunata* in higher temperature habitats would not be supported. This thermal preference apparently lower than its thermal tolerance abilities, as observed in many other vent species (Bates et al., 2010), might simply indicate that thermal conditions are not sufficient to explain the distribution of *M. fortunata* in our assemblages.

Thermal niches of the different life stages of both *R. exoculata* and *R. chacei* were greatly overlapping between each other's with no clear tendency for the small variations of the niche center position. Thermal range were mostly similar between all the life stages of *R. exoculata* and between all life stages of *R. chacei*. Moreover, thermal conditions were clearly insufficient to explain the distribution of all these life stages, except *R. exoculata* non-reproductive females and subadults. Other environmental factors, including concentrations of reduced compounds fueling symbiotic bacteria of the shrimps, are explored in the perspective of this thesis work to explain the structuration of their populations between the different types of assemblages.

Although temporal variations analyses have not been presented here, it already appears with the raw data (**Table S5.**), that some assemblages can remain extremely stable on short temporal scales (such as between PL15-A1 and PL19-A3 (7 days)); (**Table S5.**). They can also change drastically such as in the example of a sample collected in a dense aggregate of *R. exoculata* (**Fig 64G.**) that had disappeared 10 days later, replaced by an aggregate of *R. chacei* hidden between rocks (**Fig 64H.**); (**Table S5.**).

## 3.1.5 Supplementary materials

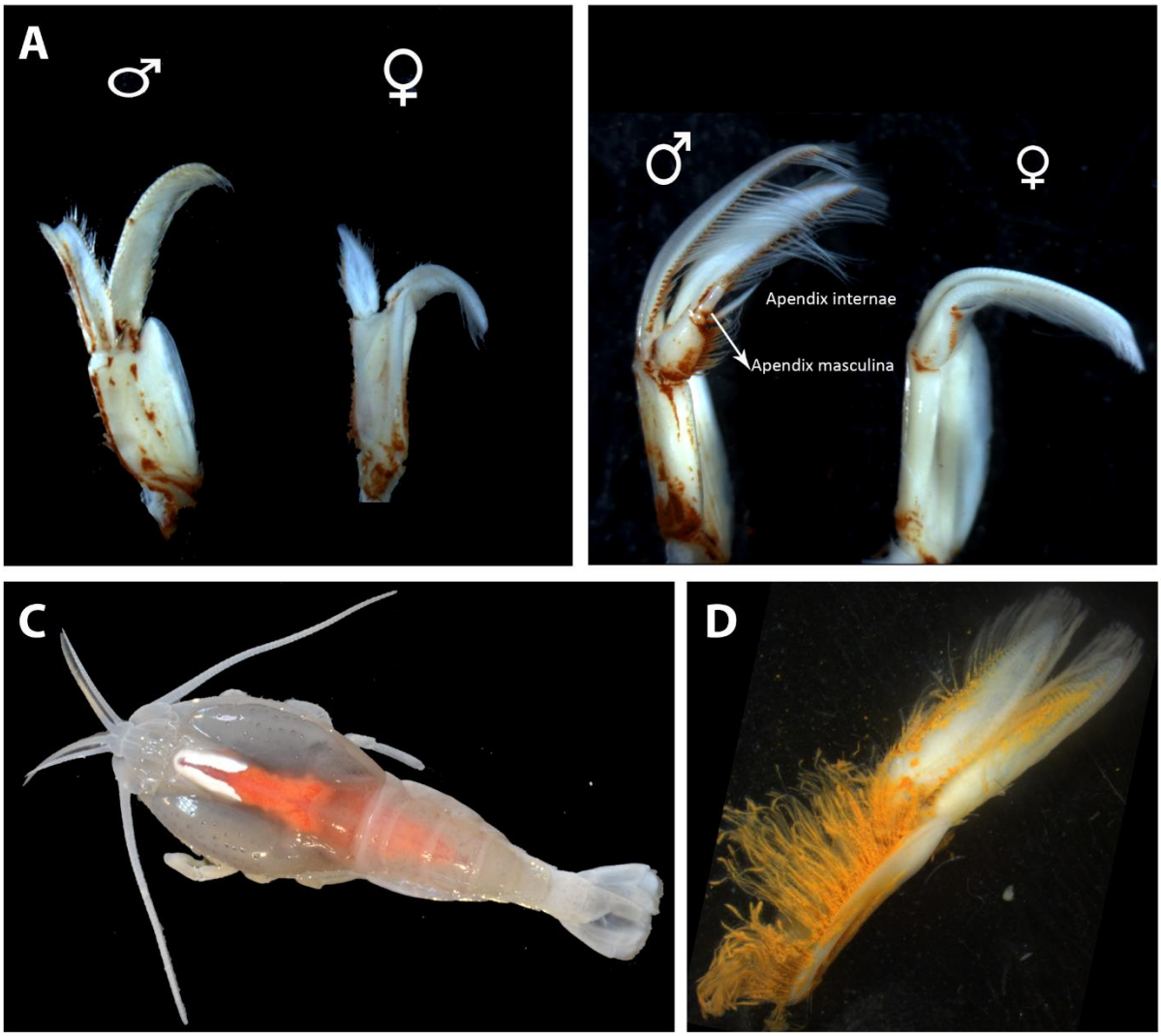


**Fig S3.** Identification of sex and reproductively active females in alvinocaridids. **A.** Morphologies of the first pleopods of males and females for *R. exoculata*. **B.** Morphologies of the second pleopods of males and females for *R. exoculata*. **C.** *R. exoculata* with developed gonads under its cephalothorax and abdomen (in pink). **D.** Morphologies of the modified second to fourth pleopods of ovigerous females for *R. exoculata*.

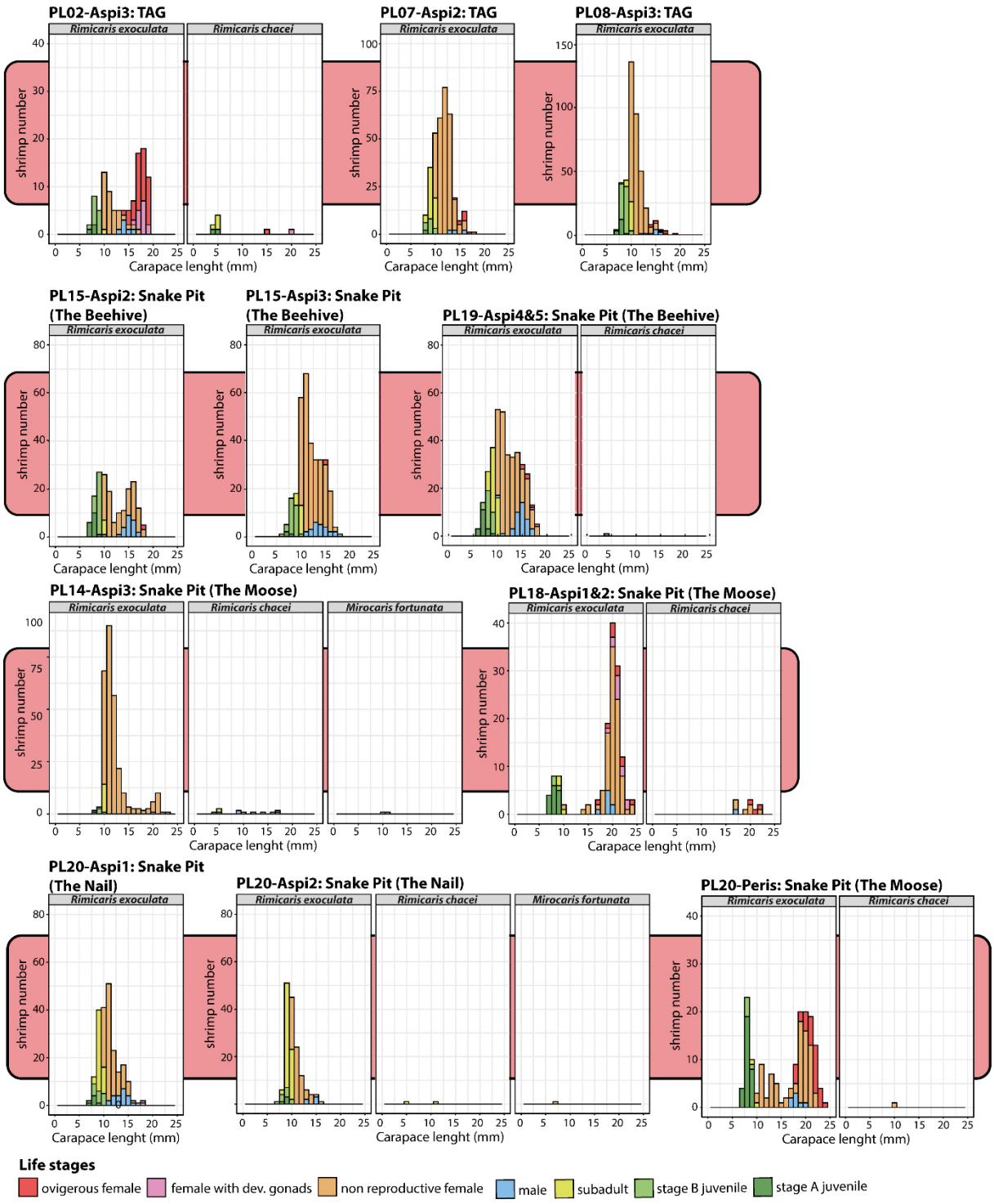


**Fig S4.** Additional size class histograms of the different dense aggregate assemblages collected for this study.

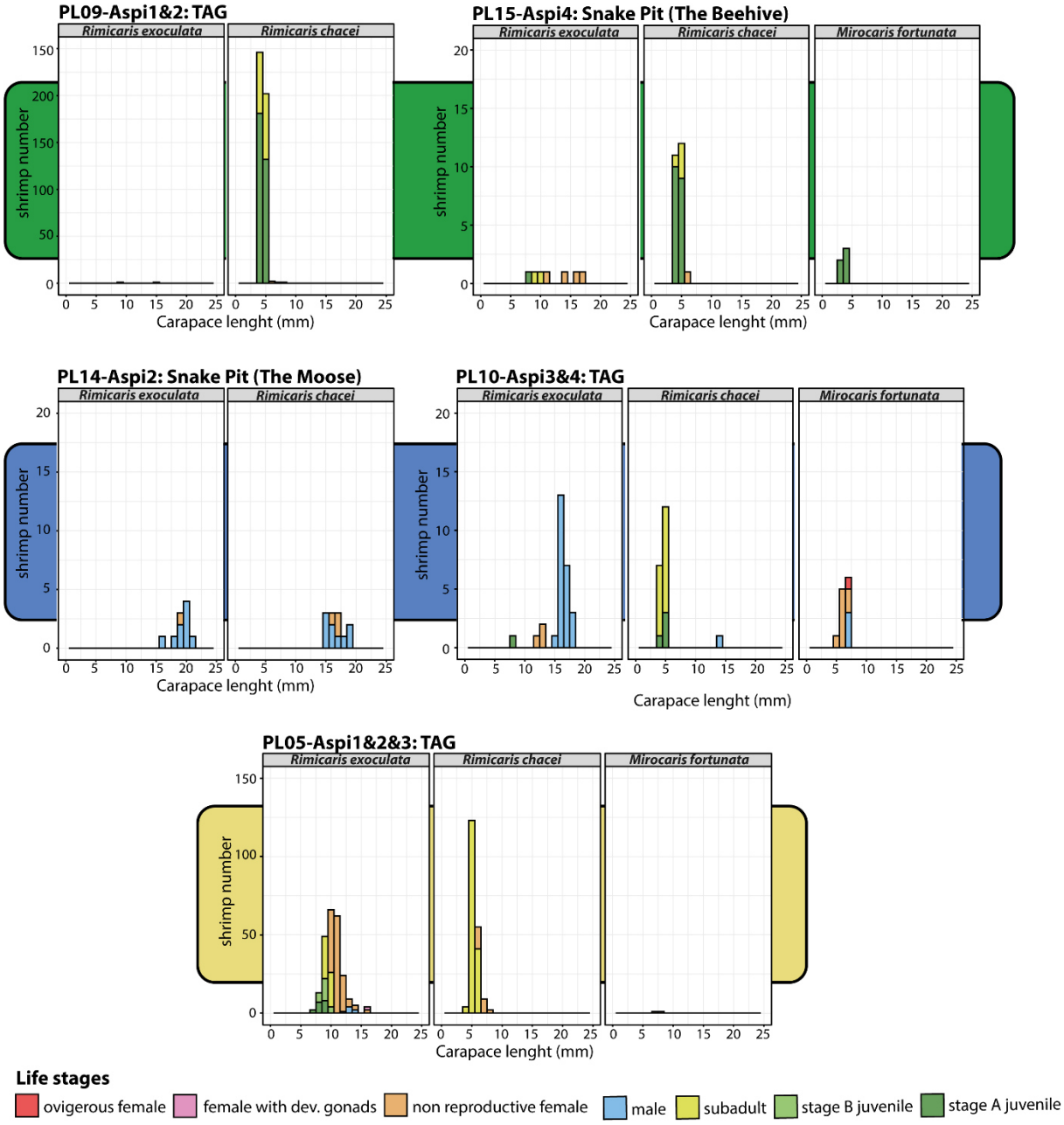


**Fig S5.** Additional size class histograms of the different assemblage types collected for this study. **Green:** R. chacei nurseries; **Blue:** Peripheral assemblages of scattered alvinocaridid individuals; **Yellow:** Scattered alvinocaridid assemblages at the vicinity of the dense aggregates of *R. exoculata*

| Vent Field / Edifice | Assemblage Type | Sample ID | Avg.T (°C) | Std.T (°C) | Min.T (°C) | Max.T (°C) |
|---|---|---|---|---|---|---|
| TAG | Dense Aggregate | PL02_A1 | 8.5 | 4.8 | 3.7 | 20.4 |
| TAG | Dense Aggregate | PL06_A1 | 20.1 | 4.6 | 11.0 | 33.0 |
| TAG | Dense Aggregate | PL08_A3 | 9.4 | 4.5 | 5.0 | 19.8 |
| TAG | Hidden Aggregate | PL08_A2 | 4.9 | 0.7 | 4.5 | 6.9 |
| TAG | Periphery | PL10_A3_4 | 3.4 | 0.3 | 3.1 | 4.1 |
| TAG | *R. chacei* nursery | PL02_A2 | 4.8 | 0.3 | 4.2 | 5.4 |
| TAG | *R. chacei* nursery | PL09_A1_2 | 3.8 | 0.5 | 3.3 | 5.3 |
| TAG | Vicinity of Aggregates | PL10_A1_2 | 8.2 | 3.9 | 4.2 | 20.7 |
| Snake Pit / The Beehive | Dense Aggregate | PL15_A2 | 7.7 | 0.8 | 6.7 | 10.1 |
| Snake Pit / The Beehive | Dense Aggregate | PL15_A3 | 20.3 | 5.9 | 11.4 | 38.1 |
| Snake Pit / The Moose | Dense Aggregate | PL16_A5 | 6.0 | 1.5 | 3.9 | 8.4 |
| Snake Pit / The Moose | Dense Aggregate | PL18_A1_2 | 9.7 | 2.1 | 5.3 | 13.1 |
| Snake Pit / The Beehive | Dense Aggregate | PL19_A4_5 | 7.0 | 1.3 | 4.9 | 9.5 |
| Snake Pit / The Nail | Dense Aggregate | PL20_A1 | 22.5 | 6.9 | 12.1 | 30.7 |
| Snake Pit / The Nail | Dense Aggregate | PL20_A2 | 14.5 | 1.5 | 8.1 | 19.0 |
| Snake Pit / The Beehive | Periphery | PL19_A1_2 | 3.6 | 0.8 | 3.3 | 6.1 |
| Snake Pit / The Nail | Periphery - *Mirocaris* | PL20_A3_4_5 | 4.4 | 0.5 | 4.2 | 5.9 |
| Snake Pit / The Beehive | *R. chacei* nursery | PL15_A4 | 7.8 | 7.6 | 3.4 | 25.2 |
| Snake Pit / The Beehive | *R. exoculata* nursery | PL15_A1 | 3.4 | 0.5 | 3.2 | 4.9 |
| Snake Pit / The Beehive | *R. exoculata* nursery | PL19_A3 | 4.8 | 0.6 | 3.9 | 6.6 |

**Table S3**. Detailed thermal conditions of each assemblage samples with its environmental conditions.

| Assemblage Type | Sample ID | *Rimicaris exoculata* | | | | | | | | | | | | *Rimicaris chacei* | | | | | | | | | | | *Mirocaris fortunata* | | | | | | |
|---|---|---|---|---|---|---|---|---|---|---|---|---|---|---|---|---|---|---|---|---|---|---|---|---|---|---|---|---|---|---|---|
| | | OF | GF | RF | NRF | Ftot | M | Sub | St. B | St. A | Imm | Ad | n | OF | GF | RF | NRF | M | Ftot | Sub | St. A | Imm | Ad | n | OF | NRF | M | AllF | Imm | Ad | n |
| Dense Aggregate | PL02-A1 | 12 | 25 | 37 | 13 | 50 | 42 | 3 | 0 | 14 | 17 | 92 | 109 | 0 | 0 | 0 | 1 | 0 | 1 | 0 | 0 | 0 | 1 | 1 | 0 | 0 | 0 | 0 | 0 | 0 | 0 |
| Dense Aggregate | PL02-A3 | 41 | 14 | 55 | 34 | 89 | 6 | 1 | 12 | 3 | 16 | 95 | 111 | 1 | 1 | 2 | 0 | 0 | 2 | 4 | 2 | 6 | 2 | 8 | 0 | 0 | 0 | 0 | 0 | 0 | 0 |
| Dense Aggregate | PL06-A1 | 40 | 9 | 49 | 111 | 160 | 15 | 17 | 28 | 3 | 48 | 175 | 223 | 0 | 0 | 0 | 0 | 0 | 0 | 0 | 0 | 0 | 0 | 0 | 0 | 0 | 0 | 0 | 0 | 0 | 0 |
| Dense Aggregate | PL07-A2 | 9 | 0 | 9 | 260 | 269 | 6 | 47 | 15 | 2 | 64 | 275 | 339 | 0 | 0 | 0 | 0 | 0 | 0 | 0 | 0 | 0 | 0 | 0 | 0 | 0 | 0 | 0 | 0 | 0 | 0 |
| Dense Aggregate | PL08-A3 | 8 | 0 | 8 | 286 | 294 | 9 | 29 | 69 | 16 | 114 | 303 | 417 | 0 | 0 | 0 | 0 | 0 | 0 | 0 | 0 | 0 | 0 | 0 | 0 | 0 | 0 | 0 | 0 | 0 | 0 |
| Hidden Aggregate | PL08-A2 | 3 | 0 | 3 | 3 | 6 | 1 | 1 | 1 | 0 | 2 | 7 | 9 | 11 | 0 | 11 | 5 | 16 | 16 | 0 | 0 | 0 | 32 | 32 | 0 | 1 | 0 | 1 | 0 | 1 | 1 |
| *R. chacei* Nursery | PL02-A2 | 0 | 0 | 0 | 0 | 0 | 0 | 1 | 0 | 0 | 1 | 0 | 1 | 0 | 0 | 0 | 0 | 0 | 0 | 80 | 44 | 124 | 0 | 124 | 0 | 0 | 0 | 0 | 0 | 0 | 0 |
| *R. chacei* Nursery | PL09-A1&2 | 0 | 0 | 0 | 0 | 0 | 1 | 0 | 0 | 1 | 1 | 1 | 2 | 0 | 0 | 0 | 4 | 0 | 4 | 135 | 313 | 448 | 4 | 452 | 0 | 0 | 0 | 0 | 0 | 0 | 0 |
| Periphery | PL09-A3 | 1 | 0 | 1 | 0 | 1 | 14 | 0 | 0 | 0 | 0 | 15 | 15 | 0 | 0 | 0 | 0 | 0 | 0 | 0 | 0 | 0 | 0 | 0 | 0 | 0 | 0 | 0 | 0 | 0 | 0 |
| Periphery | PL10-A3&4 | 0 | 0 | 0 | 3 | 3 | 24 | 0 | 0 | 1 | 1 | 27 | 28 | 0 | 0 | 0 | 0 | 1 | 0 | 15 | 4 | 19 | 1 | 20 | 0 | 8 | 3 | 8 | 0 | 11 | 11 |
| Vicinity of Aggregates | PL05-A1&2&3 | 0 | 2 | 2 | 135 | 137 | 7 | 49 | 24 | 17 | 90 | 144 | 234 | 0 | 0 | 0 | 25 | 0 | 25 | 168 | 0 | 168 | 25 | 193 | 0 | 2 | 0 | 2 | 0 | 2 | 2 |
| Vicinity of Aggregates | PL08-A1 | 0 | 0 | 0 | 9 | 9 | 3 | 6 | 3 | 0 | 9 | 12 | 21 | 0 | 0 | 0 | 4 | 0 | 4 | 9 | 0 | 9 | 4 | 13 | 1 | 0 | 0 | 1 | 0 | 1 | 1 |
| Vicinity of Aggregates | PL10-A1&2 | 0 | 0 | 0 | 15 | 15 | 7 | 1 | 1 | 0 | 2 | 22 | 24 | 0 | 0 | 0 | 1 | 2 | 1 | 37 | 1 | 38 | 3 | 41 | 4 | 1 | 0 | 0 | 0 | 0 | 0 |
| Dense Aggregate | PL15-A2 | 2 | 0 | 2 | 101 | 103 | 23 | 6 | 34 | 19 | 59 | 126 | 185 | 0 | 0 | 0 | 0 | 0 | 0 | 0 | 0 | 0 | 0 | 0 | 0 | 0 | 0 | 0 | 0 | 0 | 0 |
| Dense Aggregate | PL15-A3 | 2 | 0 | 2 | 245 | 247 | 25 | 17 | 34 | 3 | 54 | 272 | 326 | 0 | 0 | 0 | 0 | 0 | 0 | 0 | 0 | 0 | 0 | 0 | 0 | 0 | 0 | 0 | 0 | 0 | 0 |
| Dense Aggregate | PL19-A4&5 | 6 | 1 | 7 | 219 | 226 | 39 | 51 | 28 | 18 | 97 | 265 | 362 | 0 | 0 | 0 | 0 | 0 | 0 | 0 | 1 | 1 | 0 | 1 | 0 | 0 | 0 | 0 | 0 | 0 | 0 |
| Dense Aggregate | PL14-A3 | 0 | 0 | 0 | 314 | 314 | 1 | 17 | 5 | 1 | 23 | 315 | 338 | 0 | 0 | 0 | 2 | 6 | 2 | 2 | 2 | 4 | 8 | 12 | 0 | 2 | 0 | 2 | 0 | 2 | 2 |
| Dense Aggregate | PL16-A5 | 20 | 1 | 21 | 34 | 55 | 10 | 0 | 0 | 4 | 4 | 65 | 69 | 1 | 1 | 2 | 2 | 4 | 4 | 0 | 0 | 0 | 8 | 8 | 0 | 0 | 0 | 0 | 0 | 0 | 0 |
| Dense Aggregate | PL18-A1&2 | 34 | 2 | 36 | 79 | 115 | 7 | 2 | 5 | 31 | 38 | 122 | 160 | 0 | 0 | 0 | 1 | 0 | 1 | 0 | 0 | 0 | 1 | 8 | 0 | 0 | 0 | 0 | 0 | 0 | 0 |
| Dense Aggregate | PL20-P1 | 11 | 12 | 23 | 90 | 113 | 8 | 3 | 3 | 15 | 21 | 121 | 142 | 3 | 0 | 3 | 6 | 1 | 9 | 0 | 0 | 0 | 10 | 10 | 0 | 0 | 0 | 0 | 0 | 0 | 0 |
| Dense Aggregate | PL20-A1 | 0 | 1 | 1 | 121 | 122 | 23 | 48 | 16 | 6 | 70 | 145 | 215 | 0 | 0 | 0 | 0 | 0 | 0 | 0 | 0 | 0 | 0 | 0 | 0 | 0 | 0 | 0 | 0 | 0 | 0 |
| Dense Aggregate | PL20-A2 | 0 | 0 | 0 | 69 | 69 | 5 | 67 | 10 | 4 | 81 | 74 | 155 | 0 | 0 | 0 | 1 | 0 | 1 | 1 | 0 | 1 | 1 | 2 | 0 | 1 | 0 | 1 | 0 | 1 | 1 |
| Hidden Aggregate | PL14-A1 | 0 | 0 | 0 | 0 | 0 | 1 | 0 | 0 | 1 | 1 | 1 | 2 | 7 | 0 | 7 | 40 | 24 | 47 | 9 | 19 | 28 | 71 | 99 | 1 | 8 | 2 | 9 | 1 | 11 | 12 |
| *R. chacei* Nursery | PL15-A4 | 0 | 0 | 0 | 4 | 4 | 0 | 2 | 0 | 1 | 3 | 4 | 7 | 0 | 0 | 0 | 1 | 0 | 1 | 4 | 19 | 23 | 1 | 24 | 0 | 0 | 0 | 0 | 5 | 0 | 5 |
| *R. chacei* Nursery | PL17-A1&2&3 | 0 | 0 | 0 | 5 | 5 | 3 | 0 | 3 | 5 | 8 | 8 | 16 | 0 | 0 | 0 | 3 | 0 | 3 | 17 | 70 | 87 | 3 | 90 | 0 | 5 | 0 | 5 | 8 | 5 | 13 |
| *R. exoculata* Nursery | PL15-A1 | 0 | 0 | 0 | 12 | 12 | 3 | 10 | 32 | 100 | 142 | 15 | 157 | 0 | 0 | 0 | 0 | 0 | 0 | 0 | 2 | 2 | 0 | 2 | 0 | 0 | 0 | 0 | 0 | 0 | 0 |
| *R. exoculata* Nursery | PL19-A3 | 0 | 0 | 0 | 11 | 11 | 4 | 7 | 33 | 117 | 157 | 15 | 172 | 0 | 0 | 0 | 0 | 0 | 0 | 0 | 0 | 0 | 0 | 0 | 0 | 0 | 0 | 0 | 0 | 0 | 0 |
| Periphery | PL19-A1&2 | 0 | 0 | 0 | 4 | 4 | 19 | 1 | 2 | 5 | 8 | 23 | 31 | 0 | 0 | 0 | 2 | 2 | 2 | 0 | 1 | 1 | 4 | 5 | 0 | 5 | 1 | 5 | 0 | 6 | 6 |
| Periphery | PL14-A2 | 0 | 0 | 0 | 1 | 1 | 9 | 0 | 0 | 0 | 0 | 10 | 10 | 0 | 0 | 0 | 3 | 9 | 3 | 0 | 0 | 0 | 12 | 12 | 0 | 0 | 0 | 0 | 0 | 0 | 0 |
| Periphery - *Mirocaris* | PL20-A3&4&5 | 1 | 1 | 2 | 12 | 14 | 14 | 1 | 9 | 5 | 15 | 28 | 43 | 0 | 0 | 0 | 22 | 10 | 22 | 11 | 6 | 17 | 32 | 49 | 28 | 83 | 16 | 111 | 5 | 127 | 132 |

**Table S4.** Detail individual number of the different life stages for *R. exoculata*, *R. chacei* and *M. fortunata* shrimps from and Snake Pit, for the different collected assemblages in 2018. **OF:** Ovigerous females; **GF:** females with developed gonads; **RF:** Reproductively active females (**OF** + **GF**); **NRF:** Non-reproductive females; **Ftot:** All females; **M:** males; **Sub:** subadult stages; **St. B.:** stage B juveniles; **St. A.:** stage A juveniles; **Imm:** immatures life stages (juveniles + subadults); **Ad:** Adult life stages; **n:** total individuals.

| Period between sampling | Assemblage Type | Sample ID | *Rimicaris exoculata* | | | | | | | | *Rimicaris chacei* | | | | | | | *Mirocaris fortunata* | | | | |
|---|---|---|---|---|---|---|---|---|---|---|---|---|---|---|---|---|---|---|---|---|---|---|
| | | | OF | GF | NRF | M | Sub | St. B | St. A | Tot | OF | GF | NRF | M | Sub | St. A | Tot | OF | NRF | M | J | Tot |
| day 0 | Dense Aggregate | PL02-A3 | 41 | 14 | 34 | 6 | 1 | 12 | 3 | 111 | 1 | 1 | 0 | 0 | 4 | 2 | 8 | 0 | 0 | 0 | 0 | 0 |
| day +10 | Hidden Aggregate | PL08-A2 | 3 | 0 | 3 | 1 | 1 | 1 | 0 | 9 | 11 | 0 | 5 | 16 | 0 | 0 | 32 | 0 | 1 | 0 | 0 | 1 |
| day 0 | *R. exoculata* nursery | PL15-A1 | 0 | 0 | 12 | 3 | 10 | 32 | 100 | 159 | 0 | 0 | 0 | 0 | 0 | 2 | 0 | 0 | 0 | 0 | 0 | 0 |
| day +7 | *R. exoculata* nursery | PL19-A3 | 0 | 0 | 11 | 4 | 7 | 33 | 117 | 172 | 0 | 0 | 0 | 0 | 0 | 0 | 0 | 0 | 0 | 0 | 0 | 0 |
| day 0 | Dense Aggregate | PL15-A3 | 2 | 0 | 245 | 25 | 17 | 34 | 3 | 326 | 0 | 0 | 0 | 0 | 0 | 0 | 0 | 0 | 0 | 0 | 0 | 0 |
| day +7 | Dense Aggregate | PL19-A4&5 | 6 | 1 | 219 | 39 | 51 | 28 | 18 | 362 | 0 | 0 | 0 | 0 | 0 | 1 | 0 | 0 | 0 | 0 | 0 | 0 |
| day 0 | *R. chacei* nursery | PL15-A4 | 0 | 0 | 4 | 0 | 2 | 0 | 1 | 7 | 0 | 0 | 1 | 0 | 4 | 19 | 24 | 0 | 0 | 0 | 5 | 5 |
| day +5 | *R. chacei* nursery | PL17-A1&2&3 | 0 | 0 | 5 | 3 | 0 | 3 | 5 | 16 | 0 | 0 | 3 | 0 | 17 | 70 | 90 | 0 | 5 | 0 | 8 | 13 |
| day 0 | Dense Aggregate | PL18-A1&2 | 11 | 12 | 90 | 8 | 3 | 3 | 15 | 142 | 3 | 0 | 6 | 1 | 0 | 0 | 10 | 0 | 0 | 0 | 0 | 0 |
| day +2 | Dense Aggregate | PL20-P1 | 34 | 2 | 79 | 7 | 2 | 5 | 31 | 160 | 0 | 0 | 1 | 0 | 0 | 0 | 8 | 0 | 0 | 0 | 0 | 0 |

**Table S5.** Population structure variability within assemblages on short temporal scale. OF: Ovigerous females; GF: females with developed gonads; NRF: Non-reproductive females; M: males; Sub: subadult stages; St. B.: stage B juveniles; St. A.: stage A juveniles; J: undetermined juvenile stages (*M. fortunata* only).

# 3.2 Additional results

Although it is still unclear on how it will be integrated to the study, a temporal comparison at a large temporal scale could be realized as well by comparing the 2018 samples presented earlier with the samples of 2014, and also with the shrimp samples collected in 2017, that were sorted during this thesis. The number and the type of habitat samples are a bit more limited but the data should be sufficient to establish comparison at the whole population level at least for *R. exoculata*. This table summarize the samples obtained in 2017 (**Table S6**). One strong issue, though, is the absence of detailed examination on several individuals that were only identified as adults or immature specimens without any informations on their sex or juvenile stages. This create a difference between the total number of adults or immature individuals and their number per sex or per stages in some assemblages that are indicated in bold in **Table S6**.

| Vent Field / Edifice | Assemblage Type | Sample ID | *Rimicaris exoculata* | | | | | | | | | | | | *Rimicaris chacei* | | | | | | | | | | |
|---|---|---|---|---|---|---|---|---|---|---|---|---|---|---|---|---|---|---|---|---|---|---|---|---|---|
| | | | **OF** | **GF** | **RF** | **NRF** | **Ftot** | **M** | **Sub** | **St. B** | **St. A** | **Imm** | **Ad** | **n** | **OF** | **GF** | **RF** | **NRF** | **M** | **Ftot** | **Sub** | **St. A** | **Imm** | **Ad** | **n** |
| Snake Pit | Dense Aggregate | PL02-A1 | 0 | 0 | 0 | 25 | 25 | 2 | 1 | 2 | 0 | 3 | 27 | 30 | 0 | 0 | 0 | 1 | 0 | 1 | 0 | 0 | 0 | **3** | **3** |
| Snake Pit | Dense Aggregate | PL02-A4 | 0 | 0 | 1 | 697 | 698 | 5 | 182 | 47 | 11 | 240 | **713** | **953** | 0 | 0 | 0 | 0 | 0 | 0 | 0 | 0 | 0 | 0 | 0 |
| Snake Pit | Dense Aggregate | PL02-A5 | 0 | 0 | 0 | 48 | 48 | 4 | 4 | 2 | 4 | 10 | 52 | 62 | 0 | 0 | 1 | 1 | 0 | 0 | 0 | 0 | 0 | **2** | **2** |
| Snake Pit | *R. chacei* Nurseries | PL02-A2 | 0 | 0 | 0 | 3 | 3 | 1 | 0 | 0 | 0 | 0 | 4 | 4 | 0 | 0 | 0 | 0 | 0 | 0 | 2 | 100 | **122** | 0 | **122** |
| Snake Pit | Vicinity of Aggregates + Aggregate mixed | PL02-A3 | 0 | 0 | 0 | 162 | 162 | 2 | 99 | 79 | 106 | **306** | 164 | **460** | 0 | 0 | 0 | 0 | 0 | 0 | 0 | 0 | 0 | 0 | 0 |
| TAG | Dense Aggregate | PL10-A2 | 0 | 0 | 0 | 57 | 57 | 6 | 1 | 0 | 0 | 1 | 63 | **64** | 0 | 0 | 0 | 0 | 2 | 2 | 8 | 15 | **23** | 3 | **26** |
| TAG | Dense Aggregate | PL10-A5 | 0 | 0 | 0 | 131 | 131 | 8 | 2 | 2 | 2 | 6 | **154** | **160** | 0 | 0 | 0 | 0 | 0 | 0 | 0 | 0 | 0 | **3** | **3** |
| TAG | Dense Aggregate | PL13-A1-A5 | 0 | 0 | 15 | 162 | 177 | 87 | 26 | 90 | 13 | **139** | 264 | **403** | 0 | 0 | 0 | 0 | 0 | 2 | 0 | 0 | 4 | 2 | 6 |
| TAG | *R. chacei* Nurseries | PL10-A1 | 0 | 0 | 0 | 1 | 1 | 0 | 0 | 0 | 0 | 0 | 0 | 1 | 0 | 0 | 0 | 0 | 0 | 0 | 11 | 75 | **95** | 0 | **95** |

**Table S6**. Detailled individual number of the different life stages for *R. exoculata* and *R. chacei* shrimps from and Snake Pit, for the different collected assemblages in 2017 during the HERMINE cruise. **OF:** Ovigerous females; **GF:** females with developed gonads; **RF:** Reproductively active females (**OF** + **GF**); **NRF:** Non-reproductive females; **Ftot:** All females; **M:** males; **Sub:** subadult stages; **St. B.:** stage B juveniles; **St. A.:** stage A juveniles; **Imm:** immature life stages (juveniles + subadults); **Ad:** Adult life stages; **n:** total individuals.

# Chapter 4
# Giving Birth in turn

The aim of this study was to confirm the seasonality of the *R. exoculata* reproduction by comparing the data from 2014 with two new batches of ovigerous females collected in 2017 and 2018. In addition to evaluate reproductive periodicity, the objectives of this comparison were also to assess the interannual variations of the reproductive output – egg number, egg volume and brood volume – of *R. exoculata*. The large collection of ovigerous females of *R. chacei* and *R. exoculata* in 2018 also enables us to describe the reproductive characteristics of *R. chacei* for the first time as well as those of *M. fortunata* in a period of the year still unexplored for this species. Data from the 2017 expedition were collected by Dr. Pradillon whereas those collected from 2018 during the BICOSE 2 expedition were, again, part of this thesis work. Ovigerous females were sorted individually on board, and egg stages were also identification on fresh material. Measures and egg count were conducted in the laboratory.

In addition to this, this work also attempts to identify environmental cues that could potentially synchronize the seasonality of *R. exoculata* reproduction. Although previous studies (Copley and Young, 2006; Nye et al., 2013) strongly suggested that the variations of the photosynthetic surface production were synchronizing the reproduction of other alvinocaridids, many evidences do not really support this hypothesis in the case of *R. exoculata*. Among others, the strong oligotrophic character of the water column above these vent fields, the existing but very limited variations across seasons and the depth, much lower than for any studies where surface production was related to reproductive periodicity, are all weakening this hypothesis. Looking at *R. kairei* population samples available at Jamstec (Japan) gave me an opportunity to compare two sister species living at comparable lattitudes but in opposed hemispheres (*R. kairei* is found on Indian Ridges). In these contrasting locations, surface production follows an opposite seasonal pattern, and if reproduction of shrimps is driven by this factor. Then both species are expected to exhibit opposite reproductive seasonality.

A fruitful exchange with the JAMSTEC thus allowed to explore this question looking at ovigerous females of *R. kairei*, the sister species of *R. exoculata* from the Central Indian Ridge. I analysed the ovigerous females collected by Dr. Chen in 2016 (during an expedition led by the JAMSTEC), during a stay at JAMSTEC in June 2019. With these materials, interspecific variations between *R. exoculata* and its co-occurring species or with its sister species from another biogeographical region were assessed, ultimately aiming at determining whether reproductive seasonality was linked to the seasonal variations of the photosynthetic primary production around the globe, or not.

This work is still in progress, and remains uncompleted compared to the previous ones. New data of *R. kairei* could be available with the JAMSTEC video databases and the results of this study still need to be put into perspective with the current bibliography.

# 4.1 Reproductive strategies in alvinocaridid shrimps from hydrothermal vents of the Mid Atlantic Ridge and the Central Indian Ridge

## Authors and Affiliations

Pierre Methou[1,2], Watanabe, H. K., Chen, C., Marie-Anne Cambon-Bonavita[1], Florence Pradillon[2*]

[1] : Ifremer, Univ Brest, CNRS, Laboratoire de Microbiologie des Environnements Extrêmes, UMR6197, 29280 Plouzané, France

[2] : Ifremer, Centre Brest, Laboratoire Environnements Profonds (REM/EEP/LEP), ZI de la pointe du diable, 29280 Plouzané, France

[3]: X-STAR, Japan Agency for Marine-Earth Science and Technology (JAMSTEC), Kanagawa, Japan

## 4.1.1 Introduction

Deep sea chemosynthetic ecosystems, hosting very dense and specific faunal communities, are distributed widely in the ocean but also patchily, forming isolated oases of life for a specialized range of organisms (Beaulieu et al., 2013; Levin and Sibuet, 2012). Additionally, these places are also ephemeral owing to their geological instability, especially in the case of hydrothermal vents. Indeed, several extinct vent fields have been observed, and more exceptionally catastrophic eruptions that led to the collapse of entire faunal communities have also been witnessed (Fornari et al., 2012; Lalou et al., 1985; Rona et al., 1993). Particular life history traits, such as the reproduction, are therefore of critical importance for the maintenance of their population and for the establishment in other vent fields. Rather than a single strategy adapted to chemosynthetic ecosystems, it is apparent that vent and cold seeps fauna exhibit a wide diversity of reproductive patterns constrained by phylogenetic relationships (Tyler and Young, 1999; Van Dover et al., 1985).

Sampling difficulties in these ecosystems have hampered the establishment of temporal studies of reproductive patterns. These limitations have slowed down a comprehensive understanding of reproductive cycles in these environments that can only be determined by sampling at regular interval over a period of time related to the assumed periodicity of the cycle (Tyler and Young, 1999). Therefore, many studies exploring this periodicity often reported data of composite years with many months missing. For some times, it was believed that, in the absence of sunlight and thus of the seasonality induced by the sunshine (such as temperature, day length, phytoplankton blooms…) deep-sea species reproduction was continuous and independent of these seasonal factors (Orton, 1920). Nonetheless, while continuous reproduction was indeed observed in many vent and cold seep species (Copley et al., 2003; Faure et al., 2007; Hilario et al., 2005; Matabos and Thiebaut, 2010; Tyler et al., 2008), some studies suggested the existence of seasonal variations in the reproduction of others. Among them, some vesicomyid clams (Lisin et al., 1997), bathymodiolin mussels (Comtet and Desbruyères, 1998; Dixon et al., 2006; Tyler et al., 2007) and different crustaceans families (Copley and Young, 2006; Perovich et al., 2003) exhibited seasonal patterns in their gametogenesis, brooding or

spawning periods. For instance in bathymodiolin mussels – including those from Atlantic vent sites – spawning period correlates with the surface primary production, preceding the phytoplankton peak of late winter to early spring (Dixon et al., 2006; Laming et al., 2018; Tyler et al., 2007). This suggests that the surface primary production could act as a reproductive cue, synchronizing individuals to spawn/breed at the same period of the year.

With a wide geographical distribution in many cold seeps and almost all major hydrothermal vent biogeographic provinces, alvinocaridid shrimps constitute one of the major group among the endemic fauna retrieved in chemosynthetic ecosystems (Lunina and Vereshchaka, 2014; Nye et al., 2012). Although their egg remains much smaller than those of some vent decapod crustaceans like *Kiwa* crabs or *Munidopsis* squat lobsters (Marsh et al., 2015; Van Dover et al., 1985), some variability in the alvinocaridid egg size was reported with a trade-off between egg size and fecundity. The ones with the lowest fecundity – like *Alvinocaris stactophila*, *Mirocaris fortunata* – present also larger eggs than shrimp species with higher fecundity like *Alvinocaris muricola* (Copley and Young, 2006; Ramirez-Llodra et al., 2000; Ramirez-Llodra and Segonzac, 2006). Seasonality has also been confirmed in the gametogenesis and brooding periods for some of these shrimps like *A. stactophila* (Copley and Young, 2006), although this pattern remains unclear for others, such as *A. muricola* (Ramirez-Llodra and Segonzac, 2006). Like the bathymodiolin mussels, the brooding period of *A. stactophila* between winter and early spring correlates with the surface primary production (Copley and Young, 2006). A similar brooding period was also hypothesized for *R. hybisae* from the Mid Cayman Rise with ovigerous females present in high proportions in January 2012, and to a lower extend in February 2018 (around 50% and 7% of all females, respectively) (Nye, 2013; Nye et al., 2013) whereas they were not reported in August 2011 and July 2013 (Nye et al., 2013; Watanabe, personnal communication).

Reproductive features observed in *R. exoculata*, the most studied species of this family, and in one of its co-occurring species in the Mid Atlantic Ridge (MAR), *R. chacei*, were faced for a long time with contradicting evidences. While oocyte-size frequency analyses revealed an absence of synchronicity in the gametogenesis of these species, suggesting a continuous reproduction, brooding females were lacking at all the sampling periods examined at that time (Ramirez-Llodra et al., 2000). On the other hand, gametogenesis of *Mirocaris fortunata*, another co-occurring species, was also asynchronous but brooding females could be regularly sampled in different vent fields (Komai and Segonzac, 2003; Ramirez-Llodra et al., 2000). It is only recently, that a large number of brooding females were collected between January and early February 2014, at a period of the year that had not been sampled before (Hernández-Ávila, 2016). These females were found in the dense aggregates of shrimps close to the vent fluid emissions, discarding the previous theory of a brooding migration out of the harsh vent emissions (Hernández-Ávila, 2016). These findings suggest a seasonal reproduction for *R. exoculata*, like *A. stactophila* from cold seeps, although annual observations at this same period are required to confirm such pattern. Reproductive features of *R. chacei* were scarcely studied and remain unclear.

Similarly, no reproductive studies have been conducted on *R. kairei*, the sister species of *R. exoculata*, sharing a similar ecology and morphology (Watabe and Hashimoto, 2002). This species presents indeed a strongly inflated cephalothorax and lives in dense aggregates close to vent fluid emissions in the Central Indian Ridge (CIR) (Van Dover, 2001). Although both species appear very similar in their ecology, they differ markedly in their location since *R. kairei* inhabits vent fields that are

all located in the Southern Hemisphere, according to our current knowledge of its distribution. This also contrasts with all the other reproductive studies conducted on alvinocaridids, which were all distributed in the Northern Hemisphere (Copley and Young, 2006; Hernández-Ávila, 2016; Nye et al., 2013; Ramirez-Llodra et al., 2000; Ramirez-Llodra and Segonzac, 2006; Van Dover et al., 1985). More specifically, some vent fields of the CIR, such as Kairei (25°S) and Edmond (23°S), are located at opposed latitudes to those where some vent fields of the MAR hosting *R. exoculata*, such as TAG (26°N) and Snake Pit (23°N), are located. Therefore, if *R. kairei* has a seasonal reproduction like *R. exoculata*, and assuming that photosynthetic production sinking from the surface is a synchronizing factors in these species like in Bathymodiolin mussels, then, brooding periods at opposite periods of the year should be observed in these two species.

Here we expand initial observations by Hernández-Ávila et al 2016, suggesting seasonality in *R. exoculata*, by analyzing shrimps populations sampled in two additional consecutive years at slightly different periods, and by including observations in other species of the family. The aims of this study were thus (i) to confirm seasonal patterns in *R. exoculata* by assessing the pluriannual variation of its reproduction, and (ii) determine whether such seasonality was linked to regional cues by assessing the reproduction of co-occurring species of the same family, *R. chacei* and *M. fortunata*, at the same period as well as with a closely related species, *R. kairei*, but with a different location.

## 4.1.2 Materials & Methods

### 4.1.2.1 Field sampling

Shrimps were collected directly with the suction sampler of the French HOV *Nautile* (BICOSE 2, HERMINE), the HOV *Shinkai 6500* (YK16-E02) or the ROV *Victor 6000* (BICOSE). For the MAR species, samples were collected during the BICOSE expedition (10$^{th}$ January – 11$^{th}$ February 2014), HERMINE expedition (15$^{th}$ March 2017 – 28$^{th}$ April 2017) and the BICOSE 2 expedition (26$^{th}$ January 2018 – 10$^{th}$ March 2018), on board of the R/V *Pourquoi Pas?*, at the Snake Pit (23°22.1'N 44°57.1'W, 3470 m depth) and the TAG (26°08.2'N, 44°49.5'W, 3620 m depth) hydrothermal vent fields (**Fig 69A.**). *R. kairei* samples were collected during the YK16-E02 expedition (4$^{th}$ February – 2$^{nd}$ March 2016) on board of the ship R/V *Yokosuka* at the Kairei (25°19'10''S, 70°2'24''E, 2415 m depth) and Edmond (23°52'43.8''S, 69°35'.45.6''E, 3290 m depth) vent fields of the CIR (**Fig 69B.**).

Upon recovery on board the ship, ovigerous females of *R. exoculata*, *R. chacei* and *M. fortunata* were identified and individually sorted from the rest of the population. Ovigerous females include both brooding females and hatched females that had just released their larvae but still had the modified pleopods characteristic of the brooding period. The number of females examined for each species in

samples from the different vent fields and expeditions are summarized in **Table 10.** For *R. kairei*, ovigerous females were identified and sorted from the rest of the population in the laboratory.

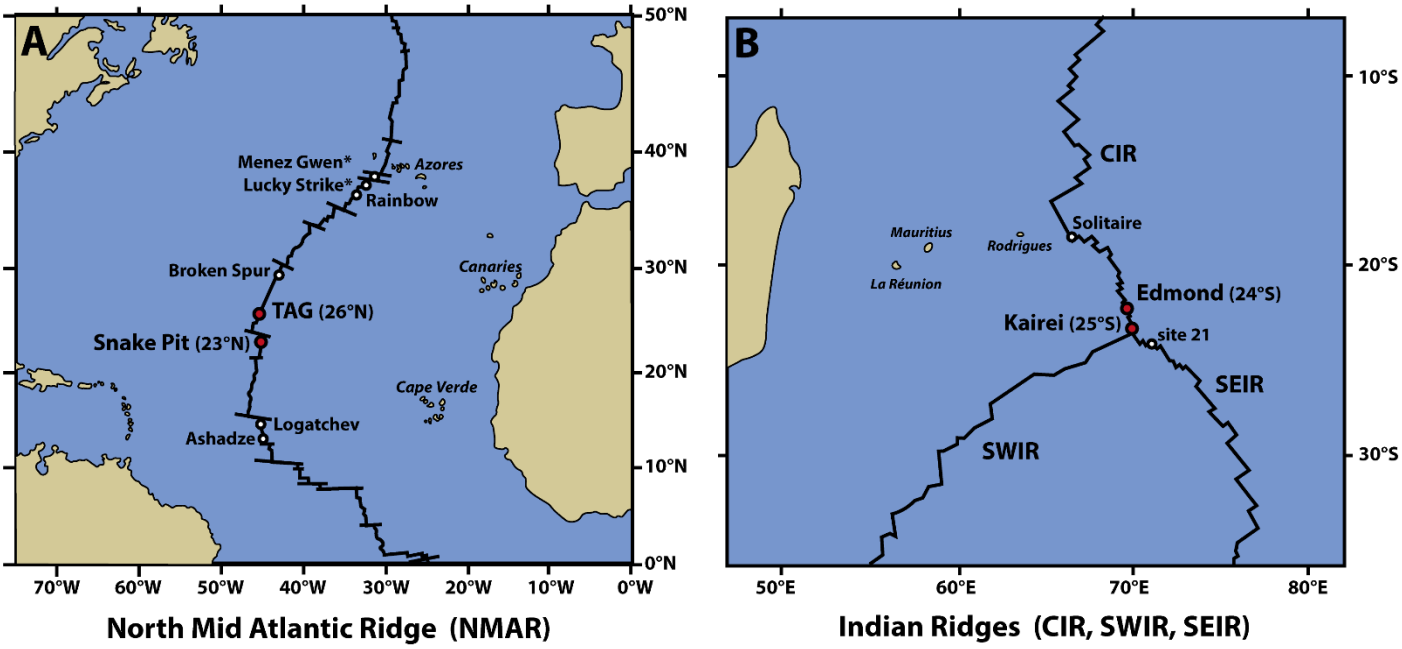


**Fig 70.** Maps of the studied areas. **A.** Map of the North Mid Atlantic Ridge (NMAR) where *R. exoculata*, *R. chacei* and *M. fortunata* have been sampled. **B.** Map of the South West Indian Ridge (SWIR), South East Indian Ridge (SEIR) and of the Central Indian Ridge (CIR) where *R. kairei* shrimps were sampled. White circle: vent fields of the areas where the studied alvinocaridids are present. Red circle: Vent fields sampled for this study. *vent fields where only *R. chacei* and *M. fortunata* are present

Egg stages in broods were identified on board for ovigerous females collected during the BICOSE 2 expedition, before being fixed in 10% neutral buffered formalin for 24h and then rinsed and stored in 80% EtOH. For shrimps of other expeditions, ovigerous females were fixed and stored in 10% formalin on board whereas the identification of egg stages was conducted in the laboratory.

Eggs in broods were classified in three developmental stages (early, mid and late) according to the classification used in (Methou et al., 2019a) and the BICOSE study (2014) (Hernández-Ávila, 2016):

- Early stage : from one-cell embryos to fully segmented embryos (blastula);
- Middle stage includes embryos at the gastrulation (a clear area starts to be visible at one pole of the egg) to embryos showing early differentiation of larval structures;
- Late stage includes embryos with advanced development of larval structures and eyespots visible through the egg envelope.

### 4.1.2.2 Shrimps and Eggs Measurements

Some brooding females harbored damaged or aborted broods and were discarded from the reproductive analysis (relative fecundity, egg and brood volumes and egg stages proportions (**Table 10.**). Carapace length (CL) was determined to the nearest 0.1 mm with Vernier calipers from the rear of the eye socket to the rear of the carapace in the mid-dorsal line.

For each brood, the total number of eggs was manually counted. Ten eggs were randomly selected, and both their maximum and minimum diameters were measured. The volume of embryos was estimated according to (Oh and Hartnoll, 2004), considering a spheroid volume as $v= (4/3)\pi.r1.r2^2$, where r1 and r2 are the half of the maximum and the minimum axis of the egg, respectively.

| **Type of females** | **Ovigerous females** | **Brooding females** | | | | | **Hatched females** | **Dammaged** |
|---|---|---|---|---|---|---|---|---|
| **Indivual number (n) or Carapace lenght (CL) ( in mm)** | n | n | mean | sd | min | max | n | n |
| *Rimicaris exoculata* (BICOSE 2014) TAG | 81 | 47 | 15.7 | 1.4 | 12 | 18.3 | 4 | 30 |
| *Rimicaris exoculata* (BICOSE 2014) Snake Pit | 55 | 45 | 17.5 | 1.4 | 15 | 20.5 | 9 | 1 |
| *Rimicaris exoculata* (HERMINE 2017) TAG | 17 | 14 | 16.8 | 0.9 | 15.3 | 18.2 | 2 | 1 |
| *Rimicaris exoculata* (HERMINE 2017) Snake Pit | 2 | 1 | - | - | - | - | 1 | 0 |
| *Rimicaris exoculata* (BICOSE 2 2018) TAG | 114 | 103 | 17 | 1.4 | 14.1 | 20.1 | 3 | 8 |
| *Rimicaris exoculata* (BICOSE 2 2018) Snake Pit | 80 | 43 | 20 | 2.4 | 15.5 | 23.8 | 14 | 23 |
| *Rimicaris exoculata* (BICOSE 2 2018) The Beehive only | 14 | 10 | 17.1 | 1.5 | 15.5 | 20.8 | 2 | 2 |
| *Rimicaris exoculata* (BICOSE 2 2018) The Moose only | 65 | 33 | 22 | 1.9 | 17.3 | 23.8 | 11 | 21 |
| *Rimicaris kairei* (YK16-E02 2016) Kairei | 51 | 45 | 20.8 | 1 | 18.2 | 23 | 2 | 4 |
| *Rimicaris kairei (YK16-E02 2016)* Edmond | 2 | 1 | - | - | - | - | 1 | 0 |
| *Rimicaris chacei* (BICOSE 2 2018) TAG | 12 | 12 | 17.3 | 2.5 | 12.9 | 20.2 | 0 | 0 |
| *Rimicaris chacei* (BICOSE 2 2018) Snake Pit | 11 | 8 | 16.2 | 3.8 | 11.8 | 21.8 | 2 | 1 |
| *Mirocaris fortunata* (BICOSE 2 2018) TAG | 3 | 2 | 9.3 | 1.5 | 8.2 | 10.3 | 0 | 1 |
| *Mirocaris fortunata* (BICOSE 2 2018) Snake Pit | 31 | 12 | 8.9 | 1.1 | 7.7 | 10.2 | 8 | 11 |

**Table 10.** Summary of the ovigerous females collected with the number of brooding females, females with hatched broods and females with damaged broods. Mean CL size of the brooding females of each species or sampling year per vent fields were also given, as well as their minimum and maximum sizes.

### 4.1.2.3 Statistical analysis

Alvinocaridid ovigerous females were grouped according to either the sampling year or species and according to their vent field origin. Visual examination of our dataset and Shapiro-Wilk normality tests revealed that the size, the egg number and the egg volume of *R. exoculata* brooding females collected during the BICOSE 2 expedition were not following a Gaussian distribution. Therefore, non-parametric tests were used for intergroup comparison, with a Kruskal-Wallis test followed by post-hoc pairwise Wilcoxon test when three or four groups were compared. All tests were performed using R version 3.5.1.

## 4.1.3 Results

### 4.1.3.1. Interannual variation of *R. exoculata* reproduction

As in 2014 (**Fig 70A.**, Spearman correlation r= 0.67, $p < 0.0001$), the realized fecundity of *R. exoculata* from 2018 correlated positively with the carapace length (CL) (**Fig 70A.**, Spearman correlation r= 0.72, $p < 0.0001$). Moreover, the slope of the relationship between the $\log_e$-transformed realized fecundity and the $\log_e$-transformed carapace length did not significantly differ between TAG and Snake Pit in 2018 (**Fig 70A.**, $F = 0.004$ $p = 0.95$) neither than between 2014 and 2018 (**Fig 70A.**, $F = 1.175$ $p = 0.28$). However, no correlation could be observed in 2017 (**Fig 70A.**, Spearman correlation r= 0.38, $p = 0.16$), although this could be related to the lower sampling effort, as their realized fecundity fall in the range of those from the other sampling years.

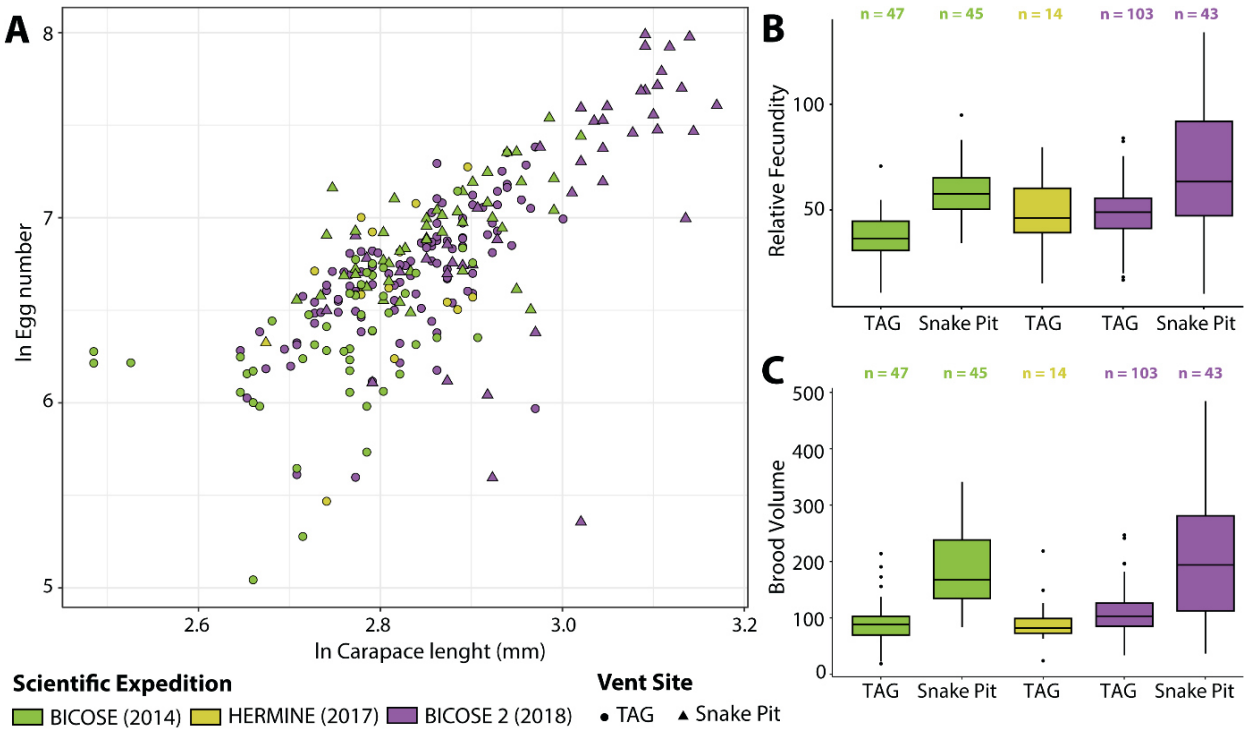


**Fig 71.** Interannual variations of *R. exoculata* fecundity between 2014 (BICOSE), 2017 (HERMINE) and 2018 (BICOSE 2) at TAG and at Snake Pit. **A.** Variation of $\log_e$-transformed minimum realized fecundity with $\log_e$-transformed carapace length **B.** Fecundity corrected for body size (carapace length). n: number of individuals measured. **C.** Brood volume, i.e. the number of egg multiplied by their individual volume.

In general, differences could be observed between the sizes of *R. exoculata* brooding females between the different sampling years for a given vent site (Kruskal-Wallis, H= 81.52, $p < 0.05$) (**Table 10.**). However, brooding females collected in 2018 were bigger than the brooding females collected in 2014 both at TAG (2018: 17.0 ± 1.35 mm; 2014: 15.7 ± 1.43 mm; Dunn's Multiple Comparison Test, $p < 0.05$) and at Snake Pit (2018: 20.0 ± 2.38 mm; 2014: 17.5 ± 1.37 mm; Dunn's Multiple Comparison Test, $p < 0.05$). This difference in body size between brooding females in 2014 and in 2018 was mostly related to the collections of individuals from The Moose edifice in 2018 only, which were significantly bigger than those collected from The Beehive edifice in 2018 (The Beehive 2018: 17.1 ± 1.53 mm; The Moose 2018: 20.8 ± 1.85 mm; Dunn's Multiple Comparison Test, $p < 0.05$). Indeed, if the individuals from the Moose are excluded from the 2018 dataset, brooding females body sizes were rather similar between the 2014 and 2018 sampling (2018: 17.1 ± 1.53 mm; 2014: 17.5 ± 1.37 mm; Dunn's Multiple Comparison Test, $p > 0.05$). No differences could be observed however between brooding females collected in 2017 with those collected in 2014 or 2018 (TAG, 2017: 17.1 ± 1.53 mm). Moreover, for a given sampling year, brooding females of *R. exoculata* were bigger at Snake Pit than at TAG, both in 2014 and in 2018, (Dunn's Multiple Comparison Test, $p < 0.05$). Unfortunately, with only one brooding female collected at Snake Pit in 2017, no comparison could be made between TAG and Snake Pit with this sampling year.

Therefore, the few differences in the realized fecundity of brooding females between the different sampling years (Kruskal-Wallis, H= 65.025 $p < 0.05$) (**Fig 70B.**) could be attributed to their variations in body size and a non-linear relationship between fecundity and body size for these species. Indeed, differences in the relative fecundity of *R. exoculata* could be observed mostly between 2014 and 2018 at TAG (2014: 37.3 ± 11.4; 2018: 49.4 ± 12.9; Dunn's Multiple Comparison Test, $p < 0.05$). Differences were also observed in the relative fecundity of the two vent fields both in 2014 (TAG: 37.3 ± 11.4; Snake Pit: 59.3 ± 13.4 mm; Dunn's Multiple Comparison Test, $p < 0.05$) and in 2018 (TAG: 49.4 ± 12.9; Snake Pit: 69.4 ± 31.2 mm; Dunn's Multiple Comparison Test, $p < 0.05$). Accordingly, whereas the greatest realized fecundity in 2014 was 1879 eggs in an individual from the Snake Pit vent field with a CL of 19.8 mm, the greatest realized fecundities in 2017 and 2018 were respectively of 1443 eggs in an individual from the TAG vent field with a CL of 18.1 mm and of 2949 eggs in an individual from the Snake Pit vent field with a CL of 22 mm. Overall, size-specific fecundity ranged from 10.8 to 94.9 eggs.mm$^{-1}$ in 2014, from 15.3 to 79.7 eggs.mm$^{-1}$ in 2017 and from 10.3 to 134 eggs.mm$^{-1}$ in 2018. Similarly, differences in brood volume could only be observed between vent fields (Kruskal-Wallis, H= 8.1146 $p < 0.05$). A larger brood volume at Snake Pit for the females collected in 2014 (TAG: 93 ± 39.4; Snake Pit: 182 ± 62 mm; Dunn's Multiple Comparison Test, $p < 0.05$) or in 2018 (TAG: 109 ± 38.5; Snake Pit: 203 ± 112 mm; Dunn's Multiple Comparison Test, $p < 0.05$), (**Fig 70C.**). No variation in the brood volumes were observed between sampling years either at TAG or at Snake Pit (**Fig 70C.**)

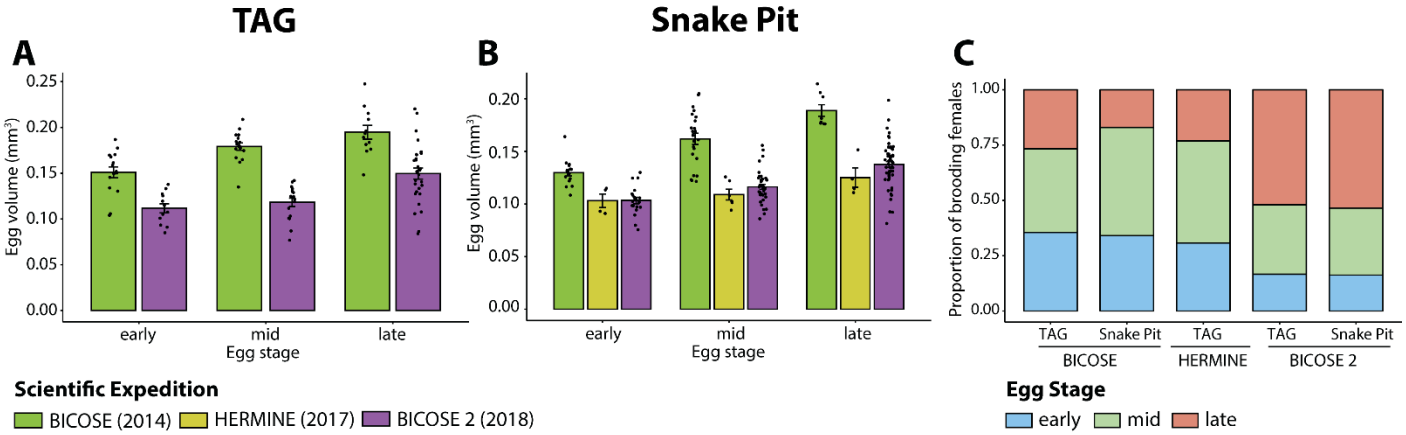


**Fig 72.** Interannual variations of *R. exoculata* egg volume and egg stages between 2014 (BICOSE), 2017 (HERMINE) and 2018 (BICOSE 2) at TAG and at Snake Pit. **A.** Egg volumes of *R. exoculata* from TAG at different egg stages. **B.** Egg volumes of *R. exoculata* from TAG at different egg stages. **C.** Egg stages proportion of *R. exoculata*.

Differences in egg volume between sampling years were also limited, either for early (Kruskal-Wallis, H= 34.21 $p < 0.05$), mid (Kruskal-Wallis, H= 60.06 $p < 0.05$), or late stage eggs (Kruskal-Wallis, H= 44.44 $p < 0.05$). Still, a larger egg volume was observed in 2014 compared to the other sampling years for both mid and late stage eggs at TAG and at Snake Pit (**Fig 71A**. and **71B**.; Dunn's Multiple Comparison Tests, $p < 0.05$). This difference was related to an observer effect, since the 2014 dataset was produced separately in a previous study (Hernández-Ávila, 2016). A sub-sample of the broods examined in the 2014 dataset were measured again by the observer who produced the 2017 and 2018, datasets. This re-examination revealed a significant difference in the calculated egg volume but also in the measured maximum and minimum diameters between the two observers (**Fig S6.**). Accordingly, no difference could be observed between the re-examined 2014 subsample and the 2017 and 2018 samples treated by the same observer (**Fig S6.**). The proportions of each developmental stage were

rather similar at TAG between 2014 and 2017 (**Fig 71C.**; $\chi^2$ = 0.546; 2 df; p > 0.05) with a majority of broods with eggs at the middle stage (2014: 37.8 %; 2017: 46.2 %), around a third of the broods with eggs at early stage (2014: 35.6 %; 2017: 30.8 %) and a minority of broods with eggs at late stage (2014: 26.6 %; 2017: 23.1 %). However, these proportions differ for 2018 compared to the 2014 sampling both at TAG (**Fig 71C.**; $\chi^2$ = 27.938; 2 df; p < 0.05) and at Snake Pit (**Fig 71C.**; $\chi^2$ = 58.493; 2 df; p < 0.05). Indeed, the majority of the 145 *R. exoculata* broods in 2018 were not at a middle stage of development but at late stage of development both at TAG (52 %) and at Snake Pit (53.5 %). Then, almost a third of the broods were at middle stage of development (TAG: 31.3 %; Snake Pit: 30.2 %) whereas broods with early stage eggs were in minority (TAG: 16.7 %; Snake Pit: 16.3 %).

### 4.1.3.2. Interspecies comparison between *R. exoculata*, its sister species and its co-occurring species

As for *R. exoculata* (**Fig 72A.**, Spearman correlation r= 0.67, p < 0.0001), the realized fecundity of *R. kairei*, *R. chacei* and *M. fortunata* correlated positively with the carapace length (CL) (**Fig 72A.**; Spearman correlation: *R. kairei*: r= 0.40, p = 0.0055; *R. chacei*: r= 0.66, p = 0.0015; *M. fortunata*: r= 0.93, p = 0.00024). Moreover, the slopes of the relationship between the $\log_e$-transformed realized fecundity and the $\log_e$-transformed body size did not significantly differ between *R. exoculata* and its co-occurring species: *R. chacei* (**Fig 72A.**, F = 1.6168 p = 0.2054). However, they significantly differ between *R. exoculata* and the two other species, *R. kairei* (**Fig 72A.**, F =6.6376 p < 0.05) and *M. fortunata* (**Fig 72A.**, F = 3.4474 p 0.0653).

We observed differences between the size of the collected individuals of *R. exoculata* and its sister species *R. kairei* (Kruskal-Wallis H= 104.11, p < 0.05) (**Table 10.**). *R. kairei* brooding females from Kairei were bigger than *R. exoculata* brooding females from TAG (*R. exoculata*: 17 ± 1.35 mm; *R. kairei*: 20.8 ± 1 mm; Dunn's Multiple Comparison Test, p < 0.05) but of similar size compared to those from Snake Pit (*R. exoculata*: 20 ± 2.38 mm; *R. kairei*: 20.8 ± 1 mm; Dunn's Multiple Comparison Test, p > 0.05). No clear variation could be observed between the relative fecundity of *R. exoculata* and *R. kairei* (Kruskal-Wallis H= 10.674, p < 0.05), (**Fig 72B.**), except a slightly higher relative fecundity for *R. kairei* from Kairei compared to *R. exoculata* from TAG (*R. exoculata*: 49.4 ± 12.9; *R. kairei*: 72.4 ± 20.2; Dunn's Multiple Comparison Test, p < 0.05). For *R. exoculata*, the greatest realized fecundity was 2949 eggs in an individual from the Snake Pit vent field with a CL of 22 mm, whereas for *R. kairei*, the greatest realized fecundity was 2439 eggs in an individual from the Kairei vent field with a CL of 21.8 mm. Overall, size-specific fecundity ranged from 10.3 to 134 eggs.mm$^{-1}$ for *R. exoculata* and from 22.6 to 112 eggs.mm$^{-1}$ for *R. kairei*. Similarly, few differences in brood volume were observed between the two species (Kruskal-Wallis H= 59.05, p < 0.05) with only larger brood volume *for R. kairei* compared to *R. exoculata* at TAG (*R. exoculata*: 109 ± 38.5; *R. kairei*: 194 ± 57.9; Dunn's Multiple Comparison Test, p < 0.05), (**Fig 72C.**). Brood volume of *R. kairei* and *R. exoculata* from Snake Pit were however similar (Dunn's Multiple Comparison Test, p > 0.05), (**Fig 72C.**).

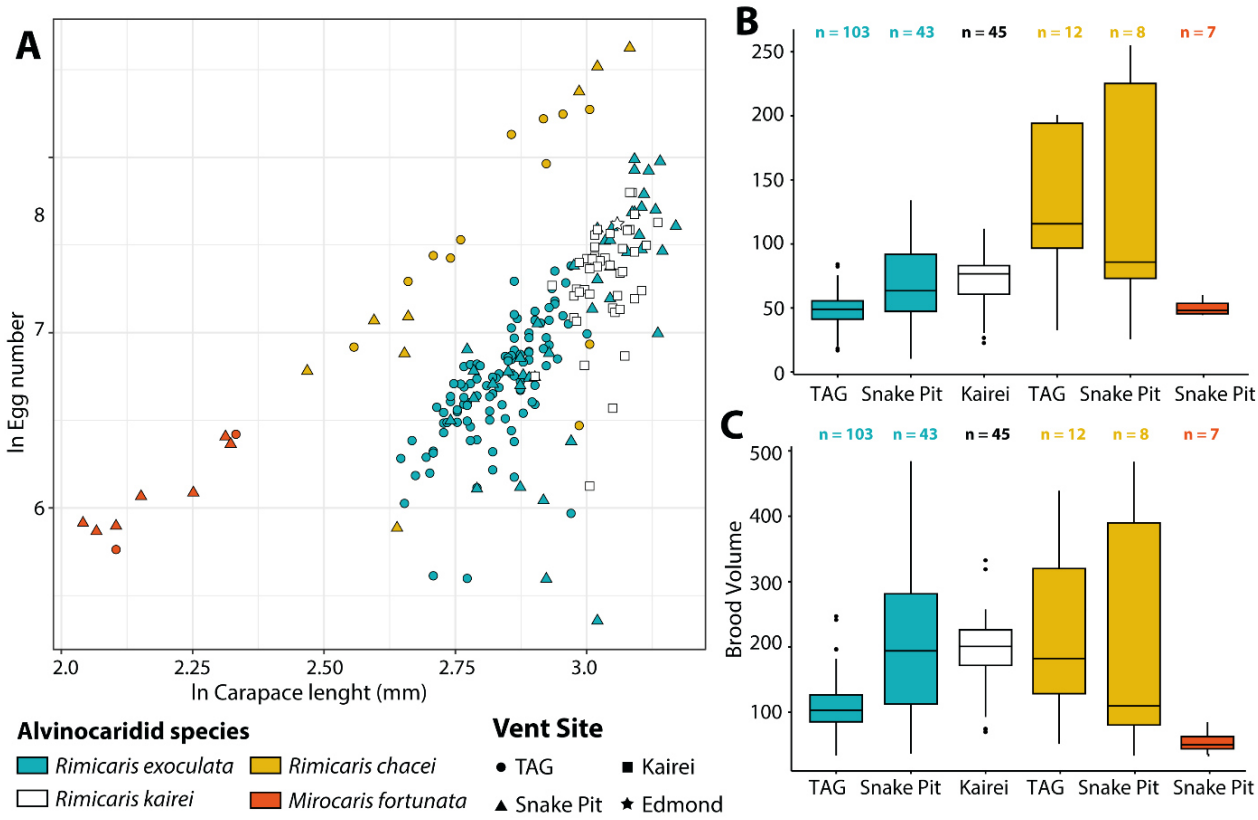


**Fig 73.** Interspecific variations of alvinocaridid fecundity between *R. exoculata*, *R. chacei* and *M. fortunata* at TAG and at Snake Pit and *R. kairei* at Kairei and Edmond. **A.** Variation of $\log_e$-transformed minimum realized fecundity with $\log_e$-transformed carapace length **B.** Fecundity corrected for body size (carapace length). **n**: number of individuals measured. **C.** Brood volume, i.e. the number of egg multiplied by their individual volume.

Differences in egg volume between *R. exoculata* and *R. kairei* were very limited (Kruskal-Wallis, $p < 0.05$) with only slightly larger egg volume for early and mid-stage eggs (Dunn's Multiple Comparison Test, $p > 0.05$) of *R. kairei* from Kairei (early: 0.120 ± 0.0156 $mm^3$; mid: 0.138 ± 0.0151 $mm^3$) compared to similar stage eggs of *R. exoculata* from TAG (early: 0.106 ± 0.0113 $mm^3$; mid: 0.120 ± 0.0133 $mm^3$), (**Fig 73A.**). The proportion of each developmental stage for *R. kairei* from Kairei was quite different from those of *R. exoculata* sampled in 2018 at TAG ($\chi^2$ = 65.161; 2 df; $p < 0.05$) or at Snake Pit ($\chi^2$ = 84.837; 2 df; $p < 0.05$), (**Fig 73B.**). Broods with eggs at early and middle stage were found in equivalent proportion (respectively 46.7% and 48.9%) whereas very few broods with late stage eggs were sampled (4.4%) in *R. kairei* (**Fig 73B.**).

Large differences in relative fecundity were observed between *R. exoculata* and its co-occurring species on the MAR (Kruskal-Wallis H= 52.38, $p < 0.05$), and were not only related to size differences (**Table 10.**). Indeed, *R. chacei* brooding females were either smaller than the *R. exoculata* brooding females for Snake Pit individuals (*R. exoculata*: 20 ± 2.38 mm; *R. chacei*: 16.2 ± 3.83 mm; Dunn's Multiple Comparison Test, $p < 0.05$) or of similar size for TAG (*R. exoculata*: 17 ± 1.34 mm; *R. chacei*: 17.3 ± 2.5 mm; Dunn's Multiple Comparison Test, $p > 0.05$). However, *R. chacei* relative fecundity was always significantly greater than relative fecundity of *R. exoculata* both at TAG (*R. exoculata*: 49.4 ± 12.9; *R. chacei*: 129 ± 59.3; Dunn's Multiple Comparison Test, $p < 0.05$) and at Snake Pit (*R. exoculata*: 69.4 ± 31.2; *R. chacei*: 132 ± 91.2; Dunn's Multiple Comparison Test, $p < 0.05$). On the

other hand, *M. fortunata* from Snake Pit were significantly smaller than *R. exoculata* or any other alvinocaridid, but significant variation could be observed in their relative fecundity (*M. fortunata* Snake Pit: 50.1 ± 6.13; Dunn's Multiple Comparison Test, $p < 0.05$). The greatest realized fecundity was 5565 eggs in an individual from the Snake Pit vent field with a CL of 21.8 mm for *R. chacei* and of 614 eggs in an individual from the TAG vent field with a CL of 10.3 mm for *M. fortunata*. Overall, size-specific fecundity ranged from 25.7 to 255 eggs.mm$^{-1}$ for *R. chacei* and from 38.8 to 60 eggs.mm$^{-1}$ for *M. fortunata*. Similarly, differences in brood volume were observed between *R. exoculata* and its co-occurring species (Kruskal-Wallis, $H= 45.33$, $p < 0.05$), although more limited than between their relative fecundity (**Fig 72C.**). Brood volumes of *M. fortunata* from Snake Pit were much smaller than those of *R. exoculata* at the same vent field (*R. exoculata*: 203 ± 112 mm; *M. fortunata*: 54.8 ± 16.8 mm; Dunn's Multiple Comparison Test, $p < 0.05$). Brood volumes of *R. chacei* were larger than *R. exoculata* at TAG (*R. exoculata*: 109 ± 38.5; *R. chacei*: 222 ± 56.1; Dunn's Multiple Comparison Test, $p < 0.05$) but were similar at Snake Pit (*R. exoculata*: 203 ± 112 mm; *R. chacei*: 215 ± 188; Dunn's Multiple Comparison Test, $p < 0.05$). No variation was found brood volumes of *R. chacei* between TAG and Snake Pit (Dunn's Multiple Comparison Test, $p < 0.05$).

No significant variation could be observed between the egg volumes of *R. exoculata* and *M. fortunata* at Snake Pit at any developmental stage (Kruskal-Wallis, $p < 0.05$), although *M. fortunata* eggs are generally smaller than those of *R. exoculata* (**Fig 73D.**). Additionally, although no increase was found between early and mid-stages of *M. fortunata* (early: 0.106 ± 0.0018 mm$^3$; mid: 0.106 ± 0.008 mm$^3$; Dunn's Multiple Comparison Test, $p < 0.05$), a clearly larger egg volume was observed for eggs at late stage (late: 0.143 ± 0.0288 mm$^3$; Dunn's Multiple Comparison Test, $p < 0.05$). In contrast, egg volumes exhibited significant differences between *R. exoculata* and *R. chacei*, eggs of the later species being significantly smaller at any stage and at any vent sites (Kruskal-Wallis, $p < 0.05$; Dunn's Multiple Comparison Test, $p < 0.05$), (**Fig 73C.** and **73D.**). Surprisingly, we did not observe a gradual increase of egg volumes between the successive developmental stages of *R. chacei*, either for TAG individuals (mid: 0.098 ± 0.0109 mm$^3$; late: 0.097 ± 0.013 mm$^3$) or for Snake Pit individuals (early: 0.089 ± 0.043 mm$^3$; mid: 0.082 ± 0.0072 mm$^3$; late: 0.093 ± 0.0131 mm$^3$) (**Fig 73C.** and **73D.**). In addition, no difference could be detected between the proportion of broods at the different developmental stages in *R. exoculata* and *R. chacei* at TAG ($\chi^2 = 84.837$; 2 df; $p < 0.05$) and at Snake Pit ($\chi^2 = 84.837$; 2 df; $p < 0.05$) or between *R. exoculata* and *M. fortunata* ($\chi^2 = 84.837$; 2 df; $p < 0.05$), (**Fig 73B.**). Proportion of broods with eggs at middle or late stage in *R. chacei* were rather similar at TAG (mid: 25 %; advanced: 41.7 %) and at Snake Pit (mid: 37.5 %; advanced: 37.5 %) whereas broods with early eggs were in minority (TAG: 8.3 %; Snake Pit: 25 %), (**Fig 73B.**). On the other hand, broods with early and middle stage eggs were similar in proportions for *M. fortunata* at Snake Pit (25 % for both) whereas broods with late eggs were the majority (50 %), (**Fig 73B.**).

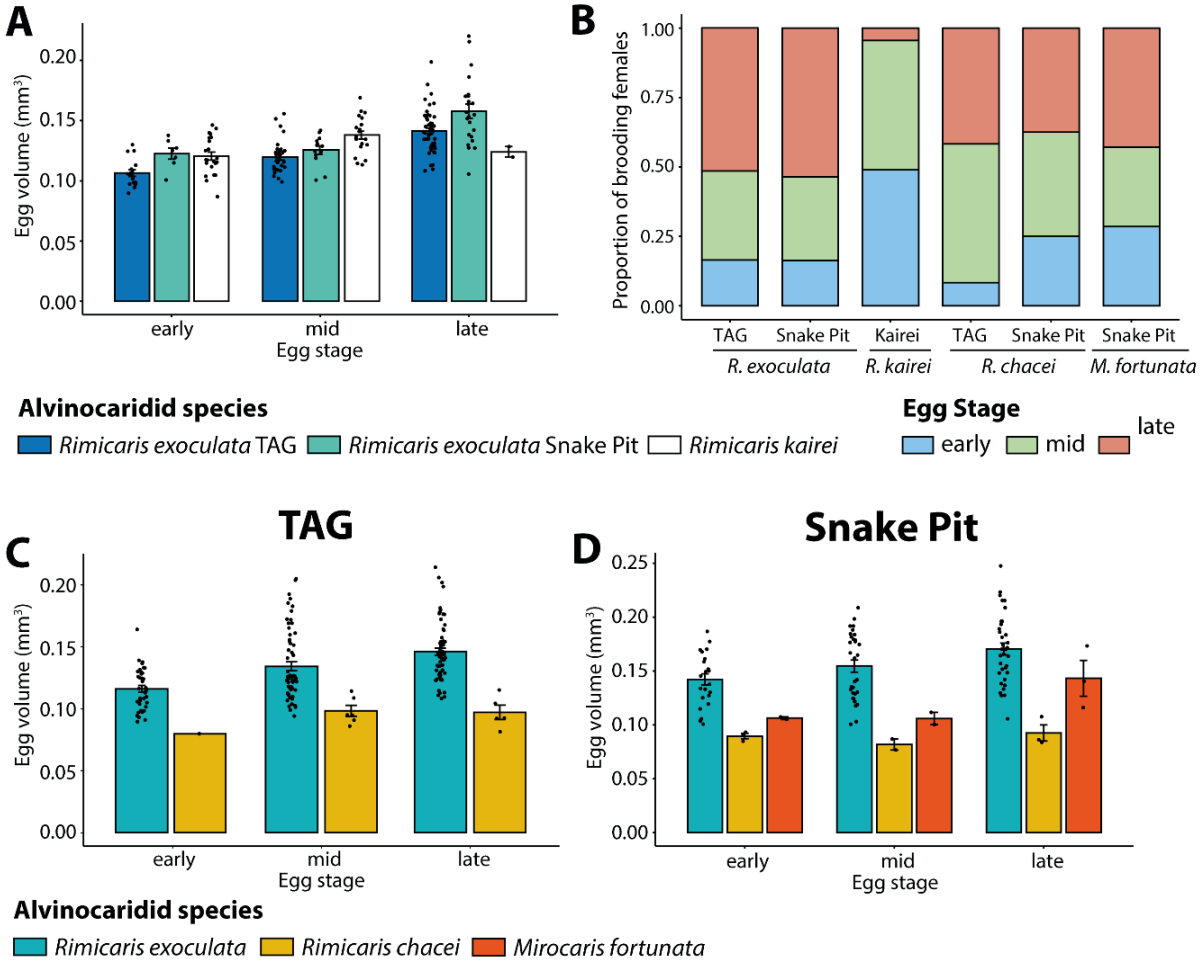


**Fig 74.** Interspecific variations of alvinocaridid egg volumes and developmental stages between *R. exoculata*, *R. chacei* and *M. fortunata* at TAG and at Snake Pit (BICOSE 2; 2018 only) and *R. kairei* at Kairei and Edmond. **A.** Egg volumes at different developmental stages of *R. exoculata* from TAG and Snake Pit compared to those of *R. kairei* from Kairei. **B.** Egg stages proportions of the different alvinocaridids per vent field. **C.** Egg volumes of co-occurring alvinocaridids from TAG at different egg stages. **D.** Egg volumes of co-occurring alvinocaridids from Snake Pit at different egg stages.

### 4.1.3.3. A review of the presence of ovigerous females in *R. exoculata*, its sister species and its co-occurring species along the different sampling years

Summarizing 20 years of sampling along the MAR, only four brooding females of *R. exoculata* only were found among the thousands collected in the period of the year between May and November: one in August 1985 and two in September 1994 at TAG and one in 2006 at the Mephisto vent site (5°S) (**Fig 74.**). It is only in March 2007, at Logatchev that a larger number of ovigerous females were collected although their reproduction was not studied at that time (**Fig 74.**). Between January and early February 2014, an important number of ovigerous were collected with 81 ovigerous females at TAG and 55 ovigerous females at Snake Pit constituting respectively 11.5 % and 4.8% of all the females collected at these vent fields. Most of these ovigerous females were brooding with 47 brooding females and 5 females with hatched broods only at TAG or 49 brooding females and 9 females with hatched broods at Snake Pit. Similarly, between February and early March 2018, many ovigerous females were retrieved as well, with 114 ovigerous females at TAG – 111 brooding and 3 hatched ones

– and 80 females at Snake Pit – 66 brooding and 14 hatched ones – constituting respectively 11% and 5.6% of all the females collected at these vent fields. These proportions of brooding females varied between 3% and 37% in individual samples collected from dense shrimp aggregates at TAG and between 0% and 29% in samples from dense shrimp aggregates at Snake Pit, over all the females collected in these assemblages. On the 5 dense aggregate assemblages collected at TAG in 2018, brooding females were always retrieved whereas brooding females were absent in only 3 dense aggregates out of the 10 collected at Snake Pit. These proportions were slightly lower in 2017 between late March and April with 18 ovigerous females at TAG – 17 brooding and 1 hatched – and 2 females at Snake Pit – one brooding and 1 hatched – constituting only 5% and 0.2% of all the females collected TAG and Snake Pit respectively. At TAG, these proportions varied between 0% and 18.8% brooding females among the total number of females depending on the aggregates, with one aggregate without any brooding females out of the three sampled aggregates. At Snake Pit, they varied between 0% and 0.3% brooding females on all the females depending on the aggregates, with three aggregate without any brooding females out of the four sampled aggregates.

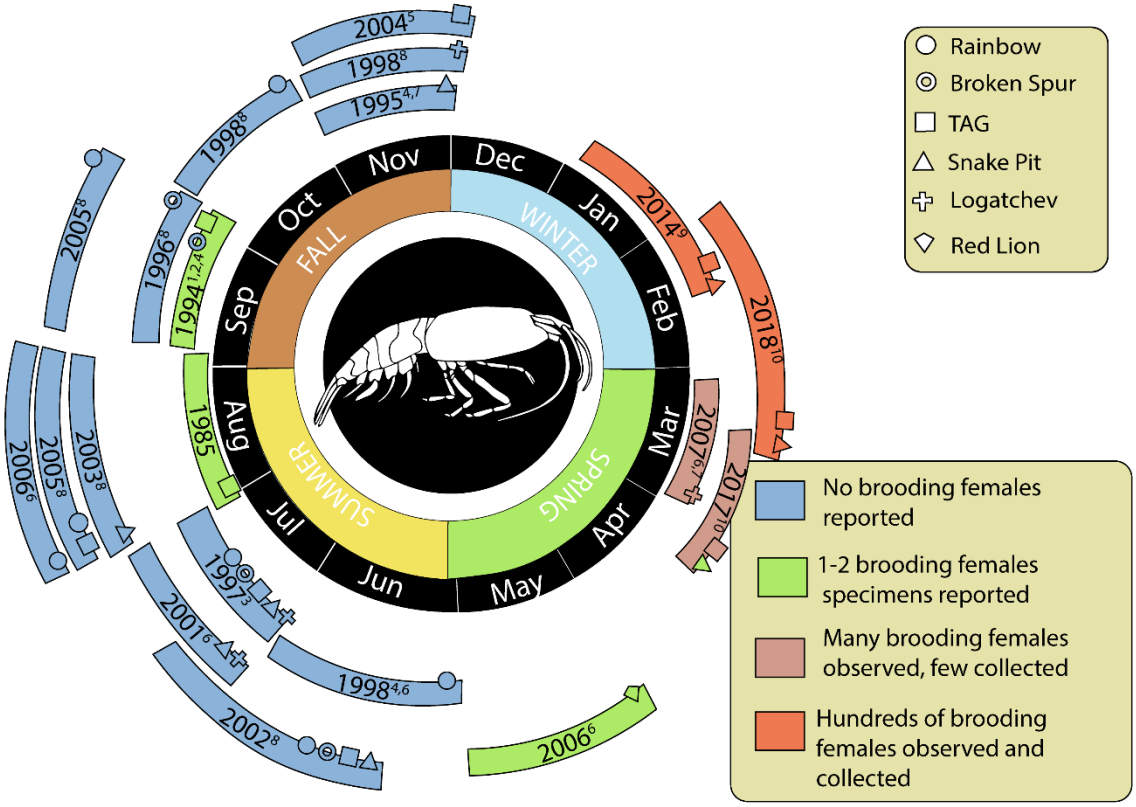


[1]Williams and Rona (1986), [2]Vereshchaka (1997), [3]Shank et al. (1998), [4]Ramirez-Llodra et al. (2000), [5]Copley et al. (2007), [6]Komai and Segonzac (2008), [7]Gebruk et al. (2010), Guri et al. (2012), [8]Lunina & Vereshchaka (2014), [9]Hernandez-Avila thesis (2016), Rapport de Campagne BICOSE (2014), [10]This work

**Fig 75.** Current knowledge on the occurrence of *R. exoculata* brooding females at different periods of the year. Illustration created by Methou from a literature review prepared by Hernández-Ávila.

As for *R. exoculata*, few brooding females of *R. chacei* have been sampled in the period of the year between May and November with only one brooding female collected in June 1994 at Lucky Strike (**Fig 75A.**). However, unlike *R. exoculata*, only few brooding females were collected between January and mid-April until 2018 with only two brooding females collected at Snake Pit in February 2014 (**Fig 75A.**). It is only in January-February 2018, that a larger number of ovigerous females were sampled, 12 – all brooding – at TAG and 11 at Snake Pit – 8 brooding and 3 hatched ones – although they represented higher proportions of their populations, respectively 22.6% and 11.2% off all females collected at TAG and at Snake Pit. On the other hand, brooding females of *M. fortunata* could be collected at almost every period of the year, especially at Lucky Strike were they are more abundant with a large number of brooding individual reported in the period between June and September (**Fig 75B.**). Similarly, between January and April, some brooding individuals were reported despite a lower sampling at these periods (**Fig 75B.**). It is only in November 1995 at Snake Pit that no brooding individual were reported (**Fig 75B.**). In January-February 2018, with a greater sampling effort, 31 ovigerous females – 22 brooding and 9 hatched ones – were collected at TAG and 3 ovigerous females – 2 brooding and 1 hatched ones – at Snake Pit representing respectively 11.8% and 21.8% of all the ovigerous females collected at TAG and Snake Pit.

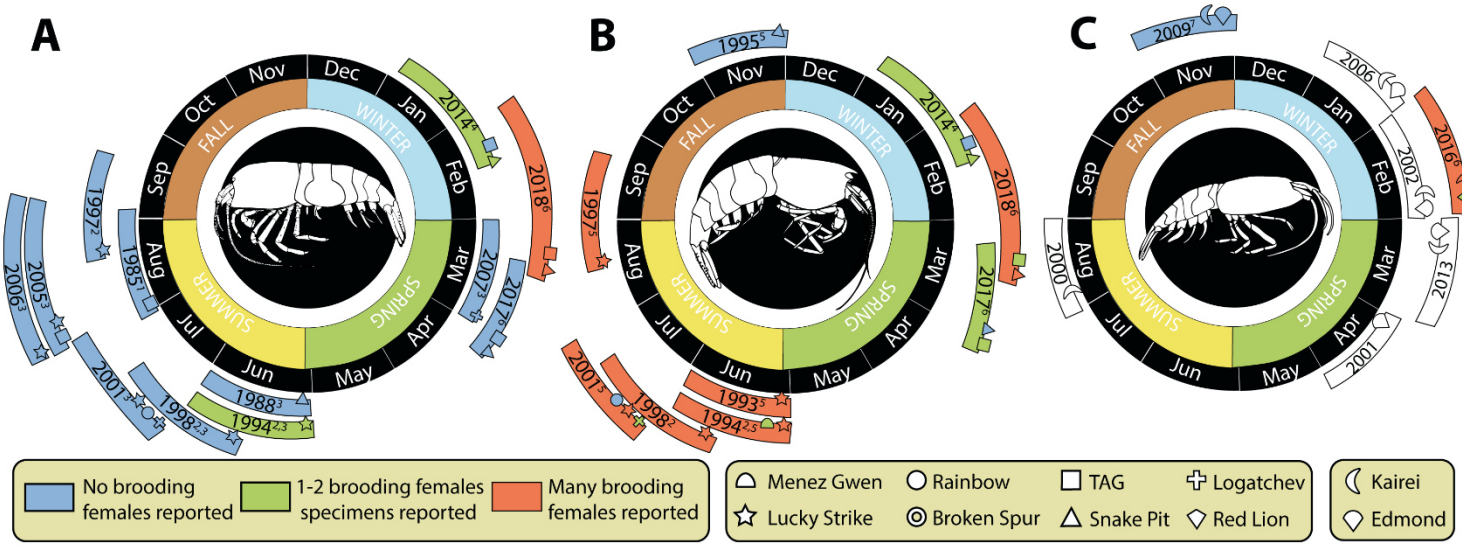


[1]Williams and Rona (1986), [2]Ramirez-Llodra et al. (2000), [3]Komai and Segonzac (2008), [4]Cruise Report BICOSE (2014), [5]Komai and Segonzac (2003), [6]This work, [7]Watanabe personnal communication

**Fig 76.** Current knowledge on the occurrence of brooding females from the other studied alvinocaridids at different periods of the year. **A.** *R. chacei*. **B.** *M. fortunata*. **C.** *R. kairei*. White bar and vent sites symbols represented the cruise for which video data are available in the JAMSTEC data bank that could possibly help us to refine our knowledge concerning the periodicity of *R. kairei* reproduction.

Unfortunately, available data from different cruises were much scarcer for *R. kairei* (**Fig 75C.**). Nonetheless, our data from February 2016, report a large presence of ovigerous females at Kairei (79 ovigerous females representing 8% of the total female population) and some ovigerous individuals at Edmond (two ovigerous females representing only 0.5% of the total female population) (**Table 11.**; **Fig 75C.**). These proportions were much more important if only ovigerous females larger than 12 mm in CL – the smallest size of ovigerous female recorded for its sister species, *R. exoculata* – were considered, representing 18.6% and 3.6% of the total female population of Kairei and Edmond, respectively (**Table 11.**). These ovigerous females were retrieved in 3 aggregates out of the five

sampled at Kairei, representing between 8.8% and 10.4% of the total female population of the different samples, and in 1 aggregates out of the four collected at Edmond, representing 1.1% of the total female population of this sample (8.7% of the total female population with CL > 12 mm). (**Table 11.**). On the other hand, ovigerous were completely absent in the collected shrimps in November 2009 (**Fig 75C.**). Other video and image datasets – and potentially shrimp samples – from JAMSTEC (in white; **Fig 75C.**) should be investigated too as well, to obtain a more detailed dataset concerning the occurrence of ovigerous females of *R. kairei*.

| | Ovigerous | Non ovigerous | Non ovigerous >12mm | %Ovigerous | %Ovigerous >12mm |
|---|---|---|---|---|---|
| **Kairei Total** | 79 | 563 | 346 | 8 | 18.59 |
| **Edmond Total** | 2 | 354 | 53 | 0.49 | 3.64 |
| **Kairei1** | 0 | 64 | 35 | 0 | 0 |
| **Kairei2** | 0 | 61 | 4 | 0 | 0 |
| **Kairei3** | 22 | 101 | 89 | 10.38 | 19.82 |
| **Kairei4** | 23 | 136 | 102 | 8.81 | 18.4 |
| **Kairei5** | 34 | 201 | 116 | 9.69 | 22.67 |
| **Edmond1** | 0 | 30 | 5 | 0 | 0 |
| **Edmond2** | 0 | 48 | 10 | 0 | 0 |
| **Edmond3** | 0 | 124 | 17 | 0 | 0 |
| **Edmond4** | 2 | 152 | 21 | 1.14 | 8.7 |

**Table 11.** Number of ovigerous and non-ovigerous – all and superior to 12 mm of CL – and proportions of ovigerous females versus the total number of females.

## 4.1.4 Directions for future discussion

No variations could be observed in the reproductive output of *R. exoculata* between our different sampling years. The few interannual differences observed for their relative fecundity were mostly related to the size of the individuals collected, the larger brooding females producing a much higher egg number than the smaller ones. Important differences in terms of egg volumes were also observed between the first year of sampling (2014) and the two others (2017 and 2018) although these differences seems related to an observer effect or an effect from the material used. Reproductive characteristics of *R. exoculata* appears then to be very stable over years *(to be put in perspective with temporal patterns in other caridean shrimps from other environments)*.

At a regional scale within the MAR, different strategies seems to exist between the different alvinocaridid species. *R. exoculata* and *R. chacei* are apparently positioned each to one end of the fecundity trade-off that exist between egg number and egg volume in alvinocaridids (**Table 12.**). Indeed, *R. chacei* a much higher relative fecundity than *R. exoculata* but also a smaller egg volume, and both exhibit a relatively similar brood volume – although it might be a bit higher for *R. chacei*. Therefore, differences in terms of maternal investment for brooding might be similar between species, although brooding length should also be considered if it differs between the two. *M. fortunata* reproductive output was quite different with a large egg size, such as *R. exoculata* and a high egg number relatively to its size, even if it remains quite low overall in comparison to its co-occurring species. The reproductive characteristics of our Snake Pit population, much bigger than those from the

Lucky Strike vent fields, did not exhibit large differences that could not be explained by their body size (**Table 12.**).

Brooding period in *R. exoculata* is confirmed to occur at least from January to early April with a total absence or a limited presence of brooding individuals between May and November. Interestingly, brooding period of *R. chacei* appears to be similar although the presence of a large number of brooding females was only confirmed between February and early March, and potentially in January too. Moreover, the absence of brooding females for this species should be taken with caution because of the important difficulty to catch these shrimps in general. On the other hand, *M. fortunata* reproduction appears to be continuous or semi-continuous with a presence of brooding females in almost every sampling: between June and September or between January and March. No informations for March, April, October and December.

Even if temporal patterns in the recruitment phase and reproductive phase of a species lifecycle are not necessarily linked, it is interesting to put in parallel, the discontinuous recruitment for *R. exoculata* and *R. chacei* with the periodic brooding periods, as well as the continuous or semi-continuous recruitment for *M. fortunata* with its continuous or semi-continuous brooding periods (Chapter 3).

At a global scale between the MAR and the CIR, *R. kairei* from the Kairei vent field exhibit a very similar reproductive output in terms of relative fecundity and egg volume – at equivalent embryonic stages – compared to its sister species *R. exoculata* from TAG or Snake Pit. Surprisingly, brooding females in this study were collected at the same period than *R. exoculata* in the month of February. Yet, these two species inhabit vent fields with opposed latitudinal positions: Kairei at 25°S and TAG and Snake Pit respectively at 26°N and 23°N. Reproduction of R. *kairei* could also be continuous unlike its sister species, however ovigerous females were completely absent from *R. kairei* samples in November 2009. More informations from available data of past expedition might clarify the periodicity of this species.

Therefore, reproduction of these two species is probably not synchronized by the seasonal patterns of the surface photosynthetic production, since they are inverted between the two hemispheres. Other environmental cues are then synchronizing the periodicity of the reproduction in *R. exoculata*, *R. kairei* as well as *R. hybisae* (Nye, 2013) – and possibly *R. chacei* – (**Table 12.**), potentially temporal patterns that are specific to hydrothermal vents. If such, this should be put in perspective with other alvinocaridids from different chemosynthetic ecosystems such as *A. stactophila* from cold seeps, as theses environments do not necessarily share the same environmental cues with hydrothermal vent ecosystems. Additionally, since reproductive studies on vent species from the South hemisphere are much less studied than those from the North, our results should also be put in perspective with other species from chemosynthetic ecosystems that exhibit seasonal patterns.

| SPECIE | *Alvinocaris muricola* (n = 9) | *Alvinocaris stactophila* (n= 55) | *Alvinocaris stactophila* (n= 65) | *Mirocaris fortunata* (n= 30) | *Mirocaris fortunata* (n= 7) | *Rimicaris exoculata* (n= 164) | *Rimicaris exoculata* (n= 98) | *Rimicaris kairei* (n= 45) | *Rimicaris chacei* (n= 12) | *Rimicaris chacei* (n= 8) | *Rimicaris hybisae* (n= 562) | *Rimicaris hybisae* (n= 397) |
|---|---|---|---|---|---|---|---|---|---|---|---|---|
| **Site** | **Congo Basin (seep)** | **Gulf of Mexico: Brine Pool IMB (seep)** | **Gulf of Mexico: Brine Pool MMB (seep)** | **MAR: Lucky Strike (vent)** | **MAR: Snake Pit (vent)** | **MAR: TAG (vent)** | **MAR: Snake Pit (vent)** | **CIR: Kairei (vent)** | **MAR: TAG (vent)** | **MAR: Snake Pit (vent)** | **MCSC: Piccard (vent)** | **MCSC: Von Damm (vent)** |
| Depth (m) | 3113-3150 | 500 | | 1690 | 3500 | 3650 | 3500 | | 3650 | 3500 | 4972 | 2294 |
| **SIZE & FECUNDITY** | | | | | | | | | | | | |
| CL (mm) Mean ± SD | 20.7 ± 2.3 | 3.77 | 3.91 | 7.17 ± 0.18 | 8.89 ± 1.04 | 16.6 ± 1.46 | 18.7 ± 2.31 | 20.8 ± 1.0 | 17.3 ± 2.50 | 16.2 ± 3.83 | 10.2 ± 1.5 | 13.9 ± 2.3 |
| Realized Fecundity Mean ± SD | 3130 ± 1180.9 | 147 | 98 | 174.7 ± 22.8 | 449 ± 104 | 773 ± 278 | 1228 ± 589 | 1553 ± 411 | 2259 ± 1208 | 2437 ± 2137 | 341.7 ± 146.2 | 1054.2 ± 229.8 |
| Size-Specific Fecundity Mean ± SD | 149.1 ± 48.0 | 39 | 25 | 24.3 | 50.1 ± 6.13 | 45.9 ± 13.9 | 63.9 ± 24.2 | 74.3 ± 18.3 | 129 ± 59.3 | 132 ± 91.2 | 30.6 ± 11.8 | 68.0 ± 13.2 |
| **EGG SIZE** | | | | | | | | | | | | |
| Mean all stage embryo size (mm) | 0.66 x 0.55 | 0.80 | 0.79 x 0.57 | 0.70 x 0.49 | 0.72 x 0.57 | 0.74 x 0.59 | 0.77 x 0.62 | 0.70 x 0.59 | 0.65 x 0.53 | 0.61 x 0.53 | 0.64 x 0.48 | 0.63 x 0.48 |
| Mean early stage embryo size (mm) | - | - | - | - | - | 0.68 x 0.57 | 0.72 x 0.61 | 0.67 x 0.58 | - | 0.60 x 0.54 | - | - |
| Mean mid stage embryo size (mm) | - | - | - | - | - | 0.73 x 0.59 | 0.73 x 0.59 | 0.72 x 0.60 | 0.65 x 0.54 | - | - | - |
| Mean late stage embryo size (mm) | - | - | - | - | 0.80 x 0.58 | 0.78 x 0.60 | 0.80 x 0.63 | - | 0.66 x 0.53 | 0.64 x 0.53 | - | - |
| **TEMPORAL & SPATIAL PATTERNS** | | | | | | | | | | | | |
| | Periphery of fluids | Periphery of fluids | Periphery of fluids | Close to fluids | Close to fluids | Close to fluids | Close to fluids | Close to fluids | Close to fluids | Close to fluids | Close to fluids | Close to fluids |
| Periodicity | - | Seasonal | Seasonal | Continuous | Continuous | Seasonal | Seasonal | Seasonal ? | Seasonal ? | Seasonal ? | Seasonal | Seasonal |
| **References** | Ramirez-Llodra & Segonzac (2006) | Copley & Young (2006) | Copley & Young (2006) | Ramirez-Llodra et al. (2000) | This work | Hernández-Ávila et al. (in prep) & this work | Hernández-Ávila et al. (in prep) & this work | This work | This work | This work | Nye et al. (2013) | Nye et al. (2013) |

**Table 12.** Summary of the documented alvinocaridids reproductive characteristics. Updated from Nye et al. (2013) with our recent results

## 4.1.5 Supplementary material

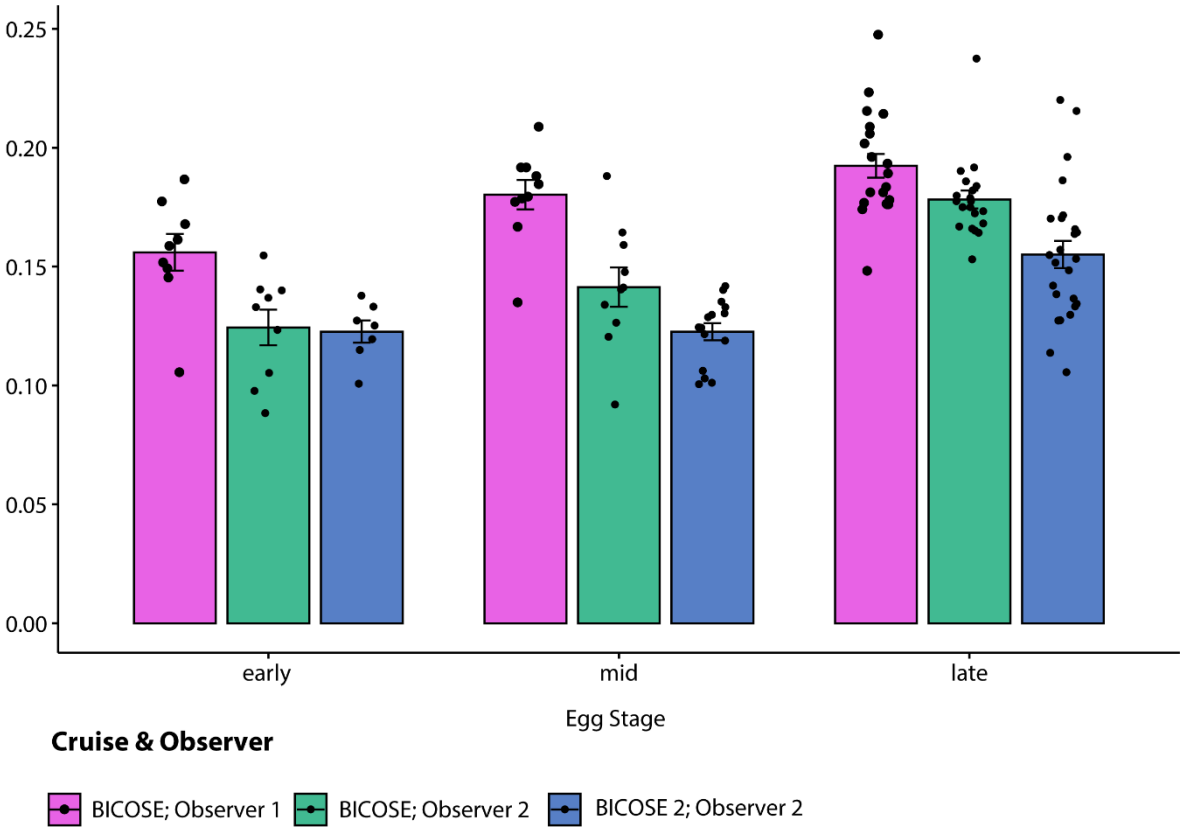


**Fig S6.** Comparison of egg volumes from 2014 (BICOSE Expedition) and from 2018 (Bicose 2) between two observers.

# The Circle of Life

*« A mesure que la partie s'avance, comment ne pas chercher à s'avouer quelles ont été la part du hasard et celle de l'inspiration ? Mais pour que soit accepté un travail, admise une nouvelle façon de penser, il faut épurer la recherche de toute scorie affective ou irrationnelle. La débarrasser de tout relent personnel, de toute odeur humaine.*

*Parcourir la voie royale qui mène une jeunesse balbutiante à une maturité épanouie. Remplacer l'ordre des évènements, des découvertes, par ce qui aurait dû être suivi si, au début, la conclusion avait été connue. Il y a un rite dans la manière de présenter les résultats scientifiques.*

*Un peu comme si l'on écrivait l'histoire d'une guerre d'après les seuls communiqués d'état major. »*

*La Statue Intérieure, Francois Jacob.*

# E.1 Discussion générale

## E.1.1 Connaissances et limitations de notre compréhension du cycle de vie des alvinocarididés

Comme résumé précédemment dans la partie présentant ce modèle d'étude (cf. partie 2.1.4), de nombreuses avancées ont pu être réalisées ces dernières années dans la compréhension du cycle de vie de la crevette hydrothermale *Rimicaris exoculata* (Cowart et al., 2017; Guri et al., 2012; Komai and Segonzac, 2008; Pond et al., 2000; Ramirez-Llodra et al., 2000; Segonzac et al., 1993; Teixeira et al., 2012) ou de celui d'autres alvinocarididés (Beedessee et al., 2013; Copley and Young, 2006; Nye et al., 2013; Ramirez-Llodra and Segonzac, 2006; Tyler and Dixon, 2000; Watanabe et al., 2016). Plus particulièrement, le travail mené par Ivan Hernández-Ávila lors d'une thèse précédente dans ce laboratoire a permis de répondre à de nombreuses interrogations qui demeuraient sans réponses jusqu'alors (Hernández-Ávila, 2016). Entre autres, la découverte en 2014 (expédition BICOSE) d'un nombre important de femelles gravides au sein des agrégats de *Rimicaris* et donc directement en contact avec les fluides hydrothermaux, a permis de rejeter complètement l'hypothèse d'une migration de celles-ci vers la périphérie. Cette hypothèse permettait d'expliquer l'absence ou la faible présence de femelles gravides observée autour des cheminées et postulait que cette migration serait liée à une nécessité de protéger les œufs des hautes températures et des émanations toxiques des cheminées hydrothermales (Ramirez-Llodra et al., 2000). Sur cette base, les travaux d'Ivan Hernández-Ávila ont donc suggéré à la place l'hypothèse d'une reproduction saisonnière s'appuyant sur le fait que cette expédition se situait dans une période de l'année (Janvier – début Février) où il n'y avait encore jamais eu de récolte de ces espèces (Hernández-Ávila, 2016). De plus, ce même travail a aussi révélé l'existence d'une distribution structurée des populations chez cette espèce avec des agrégats près des cheminées actives, majoritairement composés de femelles, des groupes de petits juvéniles autour d'émissions diffuses et des individus épars trouvés en périphérie à la base de ces cheminées, presque exclusivement composés de mâles. Son travail de thèse a aussi permis pour la première fois de décrire les premiers stades larvaires de différents alvinocarididés, dont *R. exoculata*, qui furent collectés dans l'environnement à l'aide d'une pompe à larve nouvellement développée au laboratoire (SALSA), là où les rares études précédentes sur ces stades avaient été réalisées uniquement avec des larves ayant éclos après prélèvement de leur mère (Hernández-Ávila et al., 2015). Ainsi, l'observation détaillée de l'anatomie externe de ces larves a révélé de faibles capacités natatoires (absence de pléopodes et péréopodes peu développés) ainsi qu'une lécitotrophie primaire (pièces buccales non développées, réserves lipidiques importantes) au début de leur vie larvaire (Hernández-Ávila et al., 2015). Enfin, quelques résultats préliminaires avaient pu être obtenus concernant la colonisation microbienne à la surface des œufs de *R. exoculata* au cours de leur développement (observations SEM, clonage et séquençage Sanger), mais nécessitaient d'être complétés en utilisant d'autres techniques (Hernández-Ávila, 2016).

Néanmoins de nombreuses lacunes dans la compréhension de leurs cycles de vie persistaient encore, en particulier concernant la dispersion des larves, la plupart des stades larvaires n'ayant jamais été observés. Plus particulièrement, l'hypothèse d'une saisonnalité ainsi que les limites exactes de la (des) période(s) de reproduction chez *R. exoculata* nécessitaient encore d'être confirmées par d'autres expéditions aux mêmes périodes de l'année (entre Décembre et Mars). De la même façon, bien que la distribution des plus jeunes stades juvéniles de cette espèce ait été caractérisée, le séquençage de ces

individus, correspondant à priori à des *R. chacei*, laissait supposer l'existence d'une erreur d'identification de ces stades, empêchant de confirmer l'étendue exacte de leur distribution au sein des sites hydrothermaux (Hernández-Ávila, 2016). De plus, bien que la distribution des mâles et des femelles chez *R. exoculata* semblait se faire en fonction de la distance des individus par rapport à l'émission de fluides, il restait encore à vérifier si cette organisation de leurs populations était liée à une préférence/tolérance pour certaines conditions environnementales précises. Enfin, et malgré une première étude sur le sujet (Guri et al., 2012), les mécanismes de transmission des symbiotes entre générations restaient encore très mal compris, en particulier ceux des groupes bactériens spécifiques aux communautés microbiennes du système digestif : les Mollicutes et les *Deferribacteres*.

## E.1.2 Les apports de ce travail de thèse à la compréhension du cycle de vie des *Rimicaris*

Le travail de thèse réalisé ici a permis de combler une partie des manques mis en lumière plus haut, mais aussi de répondre à certains questionnements en apportant de nouvelles informations sur une partie des étapes du cycle de vie de *R. exoculata*. En particulier, une meilleure compréhension des étapes du recrutement des stades juvéniles, de la reproduction de cette espèce ainsi que de la caractérisation des habitats des différents stades connus a pu être apportée, et a permis d'avancer de nouvelles hypothèses quant à l'acquisition des symbiotes et la dispersion.

De plus, la récolte d'un nombre important de *R. chacei* lors de l'expédition BICOSE 2 en 2018, aussi bien des stades adultes que des juvéniles, a donné la possibilité d'étendre cette étude à une autre espèce, présente sur les mêmes sites que *R. exoculata*. Se basant sur un échantillonnage plus limité, quelques informations supplémentaires furent aussi obtenues sur *M. fortunata*, une autre espèce de la même famille coexistant avec les deux autres. La comparaison de ces espèces a ainsi fait ressortir les similitudes et les divergences de leurs traits d'histoire de vie, soulignant des stratégies de cycle de vie différentes qui pourraient expliquer, en partie, la coexistence et la persistance sur le long terme de ces animaux sur les mêmes sites. Ceci a donc abouti à une réévaluation de la présentation du cycle de vie de *R. exoculata* faite précédemment (**Fig 52.**) par celle proposée ici pour *R. exoculata* (**Fig 76.**) et *R. chacei* (**Fig 77.**), résumant les quelques avancées réalisées durant cette thèse.

### E.1.2.1 Nutrition et acquisition des différents symbiotes

La présence d'assemblages bactériens sur les œufs, composés principalement ou en partie des symbiotes de *R. exoculata* avait déjà été étudiée précédemment (Cowart et al., 2017; Guri et al., 2012), tout comme les modes de nutrition de leurs stades précoces (Gebruk et al., 2000; Pond et al., 2000; Vereshchaka et al., 2000). Cependant plusieurs points nécessitaient encore d'être clarifiés, afin de déterminer le début et l'évolution de la colonisation bactérienne au cours du développement des œufs mais aussi la localisation précise de chacun des groupes bactériens pour ces stades de vie.

Afin d'y répondre, ce travail (Chapitre 1 ; (Methou et al., 2019a)), additionné aux résultats préliminaires d'Ivan Hernández-Ávila (Hernández-Ávila, 2016), a pu montrer que cette colonisation bactérienne démarre rapidement, juste après l'oviposition, avec l'observation de quelques bactéries présentes sur l'enveloppe des œufs, dès les premières divisions cellulaires. De plus, ces mêmes résultats montrent une augmentation de cette couverture bactérienne sur l'enveloppe des œufs au cours du développement embryonnaire. Cependant, celle-ci ne devient importante qu'aux stades

avancés, lorsque des structures larvaires commencent à être visibles. Parmi les bactéries colonisant ces stades, les différentes lignées de symbiotes de la cavité céphalothoracique ont été retrouvées, incluant des *Epsilonbacteraeota*, des *Gammaproteobacteria* et des *Zetaproteobacteria*, toutes localisées sur la surface des œufs. Une diversité bactérienne similaire a aussi pu être observée sur les œufs de *R. chacei* (**Fig 52.**). La comparaison des pontes provenant des sites TAG et Snake Pit a mis en évidence une forte influence du site sur la diversité bactérienne associée aux pontes de *R. exoculata*, possiblement liée à la chimie des fluides. Cette influence de la composition du fluide est d'autant plus soutenue lorsque cette comparaison est étendue à la diversité bactérienne d'une ponte de Logatchev, site dont les fluides sont riches en méthane ($[CH_4]$ = 2.1 – 3.5 mM) (Fouquet et al., 2010; Guri et al., 2012). Sur cette ponte, un nombre important de *Gammaproteobacteria* méthanotrophes a été identifié, là où ces mêmes bactéries sont absentes des pontes de *R. exoculata* provenant de TAG ($[CH_4]$ = 0.15 mM) ou Snake Pit ($[CH_4]$ = 0.062 mM). Enfin, la comparaison d'œufs localisés à différents endroits d'une même ponte a montré une forte influence de la position de l'œuf au sein de la ponte sur la couverture bactérienne, importante sur les œufs situés à l'extérieur et donc en contact direct avec le fluide, et faible avec pas ou peu de bactéries pour les œufs situés à l'intérieur, plus proches de l'abdomen de leur mère et donc ayant peu de contact avec le fluide.

En plus de cette probable influence de la composition du fluide, cette diversité est aussi fortement influencée par le type de surface colonisée avec l'existence d'assemblages bactériens spécifiques aux œufs. En effet, la diversité associée aux pontes comparée à celle du pléopode de la mère, deux surfaces soumises aux mêmes conditions environnementales, montrent que des assemblages bactériens provenant de deux pontes différentes et provenant de sites hydrothermaux différents sont plus semblables entre eux que les assemblages bactériens du pléopode et de la ponte provenant de la même mère. La raison de cette spécificité reste en revanche mal comprise et pourrait aussi bien être liée aux caractéristiques physico-chimiques de la surface de colonisation qu'à l'existence de mécanismes de sélection mis en place par la mère pour faciliter/favoriser l'installation de certaines bactéries spécifiques et limiter/empêcher le développement d'autres bactéries. Parmi eux, il semblerait que la crustine, un peptide antimicrobien exprimé à la surface des œufs et uniquement sur les parties colonisées aux stades avancés, puisse participer à cette sélection (Chapitre Annexes). Cette possible sélection active par l'animal, laisse penser que ces bactéries pourraient avoir un rôle pour les œufs, même s'il n'est pas prouvé ici. En revanche, et ce malgré la présence des mêmes lignées bactériennes que les symbiotes du céphalothorax, un rôle de détoxification est plus envisagé qu'un rôle de nutrition. Avec la couverture bactérienne qui se concentre principalement sur les œufs de l'extérieur de la ponte, celle-ci constitute une sorte de barrière entre les œufs et le milieu environnant. Dans ce contexte les bactéries pourraient avoir un rôle de protection, via leurs métabolismes. Celles-ci pourraient en effet détoxifier les composés néfastes pour ces stades de vie, notamment ceux du fluide hydrothermal. Dans le cas d'un apport nutritionnel de ces bactéries, chaque œuf aurait un apport en nourriture différent selon sa position dans la ponte suggérant donc des réserves de taille différente en fin de développement, ce qui n'a pas été observé lors des mesures pour l'étude de reproduction. L'importance des réserves ayant une influence forte sur la survie des larves, on aurait dans ce cas-ci des larves avec des potentiels différents selon la position qu'elles occupaient dans la ponte.

Bien qu'en faible nombre et retrouvées de manière irrégulière selon les pontes, des lignées d'*Entomoplasmatales* – classe des Mollicutes – correspondant à un des groupes de symbiotes du système digestif ont aussi pu être parfois identifiées. Leur absence sur les autres pontes pourrait être

liée à des limitations techniques en termes de profondeur de séquençage. Notre étude est cependant la deuxième à observer une possible présence de ces *Entomoplasmatales*, en utilisant une technique de séquençage différente et des œufs de sites différents de l'étude précédente (Cowart et al., 2017; Methou et al., 2019a). Leur localisation précise n'a en revanche pas pu être déterminée et leur réelle présence à ces stades de vie reste à démontrer. Si tel est le cas, une possible transmission maternelle durant ou précédant la période de couvaison pourra être envisagée. Concernant les autres groupes bactériens, l'absence de donnée actuelle sur les stades larvaires empêche d'établir clairement si ceux-ci peuvent être transmis de l'enveloppe, perdus après l'éclosion, à un quelconque organe hôte des larves ou si cette transmission intervient plus tard au cours de leur cycle de vie, lorsqu'elles atteignent et s'installent sur un site hydrothermal par exemple. Quelques observations microscopiques sur une larve éclose lors de la remontée sur le navire n'ont pas permis de statuer quant à la présence de bactéries à ces stades, ni sur l'existence d'un quelconque organe hôte receveur (**Fig 53.**). Cependant, ces résultats restent limités à un seul individu et sont potentiellement biaisés par le fait que son éclosion soit probablement liée à un stress de la remontée et que son développement n'ait peut-être pas été complètement terminé.

Concernant les autres stades de vie, la présence de symbiotes d'*Epsilonbacteraeota* et de *Gammaproteobacteria* colonisant les différentes pièces buccales (scaphognathites et exopodites) ainsi que les branchiostegites des stades juvéniles les plus précoces a pu être confirmée pour *R. exoculata* que et reste en cours d'investigation pour *R. chacei* (**Fig 58**.; résultats stage de M. Gueganton). La présence des symbiotes du système digestif n'a pour l'instant pas été étudiée sur d'autres stades que les stades adultes et leur localisation précise, utilisant des sondes FISH spécifiques, doit encore être précisée. Dans ce sens, les récents résultats obtenus avec une sonde *Deferribacteres* nouvellement développée laisse présager pour la suite une caractérisation précise de la présence de ces symbiotes des stades juvéniles jusqu'aux stades adultes chez *R. exoculata* et *R. chacei* (Thèse Marion Gueganton).

Les résultats isotopiques obtenus (Chapitre 2) montrent l'existence d'un changement trophique depuis un régime basé sur une nutrition non chimiosynthétique, hors de la zone d'influence hydrothermale du site, progressivement remplacé par une alimentation fournie par les symbiotes chimiosynthétiques aux stades adultes. Ainsi, ces résultats confirment ceux obtenus précédemment pour *R. exoculata* (Gebruk et al., 2000; Vereshchaka et al., 2000) et prouvent qu'un changement trophique similaire a lieu également chez *R. chacei*.

Les résultats isotopiques obtenus durant cette thèse ont aussi permis de montrer que la distribution des adultes entre zones actives et zones périphériques n'a à priori aucun effet sur leur nutrition, des femelles provenant des agrégats et des mâles provenant des agrégats ou épars à la périphérie présentant pratiquement les mêmes niches isotopiques sur un site donné (**Fig 59.**). Cette absence de distinction trophique, malgré une influence hydrothermale différente, pourrait être liée à une mobilité importante des mâles qui vont et viennent entre la périphérie et les agrégats proches du fluide ou à une maintenance d'une symbiose similaire malgré une influence du fluide amoindrie. L'analyse comparant les communautés symbiotiques des mâles (périphérie ou agrégat) et des femelles (agrégat) viendra compléter ces résultats (Thèse V. Cueff-Gauchard).

### E.1.2.2 Dispersion et développement larvaire

En raison de la difficulté à récolter les différents stades planctoniques de *Rimicaris* ou même d'alvinocarididés en général, malgré les nouveaux moyens techniques mis en place – 5 larves récoltées

lors de la mission BICOSE (2014) par la pompe SALSA; 1 larve récoltée lors de l'expédition BICOSE 2 (2018), – le travail effectué durant cette thèse s'est concentré sur la partie benthique du cycle de vie et peu d'éléments ont pu être apportés sur la phase larvaire planctonique. Ainsi cette thèse reste en accord avec le modèle de dispersion larvaire proposé par (Hernández-Ávila, 2016), à savoir une longue période de dispersion avec un développement étendu et une lécitotrophie primaire suivie par une phase planctotrophe où la larve se nourrit dans son environnement. Bien que la totalité de la durée de cette phase larvaire ne puisse être évaluée pour le moment, la durée du premier stade larvaire (sans être nourrie) pourrait s'étendre de quelques jours à plus de 100 jours selon l'espèce et les conditions de température, d'après les résultats obtenus pour deux autres alvinocarididés *Shinkaicaris leurokolos* et *A. longirostris* (Watanabe et al., 2016). Cette phase de dispersion pourrait comprendre six stades larvaires ou plus, comme c'est le cas chez d'autres crevettes caridés ayant un développement étendu (Anger, 2001). Enfin, la dispersion des larves de *Rimicaris* est probablement limitée aux zones aphotiques de l'océan de par leur tolérance physiologique aux conditions environnementales. En effet, d'après les données de (Tyler and Dixon, 2000), les larves de *M. fortunata* sont incapables de supporter des températures supérieures à 20°C à pression atmosphérique, comme c'est le cas pour les eaux de surface. Si les larves de *Rimicaris* présentent des tolérances similaires, celles-ci sont donc aussi incapables de survivre dans les zones de la colonne d'eau où la production primaire photosynthétique est la plus importante.

Malgré tout, la révision de l'identification des stades juvéniles des *Rimicaris* de la dorsale médio-Atlantique couplée à des analyses isotopiques (Chapitre 2) a indirectement révélé de nouvelles informations concernant la dispersion de *R. exoculata* et *R. chacei*.

En effet, la comparaison des niches isotopiques des premiers stades juvéniles de ces deux espèces – dont les compositions isotopiques traduisent l'influence de leur nutrition/habitat passé – a montré une claire séparation de leurs niches respectives. Cette ségrégation indique donc que ces deux espèces se nourrissent de sources trophiques différentes et/ou vivent dans des habitats différents n'occupant pas la même position dans la colonne d'eau – et donc n'étant potentiellement pas transportées par les mêmes courants non plus – durant au moins une partie de leur vie larvaire. En dehors de ces nouvelles données, une meilleure compréhension de la vie larvaire de ces espèces ne pourra être apportée que par la récolte ou l'élevage en aquarium de ces stades de vie.

### E.1.2.3 Recrutement et distribution des différents stades de vie sur les sites hydrothermaux

La distribution des stades juvéniles précoces de *R. exoculata* avait déjà été étudiée précédemment par (Hernández-Ávila, 2016) et dans une moindre mesure par (Segonzac et al., 1993). Cependant, les problèmes d'identifications entre les juvéniles *R. chacei* et *R. exoculata*, déjà identifiés par (Hernández-Ávila, 2016), ont empêché de réellement comprendre la répartition exacte de chacun au sein des sites.

La révision taxonomique de l'identification des stades juvéniles d'alvinocarididés de la ride médio-Atlantique réalisée au cours de cette thèse (Chapitre 2) a là encore permis de réévaluer la distribution de chacun des stades de vie se trouvant sur les sources hydrothermales et de comparer la structure de population de ces espèces (Chapitre 3). Cette caractérisation de leur distribution a de plus été complétée par l'acquisition de données environnementales (température, composition chimique du fluide) associées à plusieurs prélèvements de crevettes. Premièrement, il apparaît clairement

maintenant que le recrutement des juvéniles de *R. chacei* se fait à des tailles bien inférieures à celles des juvéniles de *R. exoculata* (Chapitres 2 et 3), contrairement à ce qui été admis jusqu'alors (Komai and Segonzac, 2008). De plus, bien que le nombre d'individus soit limité, il semblerait également que les juvéniles de *M. fortunata* soient recrutés à des tailles encore inférieures à celles de *R. chacei*, même si une taille minimale de ces stades pour cette espèce ne peut pas être établie avec autant de certitude que pour les deux autres. Ce recrutement apparaît chez les deux espèces de *Rimicaris* comme discontinu, avec l'existence de plusieurs cohortes, contrairement à *M. fortunata* où la présence d'une unique cohorte semble plutôt indiquer un recrutement continu (Chapitre 3). Tout comme pour les adultes, les juvéniles de *R. exoculata* et *R. chacei* occupent d'une manière générale des assemblages différents avec des juvéniles de *R. exoculata* majoritairement retrouvés au sein ou accolés aux agrégats d'adultes situés sur les édifices, tandis que les juvéniles de *R. chacei* s'agrègent à la base ou à la périphérie de ces édifices, près de sorties de fluides diffus. Les zones de recrutement semblent donc différentes entre les deux espèces, cependant quelques juvéniles de *R. exoculata* ont été retrouvés en périphérie de manière exceptionnelle tout comme une minorité de *R. chacei* a pu être récoltée dans des petits agrégats d'adultes de la même espèce. Ainsi les niches thermiques des deux espèces – reconstituées à partir des données de température associées aux différent prélèvements de crevettes – ne varient pas au cours de leur cycle de vie et sont donc les mêmes pour tous les stades de vie d'une espèce donnée.

Bien que les stades adultes soient probablement les stades les mieux caractérisés du cycle de vie de ces espèces, de nouvelles données ont pu être apportées durant cette thèse, en particulier concernant *R. chacei* (Chapitre 3). En effet, cette dernière était décrite comme vivant de manière solitaire ou en petits groupes de quelques individus (Apremont et al., 2018; Komai and Segonzac, 2008; Segonzac et al., 1993). Cependant, la découverte de petits agrégats de *R. chacei* durant l'expédition BICOSE 2, en général cachés soit entre des roches soit au sein des moulières, vient nuancer cette idée et suppose une présence plus importante de cette espèce que précédemment avancé. La structure de population de *R. exoculata* entre mâles à la périphérie et femelles au sein des agrégats, observée à TAG précédemment (Hernández-Ávila, 2016), a pu être reconfirmée 4 ans plus tard sur ce site ainsi que sur le site Snake Pit. Cependant, contrairement à ce qui avait été proposé, cette organisation ne semble pas être liée aux facteurs environnementaux du gradient de mélange, les niches thermiques étant les mêmes pour les mâles et les femelles. Bien que d'autres facteurs environnementaux mériteraient d'être considérés, il est possible que cette structuration des populations de *R. exoculata* dans les sites hydrothermaux soit le résultat d'une certaine forme d'organisation sociale chez ces espèces. Une certaine forme d'interaction sociale a d'ailleurs récemment été aussi suggérée par une autre étude décrivant les comportements d'individus incubées expérimentalement sous pression (Ravaux et al., 2019), ces derniers restant en groupe collés les uns aux autres, même en l'absence de stimuli externe. Cette structuration n'a en revanche pas été observée chez *R. chacei*, chez qui des sex ratio relativement équilibrés ont été relevés pour chaque point de prélèvement. La comparaison des niches des deux espèces a permis de mettre en évidence leurs différences avec notamment une plus large niche thermique pour *R. exoculata* englobant toute la zone de mélange entre eau de mer et fluides jusqu'à 40°C. Cette niche thermique de *R. exoculata* englobe ainsi celle des autres espèces d'alvinocarididdés avec une niche encore plus limitée pour *M. fortunata* comparé à *R. chacei*.

Enfin, le prélèvement de crevettes au même endroit mais à plusieurs jours d'intervalle a aussi permis d'évaluer succinctement les dynamiques temporelles de ces populations sur de courtes échelles de temps. Ainsi, il a pu être montré que certains micro-habitats restaient extrêmement stables

sur des périodes d'une dizaine de jours, avec les mêmes proportions de chaque espèce mais aussi de chaque stade de vie par espèce. A l'inverse, d'autres micro habitats étaient extrêmement variables, allant même jusqu'à la disparition complète d'un agrégat de *R. exoculata* pour être remplacé par un groupe de *R. chacei*. En revanche, l'absence de mesures systématiques des conditions physico-chimiques du fluide empêche à l'heure actuelle de déterminer si ces variations sont liées à des facteurs environnementaux.

### E.1.2.4 Maturité sexuelle et reproduction

D'importantes avancées ont pu être faites récemment concernant la reproduction de *R. exoculata*, notamment la découverte en 2014 d'un nombre important de femelles gravides au sein des agrégats, à une période de l'année encore jamais échantillonnée précédemment (Janvier – Début Février), suggérant l'idée d'une reproduction saisonnière pour cette espèce, qui nécessitait cependant encore d'être confirmée. De plus cette même étude a fourni une estimation de la taille moyenne à laquelle la différentiation sexuelle peut être observée chez *R. exoculata,* permettant de séparer les petits adultes des individus subadultes.

Partant de là, le travail effectué durant cette thèse (Chapitre 4) a cherché à vérifier cette saisonnalité de la reproduction de *R. exoculata* en comparant ces échantillons de 2014 avec ceux récoltés en 2017 (expédition HERMINE, fin mars – début avril, échantillons assez limités) et en 2018 (expédition BICOSE 2, février – début mars). Ces échantillonnages ont ainsi permis de confirmer la présence de femelles gravides, étendant la période de reproduction au moins de début janvier jusque début mars, supportant ainsi l'hypothèse d'une reproduction saisonnière. Comme en 2014, la présence d'au moins quelques femelles gravides fut confirmée pour pratiquement chaque prélèvement d'agrégats en février – début mars 2019 tandis que leur nombre semblait plus limité en fin mars – début avril 2017. La comparaison des femelles gravides des différentes années a montré une reproduction extrêmement stable, sans aucune variation de fécondité relative – c.à.d. le nombre d'œufs rapporté à la taille de la femelle – ou de taille des œufs – mesure du diamètre – selon les années.

De plus, l'échantillonnage de 2018 a pu permettre la récolte d'un nombre suffisamment important de femelles gravides de *R. chacei* et de *M. fortunata* pour étudier la reproduction de ces espèces et les comparer aux *R. exoculata* des mêmes sites. Ainsi des stratégies de reproduction différentes ont pu être mises en évidence entre *R. exoculata* et *R. chacei,* avec un bien plus grand nombre d'œufs par femelle chez *R. chacei* à tailles équivalentes mais avec des œufs plus petits. Comparée aux données de la littérature (Cambon-Bonavita, 2014; Komai and Segonzac, 2003, 2008; Ramirez-Llodra et al., 2000; Williams and Rona, 1986), cette reproduction apparaît comme potentiellement saisonnière pour *R. chacei* aux mêmes périodes de l'année que *R. exoculata*, cependant l'absence de femelles gravides à d'autres périodes pourrait aussi être liée à la difficulté de récolter cette espèce tout simplement. Concernant *M. fortunata*, il semblerait que tout comme son recrutement, sa reproduction soit continue, des prélèvements de femelles gravides ont effectivement été rapportés pratiquement à chaque campagne de prélèvements ayant récolté ces animaux. Ceci suggère donc que la biologie de la reproduction de ces espèces n'est pas nécessairement contrainte phylogénétiquement, contrairement à ce qui a pu être proposé pour la reproduction de certaines espèces profondes (Ramirez-Llodra et al., 2000; Tyler and Young, 1999).

Enfin sur ce sujet, l'un des résultats les plus importants de ce travail vient certainement de la comparaison de la reproduction de *R. exoculata* avec celle de son espèce sœur, *R. kairei,* vivant dans l'océan Indien. En dehors du fait qu'elles présentent une reproduction quasiment identique en termes de fécondité – nombre et volume des œufs – elles présentent toutes les deux une importante présence de femelles gravides en Février-Mars. En revanche leur répartition géographique est totalement opposée pour celles dont la reproduction a été étudiée, avec une distribution de *R. exoculata* dans l'hémisphère nord (TAG : 26°N Snake Pit : 23°N), tandis que les *R. kairei* provenaient de l'hémisphère sud (Kairei : 25°S). Etant donné l'absence de lumière et donc de photosynthèse, aucun facteur saisonnier spécifique aux sources hydrothermales n'est aujourd'hui connu. Ainsi, l'existence de reproduction saisonnière dans ces environnements a souvent été supposé être le résultat d'un pic de photosynthèse au début du printemps, qui serait perçu par ces espèces via l'augmentation d'apport de matière photosynthétique tombant au fond (Copley and Young, 2006; Dixon et al., 2006; Tyler et al., 2007). Le fait que les deux espèces sœurs de *Rimicaris* se reproduisent durant les mêmes mois bien qu'elles vivent dans des hémisphères opposés – et donc soumises à des cycles saisonniers également opposés - est extrêmement surprenant. Cela semble contredire l'hypothèse générale selon laquelle les phénomènes de reproduction saisonnière dans les environnements profonds seraient liés aux cycles saisonniers de la production photosynthétique de surface. Une autre possibilité qui n'est pas encore à exclure est que *R. kairei,* contrairement à son espèce sœur, ne présente pas une reproduction saisonnière mais continue. Cependant, une campagne ayant eu lieu dans cette zone en dehors de la période Janvier-Mars n'a pas permis d'observer ou de collecter une seule femelle gravide en Octobre-Novembre 2009 (Watanabe, communication personnelle).

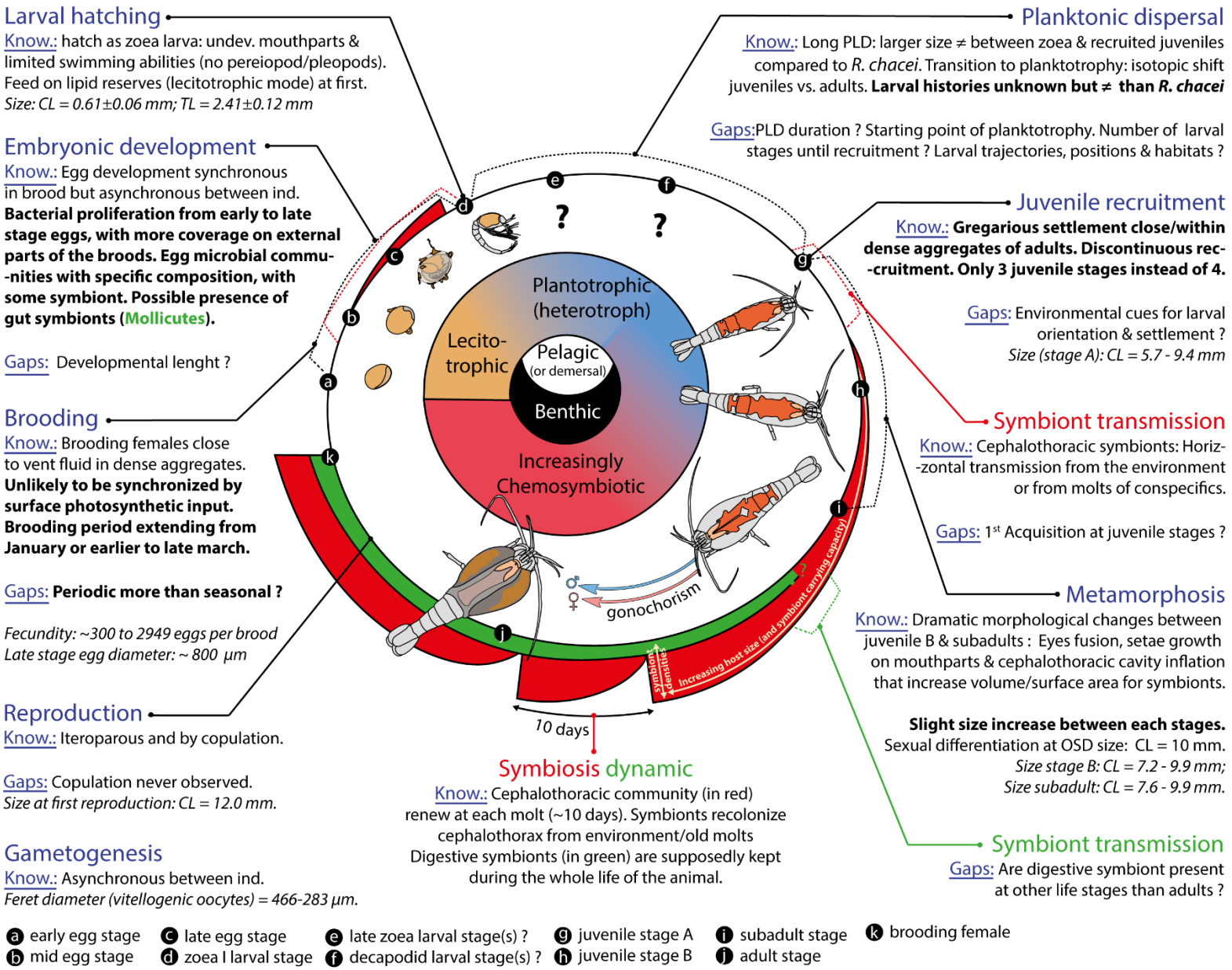


**Fig 77.** Diagram displaying currents knowledge and gaps in the lifecycle of *R. exoculata* including the new advances realized during this thesis. Largely inspired from the diagram depicting the life cycles of bathymodiolin mussels of Laming et al. (2018)

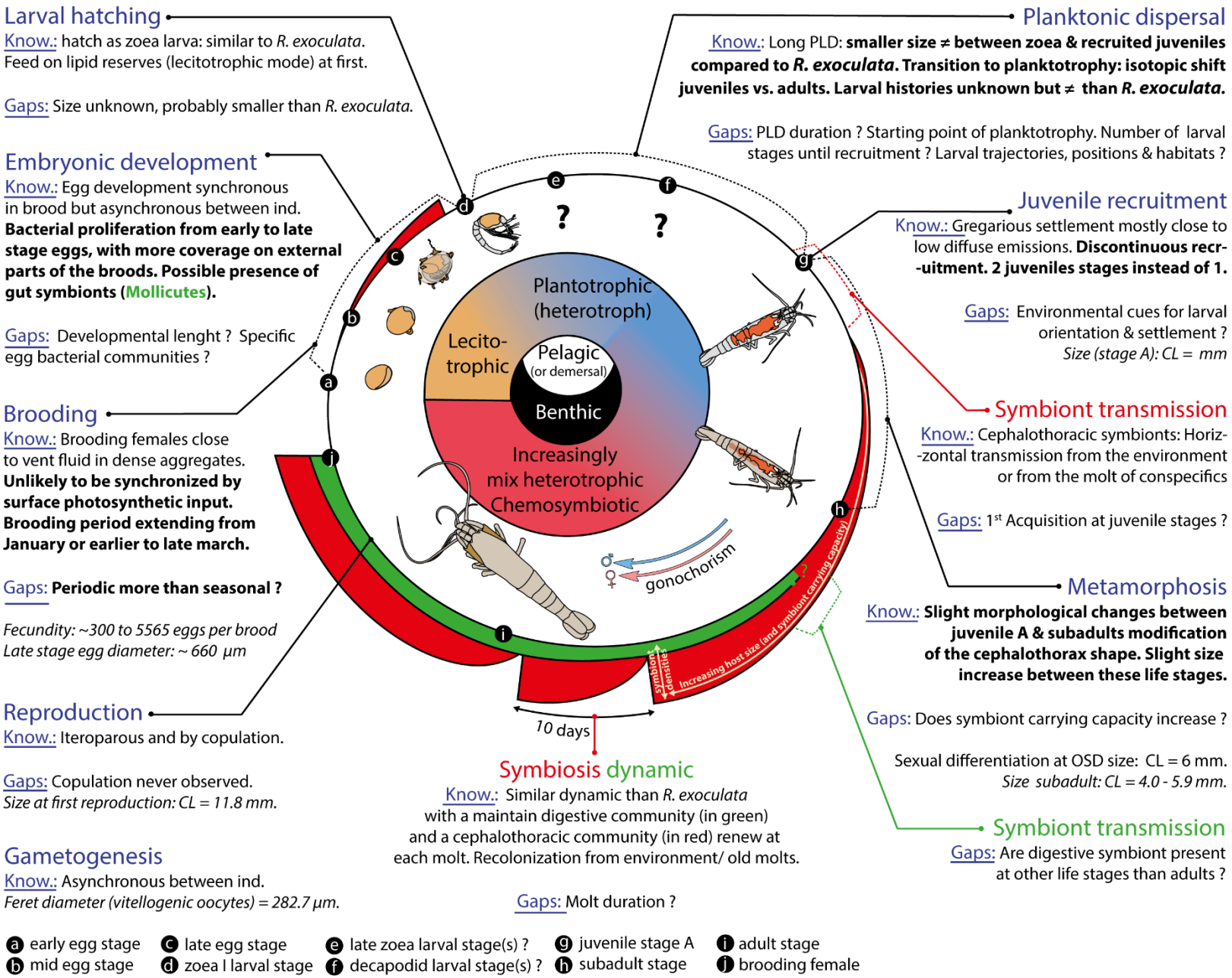


**Fig 78.** Diagram displaying currents knowledge and gaps in the lifecycle of *R. chacei* including the new advances realized during this thesis**.** Largely inspired from the diagram depicting the life cycles of bathymodiolin mussels of Laming et al. (2018)

# E.2 Perspectives et propositions de travaux futurs

## E.2.3.1 Acquisition et développement de la symbiose

Malgré les avancées réalisées durant cette thèse, de nombreuses questions restent en suspens, notamment plusieurs points concernant l'acquisition des symbiotes et leur présence aux stades précoces de la vie des crevettes *Rimicaris*. Bien qu'une spécificité des assemblages bactériens associés aux pontes de *R. exoculata* ait été démontrée, il reste à savoir si celle-ci est le résultat d'une sélection active de la part de la mère ou de l'œuf lui-même, ou si elle pourrait être le résultat du type de surface qui faciliterait l'installation de certains groupes bactériens plutôt que d'autres. Une façon de résoudre en partie ce problème serait peut-être de comparer les assemblages microbiens associés aux *R. exoculata* avec ceux associés aux *R. chacei*, à un stade de développement équivalent. En effet, en ajoutant *R. chacei* aux résultats de séquençage obtenus pour *R. exoculata* – présentés dans le chapitre 1 –, on pouvait observer une importante distinction des assemblages de la ponte de *R. chacei* et de son pléopode par rapport au reste des œufs de *R. exoculata*. Ceci suggère une plus forte influence de l'espèce que du type de surface colonisée – ponte vs pléopode. Etant donné que le type de surface chez *R. chacei* est le même que chez *R. exoculata*, ce résultat tend à rejeter l'hypothèse d'une spécificité liée au type de surface et renforce l'idée que celle-ci est liée à des mécanismes de sélection – comportement, immunité – qui diffèrent entre les deux espèces. Cependant, il est possible que les communautés bactériennes des pontes de chaque espèce diffèrent de par la position de leurs femelles gravides au sein du gradient thermique, chacune vivant en général dans une niche thermique différente de celle de l'autre (Chapitre 3). Ainsi, bien que la femelle séquencée de *R. chacei* (Rimi70) ait été récoltée au même endroit que deux autres femelles de *R. exoculata* séquencées (Rimi48 et Rimi47), il est impossible de prédire si ces deux femelles sont restées dans les mêmes environnements tout au long de leur dévelopement. Une immunité distincte entre *R. exoculata* et *R. chacei* est pourtant suggérée par l'observation de la couleur de leur hémolymphe, qui diffère entre les deux espèces (observations personnelles lors des prélèvements d'hémolymphe réalisés à bord, en collaboration avec A. Tasiemski, BICOSE 2) et devrait être confirmée par la suite par des analyses en laboratoire. De plus, les résultats obtenus sur *R. chacei* étaient limités à un seul individu et sont donc insuffisants en l'état pour confirmer cette tendance. Un nouvel échantillonnage comparant les pontes des deux espèces à différents stades de vie ou à minima à stades équivalents permettront de trancher sur la question. Ainsi, en plus de l'étude descriptive des communautés bactériennes des deux espèces, une étude comparée de leur immunité – maternelle ou de celle des œufs – serait nécessaire pour pouvoir mieux comprendre l'influence relative de l'environnement et/ou de l'immunité de l'animal sur la colonisation bactérienne de ces œufs.

Pour ce qui est des juvéniles, la transition trophique au cours de leur développement, mis en évidence à l'aide des analyses isotopiques, pourrait aussi être étudiée sous un angle anatomique, cette transition étant concomitante avec leur métamorphose en adultes, très marquée chez *R. exoculata* et moins chez *R. chacei*. Celle-ci pourrait se faire par la reconstruction anatomique tridimensionnelle de ces deux espèces à différents stades de vie/classe de taille. Ainsi à l'aide d'un micro-CT scan, il pourrait être possible de caractériser et de mesurer précisément à la fois les compartiments symbiotiques « externes » de la cavité céphalothoracique – surface des branchiostegites, des scaphognathites, exopodites – mais aussi des compartiments internes de l'animal – volume de l'estomac, du tube digestif. Ceci serait d'autant plus intéressant si cette analyse était étendue à deux autres espèces, *R. kairei* et *R. hybisae*, respectivement espèces sœurs de *R. exoculata* et *R. chacei*. En effet une forte similarité morphologique existe entre *R. kairei* et *R. exoculata*, à tel point qu'elles sont relativement difficiles à distinguer l'une de l'autre. En revanche, de nombreuses variations morphologiques peuvent

être rapidement observées entre *R. hybisae* et *R. chacei*, notamment au niveau du céphalothorax, droit chez *R. chacei* et hypertrophié chez *R. hybisae* suggérant ainsi une convergence morphologique de cette dernière avec *R. exoculata*/*R. kairei*. Cette convergence semble n'apparaitre pourtant chez *R. hybisae* qu'au cours de la métamorphose, les stades juveniles étant à première vue, en tout point similaires avec ceux de *R. chacei* (observations personnelles à partir des échantillons du JAMSTEC).

**A**

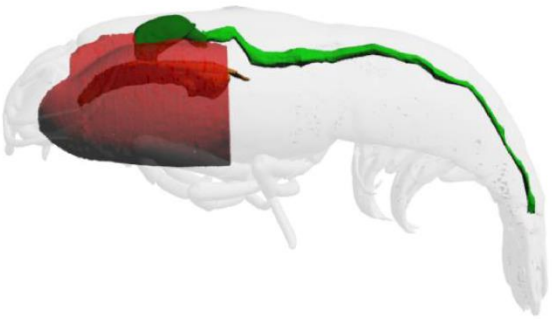

**B**

**C**

| | *R. hybisae* | *R. kairei* | *R. hybisae / R. kairei* |
|---|---|---|---|
| | $V_{org}/V_{tot}$ | $V_{org}/V_{tot}$ | $V_{org}/V_{tot}$ |
| Stomach | 0,03 | 0,01 | 4,66 |
| Digestive tube | 0,01 | 0,01 | 1,24 |
| Branchiostegite | 0,05 | 0,06 | 0,86 |
| Scaphognathite | 0,02 | 0,02 | 1,12 |

**Fig 79.** Reconstruction anatomique 3D d'alvinocarididés obtenu par CT-scan et reconstruit avec le logiciel AMIRA. **A.** Adulte de *Rimicaris kairei* du site Edmond (CL= 13.7 mm). **B.** Adulte de *Rimicaris hybisae* du site Beebe (CL = 13.8 mm). **Rouge**: Branchiostegite; **Orange**: Scaphognathite; **Vert foncé**: estomac; **Vert clair**: tube digestif. **C.** Tableau résumant les mesures du volume (estomac, tube digestif) ou la surface (branchiostegite, scaphognathite) de chacun des organes. $\mathbf{V_{org}/V_{tot}}$: Volume/surface de *R. kairei* ou *R. exoculata* par rapport au volume/surface total de l'individu. ***R. hybisae/R. kairei*** : rapport évaluant la différence de volume/surface entre les deux espèces. Résultats obtenus lors d'un séjour au JAMSEC en juin 2019 avec l'aide du Dr. Chong Chen

De plus, la reconstructions 3D de l'anatomie d'une *R. hybisae* et d'une *R. kairei* de même taille, a permis de voir que les surfaces de branchiostegites et des scaphognathite étaient similaires entre *R. hybisae* et *R. kairei* – et donc très probablement *R. exoculata* – tandis que l'estomac de *R. hybisae* se trouvait être 4.7 fois plus gros que celui de *R. kairei* (résultats préliminaires obtenus lors d'un séjour au JAMSTEC, **Fig 78**). Comparé aux observations faites pour *R. exoculata* et *R. chacei* par (Segonzac et al., 1993), la morphologie du système digestif de *R. hybisae* au stade adulte semble ainsi plus proche de celle de *R. chacei,* tandis que la morphologie de son céphalothorax se rapproche plutôt de celles de *R. exoculata* et *R. kairei*. Ainsi cette convergence anatomique de *R. hybisae* serait à priori limitée aux modifications du céphalothorax. En couplant cette étude à des observations FISH au cours du développement juvénile, il serait aussi possible de voir si ces modifications anatomiques, s'opérant au cours de la métamorphose juvénile de ces espèces, pourraient être liées à des différences en termes de colonisation symbiotique au niveau de leur céphalothorax. Si tel était le cas, on pourrait potentiellement émettre l'hypothèse que la colonisation symbiotique agirait comme un facteur

environnemental enclenchant la métamorphose chez certaines espèces, responsable de l'anatomie si particulière de leur céphalothorax.

Concernant l'acquisition des symbiotes spécifiques au système digestif, une acquisition aux stades embryonnaires des *Deferribacteres* semble être à exclure, leur présence n'ayant été démontrée dans aucune des études s'étant intéressée à ces stades (Cowart et al., 2017; Guri et al., 2012; Methou et al., 2019a). Le cas des *Entomoplasmatales* (Mollicutes) est en revanche plus complexe, avec une possible présence sur certaines pontes mais pas sur toutes. Une possibilité est qu'une transmission de ces symbiontes ait lieu pendant l'oviposition, via le mucus, ou alors dans les spermatozoïdes (tranmission paternelle), mais ni les glandes à mucus ni les gonades n'ont été encore examinées contrairement aux ovaires. Une autre possibilité serait que la transmission ne se fasse pas directement dans les ovocytes non fécondés mais au cours du développement embryonnaire pendant la phase de couvaison, ce qui pourrait expliquer une présence sur certains stades seulement. Les *Entomoplasmatales* n'étaient cependant pas plus présents sur les œufs de stades avancés que sur les œufs moins développés, la seule explication restante, outre une possible contamination, serait une profondeur de séquençage insuffisante sur certains échantillons. Dans tous les cas, si ce groupe de symbionte est bien présent à ce stade, un nombre très limité de bactéries est sûrement présent sur chaque œuf. L'utilisation du FISH sur des coupes d'œufs comme cela a été réalisé pour les *Epsilonbacteraeota,* les *Gammaproteobacteria* et les *Zetaproteobacteria*, semble être peu adapté pour localiser ce groupe de symbiote. En dehors de l'absence de sonde spécifique développée pour ce groupe (actuellement en cours, Thèse M. Gueganton), l'utilisation du FISH sur ces échantillons est mise en difficulté par de nombreux problèmes d'autofluoresence liés aux minéraux sur l'enveloppe mais aussi aux tissus animaux, en particulier les lipides des œufs, qui risquent de masquer un signal faible lors de la détection de bactéries rares. Un bel exemple d'étude ayant réussi à détecter et localiser la présence d'une très faible quantité de bactéries symbiotiques (estimation : 500 symbiotes par œufs) est celui de travaux réalisés récemment sur les œufs du bivalve *Calyptogena okutanii* (Ikuta et al., 2016). En utilisant un protocole d'hybridation *in situ* sur des œufs entiers avec des sondes spécifiques marquées au DIG, une méthode de détection colorimétrique et donc non sensible aux problèmes d'autofluorescence, cette étude a permis de localiser ces symbiotes *in toto* au niveau du pôle végétal des œufs de cette espèce. Cette présence fut confirmée par la suite avec des images TEM, montrant bien des formes de bactéries à cet endroit. Une fois les sondes spécifiques aux *Entomoplasmatales* développées au laboratoire et leur localisation précise confirmée chez les adultes, une approche similaire pourra être utilisée sur les œufs des *Rimicaris,* avec une hybridation *in situ in toto* utilisant des sondes marquées au DIG, qui pourrait être complétée par une approche TEM.

Un autre moyen de mieux comprendre les modes de transmission de ces symbiotes pourrait être d'utiliser une approche phylogénétique. En effet pour certaines espèces hydrothermales, des analyses comparant la topologie de la phylogénie des hôtes avec celle de leur(s) symbiote(s) ont permis de mettre en évidence l'existence d'une forte congruence de ces phylogénies chez certains holobiontes. Cette congruence traduit une possible co-spéciation entre l'hôte et son symbiote et un mode de transmission vertical. Inversement, une absence de congruence est généralement signe d'une transmission horizontale (Nelson and Fisher, 2000; Ozawa et al., 2017; Peek et al., 1998; Won et al., 2008). L'observation des associations bactériennes aux stades de vie précoces confirment généralement ces hypothèses, avec l'identification de bactéries associées aux œufs/embryons reflétant une transmission verticale pour ceux présentant une forte co-spéciation et un mode de transmission horizontale pour les autres (Cary and Giovannoni, 1993; Endow and Ohta, 1990; Ikuta et

al., 2016; Nussbaumer et al., 2006; Wentrup et al., 2014). Une telle approche mettant en parallèle les phylogénies des hôtes et de leurs symbiotes respectifs pourrait aussi être utilisée pour les crevettes *Rimicaris* et ainsi affiner nos hypothèses en permettant de savoir quels modes de transmission des symbiotes sont les plus probables. Ceci est particulièrement important pour les symbiotes du système digestif, pour lesquels aucune lignée proche n'a pu être retrouvée dans l'environnement jusqu'à présent, affaiblissant l'hypothèse d'une transmission horizontale. Des indices d'une potentielle co-spéciation des Entomoplasmatales et des crustacés d'une manière générale ont d'ailleurs été mis en évidence récemment. En effet, les lignées de bactéries les plus proches de symbiotes de *Rimicaris* séquencées à l'heure actuelle sont les symbiotes de l'hépatopancréas d'un isopode terrestre, et du tube digestif de deux amphipodes de la fosse des Mariannes (Cheng et al., 2019; Wang et al., 2004). Cependant les études sur la symbiose du tube digestif des alvinocarididés restent limitées pour le moment à seulement deux espèces de *Rimicaris* de l'océan Atlantique (Apremont et al., 2018; Durand et al., 2010, 2015). Une couverture plus large de cette relation symbiotique incluant des espèces d'autres régions du globe, en particulier de l'ouest Pacifique où elles sont nombreuses, mais aussi éventuellement d'autres genres comme *Alvinocaris* ou *Mirocaris* serait un prérequis à ce type d'étude phylogénétique.

### E.2.3.2 Dispersion et développement larvaire

La partie larvaire est certainement la partie la moins bien comprise du cycle de vie de *R. exoculata* et même des alvinocarididés en général. En raison de la difficulté d'échantillonnage de ces stades, peu d'avancées ont pu être réalisées durant cette thèse. De nombreux points restent ainsi à examiner, la plupart nécessitant l'élevage de larves *in vivo* et de préférence sous pression pour reconstituer les conditions environnementales du début de leur développement. Celles-ci pourraient être réalisées à l'aide de larves prélevées dans l'environnement mais aussi en incubant des larves écloses à bord provenant des pontes de *R. exoculata* gravides – qui lors de cette thèse ont servi aux études de reproduction. L'utilisation de ces dernières permettrait d'obtenir un échantillon de larve plus important, mais aussi plus homogène en terme de réplicat – même stade de développement, même espèce, variabilité génétique limitée – tandis que l'incubation en aquarium permettrait de mieux contrôler les différentes conditions environnementales. Une expérience similaire à celle réalisée sur *M. fortunata* par (Tyler and Dixon, 2000) en incubant les larves à différentes conditions de températures – au moins 20°C et 2°C, et si possible d'autres paliers à 10°C, et 15°C– et différentes conditions de pression – au moins les conditions de surface (1 atm) et celles du fond au niveau du site de prélèvement, et éventuellement d'autres paliers entre les deux – permettrait de préciser les limites de la distribution verticale de ces larves dans la colonne d'eau et si une présence de ces stades dans les eaux de surface est possible ou non.

Un autre point central qui reste à évaluer est celui du développement du système digestif après l'éclosion qui conditionne la nutrition de la larve pendant sa phase planctonique. En effet celui-ci ne semble à priori pas complètement développé, avec un œsophage et peut être un estomac, mais apparemment pas de tube digestif ouvert jusqu'au bout d'après les coupes de larves obtenues (sagittale et frontale). Ces observations ajoutées aux résultats de (Hernández-Ávila et al., 2015) qui montrent des pièces buccales non développées chez les zoés après l'éclosion, indiquent que ces larves ne peuvent probablement pas se nourrir durant les premiers moments de leur vie planctonique. La durée pendant laquelle ces larves peuvent continuer à se développer selon un mode strictement lécitotrophique, à partir de leurs réserves propres reste à déterminer. De même, le moment et le stade

de développement auxquels les larves vont basculer vers la planctotrophie demeurent inconnus. L'incubation sous pression et à 2°C d'un certain nombre de larves avec des prélèvements à intervalles réguliers – de l'ordre de quelques jours – avec une reconstruction tridimensionnelle de l'anatomie de ces larves à chaque intervalle permettrait de voir à quel moment le système digestif peut être considéré comme complétement formé et fonctionnel. En revanche, au vu de la taille des larves, la résolution obtenue avec un micro CT-Scan risque d'être insuffisant pour reconstruire proprement l'anatomie de ces stades de vie et un autre moyen d'acquisition devrait être envisagé. Il pourrait être envisagé de passer soit par une découpe sériée traditionnelle de chaque individu en entier – mais qui constituerait un travail long et fastidieux – soit par l'utilisation d'un synchrotron ou encore d'un nano CT-scan.

La durée maximale de la phase lécitotrophique, tout comme la durée totale du développement larvaire jusqu'au stade juvénile, pourraient être obtenues respectivement par une incubation sous pression des larves sans les nourrir ou dans l'autre cas, en les nourrissant de la même façon que ce qui a pu être fait pour des larves de gastéropodes par (Yahagi et al., 2017b) – mais en utilisant une nourriture adaptée pour des larves de crustacés. Chez d'autres alvinocarididés (Watanabe et al., 2016) ont observé une durée de la phase lécitotrophique – larves non nourries – , dépendante de la température, variant entre une dizaine de jours et pratiquement 100 jours, soit une durée supérieure à la plupart des missions en mer. Ainsi de telles expériences d'incubation pourraient être réalisées dans différentes conditions de température afin d'estimer la durée de vie larvaire en fonction de l'environnement rencontré par les larves au cours de leur dispersion. Cependant, au vu des durées obtenues par (Watanabe et al., 2016), et en raison de risques de l'expérimentation *in vivo*, une autre méthode pourrait aussi permettre d'estimer la durée maximale de cette phase lécitotrophique sur des durées d'incubations plus courte. Celle-ci nécessiterait de quantifier les réserves lipidiques ainsi que le taux métabolique juste après l'éclosion et à différents intervalles de temps afin d'estimer la vitesse de consommation et la durée de ces réserves lipidiques. Ces valeurs pourront aussi être comparées à d'autres espèces comme *Riftia pachyptila* (Marsh et al., 2001) ou encore entre les espèces d'alvinocarididés si plusieurs espèces sont étudiées. Ce type de comparaison permettrait de voir si des différences d'investissement maternel (en termes de ressources lipidiques) existent entre ces espèces et si cela pourrait engendrer des différences en termes de dispersion. Enfin, en plus de la durée de vie planctonique (PLD), la caractérisation de la nage de ces stades de vie serait un paramètre clé pour mieux contraindre les modèles biophysiques de dispersion et comprendre les trajectoires empruntées par la larve. On pourra ainsi déterminer leur vitesse de nage moyenne – en fonction des conditions environnementales/d'incubation – ou leur direction, – plutôt verticalement ou plutôt horizontalement – leur déplacements verticaux permettant de mieux évaluer la position qu'elles occupent dans la colonne d'eau et donc les courants que ces larves empruntent (Beaulieu et al., 2014; Epifanio et al., 1999; Yahagi et al., 2017b).

Plusieurs de ces expériences pourraient être réalisées en parallèle afin d'optimiser les temps d'incubation. Pour ce faire, toutes ces expériences *in vivo* nécessiteraient cependant le développement de nouveaux incubateurs sous pression de petites tailles, idéalement entre quatre et une douzaine, possédant un hublot d'observation ou même une caméra d'enregistrement mais aussi une ligne d'alimentation isobare comme celle installée sur l'aquarium Abyssbox afin de nourrir les larves sans pour autant dépressuriser la partie de l'aquarium où sont les larves (Shillito et al., 2015). Pour aller plus loin sur la compréhension des lieux de vie des larves et de leurs tolérances aux contextes hydrothermaux naturellement pollués, ces incubateurs permettraient aussi de réaliser sur ces larves

les mêmes tests écotoxicologiques que ceux réalisés sur les adultes de *R. exoculata* (Auguste et al., 2016), notamment en les incubant avec différentes concentrations de cuivre, afin in fine d'évaluer l'impact potentiel des rejets miniers sur leur survie et donc la capacité de dispersion/colonisation de l'espèce.

### E.2.3.3 Recrutement, reproduction et distribution des différents stades de vie sur les sites hydrothermaux

Le fait que la distribution des différents stades de vie ne soit apparemment pas structurée selon les conditions thermiques le long du gradient de mélange du fluide hydrothermal avec l'eau de mer est surprenant au vu des résultats obtenus précédemment par (Hernández-Ávila, 2016). Ces résultats obligent donc à considérer d'autres facteurs environnementaux. Par exemple, la présence et/ou l'abondance dans l'environnement de certains microorganismes spécifiques – en particulier les symbiotes de ces espèces – pourrait avoir une incidence sur la répartition des différents stades de vie de ces animaux, en particulier des juvéniles dans les zones de recrutement, s'ils n'ont pas encore acquis les symbiotes. En effet, cette présence de certains microorganismes a été montrée comme un signal environnemental fondamental pour l'installation des larves de nombreux animaux (Hadfield, 2011; Huang and Hadfield, 2003; Ritson-Williams et al., 2016; Watson et al., 2016), et pourrait jouer un rôle similaire chez *R. exoculata* et *R. chacei*. Les nombreux prélèvements d'eau avec le dispositif PLUME du *Nautile,* associés aux différents prélèvements de crevettes ainsi que de quelques roches, a pu permettre l'extraction d'ADN des communautés microbiennes entourant ces animaux (séquençage en attente). Dans un futur proche, l'analyse des données de séquençage de ces échantillons permettra d'avoir une meilleure idée de l'influence potentielle des communautés bactériennes planctoniques locales sur la distribution des *Rimicaris* tout en tenant compte des données environnementales.

Une autre approche serait d'explorer l'environnement chimique de ces espèces. En effet, les signaux chimiques sont omniprésents dans le milieu marin et constituent le « langage » principal de nombreuses espèces provenant de tous les groupes du vivant, aussi bien animal que végétal ou microbien (Hay, 2009). Dans ces écosystèmes marins, ces signaux chimiques régulent divers comportements tels que ceux impliqués dans le choix ou la recherche de nourriture, les interactions interspécifiques comme la compétition ou la prédation, la reproduction ou encore la métamorphose et le recrutement larvaire. Cette communication chimique façonne ainsi la structure des populations des différentes espèces impliquées, tout comme l'organisation des communautés, et à une plus large échelle le fonctionnement des écosystèmes (Hay, 2009). Dans l'environnement hydrothermal, les recherches en chimie se sont principalement intéressées à la chimie des fluides hydrothermaux, comment celle-ci évolue au niveau du gradient de mélange et aux facteurs sous-jacents qui contrôlent la composition de ces fluides (Barreyre et al., 2014; Charlou et al., 2010; Le Bris et al., 2006a, 2019; McDermott et al., 2018). En revanche, peu d'études se sont intéressées aux molécules organiques qui composent l'environnement proche des espèces hydrothermales et qui pourraient constituer des signaux chimiques importants dans ces écosystèmes. Ce manque de connaissances est possiblement lié aux difficultés techniques pour détecter ces molécules dans l'environnement avec les méthodes classiques de GC/MS (Chromatographie en phase gazeuse/Spéctrométrie de masse), la concentration de ces molécules étant généralement très faible ; ce à quoi s'ajoute les effets inhibiteurs du sel pour l'eau de mer qui perturbe la détection de ces molécules. Par exemple, La recherche de molécules du quorum sensing liée aux symbiontes des *Rimicaris* dans l'eau/fluide entourant ces crevettes durant une précédente thèse fut sans succès (Le Bloa, 2016; Le Bloa et al., 2017). Cependant, le

développement récent d'un nouveau protocole semble permettre d'augmenter très fortement le seuil de détection de ces molécules, de 324 fois par rapport aux méthodes de GC/MS classiques, mais aussi de retirer le sel des échantillons sans perdre pour autant toute une partie des molécules chimiques (Liebeke and Puskás, 2019; Sogin et al., 2019). Cette technique a permis ainsi de dresser le profil métabolique des molécules excrétées par les organismes alentours de plusieurs micro habitats précis, comme par exemple les eaux interstitielles des sédiments de mangroves ou de récifs coralliens, et de comparer les spécificités chimiques de chacun (Sogin et al., 2019).

Rapporté à notre structure de population, le but de cette expérience serait d'utiliser ce type de méthode pour dresser le profil métabolique des molécules chimiques qui entourent les différents micro habitats des crevettes *Rimicaris* et d'identifier des molécules d'intérêt qui ne sont retrouvées que dans un type d'habitat et qui pourraient servir de signaux chimiques pour ces espèces. Une caractérisation plus poussée de cette/ces molécule(s) pourrait permettre de déterminer son/leur origine pour savoir si elle(s) est/sont le produit d'espèces microbiennes ou des *Rimicaris* elles-mêmes ou un cocktail des deux. Ainsi il pourrait être possible de déterminer si la structuration des *Rimicaris* est le résultat de l'influence d'un facteur environnemental ou si celle-ci est le résultat d'une organisation sociale, dans le cas où l'espèce produirait et contrôlerait son propre signal. Dans un second temps, et s'il est possible de synthétiser ces molécules d'intérêt, il pourrait être intéressant d'étudier si ces molécules peuvent être détectées par la crevette, grâce aux nouvelles méthodes d'électroantennographie développées récemment (Machon et al., 2016, 2018), ou tout simplement à l'aide de tests comportementaux comme ceux réalisés à bord (équipe AMEX) durant l'expédition BICOSE 2 avec le sulfure (Cambon-Bonavita, 2018). Enfin, une fois ces tests de détection réalisés, des tests ecotoxicologiques pourraient être faits en rajoutant à ces signaux chimiques des perturbateurs qui pourraient correspondre aux rejets miniers qui auraient lieu en cas d'exploitation (Cuivre, Zinc …), et voir si la détection de ces molécules peut être perturbée par ce type de pollution. Ce type d'étude serait fondamental dans ce contexte d'exploitation minière car si de telles pollutions ne provoquent pas à priori la mort d'individus comme montré par (Auguste et al., 2016), elle pourrait affecter leurs capacités de perception de l'environnement. En effet, dans le cas où la détection de ces signaux perturbe des fonctions majeures comme celles impliquées dans la reproduction (rencontre du partenaire, accouplement …), la maintenance sur le long terme de cette espèce ne serait plus assurée.

Une autre observation étonnante lors de la campagne BICOSE 2, fut la découverte de la disparition d'un agrégat de *R. exoculata* du lieu où il avait pourtant été observé seulement 10 jours avant. A la place, un petit agrégat de *R. chacei* fut retrouvé et quelques *R. exoculata* éparses, reflétant une dynamique temporelle qui pourrait être importante chez ces espèces, même si de nombreuses zones étaient à l'inverse extrêmement stables. Ce départ des *R. exoculata* pourrait être lié à une diminution locale de l'activité hydrothermale à cet endroit, les fluides apparaissant comme moins actifs, mais l'absence de mesures des conditions environnementales lors du premier prélèvement n'a pas permis de conclure sur ce point. Ce type de prélèvements répétés à plusieurs jours d'intervalles avec à minima des mesures de températures associées permettrait d'apporter une réponse quant aux facteurs influençant cette dynamique, si de tels changements brutaux peuvent être observés à nouveau. Cependant ceci ne permettra pas d'observer l'existence de potentiels mouvements individuels si les individus quittant l'agrégat ou le groupe sont remplacés par le même type d'individus (même sexe/stade de vie). Pour cela, un marquage des individus serait nécessaire avec une observation de la même zone où les individus marqués sont retrouvés à t0 et à plusieurs jours d'intervalle. Une telle méthode fut par exemple employée pour suivre ce même type de dynamique

chez *Shinkaia crosnieri* en utilisant un colorant, le bleu brillant de Coomassie (Maruyama et al., 2018). En comptant le nombre de crabes marqués, juste après avoir appliqué le colorant *in situ* et deux jours après, cette expérience a pu montrer que les assemblages de *S. crosnieri* étaient très stables sur ces échelles de temps. En revanche du fait de sa coloration bleue, le marquage des *S. crosnieri* était très difficile à observer au fond et n'était pas stable plus de 3 jours. Un marquage par coloration pourrait être envisagé pour *R. exoculata* mais si possible avec un colorant plus stable, d'une autre couleur et non toxique pour l'environnement. Dans tous les cas, ce marquage sera limité à des échelles de temps d'une dizaine de jours maximum, du fait du cycle de mue très court de cet animal. Une autre approche qui permettrait un marquage plus précis serait d'utiliser des marqueurs acoustiques ou électroniques qui permettrai de suivre individuellement différents individus au cours de leurs mouvements sur plusieurs jours/mois comme cela peut être fait chez les abeilles, mais aussi en milieu marin ou d'autres milieux aquatiques chez différentes espèces de crustacés (González-Gurriarán et al., 2002; Guerra-Castro et al., 2011; Hubatsch, 2017; Maitland et al., 2002). Couplé avec une cartographie précise du site en identifiant la localisation des zones de fumeurs actif, cette technologie permettrait d'identifier le temps passé dans chaque micro habitat par chaque individu, l'étendue des distances parcourues par rapport aux émissions actives – certains individus de *R. exoculata* ayant été repérés à plusieurs centaines de mètres du site actif lors des plongées (observations personnelles, BICOSE 2) - mais aussi leur comportement spatial de recherche de nourriture, ces animaux se 'nourrissant' indirectement des émissions de fluides. Cependant de nombreux verrous techniques empêchent à l'heure actuelle d'envisager de telles études. En dehors de la difficulté d'obtenir une cartographie précise d'un site hydrothermal, la marge d'erreur étant de l'ordre de quelques dizaines de mètres pour ce qui est de la position du sous-marin/robot en général (échange et discussion à bord lors d'une présentation de Mathilde Pitel-Roudaut, BICOSE 2), plusieurs difficultés constituent des freins majeurs à la réalisation de ce type de suivi. Parmi eux, la difficulté de capter le signal émis par les marqueurs depuis la surface à de telles profondeurs, obligeant possiblement la mise en place de balise réceptrice au fond est un blocage important. Mais c'est surtout l'implantation de ces marqueurs, généralement interne nécessitant d'être introduit dans l'animal et donc à bord, ce qui implique la remontée et la redescente de l'animal en bonnes conditions physiologiques, qui reste probablement le principal obstacle pour lesquel de nouvelles solutions techniques doivent être envisagées.

Ainsi, les nombreuses voies de recherche dégagées ici, couplées aux développements technologiques en cours, permettront dans un futur proche de mieux cerner les mécanismes régissant les étapes clé du cycle de vie d'espèces profondes 'modèles'. Ces études, et les mises au point expérimentales et technologiques associées, accélèreront le développement des connaissances sur d'autres espèces, moins étudiées à l'heure actuelle. A terme, une meilleure connaissance générale des cycles de vie des organismes profonds permettra d'affiner les prédictions issues des approches de modélisation, notemment concernant la connectivité des populations profondes et leur résilience face aux pressions anthropiques dont le profond n'est aujourd'hui plus protégé.

*« Quand je suis sorti du jardin, l'idée m'est brusquement venue d'une expérience à faire sur la division cellulaire. Une expérience assez simple. Il suffisait de … »*

*La Statue Intérieure, Francois Jacob*

# Annex Chapter Keeping friends close

This study is the result of a collaboration established during this thesis but is not directly related to my main focus. For this study, I have provided an important help with the identification of specimens used here and collected during the Bicose 2 cruise. On board, prior to experimental procedures, I identified the shrimps to the species level, assessed their life stage, sex and performed body measurments. In the laboratory, I have also performed the embedding and the sectionning of several egg samples for the immunolabelling approach. I have also provided my recent expertise on the *Rimicaris exoculata* lifecycle and on the *Rimicaris exoculata* model in general, to participate with others to the improvement and the accurary of the introduction and the discussion developed in the paper. This article has been submited to eLife on October 2019.

# A. Antimicrobial peptides and ectosymbiotic relationships: involvement of a novel Type IIa crustin in the life cycle of a deep sea vent shrimp

## Authors and Affiliations

Simon Le Bloa[a ¥], Céline Boidin-Wichlacz[b,c ¥], Valérie Cueff-Gauchard[a], Lucile Durand[a], Rafael Diego Rosa[d], Virginie Cuvillier-Hot[c], Pierre Methou[a,f], Florence Pradillon[f], Marie-Anne Cambon-Bonavita[a], Aurélie Tasiemski[b,c]*

¥ These authors equally contributed to this work

[a]Ifremer, [a]Univ Brest, CNRS, IFREMER, Laboratoire de Microbiologie des Environnements Extrêmes, F-29280 Plouzané, France

[b]Univ. Lille, CNRS, Inserm, CHU Lille, Institut Pasteur de Lille, U1019 – UMR 8204 - CIIL - Center for Infection and Immunity of Lille, F-59000 Lille, France

[c]Univ. Lille, CNRS, UMR 8198 - Evo-Eco-Paleo, F-59000 Lille, France

[d]Laboratory of Immunology Applied to Aquaculture, Department of Cell Biology, Embryology and Genetics, Federal University of Santa Catarina, 88040-900 Florianópolis, SC, Brazil

[e]Ifremer, Centre Bretagne, Laboratoire Environnement Profond (REM/EEP/LEP), ZI de la pointe du diable, CS10070, 29280 Plouzané, France

*Correspondance to Aurélie Tasiemski, Center for Infection & Immunity of Lille, CGIM, bat: IBL, Institut Pasteur de Lille, Boulevard Louis XIV, F-59000 Lille, France, E-mail: aurelie.tasiemski@univ-lille.fr

## Abstract

The symbiotic shrimp *Rimicaris exoculata* dominates the macrofauna inhabiting the active smokers of the deep-sea mid Atlantic ridge vent fields. We investigated the nature of the host mechanisms controlling the vital and highly specialized ectosymbiotic community confined into its cephalothoracic cavity. *R. exoculata* belongs to the Pleocyemata, crustacean brooding eggs, usually producing Type I crustins. Unexpectedly, a novel anti-Gram-positive type II crustin was molecularly identified in *R. exoculata*. *Re*-crustin is mainly produced by the appendages and the inner surfaces of the cephalothoracic cavity, targeting main epibionts. Symbiosis acquisition mechanisms are still poorly understood. Yet, symbiotic communities were identified at different steps of the life cycle such as brooding stage, juvenile recruitment and molt cycle, all of which may be crucial for symbiotic acquisition and control. Here, we show a spatio-temporal correlation between the production of *Re*-crustin and the main ectosymbiosis-related life-cycle events. Overall, all our results highlight (i) a novel an unusual AMP sequence from an extremophile organism and (ii) the potential role of AMPs in the establishment of vital ectosymbiosis along the life cycle of deep-sea invertebrates.

**Keywords:** crustacean, extreme, hydrothermal vents, symbiosis, host-microbe interaction, host defense peptide, invertebrate immunity, WAP domain, life cycle.

## A.1. Introduction

In marine habitats such as in deep-sea hydrothermal ecosystems, bacterial associations with invertebrates are well-described (McFall-Ngai, 2008). The important animal biomass observed around hydrothermal vents is based on the existence of dense chemosynthetic prokaryotic communities (Desbruyères et al., 2001; Dick, 2019). Among these communities, a large number forms highly specialized symbiotic associations with metazoan hosts. These relationships are now quite well studied, *e.g.* as in the case of the bacterial community inhabiting the cephalothoracic cavity of the shrimp *Rimicaris exoculata* (Guri et al., 2012; Jan et al., 2014; Petersen et al., 2010; Ponsard et al., 2013).

By contrast, understanding the mechanisms by which hosts selectively recruit bacteria for long-term (core) or short-term (flexible) specific relationships is still a considerable challenge (Sharp and Ritchie, 2012). To date, most of the existing literature has focused on the role of immune receptors (lectins, PGRPs…) in marine symbiotic associations. A given immune receptor recognizes some families of microbes (bacteria, fungi…) on the basis of motifs of recognition (LPS, LTA, mannan…), commonly exposed on the membrane of friend and foe microorganisms (Rakoff-Nahoum and Medzhitov, 2006). However, other selective and specific host processes are required to discriminate between pathogenic or mutualistic microbes in order to selectively kill or tolerate them. Amongst the few other immune substances known to be involved in host-symbiont associations, host defense antimicrobial peptides (AMPs) represent promising actors (Franzenburg et al., 2013; Gallo and Nakatsuji, 2011; Mergaert, 2018; Salzman et al., 2010; Tasiemski et al., 2015). AMPs are chemical components that take part in both the internal and external immune defenses (*i.e.* they can be secreted in the outer parts of the body), thus playing functions in the control/establishment of ectosymbiosis as described for the hydrothermal worm *Alvinella pompejana* (Bulet et al., 2004; Maróti et al., 2011; Zasloff, 2002). From an evolutionary perspective, the adaptive diversification of AMPs at the interspecific and intraspecific levels makes them of particular interest to decipher the immune mechanisms driving bacteria-specific and environment-dependent symbioses (Gosset et al., 2014; Tennessen, 2005; Unckless et al., 2016).

The Pleocyemata shrimp *R. exoculata* (Williams and Rona, 1986) dominates the fauna at several hydrothermal vent sites of the Mid-Atlantic Ridge (MAR) (Segonzac et al., 1993). This deep-sea crustacean thrives in such hostile habitats through an association with two distinct ectosymbiotic microbial communities: one in its gut (Durand et al., 2010, 2015; Zbinden and Cambon-Bonavita, 2003) and the other in its enlarged cephalothoracic cavity (Casanova et al., 1993; Guri et al., 2012; Hügler et al., 2011; Jan et al., 2014; Petersen et al., 2010; Polz and Cavanaugh, 1995; Zbinden et al., 2004, 2008). Previous studies have demonstrated the chemotrophic role of the symbionts that colonize the cephalothoracic cavity (Gebruk et al., 2000; Polz et al., 1998; Ponsard et al., 2013; Van Dover et al., 1988). This specialized ectosymbiosis, composed of few specific bacterial lineages, mainly *Proteobacteria* and *Campylobacterota* (previously *Epsilonproteobacteria)* (Waite et al., 2008), is confined to the internal faces of the lateral carapace (branchiostegites) and the mouthparts (scaphognathites) of the cephalothorax cavity (Guri et al., 2012; Jan et al., 2014; Polz and Cavanaugh, 1995; Zbinden et al., 2004). While the gut symbiotic community also harbors *Proteobacteria* and *Campylobacterota*, other symbionts have been found in the digestive system, such as the Mollicutes or the *Deferribacteres* (Durand et al., 2010, 2015; Zbinden and Cambon-Bonavita, 2003), evoking an organ-dependent mode of selection of the symbionts by the host. Interestingly, every 10 days, the microbial community of the cephalothoracic cavity, but not of the gut, is eliminated during the molt of

the adult and ectosymbionts rapidly re-colonize the host cephalothoracic cavity (Corbari et al., 2008b; Le Bloa et al., 2017; Zbinden et al., 2008). This re-colonization process is strictly similar for each individual and strictly located on the same area of mouthparts and branchiostegites, suggesting a tight selection of the bacteria by the host (Corbari et al., 2008b; Guri et al., 2012; Zbinden et al., 2008). However, the immune mechanisms involved in this association remain mostly unknown. Only the recent work by Liu and his colleagues (Liu et al., 2019), has characterized the potential immune role of a C-type lectin, highly expressed in the scaphognathite, which could selectively recognize and agglutinate some of the cephalothoracic symbionts.

The immune system of crustaceans is based on cellular and humoral responses involving, among other substances, the production of AMPs (Destoumieux-Garzón et al., 2001). Several classes of both gene-encoded and non-ribosomally synthetized AMPs have been identified and characterized in major commercial species of decapod crustaceans (Rosa and Barracco, 2010; Smith and Dyrynda, 2015). To our knowledge, despite a particularly well-described role of these molecules in the immune response of crustaceans against pathogens (Destoumieux-Garzón et al., 2001), no studies have ever been conducted on their involvement in mutualistic symbiosis.

Crustins form a diverse and multigenic family of AMPs found in virtually all crustacean groups and in some hymenopteran insects (Tassanakajon et al., 2018). They are mainly active against Gram-positive bacteria, but their unique feature is the presence of a C-terminal whey acidic protein (WAP) domain, a conserved cysteine-rich motif (four-disulfide core or 4DSC) that exhibits antiprotease activities (Smith et al., 2008). Crustins are divided into four groups (Types I to IV) according to the presence/absence of two N-terminal structural domains: the glycine-rich and the cysteine-rich regions (Smith and Dyrynda, 2015). Type I crustins contain an N-terminal cysteine-rich region (with four conserved cysteine residues) followed by the typical C-terminal WAP domain. In addition to the cysteine-rich region, Type II crustins also harbor a highly hydrophobic glycine-rich region at the N-terminus. Comparatively, crustin members from Types III and IV are composed by one and two WAP domains, respectively, and are devoid of any other domains. Interestingly, while Type I crustins are widely distributed across decapod crustaceans (Pleocyemata and Dendrobranchiata), Type II crustins (Sub-Types IIa and IIb) are mainly present in penaeid shrimps (Dendrobranchiata) (Barreto et al., 2018).

In this study, we explored the sequence conservation of a novel glycine-rich crustin member, *Re*-crustin, produced by the extremophile Pleocyemata shrimp, *R. exoculata*. Then, we investigated expression patterns in different host tissues and throughout its life cycle in order to identify correlations with the main symbiosis related events taking place at different life stages of this vent shrimp. These events include embryonic development (Guri et al., 2012; Methou et al., 2019a), juvenile settlement into adult habitats (Methou personal observation), and through the molt cycle involving re-establishment of the symbiotic community after each molting event (Corbari et al., 2008b).

# A.2. Materials and methods

## A.2.1. Specimen collection

*Rimicaris exoculata* were collected at two MAR hydrothermal vent fields, TAG (26°08' N;-3640m) and Snake Pit (23°23' N;-3480m), with the research vessel *Pourquoi pas?* using the suction sampler of the remotely operated vehicle (ROV) Victor 6000 and the human operated submersible Nautile during the oceanographic cruises BICOSE2014 https://doi.org/10.17600/14000100 and

BICOSE2018 http://dx.doi.org/10.17600/18000004 (**Fig 79A. to 79C.**). The isobaric collection device PERISCOP (Shillito et al., 2008) was used to collect shrimps at different life stages (early and late eggs, recruited juveniles collected within adults' aggregates (**Fig 79D**), and adults at different molting stages). They were dissected aboard, and pieces were either flash frozen in liquid nitrogen before being kept at -80°C (with or without Trizol Reagent™, Invitrogen) or were kept straight after sampling at 4°C (in 4% Paraformaldehyde) until further use at the laboratory (**Fig 79E an 79F**).

## A.2.2. Molecular identification of Re-crustin

The nucleotide sequence of the Re-crustin was obtained by RT-PCR using 2 µg of template cDNA, with the forward primer 5'- GACAAACACCTCCTCCTCCTCCA -3' designed from the incomplete 5' coding sequence of a crustin sequence available in GenBank (accessing number FJ573157) and the oligo (dT)18 primer.

-cDNA synthesis: Whole animals were ground in Trizol ReagentTM using the Ultra-Turrax T25 ® (IKA). RNA was extracted according to the manufacturer's instructions. The concentration of extracted RNA was estimated with the Qubit® 3.0 Fluorometer (ThermoFisher Scientific). RNA extracts were treated by RQ1 RNase-free DNase (Promega) and used for cDNA synthesis with the RevertAid M-MuLV RT kit (ThermoFisher Scientific) according to the manufacturer's protocol. Reaction mixtures for PCR amplifications contained 0.1 µM of each primer, 0.25 mM of each desoxynucleotide triphosphate, 5× Go Taq G2 Flexi buffer (Promega), and 5 U of GoTaq G2 Flexi DNA polymerase (Promega). The PCR program involved an initial denaturation step at 95°C for 3 min, followed by 39 cycles of 95°C for 1.5 min, 55°C for 1.5 min, and 72°C for 1.5 min, with a final elongation step at 72°C for 5 min.

- Molecular cloning and sequence analysis: PCR products from each replicate were pooled and then purified with the NucleoSpin® Gel and PCR Clean-up kit (Macherey-Nagel). Purified PCR products were cloned using the TOPO-TA kit (Invitrogen, Carlsbad, CA, USA). Clones were sequenced according to the Sanger method (Sanger and Coulson, 1975) on a 310 ABI prism (Applied Biosystems). Sequences were imported into Geneious© version 8.1 software (Biomatters, available from http://www.geneious.com/). Prediction of signal peptide was performed with the SignalP 4.1 program (Petersen et al., 2011b) and the presence of conserved domains was tested using the SMART 7.0 protein analysis tool (Schultz et al., 1998) Homology searches were performed using BLAST at NCBI. Multiple alignments of the deduced amino acid sequences (Type I, Type IIa and Type IIb crustins) were generated using the MAFFT software (scoring matrix BLOSUM62) (Katoh et al., 2002). Phylogenetic analysis based on the amino acid sequences were conducted in MEGA X (Kumar et al., 2018) using the Maximum Likelihood method (complete deletion option). Trees were resampled 1,000 times.

## A.2.3. Determination of the level and site of Re-crustin gene expression by RT-qPCR

Tissues from branchiostegite, scaphognathite, gills, abdomen, stomach, hepatopancreas and eggs dissected aboard as wells as whole adults and juveniles were ground in Trizol Reagent™ using FastPrep-24® 5G (MP Biomedicals). Total RNA extraction and RT were performed as described in the previous section.

The primers used for the quantitative PCR were designed with the Primer3 Input software (http://frodo.wi.mit.edu/cgi-bin/primer3/primer3www.cgi).

- crustin primers: forward: 5'- ACTGCTGTGAGAACGGGAAC -3'; reverse: 5'-AACATGTTTGAGGGGGTCCT -3'

- *Rpl8* primers: forward: 5'- GAAGCTCCCATCAGGTGCCAAGAA -3'; reverse 5'- TTGTTACCACCACCGTGAGGATGC -3'.

The *Rpl8* gene was used as the reference gene (Cottin et al., 2010a). Real-time quantitative PCR reactions (RT-qPCR) were conducted on a LightCycler® 480 system (Roche) using a hot start enzyme. RT-qPCR assays were submitted to an initial denaturation step of 10 min at 94°C followed by 40 cycles of denaturation at 94°C for 15 s, annealing at 59°C for 1 min and extension at 72°C for 30 s. Reference and target were amplified in separated wells. After amplifications, a melting curve analysis was performed in order to confirm the specificity of the PCR products. *Re*-crustin primers generated a single and discrete peak in the dissociation curve (data not shown). A negative control and a 5-fold dilution series protocol of pooled cDNAs were included in each run. The 5-fold dilution series were used to construct a relative standard curve to determine the PCR efficiencies and for further quantification analysis. In all experiments, all primer pairs gave amplification efficiencies of 90-100%. Each reaction was run in triplicates. Analysis of relative gene expression data was performed using the ΔΔCq method (Livak and Schmittgen, 2001). For each couple of primers, a plot of the log cDNA dilution versus ΔCq was generated to validate the RT-qPCR experiments (data not shown).

## A.2.4. Immuno-location of Re-crustin protein by western blot and by immunohistochemistry

*Polyclonal antiserum*: The chemically synthesized region of *Re*-crustin (PTRFGGPPQTCSSDSSCTNNYTDK) was coupled to ovalbumin and used for the immunization procedure of two New Zealand White rabbits (Saprophyte Pathogen free) according to the protocol of Covalab™ (France).

*Protein extraction and electrophoresis:* Total proteins were isolated from the samples used for RNA extraction according to the manufacturer's instructions (Trizol Reagent™, Invitrogen). The white band containing the proteins was washed with a solution of 0.3 M guanidine hydrochloride in 95% ethanol, and then resuspended in 9.5 M urea and 2% CHAPS. The protein concentration was determined by the Bradford method using BSA as a standard (Bradford, 1976). Proteins were separated by a denaturing SDS-PAGE electrophoresis. The running gel was composed of 12% acrylamide (12% acrylamide; Tris-HCL 1.5 M, pH 8.8; 0.1% SDS; 0.1% ammonium persulfate; 0.01% TEMED) and the stacking gel was composed of 4% acrylamide (4% acrylamide; Tris-HCL 0.5 M pH 6.8; 0.1% SDS; 0.1% ammonium persulfate; 0.01% TEMED). A total of 22 µg of protein was loaded in Laemmli buffer (Tris 125 mM pH 6.8; 20% glycerol; 4% SDS and 5% β-mercaptoethanol). Gels were run at 70 V for 15 min and then at 180 V for 20 min.

*Immunoblot*: The proteins of the SDS-PAGE gel were transferred to a nitrocellulose membrane 0.2 µm (BIO RAD) by semi-dry electro blotting (0.8-1.2 mA/cm²). After transfer, the gel was stained by Coomassie Brilliant Blue R-250 (Bio Rad). The membrane was blocked for 1 h in PBS at 0.1 M containing 0.05% Tween 20 and 5% casein and was then probed with the rabbit polyclonal anti-*Re*-crustin antibody (1:300 dilution) in a the blocking solution (PBS at 0.1 M with 5% w/v nonfat dry milk) overnight at 4°C. After three washes with PBS/0.05%-Tween 20, the membrane was incubated for 1 h in the blocking solution at room temperature with the peroxidase-conjugated anti-rabbit secondary antibody Abcam (1:5000 in PBS at 0.1 M containing 0.05% Tween 20; at 1 h). A ClarityTM Western ECL

Substrate (Bio Rad) was used for the chemoluminescence visualization of the immunolabelling with a Kodak Bio Max light film.

*Immunocytochemistry and immunohistochemistry*: Eggs, juveniles and tissues were fixed aboard in 4% paraformaldehyde. Later, immunohistochemistry was performed on paraffin sections of eggs (thickness of 4µm), juveniles and adult tissues (thickness of 7µm). Consecutive paraffin sections were made with a LEICA RM 2255 microtome. Immunocytochemistry and immunohistochemistry were performed with the rabbit anti-Re-crustin (1:400) and the FITC-conjugated anti-rabbit secondary antibody (1:100; Jackson Immunoresearch Laboratories). Samples were examined using a confocal microscope (Zeiss LSM LSM780) and the Fluorescence microscope (Zeiss Axio Imager 2).

### A.2.5. Determination of antimicrobial activities

*Samples:* Branchiostegites and scaphognathites were crushed with the rotor CoolPrep, MP system (3 times 20 sec at 60 rpm) in 0.1 M PBS at 4°C. 10 µL of samples were incubated without (control) or with the anti-*Re*-crustin antibody (dilution 1:400) at 4°C for 20 min.

*Radial diffusion assay*: 10 µL of each sample were spotted onto LB-agar (Luria-Bertani) plates containing alive Gram-positive *Micrococcus luteus* or alive Gram-negative *Vibrio diabolicus* ($1x10^5$ Colony Forming Unit (CFU)/mL of LB agar). After an overnight incubation at 37°C, the activity was quantified by measuring the diameter of the bacterial growth inhibition.

## A.3. Results

### A.3.1. Re-crustin, a novel member of Type IIa crustins from the deep-sea shrimp R. exoculata

The complete nucleotide sequence of *Re-crustin* was obtained by 5'-RACE RT-PCR from total RNA extracted from the entire shrimp *R. exoculata*. The complete cDNA sequence encodes a precursor of 190 amino acid residues, which includes a 15 residues signal peptide (**Fig 80A.**). The mature polypeptide is predicted to consist of 175 residues with a calculated molecular weight of 17.82 kDa and a theoretical isoelectric point (p*I*) of about 8.5. The mature *Re*-crustin is composed by a hydrophobic glycine-rich region followed by a C-terminus containing a cysteine-rich region (with 4 conserved cysteine residues) and a single WAP domain (**Fig 80B.**). The glycine-rich region of *Re*-crustin possesses ten sequential repeats of the heptapeptide Gly-Gly-(Gly/Val)-Phe-Pro-Gly-Gln [GG(G/V)FPGQ].

Besides the presence of an N-terminal glycine-rich region, multiple sequences alignment analysis confirmed that *Re*-crustin is an authentic Type II member from the Sub-Type IIa (**Fig 81.**). The *Re*-crustin sequence showed highest homology to Type IIa crustins from other decapods from the Pleocyemata suborder, including the red cherry shrimp *Neocaridina heteropoda* (*Nh*Crustin, 67% amino acid identity), the morotoge shrimp *Pandalopsis japonica* (*Paj*-CrusIIc, 64% amino acid identity), the Japanese spiny lobster *Panulirus japonicus* (PJC1-4, 59-66% amino acid identity) and the Chinese mitten crab *Eriocheir sinensis* (*Es*crustin-1, 63% amino acid identity). Within Type II crustins from penaeid shrimp (Dendrobranchiata), *Re*-crustin was 52-59% identical to Type IIa crustins and 44-53% identical to Type IIb crustins. On the other hand, the mature *Re*-crustin displayed 36-44% identity to Type I crustins from decapods from both Pleocyemata and Dendrobranchiata suborders. Less than 30% amino acid identity was observed between *Re*-crustin and Type III (single WAP domain-containing

proteins or SWD) and Type IV crustins (double WAP domain-containing proteins or DWD). Western blot analysis from total protein extracts showed a band at the predicted molecular weight confirming (i) the specificity of the antibody designed to recognize the WAP domain of *Re*-crustin and (ii) the translation of the *Re-crustin* transcripts (**Fig 82B.**).

## A.3.2. Production sites of Re-crustin in adults

RT-qPCR and Western blot analyses were performed on exactly the same tissues from the same individuals (**Fig 82.**). Results showed the presence of both transcripts (**Fig 82A.**) and proteins (**Fig 82B.**) in the pieces of the cephalothoracic cavity. Neither the transcripts nor the proteins were detected in the gut, the hepatopancreas and the stomach. The major Re-crustin producing tissues were clearly those on which the ectosymbiotic community of the cephalothoracic cavity develops, i.e. the branchiostegites and scaphognathites. Cellular localization of Re-crustin was then investigated in these pieces of carapace colonized by symbionts using immunohistochemistry and confocal microscopy analyses (**Fig 83.**). Immunolabelling with the anti-crustin antibody provided evidence for the synthesis of Re-crustin by the epithelium cells beneath the cuticle of the branchiostegites and scaphognathites from adults (**Fig 83A. and 83C.**) and its accumulation on the cuticle that delimits the cephalothoracic cavity. Interestingly, Re-crustin covered some of intact ectosymbiotic bacteria anchored to these mouthpieces (**Fig 83C. and 83E.**).

## A.3.3. Role of Re-crustin in the antimicrobial activities of the branchiostegites and scaphognathites

Antimicrobial assays performed from crude extracts of branchiostegites and scaphognathites showed anti-bacterial activities against Gram-positive but not against Gram-negative bacteria (**Fig 84.**). Part of this antibiotic effect is reduced when the endogenous Re-crustin is blocked by adding the specific Re-crustin antibody to the extract, confirming the production of active Re-crustin in both scaphognathites and branchiostegites as well as its biological properties.

## A.3.4 Production site of Re-crustin along the life cycle of the shrimps

The transcriptomic and protein levels of Re-crustin were investigated at different stages of the shrimp life-cycle for which the colonization states by the ectosymbionts were already described (**Fig 85.**) (Guri et al., 2012; Methou et al., 2019a). In eggs, the gene is slightly expressed (**Fig 85A.**), but the protein is not detected in the western blot analysis (**Fig 85B.**). Using immunohistochemistry, which is a more sensitive method, we detect a small amount of the protein in the membrane of freshly spawned eggs (early eggs (**Fig 86A.**)). In late stages, Re-crustin was immunodetected into vesicles beneath the cell membrane (**Fig 86Ca.**) and on the bacteria that form the biofilm surrounding the eggs (**Fig 86Cb.**). RT-qPCR data using total RNAs extracted from whole juveniles combined with western blot show that Re-crustin transcripts and proteins are highly abundant at this stage (**Fig 85A.**). Re-crustin was immuno-localized on the cuticle that delimits the cephalothoracic cavity, and also in the nervous system (**Fig 87.**).

Because the life of adults is punctuated by molt cycles, the same protocol was applied to “white” adults at the beginning of their molt cycle in comparison with “red” adults at the end of their molt cycle (**Fig 88.**). In both cases, Re-crustin transcripts were not detected by RT-qPCR using RNA extracted from whole animals, probably because of an over dilution of the transcripts (**Fig 85A.**). By contrast, the protein was abundantly present in red adults at their pre-ecdysial stage while it was undetectable in adults that have just molted and are starting a new cycle (**Fig 85B.**).

Immunohistochemistry (**Fig 88.**) showed an accumulation of Re-crustin in the epidermis beneath the cuticle colonized by epibionts of red animals only (**Fig 88.**).

## A.4. Discussion

We provide here evidence for a novel biological role for gene-encoded antimicrobial host defense peptides (AMPs) in crustacean-microbe interactions. Our results revealed that the expression of a new member of the classic crustin AMP family (*Re*-crustin) is highly correlated with the establishment of the ectosymbiotic microbial communities inhabiting the cephalothoracic cavity of the extremophile deep-sea shrimp, *R. exoculata*. Different from its Pleocyemata counterparts that mainly produce Type I crustins, *R. exoculata* expresses in its tissues a N-terminal glycine-rich crustin that belongs to the Sub-Type IIa. Indeed, the Type II comprises a distinct group of crustins usually found in penaeid shrimp (Dendrobranchiata suborder) that is subdivided into two Sub-Types: Type IIa ("Crustins") and Type IIb ("Crustin-like") (Tassanakajon et al., 2018). Although unusual, the presence of Type IIa crustins has been reported for other decapod crustaceans from the Pleocyemata suborder (Kim et al., 2013; Pisuttharachai et al., 2009). On the other hand, Type IIb crustins were only described in penaeid shrimp species (Barreto et al., 2018).

The presence of a signal peptide in the *Re*-crustin precursor, together with the results obtained from the Western blot analysis, provides evidence of its processing prior to the release of the *Re*-crustin into the extracellular compartment where it exerts its biological properties. The accumulation of *Re*-crustin on the surface of some ectosymbionts, as evidenced by immunohistochemistry, also supports the extracellular secretion and clearly shows an interaction of *Re*-crustin with the ectosymbiotic community of the cephalothoracic cavity *in vivo*. This interspecific interaction appears as an important function of *Re*-crustin in *R. exoculata*. Our multiple approaches all demonstrate that *Re*-crustin is essentially produced by the mouthparts in the cephalothoracic cavity, which is hugely colonized by the ectosymbionts, (Casanova et al., 1993; Guri et al., 2012; Petersen et al., 2010; Zbinden et al., 2004). *Re*-crustin was slightly detected in the digestive tract, which is colonized by a microbial community different from the one of the cephalothoracic cavity (Durand et al., 2010, 2015). This suggests a low contribution of *Re*-crustin in this organ and underlines the importance of the molecule in the cephalothoracic cavity of *Rimicaris*. When tested for their production of antibiotics, the scaphognathites and branchiostegites showed anti-Gram-positive properties that were partially, but not only, due to *Re*-crustin, thus suggesting the synthesis of other still undiscovered antibiotics by these appendages or their associated bacteria. No activity was observed against the tested *Proteobacteria*, confirming *Re*-crustin as belonging to the Type IIa crustins which are known to be mainly active against Gram-positives (Supungul et al., 2008) while the Type IIb crustin from *Penaeus monodon* (crustin*Pm*7/Crus-like*Pm*) showed antibacterial activity against both Gram-positive and Gram-negative bacteria (Amparyup et al., 2008; Banerjee et al., 2015). Since Archaea are highly abundant in hydrothermal vents, and because their cell wall is more similar to those of Gram-positive than those of Gram-negative bacteria, an anti-Archaea activity of *Re*-crustin could be expected even if it remains to be tested when it would be technically feasible. Because they are also uncultivable, the ectosymbionts could not be used for *in vitro* antimicrobial assays. However, immunodetection with the anti-*Re*-crustin antibody showed that the AMP covers the surface of the filamentous ectosymbionts (mainly composed of Gram-negative *Proteobacteria*/*Campylobacterota*) without killing them. A control of the bacterial growth *via* bacteriostatic activities of *Re*-crustin as observed in the endosymbiostasis of beetles cannot be excluded (Masson et al., 2016).

*Re*-crustin is probably part of a cocktail of AMPs and immune receptors, such as the recently characterize type C lectin (Liu et al., 2019), acting synergistically to shape the symbiont community and to prevent the colonization of the gills by pathogens and/or competitors such as Gram-positive bacteria and also Archaea. Further investigations will have to be performed to identify the other antibiotics involved in the emblematic ectosymbiotic association of *Rimicaris*. Unexpectedly, *Re*-crustin is absent from the hemolymph in which it is generally abundantly present as a classic AMP against systemic bacterial infection of most crustaceans. Also surprisingly, neither antimicrobial nor clotting activities were observed in the hemolymph of the deep-sea shrimp, suggesting that its antimicrobial defenses are based on mechanisms somehow different from those generally observed in most crustaceans. *Re*-crustin was also immunodetected in the central nervous system (CNS). Further investigations should be performed to determine whether the expression sites are the neurons themselves or the epithelial cells infiltrated into the nervous system as documented for the crustin named PET-15 in the spiny lobster (Stoss et al., 2004). A multifunction of *Re*-crustin appears also as a potential hypothesis to explore, following *e.g.* results on the neuronal growth activities of AMPs produced by the CNS of other invertebrates (Tasiemski and Salzet, 2017).

To go further into the role of *Re*-crustin in the ectosymbiostasis of *Rimicaris*, we explored the spatio-temporal correlations between the levels of production of *Re*-crustin and the ectosymbiotic acquisition/loss/re-colonization events that punctuate the life cycle of the hydrothermal shrimp. Our data show that *Re*-crustin is already present at the surface of just spawned eggs. The synthesis is enhanced in late eggs still attached to the abdomen of the mother, as they are being colonized by a dense mat of bacteria. Interestingly, *Re*-crustin secreted by late eggs covers the bacteria forming the biofilm. The biofilm formation appears as an inducible signal for *Re*-crustin synthesis/secretion in eggs during their embryonic stages and thus may contribute to the development of the immune system. Re-crustin may also serve as an anti-competitive agent for the symbionts. During their embryonic development, *R. exoculata* egg envelopes are colonized by bacterial communities that partly differ from adult's symbiotic communities for late stage eggs (Guri et al., 2012; Methou et al., 2019a). After hatching, larvae undergo several molting events to the juvenile stage A, while dispersing in the water column before their recruitment to a new hydrothermal vent field (Guri *et al.*, 2012; Hernández-Ávila et al, 2015). Although we cannot rule out the possibility that some of the bacteria present on eggs during embryonic development are carried along during post-hatching larval life until recruitment, recruited juveniles appear to be mostly colonized anew shortly after settlement by an ectosymbiotic community *i.e.* the one of the cephalothoracic cavity in adults (Le Bloa et al., 2017). In late eggs and even much more pronounced in recruited juveniles, the peak of synthesis of *Re*-crustin corresponds to the development of a novel bacterial community. *Re*-crustin would then appear as a developmental, metamorphic signal induced by the symbiotic community in the eggs and in the juveniles stages.

Immunohistochemistry combined with RT-qPCR and western blot data also show a spatial correlation between the AMP and the symbionts, with an abundant presence of *Re*-crustin in the late eggs and in the epidermis cells beneath the cuticle of the branchiostegites and scaphognathites carrying the ectosymbionts, in recruited juveniles and in adults. As far as we know, only few studies have been devoted to the investigation of crustin expression during the early stages of crustacean's life and none were correlated with the associated bacterial community (Hauton et al., 2007; Jiravanichpaisal et al., 2007; Smith et al., 2008; Smith and Dyrynda, 2015). Hauton and colleagues have shown that Type I crustin expression levels are similar in lobster *Homarus gammarus* postlarvae stages IV and VI (Hauton et al., 2007). Larvae of the shrimp *P. monodon* have been reported to express a Type

IIb crustin transcript at high levels at all stages of development from nauplii IV through to juveniles (Barreto et al., 2018). In all reported cases, an immune function of crustins in larvae was proposed but their involvement in the symbiostasis was not investigated.

Like most crustaceans and contrary to metabole insects, *Rimicaris* still molt during their adult stage. Molting results in the complete renewal of the cuticle (including mouth appendages) together with the loss of the attached ectosymbiotic community, notably on scaphognathites and branchiostegites in our case. Interestingly, the production of *Re*-crustin by the scaphognathites and branchiostegites reaches a peak when the re-colonization occurs, corroborating the role of *Re*-crustin in the control of the symbiosis acquisition and probably in the selection of the appropriate bacteria from the habitat. Since *Rimicaris* forms large and dense colonies constituted by individuals desynchronized in their molting and development, the symbiotic bacteria remain always available within the population, such as on shed exuvia, thus allowing the horizontal transfer of the symbionts. Because *Re*-crustin accumulates on the surface of both the symbionts and the cuticle of the appendages, the molecule may also serve as a communication pathway in between the host and the bacteria thus favoring the recruitment and the horizontal transfer of the free-living symbionts.

During the extremely short molt cycle (10 days), the symbiont growth is accompanied by a progressive mineral accumulation, caused in part by the symbiont activities (Corbari et al., 2008a, 2008b). In pre-ecdysial advanced stage, the mineral crust completely surrounds the symbionts and some lysis forms can even be observed. The recovery induced by molting could "stifle" the symbionts that would no longer be able to properly feed their host. The host might thus trigger its molt to recycle its ectosymbionts. Therefore, the *R. exoculata* molt cycle could be compared to the concept of symbiotic trade-off retrieved in insects (Masson et al., 2016) whereby insects offer “board and lodging” to the endosymbionts as long as they can rely on their metabolic supply, and recycle them by autophagy and apoptosis when the cost of symbiont maintenance overcomes the provided benefits.

Our results overall highlight a novel AMP sequence from an extremophile organism and fill some knowledge gaps regarding the role of AMPs in the establishment of vital ectosymbioses that take place along the life cycle of marine organisms. *R. exoculata* enlarged cephalothoracic cavity offers a mechanic but also an immune protective environment for the symbionts against the harsh hydrothermal vent conditions and their microbial competitors while the symbionts provide nutrients via a transcuticular transfer (Ponsard et al., 2013) and maybe an immunity to the shrimp. The developmental and metamorphic role of the ectosymbiosis *via* the induced production of *Re*-crustin would have to be investigated to decipher the correlated production of the AMP with the symbiotic colonization and the transition stages of the host.

## Acknowledgments

We thank all the chief scientists, ship captains, crew and submersible teams of the oceanographic BICOSE 1 and 2 cruises for their efficiency. This work was supported by Ifremer, LabexMer and ANR Carnot EDROME Institute. We thank B. Shillito (BOREA) for the use of the pressure equipments funded by a European Community program EXOCET/D (FP6-GOCE-CT-2003-505342), and by the University Pierre et Marie Curie, under the BQR UPMC 2008. RD Rosa was founded by the Brazilian funding agencies CNPq (MEC/MCTI/CAPES/CNPq/FAPs PVE 401191/2014-1 and MCTI/CNPq

Universal 406530/2016-5) and CAPES (CIMAR 1974/2014). The authors have no conflict of interest to declare.

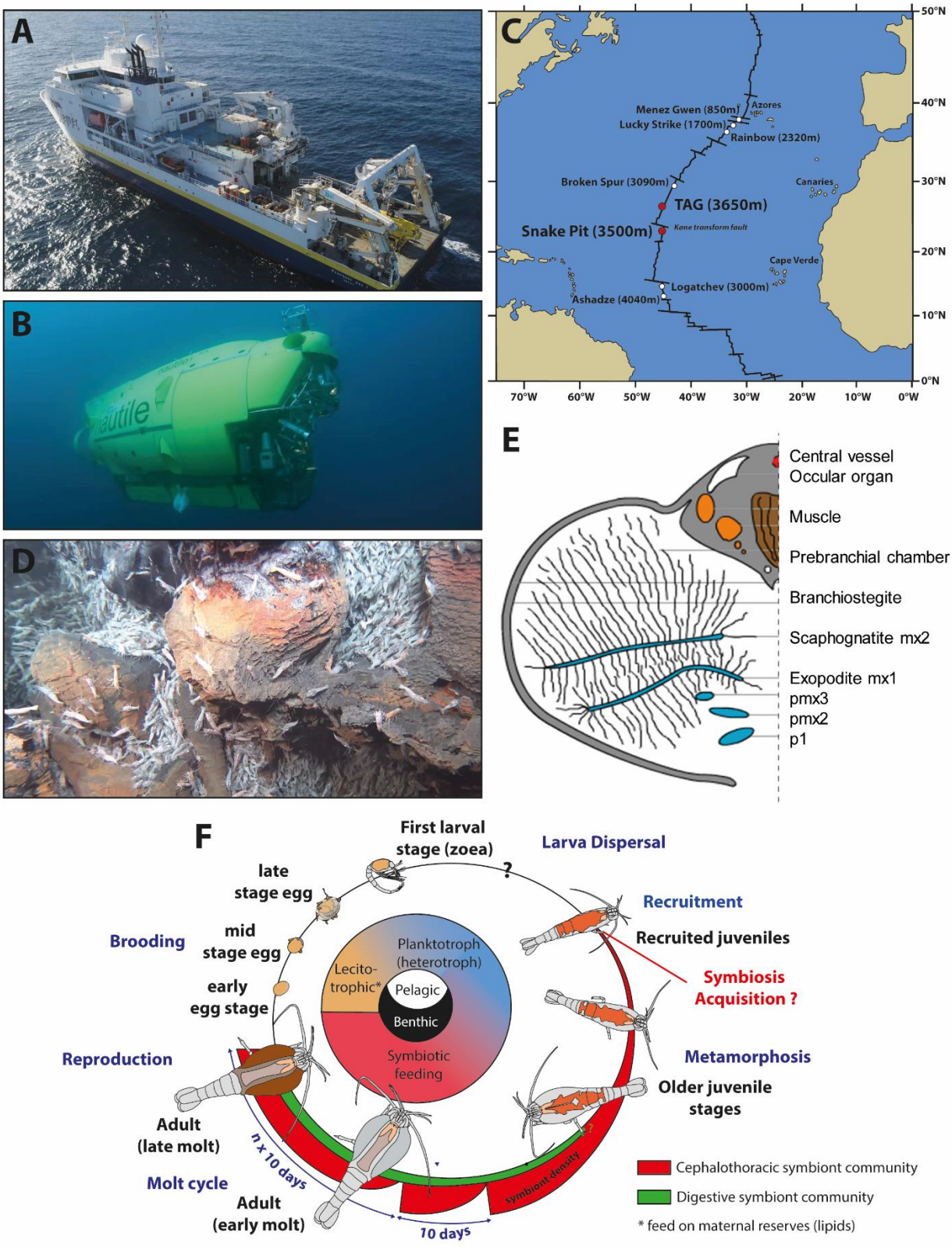


**Fig 80.** *Rimicaris exoculata* sampling and summary of its symbiotic relationships through its life cycle **A.** R/V Pourquoi pas? **B.** HOV Nautile used for sampling. **C.** Location of the two hydrothermal vent sites presently studied along the Mid-Atlantic. **D.** Suction sampling of the shrimps with the human operated submersible Nautile during the oceanographic cruise BICOSE2018. **E.** *Rimicaris exoculata* cephalothoracic chamber (modified from Segonzac et al., 1993). **F.** Life cycle of *Rimicaris exoculata*. Inspired from the figure of (Laming et al., 2018).

**A**

```
      gttcatcaccactgaaggacaaacacctcctcctccagctctctagatttctcaag -1

atgctgttattgtctttaatagctatagccaatttagctatggctttaccagaaaaggcc 60
M  L  L  L  S  L  I  A  I  A  N  L  A  M  A  L  P  E  K  A  20
caggaaacccgccactatccaggacaaggaggcgtatttccaggacaaggaggcggattt 120
Q  E  T  R  H  Y  P  G  Q  G  G  V  F  P  G  Q  G  G  G  F  40
cctggacaaggaggtggattccctggacaaggaggtggattccctggacaaggaggtgga 180
P  G  Q  G  G  G  F  P  G  Q  G  G  G  F  P  G  Q  G  G  G  60
ttccctggacaaggaggtggattccctggacaaggaggcggatttcctggacaaggaggt 240
F  P  G  Q  G  G  G  F  P  G  Q  G  G  G  F  P  G  Q  G  G  80
ggattccctggacaaggaggcggatttcctggacaaggaggtggattccctggaggatct 300
G  F  P  G  Q  G  G  G  F  P  G  Q  G  G  G  F  P  G  G  S  100
tcctcttgtaaatactggtgtagaacacctgaaaaccaagcctactgctgtgagaacggg 360
S  S  C  K  Y  W  C  R  T  P  E  N  Q  A  Y  C  C  E  N  G 120
aaccaggctcaaagaccaacccctcgtcctaccatcaggcccgggatttgcccaccagtg 420
N  Q  A  Q  R  P  T  P  R  P  T  I  R  P  G  I  C  P  P  V  140
cgaccgcagtgcccccccaccagatttggaggacccccctcaaacatgttccagtgattct 480
R  P  Q  C  P  P  T  R  F  G  G  P  P  Q  T  C  S  S  D  S  160
tcctgtaccaacaactatactgataaatgctgtttcgacagatgtcttgaagaacacgtc 540
S  C  T  N  N  Y  T  D  K  C  C  F  D  R  C  L  E  E  H  V  180
tgcaaaccacctcaacaaaatttcggccgctgaaatagtaaggaagtgaaatgaaggag 600
C  K  P  P  Q  Q  N  F  G  R  ***                           190
gtgcgacgtaacacaggcaattagccatgcatgttttgtgctaatagaaaaaaaaaaaaa 660
aaaaaaaa                                                    668
```

**B**

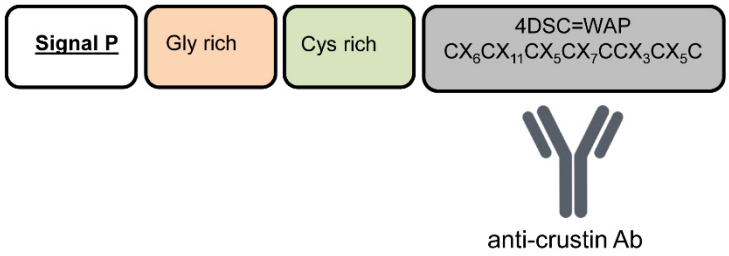


**Fig 81.** Re-crustin sequence. **A.** The full-length nucleotide (above) and predicted amino acid (below) sequences of Re-crustin cDNA from Rimicaris exoculata. The start and stop codons and the putative polyadenylation site are in bold and underlined. The signal peptide is underlined. **B.** The predicted organization of WAP domain is shown in grey boxes. The twelve conserved cysteine residues are framed.

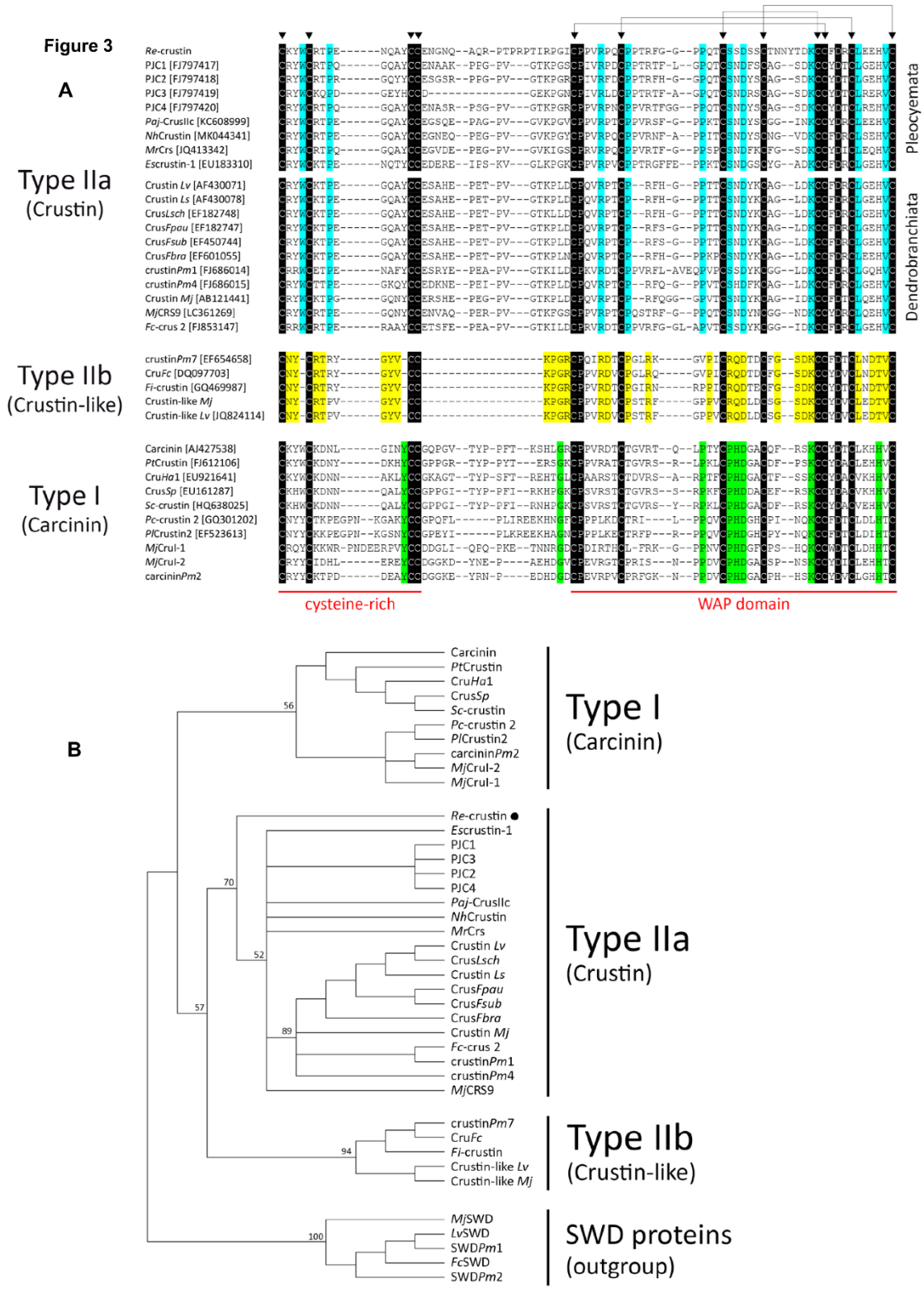


**Fig 82.** Comparison of Re-crustin with other Type I and Type II crustins from decapod crustaceans. **A.** Amino acid sequence alignments of the cysteine-rich region and the WAP domain of crustins. Identical amino acid residues are highlighted in black while specific amino acid residues found in Type IIa ("Crustin"), Type IIb ("Crustin-like") and Type I ("Carcinin") peptides are highlighted in blue, yellow and green, respectively. Triangles (▼) indicate the 12 conserved cysteine residues. **B.** Phylogenetic analysis of Type I and Type II crustins. The tree was constructed using the Maximum Likelihood method with bootstrap values calculated from 1,000 trees.

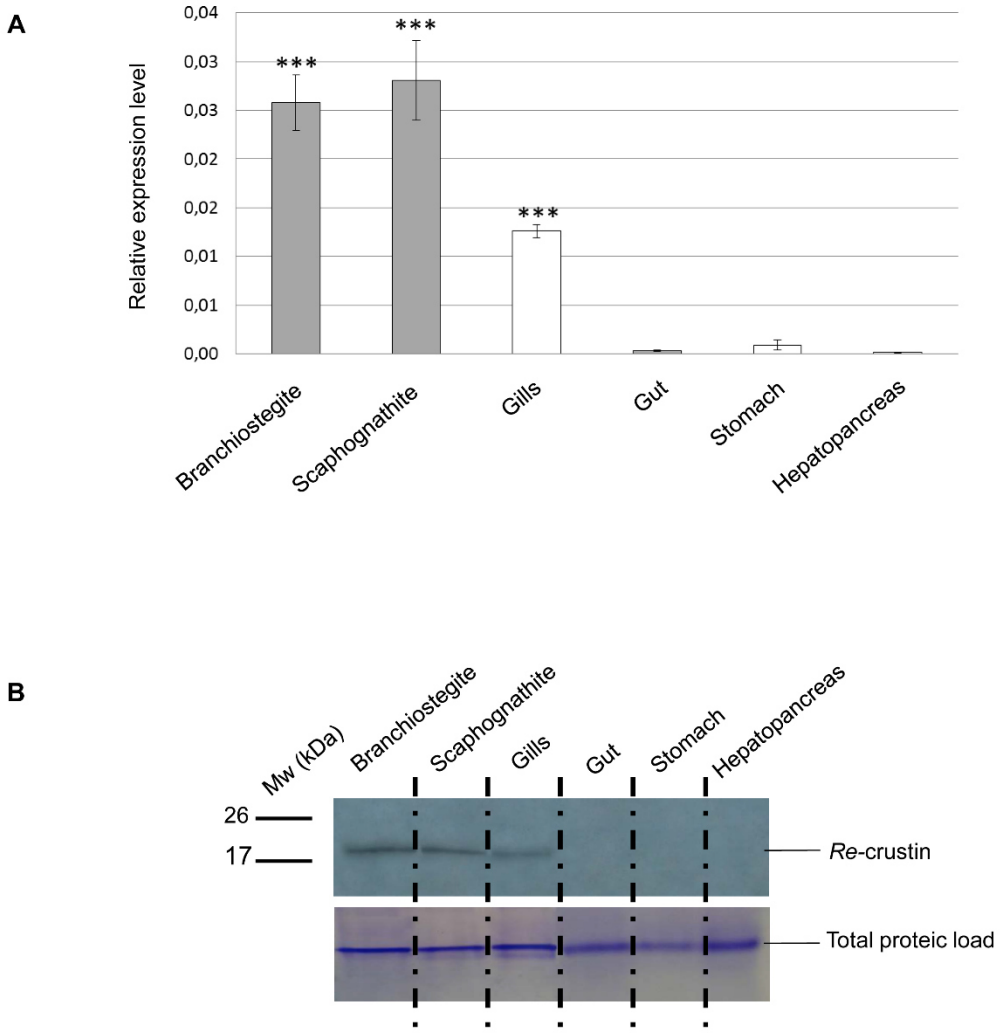


**Fig 83.** Re-crustin distribution in tissues of adults of *Rimicaris exoculata*. **A.** Quantification of the levels of expression of Re-crustin in the cephalothoracic cavity (branchiostegite; scaphognathite; gills) and in the digestive tract (gut; stomach; hepatopancreas) by RT-qPCR analysis using the ΔΔCq method. In grey symbiotic tissues. The graphs show the mean ± SEM of triplicate samples. (*$p < 0.05$; t-test). Reference (Rpl8) and target were amplified in separated wells ($n > 10$ in all cases). **B.** Western blot analysis was performed using total protein extracts from branchiostegite; scaphognathite; gills; gut; stomach and hepatopancreas dissected from adults. Immunostaining with the anti-Re-crustin antibody revealed one band of approximately 17 kDa corresponding to Re-crustin mass prediction. Mw: molecular weight markers. Equivalent well loading was assessed by a generic protein coloration of the gel (Coomassie Brilliant Blue R-250).

Figure 5

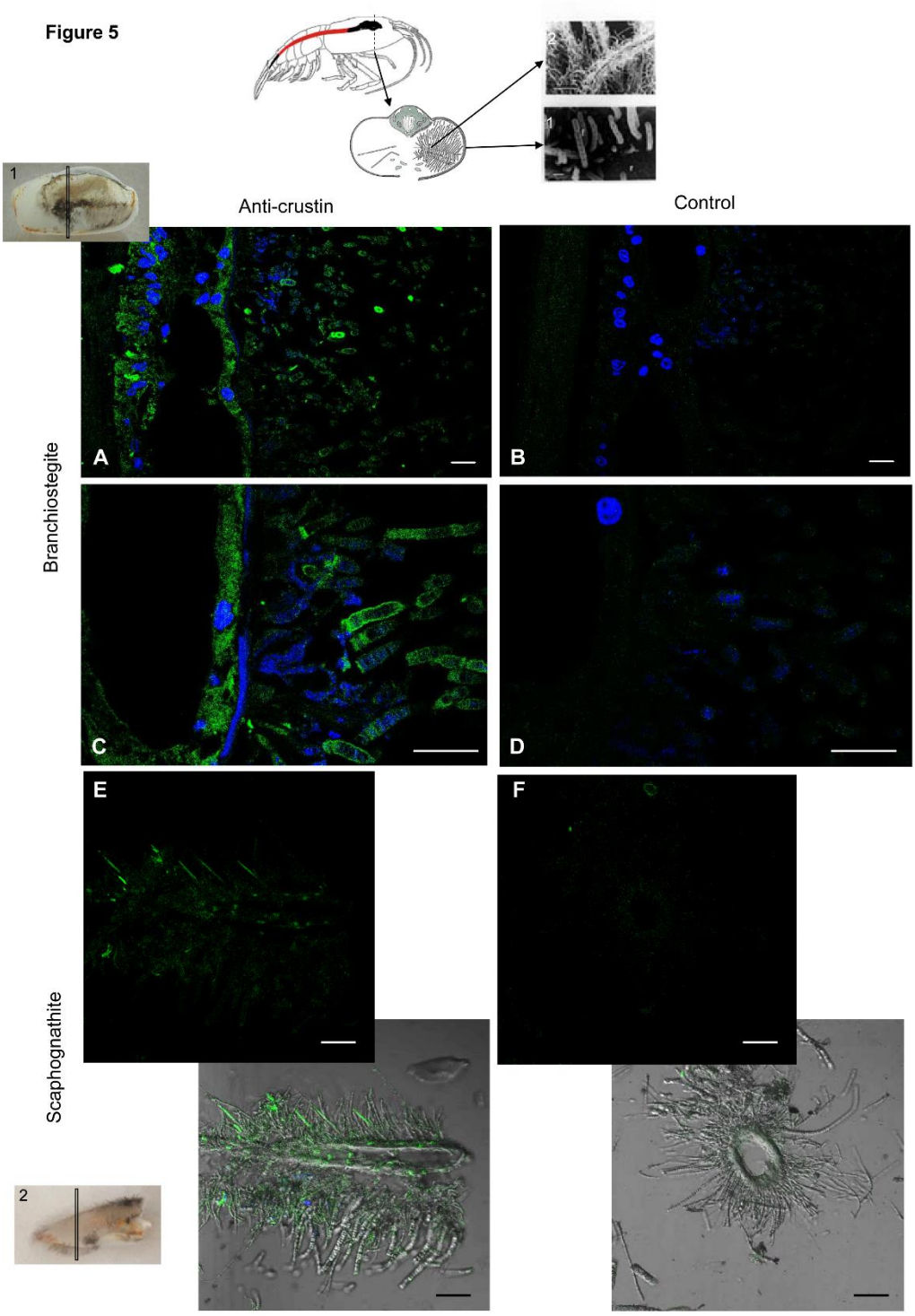


**Fig 84.** Immunolabelling on paraffin sections with a thickness of 7µm of Re-crustin on pieces of carapace colonized by bacteria. Schematic Rimicaris exoculata cephalothoracic chamber illustrated by two photos in electron microscopy (1-2) the filamentous epsilon Proteobacterial epibionts. **(A-D)** Branchiostegite and **(E-F)** scaphognathite. **(A-C)** The anti-crustin antibody specifically labels in green the tissue that lines the inside of the cephalothoracic cavity and also covers the surface of some attached bacteria. **(E)** Some bacteria attached to the scaphognathite are also labelled. **(B-D-F)** No labelling appears with the pre-immune control. Nucleic acids are labelled in blue (DAPI). The white field is superimposed in **E** and **F** to see the shadows of the structures. The observations were made using the confocal microscope, Zeiss LSM 780. Scale bars correspond to 20 µm.

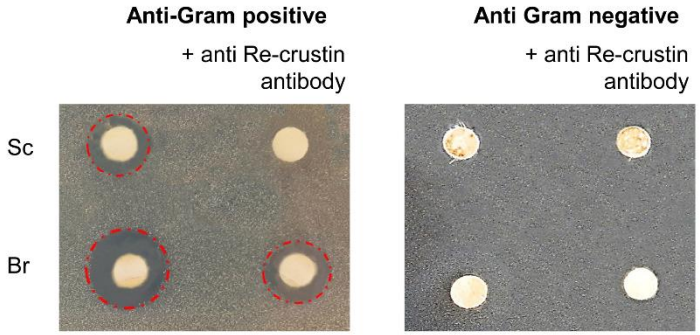


**Fig 85.** Antimicrobial activities of crude extracts of branchiostegites (Br) and scaphognathites (Sc) against Gram-positive and Gram-negative bacteria. The antibody added to the extracts acts as a blocking agent of the endogenous Re-crustin. The red circles underline the antimicrobial activities.

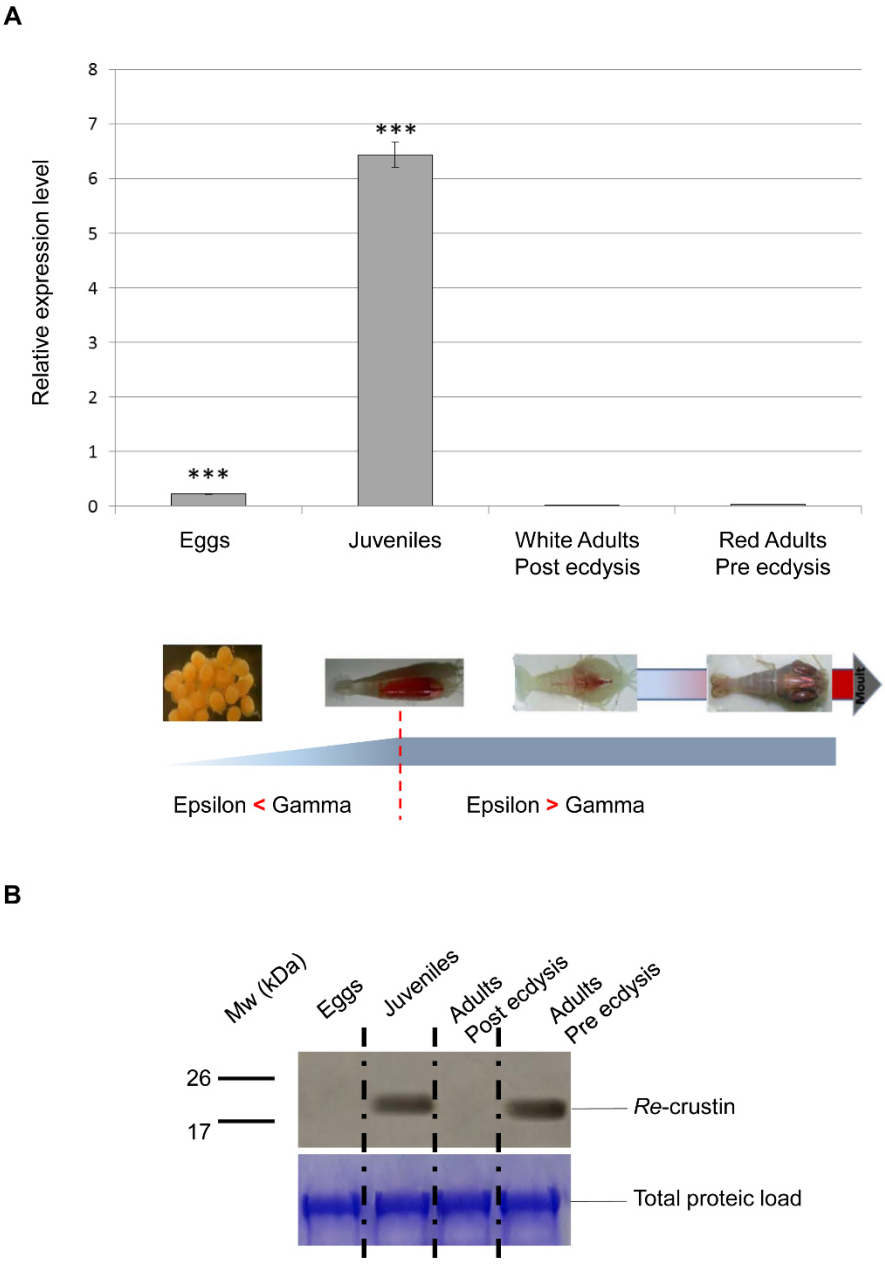


**Fig 86.** Re-crustin distribution along the *Rimicaris exoculata* life cycle and molt stages. **A.** Gene expression analysis by RT-qPCR. The graph shows the mean + SEM of triplicate samples (*, $p < 0.05$; t test). Reference (Rpl8) and targets were amplified in separated wells ($n > 10$ in all cases). **B.** Western blot analysis was performed using total protein extracts from eggs, juveniles, adults (beginning of molt cycle) and adults (end of molt cycle). Immunostaining with the anti-Re-crustin antibody revealed one band of approximately 17 kDa corresponding to Re-crustin mass prediction. Mw: molecular weight markers. Equivalent well loading was assessed by a generic protein staining of the gel (Coomassie Brilliant Blue R-250).

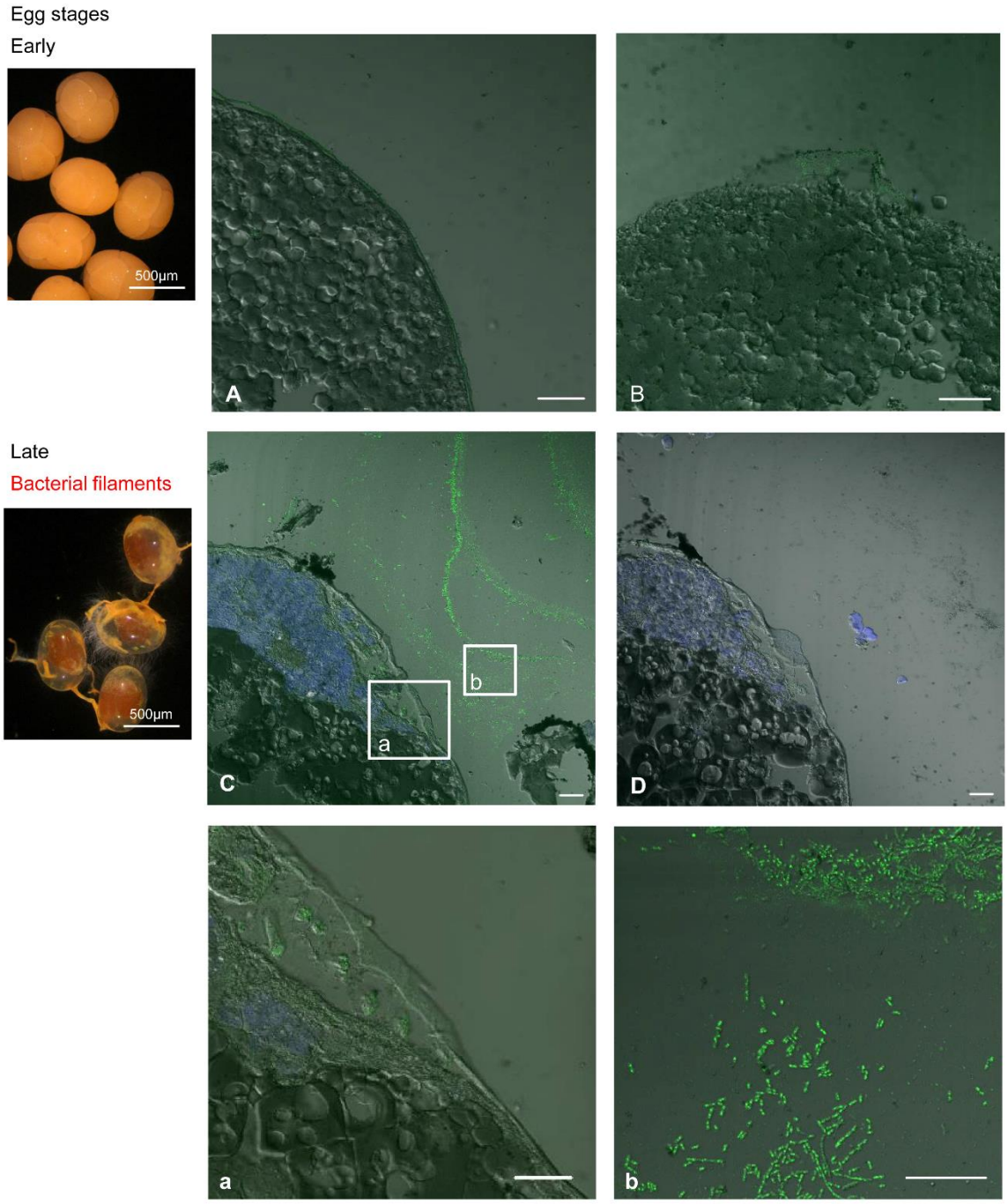


**Fig 87.** Immunolabelling on paraffin sections with a thickness of 4 µm of Re-crustin on eggs of early stages (**A-B**, no biofilm) and of late stages (**C-D**, **a-b**, orange biofilm). **A.** No labelling is visible in the panels corresponding to eggs at young stage, with the specific antibody or **B.** with the pre-immune control. On late stages, the biofilm that covers the eggs is clearly labelled (**C**, **b** for a closer view), and some vesicles containing Re-crustin are visible beneath the membrane of the egg (**C**; **a**; for a closer view). **D.** No labelling is visible with the pre-immune control. Nucleic acids are labelled in blue (DAPI). The white field is superimposed to see the shadows of the structures. The observations were made using the confocal microscope, Zeiss LSM 780. Scale bars correspond to 20 µm.

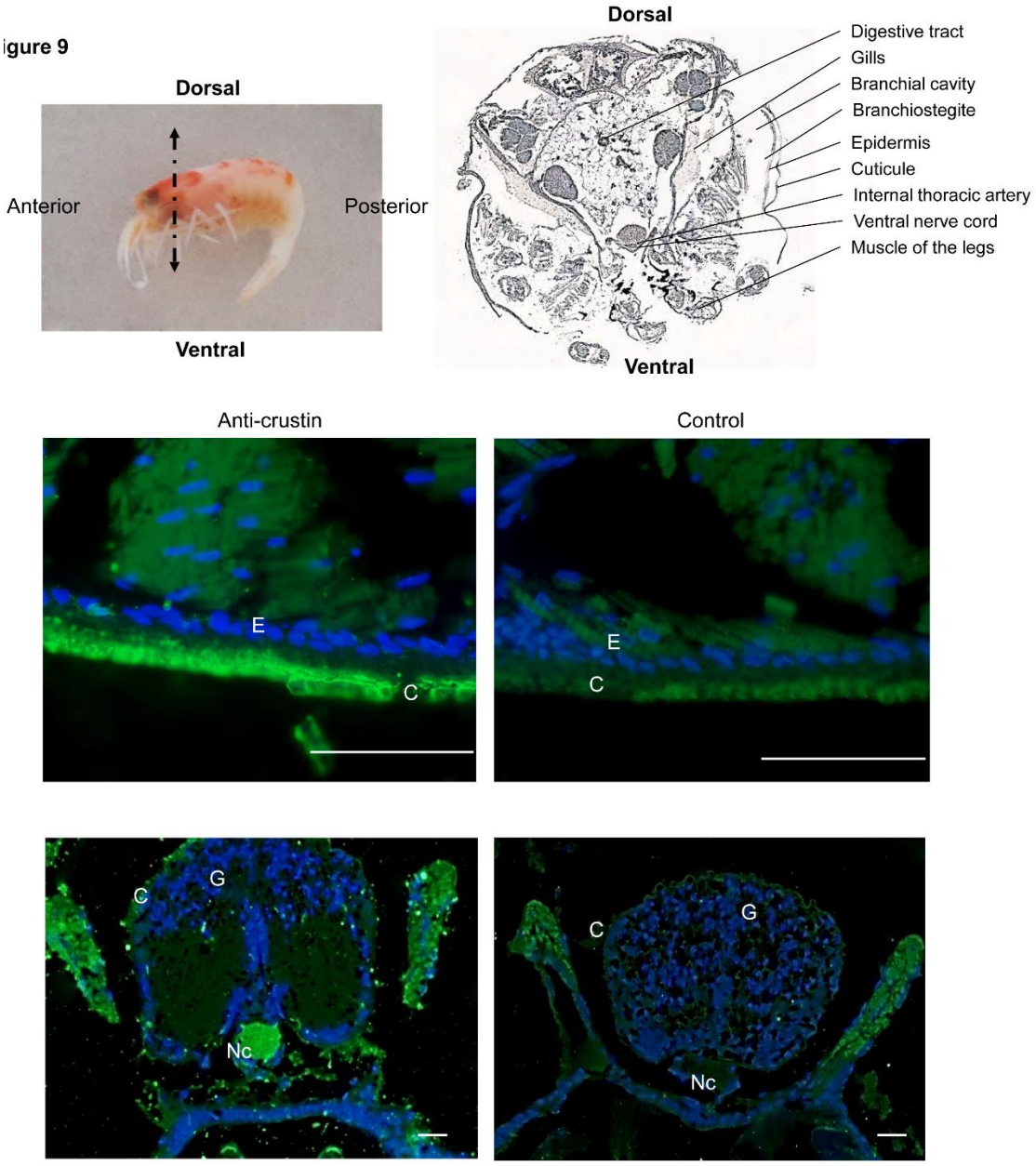


**Fig 88.** Immunolabelling on paraffin sections with a thickness of 7µm of Re-crustin on juveniles. **A.** Image of juvenile fixed in 4% paraformaldehyde to illustrate the detailed section shown on the right. The anti-crustin antibody specifically labels in green the cuticle **B.**, gills and nerve cord **C.** in juveniles. No labelling is visible in the control panels. Nucleic acids are labelled in blue (DAPI). The observations were made using the fluorescence microscope, Zeiss Axio Imager 2. Scale bars correspond to 20 µm. **Abbreviations used: C**, cuticle; **E**, Epidermis; **G**, Gills; **Nc**, nerve cord.

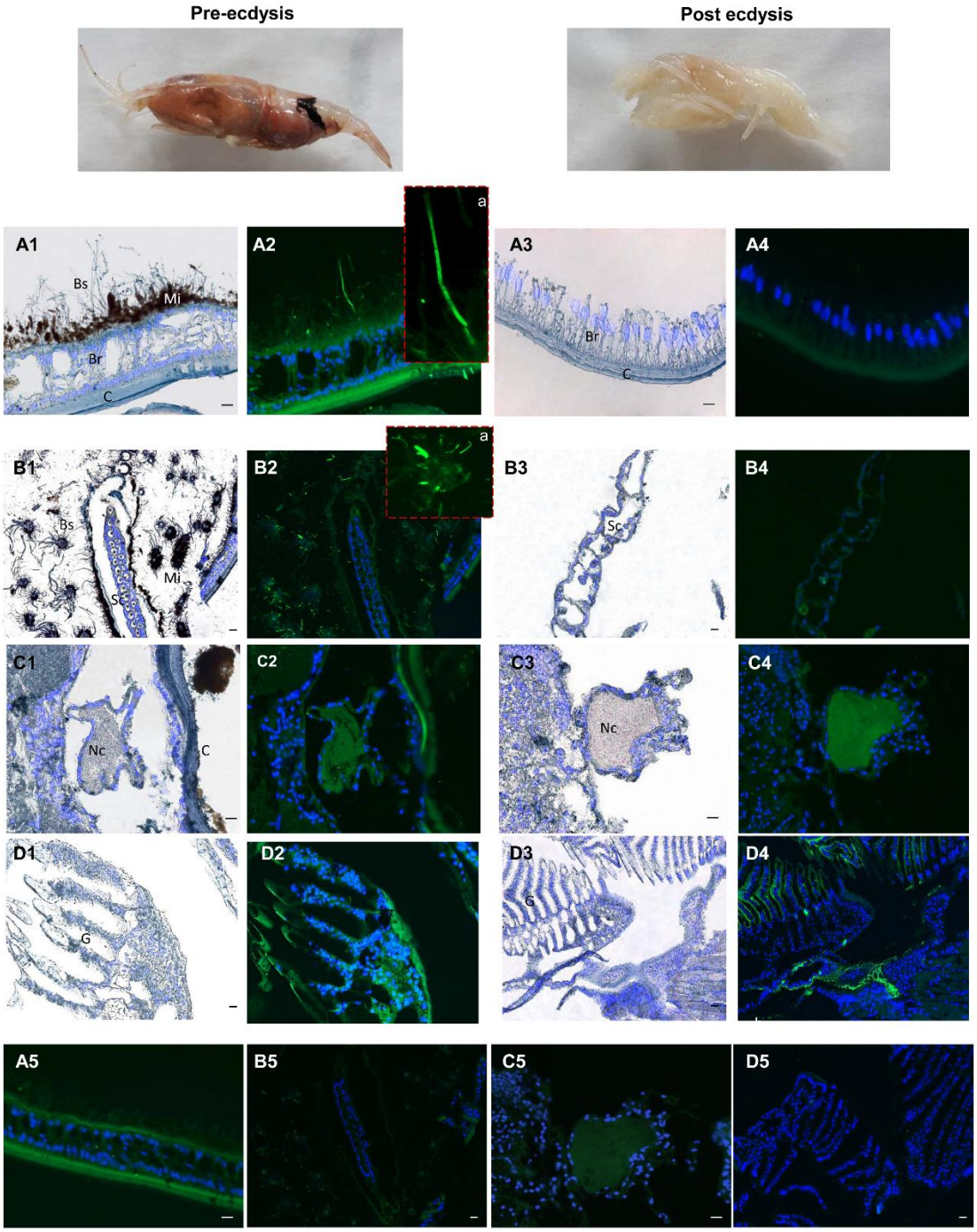


**Fig 89.** Immunolabelling on paraffin sections with a thickness of 7µm of Re-crustin in adult shrimps before and after molting. Two images present an adult shrimp at the end of the molting cycle (Pre-ecdysis) and after molting (Post-ecdysis). (**A2- a**) The anti-crustin antibody specifically labels in green the tissue that lines the inside of the cephalothoracic cavity and covers the surface of some attached bacteria at the Pre-ecdysis. (**B2- a**) Some bacteria attached to the scaphognathites are labelled at Pre-ecdysis only. An immune staining of the Re-crustin is observed in the Nerve cord (**C2- C4**) and in the gills (**D2- D4**) of adults at both the Pre- and Post-ecdysis stages. Nucleic acids are labelled in blue (DAPI). (**A5- B5-C5** and **D5**) No labelling appears with the pre-immune control. The white field is shown in **A1**, **A3**, **B1**, **B3**, **C1**, **C3** and D1, D3 to see the structures. The observations were made using the fluorescence microscope, Zeiss Axio Imager 2. The 20µm scale bars are placed on the white fields and on the pre-immune controls. **Abbreviations used : Br**, branchiostegites ; **C**, cuticle; **Bs**, Bacterial symbionts; **G**, gills; **Mi**, mineral deposits; **Sc**, scaphognathite; **Nc**, nerve cord.

# List of congress, poster and communication of this thesis

November 2019 **JAMSTEC Young Researcher Fellow Program 2020 (Job interview)**

*20 min oral presentation* **Yokohama, Kanagawa Prefecture, Japan**

## Beyond the *Rimicaris exoculata* symbioses

**Abstract:**

At the limit of tectonic plates, the deep ocean is punctuated by dense and ephemeral oases of life: the hydrothermal vent ecosystems. Unlike other marine ecosystems, they are mainly sustained by chemosynthetic primary production carried out by microorganisms, using the chemical energy from the expelled vent fluids. Many of these microorganisms are involved in symbiotic associations with many different vent faunal taxa. Chemosymbiotic animals tend to dominate visually the vent communities, forming dense aggregations around the vent chimneys. Along the Mid Atlantic Ridge, the alvinocaridid shrimp Rimicaris *exoculata* is one of the most abundant species in these ecosystems. One of the particularity of this species is its modified "head" with a strongly enlarged cephalothoracic cavity. In this cavity, the shrimp hosts large communities of chemosynthetic symbionts that provide most of its nutrition. This shrimp also possesses a second symbiotic community, with different symbionts, never retrieved in the environment, which roles are still under investigation. Less abundant, another shrimp from the same family, *R. chacei* is co-occurring with *R. exoculata*. Unlike *R. exoculata*, this shrimp does not exhibit a strongly enlarged cephalothorax but still hosts a similar symbiosis in its cephalothoracic cavity, although the symbionts only provide a part of its diet. *R. chacei* also relies on other food sources, as evidenced by its much larger stomach than *R. exoculata*. Studying these two shrimps is particularly interesting, especially when also considering a third species, *R. hybisae* from the Mid Cayman Rise that exhibits a similar morphology than *R. exoculata* with an inflated "head" but is genetically similar to *R. chacei* despite their apparent morphological differences. This suggest that the development of symbiosis and its related modifications result from anatomical convergence between *R. hybisae* and *R. exoculata*. This project aim to explore the evolutionary link between the symbioses in alvinocaridid shrimps by providing a more comprehensive view of their trophic strategies and their symbiotic relationship in shrimp from different regions of the globe. A focus will be made not only on *R. hybisae* from the Mid Cayman Rise but also on the different species from the Okinawa trough. Morphological convergence will be explored also on the internal anatomy, mainly to identify differences in the digestive system, but also how these differences may reflect the evolution of nutritional strategies. In addition, trophic strategies between the different co-occurring species of Okinawa trough will be explored to characterize species fueled by chemosynthetic symbionts. In parallel, their environmental niches will be investigated to decipher which conditions could favor the emergence of symbiotic relationships. Finally, all the data acquired during this project will be compared with those acquired on alvinocaridids from the Atlantic during previous studies and synthetized to propose a more global portrait of the trophic strategies and the symbiotic relationships of these holobionts.

June 2019 **JAMSTEC Research Discussion Seminar** (*invited by Dr. Chong Chen)*

*30 min oral presentation* **Yokosuka, Kanagawa Prefecture, Japan**

## Lifecycle ecology of the hydrothermal vent shrimps *Rimicaris exoculata* & *Rimicaris chacei*

**Abstract:**

Presented by Pierre Methou[1, 2]

1: Univ Brest, CNRS, Ifremer, Laboratoire de Microbiologie des Environnements Extrêmes, Plouzané, France

2: Ifremer, Laboratoire Environnement Profond (REM/EEP/LEP), Plouzané, France

Discovered only forty years ago, hydrothermal vents are probably some of the most surprising ecosystems of our planet. Displaying extremely harsh conditions with temperatures rising up to 400°C and high concentrations in reduced and toxic compounds, these environments are nonetheless teeming with life with dense macrofaunal communities surrounding the vent fluid emissions. Among them, the alvinocaridid shrimp *Rimicaris exoculata* is certainly one of the most well-known and emblematic species from the vent endemic fauna from the Mid Atlantic Ridge. As with many other species from those ecosystems, these shrimps house important communities of chemosynthetic bacteria living in symbiosis with their host inside the cephalothoracic cavity and the gut providing some-to-all of the shrimp nutrition. Less studied, *Rimicaris chacei*, a co-occurring species from the same vent sites but with smaller populations, is also an interesting case among the alvinocaridids, with a mixotrophic diet, halfway through symbiosis.

Hydrothermal vents are however fragile and ephemeral, prone to great geological instability, that may result cessation of the vent fluids activity. In addition, they are also fragmented, separated by tens to thousands of kms by poor and unsuitable environments for chemosynthesis, and thus *Rimicaris* symbiosis. Therefore, species survival over successive generations is greatly interlinked with their ability to successfully colonize and settle in new vent fields, implying adaptations at each level of their lifecycle. Unfortunately, and as for the rest of the vent fauna, many aspects of the alvinocaridid lifecycle remain by today poorly documented such as early development, larval dispersal and settlement or onset of symbiotic relationship. Likewise, almost no brooding female of *Rimicaris exoculata* could have been collected until recently, leaving important gaps on fundamental aspects of its reproductive biology.

The presentation will briefly expose current advances on the lifecycle ecology of the two species with a focus on their reproductive biology. Similarities with species from the Central Indian Ridge will also be addressed to discuss about their importance to provide a more global overview on the lifecycle ecology of the group.

December 2018 **Forum Careers at Sea** *(presentation of what is an early scientific career)*

*15 min oral presentation* **Oceanographic Institute of Paris, Paris, France**

1h hour of presentation with four speakers, one technician from the DYNECO laboratory at Ifremer and two others from the human resource department. Followed by 30min of exchange with the public.

November 2018 **3rd French Congress on Chemosynthetic Ecosystem (CONNECT)**

*30 min oral presentation* **Roscoff, Bretagne, France**

## Qui de l'œuf ou de la crevette ? – Evolution et spécificité des communautés bactériennes associées aux pontes de *Rimicaris exoculata* au cours du développement embryonnaire

**Abstract :**

*Rimicaris exoculata* est l'une des espèces les plus emblématiques et les plus connues de la faune endémique des sources hydrothermales. Comme beaucoup d'autres d'espèces de ces écosystèmes, les crevettes *Rimicaris* hébergent d'importantes communautés de bactéries chimiosynthétiques vivant en symbiose avec leur hôte. Celles-ci sont principalement localisées à l'intérieur du céphalothorax hypertrophié de l'animal mais aussi à l'intérieur de leur système digestif. Pour la plupart de ces partenaires symbiotiques, le mode de transmission intergénérationnel n'est toujours pas résolu et le point de démarrage de cette relation symbiotique n'est toujours pas clairement défini au cours du cycle de vie de l'hôte.

Dans cette étude, un grand nombre de femelles gravides de *Rimicaris exoculata* récolté durant la période de reproduction de l'animal, nous a permis d'explorer la diversité microbienne associée aux pontes. Combinant des techniques de microscopie et de séquençage haut débit, la présence, l'abondance relative et la diversité de ces communautés microbiennes colonisant les pontes d'œufs de *Rimicaris exoculata* ont été décrites à différent stades de développement et pour deux sites hydrothermaux.

Nos résultats révèlent, entre autres, des variations importantes de la couverture microbienne entre les pontes au cours du développement embryonnaire, mais aussi selon la répartition des œufs d'une même ponte, ceux-ci étant tous synchronisés à un même stade de développement. De plus, la comparaison de la diversité bactérienne associée aux œufs avec celle associée aux pléopodes, un tissu à priori non symbiotique et exposé à des conditions environnementales identiques, permet de mettre en évidence l'existence d'une communauté microbienne spécifique aux pontes de *Rimicaris exoculata*. Ces résultats fournissent ainsi une base pour discuter à la fois de l'acquisition potentielle des symbiontes à ce stade de développement ainsi que des potentiels rôles que pourraient avoir ces communautés bactériennes associées aux œufs pour leur hôte.

September 2018 **15th Deep Sea Biology Symposium**

*15 min oral presentation* **Monterrey, California, USA**

**Is it the Egg first or the Shrimp? – Diversity and evolution of the microbial communities colonizing broods of the vent shrimp Rimicaris exoculata throughout embryonic development**

**Abstract:**

*Rimicaris exoculata* is one of the most well-known and emblematic species from the vent endemic fauna. As with many others species from those ecosystems, *Rimicaris* shrimps house important communities of chemosynthetic bacteria living in symbiosis with their host inside the branchial cavity and the gut. For many of the symbiotic partners, transmission mode has still to be elucidated and the beginning of the symbiotic relationship is not clearly defined yet within the lifecycle of the animal. In this study, sampling of a large number of *Rimicaris exoculata* broods during the shrimp's reproductive period, has allowed us to explore the microbial diversity throughout embryonic development. Combining sequencing and microscopy techniques, the presence, relative abundance and diversity of microbial communities colonizing broods have been described in two hydrothermal vent sites for different egg stages. Our results highlight, among others, important variations in microbial communities' abundance between broods occurring throughout embryonic development but also between eggs from within a single brood, being all at the same developmental stage. Comparisons were also made between the diversity of egg communities and those found on the pleopod of the same brooding female, a non-symbiotic tissue subject to similar environmental conditions. This provides a basis to discuss both the acquisition of symbionts during this life stage and the potential roles of these bacterial communities within their host.

September 2018 **14th Night of European Research**

*4 hours with the general public* **Brest, Bretagne, France** (Océanopolis Aquarium)

October 2017 **8th Congress of the French Association of Microbial Ecology (AFEM)**

*Poster presentation* **Camaret-sur-Mer, Bretagne, France**

September 2017 **13th Night of European Research**

*4 hours with the general public* **Brest, Bretagne, France** (Océanopolis Aquarium)

*Poster realized for the laboratory*

# Quel type d'association microbienne sur les oeufs de la crevette *Rimicaris exoculata* ?

VIIIème colloque AFEM 2017 - Camaret sur mer

Pierre Methou[1,2], Ivan Hernandez-Avila[1,2], Valérie Cueff-Gauchard[1], Marie-Anne Cambon-Bonavita[1], Florence Pradillon[2]
1: Ifremer, UMR LM2E, Laboratoire de Microbiologie des Environnements Extrêmes, UBO, CNRS, F-29280 Plouzané, France
2: Ifremer, Laboratoire Environnement Profond, F-29280-Plouzané, France

LM2E UBO - CNRS - IFREMER

Ifremer

## Présentation de *Rimicaris*

*Rimicaris exoculata* est une crevette vivant sur la paroi des cheminées des sources hydrothermales de l'océan profond atlantique.

Tout près des fluides riches en composés réduits, cette espèce vit en symbiose avec des bactéries chimiosynthétique.

Bien connue à l'âge adulte, cette relation de symbiose a été jusqu'alors peu explorée au cours du cycle de vie de l'animal.

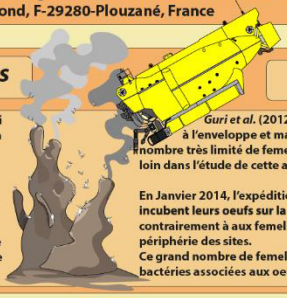

## Les oeufs chez *Rimicaris*

*Guri et al.* (2012)[1] ont montré l'existence d'une communauté bactérienne associée à l'enveloppe et majoritairement composée de Gammaprotéobactéries. Cependant le nombre très limité de femelles gravides récoltées jusqu'alors n'avait pas permis d'aller plus loin dans l'étude de cette association.

En Janvier 2014, l'expédition BICOSE permet la récolte de nombreuses femelles gravides qui incubent leurs oeufs sur la paroi des fumeurs où ils sont exposés aux fluides environnants, contrairement à aux femelles gravides d'autres crustacés hydrothermaux qui migrent en périphérie des sites.
Ce grand nombre de femelles récoltées a permis de commencer un étude plus poussée des bactéries associées aux oeufs au cours du développement embryonnaire.


Comme c'est le cas pour certains décapodes, les oeufs chez *Rimicaris exoculata* sont incubés sous l'abdomen jusqu'à l'éclosion de la larve au stade zoé.

## Un assemblage bactérien qui se développe avec l'embryon ...

La couverture bactérienne s'accroit au cours du développement embryonnaire avec un nombre de bactéries plus important sur l'enveloppe des oeufs de *Rimicaris* aux stades de développement avancés qu'aux stades précoces.

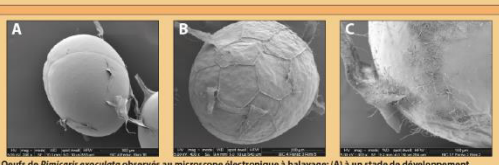


Oeufs de *Rimicaris exoculata* observés au microscope électronique à balayage; (A) à un stade de développement précoce, (B) au milieu de leur développement, (C) à un stade de développement avancé (Thèse Hernandez-Avila (2016)[2])

## Questions Scientifiques

- Quels sont les différents assemblages bactériens associés aux oeufs de *Rimicaris* ?
- Varient-ils au cours du développement ?
- Sont ils spécifiques des oeufs ?

## Avec une Diversité Spécifique ?

La "dominance" des Gammaprotéobactéries chez les oeufs n'est pas confirmée à tous les stades de développement avec une présence non négligeable d'Epsilonprotéobactéries et d'Alphaprotéobactéries selon les stades.

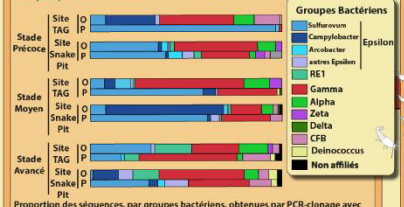


Proportion des séquences, par groupes bactériens, obtenues par PCR-clonage avec les amorces bactériennes universelles E8F/U1417R sur des oeufs (O) et le pléopode associé (P) sur différents sites hydrothermaux à différents stades de développement.

Les tests de comparaison statistiques semblent indiquer une similarité plus grande entre les communautés bactériennes des oeufs quelque soit les femelles, sites de prélevement ou stades de développement qu'entre les communautés des oeufs et des pléopodes d'une même femelle.

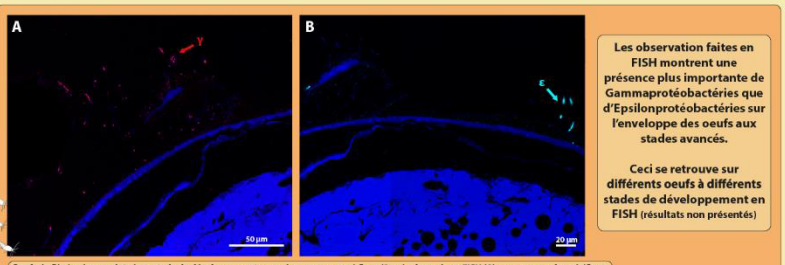


Oeufs de *Rimicaris exoculata* à un stade de développement avancé en coupes semi-fines (2µm), observés en FISH (A) avec une sonde spécifique des Gammaprotéobactéries Gam42-Cy5 (en rouge) (B) avec une sonde spécifique des Epsilonprotéobactéries Epsy914-Cy5 (en bleu clair)

Les observation faites en FISH montrent une présence plus importante de Gammaprotéobactéries que d'Epsilonprotéobactéries sur l'enveloppe des oeufs aux stades avancés.

Ceci se retrouve sur différents oeufs à différents stades de développement en FISH (résultats non présentés)

## Et si les minéraux ...

Ponte de *Rimicaris exoculata* extraite de l'abdomen de la femelle et observée sous loupe binoculaire

On observe l'accumulation de dépôts minéraux à la surface des pontes qui affecte de façon beaucoup plus marquée les oeufs situés à l'extérieur de la ponte (coloration orangée) que les autres (coloration blanche).

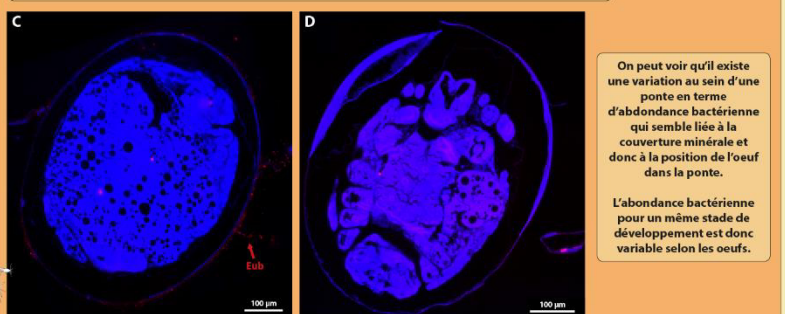


Oeufs de *Rimicaris exoculata* d'une même ponte à un stade de développement avancé en coupes semi-fines (2µm), observés en FISH avec des sondes spécifiques des Eubactéries Eub338-Cy5 (en rouge) (A) pour un oeuf à l'extérieur de la ponte soumis aux fluides et ayant d'importants dépôts minéraux (B) pour un oeuf à l'intérieur de la ponte près de l'abdomen de la femelle et ayant très peu de dépôts minéraux.

On peut voir qu'il existe une variation au sein d'une ponte en terme d'abondance bactérienne qui semble liée à la couverture minérale et donc à la position de l'oeuf dans la ponte.

L'abondance bactérienne pour un même stade de développement est donc variable selon les oeufs.

## Perspectives futures

Quel est le degré de spécifité de cette association oeuf-bactéries ? A préciser à travers des méthodes plus quantitatives. (suite à l'échec de la q-PCR, étude en NGS sur un plus grand nombre d'individus).

Les bactéries présentes sur les assemblages des oeufs sont elles chimiolithoautotrophes ? Sont elles actives ? Y a t il transfert de matière organique vers les embryons ? (Microautoradiographie)

## Conclusions préliminaires

On observe une variabilité importante de l'abondance et de la diversité des bactéries associées aux enveloppes des oeufs de *Rimicaris exoculata* qui semble refléter le temps d'exposition aux fluides hydrothermaux (accroissement avec le temps et la position des oeufs dans la ponte)

L'association aux oeufs pourrait cependant être spécifique étant donné que les communautés bactériennes de ceux-ci se distinguent de celles d'autres surfaces dont l'exposition au fluide est similaire (pléopodes de la mère)

## Références bibliographiques

[1]Guri, M., L. Durand, V. Cueff-Gauchard, M. Zbinden, P. Crassous, B. Shillito, and M.-A. Cambon-Bonavita. (2012). Acquisition of epibiotic bacteria along the life cycle of the hydrothermal shrimp *Rimicaris exoculata*. ISME J 6:597-609.

[2]Hernandez-Avila I. (Thesis), Larval Dispersal and Life Cycle in Deep Water : The Case of *Rimicaris exoculata* and related species (2016)

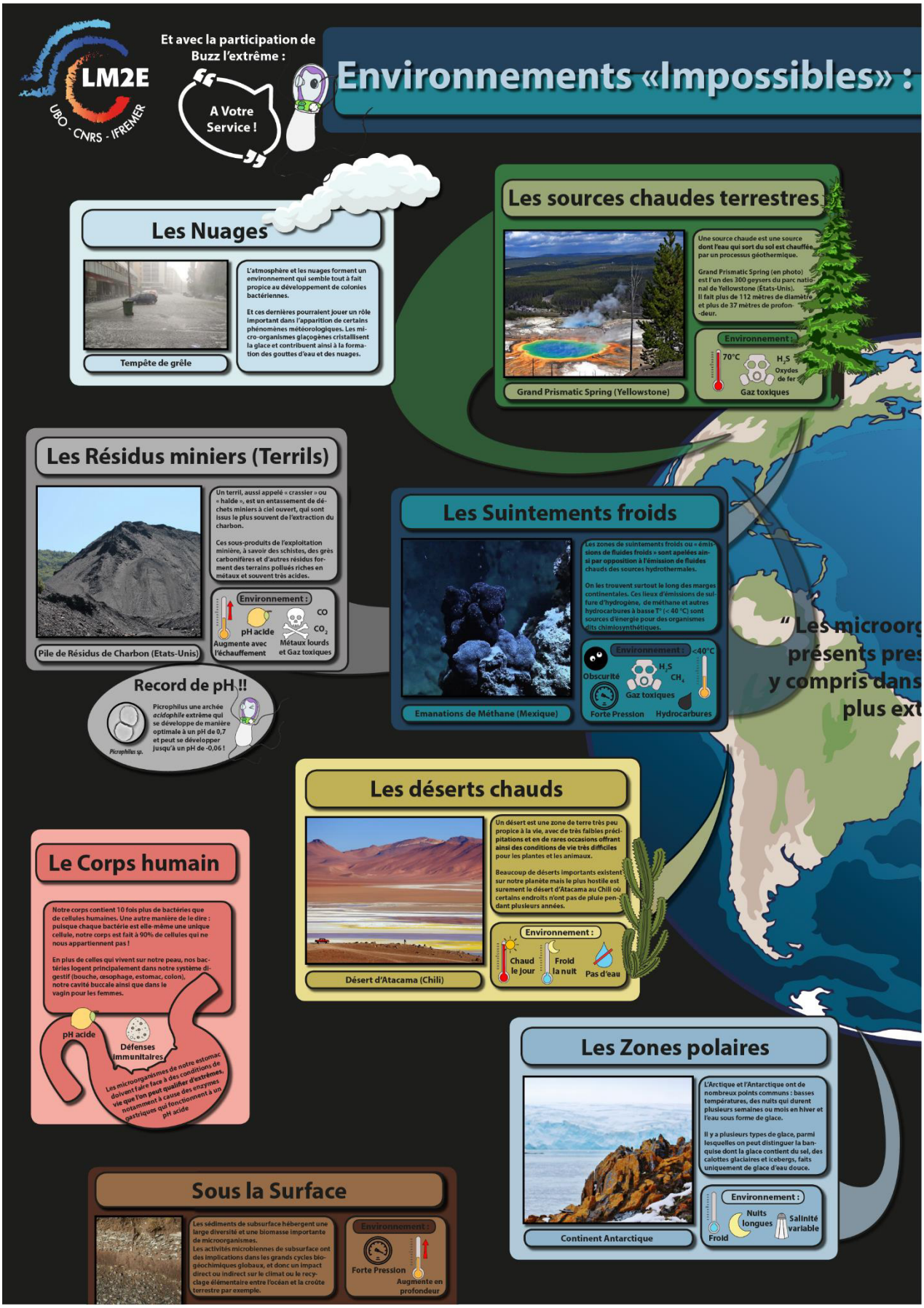
LM2E
UBO - CNRS - IFREMER
Et avec la participation de Buzz l'extrême :
A Votre Service !
Environnements «Impossibles» :
Les Nuages
Tempête de grêle
L'atmosphère et les nuages forment un environnement qui semble tout à fait propice au développement de colonies bactériennes.
Et ces dernières pourraient jouer un rôle important dans l'apparition de certains phénomènes météorologiques. Les micro-organismes glaçogènes cristallisent la glace et contribuent ainsi à la formation des gouttes d'eau et des nuages.
Les sources chaudes terrestres
Grand Prismatic Spring (Yellowstone)
Une source chaude est une source dont l'eau qui sort du sol est chauffée par un processus géothermique.
Grand Prismatic Spring (en photo) est l'un des 300 geysers du parc national de Yellowstone (États-Unis). Il fait plus de 112 mètres de diamètre et plus de 37 mètres de profondeur.
Environnement :
70°C
$H_2S$
Oxydes de fer
Gaz toxiques
Les Résidus miniers (Terrils)
Pile de Résidus de Charbon (Etats-Unis)
Un terril, aussi appelé « crassier » ou « halde », est un entassement de déchets miniers à ciel ouvert, qui sont issus le plus souvent de l'extraction du charbon.
Ces sous-produits de l'exploitation minière, à savoir des schistes, des grès carbonifères et d'autres résidus forment des terrains pollués riches en métaux et souvent très acides.
Environnement :
pH acide
CO
$CO_2$
Augmente avec l'échauffement
Métaux lourds et Gaz toxiques
Les Suintements froids
Emanations de Méthane (Mexique)
Les zones de suintements froids ou « émissions de fluides froids » sont apelées ainsi par opposition à l'émission de fluides chauds des sources hydrothermales.
On les trouvent surtout le long des marges continentales. Ces lieux d'émissions de sulfure d'hydrogène, de méthane et autres hydrocarbures à basse T° (< 40 °C) sont sources d'énergie pour des organismes dits chimiosynthétiques.
Environnement :
<40°C
Obscurité
$H_2S$
$CH_4$
Gaz toxiques
Forte Pression
Hydrocarbures
Record de pH !!
Picrophilus sp.
Picrophilus une archée acidophile extrême qui se développe de manière optimale à un pH de 0,7 et peut se développer jusqu'à un pH de -0,06 !
Les déserts chauds
Désert d'Atacama (Chili)
Un désert est une zone de terre très peu propice à la vie, avec de très faibles précipitations et en de rares occasions offrant ainsi des conditions de vie très difficiles pour les plantes et les animaux.
Beaucoup de déserts importants existent sur notre planète mais le plus hostile est surement le désert d'Atacama au Chili où certains endroits n'ont pas de pluie pendant plusieurs années.
Environnement :
Chaud le jour
Froid la nuit
Pas d'eau
Le Corps humain
Notre corps contient 10 fois plus de bactéries que de cellules humaines. Une autre manière de le dire : puisque chaque bactérie est elle-même une unique cellule, notre corps est fait à 90% de cellules qui ne nous appartiennent pas !
En plus de celles qui vivent sur notre peau, nos bactéries logent principalement dans notre système digestif (bouche, œsophage, estomac, colon), notre cavité buccale ainsi que dans le vagin pour les femmes.
pH acide
Défenses immunitaires
Les microorganismes de notre estomac doivent faire face à des conditions de vie que l'on peut qualifier d'extrêmes, notamment à cause des enzymes gastriques qui fonctionnent à un pH acide
Les Zones polaires
Continent Antarctique
L'Arctique et l'Antarctique ont de nombreux points communs : basses températures, des nuits qui durent plusieurs semaines ou mois en hiver et l'eau sous forme de glace.
Il y a plusieurs types de glace, parmi lesquelles on peut distinguer la banquise dont la glace contient du sel, des calottes glaciaires et icebergs, faits uniquement de glace d'eau douce.
Environnement :
Froid
Nuits longues
Salinité variable
Sous la Surface
Les sédiments de subsurface hébergent une large diversité et une biomasse importante de microorganismes.
Les activités microbiennes de subsurface ont des implications dans les grands cycles biogéochimiques globaux, et donc un impact direct ou indirect sur le climat ou le recyclage élémentaire entre l'océan et la croûte terrestre par exemple.
Environnement :
Forte Pression
Augmente en profondeur
" Les microorg
présents pres
y compris dans
plus ext

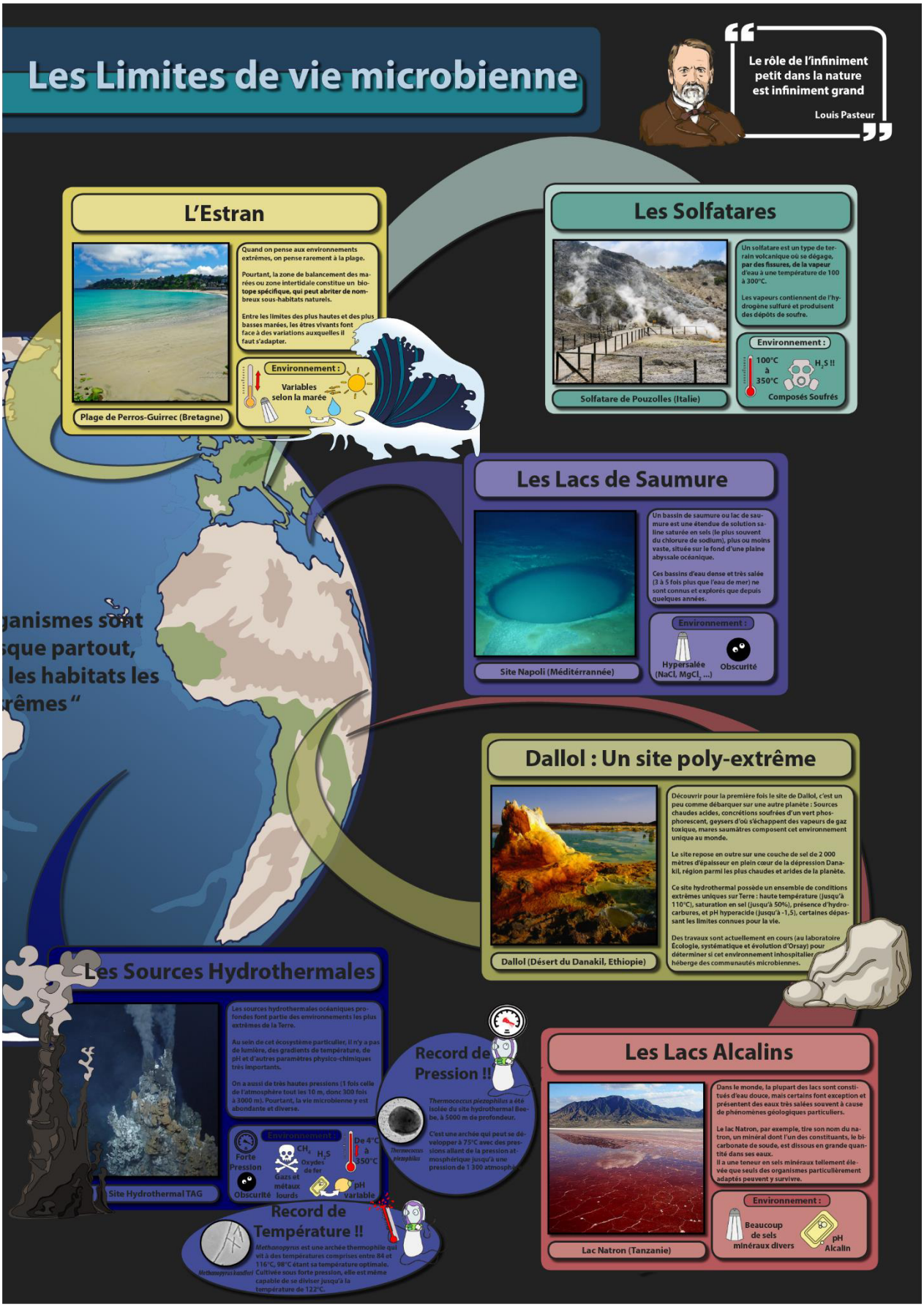
Les Limites de vie microbienne
Le rôle de l'infiniment petit dans la nature est infiniment grand
Louis Pasteur
L'Estran
Quand on pense aux environnements extrêmes, on pense rarement à la plage.
Pourtant, la zone de balancement des marées ou zone intertidale constitue un biotope spécifique, qui peut abriter de nombreux sous-habitats naturels.
Entre les limites des plus hautes et des plus basses marées, les êtres vivants font face à des variations auxquelles il faut s'adapter.
Environnement :
Variables selon la marée
Plage de Perros-Guirrec (Bretagne)
Les Solfatares
Un solfatare est un type de terrain volcanique où se dégage, par des fissures, de la vapeur d'eau à une température de 100 à 300°C.
Les vapeurs contiennent de l'hydrogène sulfuré et produisent des dépôts de soufre.
Environnement :
100°C à 350°C
H2S !!
Composés Soufrés
Solfatare de Pouzolles (Italie)
Les Lacs de Saumure
Un bassin de saumure ou lac de saumure est une étendue de solution saline saturée en sels (le plus souvent du chlorure de sodium), plus ou moins vaste, située sur le fond d'une plaine abyssale océanique.
Ces bassins d'eau dense et très salée (3 à 5 fois plus que l'eau de mer) ne sont connus et explorés que depuis quelques années.
Environnement :
Hypersalée (NaCl, MgCl2, ...)
Obscurité
Site Napoli (Méditérrannée)
ganismes sont
sque partout,
les habitats les
rêmes "
Dallol : Un site poly-extrême
Découvrir pour la première fois le site de Dallol, c'est un peu comme débarquer sur une autre planète : Sources chaudes acides, concrétions soufrées d'un vert phosphorescent, geysers d'où s'échappent des vapeurs de gaz toxique, mares saumâtres composent cet environnement unique au monde.
Le site repose en outre sur une couche de sel de 2 000 mètres d'épaisseur en plein cœur de la dépression Danakil, région parmi les plus chaudes et arides de la planète.
Ce site hydrothermal possède un ensemble de conditions extrêmes uniques sur Terre : haute température (jusqu'à 110°C), saturation en sel (jusqu'à 50%), présence d'hydrocarbures, et pH hyperacide (jusqu'à -1,5), certaines dépassant les limites connues pour la vie.
Des travaux sont actuellement en cours (au laboratoire Écologie, systématique et évolution d'Orsay) pour déterminer si cet environnement inhospitalier héberge des communautés microbiennes.
Dallol (Désert du Danakil, Ethiopie)
Les Sources Hydrothermales
Les sources hydrothermales océaniques profondes font partie des environnements les plus extrêmes de la Terre.
Au sein de cet écosystème particulier, il n'y a pas de lumière, des gradients de température, de pH et d'autres paramètres physico-chimiques très importants.
On a aussi de très hautes pressions (1 fois celle de l'atmosphère tout les 10 m, donc 300 fois à 3000 m). Pourtant, la vie microbienne y est abondante et diverse.
Environnement :
Forte Pression
Obscurité
CH4
H2S
Oxydes de fer
Gazs et métaux lourds
De 4°C à 350°C
pH variable
Site Hydrothermal TAG
Record de Pression !!
Thermococcus piezophilus a été isolée du site hydrothermal Beebe, à 5000 m de profondeur.
C'est une archée qui peut se développer à 75°C avec des pressions allant de la pression atmosphérique jusqu'à une pression de 1 300 atmosphè
Thermococcus piezophilus
Record de Température !!
Methanopyrus est une archée thermophile qui vit à des températures comprises entre 84 et 116°C, 98°C étant sa température optimale. Cultivée sous forte pression, elle est même capable de se diviser jusqu'à la température de 122°C.
Methanopyrus kandleri
Les Lacs Alcalins
Dans le monde, la plupart des lacs sont constitués d'eau douce, mais certains font exception et présentent des eaux très salées souvent à cause de phénomènes géologiques particuliers.
Le lac Natron, par exemple, tire son nom du natron, un minéral dont l'un des constituants, le bicarbonate de soude, est dissous en grande quantité dans ses eaux.
Il a une teneur en sels minéraux tellement élevée que seuls des organismes particulièrement adaptés peuvent y survivre.
Environnement :
Beaucoup de sels minéraux divers
pH Alcalin
Lac Natron (Tanzanie)

# List of supervised master students

| | |
|---|---|
| March - May 2019 | **Marion Gueganton (Engineer school, 5th year)** |
| November 2019 | **Morzina Leela (ISA international master student, Bangladesh)** |
| November 2019 | **Maialen Palazot (Engineer school, 3rd year)** |

# References

Adams, D. K., Arellano, S. M., and Govenar, B. (2012). Larval dispersal : vent life in the water column. *Oceanography* 25, 256–268. doi:10.5670/oceanog.2012.24.

Akerman, N. H., Butterfield, D. A., and Huber, J. A. (2013). Phylogenetic diversity and functional gene patterns of sulfur-oxidizing subseafloor Epsilonproteobacteria in diffuse hydrothermal vent fluids. *Front. Microbiol.* 4, 1–14. doi:10.3389/fmicb.2013.00185.

Alain, K., Postec, A., Grinsard, E., Lesongeur, F., Prieur, D., and Godfroy, A. (2010). Thermodesulfatator atlanticus sp. nov., a thermophilic, chemolithoautotrophic, sulfate-reducing bacterium isolated from a Mid-Atlantic Ridge hydrothermal vent. *Int. J. Syst. Evol. Microbiol.* 60, 33–38. doi:10.1099/ijs.0.009449-0.

Alain, K., Zbinden, M., and Bris, N. Le (2004). Early steps in microbial colonization processes at deep-sea hydrothermal vents. *Environ. Microbiol.* 6, 227–241. doi:10.1111/j.1462-2920.2004.00557.x.

Alt, J. C. (1995). "Subseafloor Processes in Mid-Ocean Ridge Hydrothennal Systems," in *Seafloor Hydrothermal Systems : Physical, Chemical, Biological and Geological Interactions*, 85–114. doi:10.1029/GM091p0085.

Amparyup, P., Kondo, H., Hirono, I., Aoki, T., and Tassanakajon, A. (2008). Molecular cloning, genomic organization and recombinant expression of a crustin-like antimicrobial peptide from black tiger shrimp Penaeus monodon. *Mol. Immunol.* 45, 1085–1093. doi:10.1016/j.molimm.2007.07.031.

Anantharaman, K., Breier, J. A., and Dick, G. J. (2016). Metagenomic resolution of microbial functions in deep-sea hydrothermal plumes across the Eastern Lau Spreading Center. *ISME J.* 10, 225–239. doi:10.1038/ismej.2015.81.

Anger, K. (2001). The biology of decapod crustacean larvae. *Crustac. Issues* 14, 417. doi:10.1651/0278-0372(2005)025.

Anger, K. (2006). Contributions of larval biology to crustacean research : A review Contributions of larval biology to crustacean research : a review. *Invertebr. Reprod. Dev.* 49, 175–205. doi:10.1080/07924259.2006.9652207.

Anger, K., Schubart, C. D., and Anger, K. (2005). Experimental Evidence of Food-Independent Larval Development in Endemic Jamaican Freshwater-Breeding Crabs. *Physiol. Biochem. Zool.* 78, 246–258.

Ansorge, R., Romano, S., Sayavedra, L., Ángel, M., Porras, G., Kupczok, A., et al. (2019). Functional diversity enables multiple symbiont strains to coexist in deep-sea mussels. *Nat. Microbiol.* doi:10.1038/s41564-019-0572-9.

Apremont, V., Cambon-Bonavita, M. A., Cueff-Gauchard, V., François, D., Pradillon, F., Corbari, L., et al. (2018). Gill chamber and gut microbial communities of the hydrothermal shrimp Rimicaris chacei Williams and Rona 1986: A possible symbiosis. *PLoS One* 13, e0206084. doi:10.1371/journal.pone.0206084.

Arellano, S. M., Van Gaest, A. L., Johnson, S. B., Vrijenhoek, R. C., and Young, C. M. (2014). Larvae from deep-sea methane seeps disperse in surface waters. *Proc. R. Soc. B* 281, 20133276. doi:10.1098/rspb.2013.3276.

Arellano, S. M., and Young, C. M. (2009). Spawning, development, and the duration of larval life in a deep-sea cold-seep mussel. *Biol. Bull.* 216, 149–162. doi:10.2307/25470737.

Assié, A. (2016). Deep Se(a)quencing : A study of deep sea ectosymbioses using next generation

sequencing.

Assié, A., Borowski, C., van der Heijden, K., Raggi, L., Geier, B., Leisch, N., et al. (2016). A specific and widespread association between deep-sea Bathymodiolus mussels and a novel family of Epsilonproteobacteria. *Environ. Microbiol. Rep.* 00. doi:10.1111/1758-2229.12442.

Assié, A., Leisch, N., Meier, D. V., Gruber-Vodicka, H., Tegetmeyer, H. E., Meyerdierks, A., et al. (2019). Horizontal acquisition of a patchwork Calvin cycle by symbiotic and free-living Campylobacterota (formerly Epsilonproteobacteria). *ISME J.* 14, 104–122. doi:10.1038/s41396-019-0508-7.

Auguste, M., Mestre, N. C., Rocha, T. L., Cardoso, C., Cueff-Gauchard, V., Le Bloa, S., et al. (2016). Development of an ecotoxicological protocol for the deep-sea fauna using the hydrothermal vent shrimp Rimicaris exoculata. *Aquat. Toxicol.* 175, 277–285. doi:10.1016/j.aquatox.2016.03.024.

Bachraty, C., Legendre, P., and Desbruyères, D. (2009). Biogeographic relationships among deep-sea hydrothermal vent faunas at global scale. *Deep. Res. Part I Oceanogr. Res. Pap.* 56, 1371–1378. doi:10.1016/j.dsr.2009.01.009.

Baker, B. J., Sheik, C. S., Taylor, C. A., Jain, S., Bhasi, A., Cavalcoli, J. D., et al. (2013). Community transcriptomic assembly reveals microbes that contribute to deep-sea carbon and nitrogen cycling. *ISME J.* 7, 1962–1973. doi:10.1038/ismej.2013.85.

Baker, E. T. (1996). Geological indexes of hydrothermal venting. *J. Geophys. Res.* 101, 13741–13753.

Baker, E. T. (2014). “Hydrothermal Plumes,” in *Encyclopedia of Marine Geosciences*, 0–11. doi:10.1007/978-94-007-6644-0.

Baker, E. T. (2017). Exploring the ocean for hydrothermal venting: New techniques, new discoveries, new insights. *Ore Geol. Rev.* 86, 55–69. doi:10.1016/j.oregeorev.2017.02.006.

Baker, E. T., Feely, R. A., Mottl, M. J., Sansone, F. T., Wheat, C. G., Resing, J. A., et al. (1994). Hydrothermal plumes along the East Pacific Rise, 8°40′ to 11°50′N: Plume distribution and relationship to the apparent magmatic budget. *Earth Planet. Sci. Lett.* 128, 1–17. doi:10.1016/0012-821X(94)90022-1.

Baker, E. T., Resing, J. A., Haymon, R. M., Tunnicliffe, V., Lavelle, J. W., Martinez, F., et al. (2016). How many vent fields? New estimates of vent field populations on ocean ridges from precise mapping of hydrothermal discharge locations. *Earth Planet. Sci. Lett.* 449, 186–196. doi:10.1016/j.epsl.2016.05.031.

Baker, E. T., Walker, S. L., Resing, J. A., Chadwick, W. W., Merle, S. G., Anderson, M. O., et al. (2017). The Effect of Arc Proximity on Hydrothermal Activity Along Spreading Centers: New Evidence From the Mariana Back Arc (12.7°N–18.3°N). *Geochemistry, Geophys. Geosystems* 18, 4211–4228. doi:10.1002/2017GC007234.

Ballard, R. D., Bryan, W. B., Heirtzler, J. R., Keller, G., Moore, J. G., and Van Andel, T. (1975). Manned Submersible Observations in the FAMOUS Area: Mid-Atlantic Ridge. *Science (80-. ).* 190.

Bandelt, H.-J., Forster, P., and Röhl, A. (1999). Median-Joining Networks for Inferring Intraspecific Phylogenies. *Mol. Biol. Evol.* 16, 37–48.

Banerjee, D., Maiti, B., Girisha, S. K., Venugopal, M. N., and Karunasagar, I. (2015). A crustin isoform from black tiger shrimp, Penaeus monodon exhibits broad spectrum anti-bacterial activity. *Aquac. Reports* 2, 106–111. doi:10.1016/j.aqrep.2015.08.009.

Barreto, C., Da Rosa Coelho, J., Yuan, J., Xiang, J., Perazzolo, L. M., and Rosa, R. D. (2018). Specific

molecular signatures for type II crustins in penaeid shrimp uncovered by the identification of crustin-like antimicrobial peptides in litopenaeus vannamei. *Mar. Drugs* 16, 5–7. doi:10.3390/md16010031.

Barreyre, T., Escartín, J., Garcia, R., Cannat, M., Mittelstaedt, E., and Prados, R. (2012). Structure, temporal evolution, and heat flux estimates from the Lucky Strike deep-sea hydrothermal field derived from seafloor image mosaics. *Geochemistry, Geophys. Geosystems* 13, 1–29. doi:10.1029/2011GC003990.

Barreyre, T., Escartin, J., Sohn, R. A., Cannat, M., Ballu, V., and Crawford, W. C. (2014). Temporal variability and tidal modulation of hydrothermal exit-fluid temperatures at the Lucky Strike deep-sea vent field, Mid-Atlantic Ridge Thibaut. *J. Geophys. Res. Solid Earth Res.* doi:10.1002/2013JB010478.Received.

Bates, A. E., Harmer, T. L., Roeselers, G., and Cavanaugh, C. M. (2011). Phylogenetic characterization of episymbiotic bacteria hosted by a hydrothermal vent limpet (lepetodrilidae, vetigastropoda). *Biol. Bull.* 220, 118–127. doi:10.1086/BBLv220n2p118.

Bates, A. E., Lee, R. W., Tunnicliffe, V., and Lamare, M. D. (2010). Deep-sea hydrothermal vent animals seek cool fluids in a highly variable thermal environment. *Nat. Commun.*, 1–6. doi:10.1038/ncomms1014.

Beaulieu, S. E., Baker, E. T., and German, C. R. (2015). Where are the undiscovered hydrothermal vents on oceanic spreading ridges? *Deep. Res. Part II Top. Stud. Oceanogr.* 121, 202–212. doi:10.1016/j.dsr2.2015.05.001.

Beaulieu, S. E., Baker, E. T., German, C. R., and Maffei, A. (2013). An authoritative global database for active submarine hydrothermal vent fields. *Geochemistry, Geophys. Geosystems* 14, 4892–4905. doi:10.1002/2013GC004998.

Beaulieu, S. E., Mullineaux, L. S., Adams, D. K., and Mills, S. W. (2009). Comparison of a sediment trap and plankton pump for time-series sampling of larvae near deep-sea hydrothermal vents. *Limnol. Oceanogr. Methods* 7, 235–248. doi:10.4319/lom.2009.7.235.

Beaulieu, S. E., Sayre-Mccord, R. T., Mills, S. W., Pradillon, F., and Watanabe, H. (2014). Swimming speeds of polychaete larvae collected near deep-sea hydrothermal vents. *Mar. Ecol.* 36, 133–143. doi:10.1111/maec.12207.

Bebianno, M. J., Cardoso, C., Gomes, T., Blasco, J., Santos, R. S., and Colaço, A. (2018). Metal interactions between the polychaete Branchipolynoe seepensis and the mussel Bathymodiolus azoricus from Mid-Atlantic-Ridge hydrothermal vent fields. *Mar. Environ. Res.* doi:10.1016/j.marenvres.2018.01.017.

Becker, C., Dick, J. T. A., Cunningham, E. M., Schmitt, C., and Sigwart, J. D. (2018). The crustacean cuticle does not record chronological age: New evidence from the gastric mill ossicles. *Arthropod Struct. Dev.* 47, 498–512. doi:10.1016/j.asd.2018.07.002.

Beedessee, G., Watanabe, H., Ogura, T., Nemoto, S., Yahagi, T., Nakagawa, S., et al. (2013). High connectivity of animal populations in deep-sea hydrothermal vent fields in the central indian ridge relevant to its geological setting. *PLoS One* 8. doi:10.1371/journal.pone.0081570.

Beinart, R. A., Gartman, A., Sanders, J. G., Luther, G. W., and Girguis, P. R. (2015). The uptake and excretion of partially oxidized sulfur expands the repertoire of energy resources metabolized by hydrothermal vent symbioses. *Proc. R. Soc. B Biol. Sci.* 282. doi:10.1098/rspb.2014.2811.

Beinart, R. A., Nyholm, S. V., Dubilier, N., and Girguis, P. R. (2014). Intracellular Oceanospirillales inhabit the gills of the hydrothermal vent snail Alviniconcha with chemosynthetic, γ-

Proteobacterial symbionts. *Environ. Microbiol. Rep.* 6, 656–664. doi:10.1111/1758-2229.12183.

Beinart, R. A., Sanders, J. G., Faure, B., Sylva, S. P., Lee, R. W., Becker, E. L., et al. (2012). Evidence for the role of endosymbionts in regional-scale habitat partitioning by hydrothermal vent symbioses. *Proc. Natl. Acad. Sci.*, 241–250. doi:10.1073/pnas.1202690109.

Belkin, S., Nelson, D. C., and Jannasch, H. W. (1986). Symbiotic Assimilation of CO in Two Hydrothermal Vent Animals, the Mussel Bathymodiolus thermophilus and the Tube Worm Riftia pachyptila. *Biol. Bull.* 170, 75–86. doi:10.2307/1537438.

Bell, J. B., Woulds, C., Brown, L. E., Sweeting, C. J., Reid, W. D. K., Little, C. T. S., et al. (2016). Macrofaunal Ecology of Sedimented Hydrothermal Vents in the Bransfield Strait, Antarctica. *Front. Mar. Sci.* 3, 1–15. doi:10.3389/fmars.2016.00032.

Bellec, L., Cambon-Bonavita, M.-A., Cueff-Gauchard, V., Durand, L., Gayet, N., and Zeppilli, D. (2018). A Nematode of the Mid-Atlantic Ridge Hydrothermal Vents Harbors a Possible Symbiotic Relationship. *Front. Microbiol.* 9, 1–12. doi:10.3389/fmicb.2018.02246.

Bellou, N., Papathanassiou, E., Dobretsov, S., Lykousis, V., and Colijn, F. (2012). The effect of substratum type, orientation and depth on the development of bacterial deep-sea biofilm communities grown on artificial substrata deployed in the Eastern Mediterranean. *Biofouling* 28, 199–213. doi:10.1080/08927014.2012.662675.

Bemis, K., Lowell, R. P., and Farough, A. (2012). Diffuse flow on and around hydrothermal vents at mid-ocean ridges. *Oceanography* 25, 182–191. doi:10.5670/oceanog.2012.16.

Beninger, P. G., and Le Pennec, M. (1997). Reproductive characteristics of a primitive bivalve from a deep-sea reducing environment: giant gametes and their significance in Acharax alinae (Cryptodonta: Solemyidae). *Mar. Ecol. Prog. Ser.* 157, 195–206.

Berg, C. J. J. (1985). Reproductive strategies of mollusks from abyssal hydrothermal vent communities. *Biol Soc Washingt. Bull* 6, 185–197. Available at: http://ci.nii.ac.jp/naid/10011208803/en/ [Accessed August 16, 2019].

Bergquist, D. C., Eckner, J. T., Urcuyo, I. A., Cordes, E. E., Hourdez, S., Macko, S. A., et al. (2007). Using stable isotopes and quantitative community characteristics to determine a local hydrothermal vent food web. *Mar. Ecol. Prog. Ser.* 330, 49–65. doi:10.3354/meps330049.

Bertrand, E. M., Keddis, R., Groves, J. T., Vetriani, C., and Austin, R. N. (2013). Identity and mechanisms of alkane-oxidizing metalloenzymes from deep-sea hydrothermal vents. *Front. Microbiol.* 4, 1–11. doi:10.3389/fmicb.2013.00109.

Billings, A., Kaiser, C., Young, C. M., Hiebert, L. S., Cole, E., Wagner, J. K. S., et al. (2017). SyPRID sampler: A large-volume, high-resolution, autonomous, deep-ocean precision plankton sampling system. *Deep. Res. Part II Top. Stud. Oceanogr.* 137, 297–306. doi:10.1016/j.dsr2.2016.05.007.

Bishop, C. D., Huggett, M. J., Heyland, A., Hodin, J., and Brandhorst, B. P. (2006). Interspecific variation in metamorphic competence in marine invertebrates: The significance for comparative investigations into the timing of metamorphosis. in *Integrative and Comparative Biology*, 662–682. doi:10.1093/icb/icl043.

Borowski, C., Giere, O., Krieger, J., Amann, R., and Dubilier, N. (2002). New aspects of the symbiosis in the provannid snail Ifremeria nautilei from the North Fiji Back Arc Basin. *Cah. Biol. Mar.* 43, 321–324.

Both, R., Crook, K., Taylor, B., Brogan, S., Chappell, B., Frankel, E., et al. (1986). Hydrothermal

chimneys and associated fauna in the Manus Back-Arc Basin, Papua New Guinea. *Eos, Trans. Am. Geophys. Union* 67, 489. doi:10.1029/eo067i021p00489.

Boutet, I., Ripp, R., Lecompte, O., Dossat, C., Corre, E., Tanguy, A., et al. (2011). Conjugating effects of symbionts and environmental factors on gene expression in deep-sea hydrothermal vent mussels. *BMC Genomics* 12, 530. doi:10.1186/1471-2164-12-530.

Bradford, M. M. (1976). A Rapid and Sensitive Method for the Quantitation Microgram Quantities of Protein Utilizing the Principle of Protein-Dye Binding. *Anal. Biochem.* 254, 248–254. doi:10.1016/0003-2697(76)90527-3.

Brazelton, W. J., Mehta, M. P., Kelley, D. S., and Baross, J. A. (2011). Physiological differentiation within a single-species biofilm fueled by serpentinization. *MBio* 2, 1–9. doi:10.1128/mBio.00127-11.

Brazelton, W. J., Schrenk, M. O., Kelley, D. S., and Baross, J. A. (2006). Methane- and sulfur-metabolizing microbial communities dominate the lost city hydrothermal field ecosystem. *Appl. Environ. Microbiol.* 72, 6257–6270. doi:10.1128/AEM.00574-06.

Brenneis, G., and Richter, S. (2010). Architecture of the nervous system in Mystacocarida (Arthropoda, Crustacea)-An immunohistochemical study and 3D reconstruction. *J. Morphol.* 271, 169–189. doi:10.1002/jmor.10789.

Breusing, C., Biastoch, A., Drews, A., Metaxas, A., Jollivet, D., Vrijenhoek, R. C., et al. (2016). Biophysical and Population Genetic Models Predict the Presence of “Phantom” Stepping Stones Connecting Mid-Atlantic Ridge Vent Ecosystems. *Curr. Biol.*, 1–11. doi:10.1016/j.cub.2016.06.062.

Breusing, C., Johnson, S. B., Vrijenhoek, R. C., and Young, C. R. (2019). Host hybridization as a potential mechanism of lateral symbiont transfer in deep-sea vesicomyid clams. *Mol. Ecol.* 28, 4697–4708. doi:10.1111/mec.15224.

Bright, M., and Bulgheresi, S. (2010). A complex journey: transmission of microbial symbionts. *Nat. Rev. Microbiol.* 8, 218–230. doi:10.1038/nrmicro2262.

Bright, M., Keckeis, H., and Fisher, C. R. (2000). An autoradiographic examination of carbon fixation, transfer and utilization in the Riftia pachyptila symbiosis. *Mar. Biol.* 136, 621–632.

Bright, M., and Lallier, F. H. (2010). The Biology of Vestimentiferan Tubeworms. *Oceanogr. Mar. Biol.* 48, 213–266. doi:10.1201/EBK1439821169-c4.

Bright, M., and Sorgo, A. (2003). Ultrastructural reinvestigation of the trophosome in adults of Riftia pachyptila (Annelida, Siboglinidae). *Invertebr. Biol.* 122, 347–368. doi:10.1111/j.1744-7410.2003.tb00099.x.

Brooke, S. D., and Young, C. M. (2009). Where do the embryos of Riftia pachyptila develop? Pressure tolerances, temperature tolerances, and buoyancy during prolonged embryonic dispersal. *Deep. Res. Part II Top. Stud. Oceanogr.* 56, 1599–1606. doi:10.1016/j.dsr2.2009.05.003.

Brucker, R. M., and Bordenstein, S. R. (2012). Speciation by symbiosis. *Trends Ecol. Evol.* 27, 443–451. doi:10.1016/j.tree.2012.03.011.

Bulet, P., Stöcklin, R., and Menin, L. (2004). Anti-microbial peptides: From invertebrates to vertebrates. *Immunol. Rev.* 198, 169–184. doi:10.1111/j.0105-2896.2004.0124.x.

Butterfield, D. A., McDuff, R. E., Mottl, M. J., Lilley, M. D., Lupton, J. E., and Massoth, G. J. (1994). Gradients in the composition of hydrothermal fluids from the Endeavour segment vent field: phase separation and brine loss. *J. Geophys. Res.* 99, 9561–9583. doi:10.1029/93JB03132.

Cambon-Bonavita, M.-A. (2014). Rapport de campagne BICOSE 2014.

Cambon-Bonavita, M.-A. (2018). Rapport de campagne BICOSE 2 2018 – Tome II.

Campbell, A. C., Alkner, K. K. F., Khadem, M., and Edmond, J. M. (1988). A Time Series of Vent Fluid Compositions From 21°N, East Pacific Rise (1979, 1981, 1985), and the Guaymas Basin , Gulf of California (1982, 1985). *J. Geophys. Res.* 93, 4537–4549.

Campbell, B. J., and Cary, C. S. (2004). Abundance of Reverse Tricarboxylic Acid Cycle Genes in Free-Living Microorganisms at Deep-Sea Hydrothermal Vents. *Appl Env. Microbiol* 70, 6282–6289. doi:10.1128/AEM.70.10.6282.

Campbell, B. J., Engel, A. S., Porter, M. L., and Takai, K. (2006). The versatile ϵ-proteobacteria: key players in sulphidic habitats. *Nat. Rev. Microbiol.* 4, 458–468. doi:10.1038/nrmicro1414.

Campbell, B. J., Polson, S. W., Allen, L. Z., Williamson, S. J., Lee, C. K., Wommack, K. E., et al. (2013). Diffuse flow environments within basalt- and sediment-based hydrothermal vent ecosystems harbor specialized microbial communities. *Front. Microbiol.* 4, 1–15. doi:10.3389/fmicb.2013.00182.

Cannat, M., Fontaine, F., and Escartín, J. (2010). Serpentinization and Associated Hydrogen and Methane Fluxes at Slow Spreading Ridges. *Geophys. Monogr.* 188, 241–264. doi:10.1029/2008GM000760.

Cary, S. C., Cottrell, M. T., Stein, J. L., Camacho, F., and Desbruyères, D. (1997). Molecular identification and localization of filamentous symbiotic bacteria associated with the hydrothermal vent annelid Alvinella pompejana. *Appl. Environ. Microbiol.* 63, 1124–1130.

Cary, S. C., and Giovannoni, S. J. (1993). Transovarial inheritance of endosymbiotic bacteria in clams inhabiting deep-sea hydrothermal vents and cold seeps. *Proc. Natl. Acad. Sci. U. S. A.* 90, 5695–5699. doi:10.1073/pnas.90.12.5695.

Cary, S. C., Shank, T., and Stein, J. (1998). Worms bask in extreme temperatures. *Nature* 391, 545–546. doi:10.1038/35286.

Casanova, B., Brunet, M., and Segonzac, M. (1993). L'impact d'une épibiose bacterienne sur la morphologie fonctionnelle de crevettes associées à l'hydrothermalisme médio-Atlantique. *Cah. Biol. Mar.* 34, 573–588.

Cavanaugh, C. M. (1981). Prokaryotic Cells in the Hydrothermal Vent Tube Worm Riftia pachyptila - Possible Chemoautotrophic Symbionts. *Science (80-. ).* 213, 340–342.

Cavanaugh, C. M., McKiness, Z. P., Newton, I. L. G., and Stewart, F. J. (2013). "Marine Chemosynthetic Symbioses," in *The Prokaryotes*, 579–607. doi:10.1007/0-387-30743-5.

Chan, C. S., Fakra, S. C., Emerson, D., Fleming, E. J., and Edwards, K. J. (2011). Lithotrophic iron-oxidizing bacteria produce organic stalks to control mineral growth: Implications for biosignature formation. *ISME J.* 5, 717–727. doi:10.1038/ismej.2010.173.

Charlou, J. L., Donval, J. P., Fouquet, Y., Jean-Baptiste, P., and Holm, N. (2002). Geochemistry of high H2 and CH4 vent fluids issuing from ultramafic rocks at the Rainbow hydrothermal field (36°14'N,MAR). *Chem. Geol.* 191, 345–359. doi:10.1016/S0009-2541(02)00134-1.

Charlou, J. L., Donval, J. P., Konn, C., Ondréas, H., Fouquet, Y., Jean-baptiste, P., et al. (2010). High Production and Fluxes of H2 and CH4 and Evidence of Abiotic Hydrocarbon Synthesis by Serpentinization in Ultramafic-Hosted Hydrothermal Systems on the Mid-Atlantic Ridge. *Geophys. Monogr. Ser. 188*.

Chaston, J., and Goodrich-Blair, H. (2010). Common Trends in Mutualism Revealed by Model Associations Between Invertebrates and Bacteria. *FEMS Microbiol. Rev.* 34, 41–58. doi:10.1111/j.1574-6976.2009.00193.x.Common.

Chavagnac, V., Leleu, T., Fontaine, F., Cannat, M., Ceuleneer, G., and Castillo, A. (2018). Spatial Variations in Vent Chemistry at the Lucky Strike Hydrothermal Field, Mid Atlantic Ridge (37°N): Updates for Subseafloor Flow Geometry from the Newly Discovered Capelinhos Vent. *Geochemistry, Geophys. Geosystems* 19, 4444– 4458. doi:10.1029/2018GC007765.

Chen, C., Copley, J. T., Linse, K., and Rogers, A. D. (2015a). Low connectivity between 'scaly-foot gastropod' (Mollusca: Peltospiridae) populations at hydrothermal vents on the Southwest Indian Ridge and the Central Indian Ridge. *Org. Divers. Evol.* 15, 663–670. doi:10.1007/s13127-015-0224-8.

Chen, C., Copley, J. T., Linse, K., Rogers, A. D., and Sigwart, J. D. (2015b). The heart of a dragon: 3D anatomical reconstruction of the "scaly-foot gastropod" (Mollusca: Gastropoda: Neomphalina) reveals its extraordinary circulatory system. *Front. Zool.* 12, 1–16. doi:10.1186/s12983-015-0105-1.

Chen, C., Linse, K., Uematsu, K., and Sigwart, J. D. (2018). Cryptic niche switching in a chemosymbiotic gastropod. *Proc. R. Soc. B Biol. Sci.* 285, 1–6. doi:10.1098/rspb.2018.1099.

Chen, C., Uematsu, K., Linse, K., and Sigwart, J. D. (2017). By more ways than one: Rapid convergence at hydrothermal vents shown by 3D anatomical reconstruction of Gigantopelta (Mollusca: Neomphalina). *BMC Evol. Biol.* 17, 62. doi:10.1186/s12862-017-0917-z.

Cheng, X., Wang, Y., Li, J., Yan, G., and He, L. (2019). Comparative analysis of the gut microbial communities between two dominant amphipods from the Challenger Deep, Mariana Trench. *Deep Sea Res. Part I Oceanogr. Res. Pap.*, 103081. doi:10.1016/j.dsr.2019.103081.

Chevaldonné, P., Desbruyères, D., and Childress, J. J. (1992). Some like it hot ... and some even hotter. *Nature* 359, 593–594. doi:10.1126/science.354.6318.1366.

Chiba, S. (2007). A review of ecological and evolutionary studies on hermaphroditic decapod crustaceans. *Plankt. Benthos Res.* 2, 107–119.

Childress, J. J., Fisher, C. R., Brooks, J. M., Kennicutt, M. C., Bidigare, R., and Anderson, A. E. (1986). A methanotropic marine molluscan symbiosis mussels fueled by gas.pdf. *Science (80-. ).* 233, 1306–1308.

Childress, J. J., Fisher, C. R., Favuzzi, J. A., and Sanders, N. K. (1991). Sulfide and Carbon Dioxide Uptake by the Hydrothermal Vent Clam, Calyptogena magnifica, and Its Chemoautotrophic Symbionts. *Physiol. Zool.* 64, 1444–1470. doi:10.1086/physzool.64.6.30158224.

Childress, J. J., and Girguis, P. R. (2011). The metabolic demands of endosymbiotic chemoautotrophic metabolism on host. *J. Exp. Biol.* 214, 312–325. doi:10.1242/jeb.049023.

Chin, C. S., Coale, H., Elrod, V. A., Johnson, S., Massoth, G. J., and Baker, E. T. (1994). In situ observations of dissolved iron and manganese in hydrothermal vent plumes, Juan De Fuca Ridge. *J. Geophys. Res.* 99, 4969–4984.

Chu, H., and Mazmanian, S. K. (2013). Innate immune recognition of the microbiota promotes host-microbial symbiosis. *Nat. Immunol.* 14, 668–675. doi:10.1038/ni.2635.

Coates, C. J., and Decker, H. (2016). Immunological properties of oxygen-transport proteins: hemoglobin, hemocyanin and hemerythrin. *Cell. Mol. Life Sci.* 74, 1–25. doi:10.1007/s00018-016-2326-7.

Colaço, A., Dehairs, F., and Desbruyères, D. (2002). Nutritional relations of deep-sea hydrothermal fields at the Mid-Atlantic Ridge: A stable isotope approach. *Deep. Res. Part I Oceanogr. Res. Pap.* 49, 395–412. doi:10.1016/S0967-0637(01)00060-7.

Colaço, A., Martins, I., Laranjo, M., Pires, L., Leal, C., Prieto, C., et al. (2006). Annual spawning of the hydrothermal vent mussel, Bathymodiolus azoricus, under controlled aquarium, conditions at atmospheric pressure. *J. Exp. Mar. Bio. Ecol.* 333, 166–171. doi:10.1016/j.jembe.2005.12.005.

Combes, C. (1995). *Interactions durables: écologie et évolution du parasitisme*. Masson. Paris: Masson Available at: https://books.google.fr/books?id=3XoQAQAAMAAJ.

Comtet, T., and Desbruyères, D. (1998). Population structure and recruitment in mytilid bivalves from the Lucky Strike and Menez Gwen hydrothermal vent fields (37°17' N and 37°50' N on the Mid-Atlantic Ridge). *Mar. Ecol. Prog. Ser.* 163, 165–177. doi:10.3354/meps163165.

Coplen, T. B. (2011). Guidelines and recommended terms for expression of stable-isotope-ratio and gas-ratio measurement results. *Rapid Commun. Mass Spectrom.* 25, 2538–2560. doi:10.1002/rcm.5129.

Copley, C. E. A., Tyler, P. A., and Varney, M. S. (1998). Lipid profiles of hydrothermal vent shrimps. *Cah. Biol. Mar.* 39, 229–231.

Copley, J., Marsh, L., Glover, A., Hühnerbach, V., Nye, V., Reid, W., et al. (2016). Ecology and biogeography of megafauna and macrofauna at the first known deep-sea hydrothermal vents on the ultraslow-spreading Southwest Indian Ridge. *Sci. Rep.* 6, 39158. doi:10.1038/srep39158.

Copley, J. T., Jorgensen, P. B. K., and Sohn, R. a. (2007). Assessment of decadal-scale ecological change at a deep Mid-Atlantic hydrothermal vent and reproductive time-series in the shrimp Rimicaris exoculata. *J. Mar. Biol. Assoc.* 87, 859–867. doi:10.1017/S0025315407056512.

Copley, J. T. P. (1998). Ecology of deep-sea hydrothermal vents.

Copley, J. T. P., Tyler, P. A., Murton, B. J., and Van Dover, C. L. (1997). Spatial and interannual variation in the faunal distribution at Broken Spur vent field (29°N, Mid-Atlantic Ridge). *Mar. Biol.* 129, 723–733.

Copley, J. T. P., Tyler, P. A., Van Dover, C. L., and Philp, S. J. (2003). Spatial variation in the reproductive biology of Paralvinella palmiformis (Polychaeta: Alvinellidae) from a vent field on the Juan de Fuca Ridge. *Mar. Ecol. Prog. Ser.* 255, 171–181. doi:10.3354/meps255171.

Copley, J. T. P., and Young, C. M. (2006). Seasonality and zonation in the reproductive biology and population structure of the shrimp Alvinocaris stactophila (Caridea: Alvinocarididae) at a Louisiana Slope cold seep. *Mar. Ecol. Prog. Ser.* 315, 199–209.

Corbari, L., Cambon-Bonavita, M. A., Long, G. J., Grandjean, F., Zbinden, M., Gaill, F., et al. (2008a). Iron oxide deposits associated with the ectosymbiotic bacteria in the hydrothermal vent shrimp Rimicaris exoculata. *Biogeosciences Discuss.* 5, 1825–1865. doi:10.5194/bgd-5-1825-2008.

Corbari, L., Zbinden, M., Cambon-Bonavita, M. A., Gaill, F., and Compère, P. (2008b). Bacterial symbionts and mineral deposits in the branchial chamber of the hydrothermal vent shrimp rimicaris exoculata: Relationship to moult cycle. *Aquat. Biol.* 1, 225–238. doi:10.3354/ab00024.

Corliss, J. B., Dymond, J., Gordon, L. I., Edmond, J. M., von Herzen, R. P., Ballard, R. D., et al. (1979). Submarine thermal springs on the galapagos rift. *Science (80-. ).* 203, 1073–1083. doi:10.1126/science.203.4385.1073.

Cottin, D., Shillito, B., Chertemps, T., Tanguy, A., Léger, N., and Ravaux, J. (2010a). Identification of differentially expressed genes in the hydrothermal vent shrimp Rimicaris exoculata exposed to

heat stress. *Mar. Genomics* 3, 71–78. doi:10.1016/j.margen.2010.05.002.

Cottin, D., Shillito, B., Chertemps, T., Thatje, S., Léger, N., and Ravaux, J. (2010b). Comparison of heat-shock responses between the hydrothermal vent shrimp Rimicaris exoculata and the related coastal shrimp Palaemonetes varians. *J. Exp. Mar. Bio. Ecol.* 393, 9–16. doi:10.1016/j.jembe.2010.06.008.

Cowart, D. A., Durand, L., Cambon-Bonavita, M. A., and Arnaud-Haond, S. (2017). Investigation of bacterial communities within the digestive organs of the hydrothermal vent shrimp Rimicaris exoculata provide insights into holobiont geographic clustering. *PLoS One* 12, e0172543. doi:10.1371/journal.pone.0172543.

Cowen, J. P., Fornari, D. J., Shank, T. M., Love, B. ., Glazer, B. . H., Treusch, A., et al. (2007). Volcanic Eruptions at East Pacific Rise Near 9°50'N. *Eos, Trans. Am. Geophys. Union* 88, 81–92.

Cowen, R. K., and Sponaugle, S. (2009). Larval Dispersal and Marine Population Connectivity. *Ann. Rev. Mar. Sci.* 1, 443–466. doi:10.1146/annurev.marine.010908.163757.

Crépeau, V., Cambon Bonavita, M. A., Lesongeur, F., Randrianalivelo, H., Sarradin, P. M., Sarrazin, J., et al. (2011). Diversity and function in microbial mats from the Lucky Strike hydrothermal vent field. *FEMS Microbiol. Ecol.* 76, 524–540. doi:10.1111/j.1574-6941.2011.01070.x.

Cronan, D. S., Moorby, S. A., Glasby, G. P., Knedler, K., Thomson, J., and Hodkinson, R. (1984). Hydrothermal and volcaniclastic sedimentation on the Tonga-Kermadec Ridge and in its adjacent marginal basins. *Geol. Soc. London, Spec. Publ.* 16, 137–149. doi:10.1144/gsl.sp.1984.016.01.10.

Cruaud, P., Vigneron, A., Pignet, P., Caprais, J.-C., Lesongeur, F., Toffin, L., et al. (2017). Comparative Study of Guaymas Basin Microbiomes: Cold Seeps vs. Hydrothermal Vents Sediments. *Front. Mar. Sci.* 4, 1–15. doi:10.3389/fmars.2017.00417.

Cuvelier, D., Beesau, J., Ivanenko, V. N., Zeppilli, D., Sarradin, P., and Sarrazin, J. (2014). First insights into macro- and meiofaunal colonisation patterns on paired wood / slate substrata at Atlantic deep-sea hydrothermal vents. *Deep. Res. Part I* 87, 70–81. doi:10.1016/j.dsr.2014.02.008.

Cuvelier, D., Pierre-Marie Sarradin, Sarrazin, J., Colaço, A., Copley, J. T., Desbruyeres, D., et al. (2011). Hydrothermal faunal assemblages and habitat characterisation at the Eiffel Tower edifice ( Lucky Strike , Mid-atlantic Ridge). *Mar. Ecol.* 32, 243–255. doi:10.1111/j.1439-0485.2010.00431.x.

Cuvelier, D., Sarrazin, J., Colaço, A., Copley, J., Desbruyères, D., Glover, A. G., et al. (2009). Distribution and spatial variation of hydrothermal faunal assemblages at Lucky Strike (Mid-Atlantic Ridge) revealed by high-resolution video image analysis. *Deep. Res. Part I Oceanogr. Res. Pap.* 56, 2026–2040. doi:10.1016/j.dsr.2009.06.006.

Danovaro, R., Company, J. B., Corinaldesi, C., D'Onghia, G., Galil, B., Gambi, C., et al. (2010). Deep-sea biodiversity in the Mediterranean Sea: The known, the unknown, and the unknowable. *PLoS One* 5. doi:10.1371/journal.pone.0011832.

Darwin, C. (1859). *On the Origin of Species by Means of Natural Selection, Or, The Preservation of Favoured Races in the Struggle for Life*. Oxford: J. Murray doi:10.1038/005318a0.

Dattagupta, S., Martin, J., Liao, S., Carney, R. S., and Fisher, C. R. (2007). Deep-sea hydrocarbon seep gastropod Bathynerita naticoidea responds to cues from the habitat-providing mussel Bathymodiolus childressi. *Mar. Ecol.* 28, 193–198. doi:10.1111/j.1439-0485.2006.00130.x.

Dattagupta, S., Schaperdoth, I., Montanari, A., Mariani, S., Kita, N., Valley, J. W., et al. (2009). A novel

symbiosis between chemoautotrophic bacteria and a freshwater cave amphipod. *ISME J.* 3, 935–943. doi:10.1038/ismej.2009.34.

de Bary, A. (1879). *Die Erscheinung der Symbiose: Vortrag gehalten auf der Versammlung Deutscher Naturforscher und Aerzte zu Cassel*. Trübner Available at: https://books.google.fr/books?id=7oQ_AAAAYAAJ.

De Busserolles, F., Sarrazin, J., Gauthier, O., Galinas, Y., Fabri, M. C., Sarradin, P. M., et al. (2009). Are spatial variations in the diets of hydrothermal fauna linked to local environmental conditions? *Deep. Res. Part II Top. Stud. Oceanogr.* 56, 1649–1664. doi:10.1016/j.dsr2.2009.05.011.

Dean, H. K. (1993). A population study of the bivalve Idas argenteus Jeffreys, 1876,(Bivalvia: Mytilidae) recovered from a submerged wood block in the deep North Atlantic Ocean. *Malacologia* 35, 21–41.

Decker, C., Olu, K., Arnaud-Haond, S., and Duperron, S. (2013). Physical Proximity May Promote Lateral Acquisition of Bacterial Symbionts in Vesicomyid Clams. *PLoS One* 8. doi:10.1371/journal.pone.0064830.

Desbruyères, D., Almeida, A., Biscoito, M., Comtet, T., Khripounoff, A., Le Bris, N., et al. (2000). A review of the distribution of hydrothermal vent communities along the northern Mid-Atlantic Ridge: dispersal vs.environmental controls. *Hydrobiologia* 440, 201–216.

Desbruyères, D., Biscoito, M., Caprais, J., Colac, A., Comtet, T., Crassous, P., et al. (2001). Variations in deep-sea hydrothermal vent communities on the Mid-Atlantic Ridge near the Azores plateau. *Deep Sea Res. Part I Oceanogr. Res. Pap.* 48, 1325–1346. doi:https://doi.org/10.1016/S0967-0637(00)00083-2.

Destoumieux-Garzón, D., Saulnier, D., Garnier, J., Jouffrey, C., Bulet, P., and Bachère, E. (2001). Crustacean immunity: Antifungal peptides are generated from the C terminus of shrimp hemocyanin in response to microbial challenge. *J. Biol. Chem.* 276, 47070–47077. doi:10.1074/jbc.M103817200.

Dick, G. J. (2019). The microbiomes of deep-sea hydrothermal vents: distributed globally, shaped locally. *Nat. Rev. Microbiol.*, 1. doi:10.1038/s41579-019-0160-2.

Dick, G. J., Anantharaman, K., Baker, B. J., Li, M., Reed, D. C., and Sheik, C. S. (2013). The microbiology of deep-sea hydrothermal vent plumes: Ecological and biogeographic linkages to seafloor and water column habitats. *Front. Microbiol.* 4, 1–16. doi:10.3389/fmicb.2013.00124.

Distel, D. L., Lee, H. K., and Cavanaugh, C. M. (1995). Intracellular coexistence of methano- and thioautotrophic bacteria in a hydrothermal vent mussel. *Proc. Natl. Acad. Sci.* 92, 9598–9602. doi:10.1073/pnas.92.21.9598.

Dittel, A. I., Perovich, G., and Epifanio, C. E. (2008). Biology of the Vent Crab Bythograea thermydron: A Brief Review. *J. Shellfish Res.* 27, 63–77. doi:10.2983/0730-8000(2008)27[63:botvcb]2.0.co;2.

Dixon, D. R., Dixon, L. R. J., and Pond, D. W. (1998a). Recent advances in our understanding of the life history of bresilid vent shrimps on the MAR. *Cah. Biol. Mar.* 39, 383–386.

Dixon, D. R., Dixon, L. R. J., and Pond, D. W. (1998b). Recent advances in our understanding of the life history of bresiliid vent shrimps on the MAR. *Cah. Biol. Mar.* 39, 383–386.

Dixon, D. R., Lowe, D. M., Miller, P. I., Villemin, G. R., Colaço, A., Serrão-Santos, R., et al. (2006). Evidence of seasonal reproduction in the Atlantic vent mussel Bathymodiolus azoricus, and an apparent link with the timing of photosynthetic primary production. *J. Mar. Biol. Assoc. United Kingdom* 86, 1363–1371. doi:10.1017/S0025315406014391.

Dixson, D. L., Abrego, D., and Hay, M. E. (2014). Chemically mediated behavior of recruiting corals and fishes: A tipping point that may limit reef recovery. *Science (80-. ).* 345, 892–897. doi:10.1126/science.1255057.

Doledec, S., Chessel, D., and Gimaret-Carpentier, C. (2000). Niche separation in community analysis: A new method. *Ecology* 81, 2914–2927.

Dong, C., Xie, Y., Li, H., Lai, Q., Liu, X., and Shao, Z. (2019). Faunal and microbial biodiversity of the newly discovered Deyin-1 hydrothermal vent field at 15°S on the southern Mid-Atlantic Ridge. *Deep. Res. Part I*, 103134. doi:10.1016/j.dsr.2019.103134.

Douglas, A. E. (1994). *Symbiotic Interactions*. Oxford: Oxford University Press Available at: https://books.google.fr/books?id=4-NBngAACAAJ.

Dray, S., and Dufour, A.-B. (2007). The ade4 Package: Implementing the Duality Diagram for Ecologists. *J. Stat. Softw.* 22, 1–19. doi:10.18637/jss.v022.i04.

Druschel, G. K., Emerson, D., Sutka, R., Suchecki, P., and Luther, G. W. (2008). Low-oxygen and chemical kinetic constraints on the geochemical niche of neutrophilic iron ( II ) oxidizing microorganisms. *Geochim. Cosmochim. Acta* 72, 3358–3370. doi:10.1016/j.gca.2008.04.035.

Duarte, S., Nunes, L., Borges, P. A. V, Fossdal, C. G., and Nobre, T. (2017). Living inside termites: an overview of symbiotic interactions, with emphasis on flagellate protists. *Arquipélago Life Mar. Sci.* 34, 21–43.

Dubilier, N., Bergin, C., and Lott, C. (2008). Symbiotic diversity in marine animals: the art of harnessing chemosynthesis. *Nat. Rev. Microbiol.* 6, 725–40. doi:10.1038/nrmicro1992.

Dunn, D. C., Van Dover, C. L., Etter, R. J., Smith, C. R., Levin, L. A., Morato, T., et al. (2018). A strategy for the conservation of biodiversity on mid-ocean ridges from deep-sea mining. *Sci. Adv.* 4, eaar4313. doi:10.1126/sciadv.aar4313.

Duperron, S. (2010). *The diversity of deep-sea mussels and their bacterial symbioses*. doi:10.1007/978-90-481-9572-5.

Duperron, S. (2017). Microbial Symbioses. *Elsevier Oceanogr. Ser.* 3, 125–132. doi:10.1016/S0422-9894(08)70386-6.

Duperron, S., Bergin, C., Zielinski, F., Blazejak, A., Pernthaler, A., McKiness, Z. P., et al. (2006). A dual symbiosis shared by two mussel species, Bathymodiolus azoricus and Bathymodiolus puteoserpentis (Bivalvia: Mytilidae), from hydrothermal vents along the northern Mid-Atlantic Ridge. *Environ. Microbiol.* 8, 1441–1447. doi:10.1111/j.1462-2920.2006.01038.x.

Duperron, S., De Beer, D., Zbinden, M., Boetius, A., Schipani, V., Kahil, N., et al. (2009). Molecular characterization of bacteria associated with the trophosome and the tube of Lamellibrachia sp., a siboglinid annelid from cold seeps in the eastern Mediterranean. *FEMS Microbiol. Ecol.* 69, 395–409. doi:10.1111/j.1574-6941.2009.00724.x.

Duperron, S., Gaudron, S. M., Rodrigues, C. F., Cunha, M. R., Decker, C., and Olu, K. (2013). An overview of chemosynthetic symbioses in bivalves from the North Atlantic and Mediterranean Sea. 3241–3267. doi:10.5194/bg-10-3241-2013.

Duperron, S., Guezi, H., Gaudron, S. M., Pop Ristova, P., Wenzhöfer, F., and Boetius, A. (2011). Relative abundances of methane- and sulphur-oxidising symbionts in the gills of a cold seep mussel and link to their potential energy sources. *Geobiology* 9, 481–491. doi:10.1111/j.1472-4669.2011.00300.x.

Duperron, S., Halary, S., Lorion, J., Sibuet, M., and Gaill, F. (2008). Unexpected co-occurrence of six

bacterial symbionts in the gills of the cold seep mussel Idas sp. (Bivalvia: Mytilidae). *Environ. Microbiol.* 10, 433–445. doi:10.1111/j.1462-2920.2007.01465.x.

Duperron, S., Quiles, A., Szafranski, K. M., Léger, N., and Shillito, B. (2016). Estimating Symbiont Abundances and Gill Surface Areas in Specimens of the Hydrothermal Vent Mussel Bathymodiolus puteoserpentis Maintained in Pressure Vessels. *Front. Mar. Sci.* 3, 1–12. doi:10.3389/fmars.2016.00016.

Duperron, S., Sibuet, M., MacGregor, B. J., Kuypers, M. M. M., Fisher, C. R., and Dubilier, N. (2007). Diversity, relative abundance and metabolic potential of bacterial endosymbionts in three Bathymodiolus mussel species from cold seeps in the Gulf of Mexico. *Environ. Microbiol.* 9, 1423–1438. doi:10.1111/j.1462-2920.2007.01259.x.

Durand, L., Roumagnac, M., Cueff-Gauchard, V., Jan, C., Guri, M., Tessier, C., et al. (2015). Biogeographical distribution of Rimicaris exoculata resident gut epibiont communities along the Mid-Atlantic Ridge hydrothermal vent sites. *FEMS Microbiol. Ecol.* 91, 1–15. doi:10.1093/femsec/fiv101.

Durand, L., Zbinden, M., Cueff-Gauchard, V., Duperron, S., Roussel, E. G., Shillito, B., et al. (2010). Microbial diversity associated with the hydrothermal shrimp Rimicaris exoculata gut and occurrence of a resident microbial community. *FEMS Microbiol. Ecol.* 71, 291–303. doi:10.1111/j.1574-6941.2009.00806.x.

Edmonds, H. N., Michael, P. J., Baker, E. T., Connelly, D. P., Snow, J. E., Langmuir, C. H., et al. (2003). Discovery of abundant hydrothermal venting on the ultraslow-spreading Gakkel ridge in the Arctic Ocean. *Nature* 421, 252–256. doi:10.1038/nature01351.

Edwards, K. J., Rogers, D. R., Wirsen, C. O., and McCollom, T. M. (2003). Isolation and Characterization of Novel Psychrophilic, Neutrophilic, Fe-Oxidizing, Chemolithoautotrophic alpha- and gamma-Proteobacteria from the Deep Sea. *Nonwovens Rep. Int.* 69, 2906–2913. doi:10.1128/AEM.69.5.2906.

Emerson, D., Rentz, J. A., Lilburn, T. G., Davis, R. E., Aldrich, H., Chan, C., et al. (2007). A novel lineage of proteobacteria involved in formation of marine Fe-oxidizing microbial mat communities. *PLoS One* 2. doi:10.1371/journal.pone.0000667.

Endow, K., and Ohta, S. (1990). Occurrence of bacteria in the primary oocytes of vesicomyid clam Calyptogena soyoae . *Mar. Ecol. Prog. Ser.* 64, 309–311. doi:10.3354/meps064309.

Epifanio, C. E., Perovich, G., Dittel, A. I., and Cary, S. C. (1999). Development and behavior of megalopa larvae and juveniles of the hydrothermal vent crab Bythograea thermydron. *Mar. Ecol. Prog. Ser.* 185, 147–154. doi:10.3354/meps185147.

Fabri, M. C., Bargain, a, Briand, P., Gebruk, a, Fouquet, Y., Morineaux, M., et al. (2011). The hydrothermal vent community of a new deep-sea field, Ashadze-1, 12 degrees 58 ' N on the Mid-Atlantic Ridge. *J. Mar. Biol. Assoc. United Kingdom* 91, 1–13. doi:10.1017/s0025315410000731.

Fanenbruck, M., Harzsch, S., and Wägele, J. W. (2004). The brain of the Remipedia (Crustacea) and an alternative hypothesis on their phylogenetic relationships. *Proc. Natl. Acad. Sci. U. S. A.* 101, 3868–3873. doi:10.1073/pnas.0306212101.

Fang, J., Uhle, M., Billmark, K., Bartlett, D. H., and Kato, C. (2006). Fractionation of carbon isotopes in biosynthesis of fatty acids by a piezophilic bacterium Moritella japonica strain DSK1. *Geochim. Cosmochim. Acta* 70, 1753–1760. doi:10.1016/j.gca.2005.12.011.

Faure, B., Chevaldonné, P., Pradillon, F., Thiébaut, E., and Jollivet, D. (2007). Spatial and temporal

dynamics of reproduction and settlement in the Pompeii worm Alvinella pompejana (Polychaeta: Alvinellidae). *Mar. Ecol. Prog. Ser.* 348, 197–211. doi:10.3354/meps07021.

Felbeck, H. (1981). Chemoautotrophic potential of the hydrothermal vent tube worm, Riftia pachyptila Jones (Vestimentifera). *Science (80-. ).* 213, 336–338. doi:10.1126/science.213.4505.336.

Ferrera, I., Banta, A. B., and Reysenbach, A. L. (2014). Spatial patterns of Aquificales in deep-sea vents along the Eastern Lau Spreading Center (SW Pacific). *Syst. Appl. Microbiol.* 37, 442–448. doi:10.1016/j.syapm.2014.04.002.

Ferry, J. G. (2012). *Methanogenesis: ecology, physiology, biochemistry & genetics*. Springer Science & Business Media.

Fiala-Médioni, A., C. Michalski, J., Jolles, J., Alonso, C., and Montreuil, J. (1994). *Lysosomic and lysozyme activities in the gill of bivalves from deep hydrothermal vents*.

Fiala-Médioni, A., and Métivier, C. (1986). Ultrastructure of the gill of the hydrothermal vent bivalve Calyptogena magnifica, with a discussion of its nutrition. *Mar. Biol.* 90, 215–222.

Fiala-Medioni, A., and Pennec, M. Le (1989). Adaptative features of the bivalve molluscs associated with fluid venting in the subduction zones off Japan. *Palaeogeogr. Palaeoclimatol. Palaeoecol.* 71, 161–167. doi:10.1016/0031-0182(89)90035-7.

Fiala-Médioni, A., Z., M., P., D., J., B., A., M., A., A.-D., et al. (2002). Ultrastructural, biochemical, and immunological characterization of two populations of the mytilid mussel Bathymodiolus azoricus from the Mid-Atlantic Ridge: evidence for a dual symbiosis. *Mar. Biol.* 141, 1035–1043. doi:10.1007/s00227-002-0903-9.

Field, E. K., Sczyrba, A., Lyman, A. E., Harris, C. C., Woyke, T., Stepanauskas, R., et al. (2014). Genomic insights into the uncultivated marine Zetaproteobacteria at Loihi Seamount. *ISME J.* 9, 857–870. doi:10.1038/ismej.2014.183.

Fisher, C. R., and Childress, J. J. (1992). Organic carbon transfer from methanotrophic symbionts to the host hydrocarbon-seep mussel. *Symbiosis* 12, 221–235.

Fisher, C. R., Childress, J. J., Oremland, R. S., and Bidigare, R. R. (1987). The importance of methane and thiosulfate in the metabolism of the bacterial symbionts of two deep-sea mussels. *Mar. Biol.* 96, 1–11.

Fisher, C. R., Takai, K., and Le Bris, N. (2007). Hydrothermal Vent Ecosystems. *Oceanography* 20, 14–23. doi:10.5670/oceanog.2007.75.

Flaherty, E. A., and Ben-David, M. (2010). Overlap and partitioning of the ecological and isotopic niches. *Oikos* 119, 1409–1416. doi:10.1111/j.1600-0706.2010.18259.x.

Fleming, E. J., Davis, R. E., Mcallister, S. M., Chan, C. S., Moyer, C. L., Tebo, B. M., et al. (2013). Hidden in plain sight: Discovery of sheath-forming, iron-oxidizing Zetaproteobacteria at Loihi Seamount, Hawaii, USA. *FEMS Microbiol. Ecol.* 85, 116–127. doi:10.1111/1574-6941.12104.

Flores, G. E., Campbell, J. H., Kirshtein, J. D., Meneghin, J., Podar, M., Steinberg, J. I., et al. (2011). Microbial community structure of hydrothermal deposits from geochemically different vent fields along the Mid-Atlantic Ridge. *Environ. Microbiol.* 13, 2158–2171. doi:10.1111/j.1462-2920.2011.02463.x.

Flores, G. E., Shakya, M., Meneghin, J., Yang, Z. K., Seewald, J. S., Geoff Wheat, C., et al. (2012). Inter-field variability in the microbial communities of hydrothermal vent deposits from a back-arc basin. *Geobiology* 10, 333–346. doi:10.1111/j.1472-4669.2012.00325.x.

Folmer, O., Black, M., Hoeh, W., Lutz, R., and Vrijenhoek, R. (1994). DNA primers for amplification of mitochondrial cytochrome c oxidase subunit I from diverse metazoan invertebrates. *Mol. Mar. Biol. Biotechnol.* 3, 294–299. doi:10.1371/journal.pone.0013102.

Forbes, E. (1843). *Report on the Mollusca and Radiata of the Aegean Sea: And on Their Distribution, Considered as Bearing on Geology*.

Fornari, D. J., Von Damm, K. L., Bryce, J. G., Cowen, J. P., Ferrini, V., Fundis, A., et al. (2012). The East Pacific Rise between 9°N and 10°N: Twenty-five years of integrated, multidisciplinary oceanic spreading center studies. *Oceanography* 25, 18–43.

Fortunato, C. S., Larson, B., Butterfield, D. A., and Huber, J. A. (2018). Spatially distinct, temporally stable microbial populations mediate biogeochemical cycling at and below the seafloor in hydrothermal vent fluids. *Environ. Microbiol.* 20, 769–784. doi:10.1111/1462-2920.14011.

Fouquet, Y., Cambon, P., Etoubleau, J., Charlou, J. L., Ondréas, H., Barriga, F. J. A. S., et al. (2010). "Geodiversity of Hydrothermal Processes Along the Mid-Atlantic Ridge and Ultramafic-Hosted Mineralization: A New Type of Oceanic Cu-Zn-Co-Au Volcanogenic Massive Sulfide Deposit," in *Diversity of Hydrothermal Systems on Slow Spreading Ocean Ridges*, 321–367. doi:10.1029/2008GM000746.

Fouquet, Y., Wafik, A., Cambon, P., Mevel, C., Meyer, G., and Gente, P. (1993). Tectonic setting and mineralogical and geochemical zonation in the Snake Pit sulfide deposit. *Econ. Geol.* 88, 2018–2036. doi:10.2113/gsecongeo.88.8.2018.

Foustoukos, D. I., and Seyfried, W. E. J. (2007). Fluid Phase Separation Processes in Submarine Hydrothermal Systems. *Rev. Mineral. Geochemistry* 65, 213–239. doi:10.2138/rmg.2007.65.7.

Frank, S. A. (1996). Host — symbiont conflict over the mixing of symbiotic lineages. *Proc. R. Soc. B* 263, 339–344.

Franzenburg, S., Walter, J., Künzel, S., Wang, J., Baines, J. F., Bosch, T. C. G., et al. (2013). Distinct antimicrobial peptide expression determines host species-specific bacterial associations. *Proc. Natl. Acad. Sci. U. S. A.* 110. doi:10.1073/pnas.1304960110.

Fry, B., Gest, H., and Hayes, J. M. (1983). Sulphur isotopic compositions of deep-sea hydrothermal vent animals. *Nature* 306.

Gabbott, P. A., and Peek, K. (1991). Cellular biochemistry of the mantle tissue of the mussel Mytilus edulis. *Aquaculture* 94, 165–176. doi:10.1016/0044-8486(91)90116-O.

Gallo, R. L., and Nakatsuji, T. (2011). Microbial symbiosis with the innate immune defense system of the skin. *J. Invest. Dermatol.* 131, 1974–1980. doi:10.1038/jid.2011.182.

Gamo, T., Chiba, H., Yamanaka, T., Okudaira, T., Hashimoto, J., Tsuchida, S., et al. (2001). Chemical characteristics of newly discovered black smoker fluids and associated hydrothermal plumes at the Rodriguez Triple Junction, Central Indian Ridge. *Earth Planet. Sci. Lett.* 193, 371–379. doi:10.1016/S0012-821X(01)00511-8.

Gardebrecht, A., Markert, S., Sievert, S. M., Felbeck, H., Thürmer, A., Albrecht, D., et al. (2012). Physiological homogeneity among the endosymbionts of Riftia pachyptila and Tevnia jerichonana revealed by proteogenomics. *ISME J.* 6, 766–776. doi:10.1038/ismej.2011.137.

Gartman, A., Yücel, M., Madison, A. S., Chu, D. W., Ma, S., Janzen, C. P., et al. (2011). Sulfide Oxidation across Diffuse Flow Zones of Hydrothermal Vents. *Aquat. Geochemistry* 17, 583–601. doi:10.1007/s10498-011-9136-1.

Gaten, E., Herring, P. J., Shelton, P. M. J., and Johnson, M. L. (1998). Comparative morphology of the

eyes of postlarval bresiliid shrimps from the region of hydrothermal vents. *Biol. Bull.* 194, 267–280.

Gaudron, S. M., Demoyencourt, E., and Duperron, S. (2012). Reproductive traits of the cold-seep symbiotic mussel Idas modiolaeformis: Gametogenesis and larval biology. *Biol. Bull.* 222, 6–16.

Gaudron, S. M., Pradillon, F., Pailleret, M., Duperron, S., Bris, N. Le, and Gaill, F. (2010). Colonization of organic substrates deployed in deep-sea reducing habitats by symbiotic species and associated fauna. *Mar. Environ. Res.* 70, 1–12. doi:10.1016/j.marenvres.2010.02.002.

Gebruk, A., Fabri, M. C., Briand, P., and Desbruyeres, D. (2010). Community dynamics over a decadal scale at logatchev, 14°45'N, mid-atlantic ridge. *Cah. Biol. Mar.* 51, 383–388.

Gebruk, A. V., Pimenov, N. V., and Savvichev, A. S. (1993). Feeding specialization of bresiliid shrimps in the TAG site hydrothermal community. *Mar. Ecol. Prog. Ser.* 98, 247–253. doi:10.3354/meps098247.

Gebruk, A. V., Southward, E. C., Kennedy, H., and Southward, A. J. (2000). Food sources, behaviour, and distribution of hydrothermal vent shrimps at the Mid-Atlantic Ridge. *J. Mar. Biol. Assoc. United Kingdom* 80, 485–499. doi:10.1017/S0025315400002186.

Gerdes, K., Arbizu, P. M., and Schwarz-schampera, U. (2019). Detailed Mapping of Hydrothermal Vent Fauna : A 3D Reconstruction Approach Based on Video Imagery. *Front. Mar. Sci.* 6. doi:10.3389/fmars.2019.00096.

Geret, F., Riso, R., Sarradin, P. M., Caprais, J. C., and Cosson, R. P. (2002). Metal bioaccumulation and storage forms in the shrimp, Rimicaris exoculata, from the Rainbow hydrothermal field (Mid-Atlantic Ridge); preliminary approach to the fluid-organism relationship. *Cah. Biol. Mar.* 43, 43–52.

Gerlach, G., Atema, J., Kingsford, M. J., Black, K. P., and Miller-Sims, V. (2007). Smelling home can prevent dispersal of reef fish larvae. *Proc. Natl. Acad. Sci.* 104, 858–863. doi:10.1073/pnas.0606777104.

German, C. R., Bowen, A., Coleman, M. L., Honig, D. L., Huber, J. A., Jakuba, M. V, et al. (2010). Diverse styles of submarine venting on the ultraslow spreading Mid-Cayman Rise. *Proc. Natl. Acad. Sci.* 107, 14020–14025. doi:10.1073/pnas.1009205107.

German, C. R., and Parson, L. M. (1998). Distributions of hydrothermal activity along the Mid-Atlantic Ridge: Interplay of magmatic and tectonic controls. *Earth Planet. Sci. Lett.* 160, 327–341. doi:10.1016/S0012-821X(98)00093-4.

Giovannelli, D., Chung, M., Staley, J., Starovoytov, V., Bris, N. Le, and Vetriani, C. (2016). Sulfurovum riftiae sp. nov., a mesophilic, thiosulfate-oxidizing, nitrate-reducing chemolithoautotrophic epsilonproteobacterium isolated from the tube of the deep-sea hydrothermal vent polychaete Riftia pachyptila. *Int. J. Syst. Evol. Microbiol.* 66, 2697–2701. doi:10.1099/ijsem.0.001106.

Girguis, P. R. (2006). Thermal Preference and Tolerance of Alvinellids. *Science (80-. ).* 312, 231–231. doi:10.1126/science.1125286.

Girguis, P. R., and Childress, J. J. (2006). Metabolite uptake, stoichiometry and chemoautotrophic function of the hydrothermal vent tubeworm Riftia pachyptila: responses to environmental variations in substrate concentrations and temperature. *J. Exp. Biol.* 209, 3516–3528. doi:10.1242/jeb.02404.

Glover, A. G., Wiklund, H., Chen, C., and Thomas, G. (2018). Managing a sustainable deep- sea ' blue economy ' requires knowledge of what actually lives there. *Elife* 7, 1–7.

Goffredi, S. K. (2010). Indigenous ectosymbiotic bacteria associated with diverse hydrothermal vent invertebrates. *Environ. Microbiol. Rep.* 2, 479–488. doi:10.1111/j.1758-2229.2010.00136.x.

Goffredi, S. K., Girguis, P. R., Desaulniers, N. T., and Childress, J. (1999). Physiological Functioning of Carbonic Anhydrase in the Hydrothermal Vent Tubeworm Riftia Pachyptila. *Biol. Bull.* 196, 257–264.

Goffredi, S. K., Gregory, A., Jones, W. J., Morella, N. M., and Sakamoto, R. I. (2014). Ontogenetic variation in epibiont community structure in the deep-sea yeti crab, Kiwa puravida: Convergence among crustaceans. *Mol. Ecol.* 23, 1457–1472. doi:10.1111/mec.12439.

Goffredi, S. K., Johnson, S., Tunnicliffe, V., Caress, D., Clague, D., Escobar, E., et al. (2017). Hydrothermal vent fields discovered in the southern Gulf of California clarify role of habitat in augmenting regional diversity. *Proc. R. Soc. B Biol. Sci.* 284, 20170817. doi:10.1098/rspb.2017.0817.

Goffredi, S. K., Jones, W. J., Erhlich, H., Springer, A., and Vrijenhoek, R. C. (2008). Epibiotic bacteria associated with the recently discovered Yeti crab, Kiwa hirsuta. *Environ. Microbiol.* 10, 2623–2634. doi:10.1111/j.1462-2920.2008.01684.x.

Goffredi, S. K., Orphan, V. J., Rouse, G. W., Jahnke, L., Embaye, T., Turk, K., et al. (2005). Evolutionary innovation: A bone-eating marine symbiosis. *Environ. Microbiol.* 7, 1369–1378. doi:10.1111/j.1462-2920.2005.00824.x.

Goffredi, S. K., Warén, A., Orphan, V. J., Van Dover, C. L., and Vrijenhoek, R. C. (2004). Hydrothermal Vent Gastropod from the Indian Ocean. *Appl. Environ. Microbiol.* 70, 3082–3090. doi:10.1128/AEM.70.5.3082.

Gonnella, G., Böhnke, S., Indenbirken, D., Garbe-Schönberg, D., Seifert, R., Mertens, C., et al. (2016). Endemic hydrothermal vent species identified in the open ocean seed bank. *Nat. Microbiol.* 1, 1–7. doi:10.1038/nmicrobiol.2016.86.

González-Gurriarán, E., Freire, J., and Bernárdez, C. (2002). Migratory Patterns of Female Spider Crabs Maja Squinado Detected Using Electronic Tags and Telemetry. *J. Crustac. Biol.* 22, 91–97. doi:10.1651/0278-0372(2002)022[0091:mpofsc]2.0.co;2.

Gosset, C. C., Do Nascimento, J., Augé, M. T., and Bierne, N. (2014). Evidence for adaptation from standing genetic variation on an antimicrobial peptide gene in the mussel Mytilus edulis. *Mol. Ecol.* 23, 3000–3012. doi:10.1111/mec.12784.

Govenar, B. (2012). Energy Transfer Through Food Webs at Hydrothermal Vents: Linking the Lithosphere to the Biosphere. *Oceanography* 25, 246–255. doi:10.5670/oceanog.2012.23.

Govenar, B., Fisher, C. R., and Shank, T. M. (2015). Variation in the diets of hydrothermal vent gastropods. *Deep. Res. Part II Top. Stud. Oceanogr.* 121, 193–201. doi:10.1016/j.dsr2.2015.06.021.

Govenar, B., Le Bris, N., Gollner, S., Glanville, J., Aperghis, A. B., Hourdez, S., et al. (2005). Epifaunal community structure associated with Riftia pachyptila aggregations in chemically different hydrothermal vent habitats. *Mar. Ecol. Prog. Ser.* 305, 67–77. doi:10.3354/meps305067.

Grzymski, J. J., Murray, A. E., Campbell, B. J., Kaplarevic, M., Gao, G. R., Lee, C., et al. (2008). Metagenome analysis of an extreme microbial symbiosis reveals eurythermal adaptation and metabolic flexibility. *Proc. Natl. Acad. Sci.* 105, 17516–17521. doi:10.1073/pnas.0802782105.

Guerra-Castro, E., Carmona-Suárez, C., and Conde, J. E. (2011). Biotelemetry of crustacean decapods: Sampling design, statistical analysis, and interpretation of data. *Hydrobiologia* 678, 1–15.

doi:10.1007/s10750-011-0828-8.

Guri, M., Durand, L., Cueff-Gauchard, V., Zbinden, M., Crassous, P., Shillito, B., et al. (2012). Acquisition of epibiotic bacteria along the life cycle of the hydrothermal shrimp Rimicaris exoculata. *ISME J.* 6, 597–609. doi:10.1038/ismej.2011.133.

Haase, K. M., Petersen, S., Koschinsky, A., Seifert, R., Devey, C. W., Keir, R., et al. (2007). Young volcanism and related hydrothermal activity at 5°S on the slow-spreading southern Mid-Atlantic Ridge. *Geochemistry, Geophys. Geosystems* 8, 1–17. doi:10.1029/2006GC001509.

Hadfield, M. G. (2011). Biofilms and Marine Invertebrate Larvae: What Bacteria Produce That Larvae Use to Choose Settlement Sites. *Ann. Rev. Mar. Sci.* 3, 453–470. doi:10.1146/annurev-marine-120709-142753.

Haeckel, E. (1866). *Generelle Morphologie der Organismen. Allgemeine Grundzüge der organischen Formen-Wissenschaft, mechanisch begründet durch die von C. Darwin reformirte Descendenz-Theorie, etc*.

Hager, K. W., Fullerton, H., Butterfield, D. A., and Moyer, C. L. (2017). Community structure of lithotrophically-driven hydrothermal microbial mats from the Mariana Arc and back-arc. *Front. Microbiol.* 8. doi:10.3389/fmicb.2017.01578.

Halary, S., Riou, V., Gaill, F., Boudier, T., and Duperron, S. (2008). 3D FISH for the quantification of methane- and sulphur-oxidizing endosymbionts in bacteriocytes of the hydrothermal vent mussel Bathymodiolus azoricus. *ISME J.* 2, 284–292. doi:10.1038/ismej.2008.3.

Hamasaki, K., Nakajima, K., Kado, R., Tsuchida, S., and Kitada, S. (2010). Number and Duration of Zoeal Stages of the Hydrothermal Vent Crab Gandalfus yunohana from Laboratory Reared Specimens. *J. Crustac. Biol.* 30, 236–240. doi:10.1651/09-3199.1.

Harmer, T. L., Rotjan, R. D., Nussbaumer, A. D., Bright, M., Ng, A. W., DeChaine, E. G., et al. (2008). Free-living tube worm endosymbionts found at deep-sea vents. *Appl. Environ. Microbiol.* 74, 3895–3898. doi:10.1128/AEM.02470-07.

Hashimoto, J., Ohta, S., Gamo, T., Chiba, H., Yamaguchi, T., Tsuchida, S., et al. (2001). First Hydrothermal Vent Communities from the Indian Ocean Discovered. *Zoolog. Sci.* 18, 717–721. doi:10.2108/zsj.18.717.

Hauton, C., Brockton, V., and Smith, V. J. (2007). In vivo effects of immunostimulants on gene expression and disease resistance in lobster (Homarus gammarus) post-larval stage VI (PLVI) juveniles. *Mol Immunol* 44, 443–450.

Hay, M. E. (2009). Marine Chemical Ecology: Chemical Signals and Cues Structure Marine Populations, Communities, and Ecosystems. *Ann. Rev. Mar. Sci.* 1, 193–212. doi:10.1146/annurev.marine.010908.163708.

Haymon, R. M., Fornari, D. J., Edwards, M. H., Carbotte, S., Wright, D., and Macdonald, K. C. (1991). Hydrothermal vent distribution along the East Pacific Rise crest (9°09'-54'N) and its relationship to magmatic and tectonic processes on fast-spreading mid-ocean ridges. *Earth Planet. Sci. Lett.* 104, 513–534. doi:10.1016/0012-821X(91)90226-8.

Hernández-Ávila, I. (2016). Larval dispersal and life cycle in deep-water hydrothermal vents : The case of Rimicaris exoculata and related species.

Hernández-Ávila, I., Cambon-Bonavita, M. A., and Pradillon, F. (2015). Morphology of first zoeal stage of four genera of alvinocaridid shrimps from hydrothermal vents and cold seeps: Implications for ecology, larval biology and phylogeny. *PLoS One* 10, 1–27.

doi:10.1371/journal.pone.0144657.

Herring, P. J. (2006). Presence of postlarval alvinocaridid shrimps over south-west Indian Ocean hydrothermal vents, with comparisons of the pelagic biomass at different vent sites. *J. Mar. Biol. Assoc. United Kingdom* 86, 125–128. doi:doi:10.1017/S0025315406012938.

Herring, P. J., and Dixon, D. R. (1998). Extensive deep-sea dispersal of postlarval shrimp from a hydrothermal vent. *Deep. Res. Part I Oceanogr. Res. Pap.* 45, 2105–2118. doi:10.1016/S0967-0637(98)00050-8.

Hessler, R. R., and Lonsdale, P. F. (1991). Biogeography of Mariana Trough hydrothermal vent communities. *Deep Sea Res. Part A, Oceanogr. Res. Pap.* 38, 185–199. doi:10.1016/0198-0149(91)90079-U.

Heywood, J. L., Chen, C., Pearce, D. A., and Linse, K. (2017). Bacterial communities associated with the Southern Ocean vent gastropod, Gigantopelta chessoia: indication of horizontal symbiont transfer. *Polar Biol.* 40, 2335–2342. doi:10.1007/s00300-017-2148-6.

Hilario, A., Metaxas, A., Gaudron, S. M., Howell, K. L., Mercier, A., Mestre, N. C., et al. (2015). Estimating dispersal distance in the deep sea: challenges and applications to marine reserves. *Front. Mar. Sci.* 2, 1–14. doi:10.3389/fmars.2015.00006.

Hilário, A., Vilar, S., Cunha, M. R., and Tyler, P. (2009). Reproductive aspects of two bythograeid crab species from hydrothermal vents in the Pacific-Antarctic Ridge. *Mar. Ecol. Prog. Ser.* 378, 153–160. doi:10.3354/meps07858.

Hilario, A., Young, C. M., and Tyler, P. A. (2005). Sperm storage, internal fertilization and embryonic dispersal invent and seep tubeworms. *Biol. Bull.* 208, 20–28.

Hiraoka, R., Komai, T., and Tsuchida, S. (2019). A new species of Alvinocaris (Crustacea: Decapoda: Caridea: Alvinocarididae) from hydrothermal vents in the Izu-Bonin and Mariana Arcs, north-western Pacific. *J. Mar. Biol. Assoc. United Kingdom*. doi:10.1017/S0025315419001097.

Holden, J., Breier, J., Rogers, K., Schulte, M., and Toner, B. (2012). Biogeochemical Processes at Hydrothermal Vents: Microbes and Minerals, Bioenergetics, and Carbon Fluxes. *Oceanography* 25, 196–208. doi:10.5670/oceanog.2012.18.

Hourdez, S., and Lallier, F. H. (2007). Adaptations to hypoxia in hydrothermal-vent and cold-seep invertebrates. *Life Extrem. Environ.*, 297–313. doi:10.1007/978-1-4020-6285-8-19.

Hourdez, S., and Weber, R. E. (2005). Molecular and functional adaptations in deep-sea hemoglobins. *J. Inorg. Biochem.* 99, 130–141. doi:10.1016/j.jinorgbio.2004.09.017.

Huang, S., and Hadfield, M. G. (2003). Composition and density of bacterial biofilms determine larval settlement of the polychaete Hydroides elegans. *Mar. Ecol. Prog. Ser.* 260, 161–172. doi:10.3354/meps260161.

Hubatsch, H. A. (2017). Movement patterns and habitat use of the exploited swimming crab Scylla serrata ( Forskål , 1775 ) Dissertation Hilke Alberts-Hubatsch.

Huber, J. A., Cantin, H. V., Huse, S. M., Mark Welch, D. B., Sogin, M. L., and Butterfield, D. A. (2010). Isolated communities of Epsilonproteobacteria in hydrothermal vent fluids of the Mariana Arc seamounts. *FEMS Microbiol. Ecol.* 73, 538–549. doi:10.1111/j.1574-6941.2010.00910.x.

Hügler, M., Petersen, J. M., Dubilier, N., Imhoff, J. F., and Sievert, S. M. (2011). Pathways of carbon and energy metabolism of the epibiotic community associated with the deep-sea hydrothermal vent shrimp Rimicaris exoculata. *PLoS One* 6. doi:10.1371/journal.pone.0016018.

Hügler, M., and Sievert, S. M. (2011). Beyond the Calvin Cycle : Autotrophic Carbon Fixation in the Ocean. *Ann. Rev. Mar. Sci.* doi:10.1146/annurev-marine-120709-142712.

Hurtado, L. A., Lutz, R. A., and Vrijenhoek, R. C. (2004). Distinct patterns of genetic differentiation among annelids of eastern Pacific hydrothermal vents. *Mol. Ecol.* 13, 2603–2615. doi:10.1111/j.1365-294X.2004.02287.x.

Husson, B., Sarradin, P. M., Zeppilli, D., and Sarrazin, J. (2017). Picturing thermal niches and biomass of hydrothermal vent species. *Deep. Res. Part II Top. Stud. Oceanogr.* 137, 6–25. doi:10.1016/j.dsr2.2016.05.028.

Hutchinson, G. (1957). Concluding remarks. in *Cold Sprig Harbor Symposia on Quantitative Biology: Yale University New Haven*, 66–77.

Ikuta, T., Igawa, K., Tame, A., Kuroiwa, T., Kuroiwa, H., Aoki, Y., et al. (2016). Surfing the vegetal pole in a small population: extracellular vertical transmission of an 'intracellular' deep-sea clam symbiont. *R. Soc. Open Sci.* 3, 160130. doi:10.1098/rsos.160130.

Imachi, H., Tasumi, E., Takaki, Y., Hoshino, T., Schubotz, F., Gan, S., et al. (2019). Cultivable microbial community in 2-km-deep, 20-million-year-old subseafloor coalbeds through ~1000 days anaerobic bioreactor cultivation. *Sci. Rep.* 9, 1–16. doi:10.1038/s41598-019-38754-w.

Inagaki, F., Takai, K., Nealson, K. H., and Horikoshi, K. (2004). Sulfurovum lithotrophicum gen. nov., sp. nov., a novel sulfur-oxidizing chemolithoautotroph within the E-Proteobacteria isolated from Okinawa Trough hydrothermal sediments. *Int. J. Syst. Evol. Microbiol.* 54, 1477–1482. doi:10.1099/ijs.0.03042-0.

Ishibashi, J., Noguchi, T., Toki, T., Miyabe, S., Takahashi, Y., Konno, U., et al. (2014). Diversity of fluid geochemistry affected by processes during fluid upwelling in active hydrothermal fields in the Izena Hole, the middle Okinawa Trough back-arc basin. *Geochem. J.* 48, 357–369. doi:10.2343/geochemj.2.0311.

Jackson, A. L., Inger, R., Parnell, A. C., and Bearhop, S. (2011). Comparing isotopic niche widths among and within communities: SIBER - Stable Isotope Bayesian Ellipses in R. *J. Anim. Ecol.* 80, 595–602. doi:10.1111/j.1365-2656.2011.01806.x.

Jacob, F. (1977). Evolution and Tinkering. *Science (80-. ).* 196, 1161–1166.

Jan, C., Petersen, J. M., Werner, J., Teeling, H., Huang, S., Glöckner, F. O., et al. (2014). The gill chamber epibiosis of deep-sea shrimp Rimicaris exoculata: An in-depth metagenomic investigation and discovery of Zetaproteobacteria. *Environ. Microbiol.* 16, 2723–2738. doi:10.1111/1462-2920.12406.

Jaspers, E., and Overmann, J. (2014). Ecological Significance of Microdiversity: Identical 16S rRNA Gene Sequences Can Be Found in Bacteria with Highly Divergent Genomes and Ecophysiologies. *Appl. Environ. Microbiol.* 70, 62. doi:10.1128/AEM.70.8.4831.

Jinks, R. N., Battelle, B. A., Herzog, E. D., Kass, L., Renninger, G. H., and Chamberlain, S. C. (1998). Sensory adaptations in hydrothermal vent shrimps from the Mid-Atlantic Ridge. *Cah. Biol. Mar.* 39, 309–312.

Jiravanichpaisal, P., Lee, S. Y., Kim, Y. A., Andrén, T., and Söderhäll, I. (2007). Antibacterial peptides in hemocytes and hematopoietic tissue from freshwater crayfish Pacifastacus leniusculus: Characterization and expression pattern. *Dev. Comp. Immunol.* 31, 441–455. doi:10.1016/j.dci.2006.08.002.

Johnson, H. P., Hutnak, M., Dziak, R. P., Fox, C. G., Urcuyo, I., Cowen, J. P., et al. (2000). Earthquake-

induced changes in a hydrothermal system on the Juan de Fuca mid-ocean ridge. *Nature* 407, 174–177. doi:10.1038/35025040.

Johnson, S. B., Warén, A., Tunnicliffe, V., Van Dover, C., Wheat, C. G., Schultz, T. F., et al. (2015). Molecular taxonomy and naming of five cryptic species of Alviniconcha snails (Gastropoda: Abyssochrysoidea) from hydrothermal vents. *Syst. Biodivers.* 13, 278–295. doi:10.1080/14772000.2014.970673.

Johnson, S. B., Young, C. R., Jones, W. J., Warén, A., and Vrijenhoek, R. C. (2006a). Migration, isolation, and speciation of hydrothermal vent limpets (Gastropoda; Lepetodrilidae) across the Blanco Transform Fault. *Biol. Bull.* 210, 140–157. doi:10.2307/4134603.

Johnson, W. S., Stevens, M., and Watling, L. (2001). Reproduction and development of marine peracaridans. *Adv. Mar. Biol.* 39, 105–260. doi:10.1016/s0065-2881(01)39009-0.

Johnson, Z. I., Zinser, E. R., Coe, A., McNulty, N. P., Woodward, E. M. S., and Chisholm, S. W. (2006b). Niche partitioning among Prochlorococcus ecotypes along ocean-scale environmental gradients. *Science (80-. ).* 311, 1737–1740. doi:10.1126/science.1118052.

Jollivet, D., Empis, A., Baker, M. C., Hourdez, S., Comtet, T., Desbruyeres, D., et al. (2000). Reproductive biology , sexual dimorphism , and population structure of the deep sea hydrothermal vent scale-worm , Branchipolynoe seepensis ( Polychaeta : Polynoidae ). *J. Exp. Mar. Bio. Ecol.* 80, 55–68.

Jones, S. E., and Lennon, J. T. (2010). Dormancy contributes to the maintenance of microbial diversity. *Proc. Natl. Acad. Sci. U. S. A.* 107, 5881–5886. doi:10.1073/pnas.0912765107.

Kádár, E., Bettencourt, R., Costa, V., Santos, R. S., Lobo-da-Cunha, A., and Dando, P. (2005). Experimentally induced endosymbiont loss and re-acquirement in the hydrothermal vent bivalve Bathymodiolus azoricus. *J. Exp. Mar. Bio. Ecol.* 318, 99–110. doi:10.1016/j.jembe.2004.12.025.

Kádár, E., Davis, S. A., and Lobo-Da-Cunha, A. (2008). Cytoenzymatic investigation of intracellular digestion in the symbiont-bearing hydrothermal bivalve Bathymodiolus azoricus. *Mar. Biol.* 153, 995–1004. doi:10.1007/s00227-007-0872-0.

Kalinka, A. T., and Tomancak, P. (2012). The evolution of early animal embryos: Conservation or divergence? *Trends Ecol. Evol.* 27, 385–393. doi:10.1016/j.tree.2012.03.007.

Katoh, K., Misawa, K., Kuma, K., and Miyata, T. (2002). MAFFT: a novel method for rapid multiple sequence alignment based on fast Fourier transform. *Nucleic Acids Res.* 30, 3059–3066. doi:10.1093/nar/gkf436.

Katz, S., Klepal, W., and Bright, M. (2011). The Osedax Trophosome : Organization and Ultrastructure. *Biol. Bull.* 220, 128–139.

Kelly, N. E., and Metaxas, A. (2008). Population structure of two deep-sea hydrothermal vent gastropods from the Juan de Fuca Ridge, NE Pacific. *Mar. Biol.* 153, 457–471. doi:10.1007/s00227-007-0828-4.

Kelly, N., and Metaxas, A. (2010). Understanding population dynamics of a numerically dominant species at hydrothermal vents: A matrix modeling approach. *Mar. Ecol. Prog. Ser.* 403, 113–128. doi:10.3354/meps08442.

Kersten, O., Smith, C. R., and Vetter, E. W. (2017). Abyssal near-bottom dispersal stages of benthic invertebrates in the Clarion-Clipperton polymetallic nodule province. *Deep. Res. Part I Oceanogr. Res. Pap.* 127, 31–40. doi:10.1016/j.dsr.2017.07.001.

Khripounoff, A., Comtet, T., Vangriesheim, A., and Crassous, P. (2000). Near-bottom biological and mineral particle flux in the Lucky Strike hydrothermal vent area (Mid-Atlantic Ridge). *J. Mar. Syst.* 25, 101–118.

Kim, B., Kim, M., Kim, A. R., Yi, M., Choi, J. H., Park, H., et al. (2013). Differences in gene organization between type I and type II crustins in the morotoge shrimp, Pandalopsis japonica. *Fish Shellfish Immunol.* 35, 1176–1184. doi:10.1016/j.fsi.2013.07.031.

Kim, S. L., and Mullineaux, L. S. (1998). Distribution and near-bottom transport of larvae and other plankton at hydrothermal vents. *Deep. Res. Part II Top. Stud. Oceanogr.* doi:10.1016/S0967-0645(97)00042-8.

Kimura, M., Uyeda, S., Kato, Y., Tanaka, T., Yamano, M., Gamo, T., et al. (1988). Active hydrothermal mounds in the Okinawa Trough backarc basin, Japan. *Tectonophysics* 145, 319–324. doi:10.1016/0040-1951(88)90203-X.

Klevenz, V., Bach, W., Schmidt, K., Hentscher, M., Koschinsky, A., and Petersen, S. (2012). Geochemistry of vent fluid particles formed during initial hydrothermal fluid-seawater mixing along the Mid-Atlantic Ridge. *Geochemistry, Geophys. Geosystems* 12, 1–23. doi:10.1029/2011GC003704.

Klose, J., Polz, M. F., Wagner, M., Schimak, M. P., Gollner, S., and Bright, M. (2015). Endosymbionts escape dead hydrothermal vent tubeworms to enrich the free-living population. *Proc Natl Acad Sci U S A* 112, 1–6. doi:10.1073/pnas.1501160112.

Knowlton, N., and Weigt, L. A. (1998). New dates and new rates for divergence across the Isthmus of Panama. *Proc. R. Soc. B Biol. Sci.* 265, 2257–2263. doi:10.1098/rspb.1998.0568.

Komai, T., Giere, O., and Segonzac, M. (2007). New Record of Alvinocaridid Shrimps (Crustacea: Decapoda: Caridea) from Hydrothermal Vent Fields on the Southern Mid-Atlantic Ridge, including a New Species of the Genus Opaepele. *Species Divers.* 12, 237–253.

Komai, T., and Giguère, T. (2019). A new species of alvinocaridid shrimp Rimicaris Williams & Rona, 1986 (Decapoda: Caridea) from hydrothermal vents on the Mariana Back Arc Spreading Center, northwestern Pacific. *J. Crustac. Biol.*, 1–11. doi:10.1093/jcbiol/ruz046.

Komai, T., and Segonzac, M. (2003). Review of the hydrothermal vent shrimp genus Mirocaris, redescription of M. fortunata and reassessment of the taxonomic status of the family Alvinocarididae (Crustacea : Decapoda : Caridea). *Cah. Biol. Mar.* 44, 199–215.

Komai, T., and Segonzac, M. (2008). Taxonomic Review of the Hydrothermal Vent Shrimp Genera Rimicaris Williams & Rona and Chorocaris Martin & Hessler (Crustacea: Decapoda: Caridea: Alvinocarididae). *J. Shellfish Res.* 27, 21–41. doi:10.2983/0730-8000(2008)27[21:TROTHV]2.0.CO;2.

Komai, T., and Tsuchida, S. (2015). New records of Alvinocarididae (Crustacea: Decapoda: Caridea) from the southwestern Pacific hydrothermal vents, with descriptions of one new genus and three new species. *J. Nat. Hist.*, 1–36. doi:10.1080/00222933.2015.1006702.

Kong, L., Ryan, W. B. F., Mayer, L., Detrick, R., Fox, P. J., and Manchester, K. (1985). Bare-rock drill sites, ODP Legs 106 and 109: Evidence for hydrothermal activity at 23°N in the Mid-Atlantic Ridge. *Eos, Trans. Am. Geophys. Union* 66, 936. doi:10.1130/0091-7613(1986)14<1004:dtsphs>2.0.co;2.

Kormas, K. A., Tivey, M. K., Von Damm, K., and Teske, A. (2006). Bacterial and archaeal phylotypes associated with distinct mineralogical layers of a white smoker spire from a deep-sea hydrothermal vent site (9°N, East Pacific Rise). *Environ. Microbiol.* 8, 909–920.

doi:10.1111/j.1462-2920.2005.00978.x.

Koschinsky, A., Garbe-Schönberg, D., Sander, S., Schmidt, K., Gennerich, H. H., and Strauss, H. (2008). Hydrothermal venting at pressure-temperature conditions above the critical point of seawater, 5°S on the Mid-Atlantic Ridge. *Geology* 36, 615–618. doi:10.1130/G24726A.1.

Koski, R. A., Jonasson, I. R., Kadko, D. C., Smith, V. K., and Wong, F. L. (1994). Compositions, growth mechanisms, and temporal relations of hydrothermal sulfide-sulfate-silica chimneys at the northern Cleft segment, Juan de Fuca Ridge. *J. Geophys. Res.* 99, 4813–4832.

Kremer, N., Schwartzman, J., Augustin, R., Zhou, L., Ruby, E. G., and Mcfall-ngai, M. J. (2014). The dual nature of haemocyanin in the establishment and persistence of the squid − vibrio symbiosis The dual nature of haemocyanin in the establishment and persistence of the squid – vibrio symbiosis. *Proc. R. Soc. Biol. Sci.* 281. doi:10.5061/dryad.cq032.

Krylova, E. M., and Sahling, H. (2010). Vesicomyidae (Bivalvia): Current taxonomy and distribution. *PLoS One* 5. doi:10.1371/journal.pone.0009957.

Kumagai, H., Nakamura, K., Toki, T., Morishita, T., Okino, K., Ishibashi, J. I., et al. (2008). Geological background of the Kairei and Edmond hydrothermal fields along the Central Indian Ridge: Implications of their vent fluids'distinct chemistry. *Geofluids* 8, 239–251. doi:10.1111/j.1468-8123.2008.00223.x.

Kumar, S., Stecher, G., Li, M., Knyaz, C., and Tamura, K. (2018). MEGA X : Molecular Evolutionary Genetics Analysis across Computing Platforms. *Mol. Biol. Evol.* 35, 1547–1549. doi:10.1093/molbev/msy096.

Kuwahara, H., Yoshida, T., Takaki, Y., Shimamura, S., Nishi, S., Harada, M., et al. (2007). Reduced Genome of the Thioautotrophic Intracellular Symbiont in a Deep-Sea Clam, Calyptogena okutanii. *Curr. Biol.* 17, 881–886. doi:10.1016/j.cub.2007.04.039.

Kvennefors, E. C. E., Leggat, W., Hoegh-guldberg, O., Degnan, B. M., and Barnes, A. C. (2008). An ancient and variable mannose-binding lectin from the coral Acropora millepora binds both pathogens and symbionts. *Dev. Comp. Immunol.* 32, 1582–1592. doi:10.1016/j.dci.2008.05.010.

L'Haridon, S., Reysenbach, A. L., Banta, A., Messner, P., Schumann, P., Stackebrandt, E., et al. (2003). Methanocaldococcus indicus sp. nov., a novel hyperthermophilic methanogen isolated from the Central Indian Ridge. *Int. J. Syst. Evol. Microbiol.* 53, 1931–1935. doi:10.1099/ijs.0.02700-0.

Laes-Huon, A., Legrand, J., Tanguy, V., Cathalot, C., Blandin, J., and Rolin, J. (2014). Long term in situ monitoring of total dissolved iron concentrations on the MoMAR observatory. *IEEE Sens. Syst. a Chang. Ocean* 17, 5270. doi:10.1109/SSCO.2014.7000366.

Lalou, C., Brichet, E., and Hekinian, R. (1985). Age dating of sulfide deposits from axial and off-axial structures on the East Pacific Rise near 12°50'N. *Earth Planet. Sci. Lett.* 75, 59–71. doi:10.1016/0012-821X(85)90050-0.

Laming, S. R., Gaudron, S. M., and Duperron, S. (2018). Lifecycle Ecology of Deep-Sea Chemosymbiotic Mussels : A Review. *Front. Mar. Sci.* 5. doi:10.3389/fmars.2018.00282.

Lanzén, A., Jørgensen, S. L., Bengtsson, M. M., Jonassen, I., Øvreås, L., and Urich, T. (2011). Exploring the composition and diversity of microbial communities at the Jan Mayen hydrothermal vent field using RNA and DNA. *FEMS Microbiol. Ecol.* 77, 577–589. doi:10.1111/j.1574-6941.2011.01138.x.

Layman, C. A., and Allgeier, J. E. (2012). Characterizing trophic ecology of generalist consumers : a case study of the invasive lionfish in The Bahamas. *Mar. Ecol. Prog. Ser.* 448, 131–141.

doi:10.3354/meps09511.

Le Bloa, S. (2016). Mode de reconnaissance hôte symbionte en milieux extrêmes : cas du modèle symbiotique Rimicaris exoculata.

Le Bloa, S., Durand, L., Cueff-Gauchard, V., Le Bars, J., Taupin, L., Marteau, C., et al. (2017). Highlighting of quorum sensing lux genes and their expression in the hydrothermal vent shrimp Rimicaris exoculata ectosymbiontic community. Possible use as biogeographic markers. *PLoS One* 12, 1–19. doi:10.1371/journal.pone.0174338.

Le Bris, N., and Gaill, F. (2007). How does the annelid Alvinella pompejana deal with an extreme hydrothermal environment? *Life Extrem. Environ.*, 315–339. doi:10.1007/978-1-4020-6285-8-20.

Le Bris, N., Govenar, B., Le Gall, C., and Fisher, C. R. (2006a). Variability of physico-chemical conditions in 9°50'N EPR diffuse flow vent habitats. *Mar. Chem.* 98, 167–182. doi:10.1016/j.marchem.2005.08.008.

Le Bris, N., Rodier, P., Sarradin, P. M., and Le Gall, C. (2006b). Is temperature a good proxy for sulfide in hydrothermal vent habitats? *Cah. Biol. Mar.* 47, 465–470.

Le Bris, N., Sarradin, P., and Caprais, J. (2003). Contrasted sulphide chemistries in the environment of 13 N EPR vent fauna. *Deep Sea Res. Part I Oceanogr. Res. Pap.* 50, 737–747. doi:10.1016/S0967-0637(03)00051-7.

Le Bris, N., Yücel, M., Das, A., Sievert, S. M., LokaBharathi, P., and Girguis, P. R. (2019). Hydrothermal Energy Transfer and Organic Carbon Production at the Deep Seafloor. *Front. Mar. Sci.* 5, 1–24. doi:10.3389/fmars.2018.00531.

Le Bris, N., Zbinden, M., and Gaill, F. (2005). Processes controlling the physico-chemical micro-environments associated with Pompeii worms. *Deep. Res. Part I Oceanogr. Res. Pap.* 52, 1071–1083. doi:10.1016/j.dsr.2005.01.003.

Le Pennec, M., and Beninger, P. G. (2000). Reproductive characteristics and strategies of reducing-system bivalves. *Comp. Biochem. Physiol. - A Mol. Integr. Physiol.* 126, 1–16. doi:10.1016/S0742-8413(00)00100-6.

Lecchini, D., Dixson, D. L., Lecellier, G., Roux, N., Frédérich, B., Besson, M., et al. (2017). Habitat selection by marine larvae in changing chemical environments. *Mar. Pollut. Bull.* 114, 210–217. doi:10.1016/j.marpolbul.2016.08.083.

Lecchini, D., Mills, S. C., Brié, C., Maurin, R., and Banaigs, B. (2010). Ecological determinants and sensory mechanisms in habitat selection of crustacean postlarvae. *Behav. Ecol.* 21, 599–607. doi:10.1093/beheco/arq029.

Lecchini, D., and Nakamura, Y. (2013). Use of chemical cues by coral reef animal larvae for habitat selection. *Aquat. Biol.* 19, 231–238. doi:10.3354/ab00532.

Lee, O. O., Wang, Y., Tian, R., Zhang, W., Shek, C. S., Bougouffa, S., et al. (2014). In situ environment rather than substrate type dictates microbial community structure of biofilms in a cold seep system. *Sci. Rep.* 4, 1–10. doi:10.1038/srep03587.

Lee, R. W., and Childress, J. J. (1994). Assimilation of Inorganic Nitrogen by Marine Invertebrates and Their Chemoautotrophic and Methanotrophic Symbionts. *Appl. Environ. Microbiol.* 60, 1852–1858.

Lee, R. W., Robert, K., Matabos, M., Bates, A. E., and Juniper, S. K. (2015). Temporal and spatial variation in temperature experienced by macrofauna at Main Endeavour hydrothermal vent

field. *Deep. Res. Part I Oceanogr. Res. Pap.* 106, 154–166. doi:10.1016/j.dsr.2015.10.004.

Leigh, J. W., and Bryant, D. (2015). POPART : full-feature software for haplotype network construction. *Methods Ecol. Evol.* 6, 1110–1116. doi:10.1111/2041-210X.12410.

Levin, L. A., Mendoza, G. F., Konotchick, T., and Lee, R. (2009). Macrobenthos community structure and trophic relationships within active and inactive Pacific hydrothermal sediments. *Deep. Res. Part II Top. Stud. Oceanogr.* 56, 1632–1648. doi:10.1016/j.dsr2.2009.05.010.

Levin, L. A., and Sibuet, M. (2012). Understanding Continental Margin Biodiversity : A New Imperative. *Ann. Rev. Mar. Sci.* 4, 79–112. doi:10.1146/annurev-marine-120709-142714.

Li, M., Jain, S., and Dick, G. J. (2016). Genomic and transcriptomic resolution of organic matter utilization among deep-sea bacteria in guaymas basin hydrothermal plumes. *Front. Microbiol.* 7, 1–13. doi:10.3389/fmicb.2016.01125.

Li, M., Toner, B. M., Baker, B. J., Breier, J. A., Sheik, C. S., and Dick, G. J. (2014). Microbial iron uptake as a mechanism for dispersing iron from deep-sea hydrothermal vents. *Nat. Commun.* 5, 1–8. doi:10.1038/ncomms4192.

Li, Y., Liles, M. R., and Halanych, K. M. (2018). Endosymbiont genomes yield clues of tubeworm success. *ISME J.* 12, 2785–2795. doi:10.1038/s41396-018-0220-z.

Liebeke, M., and Puskás, E. (2019). Drying enhances signal intensities for global gc–ms metabolomics. *Metabolites* 9, 1–8. doi:10.3390/metabo9040068.

Lilley, M. D., Butterfield, D. A., Olson, E. J., Lupton, J. E., Macko, S. A., and McDuff, R. E. (1993). Anomalous CH4 and NH4+ concentrations at an unsedimented mid-ocean-ridge hydrothermal system. *Nature* 364, 45–47.

Lilley, M. O., Butterfield, D. A., Lupton, J. E., and Olson, E. J. (2003). Magmatic events can produce rapid changes in hydrothermal vent chemistry. *Nature* 422, 878–881. doi:10.1038/nature01569.

Lin, T. J., Ver Eecke, H. C., Breves, E. A., Dyar, M. D., Jamieson, J. W., Hannington, M. D., et al. (2016). Linkages between mineralogy, fluid chemistry, and microbial communities within hydrothermal chimneys from the Endeavour Segment, Juan de Fuca Ridge. *Geochemistry Geophys. Geosystems* 18, 1541–1576. doi:10.1002/2014GC005684.Key.

Lisin, S. E., Hannan, E. E., Kochevar, R. E., Harrold, C., and Barry, J. P. (1997). Temporal variation in gametogenic cycles of vesicomyid clams. *Invertebr. Reprod. Dev.* 31, 307–318. doi:10.1080/07924259.1997.9672590.

Liu, X., Ye, S., Cheng, C., Li, H., Lu, B., Yang, W.-J., et al. (2019). Identification and characterization of a symbiotic agglutination-related C-type lectin from the hydrothermal vent shrimp Rimicaris exoculata. *Fish Shellfish Immunol.* 92, 1–10. doi:10.1016/j.fsi.2019.05.057.

Livak, K. J., and Schmittgen, T. D. (2001). Analysis of relative gene expression data using real-time quantitative PCR and the 2-ΔΔCT method. *Methods* 25, 402–408. doi:10.1006/meth.2001.1262.

Lonsdale, P. (1977). Clustering of suspension-feeding macrobenthos near abyssal hydrothermal vents at oceanic spreading centers. *Deep. Res.* 24. doi:10.1016/0146-6291(77)90478-7.

López-García, P., Duperron, S., Philippot, P., Foriel, J., Susini, J., and Moreira, D. (2003). Bacterial diversity in hydrothermal sediment and epsilonproteobacterial dominance in experimental microcolonizers at the Mid-Atlantic Ridge. *Environ. Microbiol.* 5, 961–976. doi:10.1046/j.1462-2920.2003.00495.x.

Lowell, R. P., Houghton, J. L., Farough, A., Craft, K. L., Larson, B. I., and Meile, C. D. (2015).

Mathematical modeling of diffuse flow in seafloor hydrothermal systems: The potential extent of the subsurface biosphere at mid-ocean ridges. *Earth Planet. Sci. Lett.* 425, 145–153. doi:10.1016/j.epsl.2015.05.047.

Lunina, A. A., and Vereshchaka, A. L. (2014). Distribution of hydrothermal alvinocaridid shrimps: Effect of geomorphology and specialization to extreme biotopes. *PLoS One* 9. doi:10.1371/journal.pone.0092802.

Luther, G. W., Rozan, T. F., Taillefert, M., Nuzzio, D. B., Di Meo, C., Shank, T. M., et al. (2001). Chemical speciation drives hydrothermal vent ecology. *Nature* 410, 813–816.

Lutz, R. A., Shank, T. M., Fornari, D. J., Haymon, R. M., Lilley, M. D., Von Damm, K. L., et al. (1994). Rapid growth at deep-sea vents. *Nature* 371, 663–664.

Macdonald, K. C. (1982). Mid-Ocean Ridge: Fine Scale Tectonic, Volcanic and Hydrothermal Processes Within the Plate Boundary Zone. *Annu. Rev. Earth Planet. Sci.* 10, 155–189.

Macdonald, P. D. M., and Pitcher, T. J. (1979). Age-Groups from Size-Frequency Data: A Versatile and Efficient Method of Analyzing Distribution Mixtures. *J. Fish. Res. Board Canada* 36, 987–1001. doi:10.1139/f79-137.

Macdonald, P., and Du, J. (2012). Mixdist: finite mixture distribution models. *R Packag. version 0.5-4, URL http//CRAN. R-project. org/package= Mix.*

Machon, J., Krieger, J., Meth, R., Zbinden, M., Ravaux, J., Montagné, N., et al. (2019). Neuroanatomy of a hydrothermal vent shrimp provides insights into the evolution of crustacean integrative brain centers. *Elife* 8, 1–37. doi:10.7554/elife.47550.

Machon, J., Lucas, P., Ravaux, J., and Zbinden, M. (2018). Comparison of chemoreceptive abilities of the hydrothermal shrimp Mirocaris fortunata and the coastal shrimp Palaemon elegans. *Chem. Senses* 43, 489–501. doi:10.1093/chemse/bjy041.

Machon, J., Ravaux, J., Zbinden, M., and Lucas, P. (2016). New electroantennography method on a marine shrimp in water. *J. Exp. Biol.* doi:10.1242/jeb.140947.

Macpherson, E., Jones, W., and Segonzac, M. (2005). A new squat lobster family of Galatheoidea (Crustacea, Decapoda, Anomura) from the hydrothermal vents of the Pacific-Antarctic Ridge. *Zoosystema* 27, 709–723.

Maitland, D. P., Jackson, R. L., Ladle, R. J., and Ward, P. (2002). Field considerations and problems associated with radio tracking a tropical fresh water land crab. *J. Crustac. Biol.* 22, 493–496.

Margulis, L. (1971). Symbiosis and Evolution. *Sci. Am.* 225, 48–61. Available at: http://www.jstor.org/stable/24922800.

Markert, S., Arndt, C., Felbeck, H., Becher, D., Sievert, S. M., Hügler, M., et al. (2007). Physiological Proteomics of the Uncultured Endosymbiont of Riftia pachyptila. *Science (80-. ).* 315, 247–250. doi:10.1126/science.1132913.

Maróti, G., Kereszt, A., Kondorosi, É., and Mergaert, P. (2011). Natural roles of antimicrobial peptides in microbes, plants and animals. *Res. Microbiol.* 162, 363–374. doi:10.1016/j.resmic.2011.02.005.

Marsh, A. G., Mullineaux, L. S., Young, C. M., and Manahan, D. T. (2001). Larval dispersal potential of the tubeworm Riftia pachyptila at deep-sea hydrothermal vents. *Nature* 411, 77–80. doi:10.1038/35075063.

Marsh, L., Copley, J. T., Huvenne, V. A. I., Linse, K., Reid, W. D. K., Rogers, A. D., et al. (2012).

Microdistribution of Faunal Assemblages at Deep-Sea Hydrothermal Vents in the Southern Ocean. *PLoS One* 7. doi:10.1371/journal.pone.0048348.

Marsh, L., Copley, J. T., Tyler, P. A., and Thatje, S. (2015). In hot and cold water: Differential life-history traits are key to success in contrasting thermal deep-sea environments. *J. Anim. Ecol.* 84, 898–913. doi:10.1111/1365-2656.12337.

Martin, J. W., Signorovitch, J., and Patel, H. (1997). A new species of Rimicaris (Crustacea: Decapoda: Bresiliidae) from the Snake Pit hydrothermal vent field on the Mid-Atlantic Ridge. *Proc. Biol. Soc. Washingt.* 110, 399–411.

Martin, J. W., Wall, A. R., Shank, T. I. M., Cha, H., Seid, C. A., and Rouse, G. W. (2018). A new species of Alvinocaris (Crustacea: Decapoda: Caridea: Alvinocarididae) from Costa Rican methane seeps. *Zootaxa* 4504, 418–430.

Maruyama, T., Watsuji, T., Takahashi, T., Kayama Watanabe, H., Nagai, Y., Fujiwara, Y., et al. (2018). In situ vital staining for chasing the galatheid crab Shinkaia crosnieri on deep-sea floor. *JAMSTEC Rep. Res. Dev.* 27, 87–97. doi:10.5918/jamstecr.27.87.

Masson, F., Zaidman-Rémy, A., and Heddi, A. (2016). Antimicrobial peptides and cell processes tracking endosymbiont dynamics. *Philos. Trans. R. Soc. B Biol. Sci.* 371. doi:10.1098/rstb.2015.0298.

Matabos, M., Cuvelier, D., Brouard, J., Shillito, B., Ravaux, J., Zbinden, M., et al. (2015). Behavioural study of two hydrothermal crustacean decapods: Mirocaris fortunata and Segonzacia mesatlantica, from the Lucky Strike vent field (Mid-Atlantic Ridge). *Deep. Res. Part II Top. Stud. Oceanogr.* 121, 146–158. doi:10.1016/j.dsr2.2015.04.008.

Matabos, M., and Thiebaut, E. (2010). Reproductive biology of three hydrothermal vent peltospirid gastropods (Nodopelta heminoda, N. subnoda and Peltospira operculata) associated with Pompeii worms on the East Pacific Rise. *J. Molluscan Stud. Stud.* 76, 257–266. doi:10.1093/mollus/eyq008.

McCutchan, J. H., Lewis, W. M., Kendall, C., and McGrath, C. C. (2003). Variation in trophic shift for stable isotope ratios of carbon, nitrogen, and sulfur. *Oikos* 102, 378–390. doi:10.1034/j.1600-0706.2003.12098.x.

Mcdermott, J. M., Seewald, J. S., German, C. R., and Sylva, S. P. (2015). Pathways for abiotic organic synthesis at submarine hydrothermal fields. *Proc. Natl. Acad. Sci.*, 2–6. doi:10.1073/pnas.1506295112.

McDermott, J. M., Sylva, S. P., Ono, S., German, C. R., and Seewald, J. S. (2018). Geochemistry of fluids from Earth's deepest ridge-crest hot-springs: Piccard hydrothermal field, Mid-Cayman Rise. *Geochim. Cosmochim. Acta* 228, 95–118. doi:10.1016/j.gca.2018.01.021.

McFall-Ngai, M., Heath-Heckman, E. A. C., Gillette, A. A., Peyer, S. M., and Harvie, E. A. (2012). The secret languages of coevolved symbioses: Insights from the Euprymna scolopes-Vibrio fischeri symbiosis. *Semin. Immunol.* 24, 3–8. doi:10.1016/j.smim.2011.11.006.

McFall-Ngai, M. J. (2008). Are biologists in 'future shock'? Symbiosis integrates biology across domains. *Nat. Rev Microbiol* 6, 789–792.

McGillicuddy Jr., D. J., Lavelle, J. W., Thurnherr, A. M., Kosnyrev, V. K., and Mullineaux, L. S. (2010). Larval dispersion along an axially symmetric mid-ocean ridge. *Deep. Res. Part I* 57, 880–892. doi:10.1016/j.dsr.2010.04.003.

McHugh, D. (1989). Population structure and reproductive biology of two sympatric hydrothermal

vent polychaetes, Paralvinella pandorae and P. palmiformis. *Mar. Biol.* 103, 95–106. doi:10.1007/BF00391068.

Meier, D. V. (2016). Bacterial niche adaptation at hydrothermal vents.

Meier, D. V., Pjevac, P., Bach, W., Hourdez, S., Girguis, P. R., Vidoudez, C., et al. (2017). Niche partitioning of diverse sulfur-oxidizing bacteria at hydrothermal vents. *ISME J.* 11, 1545–1558. doi:10.1038/ismej.2017.37.

Meier, D. V, Bach, W., Girguis, P. R., Gruber-vodicka, H. R., Reeves, E. P., Richter, M., et al. (2016). Heterotrophic Proteobacteria in the vicinity of diffuse hydrothermal venting. 18, 4348–4368. doi:10.1111/1462-2920.13304.

Menge, B. A. (1991). Relative importance of recruitment and other causes of variation in rocky intertidal community structure. *J. Exp. Mar. Bio. Ecol.* 146, 69–100.

Mergaert, P. (2018). Role of antimicrobial peptides in controlling symbiotic bacterial populations. *Nat. Prod. Rep.* 35, 336–356. doi:10.1039/c7np00056a.

Metaxas, A. (2004). Spatial and temporal patterns in larval supply at hydrothermal vents on the northeast Pacific Ocean. *Limnol. Ocean.* 49, 1949–1956.

Metaxas, A., and Saunders, M. (2009). Quantifying the " Bio-" Components in Biophysical Models in Marine Benthic of Larval Transport and Pitfalls Invertebrates : Advances and Pitfalls. *Biol. Bull.* 216, 257–272. doi:10.2307/25548159.

Methou, P., Hernández-Ávila, I., Aube, J., Cueff-Gauchard, V., Gayet, N., Amand, L., et al. (2019a). Is It First the Egg or the Shrimp? – Diversity and Variation in Microbial Communities Colonizing Broods of the Vent Shrimp Rimicaris exoculata During Embryonic Development. *Front. Microbiol.* 10, 1–19. doi:10.3389/fmicb.2019.00808.

Methou, P., Michel, L., Segonzac, M., Pradillon, F., and Cambon-Bonavita, M.-A. (2019b). Trophic shifts and distinct larval life in two Rimicaris shrimps from the Mid Atlantic Ridge unveiled by taxonomic reexamination of their juveniles stages.

Meyer, J. L., Akerman, N. H., Proskurowski, G., and Huber, J. A. (2013a). Microbiological characterization of post-eruption "snowblower" vents at axial seamount, juan de fuca ridge. *Front. Microbiol.* 4, 1–13. doi:10.3389/fmicb.2013.00153.

Meyer, S., Wegener, G., Lloyd, K. G., Teske, A., Boetius, A., and Ramette, A. (2013b). Microbial habitat connectivity across spatial scales and hydrothermal temperature gradients at Guaymas Basin. *Front. Microbiol.* 4, 1–11. doi:10.3389/fmicb.2013.00207.

Mills, S. W., Beaulieu, S. E., and Mullineaux, L. S. (2009). Photographic identification guide to larvae at hydrothermal vents.

Minagawa, M., and Wada, E. (1984). Stepwise enrichment of 15N along food chains : Further evidence and the relation between 615N and animal age. *Geochim. Cosmochim. Acta* 48, 1135–1140.

Mindell, D. P. (1992). Phylogenetic consequences of symbioses: Eukarya and Eubacteria are not monophyletic taxa. *BioSystems* 27, 53–62. doi:10.1016/0303-2647(92)90046-2.

Mino, S., Nakagawa, S., Makita, H., Toki, T., Miyazaki, J., Sievert, S. M., et al. (2017). Endemicity of the cosmopolitan mesophilic chemolithoautotroph Sulfurimonas at deep-sea hydrothermal vents. *ISME J.* 11, 909–919. doi:10.1038/ismej.2016.178.

Mitarai, S., Watanabe, H., Nakajima, Y., Shchepetkin, A. F., and McWilliams, J. C. (2016). Quantifying

dispersal from hydrothermal vent fields in the western Pacific Ocean. *Proc. Natl. Acad. Sci. U. S. A.* 113, 2976–2981. doi:10.1073/pnas.1518395113.

Mittelstaedt, E., Escartín, J., Gracias, N., Olive, J. A., Barreyre, T., Davaille, A., et al. (2012). Quantifying diffuse and discrete venting at the Tour Eiffel vent site, Lucky Strike hydrothermal field. *Geochemistry, Geophys. Geosystems* 13. doi:10.1029/2011GC003991.

Miyake, H., Kitada, M., Itoh, T., Nemoto, S., Okuyama, Y., Watanabe, H., et al. (2010). Larvae of deep-sea chemosynthetic ecosystem animals in captivity. *Cah. Biol. Mar.* 51, 441–450.

Miyake, H., Kitada, M., Tsuchida, S., Okuyama, Y., and Nakamura, K. I. (2007). Ecological aspects of hydrothermal vent animals in captivity at atmospheric pressure. *Mar. Ecol.* 28, 86–92. doi:10.1111/j.1439-0485.2006.00115.x.

Miyake, H., Tsukahara, J., Hashimoto, J., Uematsu, K., and Maruyama, T. (2006). Rearing and observation methods of vestimentiferan tubeworm and its early development at atmospheric pressure. *Cah. Biol. Mar.* 47, 471–475.

Miyazaki, J., Kawagucci, S., Takahashi, A., Kitada, K., Matsui, Y., Tasumi, E., et al. (2017). Deepest and hottest hydrothermal activity in the Okinawa Trough : the Yokosuka site at Yaeyama Knoll Subject Category : Subject Areas : Author for correspondence : *R. Soc. open sci.* 4.

Moalic, Y., Desbruyères, D., Duarte, C. M., Rozenfeld, A. F., Bachraty, C., and Arnaud-Haond, S. (2012). Biogeography revisited with network theory: Retracing the history of hydrothermal vent communities. *Syst. Biol.* 61, 127–137. doi:10.1093/sysbio/syr088.

Moran, N. A., and Dunbar, H. E. (2006). Sexual acquisition of beneficial symbionts in aphids. *Proc. Natl. Acad. Sci.* 103, 12803–12806. doi:10.1073/pnas.0605772103.

Morgan, J. P., and Chen, Y. J. (1993). Dependence of ridge-axis morphology on magma supply and spreading rate. *Nature* 364, 706–708. doi:10.1038/364706a0.

Mottl, M. J., Seewald, J. S., Wheat, C. G., Tivey, M. K., Michael, P. J., Proskurowski, G., et al. (2011). Chemistry of hot springs along the Eastern Lau Spreading Center. *Geochim. Cosmochim. Acta* 75, 1013–1038. doi:10.1016/j.gca.2010.12.008.

Mullineaux, L. S., Adams, D. K., Mills, S. W., and Beaulieu, S. E. (2010). Larvae from afar colonize deep-sea hydrothermal vents after a catastrophic eruption. *Proc. Natl. Acad. Sci. U. S. A.* 107, 7829–7834. doi:10.1073/pnas.0913187107.

Mullineaux, L. S., Fisher, C. R., Peterson, C. H., and Schaeffer, S. W. (2000). Tubeworm succession at hydrothermal vents: Use of biogenic cues to reduce habitat selection error? *Oecologia* 123, 275–284. doi:10.1007/s004420051014.

Mullineaux, L. S., Mills, S. W., and Goldman, E. (1998). Recruitment variation during a pilot colonization study of hydrothermal vents ( 9 ° 50 N , East Pacific Rise ). *Deep. Res. Part II* 45, 441–464.

Mullineaux, L. S., Mills, S. W., Sweetman, A. K., Beaudreau, A. H., Metaxas, A., and Hunt, H. L. (2005). Vertical, lateral and temporal structure in larval distributions at hydrothermal vents. *Mar. Ecol. Prog. Ser.* 293, 1–16. doi:10.3354/meps293001.

Naganuma, T., Otsuki, A., and Seki, H. (1989). Abundance and growth rate of bacterioplankton community in hydrothermal vent plumes of the North Fiji Basin. *Deep Sea Res. Part A, Oceanogr. Res. Pap.* 36, 1379–1390. doi:10.1016/0198-0149(89)90089-7.

Nakagawa, S., Shimamura, S., Takaki, Y., Suzuki, Y., Murakami, S. I., Watanabe, T., et al. (2014). Allying with armored snails: The complete genome of gammaproteobacterial endosymbiont.

*ISME J.* 8, 40–51. doi:10.1038/ismej.2013.131.

Nakagawa, S., and Takai, K. (2008). Deep-sea vent chemoautotrophs: Diversity, biochemistry and ecological significance. *FEMS Microbiol. Ecol.* 65, 1–14. doi:10.1111/j.1574-6941.2008.00502.x.

Nakagawa, S., Takaki, Y., Shimamura, S., Reysenbach, A., and Takai, K. (2007). Deep-sea vent epsilonproteobacterial genomes provide insight into emergence of pathogens. *Proc. Natl. Acad. Sci. U. S. A.* 104, 12146–12150.

Nakamura, K., and Takai, K. (2014). Theoretical constraints of physical and chemical properties of hydrothermal fluids on variations in chemolithotrophic microbial communities in seafloor hydrothermal systems. *Prog. Earth Planet. Sci.* 1, 1–24. doi:10.1186/2197-4284-1-5.

Nakamura, K., Watanabe, H., Miyazaki, J., Takai, K., Kawagucci, S., Noguchi, T., et al. (2012). Discovery of new hydrothermal activity and chemosynthetic fauna on the Central Indian ridge at 18°-20°S. *PLoS One* 7, 1–11. doi:10.1371/journal.pone.0032965.

Nalepa, C. A. (2015). Origin of termite eusociality: Trophallaxis integrates the social, nutritional, and microbial environments. *Ecol. Entomol.* 40, 323–335. doi:10.1111/een.12197.

Nedoncelle, K., Lartaud, F., de Rafelis, M., Boulila, S., and Le Bris, N. (2013). A new method for high-resolution bivalve growth rate studies in hydrothermal environments. *Mar. Biol.* 160, 1427–1439. doi:10.1007/s00227-013-2195-7.

Nègre-Sadargues, G., Castillo, R., and Segonzac, M. (2000). Carotenoid pigments and trophic behaviour of deep-sea shrimps (Crustacea, Decapoda, Alvinocarididae) from a hydrothermal area of the Mid-Atlantic Ridge. *Comp. Biochem. Physiol. - A Mol. Integr. Physiol.* 127, 293–300. doi:10.1016/S1095-6433(00)00258-0.

Nelson, K., and Fisher, C. R. (2000). Absence of cospeciation in deep-sea vestimentiferan tube worms and their bacterial endosymbionts. *Symbiosis* 28, 1–15.

Nercessian, O., Bienvenu, N., Moreira, D., Prieur, D., and Jeanthon, C. (2005). Diversity of functional genes of methanogens , methanotrophs and sulfate reducers in deep-sea hydrothermal environments. *Environ. Microbiol.* 7, 118–132. doi:10.1111/j.1462-2920.2004.00672.x.

Newsome, S. D., Martinez del Rio, C., Bearhop, S., and Phillips, D. L. (2008). A niche for isotopic ecology. *J. Physiol. Pharmacol.* 59, 123–134. doi:10.1890/060150.01.

Newton, I. L. G., Woyke, T., Auchtung, T. A., Dilly, G. F., Dutton, R. J., Fisher, M. C., et al. (2007). The Calyptogena magnifica Chemoautotrophic Symbiont Genome. *Science (80-. ).* 315, 998–1000. doi:10.1126/science.1138438.

Nomaki, H., Uejima, Y., Ogawa, N. O., Yamane, M., Watanabe, H. K., Senokuchi, R., et al. (2019). Nutritional sources of meio- and macrofauna at hydrothermal vents and adjacent areas : natural- abundance radiocarbon and stable isotope analyses. *Mar. Ecol. Prog. Ser.* 622, 49–65.

Nunoura, T., Chikaraishi, Y., Izaki, R., Suwa, T., Sato, T., Harada, T., et al. (2018). A primordial and reversible TCA cycle in a facultatively chemolithoautotrophic thermophile. *Science (80-. ).* 563, 559–563.

Nussbaumer, A. D., Fisher, C. R., and Bright, M. (2006). Horizontal endosymbiont transmission in hydrothermal vent tubeworms. *Nature* 441, 345–348. doi:10.1038/nature04793.

Nye, V. (2013). Life-history biology and biogeography of invertebrates in deep-sea chemosynthetic environments.

Nye, V., Copley, J. T. P., and Plouviez, S. (2012). A new species of Rimicaris ( Crustacea : Decapoda :

Caridea : Alvinocarididae ) from hydrothermal vent fields on the Mid-Cayman Spreading Centre , Caribbean. *J. Mar. Biol. Assoc. United Kingdom* 92, 1057–1072. doi:10.1017/S0025315411002001.

Nye, V., Copley, J. T., and Tyler, P. A. (2013). Spatial Variation in the Population Structure and Reproductive Biology of Rimicaris hybisae (Caridea: Alvinocarididae) at Hydrothermal Vents on the Mid-Cayman Spreading Centre. *PLoS One* 8. doi:10.1371/journal.pone.0060319.

O'Brien, C. E., Giovannelli, D., Govenar, B., Luther, G. W., Lutz, R. A., Shank, T. M., et al. (2015). Microbial biofilms associated with fluid chemistry and megafaunal colonization at post-eruptive deep-sea hydrothermal vents. *Deep. Res. Part II Top. Stud. Oceanogr.* 121, 31–40. doi:10.1016/j.dsr2.2015.07.020.

O'Connor, M. I., Bruno, J. F., Gaines, S. D., Halpern, B. S., Lester, S. E., Kinlan, B. P., et al. (2007). Temperature control of larval dispersal and the implications for marine ecology , evolution , and conservation. *Proc. Natl. Acad. Sci. U. S. A.* 104, 1266–1271.

Oh, C. W., and Hartnoll, R. G. (2004). Reproductive biology of the common shrimp Crangon crangon (Decapoda: Crangonidae) in the central Irish Sea. *Mar. Biol.* 144, 303–316. doi:10.1007/s00227-003-1205-6.

Okada, S., Chen, C., Watsuji, T., Nishizawa, M., Suzuki, Y., Sano, Y., et al. (2019). The making of natural iron sulfide nanoparticles in a hot vent snail. *Proc. Natl. Acad. Sci.*, 1–6. doi:10.1073/pnas.1908533116.

Okutani, T., Fujikura, K., and Sasaki, T. (2003). Two New Species of Bathymodiolus (Bivalvia: Mytilidae) from Methane Seeps on the Kuroshima Knoll off the Yaeyama Islands, Southwestern Japan. *Venus* 3, 97–110.

Olins, H. C., Rogers, D. R., Preston, C., Ussler, W., Pargett, D., Jensen, S., et al. (2017). Co-registered geochemistry and metatranscriptomics reveal unexpected distributions of microbial activity within a hydrothermal vent field. *Front. Microbiol.* 8, 1–18. doi:10.3389/fmicb.2017.01042.

Oliver, G., Rodrigues, C. F., and Cunha, M. R. (2011). Chemosymbiotic bivalves from the mud volcanoes of the Gulf of Cadiz , NE Atlantic , with descriptions of new species of Solemyidae , Lucinidae and Vesicomyidae. *Zookeys* 38, 1–38. doi:10.3897/zookeys.113.1402.

Oliver, P. G. (2015). Description and morphology of the "Juan de Fuca vent mussel", Benthomodiolus erebus sp. n. (Bivalvia, Mytilidae, Bathymodiolinae): "Phylogenetically basal but morphologically advanced." *Zoosystematics Evol.* 91, 151–165. doi:10.3897/zse.91.5417.

Op den Camp, H. J. M., Islam, T., Stott, M. B., Harhangi, H. R., Hynes, A., Schouten, S., et al. (2009). Environmental, genomic and taxonomic perspectives on methanotrophic Verrucomicrobia. *Environ. Microbiol. Rep.* 1, 293–306. doi:10.1111/j.1758-2229.2009.00022.x.

Opatkiewicz, A. D., Butterfield, D. A., and Baross, J. A. (2009). Individual hydrothermal vents at Axial Seamount harbor distinct subseafloor microbial communities. *FEMS Microbiol. Ecol.* 70, 413–424. doi:10.1111/j.1574-6941.2009.00747.x.

Orton, J. H. (1920). Sea-Temperature, Breeding and Distribution in Marine Animals. *J. Mar. Biol. Assoc. United Kingdom* 12, 339–366. doi:10.1017/S0025315400000102.

Ozawa, G., Shimamura, S., Takaki, Y., Takishita, K., Ikuta, T., Barry, J. P., et al. (2017). Ancient occasional host switching of maternally transmitted bacterial symbionts of chemosynthetic vesicomyid clams. *Genome Biol. Evol.* 9, 2226–2236. doi:10.1093/gbe/evx166.

Pagé, A., Tivey, M. K., Stakes, D. S., and Reysenbach, A. L. (2008). Temporal and spatial archaeal

colonization of hydrothermal vent deposits. *Environ. Microbiol.* 10, 874–884. doi:10.1111/j.1462-2920.2007.01505.x.

Page, H. M., Fiala-Medioni, A., Fisher, C. R., and Childress, J. J. (1991). Experimental evidence for filter-feeding by the hydrothermal vent mussel, Bathymodiolus thermophilus. *Deep Sea Res. Part A, Oceanogr. Res. Pap.* 38, 1455–1461. doi:10.1016/0198-0149(91)90084-S.

Pedersen, R. B., Rapp, H. T., Thorseth, I. H., Lilley, M. D., Barriga, F. J. a S., Baumberger, T., et al. (2010). Discovery of a black smoker vent field and vent fauna at the Arctic Mid-Ocean Ridge. *Nat. Commun.* 1, 126. doi:10.1038/ncomms1124.

Peek, A. S., Feldman, R. a, Lutz, R. a, and Vrijenhoek, R. C. (1998). Cospeciation of chemoautotrophic bacteria and deep sea clams. *Proc. Natl. Acad. Sci. U. S. A.* 95, 9962–9966. doi:10.1073/pnas.95.17.9962.

Pelli, D. G., and Chamberlain, S. C. (1989). The visibility of 350°C black-body radiation by the shrimp Rimicaris exoculata and man. *Nature* 337, 460–461. doi:10.1038/337460a0.

Perez, M., and Juniper, S. K. (2016). Insights into Symbiont Population Structure among Three Vestimentiferan Tubeworm Host Species at Eastern Pacific Spreading Centers. *Appl. Environ. Microbiol.* 82, 5197–5205. doi:10.1128/aem.00953-16.

Perez, M., and Juniper, S. K. (2018). Is the trophosome of Ridgeia piscesae monoclonal? *Symbiosis* 74, 55–65. doi:10.1007/s13199-017-0490-7.

Perner, M., Bach, W., Hentscher, M., Koschinsky, A., Garbe-schönberg, D., Streit, W. R., et al. (2009). Short-term microbial and physico-chemical variability in low-temperature hydrothermal fluids near 5 ° S on the Mid-Atlantic Ridge. *Environ. Microbiol.* 11, 2526–2541. doi:10.1111/j.1462-2920.2009.01978.x.

Perner, M., Gonnella, G., Hourdez, S., Böhnke, S., Kurtz, S., and Girguis, P. (2013a). In situ chemistry and microbial community compositions in five deep-sea hydrothermal fluid samples from Irina II in the Logatchev field. *Environ. Microbiol.* 15, 1551–1560. doi:10.1111/1462-2920.12038.

Perner, M., Hansen, M., Seifert, R., Strauss, H., Koschinsky, A., and Petersen, S. (2013b). Linking geology, fluid chemistry, and microbial activity of basalt- and ultramafic-hosted deep-sea hydrothermal vent environments. *Geobiology* 11, 340–355. doi:10.1111/gbi.12039.

Perovich, G. M., Epifanio, C. E., Dittel, A. I., and Tyler, P. A. (2003). Spatial and temporal patterns in development of eggs in the vent crab Bythograea thermydron. *Mar. Ecol. Prog. Ser.* 251, 211–220. doi:10.3354/meps251211.

Pester, N. J., Reeves, E. P., Rough, M. E., Ding, K., Seewald, J. S., and Seyfried, W. E. (2012). Subseafloor phase equilibria in high-temperature hydrothermal fluids of the Lucky Strike Seamount (Mid-Atlantic Ridge, 37°17'N). *Geochim. Cosmochim. Acta* 90, 303–322. doi:10.1016/j.gca.2012.05.018.

Petersen, J. M., Ramette, A., Lott, C., Cambon-Bonavita, M. A., Zbinden, M., and Dubilier, N. (2010). Dual symbiosis of the vent shrimp Rimicaris exoculata with filamentous gamma- and epsilonproteobacteria at four mid-atlantic ridge hydrothermal vent fields. *Environ. Microbiol.* 12, 2204–2218. doi:10.1111/j.1462-2920.2009.02129.x.

Petersen, J. M., Zielinski, F. U., Pape, T., Seifert, R., Moraru, C., Amann, R., et al. (2011a). Hydrogen is an energy source for hydrothermal vent symbioses. *Nature* 476, 176–180. doi:10.1038/nature10325.

Petersen, T. N., Brunak, S., Von Heijne, G., and Nielsen, H. (2011b). SignalP 4.0: Discriminating signal

peptides from transmembrane regions. *Nat. Methods* 8, 785–786. doi:10.1038/nmeth.1701.

Pflugfelder, B., Cary, S. C., and Bright, M. (2009). Dynamics of cell proliferation and apoptosis reflect different life strategies in hydrothermal vent and cold seep vestimentiferan tubeworms. *Cell Tissue Res.* 337, 149–165. doi:10.1007/s00441-009-0811-0.

Pineda, J., Hare, J. A., and Sponaugle, S. (2007). Larval transport and dispersal in the coastal ocean and consequences for population connectivity. *Oceanography* 20, 22–39.

Pisuttharachai, D., Fagutao, F. F., Yasuike, M., Aono, H., Yano, Y., Murakami, K., et al. (2009). Characterization of crustin antimicrobial proteins from Japanese spiny lobster Panulirus japonicus. *Dev. Comp. Immunol.* 33, 1049–1054. doi:10.1016/j.dci.2009.05.006.

Pizzochero, A. C., Michel, L. N., Chenery, S. R., McCarthy, I. D., Vianna, M., Malm, O., et al. (2017). Use of multielement stable isotope ratios to investigate ontogenetic movements of Micropogonias furnieri in a tropical Brazilian estuary . *Can. J. Fish. Aquat. Sci.* 373, 1–10. doi:10.1139/cjfas-2017-0148.

Plouviez, S., Jacobson, A., Wu, M., and Van Dover, C. L. (2015). Characterization of vent fauna at the mid-cayman spreading center. *Deep. Res. Part I Oceanogr. Res. Pap.* 97, 124–133. doi:10.1016/j.dsr.2014.11.011.

Plum, C., Pradillon, F., Fujiwara, Y., and Sarrazin, J. (2017). Copepod colonization of organic and inorganic substrata at a deep-sea hydrothermal vent site on the Mid-Atlantic Ridge. *Deep. Res. Part II Top. Stud. Oceanogr.* doi:10.1016/j.dsr2.2016.06.008.

Podowski, E. L., Ma, S., Luther, G. W., Wardrop, D., and Fisher, C. R. (2010). Biotic and abiotic factors affecting distributions of megafauna in diffuse flow on andesite and basalt along the Eastern Lau Spreading Center, Tonga. *Mar. Ecol. Prog. Ser.* 418, 25–45. doi:10.3354/meps08797.

Polz, M. F., and Cavanaugh, C. M. (1995). Dominance of one bacterial phylotype at a Mid-Atlantic Ridge hydrothermal vent site. *Proc. Natl. Acad. Sci. U. S. A.* 92, 7232–7236.

Polz, M. F., Robinson, J. J., Cavanaugh, C. M., Dover, C. L. Van, and Van, C. L. (1998). Trophic ecology of massive shrimp aggregations at a Mid-Atlantic hydrothermal vent site. *Limnol. Oceanogr.* 43, 1631–1638.

Polzin, J., Arevalo, P., Nussbaumer, T., Polz, M. F., and Bright, M. (2019). Polyclonal symbiont populations in hydrothermal vent tubeworms and the environment. *Proc. R. Soc. B* 286. doi:10.1098/rspb.2018.1281.

Pond, D., Dixon, D., and Sargent, J. (1997a). Wax-ester reserves facilitate dispersal of hydrothermal vent shrimps. *Mar. Ecol. Prog. Ser.* 146, 289–290. doi:10.3354/meps146289.

Pond, D. W., Gebruk, A., Southward, E. C., Southward, A. J., Fallick, A. E., Bell, M. V., et al. (2000). Unusual fatty acid composition of storage lipids in the bresilioid shrimp Rimicaris exoculata couples the photic zone with MAR hydrothermal vent sites. *Mar. Ecol. Prog. Ser.* 198, 171–179. doi:10.3354/meps198171.

Pond, D. W., Sargent, J. R., Fallick, A. E., Allen, C., Bell, M. V, and Dixon, D. R. (1999). d13C values of lipids from phototrophic zone microplankton and bathypelagic shrimps at the Azores sector of the Mid-Atlantic Ridge. *Deep. Res.* 47, 121–136.

Pond, D. W., Segonzac, M., Bell, M. V, Dixon, David, R., Fallick, A. E., and Sargent, J. R. (1997b). Lipid and lipid carbon stable isotope composition of the hydrothermal vent shrimp Mirocaris fortunata : evidence for nutritional dependence on photosynthetically fixed carbon. *Mar. Ecol. Prog. Ser.* 157, 221–231.

Ponnudurai, R., Kleiner, M., Sayavedra, L., Petersen, J. M., Moche, M., Otto, A., et al. (2016). Metabolic and physiological interdependencies in the Bathymodiolus azoricus symbiosis. *ISME J.*, 1–15. doi:10.1038/ismej.2016.124.

Ponsard, J., Cambon-Bonavita, M. A., Zbinden, M., Lepoint, G., Joassin, A., Corbari, L., et al. (2013). Inorganic carbon fixation by chemosynthetic ectosymbionts and nutritional transfers to the hydrothermal vent host-shrimp Rimicaris exoculata. *ISME J.* 7, 96–109. doi:10.1038/ismej.2012.87.

Portail, M., Brandily, C., Cathalot, C., Colaço, A., Gélinas, Y., Husson, B., et al. (2018). Food-web complexity across hydrothermal vents on the Azores triple junction. *Deep. Res. Part I Oceanogr. Res. Pap.* 131, 101–120. doi:10.1016/j.dsr.2017.11.010.

Portail, M., Olu, K., Dubois, S. F., Escobar-Briones, E., Gelinas, Y., Menot, L., et al. (2016). Food-web complexity in Guaymas Basin hydrothermal vents and cold seeps. *PLoS One* 11. doi:10.1371/journal.pone.0162263.

Portail, M., Olu, K., Escobar-Briones, E., Caprais, J. C., Menot, L., Waeles, M., et al. (2015). Comparative study of vent and seep macrofaunal communities in the Guaymas Basin. *Biogeosciences* 12, 5455–5479. doi:10.5194/bg-12-5455-2015.

Pradillon, F., Schmidt, a, Peplies, J., and Dubilier, N. (2007). Species identification of marine invertebrate early stages by whole-larvae in situ hybridisation of 18S ribosomal RNA. *Mar. Ecol. Prog. Ser.* 333, 103–116. doi:10.3354/meps333103.

Pradillon, F., Shillito, B., Young, C. M., and Gaill, F. (2001). Developmental arrest in vent worm embryos. *Nature* 413, 698–699. doi:10.1038/35099674.

Pruis, M. J., and Johnson, H. P. (2004). Tapping into the sub-seafloor: Examining diffuse flow and temperature from an active seamount on the Juan de Fuca Ridge. *Earth Planet. Sci. Lett.* 217, 379–388. doi:10.1016/S0012-821X(03)00607-1.

Raggi, L., Schubotz, F., Hinrichs, K. U., Dubilier, N., and Petersen, J. M. (2013). Bacterial symbionts of Bathymodiolus mussels and Escarpia tubeworms from Chapopote, an asphalt seep in the southern Gulf of Mexico. *Environ. Microbiol.* 15, 1969–1987. doi:10.1111/1462-2920.12051.

Rakoff-Nahoum, S., and Medzhitov, R. (2006). Role of the innate immune system and host-commensal mutualism. *Curr. Top. Microbiol. Immunol.* 308, 1–18.

Ramirez-Llodra, E., Brandt, A., Danovaro, R., De Mol, B., Escobar, E., German, C. R., et al. (2010). Deep, diverse and definitely different: Unique attributes of the world's largest ecosystem. *Biogeosciences* 7, 2851–2899. doi:10.5194/bg-7-2851-2010.

Ramirez-Llodra, E., and Segonzac, M. (2006). Reproductive biology of Alvinocaris muricola (Decapoda: Caridea: Alvinocarididae) from cold seeps in the Congo Basin. *J. Mar. Biol. Assoc. UK* 86, 1347. doi:10.1017/S0025315406014378.

Ramirez-Llodra, E., Shank, T., and German, C. (2007). Biodiversity and Biogeography of Hydrothermal Vent Species: Thirty Years of Discovery and Investigations. *Oceanography* 20, 30–41. doi:10.5670/oceanog.2007.78.

Ramirez-Llodra, E., Tyler, P. A., and Copley, J. T. P. (2000). Reproductive biology of three caridean shrimp, Rimicaris exoculata, Chorocaris chacei and Mirocaris fortunata. *J. Mar. Biol. Assoc. United Kingdom* 80, 473–484. doi:10.1017/S0025315400002174.

Ramm, T., and Scholtz, G. (2017). No sight, no smell? – Brain anatomy of two amphipod crustaceans with different lifestyles. *Arthropod Struct. Dev.* 46, 537–551. doi:10.1016/j.asd.2017.03.003.

Ramondenc, P., Germanovich, L. N., Von Damm, K. L., and Lowell, R. P. (2006). The first measurements of hydrothermal heat output at 9°50'N, East Pacific Rise. *Earth Planet. Sci. Lett.* 245, 487–497. doi:10.1016/j.epsl.2006.03.023.

Raulfs, E. C., Macko, S. A., and Van Dover, C. L. (2004). Tissue and symbiont condition of mussels exposed to varying levels of hydrothermal activity. *J. Mar. Biol. Ass. U.K.* 84, 229–234. Available at: http://journals.cambridge.org/action/displayFulltext?type=1&fid=201712&jid=&volumeId=&issueId=01&aid=201711&bodyId=&membershipNumber=&societyETOCSession=.

Ravaux, J., Cottin, D., Chertemps, T., Hamel, G., and Shillito, B. (2009). Hydrothermal vent shrimps display low expression of the heat-inducible hsp70 gene in nature. *Mar. Ecol. Prog. Ser.* 396, 153–156. doi:10.3354/meps08293.

Ravaux, J., Gaill, F., Le Bris, N., Sarradin, P., Jollivet, D., and Shillito, B. (2003). Heat-shock response and temperature resistance in the deep-sea vent shrimp Rimicaris exoculata. *J. Exp. Biol.* 206, 2345–54. doi:10.1242/jeb.00419.

Ravaux, J., Hamel, G., Zbinden, M., Tasiemski, A. A., Boutet, I., Léger, N., et al. (2013). Thermal Limit for Metazoan Life in Question: In Vivo Heat Tolerance of the Pompeii Worm. *PLoS One* 8, 4–9. doi:10.1371/journal.pone.0064074.

Ravaux, J., Léger, N., Hamel, G., and Shillito, B. (2019). Assessing a species thermal tolerance through a multiparameter approach: the case study of the deep-sea hydrothermal vent shrimp Rimicaris exoculata. *Cell Stress Chaperones* 24, 647–659. doi:10.1007/s12192-019-01003-0.

Ravaux, J., Léger, N., Rabet, N., Fourgous, C., Voland, G., Zbinden, M., et al. (2016). Plasticity and acquisition of the thermal tolerance (upper thermal limit and heat shock response) in the intertidal species Palaemon elegans. *J. Exp. Mar. Bio. Ecol.* 484, 39–45. doi:10.1016/j.jembe.2016.07.003.

Ravaux, J., Toullec, J. Y., Léger, N., Lopez, P., Gaill, F., and Shillito, B. (2007). First hsp70 from two hydrothermal vent shrimps, Mirocaris fortunata and Rimicaris exoculata: Characterization and sequence analysis. *Gene* 386, 162–172. doi:10.1016/j.gene.2006.09.001.

Reeves, E. P., Seewald, J. S., Saccocia, P., Bach, W., Craddock, P. R., Shanks, W. C., et al. (2011). Geochemistry of hydrothermal fluids from the PACMANUS , Northeast Pual and Vienna Woods hydrothermal fields , Manus Basin , Papua New Guinea. *Geochim. Cosmochim. Acta* 75, 1088–1123. doi:10.1016/j.gca.2010.11.008.

Reid, W. D. K., Sweeting, C. J., Wigham, B. D., McGill, R. A. R., and Polunin, N. V. C. (2016). Isotopic niche variability in macroconsumers of the East Scotia Ridge (Southern Ocean) hydrothermal vents: What more can we learn from an ellipse? *Mar. Ecol. Prog. Ser.* 542, 13–24. doi:10.3354/meps11571.

Reid, W. D. K., Sweeting, C. J., Wigham, B. D., Zwirglmaier, K., Hawkes, J. A., McGill, R. A. R., et al. (2013). Spatial Differences in East Scotia Ridge Hydrothermal Vent Food Webs: Influences of Chemistry, Microbiology and Predation on Trophodynamics. *PLoS One* 8, 1–11. doi:10.1371/journal.pone.0065553.

Reid, W. D. K., Watts, J., Clarke, S., Belchier, M., and Thatje, S. (2007). Egg development, hatching rhythm and moult patterns in Paralomis spinosissima (Decapoda: Anomura: Paguroidea: Lithodidae) from South Georgia waters (Southern Ocean). *Polar Biol.* 30, 1213–1218. doi:10.1007/s00300-007-0279-x.

Renninger, G. H., Kass, L., Gleeson, R. A., Van Dover, C. L., Battelle, B.-A., Jinks, R. N., et al. (1995).

Sulfide as a Chemical Stimulus for Deep-Sea Hydrothermal Vent Shrimp. *Biol. Bull.* 189, 69–76. doi:10.2307/1542456.

Reveillaud, J., Reddington, E., McDermott, J., Algar, C., Meyer, J. L., Sylva, S., et al. (2015). Subseafloor microbial communities in hydrogen-rich vent fluids from hydrothermal systems along the Mid-Cayman Rise. *Environ. Microbiol.* 18, 1970–1987. doi:10.1111/1462-2920.13173.

Reysenbach, A. L., and Shock, E. (2002). Merging genomes with geochemistry in hydrothermal ecosystems. *Science (80-. ).* 296, 1077–1082. doi:10.1126/science.1072483.

Riekenberg, P. M., Carney, R. S., and Fry, B. (2016). Trophic plasticity of the methanotrophic mussel Bathymodiolus childressi in the Gulf of Mexico. *Mar. Ecol. Prog. Ser.* 547, 91–106. doi:10.3354/meps11645.

Rieley, G., Van Dover, C. L., Hedrick, D. B., and Eglinton, G. (1999). Trophic ecology of Rimicaris exoculata: A combined lipid abundance/stable isotope approach. *Mar. Biol.* 133, 495–499. doi:10.1007/s002270050489.

Riou, V., Colaço, A., Bouillon, S., Khripounoff, A., Dando, P., Mangion, P., et al. (2010). Mixotrophy in the deep sea: A dual endosymbiotic hydrothermal mytilid assimilates dissolved and particulate organic matter. *Mar. Ecol. Prog. Ser.* 405, 187–201. doi:10.3354/meps08515.

Riou, V., Halary, S., Duperron, S., Bouillon, S., Elskens, M., Bettencourt, R., et al. (2008). Influence of CH4 and H2S availability on symbiont distribution, carbon assimilation and transfer in the dual symbiotic vent mussel Bathymodiolus azoricus. *Biogeosciences* 5, 1681–1691. doi:10.5194/bg-5-1681-2008.

Ritson-Williams, R., Arnold, S. N., and Paul, V. J. (2016). Patterns of larval settlement preferences and post-settlement survival for seven Caribbean corals. *Mar. Ecol. Prog. Ser.* 548, 127–138. doi:10.3354/meps11688.

Ritt, B., Duperron, S., Lorion, J., Sara Lazar, C., and Sarrazin, J. (2012). Integrative study of a new cold-seep mussel ( Mollusca : Bivalvia ) associated with chemosynthetic symbionts in the Marmara Sea. *Deep. Res. I* 67, 121–132. doi:10.1016/j.dsr.2012.05.009.

Rittschof, D., Forward, R. B., Cannon, G., Welch, J. M., McClary, M., Holm, E. R., et al. (1998). Cues and context: Larval responses to physical and chemical cues. *Biofouling* 12, 31–44. doi:10.1080/08927019809378344.

Ritz, D. A., Hobday, A. J., Montgomery, J. C., and Ward, A. J. W. (2011). *Social Aggregation in the Pelagic Zone with Special Reference to Fish and Invertebrates*. Elsevier Ltd doi:10.1016/B978-0-12-385529-9.00004-4.

Robidart, J. C., Bench, S. R., Feldman, R. A., Novoradovsky, A., Podell, S. B., Gaasterland, T., et al. (2008). Metabolic versatility of the Riftia pachyptila endosymbiont revealed through metagenomics. *Environ. Microbiol.* 10, 727–737. doi:10.1111/j.1462-2920.2007.01496.x.

Rogers, A. D., Tyler, P. A., Connelly, D. P., Copley, J. T., James, R., Larter, R. D., et al. (2012). The Discovery of New Deep-Sea Hydrothermal Vent Communities in the Southern Ocean and Implications for Biogeography. *PLoS Biol* 10, e1001234. doi:10.1371/journal.pbio.1001234.

Rona, P. A., Hannington, M. D., Raman, C. V., Thompson, G., Tivey, K., Humphris, S. E., et al. (1993). Active and Relict Sea-Floor Hydrothermal Mineralization at the TAG Hydrothermal. *Geology* 88.

Rona, P. A., Klinkhammer, G. P., Nelsen, T. A., Trefry, J. H., and Elderfield, H. (1986). Black smokers, massives sulphides and vent biota at the Mid-Atlantic Ridge. *Nature* 324, 698–699. doi:10.1038/320129a0.

Rosa, R. D., and Barracco, M. A. (2010). Antimicrobial peptides in crustaceans. *Isj* 7, 262–284. doi:10.1016/j.jip.2010.09.012.

Rossi, G. S., and Tunnicliffe, V. (2017). Trade-offs in a high CO2 habitat on a subsea volcano: Condition and reproductive features of a bathymodioline mussel. *Mar. Ecol. Prog. Ser.* 574, 49–64. doi:10.3354/meps12196.

Roterman, C. N., Copley, J. T., Linse, K. T., Tyler, P. A., and Rogers, A. D. (2016). Connectivity in the cold: The comparative population genetics of vent-endemic fauna in the Scotia Sea, Southern Ocean. *Mol. Ecol.* 25, 1073–1088. doi:10.1111/mec.13541.

Roterman, C. N., Lee, W., Liu, X., Lin, R., Li, X., and Won, Y. (2018). A new yeti crab phylogeny : Vent origins with indications of regional extinction in the East Pacific. *PLoS One*, 1–27.

Rouse, G. W., Goffredi, S. K., Johnson, S. B., and Vrijenhoek, R. C. (2018). An inordinate fondness for Osedax (Siboglinidae: Annelida): Fourteen new species of bone worms from California. *Zootaxa* 4377, 451–489. doi:10.11646/zootaxa.4377.4.1.

Roussel, E. G., Konn, C., Charlou, J., Donval, J., Fouquet, Y., Prieur, D., et al. (2011). Comparison of microbial communities associated with three Atlantic ultramafic hydrothermal systems ´. *FEMS Microbiol. Ecol.* 77, 647–665. doi:10.1111/j.1574-6941.2011.01161.x.

Rubin-Blum, M., Antony, C. P., Borowski, C., Sayavedra, L., Pape, T., Sahling, H., et al. (2017). Short-chain alkanes fuel mussel and sponge Cycloclasticus symbionts from deep-sea gas and oil seeps. *Nat. Microbiol.* 2, 1–11. doi:10.1038/nmicrobiol.2017.93.

Ryu, T., Woo, S., and Lee, N. (2019). The first reference transcriptome assembly of the stalked barnacle , Neolepas marisindica , from the Onnuri Vent Field on the Central Indian Ridge. *Mar. Genomics*, 0–1. doi:10.1016/j.margen.2019.04.004.

Sadosky, F., Thiebaut, E., Jollivet, D., and Shillito, B. (2002). Recruitment and population structure of the vetigastropod Lepetodrilus elevatus at 13°N hydrothermal vent sites on East Pacific Rise. *Cah. Biol. Mar.* 43, 399–402.

Salem, H., Florez, L., Gerardo, N., and Kaltenpoth, M. (2015). An out-of-body experience: The extracellular dimension for the transmission of mutualistic bacteria in insects. *Proc. R. Soc. B Biol. Sci.* 282. doi:10.1098/rspb.2014.2957.

Salerno, J. L., Macko, S. A., Hallam, S. J., Bright, M., Won, Y. J., McKiness, Z., et al. (2005). Characterization of symbiont populations in life-history stages of mussels from chemosynthetic environments. *Biol. Bull.* 208, 145–155. doi: .

Salzman, N. H., Hung, K., Haribhai, D., Chu, H., Karlsson-Sjöberg, J., Amir, E., et al. (2010). Enteric defensins are essential regulators of intestinal microbial ecology. *Nat. Immunol.* 11, 76–83. doi:10.1038/ni.1825.

Sanders, J. G., Beinart, R. a, Stewart, F. J., Delong, E. F., and Girguis, P. R. (2013). Metatranscriptomics reveal differences in in situ energy and nitrogen metabolism among hydrothermal vent snail symbionts. *ISME J.* 7, 1556–67. doi:10.1038/ismej.2013.45.

Sanger, F., and Coulson, A. (1975). A Rapid Method for Determining Sequences in DNA by Primed Synthesis with DNA Polymerase. *J. Mol. Biol.* 94, 441–448.

Sarrazin, J., and Juniper, S. K. (1999). Biological characteristics of a hydrothermal edifice mosaic community. *Mar. Ecol. Prog. Ser.* 185, 1–19. doi:10.3354/meps185001.

Sayavedra, L., Kleiner, M., Ponnudurai, R., Wetzel, S., Pelletier, E., Barbe, V., et al. (2015). Abundant toxin-related genes in the genomes of beneficial symbionts from deep-sea hydrothermal vent

mussels. *Elife* 4, 1–39. doi:10.7554/eLife.07966.001.

Schander, C., Rapp, H. T., Kongsrud, J. A., Bakken, T., Berge, J., Cochrane, S., et al. (2010). The fauna of hydrothermal vents on the Mohn Ridge (North Atlantic). *Mar. Biol. Res.* 6, 155–171. doi:10.1080/17451000903147450.

Scheirer, D. S., Shank, T. M., and Fornari, D. J. (2006). Temperature variations at diffuse and focused flow hydrothermal vent sites along the northern East Pacific Rise. *Geochemistry, Geophys. Geosystems* 7. doi:10.1029/2005GC001094.

Schmidt, C., Vuillemin, R., Le Gall, C., Gaill, F., and Le Bris, N. (2008). Geochemical energy sources for microbial primary production in the environment of hydrothermal vent shrimps. *Mar. Chem.* 108, 18–31. doi:10.1016/j.marchem.2007.09.009.

Schmidt, K., Koschinsky, A., Garbe-Schönberg, D., de Carvalho, L. M., and Seifert, R. (2007). Geochemistry of hydrothermal fluids from the ultramafic-hosted Logatchev hydrothermal field, 15°N on the Mid-Atlantic Ridge: Temporal and spatial investigation. *Chem. Geol.* 242, 1–21. doi:10.1016/j.chemgeo.2007.01.023.

Schubart, C. D., Diesel, R., and Hedges, B. (1998). Rapid evolution to terrestrial life in Jamaican crabs. *Nature* 393, 363–365. doi:10.1038/30724.

Schultz, J., Milpetz, F., Bork, P., and Ponting, C. P. (1998). SMART, a simple modular architecture research tool: Identification of signaling domains. *Proc. Natl. Acad. Sci. U. S. A.* 95, 5857–5864. doi:10.1073/pnas.95.11.5857.

Scott, J. J., Breier, J. A., Luther, G. W., and Emerson, D. (2015). Microbial iron mats at the mid-atlantic ridge and evidence that zetaproteobacteria may be restricted to iron-oxidizing marine systems. *PLoS One* 10, 1–19. doi:10.1371/journal.pone.0119284.

Seewald, J., Cruse, A., and Saccocia, P. (2003). Aqueous volatiles in hydrothermal fluids from the Main Endeavour Field, northern Juan de Fuca Ridge: Temporal variability following earthquake activity. *Earth Planet. Sci. Lett.* 216, 575–590. doi:10.1016/S0012-821X(03)00543-0.

Segonzac, M., de Saint Laurent, M., and Casanova, B. (1993). L'enigme du comportement trophique des crevettes Alvinocarididae des sites hydrothermaux de la dorsale medio-atlantique. *Cah.Biol.Mar.* 34, 535–571.

Sen, A., Becker, E. L., Podowski, E. L., Wickes, L. N., Ma, S., Mullaugh, K. M., et al. (2013). Distribution of megafauna on sulfide edifices on the Eastern Lau Spreading Center and Valu Fa Ridge. *Deep. Res. Part I Oceanogr. Res. Pap.* 72, 48–60. doi:10.1016/j.dsr.2012.11.003.

Seston, S. L., Beinart, R. A., Sarode, N., Shockey, A. C., Ranjan, P., Ganesh, S., et al. (2016). Metatranscriptional response of chemoautotrophic Ifremeria nautilei endosymbionts to differing sulfur regimes. *Front. Microbiol.* 7, 1–18. doi:10.3389/fmicb.2016.01074.

Seyfried, W. E., Seewald, J. S., and Berndt, M. E.Foustoukos, D. I. (2004). Correction to "Chemistry of hydrothermal vent fluids from the Main Endeavour Field, northern Juan de Fuca Ridge: Geochemical controls in the aftermath of June 1999 seismic events." *J. Geophys. Res. Solid Earth* 109, 1–23. doi:10.1029/2004jb003219.

Shank, T. M., Black, M. B., Halanych, K. M., Lutz, R. A., and Vrijenhoek, R. C. (1999). Miocene Radiation of Deep-Sea Hydrothermal Vent Shrimp ( Caridea : Bresiliidae ): Evidence from Mitochondrial Cytochrome Oxidase Subunit I. *Mol. Phylogenet. Evol.* 13, 244–254.

Shank, T. M., Fornari, D. J., Damm, K. L. Von, Lilley, M. D., Haymon, R. M., and Lutz, R. A. (1998a). Temporal and spatial patterns of biological community development at nascent deep-sea

hydrothermal vents ( 9 ° 50 N , East Pacific Rise ). *Deep. Res. Part II* 45, 465–515.

Shank, T. M., Lutz, R. a, and Vrijenhoek, R. C. (1998b). Molecular systematics of shrimp (Decapoda: Bresiliidae) from deep-sea hydrothermal vents, I: Enigmatic “small orange” shrimp from the Mid-Atlantic Ridge are juvenile Rimicaris exoculata. *Mol. Mar. Biol. Biotechnol.* 7, 88–96.

Sharp, K. H., and Ritchie, K. B. (2012). Multi-partner interactions in corals in the face of climate change. *Biol. Bull.* 223, 66–77. doi:10.1086/BBLv223n1p66.

Sheader, M., and Van Dover, C. L. (2007). Temporal and spatial variation in the reproductive ecology of the vent-endemic amphipod Ventiella sulfuris in the eastern Pacific. *Mar. Ecol. Prog. Ser.* 331, 181–194. doi:10.3354/meps331181.

Sheader, M., Van Dover, C. L., and Shank, T. M. (2000). Structure and function of Halice hesmonectes (Amphipoda: Pardaliscidae) swarms from hydrothermal vents in the eastern Pacific. *Mar. Biol.* 136, 901–911. doi:10.1007/s002270000300.

Sheader, M., Van Dover, C. L., and Thurston, M. H. (2004). Reproductive ecology of Bouvierella curtirama (Amphipoda: Eusiridae) from chemically distinct vents in the Lucky Strike vent field, Mid-Atlantic Ridge. *Mar. Biol.* 144, 503–514. doi:10.1007/s00227-003-1211-8.

Sheik, C. S., Anantharaman, K., Breier, J. A., Sylvan, J. B., Edwards, K. J., and Dick, G. J. (2015). Spatially resolved sampling reveals dynamic microbial communities in rising hydrothermal plumes across a back-arc basin. *ISME J.* 9, 1434–1445. doi:10.1038/ismej.2014.228.

Shillito, B., Hamel, G., Duchi, C., Cottin, D., Sarrazin, J., Sarradin, P. M., et al. (2008). Live capture of megafauna from 2300 m depth, using a newly designed Pressurized Recovery Device. *Deep. Res. Part I Oceanogr. Res. Pap.* 55, 881–889. doi:10.1016/j.dsr.2008.03.010.

Shillito, B., Jollivet, D., Sarradin, P., Rodier, P., Lallier, F., Desbruyères, D., et al. (2001). Temperature resistance of Hesiolyra bergi , a polychaetous annelid living on deep-sea vent smoker walls. *Mar. Ecol. Prog. Ser.* 216, 141–149.

Shillito, B., Le Bris, N., Hourdez, S. M., Ravaux, J., Cottin, D., Caprais, J. C., et al. (2006). Temperature resistance studies on the deep-sea vent shrimp Mirocaris fortunata. *J. Exp. Biol.* 209, 945–955. doi:10.1242/jeb.02102.

Shillito, B., Ravaux, J., Sarrazin, J., Zbinden, M., Sarradin, P. M., and Barthelemy, D. (2015). Long-term maintenance and public exhibition of deep-sea hydrothermal fauna: The AbyssBox project. *Deep. Res. Part II Top. Stud. Oceanogr.* 121, 137–145. doi:10.1016/j.dsr2.2015.05.002.

Sievert, S. M., Scott, K. M., Klotz, M. G., Chain, P. S. G., Hauser, L. J., Hemp, J., et al. (2008). Genome of the Epsilonproteobacterial Chemolithoautotroph Sulfurimonas denitrificans. *Appl. Environ. Microbiol.* 74, 1145–1156. doi:10.1128/aem.01844-07.

Sievert, S., and Vetriani, C. (2012). Chemoautotrophy at Deep-Sea Vents: Past, Present, and Future. *Oceanography* 25, 218–233. doi:10.5670/oceanog.2012.21.

Sitaraman, D., Zars, M., LaFerriere, H., Chen, Y. C., Sable-Smith, A., Kitamoto, T., et al. (2008). Serotonin is necessary for place memory in Drosophila. *Proc. Natl. Acad. Sci. U. S. A.* 105, 5579–5584. doi:10.1073/pnas.0710168105.

Slobodnika, G. B., Kolganova, T. V., Chernyh, N. A., Querellou, J., Bonch-Osmolovskaya, E. A., and Slobodkin, A. I. (2009). Deferribacter autotrophicus sp. nov., an iron(III)-reducing bacterium from a deep-sea hydrothermal vent. *Int. J. Syst. Evol. Microbiol.* 59, 1508–1512. doi:10.1099/ijs.0.006767-0.

Smith, V. J., and Dyrynda, E. A. (2015). Antimicrobial proteins: From old proteins, new tricks. *Mol.*

*Immunol.* 68, 383–398. doi:10.1016/j.molimm.2015.08.009.

Smith, V. J., Fernandes, J. M. O., Kemp, G. D., and Hauton, C. (2008). Crustins: Enigmatic WAP domain-containing antibacterial proteins from crustaceans. *Dev. Comp. Immunol.* 32, 758–772. doi:10.1016/j.dci.2007.12.002.

Snow, J., and Edmonds, H. N. (2007). Ultraslow-Spreading Ridges: Rapid Paradigm Changes. *Oceanography* 20, 90. doi:10.5670/oceanog.2007.83.

Sogin, E. M., Puskas, E., Dubilier, N., and Liebeke, M. (2019). Marine metabolomics: a method for the non-targeted measurement of metabolites in seawater by gas-chromatography mass spectrometry. *mSystems* 4, 528307. doi:10.1101/528307.

Sohn, R. A. (2007). Stochastic analysis of exit fluid temperature records from the active TAG hydrothermal mound (Mid-Atlantic Ridge, 26°N): 1. Modes of variability and implications for subsurface flow. *J. Geophys. Res. Solid Earth* 112, 1–16. doi:10.1029/2006JB004435.

Southward, E. C. (2008). The Morphology of Bacterial Symbioses in the Gills of Mussels of the Genera Adipicola and Idas (Bivalvia: Mytilidae). *J. Shellfish Res.* 27, 139–146. doi:10.2983/0730-8000(2008)27[139:tmobsi]2.0.co;2.

Southward, E. C., Tunnicliffe, V., and Black, M. (1995). Revision of the species of Ridgeia from northeast Pacific hydrothermal vents, with a redescription of Ridgeia piscesae Jones (Pogonophora: Obturata = Vestimentifera). *Can. J. Zool.* 73, 282–295. doi:10.1139/z95-033.

Spiess, F. N., Carranza, A., Cordoba, D., Cox, C., Diaz Garcia, V. M., Francheteau, J., et al. (1980). East Pacific Rise : Hot Springs and Geophysical Experimer. *Science (80-. ).* 207, 1421–1433.

Staudigel, H., Moyer, C. L., Garcia, M. O., Malahoff, A., Clague, D. A., and Koppers, A. A. P. (2006). Lō`ihi Seamount. *Earth Planet. Sci. Lett.* 23, 72–73. doi:10.1029/2005GC001222.Moore.

Stegner, M. E. J., Stemme, T., Iliffe, T. M., Richter, S., and Wirkner, C. S. (2015). The brain in three crustaceans from cavernous darkness. *BMC Neurosci.* 16. doi:10.1186/s12868-015-0138-6.

Stevens, C. J., Limén, H., Pond, D. W., Gélinas, Y., and Juniper, S. K. (2008). Ontogenetic shifts in the trophic ecology of two alvinocaridid shrimp species at hydrothermal vents on the Mariana Arc, western Pacific Ocean. *Mar. Ecol. Prog. Ser.* 356, 225–237. doi:10.3354/meps07270.

Stiller, J., Rousset, V., Pleijel, F., Chevaldonné, P., Robert, C., and Rouse, G. W. (2013). Systematics and Biodiversity Phylogeny , biogeography and systematics of hydrothermal vent and methane seep Amphisamytha ( Ampharetidae , Annelida ), with descriptions of three new species Phylogeny , biogeography and systematics of hydrothermal vent and. *Syst. Biodivers.*, 37–41.

Stokke, R., Dahle, H., Roalkvam, I., Wissuwa, J., Daae, F. L., Tooming-Klunderud, A., et al. (2015). Functional interactions among filamentous Epsilonproteobacteria and Bacteroidetes in a deep-sea hydrothermal vent biofilm. *Environ. Microbiol.* 17, 4063–4077. doi:10.1111/1462-2920.12970.

Stoss, T. D., Nickell, M. D., Hardin, D., Derby, C. D., and McClintock, T. S. (2004). Inducible Transcript Expressed by Reactive Epithelial Cells at Sites of Olfactory Sensory Neuron Proliferation. *J. Neurobiol.* 58, 355–368. doi:10.1002/neu.10294.

Strathmann, R. R. (1985). Feeding and Nonfeeding Life-History Evolution in Marine Invertebrates. *Ann. Rev. Ecol. Syst* 16, 339–361.

Streams, M. E., Fisher, C. R., and Fiala-Médioni, A. (1997). Methanotrophic symbiont location and fate of carbon incorporated from methane in a hydrocarbon seep mussel. *Mar. Biol.* 129, 465–476. doi:10.1007/s002270050187.

Sun, S., Sha, Z., and Wang, Y. (2018). Phylogenetic position of Alvinocarididae (Crustacea: Decapoda: Caridea): New insights into the origin and evolutionary history of the hydrothermal vent alvinocarid shrimps. *Deep. Res. Part I*. doi:10.1016/j.dsr.2018.10.001.

Sunamura, M., Higashi, Y., Miyako, C., Ishibashi, J. I., and Maruyama, A. (2004). Two Bacteria Phylotypes Are Predominant in the Suiyo Seamount Hydrothermal Plume. *Appl. Environ. Microbiol.* 70, 1190–1198. doi:10.1128/AEM.70.2.1190-1198.2004.

Supungul, P., Tang, S., Maneeruttanarungroj, C., Rimphanitchayakit, V., Hirono, I., Aoki, T., et al. (2008). Cloning, expression and antimicrobial activity of crustinPm1, a major isoform of crustin, from the black tiger shrimp Penaeus monodon. *Dev. Comp. Immunol.* 32, 61–70. doi:10.1016/j.dci.2007.04.004.

Suzuki, Y., Kojima, S., Watanabe, H., Suzuki, M., Tsuchida, S., Nunoura, T., et al. (2006a). Single host and symbiont lineages of hydrothermal-vent gastropods Ifremeria nautilei (Provannidae): Biogeography and evolution. *Mar. Ecol. Prog. Ser.* 315, 167–175. doi:10.3354/meps315167.

Suzuki, Y., Sasaki, T., Suzuki, M., Nogi, Y., Miwa, T., Takai, K., et al. (2005a). Novel Chemoautotrophic Endosymbiosis between a Member of the Epsilonproteobacteria and the Hydrothermal-Vent Gastropod Alviniconcha aff. hessleri (Gastropoda: Provannidae) from the Indian Ocean. *Appl. Environ. Microbiol.* 71, 5440–5450. doi:10.1128/AEM.71.9.5440.

Suzuki, Y., Sasaki, T., Suzuki, M., Tsuchida, S., Nealson, K. H., and Horikoshi, K. (2005b). Molecular phylogenetic and isotopic evidence of two lineages of chemoautotrophic endosymbionts distinct at the subdivision level harbored in one host-animal type: The genus Alviniconcha (Gastropoda: Provannidae). *FEMS Microbiol. Lett.* 249, 105–112. doi:10.1016/j.femsle.2005.06.023.

Suzuki, Y., Takai, K., Tsuchida, S., Kojima, S., Watanabe, H., Utsumi, T., et al. (2006b). Host-Symbiont Relationships in Hydrothermal Vent Gastropods of the Genus Alviniconcha from the Southwest Pacific. *Appl. Environ. Microbiol.* 72, 1388–1393. doi:10.1128/aem.72.2.1388-1393.2006.

Sylvan, J. B., Sia, T. Y., Haddad, A. G., Briscoe, L. J., Toner, B. M., Girguis, P. R., et al. (2013). Low Temperature Geomicrobiology Follows Host Rock Composition Along a Geochemical Gradient in Lau Basin. *Front. Microbiol.* 4. doi:10.3389/fmicb.2013.00061.

Sylvan, J. B., Toner, B. M., and Edwards, K. J. (2012). Life and death of deep-sea vents: Bacterial diversity and ecosystem succession on inactive hydrothermal sulfides. *MBio* 3, 1–10. doi:10.1128/mBio.00279-11.

Szafranski, K. M., Deschamps, P., Cunha, M. R., Gaudron, S. M., and Duperron, S. (2015a). Colonization of plant substrates at hydrothermal vents and cold seeps in the northeast Atlantic and Mediterranean and occurrence of symbiont-related bacteria. *Front. Microbiol.* 6, 1–14. doi:10.3389/fmicb.2015.00162.

Szafranski, K. M., Gaudron, S. M., and Duperron, S. (2014). Direct evidence for maternal inheritance of bacterial symbionts in small deep-sea clams (Bivalvia: Vesicomyidae). *Naturwissenschaften* 101, 373–383. doi:10.1007/s00114-014-1165-3.

Szafranski, K. M., Piquet, B., Shillito, B., Lallier, F. H., and Duperron, S. (2015b). Relative abundances of methane- and sulfur-oxidizing symbionts in gills of the deep-sea hydrothermal vent mussel Bathymodiolus azoricus under pressure. *Deep. Res. Part I Oceanogr. Res. Pap.* 101, 7–13. doi:10.1016/j.dsr.2015.03.003.

Takai, K., Kobayashi, H., Nealson, K. H., and Horikoshi, K. (2003). Deferribacter desulfuricans sp. nov., a novel sulfur-, nitrate- and arsenate-reducing thermophile isolated from a deep-sea

hydrothermal vent. *Int. J. Syst. Evol. Microbiol.* 53, 839–846. doi:10.1099/ijs.0.02479-0.

Takai, K., Nakamura, K., Toki, T., Tsunogai, U., Miyazaki, M., Miyazaki, J., et al. (2008a). Cell proliferation at 122 ° C and isotopically heavy CH 4 production by a hyperthermophilic methanogen under high-pressure cultivation. *Proc. Natl. Acad. Sci.* 105, 10949–10954.

Takai, K., Nunoura, T., Horikoshi, K., Shibuya, T., Nakamura, K., Suzuki, Y., et al. (2009). Variability in Microbial Communities in Black Smoker Chimneys at the NW Caldera Vent Field , Brothers Volcano , Kermadec Arc. *Geomicrobiol. J.* 26, 37–41.

Takai, K., Nunoura, T., Ishibashi, J., Lupton, J., Suzuki, R., Hamasaki, H., et al. (2008b). Variability in the microbial communities and hydrothermal fluid chemistry at the newly discovered Mariner hydrothermal field , southern Lau Basin. *J. Geophys. Res.* 113. doi:10.1029/2007JG000636.

Takaki, Y., Shimamura, S., Nakagawa, S., Fukuhara, Y., Horikawa, H., Ankai, A., et al. (2010). Bacterial lifestyle in a deep-sea hydrothermal vent chimney revealed by the genome sequence of the thermophilic bacterium deferribacter desulfuricans SSM1. *DNA Res.* 17, 123–137. doi:10.1093/dnares/dsq005.

Tandberg, A. H., Rapp, H. T., Schander, C., Vader, W., Sweetman, A. K., and Berge, J. (2012). Exitomelita sigynae gen. et sp. nov.: A new amphipod from the Arctic Loki Castle vent field with potential gill ectosymbionts. *Polar Biol.* 35, 705–716. doi:10.1007/s00300-011-1115-x.

Tasiemski, A., Massol, F., Cuvillier-Hot, V., Boidin-Wichlacz, C., Roger, E., Rodet, F., et al. (2015). Reciprocal immune benefit based on complementary production of antibiotics by the leech Hirudo verbana and its gut symbiont Aeromonas veronii. *Sci. Rep.* 5, 1–13. doi:10.1038/srep17498.

Tasiemski, A., and Salzet, M. (2017). Neuro-immune lessons from an annelid: The medicinal leech. *Dev. Comp. Immunol.* 66, 33–42. doi:10.1016/j.dci.2016.06.026.

Tassanakajon, A., Rimphanitchayakit, V., Visetnan, S., Amparyup, P., Somboonwiwat, K., Charoensapsri, W., et al. (2018). Shrimp humoral responses against pathogens: antimicrobial peptides and melanization. *Dev. Comp. Immunol.* 80, 81–93. doi:10.1016/j.dci.2017.05.009.

Teixeira, S., Cambon-Bonavita, M. A., Serrão, E. A., Desbruyéres, D., and Arnaud-Haond, S. (2011). Recent population expansion and connectivity in the hydrothermal shrimp Rimicaris exoculata along the Mid-Atlantic Ridge. *J. Biogeogr.* 38, 564–574. doi:10.1111/j.1365-2699.2010.02408.x.

Teixeira, S., Olu, K., Decker, C., Cunha, R. L., Fuchs, S., Hourdez, S., et al. (2013). High connectivity across the fragmented chemosynthetic ecosystems of the deep Atlantic Equatorial Belt: Efficient dispersal mechanisms or questionable endemism? *Mol. Ecol.* 22, 4663–4680. doi:10.1111/mec.12419.

Teixeira, S., Serrão, E. A., and Arnaud-Haond, S. (2012). Panmixia in a fragmented and unstable environment: The hydrothermal shrimp Rimicaris exoculata disperses extensively along the Mid-Atlantic ridge. *PLoS One* 7, 1–10. doi:10.1371/journal.pone.0038521.

Tennessen, J. A. (2005). Molecular evolution of animal antimicrobial peptides: Widespread moderate positive selection. *J. Evol. Biol.* 18, 1387–1394. doi:10.1111/j.1420-9101.2005.00925.x.

Thaler, A. D., and Amon, D. (2019). 262 Voyages Beneath the Sea: a global assessment of macro- and megafaunal biodiversity and research effort at deep-sea hydrothermal vents. *PeerJ* 7, e7397. doi:10.7717/peerj.7397.

Thaler, A. D., Plouviez, S., Saleu, W., Alei, F., Jacobson, A., Boyle, E. A., et al. (2014). Comparative population structure of two deep-sea hydrothermal-vent- associated decapods (Chorocaris sp.

2 and Munidopsis lauensis) from southwestern Pacific back-arc basins. *PLoS One* 9, 1–13. doi:10.1371/journal.pone.0101345.

Thaler, A. D., Zelnio, K., Saleu, W., Schultz, T. F., Carlsson, J., Cunningham, C., et al. (2011). The spatial scale of genetic subdivision in populations of Ifremeria nautilei, a hydrothermal-vent gastropod from the southwest Pacific. *BMC Evol. Biol.* 11, 372. doi:10.1186/1471-2148-11-372.

Thatje, S., Marsh, L., Roterman, C. N., Mavrogordato, M. N., and Linse, K. (2015a). Adaptations to Hydrothermal Vent Life in Kiwa tyleri, a New Species of Yeti Crab from the East Scotia Ridge, Antarctica. *PLoS One* 10, 1–20. doi:doi:10.1371/journal. pone.0127621.

Thatje, S., Smith, K., Marsh, L., and Tyler, P. (2015b). Evidence for protracted and lecithotrophic larval development in the yeti crab Kiwa tyleri from hydrothermal vents of the East Scotia Ridge, Southern Ocean. *Sex. Early Dev. Aquat. Org.* 1, 109–116. doi:10.3354/sedao00011.

Thiébaut, E., Huther, X., Shillito, B., Jollivet, D., and Gaill, F. (2002). Spatial and temporal variations of recruitment in the tube worm Riftia pachyptila on the East Pacific Rise ( 9°50'N and 13° N). *Mar. Ecol. Prog. Ser.* 234, 147–157.

Thiel, V., Hügler, M., Blümel, M., Baumann, H. I., Gärtner, A., Schmaljohann, R., et al. (2012). Widespread occurrence of two carbon fixation pathways in tubeworm endosymbionts: Lessons from hydrothermal vent associated tubeworms from the mediterranean sea. *Front. Microbiol.* 3, 1–20. doi:10.3389/fmicb.2012.00423.

Thomson, R. E., Mihály, S. F., Rabinovich, A. B., McDuff, R. E., Veirs, S. R., and Stahr, F. R. (2003). Constrained circulation at Endeavour ridge facilitates colonization by vent larvae. *Nature* 424, 545–549. doi:10.1038/nature01814.

Thomson, R. E., Subbotina, M. M., and Anisimov, M. V (2009). Numerical simulation of mean currents and water property anomalies at Endeavour Ridge : Hydrothermal versus topographic forcing. *J. Geophys. Res.* 114. doi:10.1029/2008JC005249.

Thorson, G. (1950). Reproductive and Larval ecology of marine bottom invertebrates. *Biol. Rev.* 25, 1–45. doi:10.1111/j.1469-185X.1950.tb00585.x.

Thubaut, J., Puillandre, N., Faure, B., Cruaud, C., and Samadi, S. (2013). The contrasted evolutionary fates of deep-sea chemosynthetic mussels (Bivalvia, Bathymodiolinae). *Ecol. Evol.* 3, 4748–4766. doi:10.1002/ece3.749.

Thurber, A. R. (2015). The crabs that live where hot and cold collide. *J. Anim. Ecol.* 84, 889–891. doi:10.1111/1365-2656.12398.

Thurber, A. R., Jones, W. J., and Schnabel, K. (2011). Dancing for food in the deep sea: Bacterial farming by a new species of Yeti crab. *PLoS One* 6, 1–12. doi:10.1371/journal.pone.0026243.

Tivey, M. K. (2007). Generation of Seafloor Hydrothermal Vent Fluids and Associated Mineral Deposits. *Oceanography* 20, 50–65. doi:10.5670/oceanog.2007.80.

Tivey, M. K. (2014). "Black and White Smokers Formation of Black Smoker Chimneys," in *Encyclopedia of Marine Geosciences*, 1–8. doi:10.1007/978-94-007-6644-0.

Toner, B. M., Lesniewski, R. A., Marlow, J. J., Briscoe, L. J., Santelli, C. M., Bach, W., et al. (2013). Mineralogy Drives Bacterial Biogeography of Hydrothermally Inactive Seafloor Sulfide Deposits. *Geomicrobiol. J.* 30, 313–326. doi:10.1080/01490451.2012.688925.

Trotsenko, Y. A., and Murrell, J. C. (2008). Metabolic Aspects of Aerobic Obligate Methanotrophs. *Adv. Appl. Microbiol.* 63, 183–229. doi:10.1016/S0065-2164(07)00005-6.

Tsuchida, S., Suzuki, Y., Fujiwara, Y., Kawato, M., Uematsu, K., Yamanaka, T., et al. (2011). Epibiotic association between filamentous bacteria and the vent-associated galatheid crab, Shinkaia crosnieri (Decapoda: Anomura). *J. Mar. Biol. Assoc. United Kingdom* 91, 23–32. doi:10.1017/S0025315410001827.

Tunnicliffe, V., Botros, M., De Burgh, M. E., Dinet, A., Johnson, H. P., Juniper, S. K., et al. (1985). Hydrothermal vents of Explorer Ridge, northeast Pacific. *Deep Sea Res. Part A. Oceanogr. Res. Pap.* 33, 401–412. doi:10.1016/0198-0149(86)90100-7.

Tunnicliffe, V., and Fowler, C. M. R. (1996). Influence of sea-floor spreading on the global hydrothermal vent fauna. *Nature* 379, 531–533. doi:10.1038/379531a0.

Tunnicliffe, V., and Jensen, G. R. (1987). Distribution and behaviour af the spider crab Macroregonia macrochira Sakai ( Brachyura ) around the hydrothermal vents of the northeast Pacific. *Can. J. Zool.* 65, 2443–2449.

Tunnicliffe, V., St Germain, C., and Hilário, A. (2014). Phenotypic variation and fitness in a metapopulation of tubeworms (Ridgeia piscesae jones) at hydrothermal vents. *PLoS One* 9. doi:10.1371/journal.pone.0110578.

Tyler, P. A., and Dixon, D. R. (2000). Temperature/pressure tolerance of the first larval stage of Mirocaris fortunata from Lucky Strike hydrothermal vent field. *J. Mar. Biol. Assoc. United Kingdom* 80, 739–740. doi:10.1017/S0025315400002605.

Tyler, P. A., Marsh, L., Baco-Taylor, A., and Smith, C. R. (2009). Protandric hermaphroditism in the whale-fall bivalve mollusc Idas washingtonia. *Deep. Res. Part II Top. Stud. Oceanogr.* 56, 1689–1699. doi:10.1016/j.dsr2.2009.05.014.

Tyler, P. A., Pendlebury, S., Mills, S. W., Mullineaux, L., Eckelbarger, K. J., Baker, M., et al. (2008). Reproduction of Gastropods from Vents on the East Pacific Rise and the Mid-Atlantic Ridge. *J. Shellfish Res.* 27, 107–118. doi:10.2983/0730-8000(2008)27[107:rogfvo]2.0.co;2.

Tyler, P. a., and Young, C. M. (1999). Reproduction and dispersal at vents and cold seeps. *J. Mar. Biol. Assoc. UK* 79, 193–208. doi:10.1017/S0025315499000235.

Tyler, P., Young, Æ. C. M., Dolan, Æ. E., Arellano, S. M., and Brooke, Æ. S. D. (2007). Gametogenic periodicity in the chemosynthetic cold-seep mussel ‘“ Bathymodiolus ”’ childressi. *Mar. Biol.* 150, 829–840. doi:10.1007/s00227-006-0362-9.

Unckless, R. L., Howick, V. M., and Lazzaro, B. P. (2016). Convergent Balancing Selection on an Antimicrobial Peptide in Drosophila. *Curr. Biol.* 26, 257–262. doi:10.1016/j.cub.2015.11.063.

Urakawa, H., Dubilier, N., Fujiwara, Y., Cunningham, D. E., Kojima, S., and Stahl, D. A. (2005). Hydrothermal vent gastropods from the same family (Provannidae) harbour epsilon and gamma proteobacterial endosymbionts. *Environ. Microbiol.* 7, 750–754. doi:10.1111/j.1462-2920.2005.00753.x.

Urcuyo, I. A., Bergquist, D. C., MacDonald, I. R., VanHorn, M., and Fisher, C. R. (2007). Growth and longevity of the tubeworm Ridgeia piscesae in the variable diffuse flow habitats of the Juan de Fuca Ridge. *Mar. Ecol. Prog. Ser.* 344, 143–157. doi:10.3354/meps06710.

Usher, K. M., Sutton, D. C., Toze, S., Kuo, J., and Fromont, J. (2005). Inter-generational transmission of microbial symbionts in the marine sponge Chondrilla australiensis (Demospongiae). *Mar. Freshw. Res.* 56, 125–131. doi:10.1071/MF04304.

Van Dover, C. L. (1994). In situ Spawning of Hydrothermal Vent Tubeworms (Riftia pachyptila). *Biol. Bull.* 186, 134. doi:10.2307/1542043.

Van Dover, C. L. (2001). Biogeography and Ecological Setting of Indian Ocean Hydrothermal Vents. *Science (80-. ).* 294, 818–823. doi:10.1126/science.1064574.

Van Dover, C. L. (2014). Impacts of anthropogenic disturbances at deep-sea hydrothermal vent ecosystems: A review. *Mar. Environ. Res.* 102, 59–72. doi:10.1016/j.marenvres.2014.03.008.

Van Dover, C. L., Ardron, J. A., Escobar, E., Gianni, M., Gjerde, K. M., Jaeckel, A., et al. (2017). Biodiversity loss from deep-sea mining. *Nat. Geosci.* 10, 464–465. doi:10.1038/ngeo2983.

Van Dover, C. L., Arnaud-Haond, S., Gianni, M., Helmreich, S., Huber, J. A., Jaeckel, A. L., et al. (2018). Scientific rationale and international obligations for protection of active hydrothermal vent ecosystems from deep-sea mining. *Mar. Policy* 90, 20–28. doi:10.1016/j.marpol.2018.01.020.

Van Dover, C. L., Factor, J. R., Williams, A. B., and Berg Jr., C. J. (1985). Reproductive patterns of decapod crustaceans from hydrothermal vents. *Bull. Biol. Soc. Washingt.*, 223–227. doi:10.2307/1380793.

Van Dover, C. L., and Fry, B. (1994). Microorganisms as food resources at deep-sea hydrothermal. *Limnol. Oceanogr.* 39, 51–57.

Van Dover, C. L., Fry, B., Grassle, J. F., Humphris, S., and Rona, P. A. (1988). Feeding biology of the shrimp Rimicaris exoculata at hydrothermal vents on the Mid-Atlantic Ridge. *Mar. Biol.* 98, 209–216. doi:10.1007/BF00391196.

Van Dover, C. L., Polz, M. F., Robinson, J., Cavanaugh, C. M., Kadko, D. C., and Hickey, P. J. (1997). Predatory Anemones at TAG. *Bridg. Newsl.* 12.

Van Dover, C. L., Szuts, E. Z., Chamberlain, S. C., and Cann, J. R. (1989). A novel eye in “eyeless” shrimp from hydrothermal vents of the Mid-Atlantic Ridge. *Nature* 337, 458–460. doi:10.1038/337458a0.

Veirs, S. R., McDuff, R. E., and Stahr, F. R. (2006). Magnitude and variance of near-bottom horizontal heat flux at the Main Endeavour hydrothermal vent field. *Geochemistry, Geophys. Geosystems* 7. doi:10.1029/2005GC000952.

Vereshchaka, A. L. (1996). Comparative analysis of taxonomic composition of shrimps as edificators of hydrothermal communities in the Mid-Atlantic Ridge. in *Doklady Biological Sciences* (New York: Consultants Bureau, c1965-1992.), 576–578.

Vereshchaka, A. L., Kulagin, D. N., and Lunina, A. A. (2015). Phylogeny and new classification of hydrothermal vent and seep shrimps of the family alvinocarididae (Decapoda). *PLoS One* 10, 1–29. doi:10.1371/journal.pone.0129975.

Vereshchaka, A. L., Lein, A. Y., Vinogradov, G. M., Dalton, S., and Dehairs, F. (2000). Carbon and nitrogen isotopic composition of the fauna from the Broken Spur hydrothermal vent field. *Mar. Biol.* 136, 11–17. doi:10.1007/s002270050002.

Vic, C., Gula, J., Roullet, G., and Pradillon, F. (2018). Dispersion of deep-sea hydrothermal vent effluents and larvae by submesoscale and tidal currents. *Deep. Res. Part I Oceanogr. Res. Pap.* 133, 1–18. doi:10.1016/j.dsr.2018.01.001.

Von Damm, K. L. (2004). Evolution of the Hydrothermal System at East Pacific Rise 9°50’N : Geochemical Evidence for Changes in the Upper Oceanic Crust. *Geophys. Monogr. Ser.*, 285–304. doi:doi:10.1029/148gm12.

Von Damm, K. L., Lilley, M. D., III, W. C. S., Brockington, M., Bray, A. M., O’Grady, K. M., et al. (2003). Extraordinary phase separation and segregation in vent fluids from the southern East Pacific Rise. *Earth Planet. Sci. Lett.* 206, 365–378. doi:10.1016/S0012-821X(02)01081-6.

Von Damm, K. L., Von, Oosting, S., E., Kozlowski, R., Buttermore, L., et al. (1995). Evolution of East Pacific Rise hydrothermal vent fluids following a volcanic eruption. *Nature* 375, 47–50. doi:10.1038/375047a0.

Vrijenhoek, R. C. (2009). Cryptic species, phenotypic plasticity, and complex life histories: Assessing deep-sea faunal diversity with molecular markers. *Deep. Res. Part II Top. Stud. Oceanogr.* 56, 1713–1723. doi:10.1016/j.dsr2.2009.05.016.

Waite, D. W., Vanwonterghem, I., Rinke, C., Parks, D. H., Zhang, Y., Takai, K., et al. (2017). Comparative genomic analysis of the class Epsilonproteobacteria and proposed reclassification to epsilonbacteraeota (phyl. nov.). *Front. Microbiol.* 8. doi:10.3389/fmicb.2017.00682.

Waite, T. J., Moore, T. S., Hsu-Kim, H., Tsang, J., Paschal, A. N., Waite, T. J., et al. (2008). Variation in Sulfur Speciation with Shellfish Presence at a Lau Basin Diffuse Flow Vent Site. *J. Shellfish Res.* 27, 163–168. doi:10.2983/0730-8000(2008)27[163:vissws]2.0.co;2.

Walsh, D. A., Zaikova, E., Howes, C. G., Song, Y. C., Wright, J. J., Tringe, S. G., et al. (2009). Metagenome of a Versatile Oceanic Dead Zones. *Science (80-. ).* 326, 4–6.

Wang, H., Li, H., Shao, Z., Liao, S., Johnstone, L., Rensing, C., et al. (2012). Genome sequence of deep-sea manganese-oxidizing bacterium Marinobacter manganoxydans MnI7-9. *J. Bacteriol.* 194, 899–900. doi:10.1128/JB.06551-11.

Wang, Y. R., and Sha, Z. L. (2017). A new species of the genus Alvinocaris Williams and Chace, 1982 (Crustacea: Decapoda: Caridea: Alvinocarididae) from the Manus Basin hydrothermal vents, Southwest Pacific. *Zootaxa* 4226, 126–136. doi:10.11646/zootaxa.4226.1.7.

Wang, Y., Stingl, U., Anton-erxleben, F., Geisler, S., Brune, A., and Zimmer, M. (2004). "Candidatus Hepatoplasma crinochetorum," a New, Stalk-Forming Lineage of. *Appl. Environ. Microbiol.* 70, 6166–6172. doi:10.1128/AEM.70.10.6166.

Wankel, S. D., Germanovich, L. N., Lilley, M. D., Genc, G., DiPerna, C. J., Bradley, A. S., et al. (2011). Influence of subsurface biosphere on geochemical fluxes from diffuse hydrothermal fluids. *Nat. Geosci.* 4, 461–468. doi:10.1038/ngeo1183.

Watabe, H., and Hashimoto, J. (2002). A New Species of the Genus Rimicaris ( Alvinocarididae : Caridea : Decapoda ) from the Active Hydrothermal Vent Field on the Central Indian Ridge. *Zoolog. Sci.* 19, 1167–1174.

Watanabe, H., Kado, R., and Kaida, M. (2006). Dispersal of vent-barnacle (genus Neoverruca) in the Western Pacific. *Cah. Biol. Mar.*, 353–357.

Watanabe, H., Yahagi, T., Nagai, Y., Seo, M., Kojima, S., Ishibashi, J. ichiro, et al. (2016). Different thermal preferences for brooding and larval dispersal of two neighboring shrimps in deep-sea hydrothermal vent fields. *Mar. Ecol.*, 1–8. doi:10.1111/maec.12318.

Watson, M. G., Scardino, A. J., Zalizniak, L., and Shimeta, J. (2016). Inhibition of invertebrate larval settlement by biofilm ciliates. *Mar. Ecol. Prog. Ser.* 557, 77–90. doi:10.3354/meps11825.

Watsuji, T.-O., Nakagawa, S., Tsuchida, S., Toki, T., Hirota, A., Tsunogai, U., et al. (2010). Diversity and function of epibiotic microbial communities on the galatheid crab, Shinkaia crosnieri. *Microbes Environ.* 25, 288–294. doi:10.1264/jsme2.ME10135.

Watsuji, T., Motoki, K., Hada, E., Nagai, Y., Takaki, Y., Yamamoto, A., et al. (2018). Compositional and Functional Shifts in the Epibiotic Bacterial Community of *Shinkaia crosnieri* Baba & Williams (a Squat Lobster from Hydrothermal Vents) during Methane-Fed Rearing. *Microbes Environ.* 33, 348–356. doi:10.1264/jsme2.me18072.

Watsuji, T. O., Yamamoto, A., Motoki, K., Ueda, K., Hada, E., Takaki, Y., et al. (2015). Molecular evidence of digestion and absorption of epibiotic bacterial community by deep-sea crab Shinkaia crosnieri. *ISME J.* 9, 821–831. doi:10.1038/ismej.2014.178.

Watsuji, T. O., Yamamoto, A., Takaki, Y., Ueda, K., Kawagucci, S., and Takai, K. (2014). Diversity and methane oxidation of active epibiotic methanotrophs on live Shinkaia crosnieri. *ISME J.* 8, 1020–1031. doi:10.1038/ismej.2013.226.

Webber, A. P., Roberts, S., Murton, B. J., and Hogdkinson, M. R. (2015). Geology, sulphide geochemistry and supercritical venting at the Beebe hydrothermal vent field, Cayman Trough. *Geochemistry, Geophys. Geosystems* 1, 2661–2678. doi:10.1017/CBO9781107415324.004.

Wenner, M. A., Fusaro, C., and Oaten, A. (1974). Size at onset of sexual maturity and growth rate in crustacean populations. *Can. J. Zool.* 52, 1095–1106. doi:10.1890/06-0562.1.PMID.

Wentrup, C., Wendeberg, A., Huang, J. Y., Borowski, C., and Dubilier, N. (2013). Shift from widespread symbiont infection of host tissues to specific colonization of gills in juvenile deep-sea mussels. *ISME J.* 7, 1244–1247. doi:10.1038/ismej.2013.5.

Wentrup, C., Wendeberg, A., Schimak, M., Borowski, C., and Dubilier, N. (2014). Forever competent: Deep-sea bivalves are colonized by their chemosynthetic symbionts throughout their lifetime. *Environ. Microbiol.* 16, 3699–3713. doi:10.1111/1462-2920.12597.

Wheeler, A. J., Murton, B., Copley, J., Lim, A., Carlsson, J., Collins, P., et al. (2013). Moytirra: Discovery of the first known deep-sea hydrothermal vent field on the slow-spreading Mid-Atlantic Ridge north of the Azores. *Geochemistry, Geophys. Geosystems* 14, 4170–4184. doi:10.1002/ggge.20243.

Williams, A. B., and Rona, P. A. (1986). Two New Caridean Shrimps from a Hydrothermal Field on the Mid Atlantic Ridge. *J. Crustac. Biol.* 6, 446–462.

Windoffer, R., and Giere, O. (1997). Symbiosis of the Hydrothermal Vent Gastropod Ifremeria nautilei (Provannidae) with Endobacteria-Structural Analyses and Ecological Considerations. *Biol. Bull.* 193, 381–392.

Winogradsky, S. (1887). Über Schwefelbakterien. *Britr. Biol. Pflanz* 45, 335.

Wippler, J., Kleiner, M., Lott, C., Gruhl, A., Abraham, P. E., Giannone, R. J., et al. (2016). Transcriptomic and proteomic insights into innate immunity and adaptations to a symbiotic lifestyle in the gutless marine worm Olavius algarvensis. *BMC Genomics* 17, 942. doi:10.1186/s12864-016-3293-y.

Wolff, G. H., Thoen, H. H., Marshall, J., Sayre, M. E., and Strausfeld, N. J. (2017). An insect-like mushroom body in a crustacean brain. *Elife* 6, 1–24. doi:10.7554/eLife.29889.

Won, Y.-J., Jones, W. J., and Vrijenhoek, R. C. (2008). Absence of Cospeciation Between Deep-Sea Mytilids and Their Thiotrophic Endosymbionts. *J. Shellfish Res.* 27, 129–138. doi:10.2983/0730-8000(2008)27[129:AOCBDM]2.0.CO;2.

Won, Y., Young, C. R., Lutz, R. A., and Vrijenhoek, R. C. (2003). Dispersal barriers and isolation among deep-sea mussel populations (Mytilidae: Bathymodiolus) from eastern Pacific hydrothermal vents. *Mol. Ecol.* 12, 169–184. doi:10.1046/j.1365-294X.2003.01726.x.

Wu, X., and Xu, K. (2018). Levensteiniella manusensis sp. nov., a new polychaete species (Annelida: Polynoidae) from deep-sea hydrothermal vents in the Manus Back-Arc Basin, Western Pacific. *Zootaxa* 4388, 102–110. doi:10.11646/zootaxa.4388.1.7.

Yahagi, T., Fukumori, Y., Waren, A., and Kano, Y. (2017a). Population connectivity of hydrothermal-

vent limpets along the northern Mid-Atlantic Ridge ( Gastropoda : Neritimorpha : Phenacolepadidae ). *J. Mar. Biol. Assoc. United Kingdom*, 1–7. doi:10.1017/S0025315417001898.

Yahagi, T., Kayama Watanabe, H., Kojima, S., and Kano, Y. (2017b). Do larvae from deep-sea hydrothermal vents disperse in surface waters? *Ecology* 98, 1524–1534. doi:10.1002/ecy.1800.

Yahagi, T., Watanabe, H., Ishibashi, J. I., and Kojima, S. (2015). Genetic population structure of four hydrothermal vent shrimp species (Alvinocarididae) in the Okinawa Trough, Northwest Pacific. *Mar. Ecol. Prog. Ser.* 529, 159–169. doi:10.3354/meps11267.

Yahagi, T., Watanabe, H. K., Kojima, S., and Kano, Y. (2017c). Do larvae from deep-sea hydrothermal vents disperse in surface waters ? *Ecology* 98, 1524–1534. doi:10.1111/ijlh.12426.

Yamamoto, M., and Takai, K. (2011). Sulfur metabolisms in epsilon-and gamma-proteobacteria in deep-sea hydrothermal fields. *Front. Microbiol.* 2, 1–8. doi:10.3389/fmicb.2011.00192.

Yang, C. H., Tsuchida, S., Fujikura, K., Fujiwara, Y., Kawato, M., and Chan, T. Y. (2016). Connectivity of the squat lobsters Shinkaia crosnieri (Crustacea: Decapoda: Galatheidae) between cold seep and hydrothermal vent habitats. *Bull. Mar. Sci.* 92, 17–31. doi:10.5343/bms.2015.1031.

Yang, J., Lu, B., Chen, D., Yu, Y., Yang, F., Nagasawa, H., et al. (2013). When Did Decapods Invade Hydrothermal Vents ? Clues from the Western Pacific and Indian Oceans. *Mol. Biol. Evol.* 30, 305–309. doi:10.1093/molbev/mss224.

Young, C. M. (2003). “Reproduction, Development & Life history Traits,” in *Ecosystem of Deep Oceans* Ecosystems of the World. (Elsevier Science), 381–426. Available at: https://books.google.fr/books?id=62zMI9P4Vv8C.

Young, C. M., He, R., Emlet, R. B., Li, Y., Qian, H., Arellano, S. M., et al. (2012). Dispersal of deep-sea larvae from the intra-American seas: Simulations of trajectories using ocean models. *Integr. Comp. Biol.* 52, 483–496. doi:10.1093/icb/ics090.

Yücel, M., and Luther, G. W. (2013). Temporal trends in vent fluid iron and sulfide chemistry following the 2005/2006 eruption at East Pacific Rise, 9°50’N. *Geochemistry, Geophys. Geosystems* 14, 759–765. doi:10.1002/ggge.20088.

Zal, F., Jollivet, D., Chevaldonné, P., and Desbruyères, D. (1995). Reproductive biology and population structure of the deep-sea hydrothermal vent worm Paralvinella grasslei (Polychaeta: Alvinellidae) at 13~ on the East Pacific Rise. *Mar. Biol.* 122, 637–648.

Zal, F., Leize, E., Lallier, F. H., Toulmond, A., Van Dorsselaer, A., and Childress, J. J. (1998). S-Sulfohemoglobin and disulfide exchange: The mechanisms of sulfide binding by Riftia pachyptila hemoglobins. *Proc. Natl. Acad. Sci.* 95, 8997–9002. doi:10.1073/pnas.95.15.8997.

Zal, F., Leize, E., Oros, D. R., Hourdez, S., Dorsselaer, A. Van, and Childress, J. J. (2000). Haemoglobin structure and biochemical characteristics of the sulphide-binding component from the deep-sea clam Calyptogena magnifica. *Cah. Biol. Mar.* 41, 413–423.

Zasloff, M. (2002). Antimicrobial peptides of multicellular organisms. *Nature* 415, 389–395.

Zbinden, M., Berthod, C., Montagné, N., Machon, J., Léger, N., Chertemps, T., et al. (2017). Comparative study of chemosensory organs of shrimp from hydrothermal vent and coastal environments. *Chem. Senses* 42, 319–331. doi:10.1093/chemse/bjx007.

Zbinden, M., and Cambon-Bonavita, M. A. (2003). Occurrence of Deferribacterales and Entomoplasmatales in the deep-sea Alvinocarid shrimp Rimicaris exoculata gut. *FEMS Microbiol. Ecol.* 46, 23–30. doi:10.1016/S0168-6496(03)00176-4.

Zbinden, M., Gallet, A., Szafranski, K. M., Machon, J., Ravaux, J., Léger, N., et al. (2018). Blow Your Nose, Shrimp! Unexpectedly Dense Bacterial Communities Occur on the Antennae and Antennules of Hydrothermal Vent Shrimp. *Front. Mar. Sci.* 5, 1–14. doi:10.3389/fmars.2018.00357.

Zbinden, M., Le Bris, N., Gaill, F., and Compère, P. (2004). Distribution of bacteria and associated minerals in the gill chamber of the vent shrimp Rimicaris exoculata and related biogeochemical processes. *Mar. Ecol. Prog. Ser.* 284, 237–251. doi:10.3354/meps284237.

Zbinden, M., Marqué, L., Gaudron, S. M., Ravaux, J., Léger, N., and Duperron, S. (2014). Epsilonproteobacteria as gill epibionts of the hydrothermal vent gastropod Cyathermia naticoides (North East-Pacific Rise). *Mar. Biol.* 162, 435–448. doi:10.1007/s00227-014-2591-7.

Zbinden, M., Shillito, B., Le Bris, N., de Villardi de Montlaur, C., Roussel, E., Guyot, F., et al. (2008). New insigths on the metabolic diversity among the epibiotic microbial communitiy of the hydrothermal shrimp Rimicaris exoculata. *J. Exp. Mar. Bio. Ecol.* 359, 131–140. doi:10.1016/j.jembe.2008.03.009.

Zeppilli, D., Bellec, L., Cambon-Bonavita, M.-A., Decraemer, W., Fontaneto, D., Fuchs, S., et al. (2019). Ecology and trophic role of Oncholaimus dyvae sp. nov. (Nematoda: Oncholaimidae) from the lucky strike hydrothermal vent field (Mid-Atlantic Ridge). *BMC Zool.* 4, 1–15. doi:10.1186/s40850-019-0044-y.

Zeppilli, D., Leduc, D., Fontanier, C., Fontaneto, D., Fuchs, S., Gooday, A. J., et al. (2018). Characteristics of meiofauna in extreme marine ecosystems : a review. *Mar. Biodiversity* 48.

Zeppilli, D., Vanreusel, A., Pradillon, F., Fuchs, S., Mandon, P., James, T., et al. (2015). Rapid colonisation by nematodes on organic and inorganic substrata deployed at the deep-sea Lucky Strike hydrothermal vent field (Mid-Atlantic Ridge). *Mar. Biodivers.* 45, 489–504. doi:10.1007/s12526-015-0348-2.

Zhou, Y., Zhang, D., Zhang, R., Liu, Z., Tao, C., Lu, B., et al. (2018). Characterization of vent fauna at three hydrothermal vent fields on the Southwest Indian Ridge : Implications for biogeography and interannual dynamics on ultraslow-spreading ridges. *Deep. Res. Part I*. doi:10.1016/j.dsr.2018.05.001.

Zielinski, F. U., Pernthaler, A., Duperron, S., Raggi, L., Giere, O., Borowski, C., et al. (2009). Widespread occurrence of an intranuclear bacterial parasite in vent and seep bathymodiolin mussels. *Environ. Microbiol.* 11, 1150–1167. doi:10.1111/j.1462-2920.2008.01847.x.

Zimmermann, J., Lott, C., Weber, M., Ramette, A., Bright, M., Dubilier, N., et al. (2014). Dual symbiosis with co-occurring sulfur-oxidizing symbionts in vestimentiferan tubeworms from a Mediterranean hydrothermal vent. *Environ. Microbiol.* 16, 3638–3656. doi:10.1111/1462-2920.12427.

Zimmermann, J., Wentrup, C., Sadowski, M., Blazejak, A., Gruber-Vodicka, H. R., Kleiner, M., et al. (2016). Closely coupled evolutionary history of ecto- and endosymbionts from two distantly related animal phyla. *Mol. Ecol.*, 1–21. doi:10.1111/mec.13554.

Zook, D. (2015). "Symbiosis—Evolution's Co-Author," in *Reticulate Evolution*, ed. N. Gontier (Springer US), 41–81. doi:10.1111/j.1365-294X.2011.05004.x.

Zwirglmaier, K., Reid, W. D. K., Heywood, J., Sweeting, C. J., Wigham, B. D., Polunin, N. V. C., et al. (2015). Linking regional variation of epibiotic bacterial diversity and trophic ecology in a new species of Kiwaidae ( Decapoda , Anomura ) from East Scotia Ridge ( Antarctica ) hydrothermal vents. *Microbiologyopen*, 136–150. doi:10.1002/mbo3.227.

# REFERENCES

UNIVERSITE SCIENCES BRETAGNE DE LA MER LOIRE ET DU LITTORAL

UBO Université de Bretagne Occidentale

Titre : **Cycles de vie de deux crevettes hydrothermales de la dorsale médio-atlantique : *Rimicaris exoculata* et *Rimicaris chacei***

**Mots clés:** Sources hydrothermales, crevettes *Rimicaris*, Symbioses, traits d'histoire de vie, colonisation, chimiosynthèse

**Résumé:** Les écosystèmes hydrothermaux profonds sont des oasis de vie denses où la production primaire est dépendante de la chimiosynthèse réalisée par des microorganismes, dont certains forment des symbioses avec les taxons hydrothermaux dominants. Dans cet habitat éphémère et fragmenté, ces organismes endémiques font face à un double défi : disperser à travers un environnement très différent du biotope hydrothermal, et maintenir l'association symbiotique essentielle à la colonisation de ce milieu. Les crevettes du genre *Rimicaris* dominent les communautés des sites hydrothermaux profonds de la ride médio-Atlantique. Ici, l'étude de deux espèces, *R. exoculata* et *R. chacei*, vivant en sympatrie, nous permet d'aborder des questionnements liés à leur cycle de vie et au développement de leur relation symbiotique, pour comprendre ce qui peut expliquer leur différence apparente de succès de colonisation. Aux stades de vie embryonnaire, l'étude de la prolifération bactérienne chez *R. exoculata* suggère une possible transmission précoce de certaines lignées symbiotiques. Après avoir réévalué la taxonomie des stades juvéniles des deux espèces de *Rimicaris*, différents aspects de leur structure démographique, de leur reproduction et de leur transition trophique au cours du développement juvénile vers une nutrition impliquant la chimiosynthèse bactérienne ont été étudiés. Les résultats mettent en évidence des différences aussi bien du point de vue de la vie larvaire que des processus post-recrutement. Les avancées ainsi réalisées suggèrent de nouvelles voies de recherche pour lever les verrous persistant dans la compréhension du cycle de vie de ces espèces, et soulignent l'importance de replacer nos connaissances dans la perspective de l'histoire de colonisation des systèmes hydrothermaux en étendant les approches développées ici à des espèces apparentées vivant dans d'autres régions du globe.

Title : **Lifecycles of two hydrothermal vent shrimps from the Mid-Atlantic Ridge: *Rimicaris exoculata* and *Rimicaris chacei***

**Keywords :** Hydrothermal vent, *Rimicaris* shrimps, Symbioses, Life-history traits, colonization, chemosynthesis

**Abstract:** Deep hydrothermal vent ecosystems are dense oases of life, which are mainly sustained by chemosynthetic primary production carried out by microorganisms, some of which are involved in symbioses with key dominant vent taxa. In this ephemeral and patchy habitat, endemic vent species face a double challenge: a dispersal phase through environments radically different from their vent biotope, and the transmission of symbionts that are essential to colonize vent systems. *Rimicaris* shrimps dominate communities of deep vent fields of the Mid Atlantic Ridge. Here, the study of two species, *R. exoculata* and *R. chacei*, living in sympatry, allows us to address issues related to their life cycle and the development of their symbiotic relationships, to understand what may explain the apparent difference in their colonization success. In embryonic life stages, the study of bacterial proliferation in *R. exoculata* suggests a possible early transmission of certain symbiotic lines. After reassessing juvenile stages taxonomy of both species of *Rimicaris*, different aspects of their demographic structure, reproduction and trophic transition during juvenile development towards a nutrition involving bacterial chemosynthesis were analyzed through a variety of approaches. The results highlight differences in both larval life and post-recruitment processes. The advances achieved here also open new research avenues to bridge remaining gaps still preventing a comprehensive understanding of their life cycle, while emphasizing the importance of placing this knowledge in the perspective of the colonization history of deep-sea vents by extending our approach to related species origination from other parts of the world.